

**ISOLATION AND ANALYSIS OF POLYCYCLIC AROMATIC
HYDROCARBONS (PAHs) TO DETERMINE AMBIENT AIR QUALITY
FROM DIFFERENT BIOINDICATORS: PROCESS INTENSIFICATION
APPROACH FOR SOLVENT EXTRACTION TECHNIQUES**

**THESIS SUBMITTED
BY
SHRITAMA MUKHOPADHYAY**

DOCTOR OF PHILOSOPHY (ENGINEERING)

**DEPARTMENT OF CHEMICAL ENGINEERING,
FACULTY COUNCIL OF ENGINEERING & TECHNOLOGY
JADAVPUR UNIVERSITY
KOLKATA-700032, INDIA**

2024

JADAVPUR UNIVERSITY
KOLKATA-700032, INDIA

INDEX NO.: 186/19/E

1. Title of the thesis : Isolation and analysis of polycyclic aromatic hydrocarbons (PAHs) to determine ambient air quality from different bioindicators: Process intensification approach for solvent extraction techniques.

2. Name, Designation & Institution of the Supervisors :

Dr. Ratna Dutta

Associate Professor

Department of Chemical Engineering

Jadavpur University

Kolkata-700032, India.

&

Prof. (Dr.) Papita Das

Professor

Department of Chemical Engineering

Jadavpur University

Kolkata-700032, India.

3. List of Publications in International Journals:

1. **Mukhopadhyay, S.,** Dutta, R., Das, P., 2024. Greenery planning for urban air pollution control based on biomonitoring potential: Explicit emphasis on foliar accumulation of particulate matter (PM) and polycyclic aromatic hydrocarbons (PAHs). **Journal of Environmental Management** 355, 120524.

<https://doi.org/10.1016/j.jenvman.2024.120524>

2. **Mukhopadhyay, S.,** Dutta, R., Dhara, A., Das, P., 2023. Biomonitoring of polycyclic aromatic hydrocarbons (PAHs) by *Murraya paniculata* (L.) Jack in South Kolkata, West Bengal, India: Spatial and temporal variations. **Environmental Geochemistry and Health** 45, 5761–5781.
<https://doi.org/10.1007/s10653-023-01506-x>
3. **Mukhopadhyay, S.,** Dutta, R., Dhara, A., 2021 Assessment of Air Pollution Tolerance Index of *Murraya paniculata* (L.) Jack in Kolkata metro city, West Bengal, India. **Urban Climate** 39, 100977.
<https://doi.org/10.1016/j.uclim.2021.100977>
4. **Mukhopadhyay, S.,** Dutta, R., Das, P., 2020. A critical review on plant biomonitors for determination of polycyclic aromatic hydrocarbons (PAHs) in air through solvent extraction techniques. **Chemosphere** 251, 126441.
<https://doi.org/10.1016/j.chemosphere.2020.126441>
5. Ghosh, S., Dutta, R., **Mukhopadhyay, S.,** 2023. A Review on Seasonal Changes in Particulate Matter Accumulation by Plant Bioindicators: Effects on Leaf Traits. **Water, Air, and Soil Pollution** 234, 1-18.
<https://doi.org/10.1007/s11270-023-06549-5>

4. List of Patents : Nil

5. List of Presentations in National/International Conferences :

1. Aparna Dhara, Ratna Dutta, Marshal Murmu, **Shritama Mukhopadhyay**, Efficacy of *Magnifera indica* as biomonitoring plant species for atmospheric polycyclic aromatic hydrocarbons (PAHs) and heavy metals (HMs), **National Symposium on Sustainable Technology & Management for Humanistic Growth**, jointly organized by the Faculty of Engineering & Technology, Jadavpur University and Vivekananda Institute of Environment & Management, during December 22-23, 2023, at Jadavpur University, Kolkata, India.
2. Aparna Dhara, **Shritama Mukhopadhyay**, Ratna Dutta, Polycyclic aromatic hydrocarbon pollution in the urban wetland soil in South Kolkata, **International Conference on Chemical Engineering, Innovations & Sustainability (ICEIS 2023)**, organized by the Department of Chemical Engineering, Jadavpur University, Kolkata, India, on the auspicious occasion of Centenary Celebration Program, during February, 25-27, 2023, at Jadavpur University, Kolkata, India.

3. **Shritama Mukhopadhyay**, Ratna Dutta, Aparna Dhara, Papita Das, Seasonal trends of atmospheric polycyclic aromatic hydrocarbons (PAHs) in Kolkata metro city of India: Biomonitoring using foliage of *Murraya paniculata* (L.) Jack, **International Conference on Advances in Chemical and Material Sciences (ACMS-2022)** - On the occasion of Platinum Jubilee Year of Indian Institute of Chemical Engineers, organized by Indian Institute of Chemical Engineers, Kolkata, In association with National Institute of Technology, Jalandhar, Heritage Institute of Technology, Kolkata & Osmania University College of Technology, Hyderabad, during April 14-16, 2022.
4. **Shritama Mukhopadhyay**, Aparna Dhara, Ratna Dutta, Bioindicators for monitoring of ambient air pollution and its bioremediation - A Review, **9th International Conference on Sustainable Waste Management towards Circular Economy (9th IconSWM-CE 2019)**, organised by Kalinga Institute of Industrial Technology (KIIT) (DU), Odisha, India and International Society of Waste Management, Air and Water (ISWMAW) under the Aegis of International Society of Waste Management, Air and Water (ISWMAW) at KIIT, Bhubaneswar, Odisha, India during November 27-30, 2019.

PROFORMA – 1

“Statement of Originality”

I, **Shritama Mukhopadhyay**, registered on 26th June 2019 do hereby declare that this thesis entitled “**Isolation and analysis of polycyclic aromatic hydrocarbons (PAHs) to determine ambient air quality from different bioindicators: Process intensification approach for solvent extraction techniques**” contains literature survey and original research work done by the undersigned candidate as part of Doctoral studies.

All information in this thesis have been obtained and presented in accordance with existing academic rules and ethical conduct. I declare that, as required by these rules and conduct, I have fully cited and referred all materials and results that are not original to this work.

I also declare that I have checked this thesis as per the “Policy on Anti Plagiarism, Jadavpur University, 2019”, and the level of similarity as checked by iThenticate software is 6 %.

Shritama Mukhopadhyay
Signature of Candidate:

Date : 23/07/2024

Certified by Supervisors:

(Signature with date, seal)

Ratna Dutta 23/07/24

Dr. Ratna Dutta

Associate Professor

Department of Chemical Engineering

Jadavpur University

Kolkata-700032, India.

Papita Das 23/07/24

Prof. (Dr.) Papita Das

Professor

Department of Chemical Engineering

Jadavpur University

Kolkata-700032, India.

Dr. Ratna Dutta

Associate Professor

Chemical Engineering Department

JADAVPUR UNIVERSITY

Kolkata - 700 032, India

Dr. Papita Das
Professor
Dept. of Chemical Engineering
Jadavpur University, Kolkata

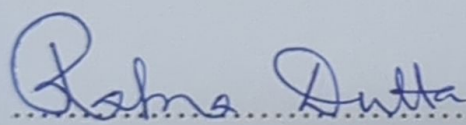


PROFORMA - 2

CERTIFICATE FROM THE SUPERVISORS

This is to certify that the thesis entitled "Isolation and analysis of polycyclic aromatic hydrocarbons (PAHs) to determine ambient air quality from different bioindicators: Process intensification approach for solvent extraction techniques" submitted by Smt. Shritama Mukhopadhyay, who got her name registered on 26th June 2019 for the award of Ph.D. (Engineering) degree of Jadavpur University is absolutely based upon her own work under the supervision of Dr. Ratna Dutta and Prof. (Dr.) Papita Das and that neither her thesis nor any part of the thesis has been submitted for any degree or any other academic award anywhere before.

(Signature of the Supervisors and
date with office seal)

 23/07/24

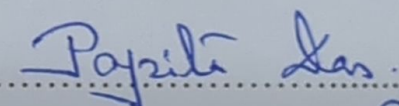
Dr. Ratna Dutta

Associate Professor

Department of Chemical Engineering

Jadavpur University

Kolkata-700032, India.

 23/07/24

Prof. (Dr.) Papita Das

Professor

Department of Chemical Engineering

Jadavpur University

Kolkata-700032, India.

Dr. Ratna Dutta

Associate Professor

Chemical Engineering Department

JADAVPUR UNIVERSITY

Kolkata - 700 032, India

 **Dr. Papita Das**
Professor
Dept. of Chemical Engineering
Jadavpur University, Kolkata

DECLARATION

I hereby declare that the thesis entitled “Isolation and analysis of polycyclic aromatic hydrocarbons (PAHs) to determine ambient air quality from different bioindicators: Process intensification approach for solvent extraction techniques” is solely the result of my own work under the guidance of Dr. Ratna Dutta, Associate Professor, and Prof. (Dr.) Papita Das of Chemical Engineering Department, Jadavpur University, Kolkata, India. Any part of the work as described herein has not been submitted for any other degree or professional qualification. Any help or information taken from other available sources has been duly acknowledged.

Shritama Mukhopadhyay

.....
Shritama Mukhopadhyay

Index No.: 186/19/E

Department of Chemical Engineering

Jadavpur University

Kolkata-700032, India.

ACKNOWLEDGEMENT

The work described in this thesis would not have been possible without the help and support from a multitude of people who always stood by my side persistently and directly or indirectly have contributed to the successful accomplishment of my thesis. Words cannot express my gratitude to all of them, but I will put in every effort to do the same.

*Above all, I would like to convey my sincere gratitude to my supervisors, **Dr. Ratna Dutta**, Associate Professor, and **Prof. (Dr.) Papita Das** of Chemical Engineering Department, Jadavpur University, Kolkata, India, for giving me the opportunity to work as a researcher and providing invaluable guidance and suggestions from time to time for pursuing the course of work. Their continuous encouragement, constant help and support, innovative thoughts and insightful advice enabled me to cultivate an interest in the research area and conduct systematic investigations on the topic using proper scientific methods for reaching arguable conclusions with facts. Their incomparable suggestions will last with continued existence as a lifelong resource of precious knowledge. I am deeply obliged to **Prof. Rajat Chakraborty**, Chemical Engineering Department, Jadavpur University, Kolkata, India, for his valuable suggestions and advice which greatly helped me in accomplishing my research work. I am also indebted to **Prof. Dipankar Halder**, Food Technology and Bio-Chemical Engineering, Jadavpur University, Kolkata, India, for providing enlightening ideas on the research subject for the improvement of the work.*

*Furthermore, I would like to acknowledge the support received from all the **faculty members** of the Department of Chemical*

Engineering, Jadavpur University, Kolkata, India, in terms of resources and facilities towards achieving successful results. I am also thankful to the technical staff members of the Department, **Mr. Jyotish Das** and **Mr. Nayan Mondal**, for their continuous cooperation and assistance.

I am very much grateful to the State Government Fellowship Scheme of Jadavpur University for providing Senior Research Fellowship during my entire tenure.

I would like to extend my heartfelt thanks to my fellow lab mates and juniors, **Ms. Aparna Dhara**, **Ms. Nabasmita Barman**, **Mr. Marshal Murmu**, **Mr. Marshal Kisku**, **Mr. Biswanath Das**, **Sk. Rakibul Hossain** and **Mr. Sayantan Ghosh**, for their sincere help and unfailing support throughout the tenure of my work.

Finally, yet importantly, I want to express my deepest gratitude to my parents (**Sri Amitava Mukhopadhyay** and **Smt. Sarmila Mukhopadhyay**) for their blessings, selfless love, commitment and help in every possible way in all the phases of my life. Their presence gave me immense courage and confidence to go ahead in life and achieve my best. A special thanks also goes to my elder sister, **Smt. Shreya Mukhopadhyay**, for her mental support, guidance and wisdom. Her presence in my life is a continuous source of encouragement, relief and happiness.

Shritama Mukhopadhyay

SHRITAMA MUKHOPADHYAY

Date: 23/07/2024

Place: Kolkata

CONTENTS

Sl. No.	Topic	Page No.
	Abstract	i-v
	List of Figures	vi-ix
	List of Tables	x-xii
Chapter 1	Introduction	1-80
1.1.	Overview	1-2
1.2.	PAHs as air pollutants: Sources, fate and exposure risks	3-19
1.2.1.	Major sources of PAHs in the natural environment	4-9
1.2.2.	Distribution and transport of PAHs in the environment	9-17
1.2.2.1.	PAHs in air	10-14
1.2.2.2.	PAHs in soil and sediment	15-16
1.2.2.3.	PAHs in water streams	16-17
1.2.3.	Exposure to PAHs and their associated risks on public health	17-19
1.3.	Traditional monitoring and biomonitoring of air pollutants	19-21
1.4.	Biomonitoring scheme: Measurement of the accumulation of PAHs in plant tissues	22-40
1.4.1.	Sample preparation techniques	22-35
1.4.1.1.	Sampling and sample pretreatment methodologies	22-23
1.4.1.2.	Solvent extraction of PAHs	23-35
	<ul style="list-style-type: none"> Factors influencing the process of PAHs extraction 	23-27
	<ul style="list-style-type: none"> USEPA promulgated methods for extraction and analysis of PAHs 	27
	<ul style="list-style-type: none"> Methods of extraction 	27-35
1.4.1.3.	Extract clean-up	35-36
1.4.2.	Analytical techniques for PAHs detection with method validation	36-40
1.5.	Biomonitoring of airborne PAHs using terrestrial vascular and non-vascular plants	41-73
1.5.1.	Vascular plants as biomonitors of atmospheric PAHs pollution	41-51
	(a) Plant leaves	41-49
	(b) Tree bark/stem/ring/trunk	49-50

Sl. No.	Topic	Page No.
1.5.2.	Role of non-vascular plants in PAHs biomonitoring	50-73
	(a) Lichens as indicators of PAHs pollution	51-60
	(b) Use of mosses for PAHs monitoring in ambient air	61-73
1.6.	Statement of the problem	74-75
1.6.1.	Objectives of the work: Overall and specific	75-78
1.6.2.	Outline of the thesis	78-80
Chapter 2	Methodology I: Assessment of biomonitoring potential of <i>Murraya paniculata</i> (L.) Jack (terrestrial plant) along major roads of South Kolkata, India	81-109
2.1.	Background	81-84
2.2.	Materials and methods	84-91
2.2.1.	Study area and site selection	84-86
2.2.2.	Sampling and processing of plant materials	87
2.2.3.	Chemicals and reagents	88
2.2.4.	Physical, biochemical, physiological and morphological characterization of plant leaves	88-90
2.2.4.1.	Dust retention capacity of plant leaves	88
2.2.4.2.	Air pollution tolerance index (APTI)	89
2.2.4.3.	Leaf lipid content	90
2.2.4.4.	SEM-EDX analysis	90
2.2.5.	PAHs analysis in plant leaves	91
2.2.6.	Statistical and correlation/regression analyses	91
2.3.	Results and discussion	91-109
2.3.1.	Dust retention capacity of <i>Murraya paniculata</i> leaves	91-94
2.3.2.	Tolerance of <i>Murraya paniculata</i> to abiotic stress	94-99
2.3.2.1.	Total chlorophyll content	94-95
2.3.2.2.	Ascorbic acid content	95-96
2.3.2.3.	Leaf extract pH	96-97
2.3.2.4.	Relative water content (RWC)	97-98
2.3.2.5.	Air pollution tolerance index (APTI)	98-99
2.3.3.	Total carotenoids content	99-100
2.3.4.	Lipid content of plant leaves	100
2.3.5.	SEM observation with energy-dispersive X-ray microanalysis	100-103

Sl. No.	Topic	Page No.
2.3.6.	PAHs detection in <i>Murraya paniculata</i> leaves for biomonitoring: A qualitative approach	103-106
2.3.7.	Statistical and correlation/regression analyses	107-108
2.4.	Conclusion	108-109
Chapter 3	Methodology II: Extraction and analysis of PAHs from bioindicators	110-129
3.1.	Background	110-111
3.2.	Materials and methods	111-122
3.2.1	Sampling and sample pretreatment	111-112
3.2.2.	Optimization of extraction factors for isolation of PAHs from plant leaves	112-116
3.2.2.1.	Extraction methods	112-115
3.2.2.2.	Selection of extracting solvent for maximum recovery of PAHs	115-116
3.2.2.3.	Optimization of extraction time	116
3.2.3.	Extract purification and concentration	116
3.2.4.	Instrumental analysis of PAHs using GC-MS and HPLC-UVD	116-122
3.3.	Results and discussion	122-129
3.3.1.	Comparison of extraction methods	122-125
3.3.2.	Choice of solvent for PAHs extraction	125-127
3.3.3.	Effect of extraction time on PAHs yield	127-129
3.4.	Conclusion	129
Chapter 4	Methodology III: Microwave-assisted Soxhlet extraction (MAE) method for PAHs isolation from <i>Murraya paniculata</i> (L.) Jack: Process optimization using response surface methodology as process intensification	130-156
4.1.	Background	130-134
4.2.	Materials and methods	134-140
4.2.1	Sample processing for extraction	134
4.2.2.	MAE of PAHs from the leaves of <i>M. paniculata</i>	135
4.2.3.	Primary selection of solvents	135
4.2.4.	Experimental design of MAE of PAHs	135-137
4.2.4.1.	Study of single parameter effects	135-136
4.2.4.2.	Parameter optimization using RSM	136-137
4.2.5	Extract clean-up and PAHs quantification by HPLC-UVD	137-140

Sl. No.	Topic	Page No.
4.3.	Results and discussion	141-156
4.3.1.	Solvent suitability in MAE	141-142
4.3.2.	Single-parameter experiments of MAE	142-145
4.3.2.1.	Effect of extraction temperature on PAHs yield	142-143
4.3.2.2.	Effect of extraction time on PAHs yield	143
4.3.2.3.	Effect of solvent-to-sample ratio on PAHs yield	143-145
4.3.3.	Optimization of MAE parameters by RSM	146-153
4.3.3.1.	Statistical modeling and model fitting with response surface analysis	146-152
4.3.3.2.	Model optimization and validation	153
4.3.4.	Comparison of optimized MAE process with classical Soxhlet technique: Process intensification	154-155
4.4.	Conclusion	156
Chapter 5	Methodology IV: Biomonitoring of PAHs by <i>Murraya paniculata</i> (L.) Jack in South Kolkata, West Bengal, India: Spatial and temporal variations	157-168
5.1.	Background	157-158
5.2.	Materials and methods	158-159
5.2.1.	Materials, sampling location and collection time	158
5.2.2.	Spatio-temporal variations of ambient PAHs: quantitative estimation and diagnostic ratios (DRs) for characterization of sources	158-159
5.3.	Results and discussion	160-167
5.3.1.	Temporal variability in PAHs concentrations	160-162
5.3.2.	Spatial variability in PAHs concentrations	162-164
5.3.3.	Source apportionment using DRs	164-167
5.4.	Conclusion	168
Chapter 6	Methodology V: Assessment of different urban plant bioindicators for urban greenery planning	169-218
6.1.	Background	169-172
6.2.	Materials and methods	172-184
6.2.1.	Location of sampling site, selection of plant species, sample collection and preservation	172-177

Sl. No.	Topic	Page No.
6.2.2.	Quantitative estimation of particulate matter (PM) retained on plant foliage and leaf waxes	177-178
6.2.3.	Analysis of leaf core attributes to discern the biomonitoring potential of the selected plant species	178-181
6.2.3.1.	Total chlorophyll, carotenoid and ascorbic acid contents	178-179
6.2.3.2.	Relative water content and foliar pH	179
6.2.3.3.	Membrane stability index and electrolyte leakage	179-180
6.2.3.4.	Leaf carbon content	180
6.2.3.5.	Protein, proline and total soluble sugar contents	180-181
6.2.4.	Air pollution tolerance index (APTI)	181
6.2.5.	Anticipated performance index (API)	182
6.2.6.	Investigation of leaf surface micromorphology	182
6.2.7.	PAHs determination in plant foliage	182-183
6.2.8.	Risk factor assessment	183-184
6.2.9.	Statistical analysis	184
6.3.	Results and discussion	184-215
6.3.1.	PM capturing potential of plant leaves: Impacts of environmental influence, leaf waxes and morphology	184-195
6.3.2.	Bioaccumulation of PAHs	195-200
6.3.3.	Carcinogenic and mutagenic risks of PAHs	201-205
6.3.4.	Analysis of biomarkers and pollution/performance indices for comparing the suitability of plant species for urban plantation	206-216
6.3.4.1.	Contents of photosynthetic pigments (chlorophyll (Chl) and carotenoids (C _{x+c}))	206-207
6.3.4.2.	Ascorbic acid (AA) content	207
6.3.4.3.	Foliar pH	207-208
6.3.4.4.	Relative water content (RWC)	208
6.3.4.5.	Membrane stability index (MSI) and electrolyte leakage (EL): Role of proline accumulation	209-210
6.3.4.6.	Leaf carbon content: Carbon allocation in stress tolerance	210
6.3.4.7.	Total soluble sugar (TSS) content	211
6.3.4.8.	Protein content	211-212
6.3.4.9.	Air pollution induced stress tolerance of plants and considerations for green belting	212-216
6.4.	Conclusion	217-218

Sl. No.	Topic	Page No.
Chapter 7	Methodology VI: Modeling of PAHs accumulation in biomonitors: Mechanistic approach	219-251
7.1.	Background	219-223
7.2.	Materials and methods	223-231
7.2.1.	Experimental design	223-224
7.2.2.	Determination of plant-air partition coefficient (K_{PA})	224-225
7.2.3.	Determination of particle-gas partition coefficient (K_P)	225-226
7.2.4.	Determination of PAHs mass transfer coefficients for air-leaf and root-leaf uptake	226-227
7.2.5.	Estimation of bioaccumulation and translocation factors	227
7.2.6.	Elucidation of plant uptake mechanism by material balance model and fugacity approach	228-231
7.2.6.1.	Material balance approach (with model assumptions)	228-231
7.2.6.2.	Fugacity approach	231
7.3.	Results and discussion	231-251
7.3.1.	Plant-air partitioning of PAHs	231-236
7.3.2.	Particle-gas partitioning of PAHs	236-238
7.3.3.	Bioaccumulation of PAHs in plant leaves	238-242
7.3.3.1.	PAHs translocation into leaf layers from foliar PM	238-240
7.3.3.2.	PAHs translocation into leaf from plant root	240-242
7.3.4.	Mass transfer coefficients of PAHs	242-243
7.3.4.1.	Mass transfer from air to plant foliage	242-243
7.3.4.2.	Diffusion from roots to plant foliage	243
7.3.5.	Determination of dC_L/dt as a model parameter of theoretical net uptake of PAHs	244
7.3.6.	Determination of evaporative loss (LEV) from PAHs uptake kinetics	244-245
7.3.7.	PAHs uptake model validation: Material balance	246-249
7.3.8.	Reconfirmation of foliar capturing capacity by fugacity approach	249-251
7.4.	Conclusion	251
Chapter 8	Summary of results, Concluding remarks and Recommendations for future work	252-263
8.1.	Summary of results and concluding remarks	252-258
8.2.	Recommendations for future work	258-263

Sl. No.	Topic	Page No.
8.2.1.	Designing of advanced and efficient extraction method of PAHs from plant matrix as improved biomonitoring protocol	258
8.2.2.	Exploitation of efficient members of plant biomonitor: Use of lower plants like lichen and bryophytes as biomonitors	259-260
8.2.3.	Biomonitoring of heavy metals (priority air pollutant) using terrestrial plant foliages	261-263
	References	264-333
	Appendix-I	334-342

Abstract

Constant bursting of the city frontiers is taking a massive toll on natural vegetation, deteriorating thereby the purity of the clean air due to the presence of hazardous pollutants in the atmosphere. Rapid industrialization and urbanization have immensely contributed to outdoor air pollution due to vehicular emission, industrial activities, power plant operations, etc., whereas, rural areas face the major problems of indoor air pollution. Among the criteria air pollutants, polycyclic aromatic hydrocarbons (PAHs) are organic compounds having two or more fused aromatic rings, released from natural as well as man-made sources. They are persistent priority pollutants and continue to last for a long time in the environment causing severe damage to human health owing to their genotoxicity, mutagenicity and carcinogenicity. The study of PAHs in the environment has therefore aroused a global concern. Biomonitoring of airborne pollutants through creation of green belts has become the only alternative to provide natural filtering barrier. Thus, plant bioaccumulators can be exploited as biomonitors for indirect assessment of air pollution. In conformity with the above facts, efficacy of specific higher terrestrial plants (generally regarded as foundation species of the ecosystem) with broad foliage-canopy structures in mitigating airborne PAHs pollution (through entrapment into their tissues) has been demonstrated, underscoring prevalent classical and modified isolation techniques (i.e., solvent extraction) coupled with proper analytical procedures for gaining an insight into the assessment of atmospheric PAHs concentrations.

As a basis for passive air pollution biomonitoring, estimation of tolerance characteristics of a terrestrial plant was the primary focus of the study to determine the potentiality of the selected plant against contaminated environment. The study was constructed to evaluate the air pollution tolerance index (APTI) of a commonly found evergreen plant species, *Murraya paniculata*, sampled from polluted places of South Kolkata, West Bengal, India, with dense population and heavy traffic, based on leaf attributes. PAHs accumulating ability of the plant species was also examined so as to establish the species' potential in monitoring of PAHs. *M. paniculata* was found to be tolerant (APTI: 19.78–31.12) towards air pollution with dust capturing potential ranging between 0.85–2.26 mg cm⁻². Correlation analysis unveiled the strong relationship of foliar dust with leaf ascorbic acid ($r^2 = 0.931$), leaf extract pH ($r = 0.985$), leaf RWC ($r = -0.822$), total carotenoids ($r = -0.862$) and total chlorophyll ($r = -0.76$). APTI was found to be correlated positively to ascorbic acid

and foliar pH and negatively to total chlorophyll and RWC. Linear variation ($r^2 = 0.97$) of APTI with PM and other pollution burden was also noticed. Therefore, it can be concluded that APTI not only points out the sustainability of a bioindicator plant under severe pollution load, but also serves as a good indicator of contamination level. Changes in leaf surface micromorphology (such as stomal blockage and guard cell deformation, rough leaf surfaces developed from epidermal undulations, degradation of crystal structures of epicuticular waxes around the stomata and entrapment of dust particles) due to particulate pollution were also endorsed by SEM observation with energy-dispersive X-ray microanalysis. Findings also revealed that *Murraya paniculata* has the tolerance and efficiency of trapping both lighter and heavier PAHs, proving its ability for biomonitoring of atmospheric pollution.

Secondly, attempts have been made for ascertaining the concentrations of atmospheric PAHs using passive biosamplers (i.e., leaves of *M. paniculata*) in preference to classical air sampling methods by virtue of solvent extraction and analytical techniques. For achieving the desired objective, mechanical stirring, sonication, Soxhlet technique and microwave-assisted Soxhlet extraction (MAE) were employed for comparison of the effectiveness of traditional and advanced extraction methods to isolate PAHs from plant leaves. Effects of extraction techniques and operational parameters (solvent and time) on the recovery levels of PAHs were also investigated. Purified extracts, acquired through silica gel column chromatography, were subjected to GC–MS and HPLC–UV analyses for qualitative and quantitative assessment of PAHs. The results displayed that the extraction yields of Soxhlet ($272.07 \mu\text{g g}^{-1}$) and MAE ($280.17 \mu\text{g g}^{-1}$) were almost comparable and highest over sonication and mechanical stirring. Keeping the objective of targeting conventional route of extraction primarily, extraction optimization of Soxhlet method revealed toluene as the most favorable solvent for PAHs (because of the strong solute-solvent interactions favoured by intermolecular dispersive forces) and 6 h of extraction time was found to be optimum for obtaining highest recoveries.

The study was then aimed at developing a process intensified route based on solvent extraction for PAHs isolation from the leaf matrix of *M. paniculata* to overcome the limitations of traditional extraction method. In this aspect, MAE was targeted and the influence of MAE parameters on extraction yield of PAHs was evaluated through process optimization by response surface methodology (RSM) incorporating Box-Behnken Design (BBD). A three-level RSM-BBD approach was applied involving three MAE factors, extraction temperature, extraction time and solvent-to-sample ratio, for attainment of the optimal conditions to reach highest yield of PAHs as a desired response. Prior to the optimization study, solvent selection criterion was fulfilled through screening experiments

using binary solvent mixtures along with preliminary experimentations on single factor effects. The combination of toluene:acetonitrile exhibited maximum yield ($283.77 \mu\text{g g}^{-1}$) of PAHs among the other solvent blends. Regarding parameter optimization by RSM, the experimental and predicted response values showed a good linear fit and a quadratic model was also developed correlating the input (independent) variables with the response. Significance of the regression model was confirmed through analysis of variance (ANOVA) (F value: 428.74; $p < 0.0001$; R^2 : 0.9982). The model represented positive effects of the linear terms and negative effects of the quadratic terms of process parameters on the response. All the interaction terms were again found to be significant with $p < 0.05$. On performing model validation, the optimized conditions for maximization of extraction yield are observed to be: extraction temperature: 45.77°C , extraction time: 11.67 min and solvent-to-sample ratio: 22.64 mL g^{-1} , thereby achieving 98% accuracy on model prediction. A comparison between conventional Soxhlet method and MAE highlighted that the former method consumes huge amount of extraction solvent (1.8-fold higher) and extraction time (30 times higher) with high energy input and CO_2 emission during the process, suggesting the improved process performance of MAE.

To identify the PAHs occurrence pattern of wide-range dispersal, spatio-temporal distribution of accumulated PAHs across the sampling sites of South Kolkata (Jadavpur (JDV), Rash Behari Connector (RBC), Exide More (EXM) and Tollygunge (TGN)) was monitored over premonsoon, postmonsoon and winter supported by pollutant source characterization using PAHs diagnostic ratios (DRs). In spatio-temporal analysis, total concentrations of PAHs in the foliar samples of *Murraya* sp. ranged from 200.98 to $550.79 \mu\text{g g}^{-1}$ dry weight, and the highest values being recorded in the samples of EXM because of daylong inexorable traffic flow/crowding increasing the burden of ambient PAHs. Widespread changes in meteorology exerted influence on seasonal concentrations of PAHs in plant leaves, and degree of PAHs contamination varied as winter > postmonsoon > premonsoon. Foliar accretion of PAHs differed in the study sites with diverse sources of emission from motor vehicles, fossil fuel and biomass burning along with other human interferences as found from source apportionment study.

For prioritizing the role of urban green infrastructures in addressing the issues of Kolkata's air quality, efficiencies of eight indigenous plants of Baishnabghata Patuli Township (BPT), southeast Kolkata, India, were explored as green barrier species and potentials of plant leaves were exploited for biomonitoring of particulate matter (PM) and PAHs. The work focused on studying PM capturing abilities ($539.32\text{--}2766.27 \mu\text{g cm}^{-2}$) of

plants (*T. divaricata*, *N. oleander* and *B. acuminata* being the most efficient species in retaining PM) along with the estimation of foliar contents of PM adhered to leaf surfaces (total sPM (large + coarse): 526.59–2731.76 $\mu\text{g cm}^{-2}$) and embedded within waxes (total wPM (large + coarse): 8.73–34.51 $\mu\text{g cm}^{-2}$). SEM imaging used to analyze leaf surfaces affirmed the presence of innate corrugated microstructures as main drivers for particle capture. Accumulation capacities of PAHs of vehicular origin (total index, $\text{TI} > 4$) were compared among the species based on measured concentrations (159.92–393.01 $\mu\text{g g}^{-1}$), which indicated *T. divaricata*, *P. alba* and *N. cadamba* as highest PAHs accumulators. Specific leaf area (SLA) of plants (71.01–376.79 $\text{cm}^2 \text{g}^{-1}$), a measure of canopy– atmosphere interface, had great relevance in PAHs diffusion. Relative contribution (>90%) of 4–6 ring PAHs to total carcinogenic equivalent and potential as well as 5–6 ring PAHs to total mutagenic equivalent and potential had also been viewed with respect to benzo[a]pyrene. In-depth analysis of foliar traits (as air pollution biomarkers) and adoption of plant–based ranking strategies (APTI and anticipated performance index (API)) provided a rationale for green belting. Each of the naturally selected plant species showed evidences of adaptations during abiotic stress to maximize survival and filtering effects for reductive elimination of ambient PM and PAHs, allowing holistic management of green spaces.

The interplay between plant-air interaction and cycling of airborne PAHs in terrestrial ecosystem determines their environmental existence and could aid in better employment of plants as biomonitoring tool for ecological restoration. In this context, dynamics of plant (*M. paniculata*) uptake mechanisms were modeled using a mechanistic framework based on material balance. Experimentally determined plant-air (K_{PA}) and particle-gas (K_{P}) partition coefficients justified the nature of PAHs partitioning into plant and particle phases. Apart from direct exchange between plant and air (manifesting high air-leaf mass transfer coefficient k_{AL} of 85 cm h^{-1} (average) and fugacity capacity of plant foliage: $0.045\text{--}1.27 \times 10^4 \text{ mol m}^{-3} \text{ Pa}^{-1}$), PM adsorption on plant leaf surfaces and uptake and movement of PAHs from foliar PM into leaf layers (cuticle and mesophyll) were observed relating to their overall foliar PM-leaf translocation factor ($\text{TF}_{\text{f/L}}$) (which is >1). Despite efficient root accumulation (with high root concentration factor (RCF): 0.72–1.12), root to leaf transfer of PAHs was found to be minimal owing to their diminished mass flow and lower values of root-leaf translocation factor ($\text{TF}_{\text{R/L}}$). After validation of the material balance model, inner tissue absorption and adsorption to the leaf-laden PM are established as the responsible routes of PAHs uptake by a biomonitor plant species from the ambient atmosphere.

Therefore, it can be conclusively opined that the present study offers a broad basis for successful selection and identification of plant biomonitors with proper improved assessment methodology for atmospheric PAHs analysis. The study findings can further assist in strengthening the prediction of bioaccumulation of atmospheric PAHs into a biomonitor plant, providing a robust and indispensable option of advanced biomonitor selection. Also, a proposition for green belting using locally available biomonitor plants has been elaborated as a sustainable foundation for the future management and planning of township, being an unrivalled solution to air pollution.

LIST OF FIGURES

Sl. No.	Figure Description	Page No.
1.	Fig. 1. Chemical structures of USEPA PAHs.	4
2.	Fig. 2. Major sources of ambient PAHs.	6
3.	Fig. 3. Source profiles of atmospheric PAHs with the contributions of emission factors across the globe.	6-9
4.	Fig. 4. Environmental fate and transport of PAHs.	10
5.	Fig. 5. Different types of biomonitors of environmental pollution and their stress responses.	21
6.	Fig. 6. Location map of the sample sites: Jadavpur (JDV), Rash Behari Connector (RBC), Exide More (EXM) and Tollygunge (TGN) in South Kolkata and control site, Champadali (CMD) in Midnapore, West Bengal, India.	86
7.	Fig. 7. <i>Murraya paniculata</i> .	87
8.	Fig. 8. SEM-EDX micrographs (a) SEM image of plant leaves of control site, (b), (c) and (d) SEM images of plant leaves of roadside areas, (e) EDX spectrum of plant leaves of control site, (f) and (g) EDX spectra of plant leaves of roadside areas.	102-103
9.	Fig. 9. GC-MS chromatograms of PAHs extracted from the leaves of <i>M. paniculata</i> of different sites a) JDV, b) RBC, c) EXM, d) TGN and e) CMD.	106
10.	Fig. 10. Variation of APTI of <i>Murraya paniculata</i> (L.) Jack with (a) total chlorophyll content of plant leaves, (b) leaf ascorbic acid content, (c) foliar pH and (d) relative leaf water content at the polluted sites.	108
11.	Fig. 11. Illustrative outlook on abiotic stress tolerance of <i>M. paniculata</i> under the exposure of ambient air pollution for greenbelt development.	109
12.	Fig. 12. Schematic representation (left) and laboratory set-up (right) of mechanical stirring.	112

Sl. No.	Figure Description	Page No.
13.	Fig. 13. Schematic representation (left) and laboratory set-up (right) of sonication extraction.	113
14.	Fig. 14. Schematic representation (left) and laboratory set-up (right) of the conventional Soxhlet apparatus used for experimentation.	114
15.	Fig. 15. Schematic diagram (left) and laboratory set-up (right) of the modified microwave oven used for extraction purposes.	115
16.	Fig. 16. Chromatogram revealing the recovery peaks of 16 EPA-PAHs.	120
17.	Fig. 17. Schematic depiction of the overall methodology.	137
18.	Fig. 18 (a-i). Representative chromatograms of PAHs extracted from plant leaves under varying conditions of extraction temperature (30-60 °C), extraction time (5-20 min) and solvent-to-sample ratio (6-30 mL g ⁻¹) in MAE.	138-140
19.	Fig. 19. Comparative study on obtained concentrations of PAHs extracted from <i>Murraya</i> leaves using different solvent mixtures.	142
20.	Fig. 20. Effects of (a) extraction temperature, (b) extraction time and (c) solvent-to-sample ratio on the concentration of extracted PAHs.	144-145
21.	Fig. 21. Predicted vs. experimental plot of responses for PAHs extraction yield.	147
22.	Fig. 22. 2D and 3D graphs of PAHs extraction yield against (a ₁) and (a ₂): extraction temperature and time, (b ₁) and (b ₂): extraction temperature and solvent-to-sample ratio and (c ₁) and (c ₂): extraction time and solvent-to-sample ratio.	150-152
23.	Fig. 23. Locational variations in individual PAHs concentrations (µg g ⁻¹ d.w.) in <i>Murraya paniculata</i> leaves with respect to three seasons (a) winter, (b) premonsoon and (c) postmonsoon.	163-164
24.	Fig. 24. Schematic view of biomonitoring of airborne PM and PAHs by plant species.	172

Sl. No.	Figure Description	Page No.
25.	Fig. 25. (a) Location of the study area (Baishnabghata Patuli Township, BPT) within Kolkata, West Bengal, India and (b) route map view of sampling at Patuli.	173-174
26.	Fig. 26. Photographs of selected terrestrial urban plant species for the study.	176-177
27.	Fig. 27. Foliar contents ($\mu\text{g cm}^{-2}$) of (a) surface PM (sPM), (b) wax PM (wPM) of different size fractions and (c) waxes of selected plant species (data are presented as mean \pm SD, n=3).	187-188
28.	Fig. 28. SEM images of abaxial and adaxial surfaces of studied plant leaves with particulate deposition.	191-195
29.	Fig. 29. Variations in leaf accumulation (mean \pm SD, n=3) of PAHs in plant species (a) % distribution of individual PAHs and (b) % fraction of PAHs of different aromatic rings with respect to total PAHs.	199-200
30.	Fig. 30. Dominant routes of POP uptake, accumulation and transport in plants along with loss mechanisms.	220
31.	Fig. 31. Flow chart for model design.	224
32.	Fig. 32. Octanol (foliage)- and water- phase concentrations (mean \pm S.D.) of PAHs.	233
33.	Fig. 33. Plot of theoretical and experimental log K_{PA} .	235
34.	Fig. 34. Plot between log K_P and log K_{OA} .	238
35.	Fig. 35. Concentrations (mean \pm S.D.) of PAHs in foliar PM, leaf cuticular wax and inner mesophyll tissue.	239
36.	Fig. 36. Concentrations (mean \pm S.D.) of PAHs in plant root obtained from equilibrium uptake study.	241
37.	Fig. 37. Variation in leaf uptake concentration (mean \pm S.D.) of PAHs over time.	245
38.	Fig. 38. Profile of cumulative loss (mean \pm S.D.) in uptake concentration of PAHs over time.	245

Sl. No.	Figure Description	Page No.
39.	Fig. 39. Variation of APTI of <i>Murraya paniculata</i> with foliar dust concentration.	253
40.	Fig. 40. Photographs of epiphytic lichen species sampled from Kolkata, India.	259
41.	Fig. 41. Variation in concentrations of PAHs isolated from lichen species with extraction time.	260
42.	Fig. 42. Heavy metal distribution (with respect to concentration in mg kg^{-1}) in lichen species.	260
43.	Fig. 43. Heavy metal distribution (with respect to concentration in mg kg^{-1}) in some higher terrestrial plants (a, b) leaves and foliar adsorbed dust particulates of <i>T. divaricata</i> , (c, d) leaves and foliar adsorbed dust particulates of <i>C. gigantea</i> , (e, f) leaves and foliar adsorbed dust particulates of <i>N. cadamba</i> and (g, h) leaves and foliar adsorbed dust particulates of <i>A. scholaris</i> .	261-262
44.	Fig. 44. Future scope of the methodology in a nutshell.	263
	Fig. A1. Plots of dCL/dt vs. CL for individual PAH congeners.	334-342

LIST OF TABLES

Sl. No.	Table Description	Page No.
1.	Table 1: Monitoring of PAHs in the ambient air.	13-14
2.	Table 2: Comparison of extraction techniques.	39
3.	Table 3: Extraction methods with solvents, purification steps and analytical techniques for assessment of PAHs).	40
4.	Table 4: Lichen species used for biomonitoring of PAHs: Sampling sites, extraction methods and solvents for extraction.	55-57
5.	Table 5: Lichen species used for biomonitoring of PAHs: Method of analysis and concentration of PAHs.	58-60
6.	Table 6: Biomonitoring of airborne PAHs using moss species with sampling sites, extraction methods and solvents used for extraction.	66-69
7.	Table 7: Biomonitoring of airborne PAHs using moss species: Method of analysis and concentration of PAHs.	70-73
8.	Table 8: National ambient air quality monitoring (NAAQM) data (average) of the study sites during sampling period (as provided by CPCB and WBPCB).	85
9.	Table 9: Physical, biochemical and physiological characteristics of <i>M. paniculata</i> (L.) Jack.	93-94
10.	Table 10: Identification of PAHs in the leaf samples of <i>M. paniculata</i> (L.) Jack by GC-MS analysis for different sampling locations.	105
11.	Table 11: Operating conditions for GC-MS analysis of PAHs using TG-5MS capillary column (Length: 30 m; I.D.: 0.25 mm; Film: 0.25 µm).	117-118
12.	Table 12: GC-MS detection of PAHs in the certified reference material.	118
13.	Table 13: Percentage recovery of 16 EPA-PAHs extracted from <i>Murraya</i> leaves.	119-120

Sl. No.	Table Description	Page No.
14.	Table 14: Calibration data of 16 EPA-PAHs.	121-122
15.	Table 15: LOD and LOQ of individual PAHs in chromatographic (HPLC) analysis.	122
16.	Table 16: Comparison between extraction methods.	125
17.	Table 17: Variation in PAHs recovery from plant leaves using different solvents in Soxhlet extraction.	127
18.	Table 18: Profiles of foliar PAHs obtained during varying time periods of extraction with optimized solvent toluene using Soxhlet technique.	128-129
19.	Table 19: Design summary with levels and experimental scale of input variables.	1362
20.	Table 20: Design of experiments with response variable.	146-1472
21.	Table 21: Analysis of variance for the predicted quadratic model.	148
22.	Table 22: Numerical optimization of PAHs extraction yield with desirability of 1.	153
23.	Table 23: Comparison between MAE and Soxhlet method.	155
24.	Table 24: Standard range of DRs applied in the study.	159
25.	Table 25: Seasonal variations in total and individual concentrations ($\mu\text{g g}^{-1}$ d.w.) of PAHs measured in <i>Murraya paniculata</i> leaves of different sites.	161
26.	Table 26: Molecular DRs with their obtained values (as mean \pm S.D.) for identification of foliar PAHs origin in the sampling sites.	166-167
27.	Table 27: Air quality information of BPT area based on the data of WBPCB monitoring station during the sampling period	175
28.	Table 28: Toxic equivalent concentrations (TEQ) of PAHs accumulated in the leaves of selected plant species.	202

Sl. No.	Table Description	Page No.
29.	Table 29: Mutagenic equivalent concentrations (MEQ) of foliar PAHs.	203
30.	Table 30: Carcinogenic potential (CP) of accumulated PAHs in the plant leaves.	204
31.	Table 31: Mutagenic potential (MP) of accumulated PAHs in the plant leaves.	205
32.	Table 32: Evaluation of leaf characteristics (as mean \pm SD) of selected plant species as potential biomarkers.	215
33.	Table 33: Anticipated Performance Index (API) of selected plant species.	216
34.	Table 34: Partition coefficients and estimated air-phase concentrations (mean \pm S.D.) of PAHs.	234
35.	Table 35: Theoretical values of log K_{OA} and log K_{PA} .	236
36.	Table 36: Particle-gas partition coefficient (K_P) (mean \pm S.D.) of PAHs.	237
37.	Table 37: Overall PAHs concentration and translocation (mean \pm S.D.) in plant foliage.	240
38.	Table 38: Root concentration and root-leaf translocation factors (mean \pm S.D.) of PAHs.	242
39.	Table 39: Individual air-leaf mass transfer coefficients (mean \pm S.D.) of 16 PAHs.	242-243
40.	Table 40: Parameter estimation for overall root-leaf mass transfer (mean \pm S.D.) of PAHs.	243
41.	Table 41: Calculated values (mean \pm S.D.) of dC_L/dt .	244
42.	Table 42: Fugacity capacities (mean \pm S.D.) of <i>Murraya</i> leaves.	250-251

Chapter 1

1. Introduction

1.1. Overview

Catastrophic disruptions in the proper functioning of the natural ecosystem wreck the pattern of lifecycle of all the living beings, thereby jeopardizing the environmental balance. Overshoot in human population, development-driven urbanization and industrialization, ever-expanding consumption of the Earth's resources, climatic variations, pollutant burden, loss of biodiversity and health anomalies are the leading edges of the global pollution. Considering the stages of evolution in every sphere of life, achieved by the human race during the past few decades, air, water and soil pollution can be singled out as the most devastating consequences of the developmental progress. Air pollution among them stands out to have the most perilous impact on the entire biosphere. Globally, indoor and outdoor air pollution are responsible for approximately 6.7 million premature deaths per annum (<https://www.who.int/data/gho/data/themes/topics/topic-details/GHO/ncd-mortality>) and 74% of all deaths (about 41 million/year) results from non-communicable diseases (NCDs) such as, heart and chronic lung disorders, cancer, stroke, diabetes, etc.; (<https://www.who.int/data/gho/data/themes/air-pollution>). In case of ambient exposure, 99% of the global population resides in polluted places exceeding the limits of World Health Organization (WHO) air quality guidelines (<https://www.who.int/data/gho/data/themes/air-pollution>). Based on the World Health Statistics, 2023, it has been predicted by WHO that by 2050 the NCD death toll would rise to 86% of the total 90 million deaths each year (a staggered increment of 90% as of 2019) (<https://news.un.org/en/story/2023/05/1136832>). Currently, presence of atmospheric pollutants such as particulate matter (PM), polycyclic aromatic hydrocarbons (PAHs), heavy metals and obnoxious gases (SO_x, NO_x, CO, O₃, etc.) has become the centre of ecumenical interest of investigation among the researchers (https://cpcbenvvis.nic.in/envis_newsletter/Air%20Quality%20of%20Delhi.pdf), so as to frame

policies and evolve low-cost and reliable technologies for meeting the sustainability goals of diminishing global burden of disease (GBD) and ensuring negation of unfavourable temporary and permanent weather fluctuations. Many pollution controlling statutory bodies worldwide formulated real-time air quality index (AQI) to apprise the concerned citizens about the periodic air quality information based on the pollutant load in the ambient air, the increase in the index with respect to the set standards being interpreted as a matter of grave concern (Suman, 2021; <https://in.usembassy.gov/embassy-consulates/kolkata/air-quality-data/>).

PAHs, a class of toxic human carcinogens and major products of incomplete combustion, emerged as a widespread concern for both developed and developing countries mainly because of the huge expansion of the transportation sector at a breakneck pace and increased use of vehicles accounting for maximum release of PAHs to the extent of approximately 46-90% than any other anthropic activity (Nikolaou, et al., 1984; Jang et al., 2013). Based on a report of WHO, nearly, 500 PAH congeners are known to be found in the urban atmosphere (WHO, 2000). The fundamental steps of airborne PAHs assessment comprise sample collection, extraction, clean-up and analysis with illustration of results (Munyeza et al., 2019). Conventional air sampling and monitoring approaches are infrequent, laborious and costly, hence often become inefficient for estimating the real-time data of ambient PAHs levels due to additional deployment time (Blasco et al., 2006; Zhou et al., 2014; Van der Wat and Forbes, 2015; Han et al., 2022_a). Moreover, phase distribution of PAHs (i.e., partitioning between gaseous and particulate phases) poses critical challenges in methodological design (from sampling to analysis), affecting the accuracy of deciphering the quantitative profiles of their presence in the atmosphere (Munyeza et al., 2019). Environmental biomonitoring using plants, on the contrary, provides principled and structured evaluation of the pollutant concentrations as well as detection/prediction of elicited plant symptoms of pollution distresses (particularly foliar expressions that are the characteristics of the toxicants) along with detrimental effects of chemical exposure for advancement of the practices of environmental protection (Badamasi, 2022; Chaudhary, 2022; Madheshiya et al., 2022). Generally, plants (both higher and lower) act as warning devices for detecting the toxicity level of air pollutants and also present early signs of severe pollution. Thus, enforcement of green belts as nature-based solution has continuously been promoted in the urban areas for air pollution mitigation (Anand et al., 2022). For instance, concerning the impact of vegetation on atmospheric pollutant removal, USA had witnessed gross annual reduction of 711000 metric tons of air pollution in past years as documented by Nowak et al. (2006).

1.2. PAHs as air pollutants: Sources, fate and exposure risks

PAHs are a wide group of lipophilic organic compounds having multiple fused aromatic rings of carbon and hydrogen with linear, angular or cluster configurations ([Ghosal et al., 2016](#)). Chemically, PAHs are usually available in unsubstituted (parent compounds) or derivatized (nitrated, oxygenated, halogenated, hydroxylated or alkyl-substituted) forms. Nitro-PAHs (NPAHs) are more toxic because of their ability to induce mutagenesis directly (mutagenic activity 100,000 times higher and carcinogenicity 10 times higher as compared to the parent ones). However, oxy PAHs (OPAHs) can cause unalterable cell injury and lethal damage through the formation of reactive oxygen species (ROS), thereby interfering with redox regulation and homeostasis. Relative toxicological potencies of chlorinated/brominated (ClPAHs/BrPAHs), alkyl and hydroxy PAHs (OH-PAHs) are also much higher than the parent PAH congeners.

PAHs can exist in both vapour phase (low molecular weight or LMW PAHs) and particulate form (high molecular weight or HMW PAHs). HMW PAHs containing 4 to 6 rings exhibit low aqueous solubility, high melting and boiling points with diminished vapour pressure, high hydrophobicity, angularity as well as electrochemical stability in comparison to LMW PAHs having 2 to 3 fused benzene rings ([Haritash and Kaushik, 2009](#); [Patnaik, 2007](#); [Obayori et al., 2013](#)). According to the United States Environmental Protection Agency (US EPA), 16 PAHs (namely, naphthalene (NAP), acenaphthylene (ACY), acenaphthene (ACE), fluorene (FLU), phenanthrene (PHE), anthracene (ANT), fluoranthene (FLA), pyrene (PYR), benzo[a]anthracene (BaA), chrysene (CHR), benzo[b]fluoranthene (BbF), benzo[k]fluoranthene (BkF), benzo[a]pyrene (BaP), dibenzo[a,h]anthracene (DB[ah]A), indeno[1,2,3-cd]pyrene (IP) and benzo[g,h,i]perylene (B[ghi]P)) have been categorized as priority organic pollutants of significant risk depending on their lethality and abundance ([ATSDR, 1995](#); [Liu et al., 2001](#)) ([Fig. 1](#)). Among them, seven PAHs including BaA, CHR, BbF, BkF, BaP, DB[ah]A and IP are classified in the carcinogenic category, of which particulate PAHs with 5-6 rings are associated with more fatal effects than those of LMW PAHs. Universally, BaP is considered as a chemical indicator of health risk assessment and has been recognized as a criteria air pollutant by the Central Pollution Control Board (CPCB), India, and also incorporated in the National Ambient Air Quality Standards (NAAQS), 2009, for continuous monitoring. Carcinogenicity and toxicity of PAHs vary with their chemical and molecular structures and can be high enough depending on seasonal or meteorological variation (especially at the start of winter), type of fuel and emission sources ([Manzetti, 2013](#)).

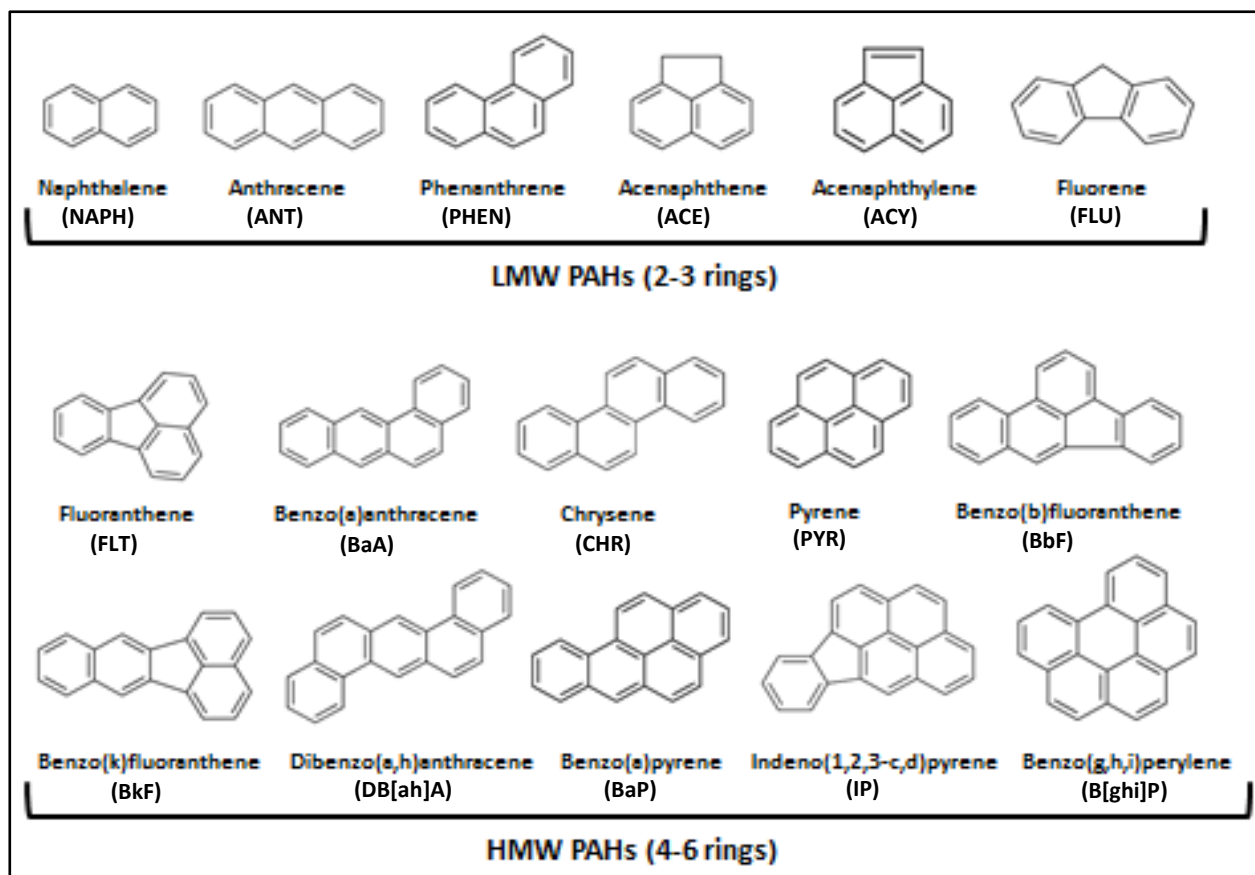


Fig. 1. Chemical structures of USEPA PAHs.

1.2.1. Major sources of PAHs in the natural environment

Industrial operations, incomplete combustion of fossil fuel (coal, oil and petrol) and wood, automobile exhausts as well as household emissions are the major contributors of PAHs to the environment (Edokpayi et al., 2016), among which incomplete combustion and vehicular activities may be contrived to be the maximum emitter of PAHs to the nature (Zhang and Tao, 2009; Peng et al., 2008). Decomposition of organic materials at elevated temperatures in an atmosphere which is inert or oxygen deficient (termed as pyrogenic decomposition) or petrogenic processes (involving petroleum & petroleum-related products and seepage of crude oil from sedimentary rocks) may also release PAHs to the environment. They can be produced either by some species of plants and bacteria or from decayed organic matter through biogenic reactions (Abdel-Shafy and Mansour, 2016). PAHs may also originate from natural sources like forest fires (Choi, 2014; Obrist et al., 2015), waste burning (Pongpiachan, 2015), biotic decomposition (Cuypers, 2001), volcanic eruptions and through discharge of hot water from hydrothermal sediments and vents (Chrysikou et al., 2008; Choi, 2014; Domingos et al., 2015).

Human activities (anthropogenic sources) such as domestic cooking, residential heating, unit operations of thermal power plants/aluminium producing factories/rubber tire manufacturing industries, municipal or industrial incinerators, oil spills and activities in oil refineries are also highly accountable for environmental pollution by PAHs ([Abdel-Shafy and Mansour, 2016](#)). Alkylated PAHs having 2- or 3- aromatic rings are mainly emitted from tobacco and wood smokes, while commercial industrial heating/boiler releases toxic heavier PAHs which are highly associated with health risks ([National Research Council, 1983](#)). Pollution sources of PAHs are represented in [Fig. 2](#).

Population of urban areas is more at risk because of their chronic exposure to PAHs with disparities in the conditions of vulnerability relative to pollutant concentrations, exposure time, emission sources and socio-economic factors, throwing open the challenges for monitoring and source attribution through qualitative (univariate/multivariate methods) and quantitative (principal component analysis (PCA), positive matrix factorization (PMF) and multiple linear regression (MLR) based) approaches ([Teixeira et al., 2012](#); [Callen et al., 2013](#)). Extensive researches have been performed universally for determination of sources in order to make an estimate of global PAHs emission over the years. Sector-wise contributions of different polluting sources in fourteen representative countries have been shown in [Fig. 3](#) for ready comparison ([Mishra et al., 2016](#); [Vestenius et al., 2011](#); [Mehmood et al., 2020](#); [Ali-Taleshi et al., 2021](#); [Siudek, 2023](#); [Jang et al., 2013](#); [Shin et al., 2022](#); [Ray et al., 2017](#); [Larsen and Baker, 2003](#); [Khan et al., 2015](#); [Masiol et al., 2012](#); [Callen et al., 2014](#); [Xing et al., 2022](#); [Wang et al., 2015a](#)). As clear from [Fig. 3](#), it can be suggested that vehicular emissions ruled the roost for most of the countries, whereas, for countries like Poland, UK, etc. biomass burning, heterogeneous combustion processes and emissions from unburned fuel had the major contributions.

PAH compounds emitted into the environment result in complex mixtures and ultimately accumulate in plant cover, soil/sediment and water/marine organisms, critically interfering with food chain and causing bioaccumulation and biomagnification ([Wagrowski and Hites, 1996](#); [Abdel-Shafy and Mansour, 2016](#)). Distribution of PAHs in the ambient atmosphere depends largely on the closeness of the polluted area to the source of emission, industrial/commercial activities and modes of dispersion. Physical and chemical characteristics, non-polar nature and lipophilicity of PAHs greatly influence their presence in the environment.

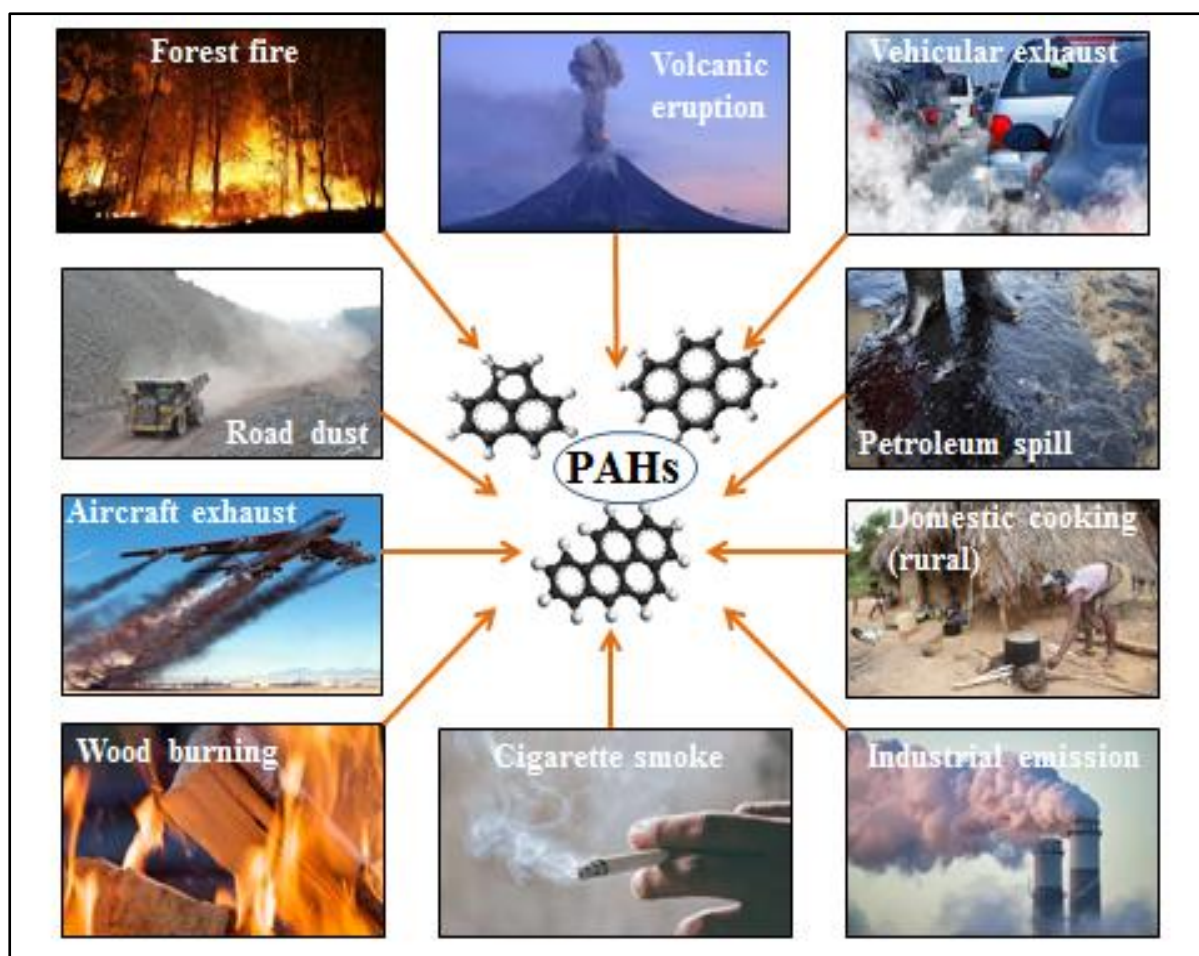
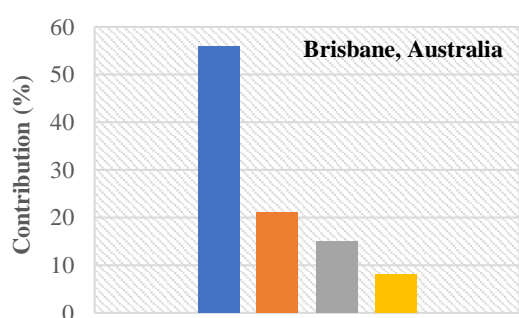
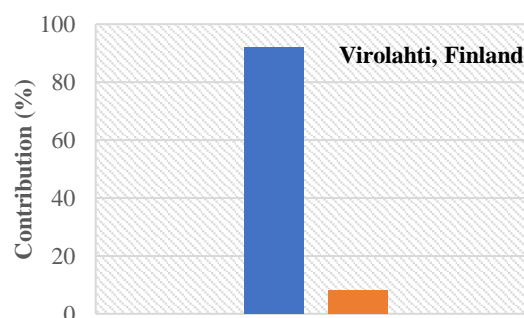


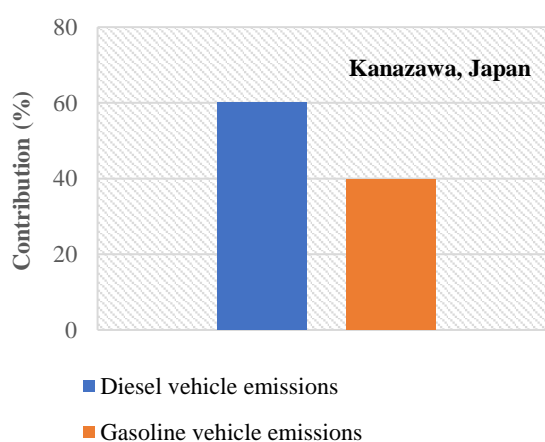
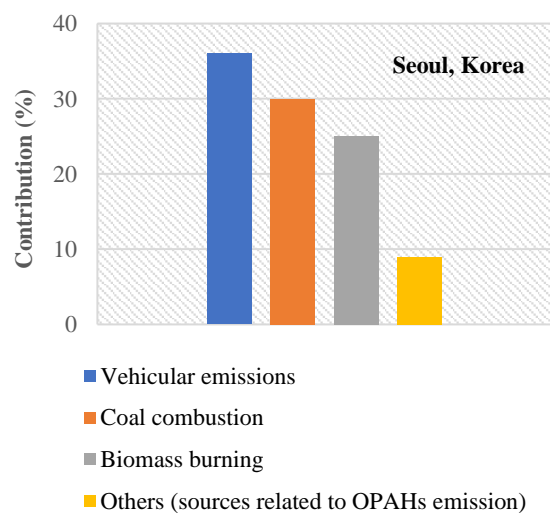
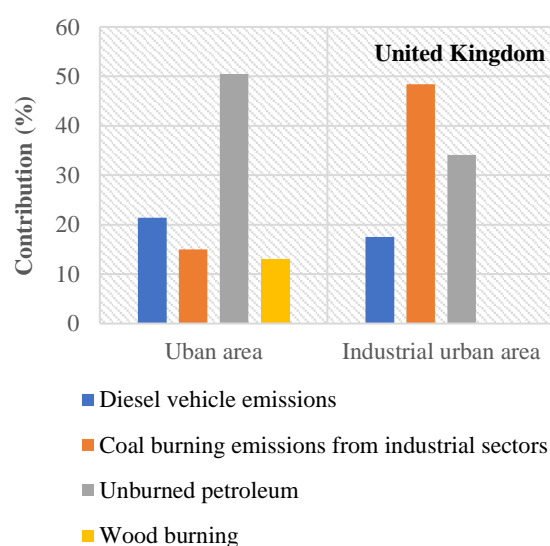
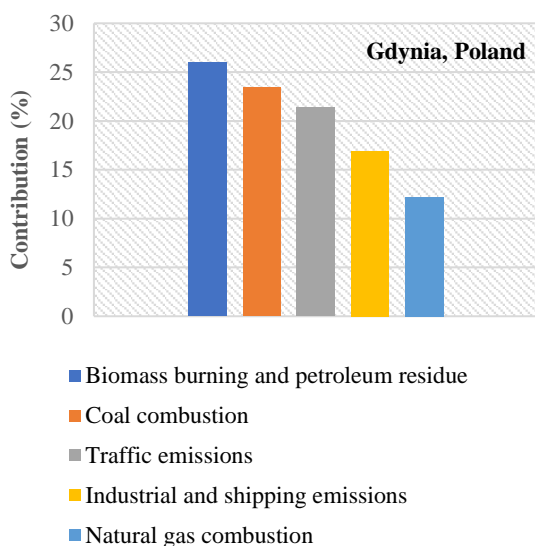
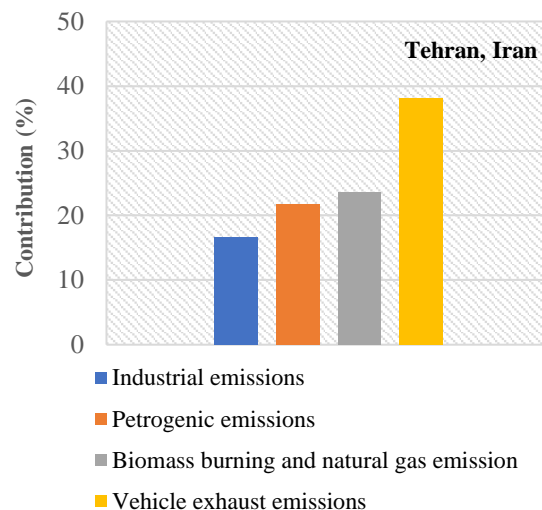
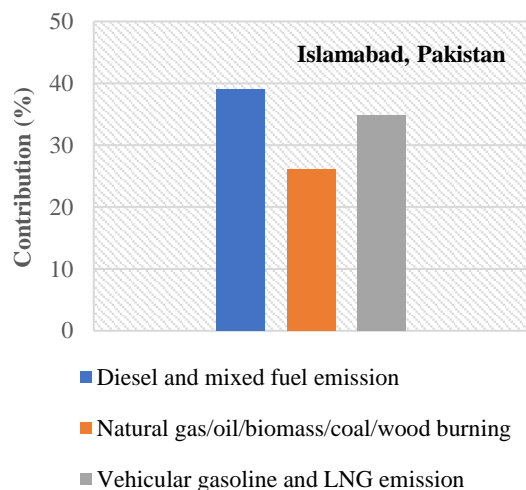
Fig. 2. Major sources of ambient PAHs.



- Vehicular emissions
- Natural gas combustion
- Petrol emissions
- Emissions from evaporative or unburned petroleum



- Combustion (fossil fuel, wood and traffic emissions)
- Others



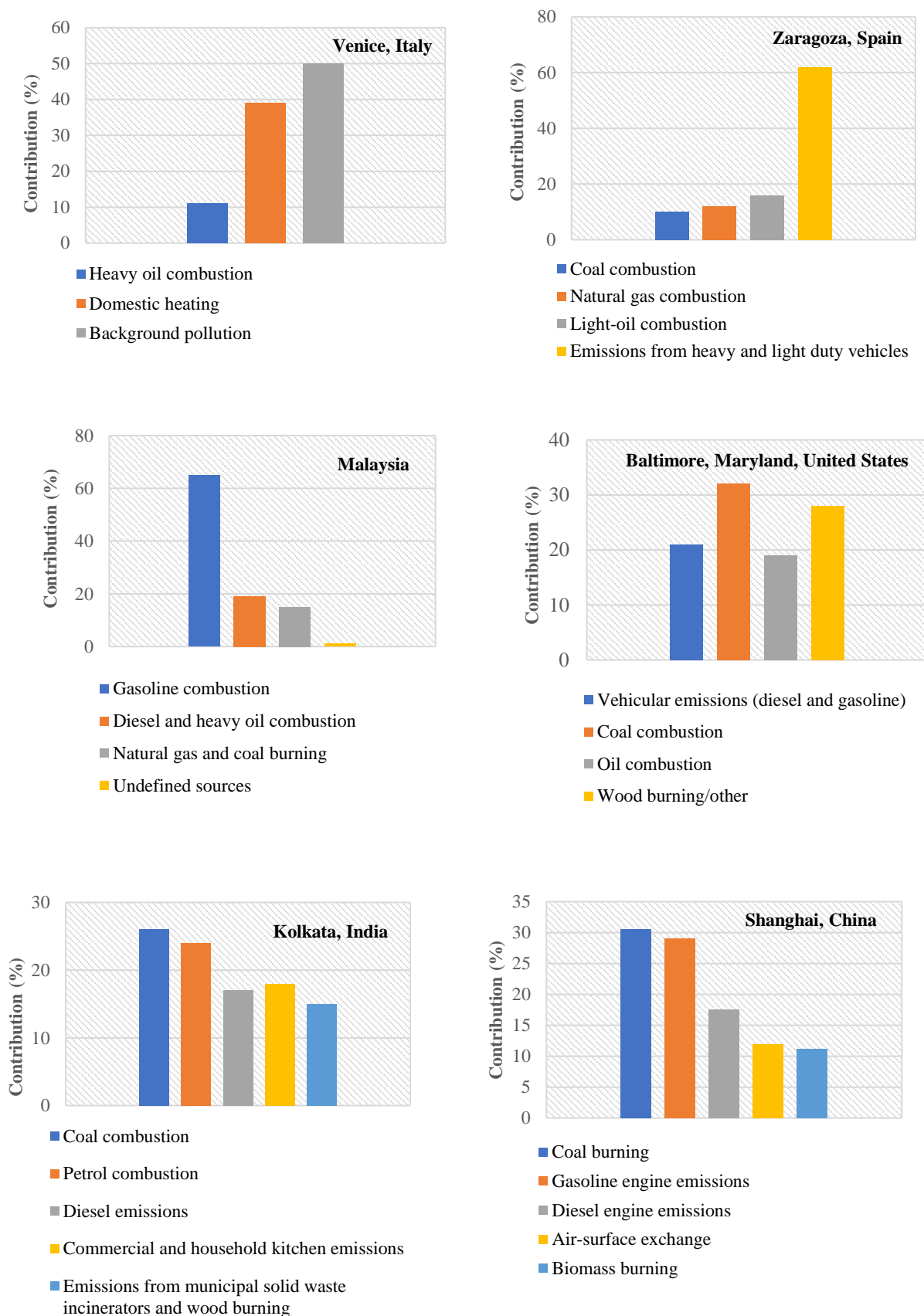


Fig. 3. Source profiles of atmospheric PAHs with the contributions of emission factors across the globe (Mishra et al., 2016; Vestenius et al., 2011; Mehmood et al., 2020; Ali-Taleshi et

al., 2021; Siudek, 2023; Jang et al., 2013; Shin et al., 2022; Ray et al., 2017; Larsen and Baker, 2003; Khan et al., 2015; Masiol et al., 2012; Callen et al., 2014; Xing et al., 2022; Wang et al., 2015a).

1.2.2. Distribution and transport of PAHs in the environment

PAHs that occur in the environment are mainly derived from petrogenic and pyrogenic processes, which require long duration for degradation. High concentrations of PAHs deposition across the various phases of environment have been confirmed in many studies. Distribution of PAHs in air, water and soil through interfacial exchange and long-range transport is depicted in Fig. 4. Atmospheric (i.e., wet, dry and gaseous) deposition mainly causes accumulation of PAHs in marine or aquatic and land-based terrestrial ecosystems (Jin et al., 2021). Fallout of air pollutants during precipitation or snowfall is referred to as wet deposition and is governed by the following expression in Eq. 1 (Viner, 2023):

$$V_{wet} = w_r \times p \quad (1)$$

where, V_{wet} is the deposition velocity, w_r is the washout ratio for particulates and p is the intensity of precipitation (rate of rainfall).

Settling of particles under the actions of turbulent mixing and Brownian diffusion, gravity, impaction and interception is regarded as dry deposition. It is also affected by wind speed, atmospheric stability, type of deposition surface and size of particulates. Dry deposition generally involves dry deposition velocity (V_d), deposition flux (F in $\text{ng m}^{-2} \text{s}^{-1}$) and surface-air concentration (C_{air} in ng m^{-3}) of aerosols and is expressed as follows (Eq. 2) (Povinec et al., 2021):

$$V_d = F / C_{air} \quad (2)$$

Gas deposition is related to the transport of pollutants between atmosphere and surfaces through vapour phase diffusion (Baldocchi et al., 1987).

Soil serves as a complex medium by acting as both a direct source or precursor and sink of pollutants, which stimulates PAHs migration till equilibrium, sorption to soil organic matter, fixation and transport into the ambience through re-volatilization (Hu et al., 2021). Soil denudation and rainwater runoff are the principal pathways of water contamination by PAHs (Qiu et al., 2019; Zhao et al., 2021). Also, variations in temperature and light intensity can cause diffusion-mediated PAHs partitioning between different interfaces (air-soil-water) (Hu

et al., 2021; Qi et al., 2023). Hence, monitoring and control of these pollutants are necessary for their toxic properties and longer half-life which form a broad spectrum of harmful end-products of degradation.

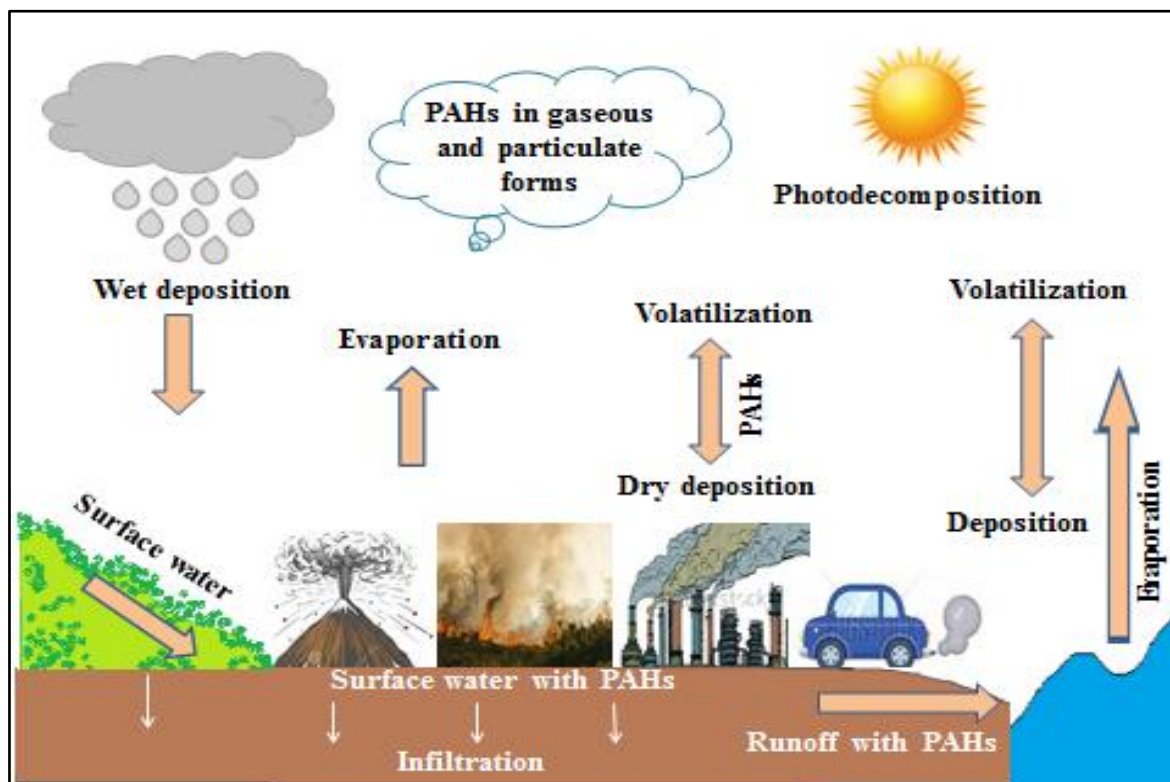


Fig. 4. Environmental fate and transport of PAHs (Ligaray et al., 2016).

1.2.2.1. PAHs in air

Global dispersion of PAHs in gaseous, particulate and droplet phases through the ambient atmosphere is the main pathway for its distribution which is influenced by their vapour pressure, dissolution, reaction with other organic compounds, solubility constant as per Henry's law and photocatalytic alterations (Birgul et al., 2011; Gocht et al., 2007; Zhong and Zhu, 2013). Existence of PAHs in gas phase or its adsorption to atmospheric aerosol particles depends on the nature of particulates and PAHs as well as temperature and relative humidity (Wang et al., 2013). Atmospheric PAH concentrations are mainly regulated by seasonality and phase partitioning, depending on temperature and PAHs vapourization where increase in temperature results in predominant PAHs equilibrium concentration in vapour phase (Kim et al., 2013). Volatile nature of LMW PAHs facilitates their abundant availability in gas phase, producing highly toxic products such as diones, nitro- and dinitro-PAHs and sulphuric acid after reacting with other criteria air pollutants (Kameda, 2011; Park et al., 2001). On the other

hand, HMW PAHs are less volatile, occurring mostly in the airborne particulate form owing to lower vapour pressure ([Kameda, 2011](#); [Kameda et al., 2005](#)). Accumulation of PAHs in ambient atmosphere is much less in summer or monsoon as compared to winter because of inversion of thermal lapse rate where air temperature increases with the increase in altitude, changes in the inversion frequency and domestic heating with deposition of particle-bound PAHs being maximum, whereas PAHs in gaseous form being predominant in summer ([Hussain et al., 2016](#); [Baek et al., 1991](#)). On the other hand, washout effects of rainfall in monsoon periods are accountable for the reduced levels of ambient PAHs pollution. PAHs fallout from the atmosphere in vapour and particle forms during precipitation by photochemical reactions is proved to be a major input of PAHs to surface waters and controls their fate in the environment ([Garban et al., 2002](#); [Bidleman, 1988](#)). It has been reported by [NAEI](#) in 2013 that the human interferences resulted in the release of approximately 621 tonnes of 16 PAHs of primary concern in UK in the year 2010 where BaP accounted for 3.23 tonnes with maximum contribution from natural emission sources (2.88 tonnes) as compared to anthropogenic activities ([Kim et al., 2013](#)). This raises the need of regulating uncontrolled combustions and implementation of cleaner fuel in the public transport.

To date, several exploratory researches on detection, identification and quantitative determination of atmospheric concentrations of PAHs have been undertaken in different countries for deeper insights into their phase and mass size distributions, atmospheric chemistry, global emission sources and health risk assessment from long-term exposure ([Table 1](#)). On that account, [Nadali et al. \(2021\)](#) proved that the concentration and gas-particle partitioning of PAHs in the ambient air were strongly dependent on diurnal as well as seasonal variations. Profound effects of different polluting sources (vehicles/combustion) on airborne PAHs levels were also evidenced by [Wang et al. \(2015_a\)](#), [Mishra et al. \(2016\)](#), [Masih et al. \(2019\)](#), [Mehmood et al. \(2020\)](#), [Ali-Taleshi et al. \(2021\)](#), [Shin et al. \(2022\)](#), [Qi et al. \(2023\)](#) and [Siudek \(2023\)](#). The results of the studies have shed light on the current status of the emission sources which is obligatory for the implementation of any strategic plan for the reduction of PAHs generation, a unified and far-sighted vision of long-lived future. The influences of climatology and meteorology as well as transboundary pollution on PAHs concentrations were again studied by [Vestenius et al. \(2011\)](#), [Gao et al. \(2013\)](#), [Khan et al. \(2015\)](#), [Ray et al. \(2017\)](#), [Liu et al. \(2017_a\)](#) and [Yang et al. \(2021\)](#) in order to pinpoint the sources of pollutants, unravel their movement in the atmosphere (through transport, dispersion and deposition) and speculate air pollution episodes. Concerning the health effects of airborne PAHs originated from a range of anthropogenic activities, high concentrations of PM_{2.5} bound

BghiP, IP, BbF and BaP induced respiratory infections (acute upper respiratory tract along with acute and chronic lower respiratory tract infections) which hampered normal breathing, genotoxicity (i.e., DNA damage) and cytotoxicity in epithelial cell lines and lung cancer as observed by [Jiang et al. \(2023\)](#).

Table 1

Monitoring of PAHs in the ambient air.

Sampling area/country	Sampling time	PAHs concentration in air (ng m ⁻³)	Remarks	References
Virolahti background station, Finland	January, 2007-September, 2008	0.14-25.3	Appreciable seasonal variations affected the concentrations of PAHs mainly emitted from combustion sources.	Vestenius et al., 2011
Urban, sub-urban and rural sites, Guangzhou, China	November-December, 2009	2.67-68.9	Weather conditions and differential emission sources influenced the temporal and spatial levels of PAHs.	Gao et al., 2013
Brisbane metropolitan area, Australia	October, 2010-August, 2012	1.17-38	Petrogenic and combustion sources were found in the study area with highest contribution from motor vehicle emissions.	Mishra et al., 2016
Shanghai, China	October, 2011-August, 2012	16.9	5-6 ring PAHs represented 56.5% of total PAHs, while 2-3 ring PAHs showed lowest abundance (12.4%). Diesel/gasoline emissions and coal burning were the predominant contributors.	Wang et al., 2015_a
Malaysia	June, 2013-February, 2014	2.79	Seasonal shifts effected PAHs occurrence and availability. Combustion and traffic sources also had significant impacts.	Khan et al., 2015
Kolkata (Indo-Gangetic Plain (IGP)) and Darjeeling (eastern Himalayan region), India	October, 2015-May, 2016	Kolkata: 37.65-146.71 Darjeeling: 5.45-36.60	Atmospheric concentrations were influenced by anthropogenic emissions and meteorological factors and differences were attributed to socio-economic backgrounds.	Ray et al., 2017
Beijing, Shanghai, Guangzhou, Nanjing, Wuhan, Taiyuan, Chengdu, Lanzhou and Xinxiang of China	October, 2013-August, 2014	3.0-580	Meteorological parameters were found to be correlated with ambient PAH levels and the emissions were dominated by vehicles (mainly driven by gasoline), household biomass burning and coal combustion.	Liu et al., 2017_a
Guangzhou, China	January, 2016-December, 2019	4.793	BghiP, IP, BbF and BaP posed highest risks with maximum exposure concentrations.	Jiang et al., 2023
Mumbai (western coast), India	September, 2016-December, 2016	Urban site: 29.36 Suburban site: 32.2	Gasoline and diesel vehicles substantially contributed to the overall PAHs concentration.	Masih et al., 2019
Islamabad, Pakistan	January-September, 2017	13.2-88.9	Vehicular emission and combustion had the major share to PAHs contribution.	Mehmood et al., 2020
Sapporo, Sagami-hara and Kirishima in Japan	Summer/winter months, 2017-2018	Sapporo: 0.31/3.35 Sagami-hara: 0.9/2.29	Air quality downfall was noticed in Shenyang and Vladivostok. The monsoonal flow (East Asian monsoon) exerted a huge impact on	Yang et al., 2021

Shenyang, China Vladivostok, Russia		Kirishima: 0.11/1.33 Shenyang: 3.72/49.7 Vladivostok: 3.05/25.3	pollutant behaviour and atmospheric interactions. Vehicle exhausts were found to be a prominent source of PAHs in all the cities.	
Tehran, Iran	March, 2018-February, 2019	Heating period: 30-49.8 Non-heating period: 18.4-26.35	Vehicular pollution represented the major source, diesel emission and gasoline exhausts being maximum in heating and non-heating periods respectively.	Ali-Taleshi et al., 2021
Hamadan, Iran	January-December, 2019	0.008-59.466	Relative humidity, wind speed and temperature were closely related to PAHs concentrations. Contribution of LMW PAHs of 3-rings was about 50%. Pyrogenic emissions and light duty vehicles were identified as the main sources.	Nadali et al., 2021
Gdynia, Poland	April-December, 2019	5.22-8.67	Local domestic heating and commercial coal combustion processes mainly contributed to PAHs concentration.	Siudek, 2023
Quingdao, Shandong Peninsula, East Coast of China	December, 2019-May, 2020 June, 2020-October, 2020	29.63	Emissions from coal combustion and waste incinerators were the primary contributors at rural sites, while, the urban areas were dominated by the traffic-related sources.	Qi et al., 2023
Seoul, Korea	May, 2020-January, 2021	3.96	Release of PAHs mostly resulted due to primary emissions from vehicles instead of secondary formation.	Shin et al., 2022

1.2.2.2. PAHs in soil and sediment

Surface soils and sediments generally get contaminated by PAH fallouts through atmospheric bulk deposition (Tao et al., 2003). This happens as these organic pollutants exhibit high affinity towards soil particles/sediments because of their lipophilicity (Kim et al., 2013). Municipal wastes or industrial wastes discharged into the environment without proper treatment are the major inputs for the contamination of surface water bodies, increasing the content of dissolved or suspended solids in water and also accumulating in the sediments (Lawal, 2017). In a study conducted by Nieuwoudt et al. (2011) in central South Africa, the total PAHs content in soil-sediment beds as analysed by GC/MS was found to be within 44-39,000 ng g⁻¹ dw in which contribution of carcinogenic PAHs amounted to 19-19,000 ng g⁻¹ dw (about 50% of the total PAHs), proving thereby that the pyrogenic sources are the major contributors of PAH pollution than petrogenic emissions.

Hydrophobic nature and partition coefficient of PAHs (i.e., octanol–water partition coefficient, K_{OW} - a measure of the difference in solubility of the PAH in the two immiscible phases at equilibrium) along with organic matter content of soil highly influence the adsorption/absorption and desorption mechanisms which govern the fate as well as mobility of PAHs in water-sediment beds (Hwang and Cutright, 2002; Hiller and Bartal 2006). Mobility of PAHs bound to soil particles in the subsurface is influenced by the particle size distribution of sorbent, soil conductivity and porosity (Riccardi et al., 2013; Abdel-Shafy and Mansour, 2016). Higher value of K_{OW} reduces the solubility of PAHs in water thereby increasing the rate of sorption to soil particles and finally affecting PAH mobility (Abdel-Shafy and Mansour, 2016). PAH concentration of 22.8 mg kg⁻¹ in soil or sediment beds is considered as the Probable Effect Concentration (PEC), above which ill effects are expected to occur frequently (<https://wrri.ncsu.edu/docs/partnerships/bmc/PAHFactSheet.pdf>). PAHs when incorporated into sediments become stagnant due to their non-polarity which prevents their dissolution in water. But formation of interstitial water organic colloids regulates the transport and distribution of PAHs in the soil/sediments by enhancing the amount of such pollutants in the aqueous phase due to their sorption onto the organic colloids which increase their mobility between pore fluids and their associated sediments (Abdel-Shafy and Mansour, 2016; Dong et al., 2012).

The unexpected surge in the levels of soil and sedimentary PAHs pollution has forced the authorities to initiate monitoring plans and controlling measures based on their abundance, nature and content, types of sources and human health or biohazards. Worldwide researches on

assessment of PAHs concentrations in such matrices, thus, furnished a scientific basis for meeting the general standards and criteria for environmental sustainability. Global trends of PAHs contamination in surface soils or in different soil layers of varied regions have been reported as 106-3148 ng g⁻¹ in Liao River Delta, Northeast China (Ma et al., 2014), 27-753 ng g⁻¹ in Yellow River Delta of coastal province of China (Yuan et al., 2014), 128.8-430.44 ng g⁻¹ in Qi'ao and Futian Nature Reserves of Greater Bay Area, a southern mega region of China (Wu et al., 2022), 10.8-4870 ng g⁻¹ in coastal wetlands of China (Yang et al., 2015), 20-225 ng g⁻¹ in Bolshezemelskaya tundra zone of Komi Republic (Yakovleva et al., 2017) and 16-12000 ng g⁻¹ in the adjacent areas of Canadian River in Cleveland, Oklahoma (Sartori et al., 2010). Concerning sediment contamination, PAHs concentrations ranged from 1.2-22.2 µg g⁻¹ in the marshes of Elizabeth River, southeast Virginia, United States (Kimbrough and Dickhut, 2006), 101.0-602.4 µg kg⁻¹ in Kvarnery Bay of Croatia (Traven, 2013), 93-431 ng g⁻¹ in Honghu Lake, Hubei Province, China (Zheng et al., 2017), 32.1-171.7 ng g⁻¹ in the areas along East China Sea (Adeleye et al., 2016), 16-31425 ng g⁻¹ in Chennai, India (Goswami et al., 2016), 5.02-981.18 µg g⁻¹ in Bhavnagar coast, Gujrat, India (Dudhagara et al., 2016) and <DL-234.3 ng g⁻¹ in mangrove sediments of South Brazil (Garcia and Martins, 2021). All such evidences are suggestive of ecosystem vulnerability and threats to human health. Anthropogenic inputs, such as petroleum pollution, biomass and coal burning, vehicle emissions, oil leakage, biogenic emissions and air-soil exchange or atmospheric deposition are likely to be the underlying factors of PAHs pollution in soil and sediments of different geographical areas. Total organic carbon (TOC) of soil organic matter (SOM) has also been found to stimulate PAHs accumulation by governing their partitioning and exchange between environmental surfaces and atmosphere.

1.2.2.3. PAHs in water streams

PAHs are the major persistent organic contaminants reaching the urban water bodies of developing metro cities due to wet or dry deposition from land-based sources, oil spillage, effluent disposal from sewage treatment plants and industries and runoff from dumping grounds and surface areas, where maximum PAHs distribution in urban areas occurs through the storm water runoff (<https://wrri.ncsu.edu/docs/partnerships/bmc/PAHFactSheet.pdf>). PAHs can also enter water streams/bodies through rains that wash off these pollutants from parking lot areas and roads, coming from tyre wear and tear, road-joint fillers, fuel leaks, auto emissions and broken pavements leading to high concentration of PAHs deposition in aquatic sediments. It is found that the tyre wear particles containing high aromatic (HA) oils, also

known as distillate aromatic extract oils (DAE), rich in PAHs, zinc and other organic compounds contribute to their release to the environment and pose severe risks to aquatic organisms due to their toxic nature. Use of tyres containing HA oils has been prohibited by the European Union (EU), which will eliminate further PAHs contamination from tyres by 98% (Wik and Dave, 2009). Presence of PAHs in water and its harmful effects on fish, amphibians, bivalves and benthic macro-invertebrates have been well documented, causing mutagenic, carcinogenic and genotoxic transformations (Connel et al., 1997). Due to their high toxicity, stable nature and lipophilicity, PAHs are transported through food chains and ultimately to the human beings (Vagi et al. 2005). Occurrence of PAHs in waterways depends on seasonal changes and is predominant in autumn and winter due to heavy traffic load and residential heating (Manoli and Samara, 1999). Maximum limit (standard) of $0.10 \mu\text{g L}^{-1}$ for total concentration of BkF, BbF, B[ghi]P, IP and $0.010 \mu\text{g L}^{-1}$ for BaP have been fixed for potable water by the European Communities (Drinking Water) Regulations, 2007 through EU Directive 98/83/EC. PAHs were generally detected in wastewater effluents and stream water using liquid-liquid extraction and GC-MS or HPLC methods. Quantum of PAHs in water streams above prescribed limit for drinking water causes potential risks to humans consuming the water. Pervasive occurrences of elevated concentrations of PAHs in aquatic environments (freshwater or marine) have been evidenced in past studies around the globe: $23.52\text{--}865.18 \text{ ng L}^{-1}$ in the Yellow River Estuary, China (Zhang et al., 2022_a), $891\text{--}1951 \text{ ng L}^{-1}$ in the Huai River of eastern China (Zhang et al., 2017_c), $0.05\text{--}65.9 \text{ ng L}^{-1}$ in the Ganges River Basin of India (Sharma et al., 2018), $688.70\text{--}4477 \text{ ng L}^{-1}$ in the Cauca River of Colombia (Sarria-Villa et al., 2016), $\text{ND}\text{--}30 \mu\text{g L}^{-1}$ in the Brahmaputra River and $\text{ND}\text{--}32 \mu\text{g L}^{-1}$ in the Hooghly River of India (Khuman et al., 2018), $235.92\text{--}10367.60 \text{ ng L}^{-1}$ in the Nile River of Egypt (Haiba, 2019) and $42\text{--}136 \text{ ng L}^{-1}$ in the surface water of Shadegan Wetland of Iran (Ashayeri et al., 2018). The authors reported the dominance of mostly LMW PAHs in water samples owing to their high water solubility and low K_{ow} . Both petrogenic and pyrogenic contaminations are accountable for PAHs inflow into the water bodies. Hence, there is an urgent need for constant monitoring and assessment of the levels of PAHs in the environment to mitigate the associated risks.

1.2.3. Exposure to PAHs and their associated risks on public health

Exposure of general population to fine particulate-bound and vapour phase PAHs, generated due to tobacco smoke, open burning, vehicular emission, residential heating or domestic cooking occurs mostly through absorption by skin, respiratory tract and gastrointestinal tract (ACGIH, 2005). Humans can develop hemolytic anemia and jaundice through consumption of

foods from crops grown in soil contaminated with PAHs because of complex nature of PAH metabolism occurring primarily in the liver and also in other tissues of human body to a lesser extent (Wang et al., 2012; Ciecierska and Obiedzinski, 2013). According to WHO, maximum acceptable concentration of benzo(a)pyrene in water should be $0.7 \mu\text{g L}^{-1}$. Teeming population of all cities may be at higher risk of PAHs exposure due to their choice of occupation and level of pollution in and around work place depending on their ever-increasing demand for survival (Caricchia et al., 1999). Individuals working in mines, metal workshop or oil refineries and also mechanics, street vendors and motor vehicle drivers are exposed to PAHs due to inhalation of exhaust fumes in their work fields (See et al., 2006). Many industrial plants producing coke, coal tar/pitch, aluminium, iron and steel, creosote, rubber, mineral oil, soot and carbon black, etc. are the major sources for human exposure to these organic pollutants (Hussain et al., 2018) which can be readily eliminated if proper remedial measures are implemented to arrest the polluting organic compounds at their emission sources. PAHs exhibit low degree of acute toxicity to human due to short-term exposure having minimum harmful effects. Occupational exposure to PAHs may cause lung, skin and bladder cancers, development of high levels of DNA adducts and mutations including non-carcinogenic but harmful effects on immune, nervous and reproductive systems (Abdel-Shafy and Mansour, 2016). Benzo(a)pyrene and benz(a)anthracene are proved to be potent carcinogenic compounds by IARC and USEPA and are used as biomarkers or indicators for environmental exposure to PAHs or carcinogenic pollution. Human health risks by drinking water from streams and lakes are rare as PAHs normally adsorb to sediment particles rather than dissolving in water (<https://wrri.ncsu.edu/docs/partnerships/bmc/PAHFactSheet.pdf>). Risk is also low from consumption of fish as PAHs do not readily bioaccumulate within vertebrates. In animals, PAHs and their metabolites induce necrosis or apoptosis in order to destroy healthy living cells (the process being referred to as cytotoxicity) depending on their aromatic ring structure, particle size and functional groups. They adversely affect the functioning of immune system, damage the genetic information within a cell causing mutations, which may lead to cancer and also interfere with normal reproduction, causing developmental toxicity in the offspring (IARC, 1983). Short-term exposure to PAHs is associated with increased risks of damaged lung function, asthma, impairment of kidney function, lysis of red blood cells and ischemic heart disease (IHD) which reduces blood flow to the heart muscle (ACGIH, 2005; ATSDR, 1995; Srogi, 2007). It also causes skin infection (Srogi, 2007), eye irritation, cataracts, nausea, vomiting and diarrhoea (Unwin et al., 2006). Anthracene, benzo(a)pyrene and naphthalene are categorized as skin allergens and sensitizers, that cause burning sensation or pain,

inflammation, redness, itching and fissures (IPCS, 1998). Chronic effects of PAHs exposure include cell disruption due to alterations in the DNA sequence, heart failure and respiratory mortality (Kuo et al., 2003). DNA fragments bound to electrophilic PAH metabolites facilitate the initiation of cancer. PAH-DNA complexes detected in leukocytes have been used as an indicator for long-term human consumption of grilled meat (Kang et al., 1995). Several studies showed that high levels of PAHs exposure to pregnant mother may cause premature birth or birth deformities with low body weight in offsprings, low IQ, improper behaviour, developmental delay and childhood asthma (Perera and Herbstman, 2011). Jung et al. (2013) showed that HMW PAHs can cause chromosomal aberrations in rodents. 1-hydroxypyrene (human metabolite of pyrene) is usually found to be excreted through urine of outdoor workers when forced to work in polluted environment, indicating acute kidney injury (Sobus et al., 2009).

Several risk indices have been used by the researchers as particular measures for assessing pollution threats in order to represent the integrated consequences of PAHs exposure. Potential toxicities of PAHs are generally expressed as mutagenic and carcinogenic equivalent concentrations with respect to benzo(a)pyrene (BaP_{MEQ} and BaP_{TEQ}) and also in reference to carcinogenic and mutagenic potential (CP and MP). Hazardous nature of mostly HMW PAHs has been confirmed in many studies with more than 90% contribution to cancer risks (Verma et al., 2022; Blaszczyk et al., 2017; Ihunwo et al., 2021). Incremental lifetime cancer risk (ILCR) and lifetime average daily dose (LADD) are often used as health risk parameters to evaluate the chances of life-threatening diseases caused via different exposure pathways (inhalation, oral or dermal) upon subjection of human population to carcinogenic pollutants for a long span of time (Ambade et al., 2021; Florencia et al., 2022). $ILCR \leq 10^{-6}$ suggests negligible probability of foreseeable risk, whereas, $ILCR > 10^{-4}$ signifies increased risk of cancer among individuals. Low to severe health risks of cancer (2.26×10^{-7} – 3.28×10^{-7} (Davoudi et al., 2021), ND – 7.21×10^{-5} (Ambade et al., 2021) and 1.3×10^{-3} – 3.7×10^{-3} (Cheng et al., 2022)) from PAHs pollution is well-reported in many investigations. Different authors have stated that the cancer risk values for individual PAH congeners may not exceed the permissible limit, but the overall cumulative risk is much higher than the threshold value (Tongo et al., 2017).

1.3. Traditional monitoring and biomonitoring of air pollutants

Detection and monitoring of PAHs in ambient air are mainly performed through direct air sampling by onsite conventional instruments such as Respirable Dust Sampler/High Volume Air Sampler and Ambient Fine Dust Sampler equipped with filter papers (fibre glass filter

paper, quartz fibre filters or polytetrafluoroethylene (PTFE) filters) at different stations near roads with heavy traffic density, at selected sites within cities, near schools/colleges, hospitals and also near probable sources of emissions (CPCB, 2003). Adsorbents like PUF disks, XAD-resins, Tenax (porous polymer adsorbent matrix), SPMDs (semipermeable membrane devices) and polymer coated glass can also be employed as passive air samplers for in-situ air sampling. However, the traditional air sampling processes as mentioned above are disadvantageous for monitoring and handling of air samples for proper analysis as expensive and sophisticated analytical equipment are required to be installed at monitoring sites with high level of maintenance along with provision for security (Blasco et al., 2006). Efficiency of air samplers for accumulating airborne pollutants also gets reduced due to their specific onsite deployment period (Zhou et al., 2014). Also, large volumes of polluted air masses should have to be sampled for continuous 24 h or more to get appreciable and measurable concentrations of PAHs. Even then it will only give information about current air quality (Van der Wat and Forbes, 2015).

Therefore, it can be opined that the simplest and most cost-effective way of assessing and determining airborne PAHs is the indirect method of employing natural bioaccumulators (organisms, groups of organisms or biological communities) as they can assimilate the pollutants from the atmosphere within their tissues and exhibit visible damages or other symptoms in response to their exposure to pollutants (Onete et al., 2010; Parmar et al., 2016). Plants' competences to respond to external stress signals vary in consonance with their biochemical, physiological and morpho-anatomical characteristics for a clean environment of the biosphere, maintaining biogeochemical cycle with ecological balance. From this perspective, plants are explored as important tools in environmental bioindication and biomonitoring depending on their pollution sensitive or tolerant nature (Achakzai et al., 2017). However, the basic difference between bioindicators and biomonitors lies in the fact that only the impact of pollution can be discerned from the bioindicators through their growth patterns, injuries developed and paucity of their diversity in a particular area, while, accumulative bioindicators/biomonitorers help make the qualitative or quantitative assessment of ambient pollution due to the presence of contaminants which reveal the level of pollution load in the environment and also provide an understanding of the anthropogenic interferences by their presence and abundant availability with long life-span in the ecosystem. Moreover, they are reproducible, can be sampled easily and applicable to those sites where heavy instruments could not be taken and installed. They are also able to monitor integrated exposure of pollutants over time. Selection of different types of bioaccumulators such as plants, animals, microbes

and macroinvertebrates, used for biomonitoring, is based on their specific responses with respect to environmental variability. Bioaccumulators and their responses to airborne pollutants are represented in Fig. 5. Plants or the above-ground organs of plants like stem, bark, ring, leaves and needles as well as lower plants such as bryophytes (e.g., mosses) and lichens are generally used as excellent biomonitors for indirectly assessing the quantum of air pollution in polluted areas, which have helped to investigate the presence of PAHs in the atmosphere. Therefore, biomonitoring of PAHs using plants, lichens and mosses has become the thrust area for environmental clean-up as they usually trap the atmospheric PAHs and mineralize or transform them into non-toxic forms, thereby eliminating them from the ambient air and improving its quality.

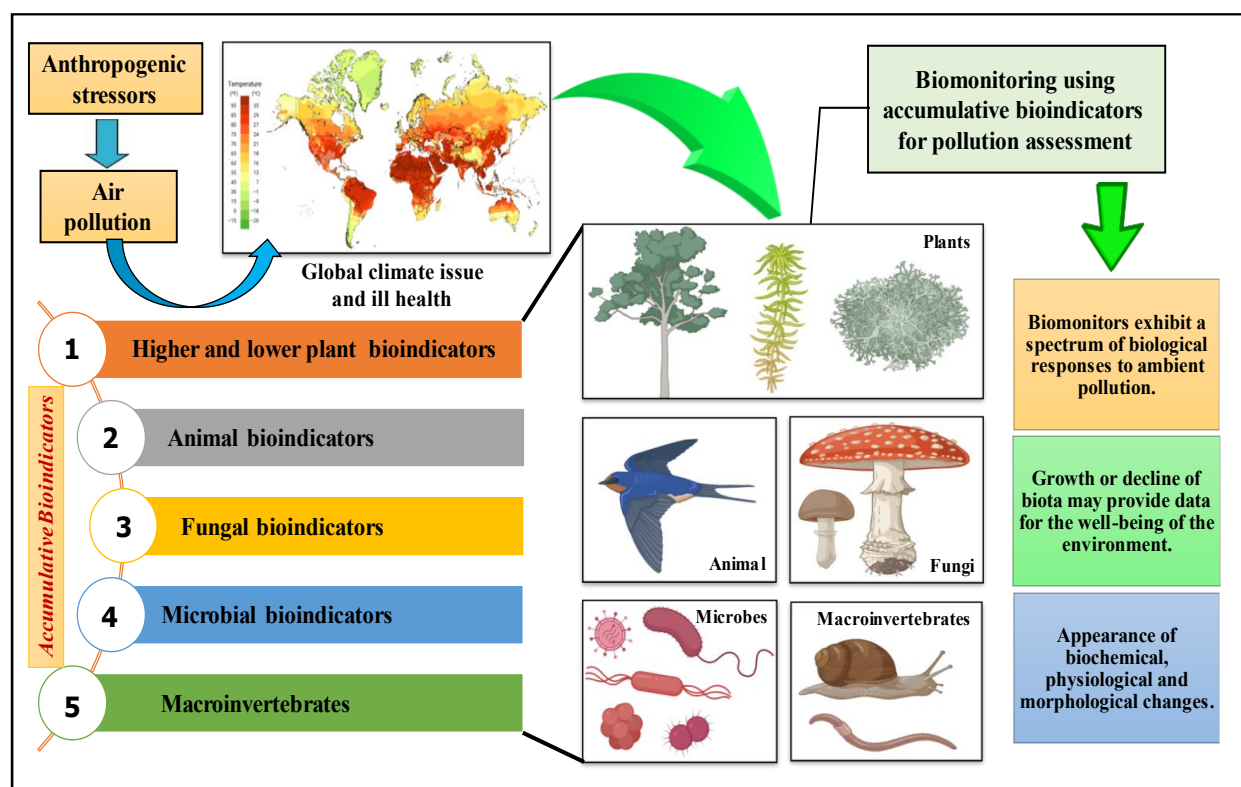


Fig. 5. Different types of biomonitors of environmental pollution and their stress responses (Parmar et al., 2016).

1.4. Biomonitoring scheme: Measurement of the accumulation of PAHs in plant tissues

The series of steps for assessment of vast range in PAHs concentrations encompasses collection of samples from selected fields, sample pretreatment, extraction and purification with proper solvents followed by analysis and interpretation of results. Investigations to obtain detectable ranges of PAHs concentration in biomonitor plants, lichens and mosses have been performed throughout the world using conventional (Soxhlet or Soxtec and ultrasonication) (Viskari et al., 1997; Holoubek et al., 2000; Migaszewski et al., 2002; Hubert et al., 2003; Augusto et al., 2010; Dolegowska and Migaszewski, 2011; Loppi et al., 2015; Studabaker et al., 2017; Yang et al., 2017; Bi et al., 2018; Oishi, 2018; Van der Wat and Forbes, 2019) as well as modified solvent-extraction techniques (microwave assisted extraction (MAE), accelerated solvent extraction (ASE)/pressurized liquid extraction (PLE), modified ultrasonic extraction, i.e. dynamic sonication assisted solvent extraction, DSASE, matrix solid-phase dispersion extraction (MSPD), SUPRAS-based microextraction and QuEChERS (quick, easy, cheap, effective, rugged and safe)) (Domeno et al., 2006; Ratola et al., 2009, 2012; Blasco et al., 2011; Schrlau et al., 2011; Foan and Simon, 2012; Fujiwara et al., 2014; Sucharova and Hola, 2014; Caballero-Casero et al., 2015; ConchaGrana et al., 2015b; Ji et al., 2019; Van der Wat and Forbes, 2019) to deliver accurate and reliable results through standardized analytical approaches like gas chromatography-mass spectrometry (GC-MS) or high performance liquid chromatography (HPLC).

1.4.1. Sample preparation techniques

1.4.1.1. Sampling and sample pretreatment methodologies

Plant sampling for biomonitoring should be based on the collection of leaves or other plant parts from healthier species. Infected (by pathogens or insects) or dead or stressed (by extreme weather conditions) plant materials need to be avoided. As far as foliage sampling (using appropriate gardening tool) is concerned, fully developed (or full grown) leaves should be taken into consideration and must involve replicate samples of minimum 40-100 leaves per sample from two to three trees for each analysis for better coverage of the study area. Duration and time of sampling should be selective pertaining to the work objective. Leaf samples should then be handled with care with their proper detachment from the petioles and placement in paper bags or polyethylene zip lock pouches before processing. It is also noteworthy that improper sampling may lead to erroneous results.

Pretreatment of biomatrices after sampling mainly involves thorough washing of unwanted debris, oven-drying or lyophilization and tissue grinding or homogenization for size reduction to produce fine powder, making it convenient for extraction process and thereby increasing the recovery efficiency (Yu et al., 2019).

1.4.1.2. Solvent extraction of PAHs

Extraction is the prime step for accurate identification and subsequent analysis of atmospheric PAHs in the environment. Mass transfer in extraction process can be extended to a certain limit beyond which further extraction or further enrichment of the extractant by solute is not possible. This depends on partition or distribution coefficient which can be defined as the ratio of concentration of an analyte in the residual matrix part to that in the extractant at equilibrium and predicts the analyte behaviour between air and matrix (McLachlan, 1999; Meylan and Howard, 2005). Conventional extraction methods like Soxhlet extraction and ultrasonication are the common methods of choice; whereas alternative extraction methods like PLE/ASE, MAE, extraction using supercritical and subcritical fluids (pressurized hot water extraction) and membrane assisted solvent extraction (MASE) are also employed which involve different organic solvents for better extraction yield (Barreca et al., 2014). Solid phase extraction (SPE) technique (one of the selective extraction processes) is primarily used for extract clean-up. Modified extraction techniques with low or no consumption of solvent have also been developed for achieving enhanced extraction efficiency, which include single-drop microextraction, cold-fiber solid-phase microextraction, MSPD, SUPRAS-based microextraction and QuEChERS extraction method (Szulejko et al., 2014). In addition to conventional organic solvents, other extraction agents including microemulsions, biosurfactants, cyclodextrins, vegetable oil or water also facilitate PAHs removal up to 47-100% (Lau et al., 2014; Lawal, 2017).

- **Factors influencing the process of PAHs extraction**

- *Nature of solvent system*

In an experimental setup, choice of appropriate solvent is the main factor affecting the extraction process, which depends on the solubility of the desired PAHs with respect to solvent polarity and solvent-matrix interactions (Chen et al., 2008). The selected solvent should be non-toxic, inflammable, chemically stable and inert to avoid reaction with the analytes. Viscosity, vapour pressure and freezing point of the solvent should be low for its user-friendly

handling and storage. The solvent should be highly selective towards PAHs than the other matrix components and should be compatible to chromatographic analysis. The matrix:solvent ratio also critically influences the process of extraction ([Luque-Garcia and Luque de Castro, 2003](#)) where the matrix should be properly submerged and saturated in adequate quantity of solvent during extraction. Better results can be obtained through high solvent:solid matrix ratio in case of conventional extraction methods, while in case of MAE, this would not yield good results owing to non-uniform temperature distribution of microwave radiation ([Tatke and Jaiswal, 2011](#)). Also, in MAE, dielectric constant (dissipation factor) of solvents governs the extent of energy absorption radiated by microwaves ([Shu and Lai, 2001](#)), thereby affecting the rate of extraction. The efficiencies of different extraction techniques may vary from one process to another.

Extraction results are greatly affected by a variety of solvent suites which may be either moderately polar like dichloromethane (DCM) or toluene or a mixture of polar and non-polar solvents according to USEPA. Loss of PAHs has been observed in several studies using DCM as solvent. On the other hand, high boiling point does not make toluene favourable for extraction ([Khan et al., 2005](#)). Other solvents which are frequently used for PAHs extraction are hexane, acetone/hexane (1:1 v/v), DCM/acetone (1:1 v/v), DCM/ethanol (1:1 v/v), n-butanol ([Hatzinger and Alexander, 1995](#)), methanol ([Codina et al., 1994](#)), chloroform, isopropanol, cyclohexane, diethyl ether and acetonitrile (ACN). Though organic solvents are effective extraction agents, they are harmful to the environment ([Khan et al., 2005](#)). Hence, ionic liquids (ILs) which are ionic compounds with low melting points and non-aqueous, are used in recent research for extraction process as green or designer solvents instead of organic solvents as they are thermally and chemically stable, able to reduce environmental pollution and enhance the selectivity of analytes and extraction efficiency ([Poole, 2004](#); [Han and Row, 2010](#); [German-Hernandez et al., 2011](#); [Xiao et al., 2018](#)). Requirement of ILs for extraction is very less (only 4-5 mL per extraction) and IL-extracts also do not need any further clean-up steps for analysis ([German-Hernandez et al., 2011](#)). However, synthesis of traditional ILs is quite difficult and costly process as compared to protic ILs and deep eutectic solvents ([Shamsuri and Abdullah, 2010](#)).

Ternary or binary solvent mixtures are also used for extraction of PAHs. [Ugwu and Ukoha \(2016\)](#) reported that high amount of targeted PAHs (mostly 2 and 4-ring PAHs) was extracted with ternary solvent system of mixed polarity (acetone + DCM + n-hexane) as compared to binary mixtures (acetone + DCM; DCM + n-hexane; and acetone + n-hexane), while both the solvent mixtures yielded same concentrations of 3 and 5-ring PAHs. These

hydrocarbons normally adhere to the matrix through physical adsorption. Other organic substances present in the mineral matrix as well as biological system tend to bind PAHs molecules through chemical and biological interactions which reduce the solvent elution ability resulting in decreased PAHs content in extracts (Delhomme et al., 2007).

➤ **Extraction time**

Proper selection of extraction time is very much necessary for economic consideration of the process and reduction of energy consumption. As the quantity of extracted analyte is generally directly proportional to the extraction time, the ‘green methods’ would be those involving less solvent, shorter duration and better yield for extraction (Dent et al., 2013). Also, mass fraction of the analytes is highly influenced by the extraction time and its proper optimization can regulate its efficiency (Dent et al., 2013). Dent et al. (2013) also reported that the organic solvent ethanol or acetone (30%) produced the most favourable condition for polyphenol extraction from dried leaves of *Salvia officinalis* (common sage leaves) at 60 °C with extraction time of 30 min. However, Wong et al. (2014) demonstrated that the total content of phenolic and flavonoid compounds for kenaf seeds extracted with 100% ethanol decreased as the extraction time increased which can be explained by the loss of antioxidants due to heat or oxygen exposure for longer periods. Mokrani and Madani (2016) showed that the increase in extraction time from 30 min to 180 min resulted in the enhancement of total phenolic compounds (TPC), 1,1-diphenyl-2-picrylhydrazyl radical-scavenging activity (DPPH-RSA) and ferric reducing power (FRP) for peach tree (*Prunus persica* L.). Any further increase in time could not boost up the recoveries following the Fick’s second law of diffusion due to equilibrium concentration reached between the solute molecules in the bulk of the solution and solid matrix. Hence, it is conferred that varying optimized time periods are required for extraction of volatile organic compounds or PAHs from different matrices depending on extraction techniques.

➤ **Temperature of extraction**

Temperature is one of the most important criteria for extraction. High temperature decreases fluid density and viscosity with decrease in surface tension, resulting in the increase in contact between solvent and targeted analytes, thereby enhancing the extraction efficiency. Increase in temperature destabilizes solute-matrix interactions, thereby increasing the solubility of solutes in the organic solvent more efficiently with improved mass transfer, rapid diffusion and better recoveries. Quantitative extraction of polar compounds can be achieved at low temperatures;

but for extraction of PAHs or hydrophobic organic compounds, high temperatures (250-300 °C) are essential ([Andersson, 2007](#)). Very high extraction temperatures (more than 300 °C) may cause damage to instruments, degrade the analytes or otherwise react at high temperatures. This may also lead to the co-extraction of other matrix components in substantial quantity with the desired PAHs, thereby compromising the purpose of selection of extraction process. There can also be blockages and pressure increase inside the equipment which will give erroneous analytical results ([Andersson, 2007](#)). Further purification of the extracted analytes may also be carried out, if necessary. Therefore, low extraction temperatures should normally be maintained to avoid denaturation of analytes along with elution of other undesired matrix components.

➤ *Effect of pressure*

Adequate pressure exerted on the solvent facilitates extraction of analytes trapped in matrix pores from the samples and also maintains the solvent in liquid phase with the help of elevated temperature. High temperature with requisite pressure reduces the surface tension of the solvent inducing it to pass through the pores as well as those areas of the matrices that are not properly exposed to the solvents due to the pore entrance blockage caused by air bubbles or water in order to make contact with the analytes for extraction ([Richter et al., 1996](#)). High pressure proves to be an added advantage for the analytes which are easily available on the matrix surface or within the pores, as seen in case of liquid chromatography. Solvent under high pressure is able to flow easily through the pores solubilizing the air bubbles and also subjecting it to intimate contact with the sample. This process is termed as adsorption chromatography for the analytes found mostly on the surface ([Richter et al., 1996](#)).

➤ *Matrix characteristics*

The matrix characteristics including particle size, chemical composition, surface area, pH, water content, total organic matter content, pore size and polarizability of analytes greatly influence analyte-matrix interactions ([Hsieh and Chang, 1997](#)). Smaller particle sizes mainly enhance the solvent flow rate as well as extraction rate owing to rapid diffusion through reduced diffusion path facing less resistance and better solvent flow across the matrix ([Amellal et al., 2001](#)). It may sometimes cause difficulties in separating the matrix from solvent after the process of extraction, which may be overcome by subsequent adoption of centrifugation or filtration steps ([Tatke and Jaiswal, 2011](#)). Also, the extent of PAHs extraction from the sample

is influenced by both its solubility in the solvent and desorption behaviour (Hsieh and Chang, 1997).

- **USEPA promulgated methods for extraction and analysis of PAHs**

The USEPA established several sampling, extraction and analytical approaches for common PAHs in which a combination of wide variety of filters (quartz filters) and adsorbents/sorbent cartridges such as Tenax, XAD-2 and polyurethane foam (PUF) have been used to draw air samples (approximately 300 m³ of air volume) efficiently over a 24 h period by employing a high-volume air sampler with a flow rate of 0.22 m³/min for acquiring adequate sample for analysis (EPA, 1999). Conventional Soxhlet extraction with appropriate solvent is normally followed for PAHs extraction from the filters and adsorbents. Further, the extract is being made concentrated by Kuderna-Danish (K-D) evaporator followed by extract clean-up with silica gel column chromatography to eliminate matrix interferences caused by the co-extracted contaminants from the sample prior to analysis by both HPLC-UV and GC-MS based on USEPA Method 610 (EPA, 1984). Standardization of the analytical instruments is essential to ensure proper analytical results for the samples within the calibration range of the instrument. If not so, then the following will have to be looked into (EPA, 1999):

- a) recalibration of instruments,
- b) adjustment of the volume of the injected samples,
- c) adjustment of concentrations of the standard solutions,
- d) adjustment of data processing system for specified retention times, etc.

Moreover, operational precision and method accuracy directly influence the sample concentration irrespective of sample matrix.

- **Methods of extraction**

- ***Mechanical agitation***

In this method samples are mechanically stirred generating turbulence for PAHs extraction by two different ways, either by placing the shake-flask on an orbital shaker or using a magnetic stirrer immersed in the shake-flask directly (Lau et al., 2010). It is a simple, economic and easy-to-handle method with minimum requirement of glass wares and solvent. It is not very much used as the extraction efficiency and quantitative results due to mechanical shaking are not satisfactory (Graham et al., 2006) owing to wide variations and less selectivity for the

assessment of PAH extracts (Berset et al., 1999). Long contact time with solvent for shaking may give proper results comparable to other methods (Kalbe et al., 2008).

➤ *Soxhlet extraction*

This technique requires more time and large volume of organic solvents, in which the solid matrix is kept in a thimble for solvent extraction via reflux cycle. The vapourized solvent after boiling is bypassed into the condenser through a distillation path, dripping back onto the solvent in the thimble after condensation. The excess solvent with the extract falls back into the boiling flask below through siphon tube (Lau et al., 2010). The solvent then starts boiling again and the process is continued till complete extraction of the analytes. Disadvantages of Soxhlet extraction include requirement of large volume of solvent, poor selectivity for PAHs, likelihood of sample carryover, non-viability of re-dissolving dry extracts, requirement of intense labour and time since the process of extraction continues up to 16-24 hours for getting better yield (Dean and Xiong, 2000). It has been reported that n-alkanes and humic substances are also coextracted with PAHs through this method integrated with GC/MS or GC/FID as identified from mass chromatograms (Graham et al., 2006). The results obtained from this technique are quite comparable to those produced by other methods with small variations having low standard deviations (Flotron et al., 2003). The percentage recovery for PAHs with more than 4 rings using this process ranges between 84–100% and increases with the increase in molecular weight (Smith et al., 2006).

Improved version of this technique (automated Soxhlet extraction method) involves two steps combining boiling and rinsing to reduce time and volume of solvent required for complete extraction. In this improved technology, solvent extraction is carried out via reflux cycle collecting the solvent with extracts below the thimble after condensation. The extraction efficiency and accuracy of this process are highly improved reaching almost up to 100% recovery (Sporring et al., 2005). Additionally, the compactness of the instrument having multiple extraction chambers ensures simultaneous extraction of PAHs from several samples (Dean and Xiong, 2000).

➤ *Ultrasonic agitation / sonication*

This technique transmits the sound energy of ultrasonic waves having 16 KHz frequency (minimum) while passing through the fluid, which causes frequent changes in the fluid density (compression and rarefaction) resulting in creation and rupture of vapour bubbles in quick succession (cavitation action). A sonicator transducer or a sonication bath can be utilized for

fluid agitation by ultrasonic waves generated by means of piezoelectric ceramics (Lau et al., 2010). Studies showed that sonication provides higher extraction efficiencies as compared to that of Soxhlet technique and is more economical and easier to operate (Sun et al., 1998). Interferences of sample matrix and other pollutants greatly influence the rate of extraction. In order to enhance the rate of extraction for PAHs, time of exposure to ultrasonic waves and power level should be monitored to prevent the degradation of organic contaminants present in the sample. Extensive exposure to sonication causes breakdown of carbonaceous particles which increases the available surface area for PAHs adsorption (Stephens et al., 1994). Centrifugation or filtration may be necessary after extraction for further isolation of PAHs from these particles.

➤ *Accelerated solvent extraction (ASE) / Pressurised fluid extraction (PFE)*

It is a newly developed technique and used for extraction of PAHs or other compounds from a complex solid or semisolid sample matrix within a very short time (5-10 min) with the help of organic solvents at elevated pressure and temperature (maintaining the temperature above atmospheric boiling point of the solvent). This process requires less time and smaller volume of solvent and shows better analyte recovery and precision than conventional methods operated under less extreme conditions. Extraction efficiency of the desired analyte increases with high temperature and pressure which keeps the solvent in a liquid state (Richter et al., 1996). High pressure (500-3000 psi) and temperature (50-200°C) allow the solvent to pass through the pores very rapidly solubilising the surrounding air bubbles and allowing the solvent to come in contact with much of the sample. In ASE system, multiple numbers of samples in extraction chambers can be run in a single batch by placing them in cartridges containing required volume of selected solvent which helps in extracting the desired compounds (Richter et al., 1996). After completion of extraction, sample is purged with nitrogen gas to remove remaining solvent and collected into a collection vessel for further concentration and analysis. It has been reported that efficiency of PAHs extraction from soil-sediment beds is much higher in ASE system as compared to traditional Soxhlet extraction technique (Wang et al., 2007) with improved accuracy of extraction, reducing RSD (relative standard deviation) down to less than 10% (Liguori et al., 2006). ASE system also offers automation and precision using less solvent volume and time which prevents vapourization of PAHs and sample contamination by avoiding the strenuous process of sample preparation (Liguori et al., 2006).

➤ ***Pressurized hot water extraction (PHWE) / Subcritical water extraction (SWE)***

This method is extensively used as an eco-friendly extraction technique which utilizes hot water under pressure as an extractant replacing organic solvents due to its non-toxic nature, easy availability and disposal and cost-effectiveness. Pressurised hot water with altered physico-chemical characteristics helps in PAHs extraction from solid matrices under high temperature (below 374.0°C-critical temperature of water-but above 100°C) and pressure (5 bar at 150°C and 86 bar at 300°C) for maintaining the liquid nature of water. Steam can also be used in the process of extraction instead of hot water ([Khan et al., 2005](#)). High temperature and pressure make the electrostatic interactions (hydrogen bonding) between water molecules feeble, resulting in lower dielectric constant and simultaneous decrease in polarity, which enhances PAHs solubility by reducing hydrophilicity of water ([Lau et al., 2010](#); [Manahan, 2005](#)). When oxidizing agents are also used with SWE method, it provides better extraction efficiency for PAHs with excellent selectivity and less or almost no coextraction of other alkanes ([Hawthorne et al., 2000](#)). This combined approach offers an extraction efficiency of 99.1–99.99%, whereas only SWE technique provides the same ranging between 79–99+% ([Dadkhah and Akgerman, 2002](#)). Heat-labile compounds are generally extracted at low temperature in the presence of other co-solvent, which works by reducing the water density by weakening the hydrogen bonding of water molecules ([Curren and King, 2001](#)). Maximum extraction of PAHs with 2-4 fused aromatic rings can be achieved by PHWE, whereas high recovery rate for PAHs having 4-7 fused benzene rings can be obtained through PLE ([Hawthorne et al., 2000](#)). Coextraction of other compounds with the desired analyte renders the extract turbid when non-selective extraction techniques like Soxhlet, PLE and MAE are employed ([Andersson, 2007](#)).

➤ ***Supercritical fluid extraction (SFE)***

Supercritical fluids having properties akin to both gas and liquid can effuse through solid matter as a gas or dissolve them as a liquid due to absence of surface tension and liquid/gas phase boundary ([Lau et al., 2010](#)). This dissolving power of supercritical fluid is utilized for extraction and fractionation of a broad spectrum of compounds ([Khan et al., 2005](#)). As for example, carbon dioxide in supercritical state (temperature 31°C and pressure 74 bar) can be used to extract PAHs from the sample matrices ([Hawthorne et al., 2000](#)). SFE involves both static and dynamic mode of operation to extract analytes from sample. Temperature, pressure and mode of operation are the main process parameters influencing extraction ([Khan et al.,](#)

2005). Degree of solvation in supercritical fluids can be controlled by regulating the pressure and temperature or with addition of modifiers like methanol (1-10%) which alters the polarity of supercritical fluid. SFE enhances the extraction kinetics and improves recovery rates as compared to conventional extraction method like Soxhlet technique (Northcott and Jones, 2000). Application of SFE in determining the desorption behaviour and abundance of carbonaceous pollutants in soil has also been reported (Hawthorne and Grabanski, 2000). Elution of highly purified extracts renders this technique very much selective with reduction in standard deviation (Lau et al., 2010). Extraction of analytes using supercritical water is constrained as it requires high temperature (>374°C) and pressure (>218 atm) causing corrosion or damage of the extraction vessel (Yang et al., 1997). Integrated SFE system may allow the analysis of the extracts directly by gas chromatography without any clean-up, thereby preventing contamination by manual handling (Berset et al., 1999).

➤ ***Solid phase extraction (SPE)***

This technique requires less time with high selectivity for PAHs extraction. Prior to extraction with a selected solvent, the samples are rinsed with another solvent to remove all the unwanted compounds present in the soil matrix (Kootstra et al., 1995). Selected sample must be subjected to sand filtration or passed through empty solid phase extraction cartridges before start of extraction in order to stop the clogging of SPE column by the soil particles (Lau et al., 2010). The washed sample containing PAHs is then kept in a collection tube for extraction. The basic principle of SPE involves adsorption of the sample onto a sorbent material (like activated charcoal or modified silica) (Sibiya et al., 2012). Studies revealed that SPE can be efficiently used for sample preparation for PAH analysis having correlation coefficients more than 0.9 with relative standard deviations between 0.8-9.1% as compared to the liquid-liquid extraction (LLE) standard deviations ranging between 1.1 to 15.1%. Using this technique, volatile PAHs like naphthalene, acenaphthylene and acenaphthene can be recovered up to 80–90% (Kootstra et al., 1995). Its advantages include high extraction rates, purification and enrichment of sample, requirement of small volume of solvent and less time compared to other sample preparation techniques (Sibiya et al., 2012). This technique can be used with automation having facilities for running multiple samples simultaneously with optimized process parameters and compatible analytical results for getting better analyte enrichment and recovery (Sibiya et al., 2012). But it has the only disadvantage of involving many steps during extraction which requires more time for method development.

Another novel extraction technique is the solid phase microextraction (SPME), a variation of SPE, which uses a small diameter fused-silica fibre having a coating of an extracting phase and covered by a protecting device for easy operation. This SPME system eliminates the use of solvents, adsorbs the PAHs from the matrix and then directly introduces the sample to the injection port of the instrument for quantitative determination. This technique is fast, simple with high extraction efficiency and enables its operation to be easily carried out at site (Lau et al., 2010). SPME requires very small amount of samples for extraction that can be easily analysed without any pretreatment. Analysis of the sample adsorbed to the fibre can also be done after few days of extraction without substantial loss of volatile components if proper storage conditions are maintained (Lau et al., 2010). Volatile PAHs having 2-4 fused-benzene rings can be easily extracted using SPME methodology (Eriksson et al., 2001).

➤ ***Thermal desorption***

This extraction technique is a solvent free approach without any requirement of high-pressure technology and is mainly applied to isolate organic contaminants from soil, sludge or sediments. It is integrated with GC and the prepared sample is directly injected into the injection port. An inert carrier gas is stopped initially till the target compounds are volatilized from the matrix into the thermal desorber by rapid heating of the injector up to required temperature between 200-500°C (Lau et al., 2010). The carrier gas then passes through the injector into the GC column, taking with it the isothermally extracted compounds, for detection and analysis. Content of PAHs in fly ash, particulate matter and polluted soil-sediment beds can also be determined using this process. This process depends on the heating method (direct or indirect), matrix and parameters like pressure, temperature, boiling point, total organic matter content, contact time and extent of mixing for efficient extraction (Renoldi et al., 2003; Ayen et al., 1994).

➤ ***Pyrolysis (Py) or high temperature distillation (HTD)***

This method involves rapid change in temperature over time in which materials undergo thermochemical decomposition above 300°C in an oxygen-controlled environment (Weidemann et al., 2018). The yield and chemical composition of the pyrolysis products depend on the characteristics of the feedstock, heating rate and residence time of the process (Zhao et al. 2013). This high temperature catalyzes the break-down of macromolecules into simple and volatile ones (Lau et al., 2010). Pyrolysis with online GC has the advantages of eliminating the purification steps, lower contamination risks, higher sensitivity and specificity,

elimination of solvent requirement and cost-effectiveness. In this technique, temperature has to be carefully optimized to prevent formation of undesirable by-products (Lau et al., 2010).

➤ ***Membrane assisted solvent extraction (MASE)***

In MASE technique prepared sample mixed with organic solvent is passed through low density polyethylene (LDPE) membrane for its separation from solvent. Solvents used should either be non-polar to avoid its loss through the membrane or very polar having lipophobic properties to prevent their passage through the membrane. Acetonitrile is generally used for PAH extraction with MASE coupled to HPLC analysis. MASE is performed offline in a vial; the extracted sample is then directly fed into the injection port of GC/MS using large volume injection LVI (Hauser and Popp, 2001). Liquid-liquid extraction with microporous membranes (e.g., supported liquid membranes (SLMs), emulsion liquid membranes and ionic liquid membranes) is employed to eliminate matrix interferences due to their hydrophobic and size-exclusive properties for analyte detection (Ncube et al., 2016; Davoodi-nasab et al., 2017; Pabby et al., 2017; Ncube et al., 2018). Potentially this technique can also be automated integrating with highly sophisticated chromatographic equipment (Barri and Jonsson, 2008). But extraction is not exhaustive in this technique (Hyotylainen and Riekkola, 2008) as the membrane pores get choked by other high molecular weight compounds (Jakubowska, 2005).

Rodil et al. (2007) showed that more than 65% recovery with relative standard deviation (RSD) of 6 to 18% can be achieved for all the sixteen priority PAHs (as listed by USEPA) by this technique. It was also found by Prieto et al. (2008) that recoveries ranging between 81–116% can be obtained for PAHs present in brackish water (estuarine) samples. Process parameters such as shaking speed, extraction temperature, time, ionic strength of extraction solvent and sample pH have to be optimized to achieve enriched analytes from the sample (Rodil et al., 2007). Membrane assisted extraction is mainly used in food and bio-analysis.

➤ ***Fluidized-bed Extraction (FBE)***

Fluidized-bed extraction (FBE) technique resembles automated Soxhlet extraction method, where an extraction vessel with a filter fixed at its bottom holds the sample. The selected solvent is put into another vessel below the sample and is heated up. Evaporation of solvent takes place through the filter which raises the temperature of the sample and penetrates it causing agitation to maintain its fluidity (Lau et al., 2010). The solvent vapour then condenses and gets collected into the vessel below, dripping back through the sample extracting analytes with it. Further concentration of collected solvent is then carried out for final analysis. The

extraction time and solvent consumption are reduced in this method under optimized conditions (Lau et al., 2010).

➤ ***Microwave-assisted extraction (MAE)***

In this technique, solvent extraction of PAHs from matrices is aided by microwave irradiation (Eskilsson and Bjorklund, 2000). Instantaneous microwave heating of the sample greatly enhances the rate of extraction due to dipole rotation and ionic conductance. Extraction solvent that can absorb microwaves is mostly preferred. Microwave heating does not cause any deterioration or denaturation of extracted compounds unless the temperature is too high (Lopez-Avila et al., 1998) and the extraction process can be conducted either in a closed vessel under controlled condition or in an open vessel under normal atmospheric condition (Camel, 2000). These methods are known as pressurized MAE (PMAE) and focused MAE (FMAE) respectively. Application of controlled pressure would raise the temperature beyond the solvent boiling point inside the closed extraction vessel and speed up the rate of extraction and yield as compared to Soxhlet technique. In open vessel, the temperature is limited by the solvent boiling point at atmospheric pressure. In this process, extraction time is reduced to 10-20 min per sample batch due to rapid microwave heating with solvent consumption of 25-50 ml per sample. Prior to analysis, clean-up steps are mainly performed at room temperature for purification of the samples after completion of the heating cycle (Khan et al., 2005). Extraction using MAE technique depends on the degree of polarization of the sample and solvent (Delhaes and Drillon, 1987). Immersion of sample matrix in a microwave transparent solvent like hexane can prevent the degradation of thermo-labile components. Bangkedphol et al. (2006) reported that PMAE method using cyclohexane:acetone (3:2) in a closed system operated for 15 min at 140% boiling point of acetone is most efficient for PAH extraction with 96.55% recovery. Advantages of this process include less requirement of solvent, better extraction yield within short duration having no influence of other compounds present in the matrix as compared to other methods (Kamankesh et al., 2015).

➤ ***QuEChERS extraction***

Being an efficient and green extraction method, QuEChERS technique works on the principle of solid-liquid extraction with salting out effects on the partitioning and distribution behaviour of analytes, comprising dispersive-SPE step and various sorbents for extract purification (Zachara et al., 2018; Agus et al., 2023). Simultaneous integration of methods, solvents, salts

and sorbents makes it a clear choice of successful extraction in shorter time in a cost-effective manner. [Sadowska-Rociek et al. \(2015\)](#) adopted QuEChERS method for PAHs extraction from chocolate samples with the application of dispersive liquid-liquid microextraction (DLLME) at clean-up stage. The authors found good efficiency of the process with 52.8-112% PAHs recoveries.

➤ *Other techniques*

High-end extraction approaches including headspace SPME (HS-SPME), cooling assisted headspace microextraction by packed sorbent method (CA-HS-MEPS) and direct immersion cold fiber SPME (DI-CF-SPME) have presently been employed for ultra-trace analysis of PAHs and their derivatives (oxy and nitro) from different solid matrices like wet/sandy/clay-sandy soil and airborne particles (especially PM_{2.5}) with less solvent volume and sample amount ([Serenjeh et al., 2020](#); [Ma et al., 2019a](#); [dos Santos et al., 2020](#); [Majd and Nojavan, 2021](#)). All the methods showed high sensitivity and undeniable process efficiency, leading to high PAHs recoveries (73-110%). On-line dynamic headspace extraction (DHS) is another modified extraction technique which demands no separate clean-up step for sample extracts. Th technique was successfully applied to complex matrices, such as fish and agal oil for the assessment of LMW PAHs ([Guiffard et al., 2020](#)).

1.4.1.3. Extract clean-up

Steps of sample clean-up with organic solvents, in several cases, are required for elimination of interferences after extraction to analyze the compounds of interest by chromatographic separation. Purification and fractionation of samples are usually carried out using column chromatography or adsorption chromatography (which relies on equilibrium separation of analytes through their partitioning between stationary and mobile phases) employing different sorbent materials like silica gel, alumina, florisil, etc. and SPE (which consists of small cartridges packed with specific sorbent material) resulting in the acceleration of analysis procedure. ([Blasco et al., 2007](#); [De Nicola et al., 2016](#); [Hussain and Hoque, 2015](#); [Ray et al., 2021](#); [Tian et al., 2019](#); [Yang et al. 2017](#)). Anhydrous sodium sulphate is also utilized in certain cases for moisture removal from sample extract during column chromatography ([Abayi et al., 2021](#)). Organic solvents which are used as eluents include n-hexane, toluene, DCM, methanol as well as different solvent combinations ([Soursou et al., 2023](#)). Efficiency of SPE clean-up with aminopropyl cartridge using solvent blend of DCM:n-hexane as eluent was reported by [Mueller et al. \(2019\)](#) who found 98% recovery for PAHs and their derivatives. Silica gel

column chromatography has also been found to be a preferred choice for many studies on PAHs determination as can be observed from high recovery percentage values (95.5-98.7% and 22.37-107.02%) (Kumari et al., 2012; Wandan et al., 2011). Gel permeation (or size exclusion) and multilayer column chromatography are also often applied for biomatrices (Bogdanovic et al., 2019). Moreover, DLLME is seldom used for purification of extracts obtained through QuEChERS method (Chen et al., 2013). Preconcentration techniques are also applied due to insufficient sensitivity of the chromatographic techniques (Li-bin et al., 2007). In general, extracts are concentrated by rotary evaporation or with inert nitrogen gas stream of high purity or using vacuum or reduced pressure (Szulejko et al., 2014).

1.4.2. Analytical techniques for PAHs detection with method validation

Various sensitive, simple and rapid analytical and biological approaches are developed and introduced for accurate determination of PAHs with respect to quantity and quality. Infrared, Raman and fluorescence spectroscopies, GC and HPLC with sensitive detectors (such as GCFID, GC-MS, GC-MS/MS, HPLC-FLD, HPLC-UVD, GC-NPD, GC-NICI/MS) are generally classified as non-biological and non-destructive analytical techniques, extensively used for the separation and detection of PAHs (Li-bin et al., 2007; Kumar et al., 2017).

Distribution of energy of a molecule with conjugated π electrons at any given moment is the basic principle of spectroscopy for analytes' characterization at molecular-level having same formula with distinct chemical structures. Hence, this technique is widely used for determination of PAHs with conjugated π electrons. Functional groups of molecules are normally detected by using spectroscopic methods which can distinguish para- and meta-derivatives. Infrared (IR) spectroscopy deals with the qualitative determination of unique functional groups associated with a molecule at characteristic frequencies or wave number between 4000 cm^{-1} and 400 cm^{-1} . Aromatic hydrocarbons containing C=C and C-H stretching represent overlapping bands in the 3100 to 2700 cm^{-1} region (Kumar et al., 2017). That is why IR spectroscopy finds its immense acceptance for PAH analysis as it can detect different molecular structures with differences in vibrational and rotational spectra of PAHs. Pakarinen et al. (2007) and Negi & Kumar (2012) have found the utility of Fourier transform infrared spectroscopy/mass spectrometry (FTIR/MS) and Fourier transform ion cyclotron resonance (FT-ICR) spectrometer in the identification and analysis of PAHs. Raman spectroscopy works on the principle of density function theory (DFT) based on vibrational, rotational and low-frequency spectra leading to characterization and analysis of desired compounds (Kumar et al., 2017). Specific spectrum for a particular PAH at a specific

wavelength can be generated using fluorescence spectroscopy with excitation wavelength range from 245 to 400 nm and emission wavelength range from 280 to 550 nm ([Christensen et al., 2005](#)). The luminescence behaviour of compounds/analytes depends on the character of the substituents, the solvent polarity, temperature and effectiveness of the fluorescence process, determined in terms of quantum yield, quenching rate constants, energy transfer, lasing ability, and radiative and non-radiative rate constants ([Fery-Forgues and Lavabre, 1999](#)) having maximum absorbance wavelength selected as the excitation wavelength ([Rivera-Figueroa et al., 2004](#)). This technique is preferred over Raman spectroscopy for its better detection through optical sensors, sensitiveness and precise analysis.

Chromatography is employed in the separation of various constituents present in a mixture and quantification thereof in the order of parts-per-million or subparts-per-million level of analytes. The constituents in the mixture move at different speeds, resulting in their separation which depends on distinct adsorption between mobile and stationary phases. Liquid chromatography (LC) facilitates the separation of polar and non-volatile compounds; the separation being highly influenced by humidity and temperature ([Kumar et al., 2017](#)). But this does not provide proper information about the distinguished spectra for each PAH as compared to GC and HPLC. LC when combined with fluorescence detector (FLD) or UV-diode array detector (DAD) or mass spectrometry (MS) has been proved to be an efficient technique for determination of PAHs content in complex mixtures ([Miege et al., 1998](#)). Another separation technique which is extensively used for quantification/identification of volatile, non-ionic and non-polar analytes is gas chromatography (GC) where inert gases are utilized as mobile phase in lieu of liquid. During separation, a rapid equilibrium, established between the stationary and mobile phases, gives highly precise analytical results within short duration. GC can only be operated with thermally stable and volatile samples which should not degrade during thermal conductivity ([Kumar et al., 2017](#)). GC-MS equipped with capillary columns (TG-5MS/HP-5MS/DB-5MS) for improved separation performance is by far widely accepted method of analysis, identification and measurement of atmospheric PAHs due to its high selectivity, sensitivity, robustness and characteristic separation of different components (resolution), having the capability of reliable detection of even lowest concentration of test sample (low limit of detection, LOD) ([Pandey et al., 2011](#)). HPLC combined with UV detection is also applied for quick separation and detection of PAHs with proper stationary (reversed phase columns) and mobile phases because of its no dependency on volatility and molecular weight of the analytes ([Agus et al., 2023](#)). It has wide acceptance for qualitative as well as quantitative

analyses. Non-detection of desired compounds in a complex mixture due to overlapping peaks can be overcome by further improvisation of the technique using various detectors.

Biological methodologies for identification of PAHs, viz. biosensor-mediated detection, microarray-based estimation, immunoassays, polymerase chain reaction and application of nanoparticles, have also gained tremendous importance in recent years owing to higher sensitivity, specificity and instantaneous recognition of PAHs during the analysis. On-site and in situ detection of PAHs can be achieved by using very simple and economic recombinant microbial biosensors which proved to be an efficient monitoring tool for environmental pollution. Instant and on-site monitoring can also be done with antibodies used against PAH recognition. Studies revealed that highly specific and sensitive real-time PCR assays can be effectively utilized for detection as well as quantification of genes in PAH-degrading bacterial population that were used as bioindicators to characterize the key enzymes catalysing the degradation ([Kumar et al., 2017](#)). Similarly, a high-throughput screening method like microarray can also be employed for determination of gene expression levels. The use of nanoparticles for PAH analysis has also resulted in increased sensitivity and limit of detection, extraction and quantification by many folds as compared to the traditional methods. [Table 2](#) and [Table 3](#) present comparisons among different extraction techniques, clean-up and analytical methods along with solvent requirements.

Analytical method validation for PAHs determination is obligatory to establish the reliability of the developed protocol with reference to data (qualitative or quantitative) accuracy and reproducibility. Validation parameters include accuracy or precision, detection and quantification limits (LOD and LOQ), linearity, range, recovery, specificity, robustness, uncertainty and ruggedness ([EU, 2011](#)). Among them, LOD and LOQ are the most crucial parameters for any analytical method and are applied when analyte concentrations are very low in sample matrices ([Agus et al., 2023](#)). Linearity describes the range of a method where the output or response falls in a direct relationship with analyte concentrations. Linearity, repeatability and specificity combinedly can indicate trueness of the measurement. Percentage of similarity of analytical results of measurement from replicate runs under the same parameter settings is referred to as method precision or accuracy. Uncertainty in measurement is another vital parameter to test for during method validation. Thus, it can be apprehended that the investigation of performance characteristics is an integral part of development of analytical method intended to be used for PAHs assessment in environmental samples.

Table 2

Comparison of extraction techniques ([Eskilsson and Bjorklund, 2000](#); [Giergielewicz-Mozajska et al., 2001](#)).

Sl. No.	Extraction technique	Extraction time	Sample size	Solvent usage	Recovery	Advantages	Disadvantages
1.	Mechanical agitation	6-12 hrs	10 g	50-200 mL	60-70%	Simple; economic; easy-to-handle.	Low selectivity; long contact time; wide variations.
2.	Soxhlet extraction	4-48 hrs	1-30 g	100-500 mL	84-100%	No filtration required.	Long extraction time; large solvent volume; clean-up steps needed.
3.	Sonication	10-60 mins	1-30 g	30-200 mL	44-76%	Multiple extractions.	Large solvent volume; repeated extractions; clean-up steps needed.
4.	ASE/PFE	5-25 mins	2-15 g	15-40 mL	95-100%	Low solvent volume; less time required.	High cost; high pressure and temperature requirement.
5.	PHWE/SWE	2.5 hrs	4 g	50-60 mL	90-100%	Better extraction efficiency; eco-friendly; high selectivity.	High pressure and temperature needed; not effective for HMW PAHs.
6.	SFE	30 mins-2 hrs	1-5 g	8-50 mL	90-95%	Low solvent volume; selective; no clean-up.	High pressure and temperature; corrosion of extraction vessel.
7.	SPE	30 mins	5 g	10-50 mL	80-90%	High extraction rates; low solvent volume; less time.	Multiple steps required during extraction for method development.
8.	MASE	30-60 mins	0.05-50 ng	500-800 μ L	81-116%	Simple and fast; no clean-up; re-usage of membranes after cleaning.	Extraction not exhaustive; choking of membrane pores by other HMW compounds.
9.	MAE	10-20 mins	1-10 g	25-50 mL	>95%	Fast with multiple extractions; low solvent volume.	Clean-up needed; requirement of microwave absorbing solvent; additional time for cooling down of vessel.

Table 3

Extraction methods with solvents, purification steps and analytical techniques for assessment of PAHs (Szulejko et al., 2014; Balampanis et al., 2017).

Sl. No.	Extraction technique	Solvent	Purification/Clean-up process	Detection/Analysis
1.	Mechanical agitation	Hexane, hexane:acetone, toluene, t-butanol, 2-propanol.	Silica gel or alumina column chromatography.	HPLC-UV, HPLC-FLD, GC-MS
2.	Soxhlet extraction	DCM, hexane, toluene, hexane:acetone (1:1), diethylether, cyclohexane, acetone.	Silica gel, alumina column chromatography or solid phase extraction, liquid-liquid extraction with DMSO or DMF and water.	HPLC-UV, GC-MS, GC-FID, HPLC-fluorescence.
3.	Sonication	Cyclohexane, DCM, hexane.	Thin layer chromatography on silica gel, liquid-liquid extraction with DMF and water, silica gel or alumina chromatography columns.	GC-FID or GC-MS, HPLC-fluorescence.
4.	ASE/PFE	DCM, hexane, acetone, toluene.	Silica gel or alumina column chromatography.	HPLC-fluorescence, GC-MS, GC-MS/MS.
5.	PHWE/SWE	Hot water under pressure	Silica gel or alumina column chromatography.	HPLC-UV, GC-ECD, GC-MS.
6.	SFE	Supercritical fluids (e.g. CO ₂ in supercritical state)	Gel permeation chromatography, Florisil column clean-up.	HPLC-MS
7.	SPE	Hexane, methanol, ethyl acetate, isopropyl alcohol, methylene chloride.	Solid-phase extraction cartridge.	HPLC-MS, GC-MS
8.	MASE	Cyclohexane, methanol, ethyl acetate, DCM, diisopropyl ether.	Clean-up not required.	GC-ECD, GC-MS
9.	MAE	Hexane, DCM, acetonitrile, acetone, hexane:acetone (1:1).	Gel permeation chromatography, Solid-phase extraction cartridge, adsorption chromatography, MAE-solid bar microextraction clean-up.	HPLC-MS, GC-MS, HPLC-UV.

1.5. Biomonitoring of airborne PAHs using terrestrial vascular and non-vascular plants

1.5.1. Vascular plants as biomonitors of atmospheric PAHs pollution

Improved air quality can be obtained through biomonitoring strategy by developing urban forests and greenbelts around habitats or industrial premises, mitigating the impacts of pollution on ecosystem generated due to release of persistent organic pollutants in the ambient air. For this purpose, various trees, shrubs, grasses, vegetation cover and green walls or green roofs are effectively utilized as accumulative phytoindicators as well as PAHs scavengers reducing the contaminant levels in the atmosphere (Currie and Bass, 2008). Therefore, tree bark, stem, ring, plant leaves and conifer needles can be very much effective as biomonitoring tools in identifying the potential risks of polluted atmosphere and understanding of local and global pollution patterns (Nobel et al., 2005).

a) Plant leaves

It has been demonstrated that the leaves of evergreen or deciduous plants and shrubs can accumulate particle or vapour-phase PAHs either in the waxy cuticular layer on the foliar surfaces or via stomatal diffusion into leaf inner tissues (Fellet et al., 2016). The process of absorption or adsorption by plant leaves is regulated by particulate or gaseous nature of PAHs, specific surface area of leaves, total lipid content in foliar tissues, octanol-air partition coefficient, foliar dust concentration, stomatal density and atmospheric conditions like pressure and temperature (Slaski et al., 2000). Influence of meteorological factors, specific leaf area (SLA), leaf area index (LAI) as well as leaf density on PAHs absorption by deciduous tree species (hazelnut and maple) was examined by Terzaghi et al. (2015). The authors observed that PAHs uptake rate varies directly with SLA, whereas LAI is species dependent.

Early detection of plant tolerance and sensitivity for distinguishing suitable biomonitors is imperative to assess the intrinsic ability of plants to counter the effect of pollution arising from abiotic stress. Thus, air pollution tolerance index (APTI) is a useful means for proper selection of tolerant plant species for sustainable plantation, which varies with total contents of leaf chlorophyll, ascorbic acid, relative water content and leaf extract pH (Singh and Rao, 1983). Plant species are grouped under three different classes depending on index values: sensitive (or bioindicators: $APTI < 10$; vulnerable to toxicity and only deliver information on the quality of environment), intermediate ($10 < APTI < 16$) and tolerant (or biomonitors: $APTI > 17$; survive harsh climates and beneficial for green infrastructure activities to ensure

ecological balance) (Singh et al., 1991). The APTI is expressed as follows (Eq. 3) (Prajapati and Tripathi, 2008_b):

$$APTI = \frac{A \times (T + P) + R}{10} \quad (3)$$

where, A is the ascorbic acid content (mg/g), T is the total content of leaf chlorophyll (mg/g), P is the leaf extract pH and R is the relative water content (%).

In addition to APTI, anticipated performance index (API) has also been considered as a grading-based performance indicator for plant species, taking account of APTI, biological traits and socioeconomic importance of plants, for sustainable development of urban green spaces (Banerjee et al., 2022). Singh et al. (1991) studied 69 plant species (herbs, shrubs and trees) in the urban-industrial belts of Varanasi, India, and found that the species like *Calotropis gigantea*, *Catharanthus roseus*, etc. were tolerant towards air pollution with high APTI values, whereas *Dalbergia sissoo* (Indian rosewood), *Lobelia chinensis*, *Carissa carandas*, *Chrozophora rottleri*, etc. were sensitive species having low APTI values. PAHs concentration in the leaves of six evergreen ornamental shrubs *Elaeagnus x ebbingei*, *Ilex aquifolium*, *Laurus nobilis*, *Ligustrum japonicum*, *Photinia x fraserii* and *Viburnum lucidum*, used for arboreous landscaping, was investigated by Fellet et al. (2016) in Italy during winter. The authors applied ultrasonic extraction with the leaf samples using DCM as the extraction solvent to determine the PAHs content. GC-MS technique in selective ion monitoring (SIM) mode was employed for its quantification. Mean PAHs recoveries were found to be 46-94%. They found that the total concentration of PAHs in plant leaves ranged between 201 and 585 $\mu\text{g kg}^{-1}$ in the sites around public parks and 366-1258 $\mu\text{g kg}^{-1}$ in high traffic congested areas with maximum contributions from phenanthrene, naphthalene, fluoranthene, fluorene and pyrene constituting about 87.6% (PHE: 54.7%; NAP: 8.5%; FLT: 12%; FLN: 7.6%; PYR: 4.7%) of total PAHs in public parks and 89.1% (PHE: 51.3%; NAP: 13.2%; FLT: 9.5%; FLN: 10.4%; PYR: 4.8%) in dense traffic areas. The authors observed in their study that the most efficient plant groups for mitigation of traffic pollution were *Elaeagnus x ebbingei*, *L. japonicum* and *L. nobilis* and confirmed their tolerance to air pollution with high APTI. Biomonitoring of PAHs using *Cinnamomum camphora* leaves was studied by Yang et al. (2017) in Shanghai, China, during summer and winter to evaluate PAHs stress in different tissues of camphor leaves and identify the point sources of emission. Determination of PAHs content in foliar dust and mesophyll tissue was carried out by employing Soxhlet extraction technique using a solvent mixture of DCM and acetone (1:1) for 18 h, followed by GC-MS analysis. Average concentrations of PAHs were 3868 ng g^{-1} in foliar dust, 1239 ng g^{-1} in cuticular wax and 134 ng g^{-1} in mesophyll

tissue during summer; whereas in winter the mean concentrations were 4076 ng g⁻¹, 4317 ng g⁻¹ and 194 ng g⁻¹ in foliar dust, cuticular wax and mesophyll tissue respectively. Diverse meteorological parameters, location and seasonal variations along with leaf wax content facilitated the changes in the distribution pattern of PAHs in the leaves. The authors demonstrated that the vehicular emissions were the major sources of contamination which affected the plant leaves, indicating poor air quality of Shanghai megacity.

Orecchio (2007) examined the feasibility of ultrasonication for the extraction of PAHs from the leaves of *Quercus ilex* L. (evergreen oak), sampled in the provinces of a populated town Palermo in Italy, using DCM for 20 min associated with GC-MS analysis for quantitative and qualitative determination. Total concentration of 16 priority PAHs (proposed by USEPA) and perylene ranged from 92 to 1454 µg kg⁻¹ d.w. which signifies that the *Quercus* leaves have the potential to be effective bioaccumulators to evaluate the integrated levels of PAHs in air over a large span of time. The percent recovery of deuterated PAHs ranged between 76 and 102% which validated the efficiencies of extraction and analytical methods. The author also suggested that these leaves can effect biodegradation of airborne PAHs due to the presence of thick cuticle and dense stellate hairs on the leaf surface. Similar study was also carried out in Southern Italy (in Naples and Salerno region) by De Nicola et al. (2011) using oak leaves (*Quercus ilex* L.) and employing a sonicator for 3 min with DCM:acetone (1:1) as PAHs extractant, analyzing the same with GC-MS technique. The percentage recoveries of deuterated PAHs varied between 66 and 72%. The mean PAHs concentration measured in plant leaves was in the range of 500-8500 ng g⁻¹ d.w. as investigated by the authors, which undoubtedly proved their efficacy in biomonitoring of air pollution. Again, De Nicola et al. (2016) demonstrated the positive role of *Quercus robur* L. (pedunculate oak) leaves and *Pinus pinaster* (maritime pine) needles, collected from NW Spain, for the formulation of a European standard for biomonitoring purpose. The authors applied an improved and modified extraction technique MSPD involving different purification sorbent materials such as florisil with PSA (primary secondary amine) for oak and florisil bonded with silica for pine leaves. DCM and hexane were considered as elution solvents for PAHs. 90-120% recovery was achieved for most of the PAHs after analyzing by GC-MS/MS even up to low limits of quantification (<3 ng g⁻¹ for pine needles and <1.5 ng g⁻¹ for *Quercus* leaves using only 250 mg of plant matrix). This MSPD technique is inclusive of both extraction and clean-up and can be recommended for standardization of the protocol to assess PAHs concentration in plant leaves for its high precision and sensitivity. Hubert et al. (2003) reported a novel single-step clean-up procedure for PAHs analysis in evergreen coniferous pine needles (*Pinus sylvestris* L.) and deciduous

maple tree leaves (*Acer campestre*) which involved size-exclusion chromatography (SEC) or gel permeation chromatography (GPC) for the plant extract obtained from Soxhlet extraction with n-hexane for 20 h. The advantages of the improvised technique as stated by the authors are distinct and sharp peaks in GC-MS chromatogram, short run time and less consumption of solvent with substantial increase in the percentage of PAHs recoveries from plant leaves when compared with the conventional purification techniques. The good performance characteristics would help to identify the biomonitoring capability of plant leaves and accurately predict the PAHs burden in the atmosphere.

[Kargar et al. \(2017\)](#) assessed ultrasonic extraction of PAHs from pine tree leaves (*Pinus* spp.) using acetone/hexane (1:1) as extraction solvent and quantified the analytes by GC technique and confirmed the potential of pine leaves as candidate biomonitors with PAHs accumulation of 139-854 $\mu\text{g kg}^{-1}$ d.w. Three-ringed PAHs were found to be predominant in plant leaves which proved pyrogenic and petrogenic sources of emission as major contributors. Usefulness of pine needles as ideal air quality biomonitors for identification and evaluation of PAHs pollution was also demonstrated by [Lehndorff and Schwark \(2010\)](#) and [Oishi \(2018\)](#). Morphological and physiological characteristics of plant leaves, seasonal variation of weather, effects of temperature and rainfall also play an important role in the uptake and accumulation of PAHs from the atmosphere as examined by [Zhao et al. \(2018\)](#) and [Tian et al. \(2019\)](#). Leaves of urban greening plant species such as *Sabina chinesis*, *Cedrus deodara*, *Magnolia grandiflora*, *Metasequoia glyptostroboides*, *Ginkgo biloba*, *Cinnamomum camphora*, *Salix babylonica*, *Platanus acerifolia* ([Tian et al., 2019](#)) and *Salix matsudana* ([Zhao et al., 2018](#)), which include both evergreen and deciduous trees as well as broadleaf and conifer trees, were studied by the authors to evaluate the concentrations of each individual PAH compound accumulated in them by employing supercritical fluid extraction using CO_2 and hexane and ultrasonication with DCM respectively. [Zhao et al. \(2018\)](#) reported that the distribution and composition profiles of PAHs in *S. matsudana* leaves changed in response to atmospheric conditions and leaf parameters and succeeded in proving their mettle to become effective accumulative phytoindicators. On the other hand, the mean PAHs concentration in other tree species ranged between 300 and 2000 ng g^{-1} with maximum accumulation in coniferous trees (*Sabina chinesis* and *Cedrus deodara*) as compared to that in broadleaf species ([Tian et al., 2019](#)). Therefore, all the findings made by the authors furnish a theoretical framework for the initiation of a plant-based ambient air quality monitoring system depending on the selection of proper plant groups which are highly capable of adsorbing or absorbing airborne pollutants.

Espenshade et al. (2019) evidenced that the leaves of *Platanus x hispanica* trees (hybrid of *Platanus orientalis* and *Platanus occidentalis*) are also competent enough in scavenging the atmospheric POPs. Tree foliage of *Eucalyptus rostrata*, *Pinus radiata*, *Populus hybridus*, *Tillandsia capillaris* and grass cultures of *Lolium multiflorum* for passive accumulation of PAHs are also intensely studied by Rodriguez et al. (2010), Rodriguez et al. (2012) and Wannaz et al. (2013) for their efficacy in biomonitoring. Also, in a study conducted in Brazil, biomonitoring efficiency of *Lolium multiflorum* ‘Lema’ and tropical tree species (*Tibouchina pulchra* and *Psidium guajava* ‘Paluma’) was compared in which *L. multiflorum* exhibited greater potential of accumulating atmospheric PAHs from the polluted region exposed to anthropogenic emissions (Rinaldi et al., 2012). The authors also reported that the grass species *L. multiflorum* showed high affinity for both HMW and LMW PAHs depending on climatic conditions (i.e., summer and monsoon periods for HMW PAHs and winter or colder periods for LMW PAHs). A similar study was carried out in Argentina (Cordoba city) by Rodriguez et al. (2015) with *Lolium multiflorum* species to study their effectiveness as biomonitors and physiological responses against PAHs near pollution emitting sources. The grass cultures were subjected to ultrasonic extraction with n-hexane and acetone mixture (1:1, v/v) followed by HPLC analysis coupled to fluorescence detection. The authors reported that the total PAHs concentration ranged from 348 to 464 ng g⁻¹ dry d.w. in dry season and 362-459 ng g⁻¹ d.w. in wet season. Green leafy vegetables such as spinach, Chinese cabbage, Shanghai green cabbage and romaine and crop plants including maize, soybean and potato leaf surfaces displayed higher PAHs uptake, which proved their ability in accumulating the contaminants in their tissues, thereby reflecting the impact of anthropogenic activities (Sun et al., 2018; Chen et al., 2019; Jia et al., 2019). Schrlau et al. (2011) also focused on passive air sampling and assessed PLE along with GC-MS analysis in order to detect the presence of semi-volatile PAHs in conifer needles including *Tsuga*, *Pseudotsuga*, *Abies*, *Picea* and *Pinus* and demonstrated that the flat and broad needles could accumulate up to 71 times higher PAHs than narrow and round needles. Impact of PAHs, released from traffic exhausts, on the leaves of a medicinal plant, paper mulberry (*Broussonetia papyrifera*), was studied by Xi et al. (2013) in South China, with the help of ASE using DCM and acetone as solvents. The authors reported the mean PAHs concentration as 2.7-800 ng g⁻¹ d.w. in heavy traffic areas and opined that the trees in these areas should remain in place for biomonitoring, not to be consumed for medicinal purposes to avoid human health hazards. PAHs accumulation potential of biomonitor plants like Scots pine (*Pinus sylvestris* L.) needles, wild rosemary (*Rhododendron tomentosum* Harmaja) and birch (*Betula* spp.) leaves was investigated by Metrak et al. (2016) based on solvent extraction

technique using DCM. Wild rosemary leaves were found to be the highest accumulator of both heavier as well as lighter PAHs as compared to Scots pine needles and birch leaves.

Holm oak leaves (*Quercus ilex*), Scots pine (*Pinus sylvestris* L.), mountain pine (*Pinus mugo* Turra), Norway spruce (*Picea abies* (L.) H. Karst), silver fir (*Abies Alba* Mill.), Masson pine trees (*Pinus massoniana* L.) and *Piptadenia gonoacantha* (tropical shrub of legume family) were also utilized for improved biomonitoring of regional airborne PAHs by many scientists based on their specific morphological and ecophysiological characteristics (Migaszewski et al., 2002; De Nicola et al., 2005, 2013; Sun et al., 2010; Papa et al., 2012; Domingos et al., 2015; Kuang et al., 2015; Chropenova et al., 2016; Anna et al., 2018). Tropical plant species such as *Croton floribundus* and *Astronium graveolens* were also examined for indirect assessment of PAHs pollution (passive biomonitoring) in southeastern regions of Brazil by Nakazato et al. (2018). Murakami et al. (2012) studied five tree species namely, *Ginkgo biloba* L., *Zelkova serrata* Makino, *Liriodendron tulipifera* L., *Prunus yedoensis* Matsum and *Magnolia kobus* DC for biomonitoring of PAHs and found that the ginkgo leaves accumulated about 97% of PAHs from the roadside air (about 80% in the wax and 17% in the inner tissues). Ratola et al. (2009) tested the efficiencies of MAE and ultrasonic extraction (USE) for the detection of 16 EPA-PAHs in two pine trees including *Pinus pinaster* Ait. and *Pinus pinea* L. (mainly needles and bark were utilized), collected from Portugal and Spain, and quantified PAHs concentrations using GC-MS technique. The authors reported recoveries of 70-130% for most of the PAHs, except for indeno[1,2,3- cd]pyrene, dibenzo[a,h]anthracene and benzo[ghi]perylene that are heavier PAHs. Predominant PAHs accumulated in pine needles and bark were PHE, FLT, NAP and PYR having concentration ranging between 213 and 1773 ng g⁻¹ d.w. Pine needles were found to be more potent biomonitors of PAHs, entrapping 2-17 times higher pollutants as compared to its bark. Seasonal and yearly variations of PAHs accumulation in pine needles namely, *Pinus pinaster* Ait. and *Pinus pinea* L., ranging from 71 to 1212 ng g⁻¹ d.w., are also influenced by needle age as examined by Ratola et al. (2010). Again, Ratola et al. (2011) investigated the monitoring ability of *Pinus pinaster* Ait. and *Pinus pinea* L. and observed that the *P. pinaster* needles accumulated more than twice the total PAHs as compared to *P. pinea* needles and hence, should be considered for the development of green infrastructures. In another study, Ratola et al. (2012) explored MAE combined with headspace solid-phase microextraction (MAE-HS-SPME) with GC-MS analysis for quantification of PAHs from the same pine trees. PAHs recoveries ranged between 70 and 110% for *P. pinaster* and 75-129% for *P. pinea*. Accumulation of particulate PAHs was more prominent in pine bark, whereas dominance of gaseous PAHs was observed in pine

needles. The method adopted by the authors proved to be more advantageous over current approaches for determination of PAHs from pine needles and bark.

Role of bioaccumulator plant species in monitoring of long-term (chronic) PAHs atmospheric pollution is well documented with the leaves of *Robinia pseudoacacia* and *Melaleuca leucadendra* (evergreen Australian native tree) by [Muller et al. \(2001\)](#) and [Capozzi et al. \(2017\)](#). Three deciduous tree species (oak, ash and hazel), creating canopy and understorey formation in woodland, were examined for PAHs deposition in their leaves by [Howsam et al. \(2000\)](#) and [Howsam et al. \(2001\)](#). Hazel leaves in understorey accumulated higher proportion of 4-, 5- and 6-ring PAHs than oak and ash leaves in the canopy due to the filtering effect through it and air turbulence which helped in the deposition of particulate PAHs. Soxhlet extraction using ether:hexane mixture (1:9) was performed by [Bi et al. \(2018\)](#) with bamboo leaves (*Phyllostachys edulis*) for 16 h in order to test their potential for bioremediation of airborne PAHs in the suburban areas of South China. They reported significant reduction in PAHs content in the atmosphere near the vicinity of bamboo forests which improved the air quality both in hazy and sunny weather. [Chun \(2011\)](#) established a correlation between PAHs concentration levels in air (C_a , ng m^{-3}) and needles of *Pinus koraiensis*, Korean pine species (C_p , ng g^{-1} d.w.) and concluded that the $\log K_{oa}-C_p/C_a$ (K_{oa} : octanol-air partitioning coefficient) model can be utilized for determining the PAHs content in air using accumulated concentrations of PAHs in pine needles (passive air samplers). Soxhlet apparatus was employed for PAHs extraction using DCM for 24 h with subsequent GC-MS analysis. PAHs recovery rate was found to be 42.5-105.1% with coefficient of variation (CV) ranging from 5.3 to 14.8% for the tested samples. A comparative study on PAHs accumulation in oak (*Quercus palustris*) leaves and pine (*Pinus nigra*) needles, executed by [Klingberg et al. \(2022\)](#) in the Swedish city of Gothenburg, revealed better efficiency of conifer needles than that of oak leaves with more accumulation of PAHs (both vapour phase and particle-bound) in three-year-old needles in comparison to one-year-old needles. ASE using DCM combined with semipermeable dialysis membrane process and open adsorption column chromatography (with n-hexane:DCM) was followed for sample extraction and clean-up coupled to GC (high resolution)-MS (low resolution) detection. The authors stated that the leaf-air partitioning of LMW PAHs was found to be governed by the equilibrium processes for both the species and proved a positive correlation between $\log K_{OA}$ and concentration ratio of $\text{PAH}_{\text{plant}}/\text{PAH}_{\text{air}}$. [Luo et al. \(2020\)](#) aimed to compare the variabilities of PAHs accumulation in the needles of three coniferous trees (fir, spruce and pinus) of different ages throughout the time of their life cycle. An ASE method (employing DCM:hexane, 1:1) for PAHs extraction was proposed by the

authors with subsequent silica gel/alumina column chromatography and GC-MS analysis for sample purification and PAHs quantification respectively. The accumulated concentrations (ng g^{-1} d.w.) varied between 34-206, 32-162 and 64-89 for fir, spruce and pinus respectively. Needle age-dependent gradual increase in the concentrations of LMW PAHs (having highest proportion: 61-94% of total PAHs) was observed by the authors, while on the contrary, contents of HMW PAHs remained unaffected. Effect of seasonal changes and distribution profile of PAHs were studied by [Prajapati and Tripathi \(2008c\)](#) in Varanasi, India using *Ficus benghalensis* (Indian Banyan tree) leaves. PAHs concentrations were maximum (two times higher) in winter than summer and monsoon as determined through sonication treatment in DCM-acetone and GC-MS. This proves the efficacy of Indian Banyan tree (abundantly available across India) as biomonitor species of PAHs pollution. Role of celery plant leaves (*Apium graveolens* var. *secalinum* L.) in the uptake of anthracene and benzo[k]fluoranthene is also presented by [Wieczorek et al. \(2015\)](#). Detection of non-polar PAHs extracted from conifer needles (*Pinus nigra* and *Cedrus atlantica*) by GC-MS/MS and liquid chromatography-tandem mass spectrometry (LC-MS/MS) after subjecting the samples to ASE, SPE and solid-phase microextraction was accomplished by [Al-Alam et al. \(2017\)](#). Same order of PAHs accumulation was observed in both the needles (36 ng g^{-1} of total PAHs with 15 ng g^{-1} NAP). It is also reported that the leaves of higher plants like non-woody annual and perennial species (*Newboulda laevis*, *Citrullus colocynthis*, *Nephrolepis bisserata*, *Manihot esculenta*, *Pennisetum purpureum*, *Zea mays*, *Mangifera indica* and *Mimosa pudica*) also act as good phytoremediators of PAHs pollution with accumulated concentration ranging from 365 to $2870 \mu\text{g kg}^{-1}$ ([Sojinu et al., 2010](#)). Bioaccumulation of PAHs in the mature leaves of shrubs like *Photinia*, *Mahonia*, *Loropetalum*, *Hypericum*, *Rhododendron* and *Pinus* was studied by [Li et al. \(2017\)](#) through ultrasonic extraction with n-hexane:acetone mixture (1:1) integrated with HPLC-FLD detection. The measured concentrations of PAHs in plant leaves varied between 0.1 and 1000 ng g^{-1} d.w. The authors demonstrated that the absorption of PAHs by plant leaves has a strong correlation with the morphologies of leaf surfaces (foliage properties) as well as cuticular waxes. Leaves of *Murraya paniculata* (Orange jasmine) as candidate biomonitors of PAHs had been studied by [Karnchanasest and Satayavibul \(2005\)](#) in Bangkok. It was found by the authors that the LMW PAHs in gaseous or vapour phase (correlation coefficient $r^2 > 0.7$) readily diffused through the plant leaves than HMW PAHs owing to their particulate forms with lower correlation coefficient ($r^2 < 0.6$). Determination of PAHs content in the leaves of *Tilia cordata* Mill (small-leaved lime) and *Populus robusta* (hybrid poplar) using HPLC-FLD was performed by [Klamerus-Iwan et al. \(2018\)](#) in the urban areas of Poland (Cracow city).

Acenaphthylene (ACY) and phenanthrene (PHE) were the governing PAHs in both the plant leaves; source of accumulation being the solid fossil fuel as well as biomass burning. Moreover, the authors also observed that the leaf water capacity was directly proportional to PAHs content.

b) Tree bark/stem/ring/trunk

Tree barks can also be relied upon as passive air samplers for biomonitoring of atmospheric PAHs due to their folded and layered structures with large surface area, high partition coefficient values, high sorption capacity, long life span, rough and highly porous surface and abundance nature, that can be utilized for the evaluation of spatio-temporal trends of pollutants with their diverse emission sources, depending on the level of pollution and type of species as well as associated human health risks (Chrabaszcz and Mroz, 2017; Niu et al., 2019_a, 2019_b). Absorption of PAHs by pine bark (*Pinus*) was studied by Orecchio et al. (2008) to investigate the air quality of Palermo (Sicily, Italy) through Soxhlet extraction using DCM with subsequent GC-MS analysis. The results showed a high concentration of PAHs (1015 $\mu\text{g kg}^{-1}$ d.w. of bark) in the area with dense traffic movement. The feasibility of pine barks (Scots pine, *Pinus sylvestris* L.) for monitoring of atmospheric PAHs pollution was also assessed by Schulz et al. (1999) and they suggested that the pine barks can be successfully utilized as biomonitors for determination of airborne organic pollutants. Zhou et al. (2014) briefly discussed the efficiency of ASE with acetone-hexane mixture and GC-MS technique for monitoring of PAHs in the ambient air of Southern Jiangsu, China, by employing the tree barks of *Cinnamomum camphora* for identification of emission sources. Results of statistical modeling revealed that the vehicular exhausts, fossil fuel combustion and industrial activities were responsible for PAHs deposition in tree bark having total concentration of 6-1560 ng g^{-1} d.w. Monitoring of airborne PAHs with corks of bark pocket developed in Longpetiole Beech (*Fagus longipetiolata*) tree trunk was evaluated by Wang et al. (2004) in south-eastern China. The study revealed that the atmosphere in that area of China was highly contaminated with PAHs pollution. Long-term changes in atmospheric PAHs levels in Chengdu plain of southwest China as recorded in the annual rings of *Ginkgo biloba* L. were evaluated through optimized ASE (more efficient than ultrasonic or Soxhlet extraction) followed by GC-MS analysis by Yin et al. (2011). The study revealed that the trunk tissue of ginkgo plant provided maximum information about the regional historical pollution pattern in comparison with leaf, bark and host soil, the main route of uptake being particulate and gaseous PAHs absorption through tree foliage. Tree barks of *Tipuana* (rosewood) and *Sibipiruna* (perennial flowering plant of legume

family) plants are also known to accumulate large quantities of LMW PAHs as well as fluoranthene and coronene, signifying greater impacts of automobile exhausts and industrial emission (Pereira et al., 2019). Bark, stem wood, twigs and leaves of forest trees *Vismia cayennensis* (small flowering tree or shrub) were assessed by Krauss et al. (2005) for source apportionment of airborne PAHs in a tropical rain forest in Brazil (Manaus city). The total concentration of PAHs in plants ranged up to 1000 $\mu\text{g kg}^{-1}$ having naphthalene contribution of more than 90% along with phenanthrene and perylene. Maximum accumulation was observed in leaves followed by bark, twigs and stem wood. The authors suggested that despite deposition of only atmospheric PAHs, plants might have also produced naphthalene, phenanthrene and perylene due to their metabolic reactions. In a study, conducted by Pereira Netto et al. (2007) in Brazil using *Terminalia catappa* L. (Combretaceae) tree bark, samples were subjected to extraction by ultrasonication in DCM and identified by high resolution GC-MS. Total PAHs concentration in tree bark varied between 242 and 1640 ng g^{-1} , 3-4 ring compounds like phenanthrene, fluoranthene and pyrene being the predominant PAHs in the samples. The authors could not find any correlation between total PAHs levels with location and distance of the trees from the emission sources and suggested that these tree barks were not suitable for proper assessment of atmospheric PAHs levels. It has been reported by Birke et al. (2018) that the outer bark layer of oak tree (*Quercus* sp.), sampled from different areas of Germany, assimilated higher concentrations of PAHs, signifying heavy atmospheric pollution load in urban and surrounding areas. Quantification of oxygenated and nitrated PAHs (OPAHs and NPAHs) in the external surface of tree barks (*Tipa* sp.), collected from the province of Buenos Aires, Argentina, using ultra high performance liquid chromatography-atmospheric pressure chemical ionization-tandem mass spectrometry (UHPLC-APCI-MS/MS) after MAE with methanol:toluene mixture was done by Fujiwara et al. (2014). Bark PAHs (OPAHs) concentration as detected by the authors ranged from 0.18 to 0.72 $\mu\text{g g}^{-1}$.

1.5.2. Role of non-vascular plants in PAHs biomonitoring

Non-vascular plants represent a broad spectrum of organisms of ancient origin, namely bryophytes, lichens, terrestrial algae and cyanobacteria with no vascular tissues. Being adaptable with their anatomical structures, metabolic processes and nutrient absorption from the atmosphere, they can respond quickly to the changing environment and climatic conditions and sustain their growth in different habitats (epiphytic or lithic), in arid/tundra regions and also in high altitudes. Moreover, they are known to provide yeoman service in maintaining the functioning of ecosystem so as to aid in the biogeochemical cycles of carbon, nitrogen and

water, regulate soil temperature and albedo, thereby helping in the control of ecological interactions of food webs. Thus, application of lower plants (particularly lichens and mosses) having cosmopolitan distribution as biological monitors of air pollution garnered a lot of attention for determining the levels of contamination in different geographical zones and human impacts on vegetation and landscapes.

a) Lichens as indicators of PAHs pollution

Apart from higher plants, efficacy of epiphytic lichens - symbiotic association between algae (Cyanobacteria or Chlorophyceae) and fungi (Ascomycetes or Phycomycetes or Basidiomycetes) - in biological monitoring of air quality is also well established since 1866 (Nylander, 1866). Lichens that mostly contribute to biomonitoring and remediation are classified as crustose (having firm attachment with the substrates), foliose (having leaf-like structures) and fruticose (having bushy growth structures) (Mohamed et al., 2016). Among the species, fruticose are found to be very sensitive to air pollution, foliose exhibit moderate responses to pollutants and crustose are assumed to have tolerant nature (Fenton, 1964). Foliose lichens are best known for accumulating high amounts of PAHs due to their large surface area-to-volume ratio. Designated as ‘permanent control systems’ by several researchers, lichens often create coloured patches (green, grey, orange and red) on tree surfaces or rocks based on the pigments produced, are highly sensitive to atmospheric pollution level and potent persistent accumulators of airborne pollutants in their tissues having no process of excretion (Conti and Cecchetti, 2001; Blasco et al., 2008). For sustenance and growth of lichens, the symbionts green algae containing chlorophyll are involved in the production of nutrients, assimilating water and minerals from fungi due to mutualistic interaction. Absence of cuticles or stomata makes them highly dependent on the surrounding environment for nutrition, thereby accumulating atmospheric contaminants over their entire surface (surface absorption) for easy penetration into their thalli. Their slow growth is characterized with uniform morphology and no shedding of parts during their entire life span (Conti and Cecchetti, 2001). Lichens are mainly involved in the synthesis and liberation of lipid metabolites onto their cell surfaces which are akin to the plant waxy cuticles behaviourally. The hydrophobic or lipophilic PAHs are attracted towards these lipid metabolites triggering lichens’ assimilation of pollutants into their tissues for further metabolic actions (Oksanen, 2006). Degree of air pollution can be ascertained through the assessment of the physiological damages caused to the lichen species due to alterations in photosynthetic rate, chlorophyll content and hormone production along with reduction in ATP (adenosine triphosphate). Bioindication using lichens involves either

mapping of lichen diversity or lichen flora in an area under study or sampling of individual lichen species for quantitative determination of pollutants in their thalli. They can also be transplanted from less polluted regions to more polluted ones for studying their structural changes which reflect bioconcentration of pollutants leading to pollution load (Gries, 1996). Index of atmospheric purity (IAP) is also a useful quantitative biomonitoring tool for correlating the lichen diversity with the ambient air pollution levels in which factors such as number of lichen species, frequency of their occurrence, area coverage and lichen sensitivity towards pollutants are considered to have an understanding of the air quality (Jayalal et al., 2016). The expression for calculating IAP is as follows (Eq. 4):

$$IAP = \sum_{i=1}^n \frac{Q_i \times f_i}{10} \quad (4)$$

where, n is the number of lichen species recorded in a study area; Q is the ecological index or average number of species which coexist with each species and f is the frequency of each species.

The more the IAP values ($IAP > 50$; Level E), better is the air quality with high richness of lichen species. IAP value zero ($0 \leq IAP \leq 12.5$; Level A) signifies total absence of lichen diversity (a condition called lichen desert), indicating worst air quality. IAP values between 25 and 37.5 indicate moderate air pollution level (Level C) (Yatawara and Dayananda, 2019). PAHs profiles in lichens can be attributed to Toxic Equivalency Factors (TEFs) (product of toxicity and concentration of individual PAHs which is generally compared with Benzo(a)pyrene as a standard carcinogenic PAH) which helps in the assessment of carcinogenicity of individual PAHs (Nisbet and Lagoy, 1992). It also reflects the extent of absorption of heavier and lighter PAHs by lichens directly from the atmosphere based on the fact that increased toxicity corresponds to the presence of large number of fused aromatic rings. Earlier lichens have been mainly exploited for biomonitoring of inorganic pollutants like SO_2 , heavy metals, fluoride and radionuclides, but now focus has also been given on monitoring of organic pollutants, specifically PAHs, to identify the qualitative as well as quantitative status of atmospheric pollution through solvent extraction techniques associated with effective analytical procedures. Holt and Miller (2011) demonstrated through their experiments that severely poor air quality can be ascertained by the abundance of lower plants like lichen *Lecanora conizaeoides* in a particular area, associated with drastic fall in its chlorophyll content. Traditional Soxhlet and ultrasonic extraction techniques using various organic solvents like DCM, ACN, cyclohexane and n-hexane (H) have been in use since long for

extraction of PAHs from lichen biomonitors (Shukla and Upreti, 2009; Augusto et al., 2010; Loppi et al., 2015; Puy-Alquiza et al., 2016; Graney et al., 2017; Studabaker et al., 2017; Zounggran et al., 2018; Landis et al., 2019; Van der Wat and Forbes, 2019; Vitali et al., 2019). Recently, rapid, robust, economic, simple, sensitive, accurate and eco-friendly methods of extraction such as MAE, ASE/PLE, DSASE and QuEChERS extraction have been developed and introduced with ease for better extraction efficiency (Domeno et al., 2006; Blasco et al., 2011; Schrlau et al., 2011; Kodnik et al., 2015; Cecconi et al., 2019; Ji et al., 2019; Van der Wat and Forbes, 2019). Soxtec or automated Soxhlet extraction was employed by Migaszewski et al. (2002) and Nascimbene et al. (2014) for PAHs extractions from lichen thalli using DCM and hexane:acetone mixture (H:A) respectively. Though performance of this method was satisfactory, the same was not used subsequently by any researcher till date because of shifting of attention towards green methods which are faster, energy-efficient and consume less volume of solvents. Application of PLE/ASE followed by proper clean-up steps for extract concentration using lichens was also investigated by Schrlau et al. (2011), Kodnik et al. (2015) and Ji et al. (2019) for accurate detection of PAHs. Domeno et al. (2006) employed DSASE, static ultrasonic extraction and Soxhlet extraction techniques for determination of 16 EPA-PAHs in lichen biomonitors (*Xanthoria parietina*) with suitable clean-up steps (applying column chromatography with adsorbent alumina and anhydrous sodium sulphate) to evaluate the efficiency of DSASE method. The study reported that the DSASE method (with PAHs recovery: 69-97%) is the best suited as compared to other classical techniques (static extraction: 69-92% recovery and Soxhlet extraction: 65-89% recovery), as it requires less extraction time and less solvent volume, thereby providing better extraction yield. Moreover, sample handling is also easy with minimum losses due to single step extraction process at reduced costs. In this context, Van der Wat and Forbes (2019) utilized four different sample extraction techniques, namely ultrasound assisted solvent extraction (UASE), Soxhlet extraction, MAE and QuEChERS extraction using lichen species *Parmotrema austrosinense* (Zahlbr.) Hale to study relative concentrations of PAHs and identify the appropriate method of extraction. SPE cartridges were used by the authors for extract purification. The authors reported that the QuEChERS technique and MAE produced encouraging results of PAHs extraction quantitatively in comparison to the other two methods. The lichen species used for the investigation proved very much effective in absorbing both LMW and HMW PAHs from the atmosphere. The authors also recommended that a single step purification process may not be effective due to chlorophyll interferences in the extract for which further studies are necessary to be undertaken. Loppi et al. (2015) compared PAHs accumulation in transplanted lichens

with the results obtained from passive gas-phase samplers (PUFs). It was concluded by the authors that the accumulation of particulate PAHs was more prominent in lichen transplants than PUFs. Quantitative assessment of atmospheric pollution levels can also be obtained directly through biomonitoring with lichen species. [Blasco et al. \(2006\)](#) proved that the PAHs generating from high temperature combustion of organic fuel are mainly accumulated in lichens due to heavy vehicular emissions as prime contributor. Diverse corticolous lichen species of genera *Arthonia*, *Chrysothrix*, *Cryptothecia*, *Dirinaria*, *Myriotrema*, *Pertusaria*, *Pyrenula*, *Pyxine*, *Sarcographa*, *Graphis*, *Megalospora*, *Parmotrema*, *Porina*, *Leptogium*, *Physcia*, *Platythecium*, *Cresponia*, *Heterodermia*, *Pyrenocarp*, *Chapsa*, *Dictyonema*, *Lecanora*, *Ocellularia*, *Collema* and *Leptotrema*, found in both rural and semi-urban/urban localities of tropical countries, can be considered to be potential pollution indicators for air quality monitoring ([Yatawara and Dayananda, 2019](#)). Hence, feasibility of different extraction techniques to concentrate PAHs from sample matrix was examined by several researchers based on selective and specific lichen species which are capable of absorbing pollutants from the atmosphere. The results of reported PAHs studies using lichen biomonitors in different countries are summarized in [Table 4](#) and [Table 5](#).

Table 4

Lichen species used for biomonitoring of PAHs: Sampling sites, extraction methods and solvents for extraction.

Lichen species	Sampling area/country	Extraction methodology adopted for PAHs	Solvents used for extraction of PAHs	References
<i>Parmotrema austrosinense</i> (Zahlbr.)Hale	Pretoria, South Africa	Soxhlet extraction for 6 h USAE for 15 min MAE QuEChERS extraction for 30 min	DCM, ACN DCM, H:A (1:1, v/v) DCM, H:A (1:1, v/v) DCM, H:A (1:1, v/v), H:DCM (1:1, v/v)	Van der Wat and Forbes, 2019
<i>Xanthoria parietina</i>	Zaragoza city, Spain	DSASE for 10 min Static ultrasonic extraction for 1h Soxhlet extraction for 6 h	H, cyclohexane, DCM, MeOH, toluene DCM DCM	Domeno et al., 2006 Domeno et al., 2006 Domeno et al., 2006
	Latium region, Central Italy Sines region, SW Coastal Portugal	Ultrasonication for 30 min Soxhlet extraction for 24 h	Cyclohexane ACN	Vitali et al., 2019 Augusto et al., 2010
<i>Evernia prunastri</i> L. (Ach.)	Molise region, Southern Italy	Soxhlet extraction for 24 h	n-Hexane	Loppi et al., 2015
<i>Hypogymnia physodes</i> (foliose)	Athabasca Oil Sands Region, Alberta, Canada	Ultrasonication for 30 min	Cyclohexane	Studabaker et al., 2017 ; Landis et al., 2019 ; Graney et al., 2017
	Holy Cross Mountains, South-Central Poland	Liquid–solid extraction using Soxtec apparatus	DCM	Migaszewski et al., 2002
<i>Parmotrema dilatatum</i>	Abidjan City, Ivory Cost	Soxhlet extraction for 12 h	DCM	Zoungranan et al., 2018
Fruticose (<i>Bryoria furcellata</i> ,	Athabasca Oil Sands	Ultrasonication for 30 min	Cyclohexane	Graney et al., 2017

<i>Cladina mitis</i> , <i>Evernia mesomorpha</i>) and foliose <i>Tuckermannopsis americana</i>	Region, Alberta, Canada			
<i>Cetrariella deliseia</i>	Yamal-Nenets autonomous region, Russian Arctic	Accelerated solvent extraction for 45 min	Acetone:DCM (1:4, v/v)	Ji et al., 2019
<i>Pseudevernia furfuracea</i> (L.) Zopf	Dolomites, NE Italy	Automated Soxhlet extraction for 60 min	Acetone:Hexane (1:1, v/v)	Nascimbene et al., 2014
	Carnic pre-Alps, NE Italy	Accelerated solvent extraction for 30 min	DCM:Acetone (1:1, v/v)	Kodnik et al., 2015
<i>Pseudevernia furfuracea</i> var. <i>furfuracea</i> (L.) Zopf.	Carnic Alps, Lateis, NE Italy	Microwave extraction	Hexane:DCM (1:1)	Cecconi et al., 2019
<i>Parmotrema hypoleucinum</i> (Steiner) Hale	Sines region, SW Coastal Portugal	Soxhlet extraction for 24 h	ACN	Augusto et al., 2010
<i>Platismatia glauca</i> , <i>Bryoria</i> sp., <i>Xanthoparmelia</i> (rock lichen), <i>Masonhalea richardsonii</i> (tundra lichen), <i>Hypogymnia</i> sp., <i>Letharia</i> sp., <i>Alectoria</i> sp., <i>Flavocetraria</i> sp.	Alpine and arctic sites, Western U.S. national parks	Pressurized liquid extraction (PLE)	DCM	Schrlau et al., 2011
<i>Xanthoparmelia mexicana</i> (Gyeln.) Hale	Guanajuato city, Mexico	Ultrasonic extraction for 2 h	ACN	Puy-Alquiza et al., 2016
<i>Phaeophyscia hispidula</i>	DehraDun City,	Soxhlet extraction for 16 h	DCM	Shukla and Upreti, 2009

Garhwal Himalayas, India				
<i>Parmelia sulcata</i> Tayl., <i>Evernia prunastri</i> (L.) Ach., <i>Ramalina farinacea</i> , <i>Pseudevernia furfuracea</i> (L.) Zopf., <i>Usnea</i> sp. and <i>Lobaria pulmonaria</i> (Schreb.) Hoffm.	Aspe and Aragon valleys, Central Pyrenees	DSASE	Hexane	Blasco et al., 2011

Note: To be read in conjunction with [Table 5](#).

Table 5

Lichen species used for biomonitoring of PAHs: Method of analysis and concentration of PAHs.

Lichen species	Method of analysis of extracted PAHs	Concentration of PAHs (dry weight basis)	References
<i>Parmotrema austrosinense</i> (Zahlbr.)Hale	GC-MSD	633 ng/g	Van der Wat and Forbes, 2019
<i>Xanthoria parietina</i>	GC-MS	340 ng/g	Domeno et al., 2006
	GC-MS HPLC-FLD, HPLC-DAD/V–UV	113x10 ³ -183x10 ³ ng/kg 167.3-256.3 ng/g	Vitali et al., 2019 Augusto et al., 2010
<i>Evernia prunastri</i> L. (Ach.) (fruticose)	GC-MS	19-683 ng/g	Loppi et al., 2015
<i>Hypogymnia physodes</i> (foliose)	GC-SIM-MS GC-TOF-MS GC-MS GC-MSD	12-482 ng/g <20 - >400 ng/g 2-30 ng/g 1184–2253 ppb	Studabaker et al., 2017 Landis et al., 2019 Graney et al., 2017 Migaszewski et al., 2002
<i>Parmotrema dilatatum</i>	HPLC	1-62 ng/g	Zounggran et al., 2018

Fruticose (<i>Bryoria furcellata</i> , <i>Cladina mitis</i> , <i>Evernia mesomorpha</i>) and foliose <i>Tuckermannopsis americana</i>	GC-MS	2-30 ng/g	Graney et al., 2017
<i>Cetrariella deliseia</i>	GC-QqQ-MSD	147.3-194.4 ng/g	Ji et al., 2019
<i>Pseudevernia furfuracea</i> (L.) Zopf	GC-MS	186-2129.5 ng/g	Nascimbene et al., 2014
	GC-MS	48.22-272.73 ng/g (Summer), 289.73-1575.85 ng/g (Winter)	Kodnik et al., 2015
<i>Pseudevernia furfuracea</i> var. <i>furfuracea</i> (L.) Zopf.	GC-MS triple quadrupole	185.4 ± 23.7-4023.2 ± 1164.4 ng/g	Cecconi et al., 2019
<i>Parmotrema hypoleucinum</i> (Steiner) Hale	HPLC-DAD/V-UV HPLC-FLD	95.5-873.8 ng/g, 442.6-562.0 ng/g	Augusto et al., 2010
<i>Platismatia glauca</i> , <i>Bryoria</i> sp., <i>Xanthoparmelia</i> (rock lichen), <i>Masonhalea richardsonii</i> (tundra lichen), <i>Hypogymnia</i> sp., <i>Letharia</i> sp., <i>Alectoria</i> sp., <i>Flavocetraria</i> sp.	GC-MS	22.3-91800 ng/g lipid	Schrlau et al., 2011
<i>Xanthoparmelia mexicana</i> (Gyeln.) Hale	GC-TQ MS	522-3571 ng/g	Puy-Alquiza et al., 2016

<i>Phaeophyscia hispidula</i>	HPLC-UVD	3.38-25.01 µg/g	Shukla and Upreti, 2009
<i>Parmelia sulcata</i> Tayl., <i>Evernia prunastri</i> (L.) Ach., <i>Ramalina farinacea</i> , <i>Pseudevernia furfuracea</i> (L.) Zopf., <i>Usnea</i> sp. and <i>Lobaria pulmonaria</i> (Schreb.) Hoffm.	GC-MS	238 ± 10-6240 ± 356 ng/g	Blasco et al., 2011

Note: To be read in conjunction with [Table 4](#).

b) Use of mosses for PAHs monitoring in ambient air

Another group of lower plants, bryophytes - mainly mosses - are also considered as indispensable tools for monitoring of ambient air quality owing to their potential for surface accumulation of toxic xenobiotic compounds like PAHs along with uptake of water and nutrients directly from the atmosphere (dry and bulk atmospheric deposition) based on their constitutional structures which are devoid of any roots or wax-like cuticles (having ectohydric nature) (Foan and Simon, 2012). In comparison with higher terrestrial (vascular) plants, mosses exhibit more spontaneous and sensitive responses with respect to environmental stress due to PAHs burden, having direct influence on their mode of reproduction, diversity, habitat and sustenance for growth (Krommer et al., 2007). They have strong affinity for cationic exchanges and allow huge deposition of atmospheric pollutants (far exceeding their physiological requirement) on their surface due to high surface-to-volume ratios (Domeno et al., 2012). Broadly two types of mosses are generally encountered, namely pleurocarpous and acrocarpous, for biomonitoring studies. Pleurocarpous mosses (*Pleurozium schreberi*, *Hylocomium splendens*, *Hypnum cupressiforme*, *Pseudoscleropodium purum*, *Eurynchium* sp., etc.) are characterized with heavily branched stems, resembling densely matted structures, whereas acrocarpous mosses (*Ceratodon purpureus*, *Polytrichum* sp., *Funaria hygrometrica*, etc.) are rarely branched and erect having a central stem and can thrive in dry environment as compared to pleurocarpous mosses (Fabure et al., 2010). Pleurocarpous mosses are widely used in most of the studies for analysis of atmospheric PAHs due to their matted structures which segregate them from the soil-sediment layer. However, they are rarely distributed in urban areas owing to their high sensitivity towards polluted environment and dry weather conditions (Harmens et al., 2013). Sensitive mosses have been reported to have slow growth rates with low metabolic activities but resistant species have high growth rates with greater capacity for detoxification of the absorbed pollutants (Gilbert, 1970; Bharali and Bates, 2006).

Researchers had been utilizing moss samples for quantification of PAHs in the ambient air by employing several sample preparation techniques such as extraction and clean-up with appropriate solvents for achieving optimum analytical results. Extraction using classical Soxhlet or Soxtec apparatus is time intensive (16-24 h), requiring large volumes of purified organic solvents (100-200 mL) (Concha-Grana et al., 2015_a). Therefore, modified and improved techniques such as MAE, ASE/PLE, ultrasonication/DSASE, MSPD and SUPRAS-based microextraction have been in great demand as potential alternatives for obtaining maximum PAHs recoveries from sample matrices. These powerful techniques consume less

solvent and offer better analyte recovery within short extraction time by improving the contact between analytes and extractant. Accumulation of both LMW and HMW PAHs was observed in mosses through PLE/ASE in diverse (urban/sub-urban, rural or industrial) areas of Spain, Czech Republic, France, Switzerland and Poland by different groups of researchers in order to evaluate the bioaccumulative potential of different moss species for identifying the emission sources (Galuszka, 2007; Foan and Simon, 2012; Foan et al., 2014, 2015; Sucharova and Hola, 2014). Foan and Simon (2012) compared Soxtec extraction technique with PLE using the species *Isoetecium myosuroides* Brid. and found PAHs concentrations more or less in the same range (220-234 ng g⁻¹) with recoveries ranging between 67 and 77%. However, PLE proved to be a highly selective technique with the reduction of both extraction time and solvent consumption. The authors applied the optimized PLE technique to other two pleurocarpous moss species *Hypnum cupressiforme* Hedw. and *Hylocomium splendens* (Hedw.) Schimp and observed that *H. cupressiforme* Hedw. accumulated lower concentrations of fluorene (FLR), benzo(a)anthracene (B(a)A), benzo(b)fluoranthene (B(b)F), benzo(k)fluoranthene (B(k)F), benzo(a)pyrene (B(a)P), dibenzo[a,h]anthracene (D(ah)A) and benzo [ghi]perylene (B(ghi)P) than the later one except PYR which was higher in *Hypnum*. According to Galuszka (2007) also, *Hylocomium splendens* showed high concentrations of PAHs compared to *Pleurozium schreberi* (Brid.) Mitt. and proved itself to be a better biomonitor. Zechmeister et al. (2006) showed in a road tunnel experiment in Vienna, Austria, that the presence of *Hylocomium splendens* (commonly known as glittering woodmoss), a perennial clonal moss, is indicative of heavy pollution due to automobile emissions. Sucharova and Hola (2014) tested air-dried and freeze-dried samples and demonstrated that the 3-ring PAHs (ACE, ACY, FLR, PHE, and ANT) were predominant in moss samples due to heavy traffic exhausts near highways in air-dried samples. Seasonal variations and environmental parameters like rainfall, elevation and wind turbulence also do have influences on PAHs accumulation in mosses (Foan et al., 2014, 2015). A novel extraction technique MSPD using devitalized moss clone samples and mossphere of *Sphagnum palustre* L. clones followed by PTV-GC-MS/MS analysis was employed by Concha-Grana et al. (2015b) and Aboal et al. (2020) to investigate the usefulness of moss clones or mossphere technique for monitoring PAHs levels as well as to validate the suitability of the extraction procedure. Homogeneous moss clones were preferred due to their lower variabilities in genetic, structural and biochemical compositions over time. Concha-Grana et al. (2015b) reported good PAHs recoveries in the range of 77-116% for *Sphagnum palustre* L. clones and 73-102% for natural moss species *Sphagnum* sp. and *Hypnum cupressiforme*. The authors also suggested the applicability of this innovative extraction

technique for quantitative determination of PAHs in different moss and lichen species. On the other hand, [Aboal et al. \(2020\)](#) concluded that the mossphere device is suitable for monitoring of 4-, 5- and 6- ring PAHs that are mainly related to wet or dry deposition, rendering it to be an effective phytosampling tool. The percentage recovery for PAHs with more than 4 rings using Soxhlet extraction ranges between 84 and 100% and increases with the increase in molecular weight ([Smith et al., 2006](#)). The results obtained from Soxhlet technique are quite comparable to those produced by other modified methods with small variations having low standard deviations ([Flotron et al., 2003](#)). For these reasons researchers from different countries still use this classical technique for qualitative or quantitative assessment of PAHs accumulated in mosses.

Varying degrees of PAHs concentrations have been reported depending on the type of species and sampling locations ([Viskari et al., 1997](#); [Holoubek et al., 2000](#); [Krommer et al., 2007](#); [Migaszewski et al., 2009](#); [Skert et al., 2010](#); [Dolegowska and Migaszewski, 2011](#); [Colabuono et al., 2015](#); [Oishi, 2018](#)). In order to avoid matrix interferences from pigments and organic matter, [Blasco et al. \(2011\)](#) devised a new modified technique DSASE for determination of PAHs in lichens, which was further extended to moss samples also by [Domeno et al. \(2012\)](#) for the analysis of nitrated derivatives of PAHs (NPAHs) due to their high toxicity leading to carcinogenic impacts. The authors observed very low concentrations of NPAHs (41-315 ng g⁻¹) as compared to parent compounds (188-1733 ng g⁻¹) with 75-98% recovery. [Vukovic et al. \(2015\)](#) for the first time applied the moss bag technology in Belgrade, Serbia, using *Sphagnum girgensohnii* Russow and *Hypnum cupressiforme* Hedw. for studying the spatio-temporal trend of PAHs distribution in urban air through sonication extraction. The most common PAHs found in moss samples include NAP, PHE, FLA, PYR, CHR, B(b)F, B(k)F, B(a)P and I(cd)P, confirming that the moss bags can be used as a potential tool for mitigating air pollution. [Capozzi et al. \(2017\)](#) also proved that moss bags could reveal information about the short-term deposition of PAHs from pyrogenic sources. A study conducted by [Otvos et al. \(2004\)](#) in Hungary revealed that 99% of PAHs accumulated in mosses was LMW PAHs generated from heavy vehicular emissions, having no significant relation with population distribution. Presence of 16 EPA-PAHs was assessed in epiphytic moss *Leptodon smithii* Hedw. by [De Nicola et al. \(2013\)](#) by employing ultrasonication with GC-MSD analysis. The authors found low levels of PAHs in mosses as compared to plant leaves due to their different bioaccumulative capabilities which are regulated by their morphological and physiological properties. [Caballero-Casero et al. \(2015\)](#) focused on supramolecular solvents other than organic solvents for simultaneous extraction of PAHs from

mosses (as indicated in [Table 6](#) and [Table 7](#)) and elimination of matrix interferences. The authors synthesized the supramolecular solvents by mixing decanoic acid, tetrahydrofuran (THF) and water in adequate proportions, thereby producing colloidal aggregates through self-assembly and coacervation. This caused a phase separation due to lesser density of SUPRAS which favoured their isolation from the equilibrium solution. SUPRAS-based microextraction process does not require any sophisticated laboratory instruments, only simple equipment would serve the purpose of sample treatment. This method yielded better recoveries ranging between 89 and 108% within 5 min using only 800 mL of SUPRAS. The results prove it to be an efficient technique but the use of SUPRAS for extraction needs further investigation with other complex matrices. Herbarium mosses, preserved during three periods 1879-1881, 1973-1975 and 2006-2007, were also explored by [Foan et al. \(2010\)](#) to examine the long-term or chronic PAHs inputs with the help of Soxtec extraction technique in the northern areas of Spain. The specimens were sampled from the Natural Park of Bertiz, Navarra, Spain, and preserved in the Herbarium PAMP of the University of Navarra. The authors' intention was to study the evolution of the anthropogenic emissions spanning over the centuries and observed that mainly charcoal production for old foundries and biomass burning for domestic purposes were responsible for LMW PAHs deposition during 19th century. The scenario started changing in the 20th century due to the advent of industrial revolution, building of power stations using fossil fuels, tremendous increase in population, development of other infrastructures and invention of cars, steam engines for railways, etc. which contributed to overall ambient pollution levels to a global extent. PAHs determinations in mosses by Soxtec technique were also carried out by [Migaszewski et al. \(2002\)](#) in the mountainous regions of Southern Poland and they noticed no appreciable change in the air quality of south-central Poland since 1998 till the date of experiment. Active moss biomonitoring studies with the application of MAE were undertaken by [Ares et al. \(2009\)](#) and [Ares et al. \(2011\)](#) in different areas of Spain using pleurocarpous moss *Pseudoscleropodium purum* (Hedw.) M. Fleisch. Their findings indicated that the bioconcentration of PAHs in mosses decreased exponentially with the distance from the source of emission, deposition being encouraging up to 1 Km from the source. [Concha-Grana et al. \(2015a\)](#) also studied MAE with *Pseudoscleropodium purum* (Hedw.) M. Fleisch., *Sphagnum* sp. and *Hypnum cupressiforme* and obtained desirably accurate recoveries between 83 and 108%, uncertainty being less than 20%. Use of PTV detector along with tandem mass spectrometry enhanced the sensitivity and selectivity of the process. PAHs content along with other details as obtained from different moss species by many researchers worldwide have all been referenced in [Table 6](#) and [Table 7](#). Therefore, it can

be concluded that the terrestrial mosses as passive samplers of atmospheric PAHs pollution have got global recognition from the research communities for biomonitoring surveys and environmental remediation.

Table 6

Biomonitoring of airborne PAHs using moss species with sampling sites, extraction methods and solvents used for extraction.

Moss species	Sampling area/country	Extraction methodology adopted for PAHs	Solvents used for extraction of PAHs	References
<i>Isoetecium myosuroides</i> Brid., <i>Hypnum cupressiforme</i> Hedw., <i>Hylocomium splendens</i> (Hedw.) Schimp	Navarra, Spain	Pressurized liquid extraction for 10 min, Soxtec extraction for 3h	n-Hexane n-Hexane	Foan and Simon, 2012
<i>Pleurozium schreberi</i> (Brid.) Mitt.	Czech Republic	Accelerated solvent extraction	n-Hexane	Sucharova and Hola, 2014
<i>Pseudoscleropodium purum</i> (Hedw.) M. Fleisch., <i>Sphagnum</i> sp., <i>Hypnum cupressiforme</i>	Galicia, NW Spain	Microwave extraction for 16 min	Hexane:Acetone (90:10)	Concha-Grana et al., 2015a
<i>Sphagnum palustre</i> L. moss clones, Natural moss of same genus <i>Sphagnum</i> sp., Natural species of <i>Hypnum cupressiforme</i>	Five different locations, Spain	Matrix solid-phase dispersion extraction for 3 min	DCM:Hexane (20:80)	Concha-Grana et al., 2015b
<i>Fissidens crassipes</i> Wilson ex Brunch & Schimp., <i>Plagiomnium undulatum</i> (Hedw.) T. J. Kop., <i>Leucodon sciuroides</i> (Hedw.) Schwagr., <i>Distichium capillaceum</i> (Hedw.) Brunch & Schimp., <i>Pleurochaete squarrosa</i> (Brid.) Lindb.	Cordoba and Jaen provinces, Spain	SUPRAS-based microextraction for 5 min	Decanoic acid/THF/Water	Caballero-Casero et al., 2015
<i>Sanionia uncinata</i> , <i>Warnstorfia sarmentosa</i> , <i>Brachitecyum</i> sp., <i>Syntrichia princeps</i>	Adjacent to Brazilian Antarctic Station, Admiralty Bay, King George Island	Soxhlet extraction for 8h	n-Hexane:Methylene chloride (1:1, v/v)	Colabuono et al., 2015

<i>Hypnum cupressiforme</i>	Navarra, Spain	DSASE	Pure hexane	Domeno et al., 2012
<i>Scleropodium purum</i> , <i>Hypnum cupressiforme</i> , <i>Abietinella abietina</i>	Man and Biosphere Reserve Wienerwald, Austria	Soxhlet extraction	n-Hexane	Krommer et al., 2007
<i>Hylocomium splendens</i> (Hedw.) Schimp.	Bertiz Nature Reserve, NW Navarra, Spain	Pressurized liquid extraction	n-Hexane	Foan et al., 2015
<i>Hypnum cupressiforme</i>	Hungary	Ultrasonic extraction	n-Hexane:Acetone (1:1, v/v)	Otvos et al., 2004
Moss bags of <i>Sphagnum girgensohnii</i> Russow and <i>Hypnum cupressiforme</i> Hedw.	Belgrade urban area, Serbia	Ultrasonication for 5 min	DCM	Vukovic et al., 2015
<i>Hypnum cupressiforme</i> Hedw.	European countries including France, Spain, Switzerland	Pressurized liquid extraction	n-Hexane	Foan et al., 2014
Red-stemmed feather moss <i>Pleurozium</i> <i>schreberi</i>	Central Finland	Soxhlet extraction for 16h	DCM	Viskari et al., 1997
<i>Hypnum cupressiforme</i> L. ex Hedw.	Kosetice observatory of Czech Hydrometeorological Institute, Valasske Mezirici, Vresova, Czech Republic	Soxhlet extraction for 8h	DCM	Holoubek et al., 2000
<i>Hylocomium splendens</i> (Hedw.) B.S.G., <i>Pleurozium</i> <i>schreberi</i> (Brid.) Mitt.	Holy Cross Mountains (Poland), Wrangell–Saint Elias National Park and Preserve (Alaska),	Soxhlet extraction	DCM	Migaszewski et al., 2009

	Denali National Park and Preserve (Alaska)			
<i>Pseudoscleropodium purum</i> (Hedw.) M. Fleisch.	Galicia, NW Spain	Microwave extraction for 30 min	Hexane:Acetone (1:1)	Ares et al., 2009
Herbarium mosses including <i>Dicranum scoparium</i> Hedw., <i>Hypnum cupressiforme</i> Hedw., <i>Thamnobryum alopecurum</i> Hedw. Gangulee, <i>Thuidium tamariscinum</i> Hedw. Schimp.	Navarra, Northern Spain	Soxtec extraction	n-Hexane, cyclohexane, DCM	Foan et al., 2010
<i>Leptodon smithii</i> Hedw.	Italian regions Campania and Tuscany	Sonication	DCM:Acetone (1:1; v/v)	De Nicola et al., 2013
<i>Hylocomium splendens</i>	Holy Cross Mountains, South-Central Poland	Soxtec extraction	DCM	Migaszewski et al., 2002
<i>Racomitrium lanuginosum</i> (Hedw.) Brid.	Central Japan	Soxhlet extraction	Acetone (for >2h) Toluene (for 16h)	Oishi, 2018
<i>Hylocomium splendens</i> (Hedw.) B.S.G., <i>Pleurozium schreberi</i> (Brid.) Mitt.	Holy Cross Mountains, South-Central Poland	Accelerated solvent extraction	DCM	Galuszka, 2007
<i>Hylocomium splendens</i> (Hedw.) B.S.G., <i>Pleurozium schreberi</i> (Brid.) Mitt.	Kielce Area, South-Central Poland	Soxhlet extraction	DCM	Dolegowska and Migaszewski, 2011
<i>Hypnum cupressiforme</i> moss bags	Naples, Italy	Sonication for 20 min	DCM	Capozzi et al., 2017

<i>Pseudoscleropodium purum</i> (Hedw.) M. Fleisch. Moss bags	Canary Island, Spain	Microwave extraction	Hexane:Acetone	Ares et al., 2011
<i>Hypnum cupressiforme</i> moss bags	Basovizza, Trieste, North eastern Italy	Extraction with microsoxhlet system	Cyclohexane	Skert et al., 2010
Mossphere filled with <i>Sphagnum palustre</i> clone	Southern Italy, North-West Spain	Matrix solid-phase dispersion extraction	DCM:Hexane (20:80)	Aboal et al., 2020

Note: To be read in conjunction with [Table 7](#).

Table 7

Biomonitoring of airborne PAHs using moss species: Method of analysis and concentration of PAHs.

Moss species	Method of analysis of extracted PAHs	Concentration of PAHs (dry weight basis)	References
<i>Isoetecium myosuroides</i> Brid., <i>Hypnum cupressiforme</i> Hedw., <i>Hylocomium splendens</i> (Hedw.) Schimp	HPLC-FLD	233.5 ng/g; 220.3 ng/g 130 ng/g 133.3 ng/g	Foan and Simon, 2012
<i>Pleurozium schreberi</i> (Brid.) Mitt.	GC-IT-MS	4-100 ng/g	Sucharova and Hola, 2014
<i>Pseudoscleropodium purum</i> (Hedw.) M. Fleisch., <i>Sphagnum</i> sp., <i>Hypnum cupressiforme</i>	GC-MS/MS	50.7 ng/g; 93.1 ng/g	Concha-Grana et al., 2015a
<i>Sphagnum palustre</i> L. moss clones, Natural moss of same genus <i>Sphagnum</i> sp., Natural species of <i>Hypnum cupressiforme</i>	PTV-GC-MS/MS	1.105 µg/g 77.35 ng/g 148.4 ng/g	Concha-Grana et al., 2015b
<i>Fissidens crassipes</i> Wilson ex Brunch & Schimp., <i>Plagiomnium undulatum</i> (Hedw.) T. J. Kop., <i>Leucodon sciuroides</i> (Hedw.) Schwagr., <i>Distichium capillaceum</i> (Hedw.) Brunch & Schimp., <i>Pleurochaete squarrosa</i> (Brid.) Lindb.	LC-FLD	17 ± 1 µg/kg; 38.1 ± 0.6 µg/kg 26.1 ± 0.3 µg/kg 22 ± 1 µg/kg 12 ± 1 µg/kg 97 ± 2 µg/kg	Caballero-Casero et al., 2015
<i>Sanionia uncinata</i> , <i>Warnstorfia sarmentosa</i> , <i>Brachitecyum</i> sp., <i>Syntrichia princeps</i>	GC-SIM-MS	544 ± 457 ng/g; 126-254 ng/g; 955 ng/g Not detected	Colabuono et al., 2015

<i>Hypnum cupressiforme</i>	APGC-Q-TOF-MS	188-1733 ng/g; 41-315 ng/g (NPAHs)	Domeno et al., 2012
<i>Scleropodium purum</i> , <i>Hypnum cupressiforme</i> , <i>Abietinella abietina</i>	GC-MSD (SIM mode)	120-730 ng/g	Krommer et al., 2007
<i>Hylocomium splendens</i> (Hedw.) Schimp.	HPLC-FLD	133.3 ng/g	Foan et al., 2015
<i>Hypnum cupressiforme</i>	HPLC-UV (LMW PAHs) HPLC-FLD (HMW PAHs)	0.1567-10.45*10 ⁴ mg/kg	Otvos et al., 2004
Moss bags of <i>Sphagnum girgensohnii</i> Russow and <i>Hypnum cupressiforme</i> Hedw.	GC-MSD	42-178 ng/g 80-249 ng/g	Vukovic et al., 2015
<i>Hypnum cupressiforme</i> Hedw.	HPLC-FLD	98.1-697.8 ng/g	Foan et al., 2014
Red-stemmed feather moss <i>Pleurozium</i> <i>schreberi</i>	GC-MSD	139.9-493.9 ng/g FW	Viskari et al., 1997
<i>Hypnum cupressiforme</i> L. ex Hedw.	HRGC-MSD	<0.3 ± 4700 ng/g 229 ± 10,222 ng/g <0.3 ± 16,733 ng/g	Holoubek et al., 2000
<i>Hylocomium splendens</i> (Hedw.) B.S.G., <i>Pleurozium</i> <i>schreberi</i> (Brid.) Mitt.	GC-MSD	523-2970 µg/kg; 473-2610 µg/kg 80-3010 µg/kg; 215-3390 µg/kg 140-1890 µg/kg; 266-1510 µg/kg	Migaszewski et al., 2009
<i>Pseudoscleropodium purum</i> (Hedw.)	GC-MS (MS/MS mode)	265.7321 ng/g (sample storage	Ares et al., 2009

M. Fleisch.		at -30 °C) 359.72 ng/g (sample storage at room temperature)	
Herbarium mosses including <i>Dicranum scoparium</i> Hedw., <i>Hypnum cupressiforme</i> Hedw., <i>Thamnobryum</i> <i>alopecurum</i> Hedw. Gangulee, <i>Thuidium</i> <i>tamariscinum</i> Hedw. Schimp.	HPLC-FLD	782.8-2009.1 ng/g (19th century) 206.1-464.6 ng/g (20th century) 86.0-372.5 ng/g (21st century)	Foan et al., 2010
<i>Leptodon smithii</i> Hedw.	GC-MSD	124.82-380.98 ng/g 72.33-154.18 ng/g	De Nicola et al., 2013
<i>Hylocomium splendens</i>	GC-MSD	587-622 ppb	Migaszewski et al., 2002
<i>Racomitrium lanuginosum</i> (Hedw.) Brid.	GC-HRMS	55.9-272.4 ng/g	Oishi, 2018
<i>Hylocomium splendens</i> (Hedw.) B.S.G., <i>Pleurozium schreberi</i> (Brid.) Mitt.	GC-MSD	238-1629 ng/g 183-822 ng/g	Galuszka, 2007
<i>Hylocomium splendens</i> (Hedw.) B.S.G., <i>Pleurozium schreberi</i> (Brid.) Mitt.	GC-MSD	558-4457 mg/kg 643-3086 µg/kg	Dolegowska and Migaszewski, 2011
<i>Hypnum cupressiforme</i> moss bags	GC-MSD	79.53-294 ng/g	Capozzi et al., 2017
<i>Pseudoscleropodium purum</i> (Hedw.) M. Fleisch. Moss bags	GC-MS (MS/MS mode)	0.310-1954 ng/g	Ares et al., 2011
<i>Hypnum cupressiforme</i> moss bags	HPLC-FLD	164-2871 ng/g	Skert et al., 2010

Mossphere filled with <i>Sphagnum palustre</i> clone	PTV-GC-MS/MS	1.506-46.768 ng/m ³	Aboal et al., 2020
--	--------------	--------------------------------	------------------------------------

Note: To be read in conjunction with [Table 6](#).

1.6. Statement of the problem

Since conventional equipment-based air sampling and air quality analysis are lengthy and uneconomic processes due to installation and maintenance of bulky instruments onsite; monitoring of ambient air quality through plant biomonitors has been in vogue for a long time. Moreover, recently it has gained momentum worldwide due to sudden enormous increase in the levels of atmospheric pollution over the past few years as a consequence of unbounded industrial and human activities. Suitable selection of biomonitor plants is the foremost criteria of biomonitoring protocol which depends on type of pollutants under study, test species, plant characteristics and areas under investigation. These bioaccumulators respond sensitively to contaminants developing damage, symptoms or injuries in their host organs, which provide strong reasons for their use as effective biomonitoring tools for controlling the pollution effects on living biota. Their abundance in nature, affordability, long life span, greater efficacy in monitoring of heavy anthropogenic impacts and eco-friendliness make them the prime choices for their utilization as ecological indicators over conventional measurement techniques. Recently, Real-time Air Quality Index (AQI) of Kolkata is > 150 (as measured by Kolkata-US consulate) which indicates very high pollution load with unhealthy environmental condition. Therefore, measurement of concentration of PAHs in air is of paramount concern in Kolkata to determine air quality. However, less work has been actually reported in recent past on biomonitoring using abundant and indigenous plant species along roadsides of Kolkata to get a detailed idea of ambient PAHs profile as a basis of green belting proposal and efficient protocol of isolation of PAHs from plant matrix. Development of traditional and a process intensified extraction-purification-analysis route for determination of PAHs content in biomonitors, based on economic, efficient, robust and time-effective extraction techniques using suitable solvents are indeed important and preferred as environmentally favourable method. Optimization of the extraction and clean-up techniques using multivariate approaches should be carried out in order to achieve authentic and reproducible results. Validation of the extraction technique is necessary for assessing the extraction regime to ensure better analyte recoveries and stable measurements over time, elevating the levels of sensitivity and specificity of analytical procedures. Another important focus area may be the scrutinizing of different available roadside plants for selection of one or few species that can be considered as green belting members outperforming others among the lot. Furthermore, it is imperative to establish PAHs distribution characteristics in biomonitor tissues and ambient air based on their partitioning behavior to identify the widespread pattern of occurrences of the pollutants in the

area under study. Effect of environmental and meteorological parameters and seasonal flux on uptake efficiency of organic pollutants by bioaccumulators should also be properly studied through actual field works. Thus, accurate identification of air pollution hotspots through bioindication would be a critical step in implementing stringent measures for environmental protection, management and sustainable development.

Conforming to the aforestated issues, selection of plant bioindicators with substantial biomonitoring potencies was accomplished for South Kolkata pollution hotspots based on complete characterization (physical, biochemical, physiological and morphological) results obtained for those plant leaves. Comprehensive studies on performance evaluation of conventional (Soxhlet) and process intensified extraction (microwave-assisted Soxhlet extraction (MAE)) techniques followed by high-end instrumental analysis were further undertaken for supporting the objective of establishing appropriate isolation protocols for PAHs from biomonitor plant tissues. Variations in the profiles of ambient PAHs were investigated corresponding to their spatio-temporal distribution behaviour. Moreover, PAHs uptake by plant foliage was modeled with respect to their partitioning behavior between air and plant matrix. Conclusively, in order to devise a green belting proposal, a large number of plant bioindicators was taken under consideration in this study to examine their performances as PAHs biomonitors.

1.6.1. Objectives of the work: Overall and specific

The overall and specific research objectives for achieving the broader outcomes have been stated below.

I. Ecophysiological evaluation for the assessment of biomonitoring potential (i.e., air pollution tolerance) of a terrestrial plant *Murraya paniculata* in traffic congested South Kolkata, India.

- Careful selection of four different study sites in South Kolkata, West Bengal, India, on the basis of pollution load supported by national ambient air quality data of central and state pollution control boards (CPCB and WBPCB). Selection of a control site in a remote area of East Midnapore, West Bengal, India, with minimal pollution load for data comparison.
- Identification of a dominant perennial plant species of shrub variety (*M. paniculata*) along the roadsides of the study areas and collection of plant leaves as sample.
- Pretreatment of plant samples prior to target analysis.

- Characterization study of plant leaves with respect to physical (dust retention capacity), biochemical (chlorophyll, carotenoids, ascorbic acid and lipid), physiological (leaf pH and moisture content) and morphological (leaf surface microstructures) attributes.
- Estimation of air pollution tolerance index (APTI) of *M. paniculata* for better indication of its biomonitoring potential.
- Isolation of PAHs from leaf matrix to detect their presence in plant foliage as a further step towards clear understanding of plant tolerance and bioaccumulative nature.

II. Determination of PAHs in biomonitor tissues by means of solvent extraction and analytical protocols.

- Application of four different solvent extraction methods including mechanical stirring, Soxhlet method, sonication and microwave-assisted Soxhlet extraction (MAE) for evaluation of their efficiencies in acquiring high PAHs yield from *Murraya* leaves after sample processing.
- Selection of suitable solvents with desirable properties and high extraction performance for PAHs recovery.
- Optimization of extraction time to intensify the yield of PAHs from *M. paniculata*.
- Development of a purification procedure of column chromatography using silica gel for sample extracts.
- Qualitative analysis of PAHs using GC-MS based on the characteristic parameters, such as retention time and quantification ions.
- Quantitative analysis of PAHs using HPLC-UV based on the development of a processing method of quantitation for concentration measurement.
- Validation of the analytical method of HPLC in terms of quality checks, recoveries and LOD/LOQ for checking the accuracy and reliability of analysis.

III. Development of microwave-assisted Soxhlet extraction (MAE) technique as a process intensified approach for PAHs isolation from the plant leaves of *M. paniculata* and optimization of extraction methodology.

- Selection of proper solvents for MAE experiments based on the polarity and nature of target PAHs.
- Comprehensive study on determination of individual effects of MAE variables (extraction temperature, extraction time and solvent-to-sample ratio) on PAHs extraction yield.

- Optimization of MAE conditions using response surface methodology (RSM) with Box-Behnken design for evaluating the optimal values of input variables for enhanced yield.
- Estimation of PAHs yield based on the analyzed concentrations of PAHs in HPLC.
- Establishment of MAE as an intensified approach of PAHs extraction over traditional Soxhlet method relating to energy efficiency, economy and yield enhancement (basic aspects of process intensification).

IV. Analysis of spatio-temporal variations of PAHs accumulated in the foliage of *M. paniculata* in South Kolkata, India.

- Determination of spatial distribution of PAHs based on their foliage concentrations at four different pollution hotspots (urban sites) identified in South Kolkata.
- Determination of temporal variations in PAHs concentrations based on seasonal effects, considering the meteorology of premonsoon, postmonsoon and winter.
- Identification of PAHs emission sources in the study areas using diagnostic ratios (DRs).

V. Screening of urban plant bioindicators for their performance in urban greenery planning.

- Investigation of PM capturing efficiencies of eight different urban roadside plant species (*N. oleander*, *T. divaricata*, *C. gigantea*, *B. acuminata*, *P. longifolia*, *A. scholaris*, *N. cadamba* and *P. alba*) of South Kolkata based upon the mass concentrations of leaf surface-bound and wax-embedded PM of large (PM₁₀₋₁₀₀) and coarse (PM_{2.5-10}) fractions.
- Extensive investigation of the synergistic effects of plant surface characteristics (including leaf surface microstructures, leaf waxes and properties of leaf lamina) on PM retention.
- Analysis of the pattern of bioaccumulation of PAHs in all the selected species through the estimation of variabilities in their distribution percentage and ring structures.
- Estimation of specific leaf area (SLA) as an important characteristic parameter of plants affecting PAHs accumulation.
- Evaluation of carcinogenicity and mutagenicity of individual PAHs for risk assessment based on their toxic and mutagenic equivalency factors.
- Analysis of abiotic stress biomarkers of plants to predict their responses towards PM and PAHs pollution and aid in the selection of tolerant species.

- Performance evaluation of the studied plants as green barrier species through APTI and anticipated performance index (API).

VI. Partitioning behavior of PAHs between air and plant matrix and assessment of PAHs uptake by the foliage of a biomonitor plant (*M. paniculata*) using a mechanistic approach-based material balance model.

- Determination of plant-air (K_{PA}) partition coefficients of PAHs for demonstrating PAHs uptake capacity of plants.
- Determination of particle-gas (K_P) partition coefficients of PAHs for indicating their potential of adsorption to foliage-laden particulates.
- Assessment of PAHs bioaccumulation in a biomonitor plant foliage through multiple uptake pathways, highlighting their translocation behaviour in PM-to-leaf and root-to-leaf interfaces.
- Investigation of the main routes of PAHs scavenging by the biomonitor plant species for effective removal of pollutants from the ambient air and determination of calculated uptake rate of PAHs along with theoretical uptake rate by plant biomonitors.
- Comparison of theoretical and calculated uptake rates of PAHs to validate the predictive model.
- Estimation of fugacity capacities to confirm the role of plant leaves in PAHs sorption.

1.6.2. Outline of the thesis

The outline of all the chapters of the PhD thesis has been presented.

Chapter 2 presents the descriptive analysis of functional traits of plant leaves of *M. paniculata*, collected from both urban (South Kolkata, India) and control/reference sites (East Midnapore, India), and assessment of APTI for the selected species to ascertain its tolerance and biomonitoring potential which has been exploited for determination of PAHs distribution in plant tissues for further confirmation.

Chapter 3 highlights the isolation techniques of PAHs from biomonitor (*Murraya* plant) tissues employing solvent extraction methods and chromatographic analysis. Optimization of extraction factors (relating to extraction methods (mechanical stirring, sonication, Soxhlet and MAE), extraction solvent and extraction time for PAHs isolation has been emphasized. Development of silica gel column cleanup as an extract purification step and

procedures of GC-MS and HPLC-UVD for PAHs analysis has also been elaborated. Additionally, HPLC method validation is provided for quality analysis.

Chapter 4 focuses on process intensification on the conventional Soxhlet method aided by MAE with special emphasis on design and optimization of MAE process parameters (extraction temperature, extraction time and solvent-to-sample ratio) using RSM approach for increased PAHs extraction yield from the leaf matrix of *M. paniculata*. From the view point of sustainability, advantages (such as cost, energy and time efficient, green and safer technique with high yield and less requirement of solvent) of MAE as a process intensified route have been established beyond doubt.

Chapter 5 highlights the spatial and temporal distribution trends of foliar PAHs in *M. paniculata* concerning site- and season- specific characteristics. Strong dependence of such variation on emission sources and climatic (premonsoon, postmonsoon and winter) conditions has also been portrayed. Moreover, this chapter provides descriptions on source analysis by DRs based on locational and seasonal variations.

Chapter 6 deals with assessment of the performance of different urban plant bioindicators of diverse nature to act as green belting species for strategic planning of urban greenery. Potential of the investigated plants for foliar accumulation of PM and PAHs has been demonstrated based on the properties of accumulative leaf surfaces, SLA and pollutant nature. Besides, risk factor analysis of PAHs is again provided for expressing their toxicity, carcinogenicity and mutagenicity. Explanation and justification of abiotic stress tolerance or adaptation by plants for their application in urban green belt formation through quantification of the relationships among stress-responsive biomarkers, APTI and API are given in this chapter.

Chapter 7 sheds light on the elucidation of plant-air and particle-gas partitioning behaviour of PAHs for investigating the effects of leaf lipids and organic matter of foliar particulates on PAHs distribution. Different pathways of translocation of PAHs (foliar PM to plant leaves and roots to plant leaves) are further highlighted. This chapter again provides thorough descriptions and interpretations of multiple pathways of PAHs uptake and their extent of contribution to total foliage accumulation based on a material balance model (mechanistic framework). Fugacity approach-based confirmation of plant uptake capacity is also presented.

Chapter 8 highlights the summary of results of the research study, concluding remarks of the entire research work and gives recommendations for some new dimensions in the future work.

An appendix section as **Appendix-I** has been provided at the end of the PhD thesis after ‘References’. This section presents the graphical depiction of variation between rate of change of PAHs concentration in plant leaves (dC_L/dt) and overall foliar PAHs concentration (C_L) for all the 16 EPA-PAHs.

Chapter 2

2. Methodology I

Assessment of biomonitoring potential of Murraya paniculata (L.) Jack (terrestrial plant) along major roads of South Kolkata, India

2.1. Background

Unplanned depletion of agricultural, water and forest lands in and around Kolkata, India, for expansion of city's boundaries to accommodate rapidly growing population including human migration from other places is the primary cause behind the destruction and decay of century-old natural ecosystem. Environmental worsening due to the diversified presence of xenobiotics, gaseous pollutants, heavy metals, persistent organic pollutants (POPs) such as polycyclic aromatic hydrocarbons (PAHs) and dust or particulate matter (PM) imposes toxic air effects on the residents together with native flora and fauna ([Haque and Singh, 2017](#)). The situation is also aggravated owing to relentless activities for the construction of infrastructures and industries, power sectors, high traffic density, growth of slum-like settlements, reducing open spaces and boundless emission (local and transboundary) of air pollutants, increasing their level in the atmosphere manifold ([Haque and Singh, 2017](#)). Air suspended PM and PAHs are among the deadly air pollutants that are genotoxic in nature. PM has been classified as Group I human carcinogen by The International Agency for Research on Cancer ([IARC, 2013](#)). PAHs are a group of hydrophobic organic compounds, ubiquitously present in different environmental compartments and mainly derived from either incomplete combustion of fossil fuels and biomass (anthropogenic inputs) or natural emissions ([Mukhopadhyay et al., 2020](#)). Their recalcitrance and persistence in nature make them highly toxic and carcinogenic for which they

have been prioritized as hazardous pollutants by US Environmental Protection Agency (USEPA) (Guidotti et al., 2003; Ghosal et al., 2016). Gas-particle partitioning of PAHs governs their atmospheric mass distribution (gas-phase PAHs are mostly of low molecular weight (LMW PAHs), while high molecular weight or HMW PAHs are adsorbed on PM). Epidemiological studies revealed that the detrimental effects of these pollutants on human beings are linked to the impairment of human reproductive and excretion systems, acute respiratory infections, cardiovascular diseases and cancerous growth in different organs (like skin, lungs and bladder) (Detmar and Jurisicova, 2010).

In this context, detail and elaborate study of air biomonitoring using passive plant samplers has been the prime concern for recognition and estimation of even small-scale environmental changes in the spatio-temporal trends of the pollutants in air (Garty, 2001). Onsite deployment of direct-reading instruments or air samplers makes the process costly on account of their long operating time and requirement for skilled supervision in monitoring the air supply lines (Blasco et al., 2006). Plants with large leaf surface area act as natural receptors and bioaccumulators of airborne pollutants, initiating adaptive responses which involve modifications in plant biochemistry, physiology and morphology (Rai, 2016). Green belts along the roadways alleviate outdoor air pollution simply through impingement, absorption, accumulation and uptake of contaminants through stomata, improving air quality in high density cities (Prajapati and Tripathi, 2008_a). Indigenous perennial plants for urban landscaping are usually selected based on their availability, adaptability, hassle-free preservation and hardiness (Rai, 2016). Such plants should also not produce and disperse copious amount of pollens provoking allergic reactions in human beings.

Singh et al. (1991) for the first time introduced a factor, namely Air Pollution Tolerance Index (APTI) with respect to plants to investigate their vulnerability towards airborne organic and inorganic pollutants. According to their study, the evaluation of APTI can be related to biochemical and physiological parameters of plants, such as ascorbic acid, chlorophyll content, relative water content and leaf-extract pH, which signifies their tolerance or sensitivity to environmental changes. Based on APTI value, plant groups can be classified as sensitive (APTI<10) intermediate (10<APTI<16) and tolerant (APTI>17) species (Singh and Rao, 1983). Several studies had been conducted by researchers across the globe on APTI of plants, considering tropical dry deciduous forest trees (*Shorea robusta*, *A. auriculiformis*, *Eucalyptus globulus*, *A. indica*), naturally grown tree species (*Psidium guajava*, *Magnifera indica*, *Ficus benghalensis*, *Delonix regia*, etc.), climber plants, trees with broad canopy, flowering plants of Apocynaceae family (*Alstonia scholaris*, *Nerium oleander*, *Tabernaemontana coronaria*,

Thevetia peruviana), herbaceous plants, etc. for urban greenery (Pandey et al., 2016; Kaur and Nagpal, 2017; Nadgorska-Socha et al., 2017; Chaudhary and Rathore, 2018; Karmakar and Padhy, 2019; Mukherjee et al., 2020). Dust capturing capacities of plant leaves are also exploited for trapping particulate pollutants from the atmosphere. Numerous plant species and their parts (leaves, conifer needles, tree barks, trunk and ring) have already been investigated as PAHs biomonitors and scavengers globally (Migaszewski et al., 2002; Sun et al., 2010; Zhao et al., 2018).

Murraya paniculata (L.) Jack or Orange Jasmine (commonly known as ‘Kamini’ in West Bengal, India) has been in use since long for its medicinal values and high percentage of essential oil (91.5%) that possesses antimicrobial and antifungal properties due to the presence of oxygenated sesquiterpenoids (Dosoky et al., 2016; Arya et al., 2017). *Murraya* species is widely used for hedging in India as well as Australia and its neighbouring countries and not known to produce allergens that may harm the surrounding people. Biomonitoring potential of Kamini has not been properly explored to its fullest extent and very few investigations had been carried out over the world for the assessment of pollution effects on the ecosphere using this species. Most of the studies related to air pollution in Kolkata are focused on direct air sampling till date (Ray et al., 2017; Haque and Singh, 2017; Ray et al., 2019) and very scanty details with recent reports are available on PAHs profiles present in the ambient air of the city along with paucity of information related to its source apportionment. There have been meagre attempts in Kolkata so far for air pollution monitoring using plant bioaccumulators or biomonitors (which may be referred to as pollutants’ sink or store house of information related to pollution history) for qualitative and quantitative determination of airborne PAHs.

The present study reports the first effort as field study of South Kolkata, India, to assess the potential of *Murraya paniculata* (L.) Jack to work as an effective biomonitor of air quality affected by PAHs. This may be proved as a sustainable approach over traditional protocol of monitoring and control. This study primarily aimed at determination of APTI for the plant species and effect of plant parameters on APTI to prove its worth in biomonitoring. The species ability to serve as a biomonitor was further judged through the analysis of one of the criteria air pollutants, PAHs, accumulated in plant leaves. Four different urban sampling locations were primarily focused, results of which were then compared to a control or reference site for depicting the variations in plant performance under pollution load. Lipophilic characteristics of PAHs make them suitable to be translocated into lipid-rich tissues of plant leaves, even if they are non-detectable through air sampling due to quick dispersal by wind flow. Probable

sources influencing PAHs accumulation in air were also recognized which would aid in controlling PAHs release at the point of emission.

2.2. Materials and methods

2.2.1. Study area and site selection

The study was carried out in the city of Kolkata (22°34'21.5220"N, 88°21'50.0112"E), West Bengal, India. Sampling campaign was conducted during winter months (December, 2019–January, 2020: peak periods of pollution having high Real-time Air Quality Index (AQI) values of 200–400) under stable weather conditions when thermal inversion, low vertical mixing and wind turbulence and less volatilization or photodegradation were predominant. The study covered four sites within the southern part of the city (South Kolkata) including areas near Jadavpur University, Jadavpur (JDV); on Rash Behari (RB)-Connector near Bakultala Bus Terminus (RBC); at Exide More (EXM) and in Tollygunge (TGN) which are corresponded to the nearby national ambient air quality monitoring (NAAQM) stations run by Central Pollution Control Board (CPCB), India and West Bengal Pollution Control Board (WBPCB), India. Mean NAAQM data (involving four major criteria air pollutants: PM₁₀, PM_{2.5}, NO₂ and SO₂) of the study areas as provided by the CPCB and WBPCB during sampling period have been displayed in [Table 8](#). A location map of the study areas has been shown in [Fig. 6](#). The sampling points are chosen based on the rising level of pollution loads associated with devastating consequences and mainly characterized by heavy traffic density, urban or residential settlements, commercial establishments, shops, restaurants, bakeries, battery production units, etc. Kolkata has been selected as the study area since limited data on biomonitoring of airborne PAHs is available till date. A control area was selected about 90 km away from Kolkata city in Champadali, Panskura (CMD), a remote semi-urban and village area in close proximity to the river Kansabati in East Midnapore, West Bengal, India with very low air pollution levels due to minimum traffic, less industries, scanty crowd and huge open spaces. The control site, CMD is also spotted in [Fig. 6](#).

Table 8

National ambient air quality monitoring (NAAQM) data (average) of the study sites during sampling period (as provided by CPCB and WBPCB) (Ref.: <https://app.cpcbcr.com/ccr/#/caaqm-dashboard-all/caaqm-landing>; <http://emis.wbpcb.gov.in/airquality/citizenreport.do>).

Site	Geographical coordinates	Average NAAQM data					
		PM ₁₀ (µg m ⁻³)	PM _{2.5} (µg m ⁻³)	NO ₂ (µg m ⁻³)	SO ₂ (µg m ⁻³)	Air quality index (with respect to PM _{2.5})	Air quality status
	Permissible limit (24-hourly average)	100	60	80	80		
JDV	22°29'57.5"N; 88°22'18.7"E	251.70	113.19	57.97	9.52	201-300	Poor
RBC	22°31'09.4"N; 88°22'53.0"E	231.44	143.70	44.55	12.32	301-400	Very poor
EXM	22°32'29.3"N; 88°20'38.2"E	271.51	147.20	82.64	12.06	301-400	Very poor
TGN	22°29'33.9"N; 88°20'43.4"E	221.98	111.37	72.28	16.93	201-300	Poor
CMD (control site)	22°23'41.1"N; 87°44'30.8"E	57.32	42.66	32.87	17.86	51-100	Satisfactory

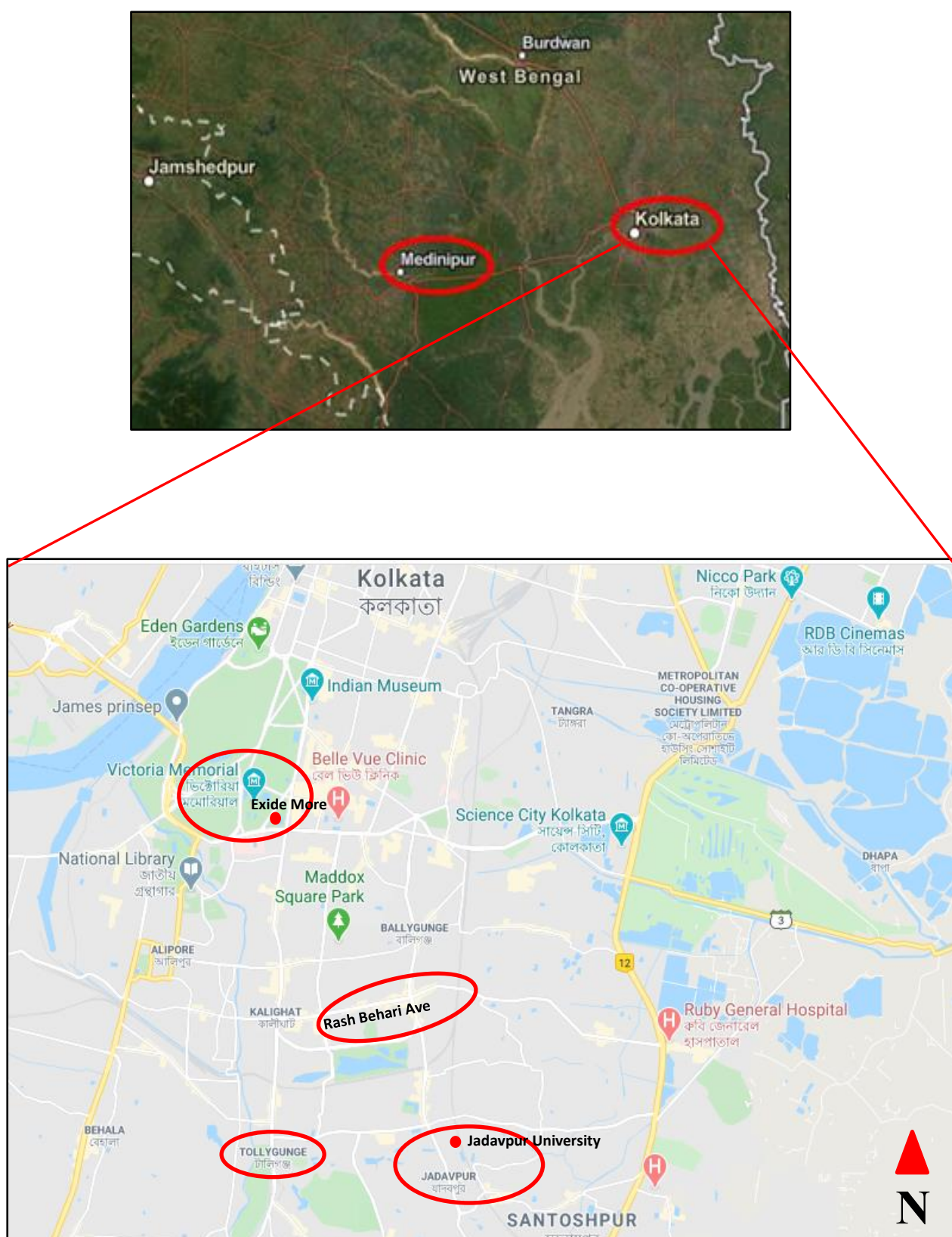


Fig. 6. Location map of the sample sites: Jadavpur (JDV), Rash Behari Connector (RBC), Exide More (EXM) and Tollygunge (TGN) in South Kolkata and control site, Champadali (CMD) in Midnapore, West Bengal, India.

2.2.2. Sampling and processing of plant materials

Small twigs of *Murraya paniculata* (L.) Jack, an ornamental, tropical evergreen flowering tree or shrub (Fig. 7) of family Rutaceae, having waxy leaf surfaces, widely grown as a garden plant, were severed during morning rush hours from the branches of 2–3 individual *Murraya* trees of same species located in each selected zone with pruning shears at a height of 1–3 m from the ground. Six replicates of samples for each location were considered for analysis. The leaves were randomly plucked by hand using sterile gloves to reduce the contact with tree foliages for avoiding exogenous contamination, put in polyethylene bags and immediately transported to the laboratory for storage till further processing and analysis. Leaf samples, after collection, were carefully washed with distilled water three to five times to remove accumulated dust or soil particles from leaf surfaces, spider webs, aphids, insect eggs and other foliage debris and dried using a lyophilizer (Eyela, Singapore; Model: FDU-1100) (freeze-drying) under vacuum for 24 h to avoid degradation of matrix components including pigments, analytes and other volatile organic compounds (de Koning et al., 2009). Dried leaves were then manually crushed with mortar and pestle to obtain powdered homogeneous sample which would enhance the kinetics of analyte extraction by reducing the diffusion pathways and increasing the contact surface area between the sample and solvent (de Koning et al., 2009).



Fig. 7. *Murraya paniculata*.

2.2.3. Chemicals and reagents

A standard mix containing all the 16 EPA-PAHs (acenaphthene, acenaphthylene, anthracene, benzo[a]anthracene, benzo[b]fluoranthene, benzo[k]fluoranthene, benzo[ghi]perylene, benzo[a]pyrene, chrysene, dibenzo[a,h]anthracene, fluoranthene, fluorene, indeno[1,2,3-cd]pyrene, naphthalene, phenanthrene and pyrene; Polynuclear aromatic hydrocarbons 16 solution, analytical standard in acetonitrile; $10\text{ }\mu\text{g mL}^{-1}$) was purchased from Sigma-Aldrich (St. Louis, Missouri, United States) for determination of PAHs in the tested samples. Highly pure HPLC grade ($\geq 99.9\%$ purity) methanol, ethanol, n-hexane, acetone, chloroform and extractant toluene along with LC-MS grade deionized water used were acquired from Merck (Darmstadt, Germany). 2, 6-dichlorophenol indophenol (DCPIP) dye of AR/ACS grade ($\geq 98\%$ by assay), used in titrimetry, was procured from Loba Chemie (India). All the other chemicals, reagents and materials of high purities (namely, oxalic acid, ascorbic acid (both are of ACS reagent grade with assay $\geq 99\%$), glutaraldehyde ($\geq 98\%$ by TLC), sodium phosphate buffer (ACS reagent grade, $\geq 98\%$), silica gel (100–200 mesh, pore size $25\text{ }\text{\AA}$, high purity grade) and Na_2SO_4 (anhydrous for analysis, ACS, $\geq 99\%$)) employed for characteristics analysis and extract clean-up were also supplied from Merck (Darmstadt, Germany).

2.2.4. Physical, biochemical, physiological and morphological characterization of plant leaves

2.2.4.1. Dust retention capacity of plant leaves

Foliar accumulation of dust was evaluated by following a gravimetric method. The fresh leaves were thoroughly washed with distilled water and the washed-out solutions were then filtered through Whatman cellulose filters (Grade 1) which were previously weighed dry to constant weights. Dust laden wet filter papers were again oven-dried and weighed. The difference in weights between the two stages of the filters gave the weight of dust (mg) on the plant leaves. Leaf surface areas (cm^2) were also determined by tracing out the impression of individual leaf on graph paper (Prajapati and Tripathi, 2008_a). Specific leaf area was calculated using the ratio of leaf area to leaf dry mass in $\text{cm}^2\text{ g}^{-1}$. Dust capturing or retention capacity of the plant leaves was estimated afterwards using the ratio of weight of dust to total leaf area (Jiao et al., 2004; Yang et al., 2017). Foliar dust concentration or dust load was finally expressed in terms of mg cm^{-2} .

2.2.4.2. Air pollution tolerance index (APTI)

In the present study, APTI was calculated to investigate the tolerance of *Murraya paniculata* to air pollutants, based on biochemical (ascorbic acid and total chlorophyll contents) and physiological (namely, leaf extract pH and relative water content) factors according to the formula given by [Singh and Rao \(1983\)](#) and [Singh et al. \(1991\)](#) as discussed in Chapter 1 in [Eq. 3](#).

For leaf extract pH, 2 g of powdered leaf sample (in every case) was initially homogenized in 20 mL of deionized water. The homogenate was then centrifuged and pH of the supernatant was measured using a calibrated digital pH meter FP20 (Mettler-Toledo, Schwerzenbach, Switzerland) ([Prasad and Rao, 1982](#)).

The quantitative determination of leaf ascorbic acid contents was performed by a titrimetric method using DCPIP dye solution ([Zubeckis, 1962](#); [Hughes, 1983](#); [CoSeteng et al., 1989](#); [Roy et al., 2020](#)). In brief, 2 g of dried, ground plant leaves (for each sample) were homogenized in 100 mL of 4% oxalic acid extracting solution for continuously 30 min. The samples were then immediately titrated against the titrant dye solution after centrifugation of the homogenates till the endpoint (distinct pink colour) was reached which persisted for about 30 s. Standardization of the dye solution was also done by titrating against a standard ascorbic acid solution of known volume and strength.

Total chlorophyll contents in plant leaves were assayed in accordance with the methods described by [Arnon \(1949\)](#) and [Sudhakar et al. \(2016\)](#). Homogenized samples (~1 g d.w.) were macerated in 20 mL of 80% acetone and sequential chlorophyll extractions were carried out thrice. The absorbances of the supernatants collected after filtration were read at 663, 645 and 470 nm for chlorophyll a and b and carotenoids ([Lichtenthaler and Wellburn, 1983](#); [Lichtenthaler, 1987](#); [Lichtenthaler and Buschmann, 2001](#)) respectively using a UV/Vis spectrophotometer (PerkinElmer, Massachusetts, United States; Model: L365) and coefficients of absorption were used for the measurement of chlorophyll and carotenoids contents.

RWCs of fresh leaves were analyzed as per the protocol developed by [Henson et al. \(1981\)](#) and [Pathak et al. \(2011\)](#). Samples of fresh leaves were washed clean after collection and fresh weights thereof were recorded. They were then submerged in deionized water and kept overnight at room temperature for saturation. The turgid weights of the samples were obtained after blotting the leaves surface dry. Subsequently, the leaf samples were oven-dried at 70 °C to constant dry weights which were also noted for the estimation of RWC.

2.2.4.3. Leaf lipid content

Leaf lipid contents were determined following the method of Bligh and Dyer (Bligh and Dyer, 1959) which is a gravimetric method based on solvent extraction. Prior to lipid extraction, intracellular chlorophyll was removed using ethanol, as otherwise, presence of chlorophyll would erroneously increase the total lipid content in the final extract (intense green in nature) due to its structural similarity with lipids. On the other hand, same solvents (chloroform:methanol mixture) used for lipid extraction would also extract the chlorophyll simultaneously (Lloyd and Tucker, 1988; Archanaa et al., 2012). Hence, powdered leaf samples (1 g each time) were extracted with 20 mL of ethanol 4–5 times with subsequent centrifugation for complete removal of chlorophyll till the supernatant became colourless (Archanaa et al., 2012). The pellets (biomass) were then dried for Bligh and Dyer method of lipid extraction. 30 mL of chloroform:methanol mixture (20:40) was added to the dried biomass followed by the addition of chloroform and water separately. Two layers of organic and aqueous phases were formed where the lipids were extracted in the chloroform or organic layer and the non-lipid parts were solubilized in the methanol-water or aqueous layer (Bligh and Dyer, 1959). An aliquot of chloroform (of known volume) was evaporated to dryness at 50–60 °C and weighed for quantification of lipid contents. All the data were calculated and tabulated as mean \pm standard deviation, mean value being presented based on six replicate values.

2.2.4.4. SEM-EDX analysis

Macromorphology of plant leaves was investigated visually to understand the extent of damage caused by the dust particles. Surface micromorphologies with the deposition of particulates and elemental composition of homogenized plant leaves were examined by scanning electron microscopy (SEM, Hitachi S-3400 N) with energy-dispersive X-ray microanalysis (EDX Micro Analyser, Horiba). A standard procedure for sample preparation was followed which involved chemical fixation of the plant leaves in glutaraldehyde and sodium phosphate buffer, dehydration of specimens in graded series of ethanol with simple air-drying under vacuum in a desiccator and mounting of samples on aluminium stubs coated with gold for visualization under SEM (Pathan et al., 2008; Fellet et al., 2016; Skrynetska et al., 2019). Six replicates of samples collected from different sites were studied for ascertaining the morphologies of leaf surfaces. Electron probe X-ray microanalysis (EDX) was also performed for quantitative analysis of the elements present in the foliage at the microscopic level (Skrynetska et al., 2019). SEM analyses were performed at 500 \times –4000 \times magnification at 15 kV accelerating voltage on selected point locations.

2.2.5. PAHs analysis in plant leaves

Isolation of PAHs from homogenized plant leaves was accomplished by means of solvent extraction method with toluene using Soxhlet apparatus. The extracted solutions were purified using silica gel column chromatography for accurate and reliable analysis and the fractions enriched with PAHs were eluted with n-hexane. The chromatographic fractions were evaporated under vacuum using a Buchi Rotavapor and consequently, the dried residues were dissolved in HPLC grade methanol for analysis by gas chromatography–mass spectrometry in a Thermo Scientific Trace 1300 gas chromatograph (GC) connected with a single quadrupole mass spectrometer (MS) (Thermo Scientific, USA) operated in electron impact ionization mode. The column used was a TG-5MS capillary column having dimensions: 30 m × 0.25 mm × 0.25 μm (Thermo Scientific, USA). Identification of the selected contaminants [qualitative analysis on the basis of retention time (RT, min) and quantification ion (m/z)] was carried through proper standardization of the GC–MS system with a certified reference material (Sigma-Aldrich, USA), ensuring measurement reproducibility (EPA, 1984; Dong et al., 2012).

2.2.6. Statistical and correlation/regression analyses

One-way analysis of variance (ANOVA) was accomplished in MS Excel 2010 by taking into consideration the leaf parameters and APTI of different sites to analyze the statistical significance of the data obtained. A correlation test was executed to quantify the strength of relationship between the foliar dust load and plant biochemical and physiological parameters. Data fitting by linear regression analysis and power law model was performed in order to investigate the impact of leaf pH and ascorbic acid on APTI and variation at different sites. MS Excel 2010 was used for both the cases (Pandey et al., 2015_a, 2016; Achakzai et al., 2017). The whole experiment was repeated three times in order to collect the time dependent data and each run was carried out in triplicate. Goodness of fit was judged by enumerating the Coefficient of Determination (R^2) and Correlation Coefficient (r).

2.3. Results and discussion

2.3.1. Dust retention capacity of *Murraya paniculata* leaves

Dust interception efficiency of plant leaves depends on plant species, leaf surface micromorphology, specific leaf area, leaf orientation and its arrangement on the stem (which is also referred to as phyllotaxy), external features such as presence of hairs or trichomes, cuticles and petioles, pattern of venation, distribution of leaf crowns in the canopy of trees,

stomatal density and epicuticular or cuticular waxes. In addition, meteorological parameters like weather or climatic conditions, wind velocity and direction as well as man-made interferences also influence foliar dust accumulation (Prajapati and Tripathi, 2008_a; Shi et al., 2016). In the present study, amount of dust adsorbed on the leaves of *M. paniculata* ranged from 0.85 ± 0.04 – 2.26 ± 0.02 mg cm⁻² in winter months. Apart from traffic emissions and commercial activities in Kolkata, air quality drop in winter is also prominent due to uncontrolled burning of solid fuels or biomass for heating, dust storms and endless bursting of firecrackers during Diwali festival at the advent of winter season which were responsible for high dust deposit on *Murraya* leaves. Wettability of plant leaves due to fog, dews or precipitation and low air turbulence or atmospheric stability inhibiting pollutant transport in winter can also be singled out as reasons for high dust retention by *Murraya paniculata*. As represented in Table 9, concentration of foliar dust is maximum at EXM as compared to other three sites owing to the existence of an urban crossing of many roads (busiest area) with very high vehicular density throughout the day and unavoidable road traffic congestion in rush hours (emitting particulate pollutants such as heterocyclic compounds, hydrocarbons, PAHs and their derivatives, metals, inorganic sulphates and nitrates) coupled with other reasons as explained above. Sparse distribution of trees at EXM also contributed to highest dust load on the targeted plants along the roadsides. Other locations are comparatively more covered by roadside plants which proved to be the front defense line against pollution from vehicular emissions in urban areas. Dust distribution pattern in plant leaves among the sites was obtained as follows: foliar dust load_{EXM} (2.26 ± 0.02 mg cm⁻²) > foliar dust load_{TGN} (1.05 ± 0.02 mg cm⁻²) > foliar dust load_{JDV} (0.95 ± 0.02 mg cm⁻²) > foliar dust load_{RBC} (0.85 ± 0.04 mg cm⁻²). Lowest foliar dust concentration, as expected, was obtained from the control site CMD (0.025 ± 0.01 mg cm⁻²), far away from traffic congestion. All these findings are indicative of significant dust-borne pollution in every sampling location of South Kolkata. All the data of Table 9 have been compared with those of the control site in order to reveal the extent of atmospheric pollution in the urban zones of South Kolkata and degree of exposure for the entire population. The measured concentrations of dust deposition on the perennial *Murraya* leaves far surpassed the values obtained by Prajapati and Tripathi (2008_a) for both deciduous and evergreen plants such as *Dalbergia sissoo*, *Magnifera indica*, *Psidium guajava*, *Ficus benghalensis*, *Ficus religiosa* and *Dendrocalamus strictus* growing in the central parts of the Varanasi city, Uttar Pradesh, India (0.025 – 0.05 mg cm⁻²) and Yang et al. (2017) for evergreen dominant tree species *Cinnamomum camphora* of Shanghai, China (0.02 – 0.65 mg cm⁻²). Bharti et al. (2018) investigated 25 plant species of Talkatora Industrial Area, Lucknow, Uttar Pradesh, India and

reported high dust concentration (5.7 mg cm^{-2}) for evergreen *Moringa oleifera* leaves having rough surfaces and short petiole and low values for *Acacia nilotica* (0.10 mg cm^{-2}), indicating that the dust retention is strictly dependent on specific plant species as well as other leaf morphologies. In comparison to others, *Murraya* leaves exhibited high dust capturing potential due to the presence of reticulate venation leading to rough leaf surfaces, small petioles, waxy coating and associated foliar trichomes (Hall et al., 2018) which facilitated greater adhesion of dust particles.

Table 9

Physical, biochemical and physiological characteristics of *M. paniculata* (L.) Jack.

Parameters	Locations				
	JDV	RBC	EXM	TGN	CMD (Control site)
Foliar dust concentration (mg cm^{-2})	0.95 ± 0.02	0.85 ± 0.04	2.26 ± 0.02	1.05 ± 0.02	0.025 ± 0.01
Total Chlorophyll ($\text{mg g}^{-1} \text{ d.w.}$)	1.72 ± 0.03	2.10 ± 0.01	1.23 ± 0.02	1.41 ± 0.03	2.18 ± 0.01
Specific leaf area ($\text{cm}^2 \text{ g}^{-1}$)	554.23	662.13	463.18	466.67	724.14
Ascorbic acid ($\text{mg g}^{-1} \text{ d.w.}$)	20.45 ± 1.31	18.18 ± 1.34	27.27 ± 1.20	22.73 ± 1.27	13.64 ± 1.42
Leaf extract pH	6.84 ± 0.04	6.69 ± 0.01	7.50 ± 0.06	6.94 ± 0.02	6.98 ± 0.04
Relative water content (%)	76.21 ± 0.57	78.71 ± 0.74	73.15 ± 1.12	74.98 ± 1.29	72.90 ± 1.44
APTI	25.13 ± 1.06	23.85 ± 1.21	31.12 ± 0.72	26.48 ± 0.91	19.78 ± 1.20
Total Carotenoids	0.59 ± 0.17	0.62 ± 0.03	0.42 ± 0.09	0.49 ± 0.13	0.60 ± 0.02

	(mg g ⁻¹ d.w.)				
Lipid	36.33±1.22	119.60±1.17	26.19±1.16	128.92±2.46	20.37±1.19
	(mg g ⁻¹ d.w.)				

2.3.2. Tolerance of *Murraya paniculata* to abiotic stress

2.3.2.1. Total chlorophyll content

Photosynthetic rate of plants, biomass growth and productivity are directly regulated by the chlorophyll content of plants which is influenced by leaf age, degree of pollution, plant species and environmental factors such as ambient temperature, light intensity, drought or aridity, salt-induced osmotic stress, foliar accumulation of aerosols and soil contamination (Zhang et al., 2016; Nadgorska-Socha et al., 2017). In the proposed work, content of total chlorophyll (TCh) varied between 1.23 ± 0.02 – 2.10 ± 0.01 mg g⁻¹ among all the studied sites (as evident from Table 9). The study clearly reveals that the total chlorophyll content is inversely proportional to the foliar dust concentration which may be due to the fact that increase in dust load decreases the rate of chlorophyll synthesis because of (a) shading effect or inaccessibility of sunrays to the chlorophyll (absorber of sunlight) owing to dust barrier, preventing the enzyme activity of chlorophyll synthase from chlorophyll biosynthesis and increasing the production of catabolic enzyme chlorophyllase responsible for chlorophyll degradation, (b) alkaline environment created by diffused dust particulates, production of cytotoxic free radicals and formation of crust on plant leaf surfaces due to hydration, denaturing the chemical structures of chlorophyll and (c) clogging of stomatal pores, thereby reducing the rates of CO₂ transfer, carbon assimilation and transpiration (Wellburn et al., 1972; Petkovsek et al., 2007; van Heerden et al., 2007; Prajapati and Tripathi, 2008_a; Prajapati, 2012; Sett, 2017; Peng et al., 2019; Roy et al., 2020). Such phenomena reduce photosynthetic activity, influencing consequently the growth of the plant which, in turn, is related to specific leaf area (SLA) (Liu et al., 2017_b). Differences in tree growth were also evidenced among the study sites based on the values of SLA. SLA values were low at the polluted sites (JDV, RBC, EXM and TGN) unlike the control site (CMD) (ref. Table 9). This implies retarded plant growth at the polluting places as opposed to the control site since low SLA is a manifestation of stunted plant growth (Dwyer et al., 2014). Further, reduction in total chlorophyll content of *Murraya* leaves due to adherence of huge amount of dust particulates on the leaf surfaces was observed at polluted sites as compared to the unpolluted or rural site, the reason being the nominal dust deposition on the foliage of

the tree species at the control site. The trend of chlorophyll concentration as evaluated from the experimental study (Table 9) based on sampling locations was established as: $TCh_{EXM} (1.23 \pm 0.02 \text{ mg g}^{-1}) < TCh_{TGN} (1.41 \pm 0.03 \text{ mg g}^{-1}) < TCh_{JDV} (1.72 \pm 0.03 \text{ mg g}^{-1}) < TCh_{RBC} (2.10 \pm 0.01 \text{ mg g}^{-1})$. At the control site, TCh and SLA values were maximum and found to be $2.18 \pm 0.01 \text{ mg g}^{-1}$ and $724.14 \text{ cm}^2 \text{ g}^{-1}$ respectively. Likewise, lowest chlorophyll content and SLA of the plant leaves at EXM are attributable to highest deposition of atmospheric dust particles on tree foliage. The TCh values presented in Table 9 are in good agreement with the amount of dust load on the leaves in each location. Similar results were obtained by Karmakar and Padhy (2019) in their study with deciduous trees at Barjora forest, Bankura, India and control site Ballavpur Wildlife Sanctuary (BWLS), Birbhum, India. The authors reported lower concentrations of total chlorophyll (mg g^{-1} fresh weight) for *Shorea robusta* Gaertn. (1.06 ± 0.08), *A. auriculiformis* Benth. (1.06 ± 0.16), *Eucalyptus globulus* Labill. (1.05 ± 0.16) and *A. indica* A. Juss. (1.15 ± 0.09) at Barjora forest as compared to the reference site BWLS (*S. robusta*: 1.92 ± 0.16 ; *A. auriculiformis*: 1.71 ± 0.27 ; *E. globulus*: 1.35 ± 0.08 ; *A. indica*: 1.29 ± 0.14). Pandey et al. (2016) examined 24 climber plant species of Varanasi city, Uttar Pradesh, India, and also observed lower chlorophyll content at the polluted urban sites (2.98 ± 0.03 – $11.82 \pm 0.84 \text{ mg g}^{-1}$), whereas higher chlorophyll levels (3.89 ± 0.87 – $11.58 \pm 0.92 \text{ mg g}^{-1}$) were detected at the control site. Therefore, it can be conferred that the decreased content of plant chlorophyll is a pointer towards heavy atmospheric pollution, but high chlorophyll content of plants even in polluted environment is indicative of their tolerance to hazardous contaminants (Ogunkunle et al., 2015).

2.3.2.2. Ascorbic acid content

Elevated level of leaf ascorbic acid content is indicative of air quality degradation and also assists in the selection of plant species applicable for biomonitoring air pollution. Absorption of airborne pollutants by the plant leaves induces excessive formation of reactive oxygen species (ROS) within plant cells. Ascorbic acid (which is found in rapidly growing parts of all the plants) can effectively degrade ROS and controls overexpression of genes linked with stress responses, thereby enhancing the tolerance level in plants under polluted conditions (Hossain et al., 2012; Singh et al., 2016a; Pathak et al., 2019). It also controls plant growth and development, enzyme activity, photosynthesis and transpiration, redox signaling pathways in chloroplasts, integrity and stability of plasma membranes for the survival of cells, RWC of plants and leaf senescence or aging (Akram et al., 2017). In relevance to the aforesaid facts, high ascorbic acid contents (18.18 ± 1.34 – $27.27 \pm 1.20 \text{ mg g}^{-1}$) of plant leaves were obtained

from heavily contaminated zones (EXM, TGN, JDV and RBC), which are much higher than what is recorded from the reference site CMD ($13.64 \pm 1.42 \text{ mg g}^{-1}$) as indicated in [Table 9](#). Highest increase in leaf ascorbic acid content was observed at EXM ($27.27 \pm 1.20 \text{ mg g}^{-1}$) when compared to the other three sites (TGN: $22.73 \pm 1.27 \text{ mg g}^{-1}$; JDV: $20.45 \pm 1.31 \text{ mg g}^{-1}$; RBC: $18.18 \pm 1.34 \text{ mg g}^{-1}$). Significant breakdown of chlorophyll at the polluted sites is a definite marker of plant leaf senescence under abiotic stressors which is effectively combatted and controlled by increased level of ascorbic acid content in the foliar tissues to help them thrive in the polluted environment. Therefore, it is clear that highest dust load ($2.26 \pm 0.02 \text{ mg cm}^{-2}$) and lowest concentration of chlorophyll ($1.23 \pm 0.02 \text{ mg g}^{-1}$) are responsible for highest ascorbic acid content at EXM which is a typical response of defense mechanism for the tolerant plant species under stress. Correspondingly, distribution and uptake of atmospheric dust particles by the leaves of *Murraya paniculata* leading to ROS-mediated denaturation of chlorophyll acted as a signal for overproduction of ascorbic acid in the plant leaves at the sampling points which, in turn, amplify their tolerance level against ambient air pollution during colder periods. In this context, it can be inferred that the lowest amount of ascorbic acid and maximum chlorophyll content of plant leaves are associated with less polluted atmosphere at the reference site. The above study has also been validated by the findings of [Thawale et al. \(2011\)](#), [Gupta et al. \(2016\)](#), [Pandey et al. \(2016\)](#), [Bharti et al. \(2018\)](#), [Karmakar and Padhy \(2019\)](#) and [Roy et al. \(2020\)](#).

2.3.2.3. Leaf extract pH

Alkalinity determines the tolerance level of plant species through detoxification mechanism developed in the plant under polluted conditions. Stomatal activity of plant leaves, proper functioning of different enzymes, photosynthetic efficiency and cell expansion are also influenced by the leaf tissue pH ([Jia and Davies, 2007](#); [Yan-ju and Hui, 2008](#); [Thawale et al., 2011](#); [Sen et al., 2017](#); [Karmakar and Padhy, 2019](#); [Karmakar et al., 2021](#)). In the polluted environment, pH of the plant leaves decreases or becomes acidic due to high contents of SO_x and NO_x in the ambient air. Sensitive plants are more susceptible to acidic pollutants which readily diffuse through the stomatal opening (process of gaseous exchange) and form nitrous acid, sulphurous acid and nitric acid after dissolution of the acidic pollutants in the aqueous sub-cellular compartments of leaf tissues, thereby lowering the foliar pH ([Bligny et al., 1997](#)). Conversely, abiotic stress tolerant plant species maintain high levels of pH which favours the conversion of hexose sugars such as glucose and galactose into ascorbic acid for their adaptation and resistance. In the proposed study, relative values of foliar extract pH were found

to be in the alkaline range (6.69 ± 0.01 – 7.50 ± 0.06) both at the urban and control sites (ref. [Table 9](#)). Plant species collected from the reference site displayed higher pH (6.98 ± 0.04) than that sampled from the polluted sites except EXM ([Table 9](#)). This may be attributed to the highest deposition of suspended particulate matter (SPM) on plant leaf surfaces at EXM because of higher anthropogenic influences affecting biotic communities in contrast to other three sampling points ([Roy et al., 2020](#)). On the other hand, plant leaves at the control site were subject to less stressful habitats which enabled them to maintain an optimal pH value (optimum pH range: 6–7) for their health and growth ([Bacon et al., 1998](#)). This also supported them in acquiring air pollution tolerance for survival in the changing environment ([Escobedo et al., 2008](#)). Hence, plants having alkaline leaf-extract pH even in the stressed conditions are said to be more tolerant and counter the atmospheric pollution effectively which is also apparent from the present study. The outcome of the study is in accordance with those of [Karmakar and Padhy \(2019\)](#) who considered the trees of tropical dry deciduous forests for urban greening (control site: 4.67 ± 0.07 – 5.72 ± 0.08 and polluted site: 4.49 ± 0.11 – 5.58 ± 0.16) and [Pandey et al. \(2016\)](#) who adopted climber trees or vines for developing strategies of vertical gardens in Varanasi, India (rural site: 6.12–7.85 and urban site: 5.80–6.53).

2.3.2.4. Relative water content (RWC)

Plant responses to abiotic stress are correlated to leaf RWC (water status in plants) which helps to regulate the physiological functions or processes (mainly growth and metabolism) of plants ([Kaur and Nagpal, 2017](#)). Under environmental stress (such as drought or aridity and burden of aerial emissions), high leaf water content assists in homeostatic regulation in plants in which a physiological balance prevails inside the cells for their viability ([Agarwal and Tiwari, 1997](#); [Karmakar et al., 2021](#)). High pollution load increases the permeability of protoplasm, causing depletion of water and dissolved nutrients from the plant cells, ultimately leading to leaf senescence at early stage ([Agarwal and Tiwari, 1997](#)). Effectually, cell permeability is altered due to the increased tendency of leakage through the damaged cell membrane which also renders the pumps and transporters ineffective for the flow of ions and solutes ([Trivedi and Sati, 2013](#)). Additionally, acidity of plant leaf cell sap gets reduced due to high RWC which increases their tolerance against pollution and helps them fight drought condition ([Gupta et al., 2016](#); [Rai, 2016](#); [Kaur and Nagpal, 2017](#); [Sen et al., 2017](#); [Mina et al., 2018](#)).

Murraya paniculata showed an increase in RWC (in %) at the polluted areas (73.15 ± 1.12 – 78.71 ± 0.74) than that of the control site (72.90 ± 1.44) ([Table 9](#)). Transpiring leaves, while in a state of full turgidity, will have RWC approximately 98% and it gets reduced to

about 30–40% in plant leaves during dehydrated conditions or at the stage of dying, whereas, at the initial phase of wilting (drooping, folding and rolling of leaves due to loss of water from plant cells), RWC is found to be in the range of 60–70% depending on plant species (Arndt et al., 2015). However, levels of atmospheric humidity fall in winter months, having a stronger influence on the process of transpiration and RWC. At low relative humidity, increased loss of water facilitates stomatal closure by the plant leaves hampering the uptake of CO₂ and causing plant growth impairment. Among the four contaminated sampling sites, plant leaves at EXM exhibited lowest RWC ($73.15 \pm 1.12\%$) as dust load was found to be highest due to significant air pollution stress. Though, in winter, RWC is below 90% for the plant species in all the sites, it can be explicitly stated that 70–80% of RWC even in adverse environmental conditions was enough for their acclimation and tolerance, since it is a species-specific physiological trait. Thus, the results depicted in Table 9 dictate the alarming status of the sampling locations and the tolerance capacity of the plant species to counteract the hazardous effects of air pollution.

2.3.2.5. Air pollution tolerance index (APTI)

APTI is a measure of plant's capacity to attenuate air pollution having deleterious effects on ecosystem and biodiversity. Variation in plant responses depends on characteristics of species and meteorological conditions of a particular area. A preliminary screening test is therefore carried out by means of APTI for the selection of plant species as environmental biomonitors on the basis of their air pollution tolerance. APTI values obtained for *M. paniculata* ranged from 19.78 ± 1.20 to 31.12 ± 0.72 among the sampling sites (Table 9) and were also observed to change with the level of pollution in the ambient air (i.e. higher the pollution burden, more is the tolerance index). It was higher at polluted sites and relatively lower at the reference site based upon considerable variability in plant parameters. Highest ascorbic acid content at EXM (in view of maximum dust deposits and least chlorophyll content) resulted in highest APTI value (31.12 ± 0.72) specifying increased levels of air pollutants. Higher index values imply high tolerance of plants, competent enough to withstand environmental pollution with less visible damage or external injury and thus, it can be comprehended that the species of *Murraya paniculata* is tolerant towards air pollution with APTI > 17 at every site under study and can be advantageously utilized as a biomonitor which permits both qualitative and quantitative assessment of eco-health for accurate estimates of air pollutant exposure. Sensitive species of plants, categorized by APTI < 10, cannot normally be applied for biomonitoring, but are exploited as biological indicators which can only give stress indication through alterations in their developmental patterns and functional parameters and cannot sustain their growth in

unfavourable circumstances. Hence, development of green infrastructures by employing such tolerant ornamental roadside plants as eco-sustainable tool is highly recommended for monitoring and abatement of air pollution along with ecological restoration of urban environment, *Murraya paniculata* being one of the best options.

2.3.3. Total carotenoids content

Contents of carotenoids in plant leaves can be considered to be the principal determinant for assessing the physiological state of plants under pollution stress and function as accessory light-harvesting pigments, provide photoprotection, help plant colouration and regulate cell proliferation, floral induction and development (Das and Roychoudhury, 2014; Li et al., 2020). Carotenoids (i.e. carotenes and xanthophylls) possess antioxidative properties to shield plants from oxidative stress by effectively scavenging ROS and also prevent chlorophyll disruption by photo-oxidation through epoxide cycle (Sifermann-Harms, 1987; Truscott, 1990). Despite that, increase in pollutant concentrations makes them vulnerable to oxidative cleavage by ROS resulting in the formation of oxidized products, some of which are bioactive triggering variations in gene expression to raise tolerance in plants exposed to air pollution (Havaux, 2013). On the other side, under serious threats, the protective mechanism may become progressively inefficient causing cell death including pigment degradation (Senser et al., 1990).

In the current study, the total amount of carotenoids was also affected by heavy air pollution. The trend of variations for both carotenoids and chlorophyll are more or less comparable as defined in Table 9. Plant leaves with highest load of road dust at EXM showed extreme reduction in the content of carotenoids ($0.42 \pm 0.09 \text{ mg g}^{-1}$) than the other sites. JDV and TGN followed the same trend, denoting low carotenoid levels with the increase in airborne dust. A slight deviation from the trend was noted at RBC where the carotenoid content ($0.62 \pm 0.03 \text{ mg g}^{-1}$) was marginally higher than the control site ($0.60 \pm 0.02 \text{ mg g}^{-1}$). This may be credited to the fact that the concentrations of some of the xanthophyll compounds do not get affected and proportions of some compounds may even get increased in stressful environment (Mibei et al., 2017; Shah et al., 2019). Decline in the concentration of plant leaf carotenoids due to hindrance in photosynthesis caused by the phytotoxicity of air pollutants is also demonstrated by many researchers (Rajput and Agrawal, 2005; Tiwari et al., 2006). Dreadful effects of automobile and coal smoke pollution on the pigment contents of *Shorea robusta* (Sal), *Mallotus philippinensis* (Rohini) and *A. indica* were also studied by Swami et al. (2004) and Iqbal et al. (2010_a, 2010_b) respectively. As a result, it can be opined that the plant defense mechanism cannot be modulated by carotenoids only but is highly dependent on the ascorbic

acid level as it forms the first line of plant's protection against the oxidative injury (Chaudhary and Rathore, 2018) and it is also clearly reflected in the present study for *Murraya paniculata*.

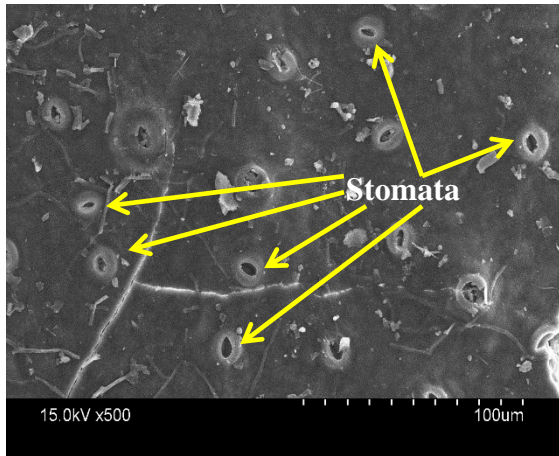
2.3.4. Lipid content of plant leaves

Leaf lipids respond to abiotic stresses by firstly giving signals on stress initiation and secondly, mitigating cellular injury via membrane lipid remodelling and regaining of membrane stability, fluidity, permeability and integrity (Balogh et al., 2013; Moradi et al., 2017). These have also been proved as the main domains for accumulation, absorption, partitioning and digestion of organic pollutants (such as PAHs) in plant leaves from air due to their lipophilicity (Hwang and Wade, 2008; Zhang and Zhu, 2009), the process being influenced by temperature variations (Simonich and Hites, 1994_a). Transport of hydrophobic organic compounds from cuticles to the inner leaf tissues gets interrupted due to low permeability and high sorption ability of cuticles, leading to the dissolution of compounds in the amorphous cuticular phase (Li et al., 2010). In this study, foliar lipid yield ranged from 26.19 ± 1.16 to 128.92 ± 2.46 mg g⁻¹ at the sites of pollution (Table 9). Higher plants may undergo changes in leaf lipid composition and content according to their physiology and different environmental, meteorological and anthropogenic factors (Kuiper, 1985). The lipid contents of plant leaves in different polluted areas did not follow any specific trend in this study. High content of plant leaf lipids at the polluted sites than the reference site (20.37 ± 1.19 mg g⁻¹) can be considered as a good predictor for the presence of persistent organic pollutants including PAHs and is a salient feature of plant tolerance to pollution stress. The results have also been corroborated by the study carried out by Li et al. (2017) with perennial plants where the authors had concluded that PAHs accumulation was highest in *Mahonia* sp. having least lipid content and conversely, *Hypericum* sp. with maximum lipid content showed bioaccumulation of PAHs to a lesser degree. Contribution of lipid microstructures along with the surface morphology of wax layer, in addition to lipid content, might also be a controlling factor for uptake mechanism and diffusion rate of organic pollutants into the plant leaves by providing a sharp concentration gradient as reflected in the results illustrated in Table 9 (Li et al., 2017).

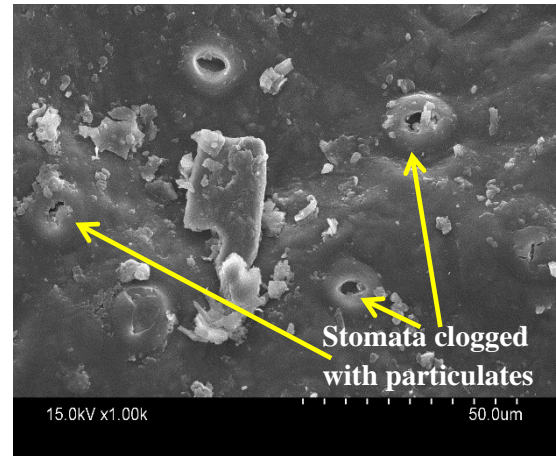
2.3.5. SEM observation with energy-dispersive X-ray microanalysis

Surface accumulation of atmospheric particulates on tree foliage is determined by the size and nature of particles and properties of the surfaces to which they adhere (Liang et al., 2017). Plant interactions with the atmosphere are directed via stomata — dynamic interface between plant leaves and air. *Murraya* leaves were found to develop distresses, though on a lesser extent,

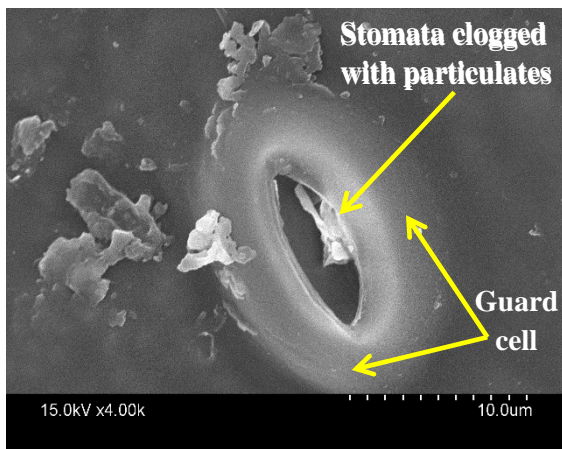
such as coloured patches (brown or yellow), surface lesions, black spots and curling owing to PM pollution. At the control site, negligible clogging of stomatal pores was seen (Fig. 8(a)), while, in the environmentally polluted sites, heavy stomatal blockages by dust were found because of roadside air pollution (Fig. 8(b), (c) and (d)). Deposition of non-uniform and flaky dust particles, both fine and coarse, was detected near the inner walls of the stomata or at the periphery of guard cells (Fig. 8(c) and (d)), distribution of particles being different with respect to locations. Similar observation was made by Skrynetska et al. (2019) and Roy et al. (2020) in and around Southern Poland and Ranchi (commercial area, India), respectively. Deformity of guard cells, surface roughness, degradation of epicuticular wax structures surrounding the stomatal aperture and embedment of dust particles throughout the surfaces were also noticed further as intense effects of vehicular air pollutants. EDX spectral analysis showed that the vast surfaces of plant leaves from the rural region CMD mostly contain calcium (Ca: 5.87 wt %), magnesium (Mg: 0.21 wt %), manganese (Mn: 0.15 wt %), chloride (Cl^- : 0.12 wt %), potassium (K: 0.95 wt %), silicon (Si: 0.25 wt %), carbon (C: 50.67 wt %) and oxygen (O: 41.79 wt %) (ref. Fig. 8(e)), probably from the plants' uptake of subsoil water as well as atmospheric absorption for ionic balance and growth. Presence of both heavy metals and atmospheric trace elements such as mercury (Hg: 0.92 wt %), cobalt (Co: 0.15 wt %), zinc (Zn: 0.33 wt %), iron (Fe: 0.15 wt %), Ca (3.27–4.85 wt %), Mg (0.28–0.29 wt %), K (0.49–0.99 wt %), Cl^- (1.03–1.24 wt %), Si (0.35–0.54 wt %) and aluminium (Al: 0.16 wt %) was evidenced in the surfaces of plant leaves of urban locations contaminated by vehicular exhausts and dust (Fig. 8(f) and (g)). Besides these, peaks of sodium (Na), nickel (Ni) and antimony (Sb) were also identified. It may be noted that the trace elements (including Zn, Al, Ni, Mg, Ca, K, Cl^- , Si, Na) might have originated from vehicular emissions, soil dust, tyre wears and broken road dust (Lin et al., 2005; Duong and Lee, 2011; Weerakkody et al., 2018a). High concentrations of major elements, C (51.30–52.93 wt %) and O (40.01–41.99 wt %), may be attributable to two reasons — bioaccumulation of mutagenic PAHs, and secondly plant growth requirements (Weerakkody et al., 2018a). Bulk composition of trace elements as obtained in the study can serve dual purposes of activating ROS scavenging enzymes and synthesizing plant hormones for their protection against ROS-induced damage, thereby increasing plant tolerance in adverse growing conditions (Khan et al., 2018). Acquisition of gold (Au) peaks in the spectra may be due to the sputter coating of samples with gold for better quality images at high voltage of SEM.



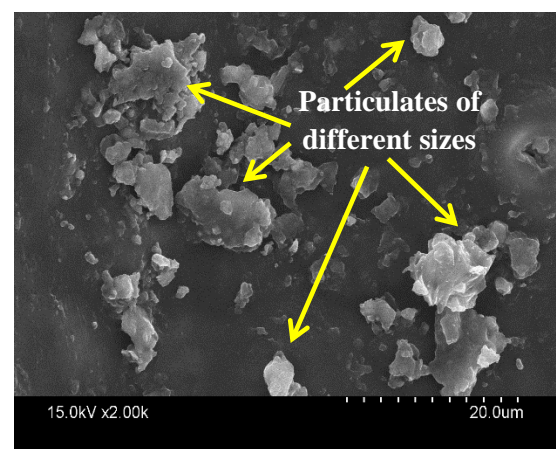
(a)



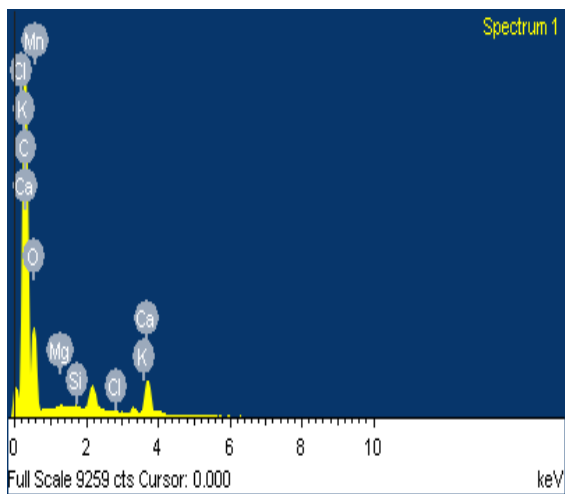
(b)



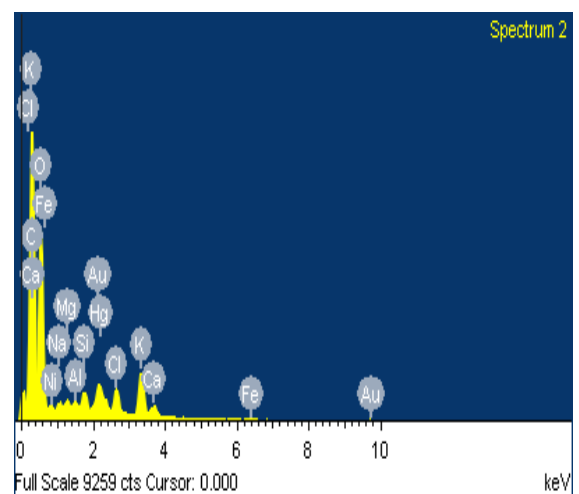
(c)



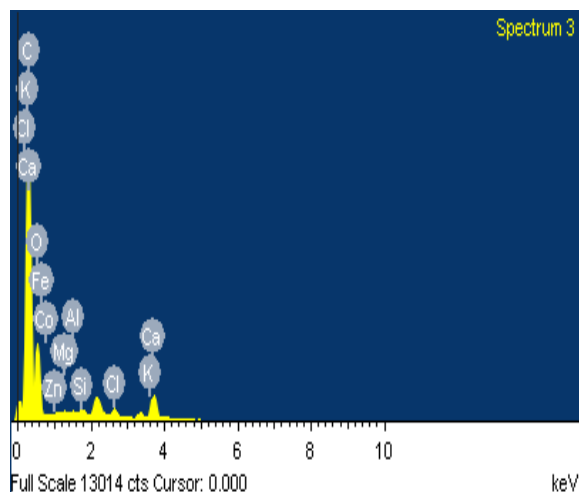
(d)



(e)



(f)



(g)

Fig. 8. SEM-EDX micrographs (a) SEM image of plant leaves of control site, (b), (c) and (d) SEM images of plant leaves of roadside areas, (e) EDX spectrum of plant leaves of control site, (f) and (g) EDX spectra of plant leaves of roadside areas.

2.3.6. PAHs detection in *Murraya paniculata* leaves for biomonitoring: A qualitative approach

Passive monitoring of air pollution through tolerant tree species that can endure the imposed stress is very much crucial for environmental clean-up by mass greening in urban spaces, practical estimation of pollutants along with the identification of their contributing sources and improvement of microclimates in megacities. PAHs in urban air is highly dominated by human interventions and meteorology which have direct impact on humidity, ambient temperature, mixing height, cloudiness, intensity and frequency of rain and wind speed, governing the dispersal of PAHs from diverse emission sources. The field study with biomonitor plant *Murraya paniculata* in the urban sites of South Kolkata revealed remarkable differences in PAHs contamination (Table 10). Due to the presence of isomers, PHE and ANT, BaA and CHR and BbF and BkF (having same quantitation ions) completely co-eluted at the same retention time during GC–MS analysis (Table 10). On the other hand, DB[ah]A and IP, though co-eluted very closely, could be easily identified for their different quantitation ions from the mass spectrum. PAHs peaks were also confirmed by comparison with library spectra. The sample chromatograms of leaf-extracted PAHs from the five different sites are presented in Fig. 9.

The plant uptake and accumulation of both LMW and HMW PAHs in the leaf tissues (favoured by biotic and abiotic factors: lipid concentration of plant leaves, surface area of

leaves, state of PAHs and partition coefficient) proved it to be a good and dependable biomonitoring agent for airborne PAHs. [Table 10](#) gives a clear picture of urban air quality concerning PAHs and it is definitely worse than that of the control site CMD due to multiple anthropogenic stressors and enormous number of vehicles on roads releasing large number of PAHs in the atmosphere. [Ray et al. \(2017\)](#) proposed that the loading of PAHs in the atmosphere of Kolkata is commonly related to diesel and petrol combustion (17–24%), burning practices with wood and coal (15–26%) as well as exhausts from residential kitchens and commercial food stalls down the roads (18%). Abundance of ACY, FLU, ANT, PYR, and PHE in the plant samples collected from JDV, RBC, EXM and TGN suggest substantial effects of heavy traffic volume with elaborate road network at all the selected sites ([Ravindra et al., 2008a](#)). Existence of BaA, BbF, BkF, PHE, CHR, IP and B[ghi]P in the plant leaves of RBC may represent vehicular activity using petrol, diesel and natural gas, signifying plying of both heavy-duty and light-duty motor vehicles through the study point ([Zhu and Wang, 2005](#)). JDV area appears to be a food hub with a large scale of restaurants and street food vendors lining up the roadsides. Hence, cooking oil fumes or cooking soot are assumed to be the predominant sources of LMW PAHs such as PHE, FLU, NAP, PYR at JDV apart from automobile exhaust emissions. Studies have also demonstrated that PAHs emission from cooking sources account for approximately 20–40% in metro cities ([Huang et al., 2010](#); [Liu et al., 2012](#)). LMW and HMW PAHs in the *Murraya* tree leaves of TGN are associated with a combined source of vehicle emissions and garbage burning with leaf litters or wood remnants from the green belts by the side of the roads. [Kakareka et al. \(2005\)](#) and [Yu et al. \(2007\)](#) stated that PHE, BbF and BkF are the main components of open field burning of rice straw, affecting air quality and visibility. Most of the HMW PAHs recognized at EXM (PYR, BaP, BbF, BkF, IP, DB[ah]A and B[ghi]P) are believed to be released from coal, wood and biomass combustion by the squatter and slum communities, generating more SPM in the air ([Ray et al., 2017](#)). PAHs having molecular masses 178 and 202 are often used for differentiating petroleum and combustion sources ([Budzinski et al., 1997](#)). The occurrence of NAP, PHE, ANT, FLA and PYR in the leaves of control site can be ascribed to household burning of woods, long-range transport of PAHs from other anthropogenic sources through wind flow and synthesis of PAHs by plant metabolism ([Krauss et al., 2005](#); [Papa et al., 2012](#)). Leaf accumulation of potentially carcinogenic PAHs (BaA, BaP, BbF, BkF, CHR, D[ah]A and IP) at the polluted sites raises the need for proper exercise of the control on the sector-wise emissions of pollutants and use of cleaner fuels for transport. In most cases, BaP is used as an indicator for total carcinogenic PAHs exposure as carcinogenicity of other PAHs is less than BaP ([Ohura et al., 2004](#)).

Table 10

Identification of PAHs in the leaf samples of *M. paniculata* (L.) Jack by GC-MS analysis for different sampling locations.

EPA-PAHs	Retention time (min)/Quantification ion (m/z) of PAHs in the Certified Reference Material	Retention time (min)/Quantification ion (m/z) of identified PAHs in the tested samples				
	JDV	RBC	Locations			CMD (Control site)
			EXM	TGN		
Naphthalene (NAP)	6.23, 6.74/128	6.07/128.61	6.73/128.52	6.94/128.77	6.66/128.67	6.76/128.01
Acenaphthylene (ACY)	10.23/152	—	10.29/152.25	10.50/152.26	10.42/152.30	—
Acenaphthene (ACE)	10.60/154	10.84/154.07	—	—	—	—
Fluorene (FLU)	12.89/166	12.75/166.03	12.28/166.50	—	12.54/166.16	—
Phenanthrene (PHE)	15.37/178	15.66/178.35	—	15.80/178.56	15.47/178.08	15.06/178.00
Anthracene (ANT)	15.37/178	15.66/178.35	—	15.80/178.56	15.47/178.08	15.06/178.00
Fluoranthene (FLA)	19.30/202	19.63/202.76	—	—	—	19.03/202.81
Pyrene (PYR)	20.59/202	20.88/202.51	20.72/202.58	20.72/202.62	—	20.30/202.70
Benzo[a]anthracene (BaA)	24.96/228	24.25/228.61	24.09/228.92	—	—	—
Chrysene (CHR)	24.96/228	24.25/228.61	24.09/228.92	—	—	—
Benzo[b]fluoranthene (BbF)	28.37/252	—	28.42/252.62	28.58/252.68	28.14/252.92	—
Benzo[k]fluoranthene (BkF)	28.37/252	—	28.42/252.62	28.58/252.68	28.14/252.92	—
Benzo[a]pyrene (BaP)	29.69/252	—	—	29.29/252.42	—	—
Dibenzo [a,h]anthracene (DB[ah]A)	36.75/278	—	36.20/278.26	36.94/278.00	36.30/278.01	—
Indeno[1,2,3-cd]pyrene (IP)	36.75/276	—	36.20/276.03	36.94/276.70	36.30/276.81	—
Benzo[g,h,i]perylene (B[ghi]P)	38.89/276	38.57/276.97	38.33/276.22	38.67/276.59	—	—
Total no. of extracted PAHs	16	10	11	11	9	5

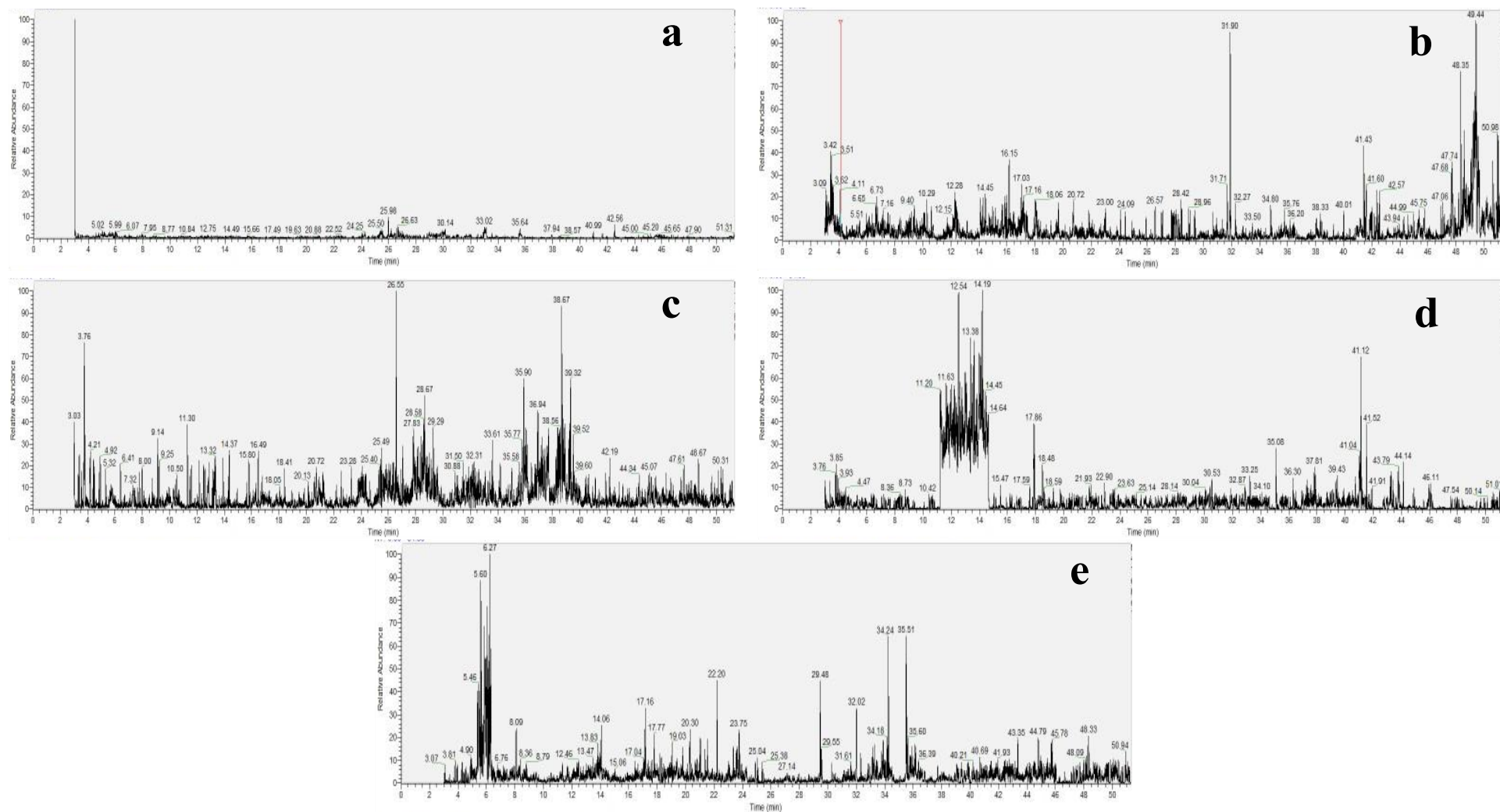


Fig. 9. GC-MS chromatograms of PAHs extracted from the leaves of *M. paniculata* of different sites a) JDV, b) RBC, c) EXM, d) TGN and e) CMD.

2.3.7. Statistical and correlation/regression analyses

One way ANOVA results demonstrated that statistically significant differences were present among the biochemical and physiological factors (total chlorophyll, ascorbic acid, leaf extract pH and RWC) and APTI of different sites (as $p < 0.05$ and $F > F_{\text{crit}}$). Therefore, exact correlation between APTI and different parameters effected by abiotic stress can be developed from the obtained data. The study of the plant samples from the polluted areas revealed that strong positive correlations exist between foliar dust load with leaf ascorbic acid content ($r=0.931$) and leaf extract pH ($r=0.985$). Higher the dust load on tree foliage, higher will be the ascorbic acid content under high pH (alkaline condition), rendering the plant more tolerant. Contrarily, strong negative correlations have been observed to exist with leaf RWC ($r=-0.822$) and total carotenoids content ($r=-0.862$). Moreover, a good negative correlation has also been found between accumulated dust loads and total chlorophyll content ($r=-0.76$). Negative correlations suggest that the higher values of dust deposition on plant leaf surfaces are associated with loss of plant pigments and low RWC as described earlier. Fig. 10(a–d) represents the plots of APTI with plant functional parameters for the polluted sites, wherein it was found that the APTI is strongly dependent on ascorbic acid content ($R^2=0.9766$), leaf tissue pH ($R^2=0.9958$), RWC ($R^2=0.8874$) and total chlorophyll content ($R^2=0.8521$), justifying the objective of the study. The goodness of fit of the expected outcome for different biochemical and physiological parameters is determined by the R^2 value (which is close to unity), signifying good fit. The results of the study showed that high positive correlations of APTI exist with ascorbic acid and foliar pH and negative correlations with RWC and total chlorophyll in case of *Murraya paniculata* species.

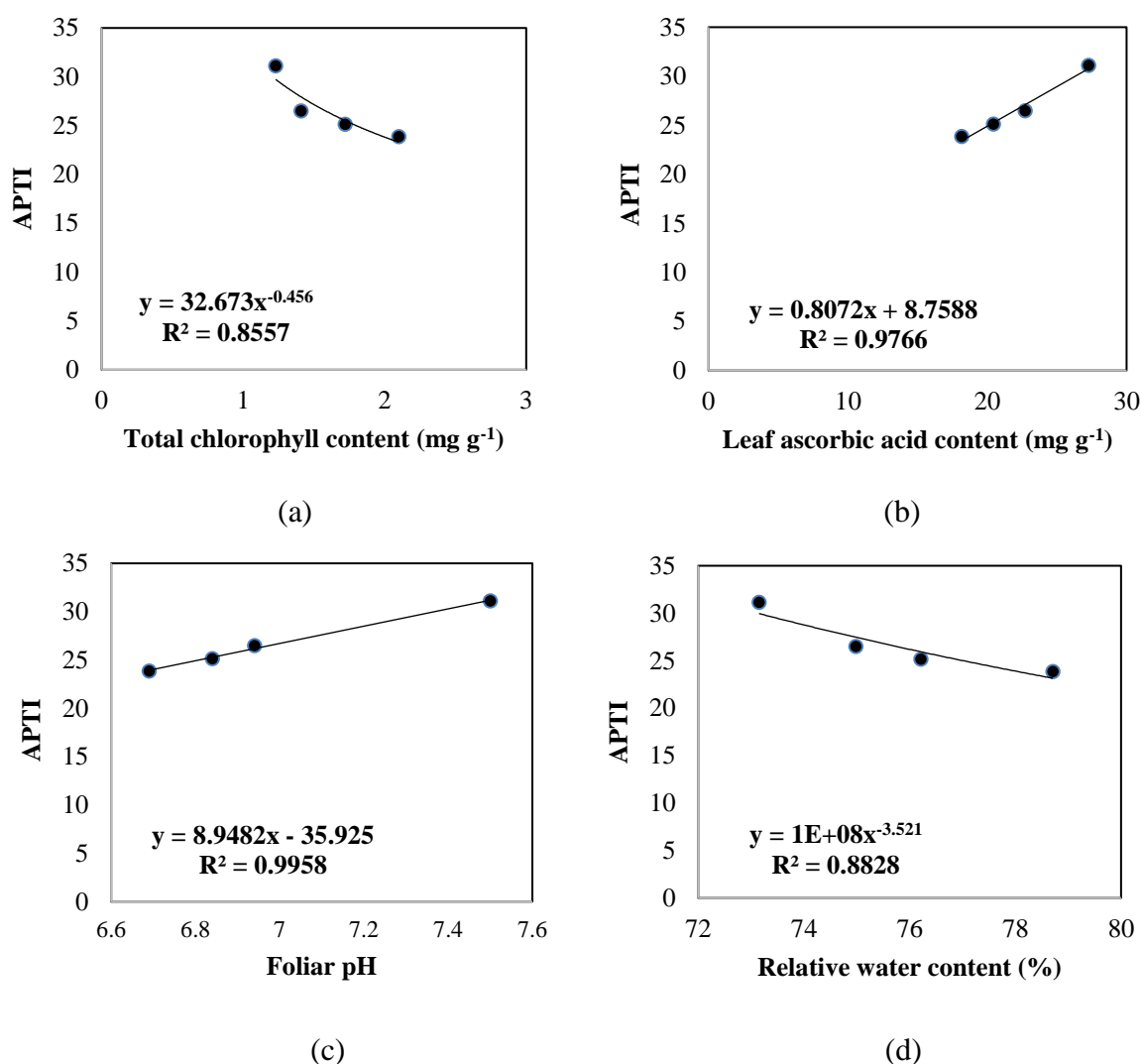


Fig. 10. Variation of APTI of *Murraya paniculata* (L.) Jack with (a) total chlorophyll content of plant leaves, (b) leaf ascorbic acid content, (c) foliar pH and (d) relative leaf water content at the polluted sites.

2.4. Conclusion

The present study highlights the ecophysiological features of *Murraya paniculata* (L.) Jack in response to inimical environmental factors such as presence of PM, PAHs, etc. influencing plant growth, cellular metabolism, reproduction and sustenance, which have been examined to ascertain the plant biomonitoring potential. Presence of highest concentration of foliar dust and maximum number of PAH congeners in one of the sample sites (EXM) referred to the highest pollution load compared to other selected sites. Reduction in leaf chlorophyll and carotenoid contents at the selected sampling sites (distinctly higher in EXM site) compared to control site (CMD) ensued from abiotic stressors, causing premature leaf senescence and restricting plant growth and diffusive resistance mechanism due to clogged stomata or deformed guard cells

with respect to unaffected condition available at CMD. To withstand pollution load, the plant showed several responses like increased production of ascorbic acid, high leaf extract pH and high RWC having highly pronounced impact on plant tolerance which helped the plant inhabit the extreme environment (Fig. 11) and thus eventually carries higher APTI values. Moreover, variation of APTI is in line with leaf intercepted PM and other pollution burden. The said plant not only shows bioindicator behavior which is evident from the APTI value of the species collected from control site (>17), but also shows biomonitoring behavior by adapting to the environment with high pollution load (where APTI changes from 19.78 up to 31.12). So, it can be affirmed that the tree species *M. paniculata* is a biomonitor of worth for assessing and minimizing environmental contamination as its tolerance index is much above the limiting value ($APTI > 17$). The hydrophobic character of plant leaf lipids facilitated sorption of PAHs at the study sites since they behave similarly to lipids, plant resistance being also highly dependent on lipid stores. The selected plant species can easily germinate and grow in harsh situations with minimal practical maintenance, which would offer an eco-friendly, economic and highly effective alternative to conventional air sampling approaches, paving the way for redemption of breathable air quality with the help of locally available common flora. Thus, explicit study on extraction and analysis of PAHs as techniques of isolation from the tissues of such biomonitor plant *M. paniculata* has been targeted in the next chapter (Chapter 3).

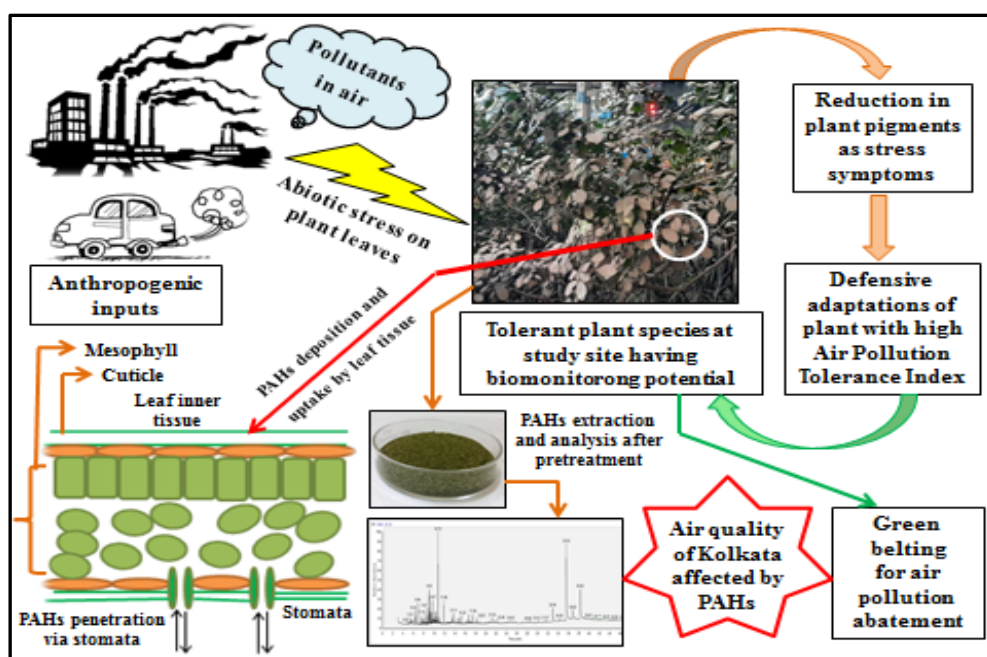


Fig. 11. Illustrative outlook on abiotic stress tolerance of *M. paniculata* under the exposure of ambient air pollution for greenbelt development.

Chapter 3

3. Methodology II

Extraction and analysis of PAHs from bioindicators

3.1. Background

Polycyclic aromatic hydrocarbons (PAHs) are lipophilic environmental carcinogens having pernicious impact on public health owing to their long presence and resistance to biodegradation (Bostrom et al., 2002; IARC, 1983; Mallah et al., 2022; Patel et al., 2020; Zheng et al., 2018). Anthropogenic pollution has been the key contributor of airborne PAH emissions and is a menace to ecosystem sustainability. Biomonitoring strategies as eco-based solution are thus broadly adopted for improving air quality on account of process economy, simple sampling procedures and wide scope of experimental maneuvering (Capozzi et al., 2016; Jiang et al., 2018; Swislawski et al., 2021). Identification and quantification of PAHs after extraction or isolation are the major requirements of biomonitoring for understanding the degree of pollution and state of changes occurring in the environment (Mukhopadhyay et al., 2020). Complex structural characteristics and diversity of plant matrices make the process of target analyte extraction difficult (as there are possible chances of coextraction of plant pigments and other organic compounds), and hence, in quality analysis, sample preparation is a vital step toward recovery (Domeno et al., 2012; Steiner et al., 2020). Traditional Soxhlet and process intensified extraction approaches (assisted with ultrasonication, supramolecular solvents, supercritical and subcritical fluids, microwave heating, high pressure and temperature, etc.) with gas or liquid chromatographic analysis proved to be indispensable for true detection of PAHs in sample materials (Barreca et al., 2014; Szulejko et al., 2014). Maximum usage of organic solvents (e.g., acetone, hexane, dichloromethane, petroleum ether and toluene) has also been noticed in numerous extraction applications (Birke et al., 2018;

Kargar et al., 2017; Klingberg et al., 2022; Niu et al., 2019_b; Oishi, 2018; Sari et al., 2021; Yang et al., 2017).

There is a pressing need for detailed examination of performance characteristics of analytical techniques for advancement of laboratory-based standardization protocols and quality assurance/control checks when dealing with desired matrices of heterogeneous composition (Steiner et al., 2020). It is very common that the extracted solutions would always contain some impurities and interferents, tampering with the analytical outcome and inducing experimental bias which generates false positive results (leading to faulty interpretation or erroneous data due to overlapping peaks of matrix components masking the analyte of interest) during PAHs quantitation. Therefore, the impure extracts often require effective purification and concentration stages to increase the sensitivity and accuracy of the analysis with reduction in the source of experimental bias (Gerssen et al., 2009). Extract clean-up procedures involving adsorbents or solid-phase extraction cartridges are generally used for complex matrices (Blasco et al., 2007; De Nicola et al., 2016; Hussain and Hoque, 2015; Ray et al., 2021; Tian et al., 2019; Yang et al., 2017). Critical evaluation of extraction process parameters through optimization studies is of utmost importance to maximize the extraction yield and deduce the interactive influences of the operating variables. Single factor and multivariate optimization (using Box–Behnken, Taguchi, Plackett–Burman, full factorial, central composite or combined designs) are well-recognized techniques for improvement of the efficacy of sample preparation methodologies (Fazeli et al., 2020; Foan and Simon, 2012; Frempong et al., 2021; Scaramboni et al., 2021). Hence, the main aim of this work was to provide a comprehensive comparative analysis of Soxhlet extraction with other methods [viz. mechanical stirring, sonication and microwave-assisted Soxhlet extraction (MAE)] for performance validation in PAHs recovery from the leaves of *Murraya paniculata* (L.) Jack and to optimize the suitability of extracting solvents and extraction time with the objective of determining the optimum extraction conditions for maximized PAHs yield.

3.2. Materials and methods

3.2.1. Sampling and sample pretreatment

Precisely, small branches, facing the roads, from 2 to 3 *Murraya* plant species (on the basis of availability) within 2–3 m height from the road level at JDV area were sampled with hand pruners for maximum pollution effects (Tian et al., 2019; Yang et al., 2017). After collection, healthy and mature leaves were hand-picked using nitrile (sterile) gloves to prevent external contamination through direct contact and subsequently stored in polyethylene zip lock pouch

bags for direct shipment to the testing laboratory. Replicate samples were also taken from each zone for robust analytical measurements.

Pretreatment of the plant leaves involved prewashing, drying and grinding for acquiring desired performance of the process. After washing of the dry mud and other residues from plant foliage, samples were lyophilized (Lyophilizer, Eyela FDU-1100) and dry leaf powder was produced thereafter with a porcelain mortar and pestle for long-term preservation.

3.2.2. Optimization of extraction factors for isolation of PAHs from plant leaves

3.2.2.1. Extraction methods

Mechanical stirring

Freeze-dried samples of leaves [10 g on dry weight (d.w.) basis] were extracted with 120 mL of high-purity n-hexane (primary solvent generally employed for all analyte groups) in an Erlenmeyer flask for 6 h at room temperature using a magnetic stirrer (Remi 2MLH) at moderate speed (Fig. 12). The extracts were then passed through Whatman Grade 1 filter papers for filtration. The entire process was repeated thrice to ensure complete extraction of target PAHs and the filtered extracts were combined together for further purification and analysis.

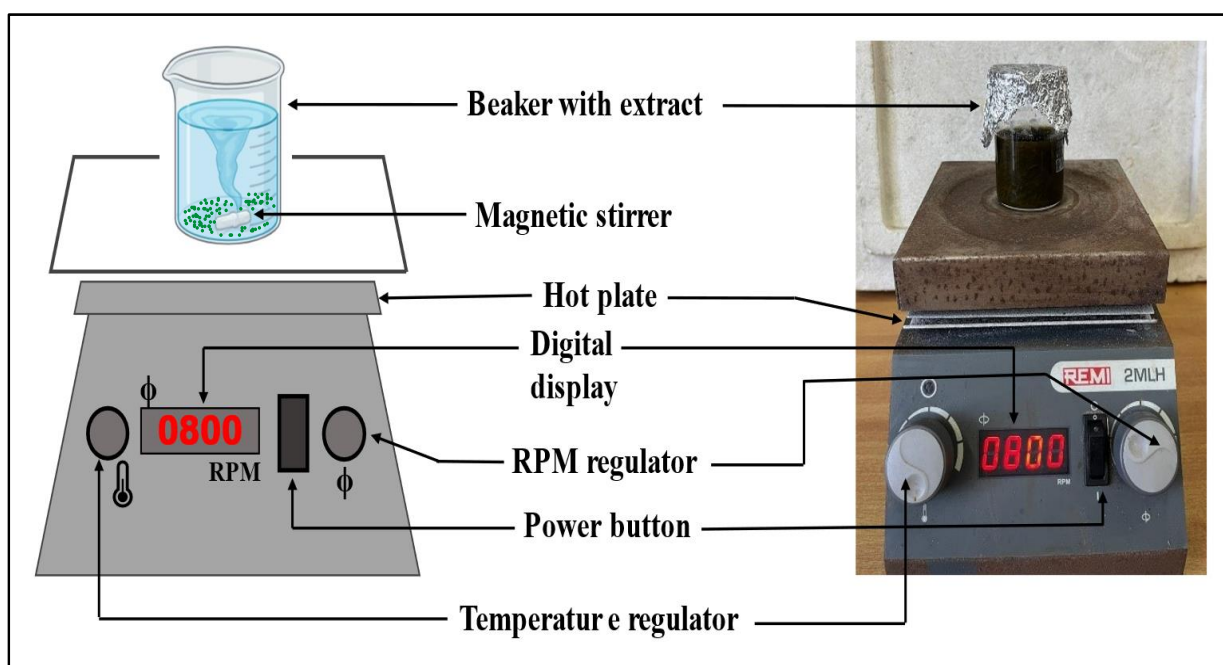


Fig. 12. Schematic representation (left) and laboratory set-up (right) of mechanical stirring.

Sonication

About 5 g of sample (leaf dry mass) was sonicated with a probe (or sonotrode MS7 of tip diameter 7 mm) sonicator [Ultrasonic Processor UP50H (50 W, 30 kHz), Hielscher Ultrasonics, Germany] (Fig. 13) at 70% amplitude for 30 min utilizing n-hexane as solvent. Pulsed mode of sonication was applied for extraction to minimize heat generation (Delacour et al., 2019). Six cycles of 5 min sonication with subsequent 5 min of rest period were carried out, and 30 mL of fresh solvent being added to the system in each cycle. Temperature as recorded during the operation was in the range of 25–35 °C. The processing conditions given by Benson et al. (2018) and Herrera-Pool et al. (2021) were followed with some amendments. After consecutive extractions, all the sample extracts were recovered, integrated and centrifuged (Remi R-8 M Plus laboratory centrifuge) at 2800 rpm for 15 min. The supernatant was collected afterward and stored in a borosilicate glass reagent bottle with screw cap at 4 °C for future investigation.

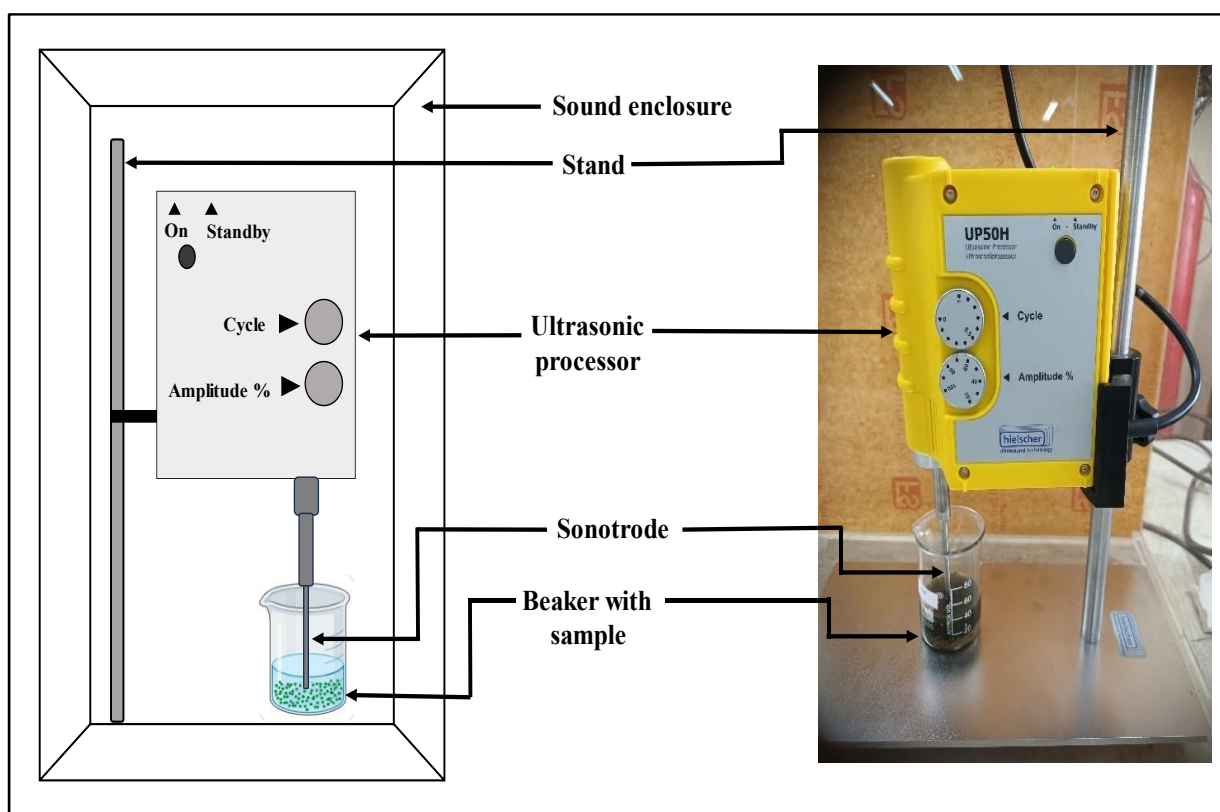


Fig. 13. Schematic representation (left) and laboratory set-up (right) of sonication extraction.

Soxhlet extraction

10 g (d.w.) of sample was Soxhlet extracted for 6 h in 120 mL of n-hexane. A filter paper thimble containing the solid plant matrix was loaded in the main extractor chamber of the apparatus (Fig. 14) for continuous extraction by solvent reflux; the exhaustive extraction cycles being repeated several times throughout the duration at boiling point temperature of the solvent. The final extract was then refrigerated for further separation and clean-up to get active PAHs fraction.

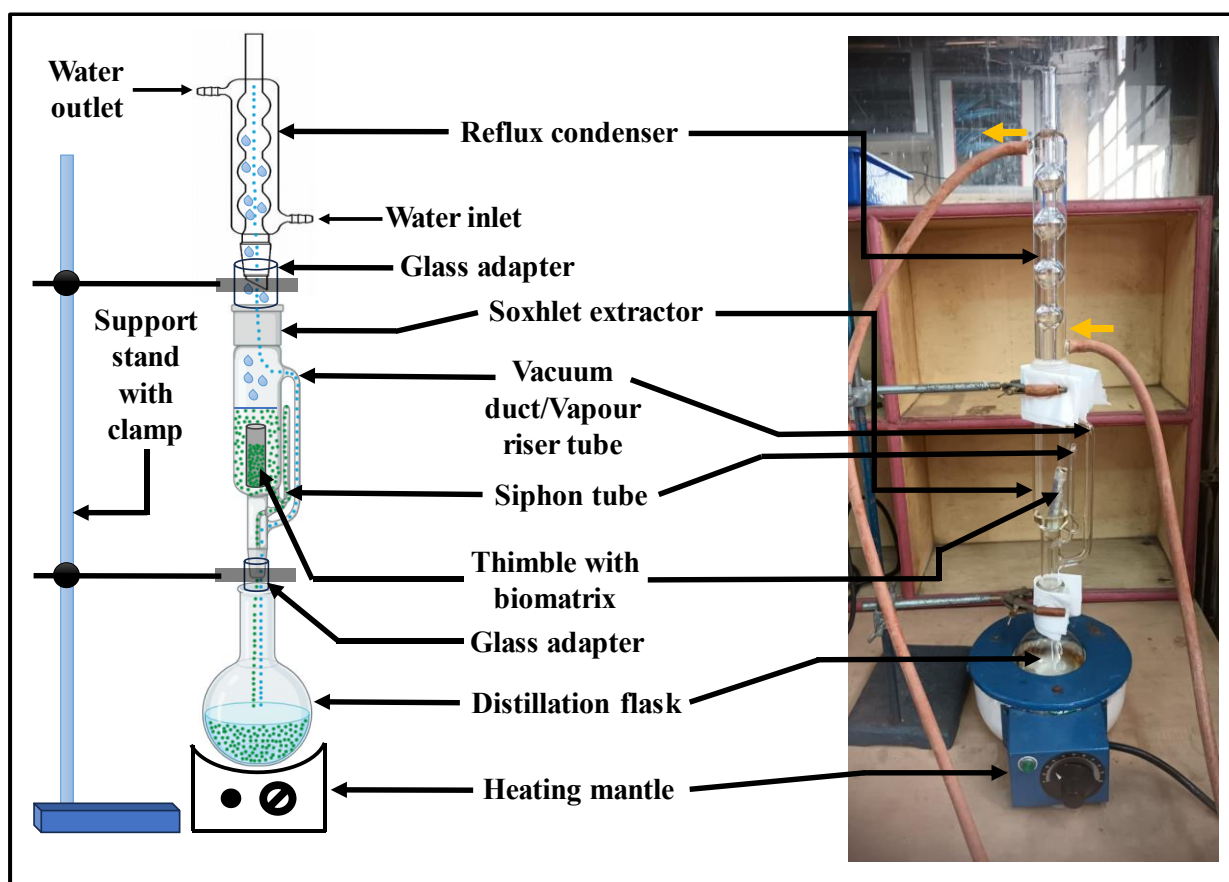


Fig. 14. Schematic representation (left) and laboratory set-up (right) of the conventional Soxhlet apparatus used for experimentation.

Microwave-assisted Soxhlet extraction (MAE)

A microwave extractor [Microwave synthesis/extraction system, Model: NuWav-Uno (11-19/Uno-112), NutechAnalytical Technologies, Pvt. Ltd., Kolkata] was deployed for PAHs extraction (Fig. 15). The methodology adopted in the study was slightly modified from the procedures recommended by Herbert et al. (2006) and Ratola et al. (2009). Lyophilized

samples (~3 g) were mixed with 90 mL of n-hexane:acetone mixture (9:1 v/v) for extraction up to 30 min under 500 W microwave power, 50 °C temperature and 500 rpm stirring speed. After extraction, the extract was filtered and the filtrate was then transferred to a borosilicate glass bottle for sample storage.

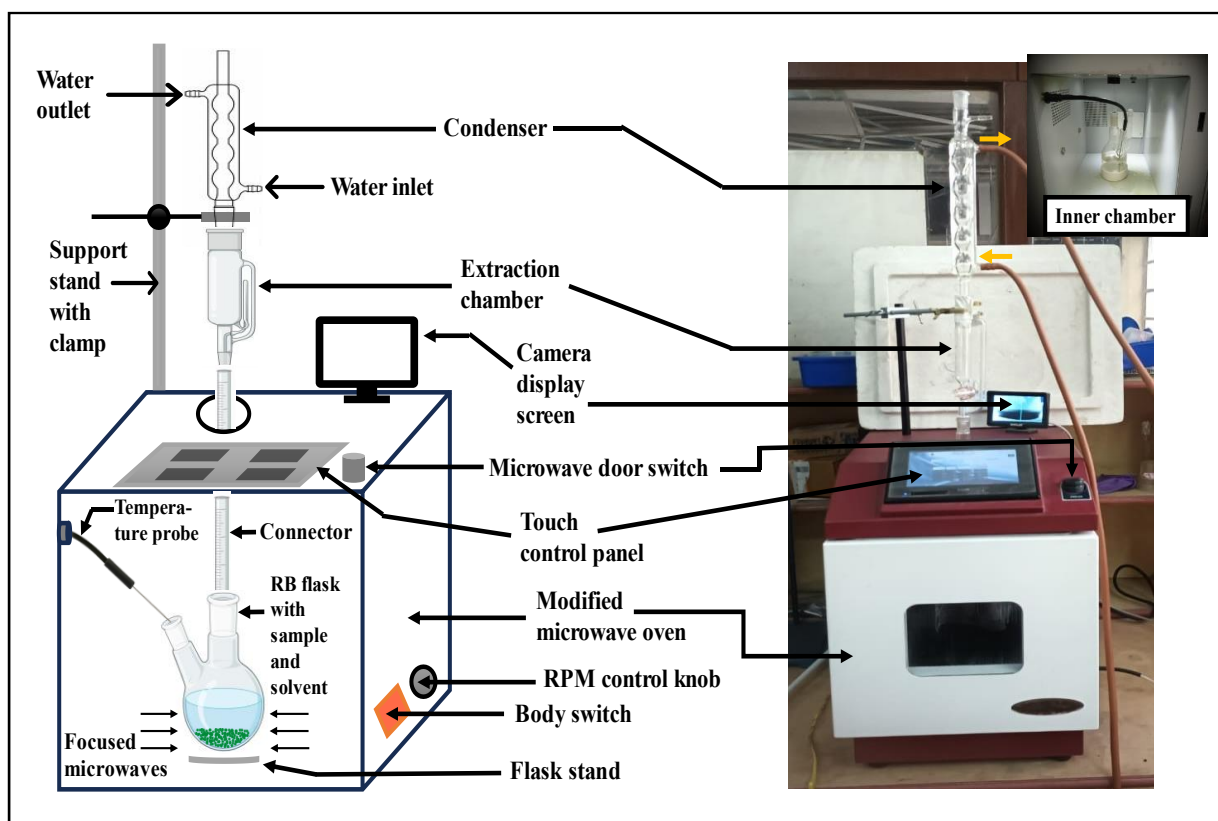


Fig. 15. Schematic diagram (left) and laboratory set-up (right) of the modified microwave oven used for extraction purposes.

3.2.2.2. Selection of extracting solvent for maximum recovery of PAHs

After validation of the favorable method, efficiencies of various solvents with different polarities (from polar to non-polar range) were analyzed in respect of their interactions with the plant matrix and PAHs extraction ability. Extraction experiments were conducted for 6 h with five separate solvent systems: acetone (relative polarity, RP: 0.355), dichloromethane (DCM) (RP: 0.309), n-hexane (RP: 0.009), toluene (RP: 0.099) (Reichardt and Welton, 2010) and acetone:n-hexane (1:1 v/v) (Merck, Darmstadt, Germany), for the purpose of identifying the best extraction solvent for highest analyte recoveries. In case of binary mixture, solvent composition in volume % has a bearing on the measurement of polarity (Zalewski et al., 1991).

3.2.2.3. Optimization of extraction time

The extraction time was optimized with the best-suited solvent to ascertain the equilibrium time for maximization of PAHs yield. Extractions were designed for 5 h, 6 h, 7 h and 8 h duration, and recoveries of all the analytes were compared among the designed experiments.

3.2.3. Extract purification and concentration

Extract clean-up was achieved through silica gel column chromatography to fractionate PAHs from matrix interferences. The extracts were loaded on a chromatographic column fitted to a retort stand and filled with anhydrous sodium sulfate (2 g; assay $\geq 99.0\%$) and preheated silica gel (10 g; 100–200 mesh, chromatographic quality). However, before packing of the column, silica gel slurry was prepared each time in the same organic solvent as used for sample extraction. Cotton plugging was also done at the bottom of the column to maintain a uniform level of silica gel throughout the process. Once the silica bed was in form, excess solvent was drained out taking precaution to avoid development of cracks in the bed. The column was conditioned with 25 mL of n-hexane before purification. In every case, sample extract of volume 8 mL was passed through the silica column and PAHs were eluted with 25 mL of n-hexane in polypropylene vials with screw cap. The eluates were concentrated within a rotary evaporator (Buchi R-3 Rotavapor) under reduced pressure, resuspended in methanol (HPLC grade, assay $\geq 99.9\%$) to make up the final volume to 4 mL and stored in a refrigerator till analysis.

3.2.4. Instrumental analysis of PAHs using GC-MS and HPLC-UV

Purified extracts were analyzed by GC–MS (Gas chromatograph with Quadrupole mass analyser, Thermo Fisher Scientific, United States; Model: Trace GC Ultra; Model No.: 320080111) for proper identification of PAHs at low levels. GC–MS was equipped with a Thermo Scientific TG-5MS capillary column coated with 5% diphenyl/95% dimethyl polysiloxane (Length: 30 m; I.D.: 0.25 mm; Film: 0.25 μm ; Maximum temperature: 330/350 $^{\circ}\text{C}$) and the oven temperature programme followed in the present study for qualitative assessment was in line with the EPA Method 610 (EPA, 1984) and the one suggested by Dong et al. (2012). For obtaining high resolution analyte peaks, temperature programme was maintained as follows: initial temperature kept at 40 $^{\circ}\text{C}$ for 1 min; then increased to 120 $^{\circ}\text{C}$ at a temperature ramping of 25 $^{\circ}\text{C min}^{-1}$ and held for 5 min; again, raised to 160 $^{\circ}\text{C}$, temperature ramping being 10 $^{\circ}\text{C min}^{-1}$ and held for 5 min; ultimately, final temperature was raised to 300

°C at the rate of 5 °C min⁻¹ and held for 15 min. The GC–MS instrument conditions are given in [Table 11](#). Mass spectra of PAHs were detected using electron impact ionization (EI) detector and selected ion monitoring (SIM) mode for their high level of accuracy, specificity and sensitivity, maintaining the detector temperature at 280 °C. Xcalibur™ software (Thermo Fisher Scientific) was used for the analysis of analyte peaks. PAHs were identified by comparing the retention time (RT) of individual PAHs in each sample with that of the pure components in the PAHs standard mix. Quantification (mass) ions (m/z) were also recorded from mass spectra for confirmation of the presence of target PAHs in the test samples. RT and ions of the individual PAH congeners in standard mix are given in [Table 12](#). Structural determination of PAHs was also simultaneously carried out from MS library.

Qualitative analysis had been conducted using proper quality control and assurance checks and following EPA Method 610 ([EPA, 1984](#)). All the glassware used in the experiment were thoroughly rinsed with HPLC grade methanol and baked in oven for about 6–8 h. Method feasibility was checked through procedural spike blank runs for every set of samples using the same analytical protocol. It was ensured that the target compounds were absent in the procedural blanks for avoidance of method interferences. Duplicate samples were also run to verify the efficiencies of sampling, extraction and analysis.

Table 11

Operating conditions for GC-MS analysis of PAHs using TG-5MS capillary column (Length: 30 m; I.D.: 0.25 mm; Film: 0.25 µm).

GC	
Carrier gas	Helium (99.99%); flow rate: 1 mL min ⁻¹ ; linear velocity: 10 mL s ⁻¹
Operation mode	Constant pressure
Inlet temperature	40 °C
Oven temperature	300 °C
Temperature Program	40-120-160-300 °C
Injection volume	1 µL
Split ratio	Operated at split less mode
Run time	51 min

MS	
Transfer line temperature	280 °C
Source temperature	200 °C
Solvent delay	3 min
Scan mass range	30-600 m/z

Table 12

GC-MS detection of PAHs in the certified reference material.

EPA-PAHs	RT (min)/Quantification ion (m/z) of PAHs in the analytical standard mix
NAP	6.23, 6.74/128
ACY	10.23/152
ACE	10.60/154
FLU	12.89/166
PHE	15.37/178
ANT	15.37/178
FLA	19.30/202
PYR	20.59/202
BaA	24.96/228
CHR	24.96/228
BbF	28.37/252
BkF	28.37/252
BaP	29.69/252
DB[ah]A	36.75/278
IP	36.75/276
B[ghi]P	38.89/276

PAHs were also eventually quantified using a high performance liquid chromatograph (HPLC, Waters, USA) coupled to UV detection at 254 nm (Waters 2489 UV/Visible detector) and associated with a reversed phase Waters PAH C18 Column, S-5 μm (4.6 mm i.d. \times 250 mm length) for separation of PAHs and a binary pump (Waters 1525) for drawing two solvents together under high pressure (maximum limit: 5000 psi) creating a gradient. Injector port of the HPLC system was fitted to a 20 μL loop with a sample injection volume of 20 μL .

Acetonitrile (ACN) and water of HPLC grades were used as mobile phases, and the gradient elution was programmed at a flow rate of 1.5 mL min⁻¹ as per the following protocol: 50% ACN for initial 5 min, then increased to 100% in 20 min and maintained for 28 min, again reduced to 50% within 32 min and held for 37 min (Waters Corporation, 2008). Column temperature was set at 30 °C with a total run time of 37 min. The method as described above was based on the guidelines of EPA Method 550.1. Breeze² software was employed for data acquisition and processing. RTs of the sample peaks were compared to that of the injected reference standards for recognizing the analytes of interest. A processing method was further developed for determination of concentrations of PAHs in test samples with respect to the certified standard mix [with 10 µg each mL⁻¹ of 16 EPA-PAHs, such as naphthalene (NAP), acenaphthylene (ACY), acenaphthene (ACE), fluorene (FLU), phenanthrene (PHE), anthracene (ANT), fluoranthene (FLA), pyrene (PYR), benzo[a]anthracene (BaA), chrysene (CHR), benzo[b]fluoranthene (BbF), benzo[k]fluoranthene (BkF), benzo[a]pyrene (BaP), dibenzo[a,h]anthracene (DB[ah] A), indeno[1,2,3-cd]pyrene (IP) and benzo[g,h,i]perylene (B[ghi]P)]. Quality of the analytical results had been verified by assessing calibration standards, method blanks and spiked samples periodically during the study under similar experimental conditions. Absence of analytes in the blank samples was confirmed, and replicate samples were also tested for method accuracy and validation. The mean recoveries of PAHs in spiked samples varied between 78 and 99% (Table 13) and the corresponding HPLC chromatogram has been shown in Fig. 16. Percentages of recovery of PAHs extracted from test samples were determined against a standard solution as follows (Eq. 5) —

$$Recovery (\%) = \frac{\text{Measured concentration of extracted PAHs}}{\text{Spiked concentration of standard PAHs (}=10 \mu\text{g mL}^{-1}\text{)}} \times 100 \quad (5)$$

Table 13

Percentage recovery of 16 EPA-PAHs extracted from *Murraya* leaves.

PAHs	Recovery (%)
NAP	90.12
ACY	97.57
ACE	90.61
FLU	85.32
PHE	93.43

ANT	95.85
FLA	77.75
PYR	84.31
BaA	91.13
CHR	99.43
BbF	82.97
BkF	87.59
BaP	92.90
DB[ah]A	78.24
IP	86.70
B[ghi]P	80.84

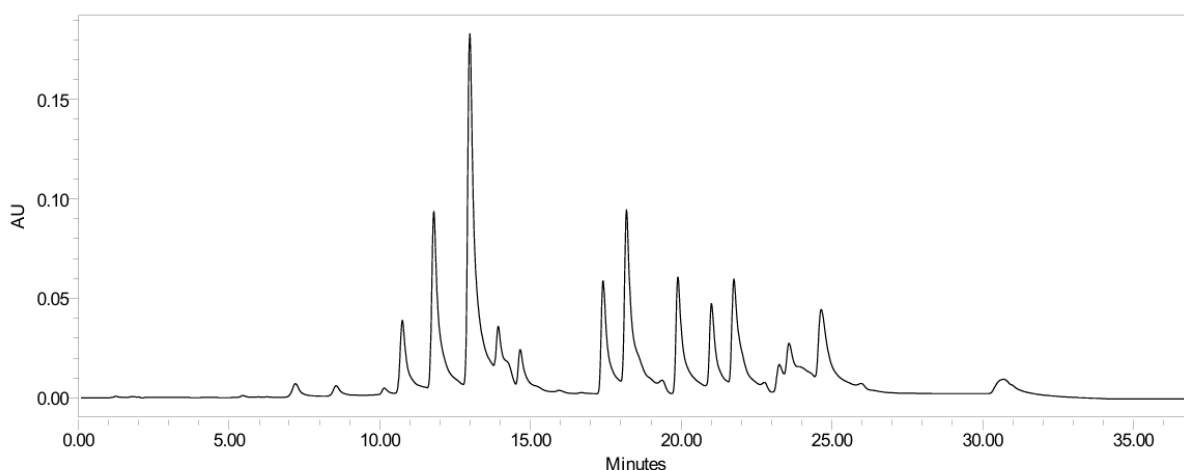


Fig. 16. Chromatogram revealing the recovery peaks of 16 EPA-PAHs.

The limits of detection (LOD) and limits of quantification (LOQ) of individual PAHs as calculated with the following equations (Eqs. 6, 7 and 8) based on the slope of calibration curve (peak area vs. concentration) (ref. Table 14) using regression statistics (Deokar et al., 2016; Saadati et al., 2013) for the analytical method are shown in Table 15.

$$LOD = \frac{3.3 \times S}{b} \quad (6)$$

$$LOQ = \frac{10 \times S}{b} \quad (7)$$

where, S = Standard deviation of the intercept and

b = Slope of the calibration curve.

Standard deviation of the intercept can again be calculated using the expression given below—

$$S = SE \times \sqrt{N} \quad (8)$$

where, SE = Standard error of the intercept (can be estimated from regression analysis) and

N = Number of observations.

Table 14

Calibration data of 16 EPA-PAHs.

PAHs	Regression equation (y = Peak area ($\mu\text{V} \cdot \text{sec}$), x = PAHs concentration ($\mu\text{g mL}^{-1}$))	Coefficient of determination (R^2)	Concentration range of calibration ($\mu\text{g mL}^{-1}$)
NAP	$y = 124667x + 2E + 06$	0.9818	0.05-10
ACY	$y = 242594x + 211805$	0.9903	0.05-10
ACE	$y = 209393 - 63262$	0.9928	0.05-10
FLU	$y = 176111x + 2E + 06$	0.9935	0.05-10
PHE	$y = 166853x + 4E + 06$	0.9858	0.05-10
ANT	$y = 327606x + 441572$	0.994	0.05-10
FLA	$y = 27837x + 370709$	0.9926	0.05-10
PYR	$y = 46273x + 32877$	0.9972	0.05-10
BaA	$y = 55077x + 795163$	0.9828	0.05-10
CHR	$y = 240344x - 13505$	0.9885	0.05-10
BbF	$y = 241876x - 15158$	0.9936	0.05-10
BkF	$y = 909462x - 161282$	0.994	0.05-10
BaP	$y = 778914x + 569110$	0.9862	0.05-10
DB[ah]A	$y = 326264x + 925712$	0.9919	0.05-10
IP	$y = 108684x + 105425$	0.9866	0.05-10
B[ghi]P	$y = 630367x + 1E + 06$	0.9965	0.05-10

Table 15

LOD and LOQ of individual PAHs in chromatographic (HPLC) analysis.

EPA-PAHs	LOD ($\mu\text{g g}^{-1}$)	LOQ ($\mu\text{g g}^{-1}$)
NAP	0.003	0.09
ACY	0.002	0.06
ACE	0.002	0.06
FLU	0.002	0.05
PHE	0.003	0.08
ANT	0.002	0.05
FLA	0.002	0.06
PYR	0.001	0.03
BaA	0.003	0.09
CHR	0.002	0.07
BbF	0.002	0.05
BkF	0.002	0.05
BaP	0.003	0.08
DB[ah]A	0.002	0.06
IP	0.003	0.07
B[ghi]P	0.001	0.04

3.3. Results and discussion

3.3.1. Comparison of extraction methods

Four distinct extraction methods were compared relating to ease of application, selectivity, extraction efficiency and yield. The results of PAHs extraction acquired with different methods are indicated in [Table 16](#). Both Soxhlet ($272.07 \pm 26.15 \mu\text{g g}^{-1}$) and MAE ($280.17 \pm 15.46 \mu\text{g g}^{-1}$) techniques outperformed sonication ($173.61 \pm 13.02 \mu\text{g g}^{-1}$) and mechanical stirring ($122.06 \pm 5.19 \mu\text{g g}^{-1}$) with respect to total PAHs yield based upon specific macroscopic and microscopic reasons. Mass spectral confirmation of PAHs detected in all the optimization studies (refer [Tables 16, 17](#) and [18](#)) was also validated through GC–MS analysis

with reference to the results presented in [Table 12](#) for analytical standard mix. Mass transfer of PAHs from the solid plant matrix to the extraction solvent is regulated by the mechanisms of convection and diffusion. Moreover, PAHs concentration difference between the leaf matrix and solvent is the driving force which controls the rate of extraction ([Pinelo et al., 2006](#)).

Soxhlet technique is a semi-batch process involving temperature acceleration ([de Castro and Ayuso, 2000](#)). Elevated temperature in Soxhlet extraction expedites the kinetics of mass transfer by increasing the solubility of solute in the solvent and hence, improves the extraction efficiency. Besides, high temperature (1) reduces solvent density, viscosity and surface tension which assists in better solvent selectivity, wettability, diffusivity and penetrability for maintaining contact with the solid surface, (2) drastically alters the surface equilibrium by denaturing the analyte–analyte (cohesive) and analyte–matrix (adhesive) interactions owing to the reduction in activation energy of desorption, (3) enhances the solvation power of solvent and (4) allows analyte diffusion into the surface of the matrix along with the mass transfer of targeted solutes into the extracting solvent ([Malik and Mandal, 2022](#)). Thus, in Soxhlet method, complete extraction of desired PAHs was possible by virtue of multiple siphoning as the solvent could reach the active sites of the matrix more easily at high temperature and the rapid rate of diffusion promoted mass transfer of PAHs which, in turn, increased the extraction rate. Furthermore, a favorable PAHs concentration gradient (almost constant) was maintained via continuous recycling of fresh solvent through the matrix (with the aid of boiling and condensation) which prevented PAHs saturation in the extractant making the extraction process exhaustive in nature, enhanced the transfer equilibrium and eventually the mass transfer rate in Soxhlet technique ([Malik and Mandal, 2022](#)).

In MAE, application of electromagnetic energy (microwaves) to the sample matrix caused damage to the structure of cell membrane, thereby increasing the maximum release of PAHs into the solvent as in the case of Soxhlet. Homogeneous heating by ionic conduction and thermal agitation due to dipole rotation improved the diffusion of solvent into the sample and stimulated the partitioning of PAHs from the matrix to the extractant ([Veggi et al., 2013](#)). Induced heat in MAE caused evaporation of residual moisture present in the sample, creating appreciable intracellular pressure which ruptured the cell walls of the leaf matrix and enhanced the leaching of PAHs ([Ngamkhae et al., 2022](#)). Increased solubility of PAHs, solvent dispersion and selectivity because of high temperature also raised the extraction efficiency without degradation of analytes. Additionally, the unidirectional flow of heat and mass transfer to the outer side of the cells was responsible for high extraction yield along with reduction in process time and energy loss ([Veggi et al., 2013](#)).

Sonication technique transmits the sound energy of ultrasonic waves while propagating through the fluid mix, promoting high solvent inflow into plant matrix, intimate contact between them and rate of mass transfer of analytes. Wave propagation also causes frequent changes in the fluid density (compression and rarefaction) resulting in creation and rupture of vapor bubbles in quick succession (cavitation action) throughout the solvent. Bursting of such bubbles facilitated cell wall breakdown and simultaneous release of PAHs into the extraction solvent. [Smith et al. \(2006\)](#) reported that the ultrasonic-assisted extraction (UAE) is not very much effective for LMW PAHs as compared to Soxhlet and microwave-assisted extraction (MAE) owing to low recovery rates varying between 44 and 76%. In the present study also, recovery of LMW PAHs (NAP, ACY, ACE, FLU, PHE and ANT) through sonication was not satisfactory [only ACY and ACE could be detected (ref. [Table 16](#))] due to, probably, the lower temperature range (25–35 °C) of the process ([Ngamkhae et al., 2022](#)).

Mechanical stirring or agitation at room temperature (in a simple shake flask placed on a magnetic stirrer) is an easy extraction technique with low requirements for glassware. However, the stirring method could not efficiently extract the HMW PAHs and the extraction efficiency was appreciably lower than the other methods (ref. [Table 16](#)) because of poor selectivity for PAHs, giving inappropriate results ([Berset et al., 1999](#); [Graham et al., 2006](#)). Normally, faster extraction occurred initially when the difference in PAHs concentration was maximum. But gradually, the extraction rate decelerated with the decrease in concentration difference, thereby causing a sharp decline in the rate of mass transfer. The extended extraction time did not further increase the yield once the saturation point was reached ([Kalbe et al., 2008](#)). Considerably higher rate of solvent evaporation was also witnessed in agitation extraction, leading to PAHs losses during evaporation.

The above-cited benefits rendered Soxhlet and MAE more effective over other techniques. [Cicero et al. \(2000\)](#) also obtained comparable recoveries in both the cases for the extraction of polychlorinated biphenyl (PCB) congeners from marine sediments. The highest extraction yield of bioactive compounds was again recorded by [Ngamkhae et al. \(2022\)](#) with MAE in contrast to UAE. A comparative study between MAE and UAE by [Ratola et al. \(2009\)](#) for PAHs extraction from pine needles and bark showed relatively same recovery results for the two methods. Hence, sonication might give better results with high extraction efficiency in some other species under optimized extraction conditions. Many studies have suggested high recoveries of PAHs from leaf matrices of various plant species (*Pinus sylvestris*, *Acer campestre*, *Pinus koraiensis*, *Cinnamomum camphora* and *Phyllostachys edulis*) using Soxhlet extraction ([Bi et al., 2018](#); [Chun, 2011](#); [Hubert et al., 2003](#); [Yang et al., 2017](#)). Therefore, in

this study, all the other experiments were carried out with the Soxhlet technique. But, considering the aforesaid advantages and extraction yield of MAE, design and optimization of its parameters have also been performed and discussed in the next chapter.

Table 16

Comparison between extraction methods.

EPA-PAHs	PAHs concentration ($\mu\text{g g}^{-1}$ d.w.) in the leaf extracts obtained with different methods			
	Mechanical stirring	Sonication	Soxhlet extraction	MAE
NAP	8.56 \pm 1.92	nd	35.93 \pm 3.19	nd
ACY	9.84 \pm 1.97	5.07 \pm 1.57	8.60 \pm 1.02	68.67 \pm 4.96
ACE	nd	54.00 \pm 11.31	1.38 \pm 0.59	34.62 \pm 7.98
FLU	48.90 \pm 9.09	nd	nd	nd
PHE	5.38 \pm 1.61	nd	7.07 \pm 0.91	1.26 \pm 0.19
ANT	28.74 \pm 4.34	nd	46.92 \pm 9.77	1.05 \pm 0.34
FLA	19.54 \pm 2.19	2.10 \pm 0.83	51.13 \pm 5.77	2.34 \pm 0.32
PYR	nd	1.65 \pm 0.49	16.85 \pm 3.17	0.21 \pm 0.02
BaA	nd	0.96 \pm 0.36	3.05 \pm 0.38	0.60 \pm 0.28
CHR	nd	0.18 \pm 0.06	2.52 \pm 0.23	0.15 \pm 0.02
BbF	0.18 \pm 0.11	0.57 \pm 0.04	0.85 \pm 0.24	0.24 \pm 0.06
BkF	0.56 \pm 0.18	0.36 \pm 0.13	2.24 \pm 0.40	0.33 \pm 0.11
BaP	0.36 \pm 0.06	0.15 \pm 0.06	nd	0.84 \pm 0.17
DB[ah]A	nd	0.24 \pm 0.04	4.68 \pm 1.63	62.10 \pm 8.59
IP	nd	38.64 \pm 8.32	34.96 \pm 7.49	45.06 \pm 5.18
B[ghi]P	nd	69.69 \pm 11.79	55.89 \pm 4.01	62.70 \pm 5.32
Total PAHs concentration	122.06 \pm 5.19	173.61 \pm 13.02	272.07 \pm 26.15	280.17 \pm 15.46

**Optimization studies done using the plant samples of JDV site only. For other experimental runs, optimized parameters were used.

‘nd’: Not detected.

3.3.2. Choice of solvent for PAHs extraction

Separation by solid–liquid extraction is greatly influenced by solvent selection, considering solubility, concentration and nature of analytes, capacity of solvents to penetrate and interact with the sample matrix, net polarities of solvents (correlated with their dipole moments, dielectric constant, viscosity, surface tension and cohesive energy density) and kinetic processes of mass transfer (Baskar et al., 2019). High solute distribution coefficient with minimized solvent losses plays a crucial role in solvent selection, and solubility of solute is also mediated by the physicochemical properties and chemical structures of both the solute and

solvent (Bonventre, 2014). Table 17 portrays the Soxhlet-based PAHs yields against the studied solvents, and the observed trend was: extraction yield ($103.70 \pm 4.47 \mu\text{g g}^{-1}$)_{with acetone} < extraction yield ($127.79 \pm 5.34 \mu\text{g g}^{-1}$)_{with acetone:n-hexane} < extraction yield ($148.06 \pm 19.37 \mu\text{g g}^{-1}$)_{with DCM} < extraction yield ($256.35 \pm 6.39 \mu\text{g g}^{-1}$)_{with n-hexane} < extraction yield ($279.49 \pm 16.93 \mu\text{g g}^{-1}$)_{with toluene}.

Inefficiency of acetone to extract HMW PAHs (yield: $43.50 \mu\text{g g}^{-1}$) is evident from Table 17. Similarly, analysis of the extracts obtained with DCM and acetone:n-hexane mixture specified the presence of mainly LMW PAHs (96.48 and $79.20 \mu\text{g g}^{-1}$, respectively) and very few HMW PAHs (only BaP, DB[ah]A and IP). But, toluene and n-hexane showed higher selectivity by extracting maximum amount of LMW (117.83 and $103.80 \mu\text{g g}^{-1}$, respectively) and HMW PAHs (161.66 and $152.55 \mu\text{g g}^{-1}$, respectively) from leaf samples. It can be clearly seen that the non-polar solvents were more suitable for the extraction of PAHs. For acetone:n-hexane mixture, although good PAHs recoveries have been reported in case of other solid matrices (Haleyur et al., 2016; Janska et al., 2004), yet, in the current study, lower extraction output was attained when compared with toluene and n-hexane separately. This could have resulted from the complexity of plant cell membrane composed of non-polar lipid tails restricting the transmembrane permeation of polar acetone molecules to a certain degree and hindering, thereby, the diffusion path of n-hexane through the plasma membrane for extraction of PAHs (Orsi et al., 2009; Shinoda, 2016). So, the above phenomenon had affected the extraction efficiency to a great extent. Least extraction capacity of acetone for non-polar PAHs can be ascribed to its high polarity as solvent extraction works on the basic principle of ‘like dissolves like’ (law of similarity and miscibility which states that a solute better dissolves in a solvent having close relative value of polarity) (Kamarudin et al., 2021) and impermeability of biological membrane with lipid bilayer limiting the free entry of highly polar molecules. DCM is a moderately polar solvent and thus, exhibited lower extraction recovery of hydrophobic PAHs. In addition, it is not recommended to be used as an extraction solvent on account of its volatility (boiling point: 39.6°C) which caused huge solvent loss in Soxhlet method. In contrast, toluene and n-hexane being most non-polar in nature (having low dipole moments), diffusion across the hydrophobic core of lipid bilayer enhanced the extraction performance. According to the results obtained (Table 17), toluene has been proved to be an ideal solvent which solvated almost all the lipophilic PAHs molecules of the matrix completely by means of dispersion interactions. Good relative yields of PAHs from the samples of tree bark, pine needles and moss species with the application of toluene in Soxhlet technique were also documented by Birke et al. (2018) and Oishi (2018). Alternatively, during dynamic sonication-

assisted extraction of PAHs from lichen samples, toluene did not show adequate method efficiency implying the significances of the process and matrix properties on extraction yield (Domeno et al., 2006).

Table 17

Variation in PAHs recovery from plant leaves using different solvents in Soxhlet extraction.

Concentration ($\mu\text{g g}^{-1}$ d.w.) of PAHs extracted from leaf matrix with various solvents					
EPA-PAHs	Acetone	DCM	n-Hexane	Toluene	Acetone: n-Hexane (1:1)
NAP	13.59 \pm 4.24	29.05 \pm 6.61	29.10 \pm 4.55	36.34 \pm 3.34	27.89 \pm 4.18
ACY	3.32 \pm 1.59	18.69 \pm 2.66	5.70 \pm 3.45	nd	nd
ACE	nd	1.43 \pm 0.53	10.94 \pm 3.94	1.13 \pm 0.32	nd
FLU	nd	0.36 \pm 0.17	nd	24.26 \pm 4.09	17.02 \pm 3.24
PHE	7.88 \pm 2.27	2.42 \pm 0.58	16.48 \pm 2.05	28.33 \pm 4.09	14.12 \pm 1.42
ANT	35.41 \pm 4.17	44.53 \pm 5.62	41.58 \pm 5.28	27.77 \pm 5.30	20.18 \pm 2.84
FLA	nd	32.34 \pm 5.75	31.39 \pm 9.49	18.34 \pm 4.79	9.87 \pm 4.15
PYR	19.12 \pm 1.99	nd	19.94 \pm 6.45	14.17 \pm 4.78	nd
BaA	20.84 \pm 3.79	nd	2.24 \pm 1.09	14.56 \pm 2.35	nd
CHR	3.54 \pm 1.26	nd	4.24 \pm 1.43	29.76 \pm 5.27	nd
BbF	nd	nd	11.83 \pm 6.01	18.94 \pm 3.80	nd
BkF	nd	nd	2.99 \pm 1.48	16.63 \pm 2.15	nd
BaP	nd	2.36 \pm 0.74	nd	15.82 \pm 3.69	12.74 \pm 2.99
DB[ah]A	nd	6.42 \pm 3.08	6.49 \pm 2.40	12.46 \pm 0.91	15.16 \pm 6.06
IP	nd	10.46 \pm 1.61	26.98 \pm 4.36	2.90 \pm 0.54	10.81 \pm 1.29
B[ghi]P	nd	nd	46.45 \pm 5.36	18.08 \pm 1.29	nd
Total PAHs concentration	103.70 \pm 4.47	148.06 \pm 19.37	256.35 \pm 6.39	279.49 \pm 16.93	127.79 \pm 5.34

3.3.3. Effect of extraction time on PAHs yield

It is necessary to optimize the extraction period in order to protect the analytes, reduce energy consumption and cost of the process. So, duration of extraction demonstrated a strong impact on the effective recovery of PAHs from *Murraya* leaves. The performance of the extraction experiments at different time intervals employing toluene is depicted in Table 18. The results revealed that the efficient extraction time (i.e., when equilibrium condition achieved between inside and outside of the solid matrix following convective mass transfer) for obtaining the

highest number and quantity of extracted PAHs was up to 6 h (yield: $274.24 \pm 4.20 \mu\text{g g}^{-1}$), beyond, which, the extraction efficacy reduced (ref. Table 18). Majority of LMW PAHs were not detected in 5 h of experimental run (only NAP and ACY present), probably due to the reason that the extraction equilibrium had not reached (i.e., persistence of a non-equilibrium state between the matrix and the solvent) at that time for all the analytes. Typically, exposure to longer extraction time disrupts plant cell membrane, enhancing the release as well as diffusion of PAHs into the solvent (Christou et al., 2021). However, extraction time exceeding the optimum value can lead to break down or conversion of target analytes owing to heat accumulation. Hence, temperature overshoot with the increase in time might have induced PAHs vaporization or thermal decomposition in the course of 7 h (yield: $149.86 \pm 10.13 \mu\text{g g}^{-1}$) and 8 h (yield: $116.61 \pm 7.54 \mu\text{g g}^{-1}$) of extractions and consequently lowered the recovery. Thus, 6 h of extraction was chosen as the optimum time for further considerations. Prolonged extraction periods were not examined as increase in time may not further affect the extraction process or may degrade or transform the analytes. Comparable extraction period has also been studied by Domeno et al. (2006) and Ray et al. (2021) using lower (*Xanthoria parietina*) and higher plant species (evergreen trees and shrubs) for PAHs determination via Soxhlet method, respectively.

Table 18

Profiles of foliar PAHs obtained during varying time periods of extraction with optimized solvent toluene using Soxhlet technique.

EPA-PAHs	Concentration ($\mu\text{g g}^{-1}$ d.w.) of PAHs in time course of extraction			
	5 h	6 h	7 h	8 h
NAP	13.89 ± 3.45	29.81 ± 5.20	15.09 ± 2.24	12.11 ± 3.27
ACY	27.85 ± 3.82	nd	23.48 ± 5.04	nd
ACE	nd	33.78 ± 7.64	nd	nd
FLU	nd	16.59 ± 2.64	nd	nd
PHE	nd	19.39 ± 4.65	nd	nd
ANT	nd	28.75 ± 5.45	nd	nd
FLA	nd	30.62 ± 5.88	nd	nd
PYR	47.54 ± 7.84	nd	37.39 ± 3.13	32.93 ± 4.77
BaA	nd	14.30 ± 3.61	nd	nd
CHR	nd	8.81 ± 2.09	nd	nd
BbF	7.13 ± 3.42	2.94 ± 0.49	15.11 ± 4.09	25.50 ± 4.93
BkF	9.76 ± 3.02	1.92 ± 0.31	9.00 ± 1.51	21.02 ± 3.69
BaP	14.17 ± 4.01	30.54 ± 3.83	15.66 ± 2.45	9.67 ± 2.72

DB[ah]A	19.29±7.06	20.75±4.73	23.04±4.11	13.98±4.21
IP	12.67±3.17	17.02±4.77	11.09±4.25	1.40±0.35
B[ghi]P	nd	19.02±3.33	nd	nd
Total PAHs				
concentration	152.30±6.44	274.24±4.20	149.86±10.13	116.61±7.54

3.4. Conclusion

Performance of monitoring potential of plant biomonitors lies in accurate determination of PAHs in bio-matrices for air pollution monitoring using comprehensive extraction protocols and for such purpose detailed analytical approaches are of great relevance. The work presented in this chapter shows a complete roadmap of conducting extraction of PAHs, followed by purification and instrumental analysis (by GC-MS and HPLC). Standardized extraction techniques are usually aimed for effective and quantitative isolation of analytes from the matrix with proper solvent consumption. Process costing, usability and solvent volume are the principal factors to be considered for an extraction process. In this aspect, four different methods were tested for their efficacy in extracting PAHs from the leaves of an evergreen species *Murraya paniculata* exposed to traffic hotspots. Among the methods investigated, Soxhlet and MAE exhibited high efficiencies of PAHs extraction. Soxhlet extraction with toluene ensured high selectivity and yielded maximum number and quantity of non-polar parent PAHs. The optimized extraction time of 6 h can certainly be claimed as the equilibration time for PAHs. Although this chapter confirms the aim of establishing Soxhlet extraction as a traditional and efficient member of solid-liquid extraction category for PAHs isolation from plant matrix, but it is noteworthy that MAE may be a far more efficient alternative over it. Therefore, detailed and critical study on MAE method for isolation of PAHs from plant matrix was carried out as process intensification study which is presented in the following chapter (Chapter 4).

Chapter 4

4. Methodology III

*Microwave-assisted Soxhlet extraction (MAE) method for PAHs isolation from *Murraya paniculata* (L.) Jack: Process optimization using response surface methodology as process intensification*

4.1. Background

Analysis of PAHs in environmental biomonitors is a challenging endeavor on account of the complex structural organization of the biomatrices and relatively low pollutant levels. To this end, isolation of target PAHs from the matrix and obtainment of the concentrations preferably above the limits of detection (LODs) would be of primary importance ([Sanchez-Prado et al., 2010](#)). Extraction of analytes from the pretreated matrix generally follows, firstly, desorption, then diffusion of solvent through the matrix pores and finally dissolution in the solvent (solvation). Of the three steps stated above, desorption is the key determinant of the overall extraction process, though the recovery may be hindered due to shortcoming of any of the steps ([Sanchez-Prado et al., 2010](#)). Hence, sample preparation becomes an integral part of analyte detection. The main considerations for the selection of extraction techniques should be highest yield and extraction efficiency in less time with low solvent volume and maximum reproducibility. Soxhlet extraction has been the most commonly applied technique for isolating PAHs from solid matrix, the process being time- and energy- intensive with consumption of huge volume of solvent ([Ramirez-Brewer et al., 2024](#)). Thus, microwave-assisted extraction

(MAE) obviates the above intrinsic disadvantages of Soxhlet method, yielding comparable recovery efficiency with less time and solvent volume, thereby reducing generation of wastes (Martinez-Ramos et al., 2020). Additionally, MAE involves the usage of minimum sample quantity with reduction in electrical energy and cost (Quintana et al., 2021). Application of microwaves enhances the heating performance through direct transfer of the microwave energy to the solution maintaining a minimum temperature gradient (Cao et al., 2024), in comparison to conventional heating methods where heat transfer to the solution takes place by the phenomenon of surface heating after the vessels are heated to a temperature.

Being electromagnetic and non-ionizing radiation, microwave energy generates molecular agitations arising from ionic conduction and dipole rotation (Bahndral et al., 2024). Exposure to microwaves as energy carriers causes rapid heating of the solvent-sample mixture, stimulating the partitioning of the desired analytes into the solvent from the matrix. Increase in temperature due to heat generation is facilitated by the medium resistance to flow of ions that causes random collisions between molecules which is brought about by the frequent changes of ionic movement due to rotation of dipoles to align in the direction of the electrical field (Zhao et al., 2023). Moreover, the dielectric constant of the solvent positively influences the generation of heat in the sample under MAE conditions. The high dielectric constant of the solvent, which reflects its capacity to absorb microwaves, increases the rate of heating by liberating more heat energy at a certain frequency. This relates the dependence of microwave heating on solvent choice and matrix. Besides, MAE offers both volumetric (i.e., faster and uniform heating of the whole system) and selective (i.e., rapid heating of specific components of a multicomponent mixture, thereby changing the processes of heat and mass transfer in the course of extraction through temperature gradients) heating effects (Sanchez-Prado et al., 2010). Microwave heating disrupts the structural organization of the biomatrix (by breaking the analyte-matrix bonds) by causing a huge difference in chemical potential between the solid matrix and bulk which forces the solvent or extractant to diffuse through the cellular structure and increases the cellular pressure, resulting in cell rupture and improving analyte extraction (Mason et al., 2011; Araujo et al., 2021). Furthermore, transport of heat and mass through parallel flow also provides higher extraction yield in MAE. Polar solvents having high dielectric losses act as microwave absorbers and are frequently used in MAE processes either singly or in mixtures (Putra et al., 2021). However, in case of PAHs, combinations of polar (for heating the solvent in contact with the solid sample) and non-polar (for extraction of non-polar analytes) solvents in varying volume percentages are commonly applied. Besides, sample matrices having high water content or dielectric loss can also be subjected to MAE by

employing a microwave non-absorbing solvent ([Madej, 2009](#)). MAE can be operated either in an open vessel mode (focused MAE which shows direct influence of solvent boiling point on maximum operating temperature at atmospheric pressure) or in a closed chamber (pressurized MAE which involves pressure mediated temperature acceleration) ([Nobrega et al., 2002](#)).

MAE parameters affecting the performance and efficiency of the process constitute volume and nature of the extracting solvent, matrix, sample weight, irradiation time, temperature and microwave power ([Ramirez-Brewer et al., 2024](#)). Solvents used in MAE should exhibit good absorption characteristics of microwave energy, should convert it to heat energy depending on dielectric factor loss, need to be highly selective to target analytes, thereby reducing the undesirable matrix effects and should have high capacity to interact with the matrix, rendering increased mass transfer and leaching of the compounds of interest from the matrix into the extractant. The ability of the solvents to absorb microwaves is correlated to their dielectric constant which specifically indicates the bulk polarity of the solvents (i.e., higher the dielectric constant, more is the polarity and absorption). For MAE, the amount of solvent required is determined by the sample weight and nature of matrix. Lower solvent volume is always preferred; however, it has to be adequate enough to immerse the sample completely. Unlike traditional extraction processes which consume huge amount of solvents for maximum analyte recovery, MAE can serve the purpose with minimal solvent quantity. Recovery efficiency may deteriorate if large volumes are used because of insufficient dissolution of analytes in the solvent resulting from improper mixing by the microwaves ([Madej, 2009](#); [Camel, 2000](#); [Camel, 2001](#)). Content of water (with high dipole moment) in the biomaterials/biomatrices is considered to be crucially important as it increases the penetrability of the microwaves, causing efficient heating of the sample. On the other hand, ferrous and organic carbon contents of the matrix are known to interfere with the extraction process ([Sanchez-Prado et al., 2010](#)). Regarding microwave power and exposure time, nature of both sample and solvent aids in their selection. High power can reduce the extraction time, but degradation of analytes can also take place concurrently at a very high power, lowering the extraction efficiency. In focused MAE, high power leads to excessive boiling of the solvent within a short span of time and hence affects extraction by limiting the contact between solvent and sample. MAE yields better analyte recoveries in shorter time period of extraction owing to the heating mechanism when compared to conventional extractions. It is also noteworthy that the extended extraction time beyond the optimum value may not further exert any influence on extraction process after equilibrium has reached or perhaps even scale down the target compound recovery. Again, high operating temperature in MAE favours the process of

extraction by disturbing the analyte-analyte or cohesive and analyte-matrix or adhesive interactions, reducing solvent viscosity and surface tension by weakening the solvent intermolecular interactions and enhancing solvent penetration and diffusivity, thereby increasing the dissolution of the analytes into the solvent after desorption from the matrix. But, pressure (which is directly related to temperature) remains a concern when dealing with closed vessel MAE and more specifically, thermolabile or heat-sensitive substances deserve particular attention ([Sanchez-Prado et al., 2010](#)).

From the purview of maximization of MAE yield in minimal time with reduced cost, suitable experimental designs with proper optimization of the extraction variables (as mentioned above) are the fundamental requirements. The conventional univariate optimization approach, where a single parameter is varied at a given time keeping other parameters unchanged, renders itself arduous, lengthy, expensive and inadequate for not being able to read the interactions between the factors ([Jovanovic et al., 2023](#)). Thus, implementation of multivariate designs, in which controlling factors are simultaneously varied, is more frequently carried out for improving the performance of extraction for their accuracy, promptness and economy. Among the multivariate ones, full factorial and fractional designs are most commonly used, but are limited to only two factor levels. However, for better results, response surface methodology (RSM) shall have to be resorted to as it integrates a set of statistical and mathematical tools for the development of empirical models and data fitting for close approximation with the experimental output ([Jovanovic et al., 2022](#)). It also accounts for the precise evaluation of combined effects of different variables and interactions thereof in order to have a complete idea about the optimal process conditions for achieving desired responses with less trial runs and process time ([Teslic et al., 2019](#)). Second-order Box-Behnken design (BBD) of RSM is more advantageous and efficient since it provides quadratic response surface model employing three-level incomplete factorial designs and the structural arrangement takes into consideration a central point and the middle points of the edges of a cube in a factorial design, excluding combinations of the factors at their extreme levels (maximum or minimum) which might result in uncertain and inappropriate test runs with unsatisfactory response ([Gaur et al., 2014](#); [Mishra and Aeri, 2016](#)). In BBD, the number of experiments is represented by the following expression (Eq. 9) ([Grosso et al., 2014](#)):

$$N = 2k(k - 1) + C_0 \quad (9)$$

where, k and C₀ are the numbers of factors and central points respectively.

Various reports are available on RSM for determining the optimum conditions of the factors affecting MAE of mostly bioactive compounds from different matrices and for the enhancement of the quality attributes of formulation of any product isolated using MAE as a green technique (Mary Leema et al., 2022; Shende et al., 2024; Bansod et al., 2023). But, from the perspective of biomonitoring of airborne pollutants, recent studies on design and optimization of process variables of MAE based on RSM for isolation of PAHs from plant leaves are very scarce. MAE and microwave-assisted headspace solid- phase microextraction have been previously used successfully by Ratola et al. (2009) and Ratola et al. (2012) respectively for the extraction of PAHs from pine trees. The extraction techniques exhibited high recoveries of PAHs (70-130%) with enhanced method efficiency. MAE of PAHs from sediment and source rock samples was also reported earlier by Cresswell and Haswell (1999), Letellier et al. (1999) and Prevot et al. (2001) using various extraction solvents and nonionic surfactant solutions. The authors suggested the suitability of the approach for quantitative determination of PAHs with high extraction yield, less extraction time and solvent usage. Thus, the broad of goal of the current study is to establish the MAE method as process intensification over traditional Soxhlet method. Hence, studies have been carried out to investigate the effects of MAE parameters on the selective recovery of PAHs from the plant leaves of *Murraya paniculata*, a familiar plant of high medicinal value having appreciable contribution towards biomonitoring of air quality as nature-based solution. A three-factor Box-Behnken design (BBD) for optimization of MAE conditions (i.e., extraction temperature, time and solvent-to-sample ratio) has been employed for maximum PAHs yield considered as a response factor. The results have also been compared with those of the traditional Soxhlet extraction to establish the potential of MAE in PAHs recovery over other methods to instill credulity about its efficacy in the field of environmental monitoring.

4.2. Materials and methods

4.2.1. Sample processing for extraction

The fresh leaves of *Murraya paniculata* were collected from the areas near Eastern Metropolitan Bypass, a central roadway in south eastern Kolkata, India, in the month of May, 2023. Prior to the process of extraction, the leaves were fully washed in deionized water and subjected to oven drying in a laboratory hot air oven at 50-60 °C for 48 h. Leaf powder was made thereafter from dried plant materials by grinding them in a mortar and pestle and stored at normal temperature in airtight zipper bags for subsequent analysis.

4.2.2. MAE of PAHs from the leaves of *M. paniculata*

PAHs extraction was carried out in a microwave extractor [Microwave synthesis/extraction system, Model: NuWav-Uno (11-19/Uno-112), NutechAnalytical Technologies, Pvt. Ltd., Kolkata] combined with a Soxhlet apparatus (i.e., reflux system). The original photograph and schematic representation of MAE has been shown in Chapter 3. Sample extraction was aided by microwave heating with appropriate temperature control. The current study was conducted by varying the process variables including extraction temperature, time and solvent-to-sample ratio in stages. The round bottom (RB) flask holding the sample and extractant was placed inside the oven and connected to an extractor which, in turn, was externally fitted with a condenser attached to a continuous flow of water for cooling. The obtained extracts were subjected to filtration using Whatman filter paper upon completion and preserved to avoid loss of target analytes.

4.2.3. Primary selection of solvents

Screening experiments were initially performed for the selection of best solvent for the extraction of PAHs using binary mixtures of n-hexane:acetone, n-hexane:dichloromethane, n-hexane:ethyl acetate, toluene:acetonitrile and toluene:tert-butanol (blends of polar and non-polar solvents). All the HPLC grade solvent blends were prepared based on volume ratios, i.e., in the proportion of 1:1 (v/v). In microwave treatment, 3 g of powdered leaf sample was added to 90 mL of extraction solvent in a 250 mL RB borosilicate glass flask and extracted for 30 min at 500 W power and 50 °C temperature under a stirring speed of 500 rpm (Herbert et al., 2006; Ratola et al., 2009). The recovered leaf extracts were then analyzed for PAHs contents.

4.2.4. Experimental design of MAE of PAHs

4.2.4.1. Study of single parameter effects

The single factor designs were conceived after preliminary solvent selection for studying the effects of process parameters on foliar PAHs extraction at distinct levels, which involved single parameter testing, one at a time, in place of changing multiple factors concurrently (Ye et al., 2023). Three independent variables were considered for the design at different extents: extraction temperature varied at 30, 35, 40, 45, 50, 55, 60, 65 and 70 °C, extraction time varied at 5, 7.5, 10, 12.5, 15, 17.5, 20, 22.5 and 25 min and solvent-to-sample ratio varied at 30:5 (=6), 45:5 (=9), 60:5 (=12), 75:5 (=15), 90:5 (=18), 105:5 (=21), 120:5 (=24), 135:5 (=27) and 150:5 (=30) (mL g⁻¹). All experimental runs were taken in triplicates for reproducible results. The selection of the operating range for each factor was made on the basis of the scientific

outcome of previously published literatures in the field (Katoch et al., 2023; Mary Leema et al., 2022; Mishra and Aeri, 2016) and some laboratory groundwork.

4.2.4.2. Parameter optimization using RSM

In this study, the process of MAE to isolate PAHs from *Murraya* leaves was optimized using BBD approach of RSM and the parameter effects on extraction performance and PAHs yield were also evaluated (Shende et al., 2024; Wen et al., 2015; Katoch et al., 2023; Tomasi et al., 2023). The range of independent variables, extraction temperature, extraction time and solvent-to-sample ratio was defined in accordance with the results of single factor experimental designs for acquiring the desired or optimal conditions of extraction (ref. Table 19).

Table 19

Design summary with levels and experimental scale of input variables.

Independent variables			Factor level		
Factor	Name	Units	Lower value (-1)	Central value (0)	Higher value (1)
A	Extraction temperature	°C	30	45	60
B	Extraction time	min	5	12.5	20
C	Solvent-sample ratio	mL g ⁻¹	6	18	30

PAHs extraction yield in terms of concentration (µg g⁻¹) was chosen as the response or dependent variable for the study. Design of experiments was carried out using Design Expert 6.0 software which allowed for 17 randomized trial runs based on three-factor, three-level (-1, 0 and 1 for each factor) BBD technique. The runs were repeated in replicate experiments for accurate measurements. A quadratic polynomial model equation involving response and input variables was developed with three main effects, three quadratic effects, three interaction effects and one model constant. Checking and validation of model adequacy and fitting were substantiated by F-test, coefficient of determination (R²) and analysis of variance (ANOVA). The model equation can be represented in a generalized form as follows (Eq. 10) (Katoch et al., 2023):

$$Y = \beta_0 + \beta_1 \times A + \beta_2 \times B + \beta_3 \times C + \beta_{11} \times A^2 + \beta_{22} \times B^2 + \beta_{33} \times C^2 + \beta_{12} \times AB + \beta_{13} \times AC + \beta_{23} \times BC \quad (10)$$

where, Y denotes the process response, i.e., concentration of PAHs ($\mu\text{g g}^{-1}$); β_0 is the model constant; A, B and C represent the extraction parameters; and β_1 , β_2 , β_3 , β_{11} , β_{22} , β_{33} , β_{12} , β_{13} and β_{23} are the linear, quadratic and interaction factor coefficients.

4.2.5. Extract clean-up and PAHs quantification by HPLC-UVD

The filtered extracts of MAE were subjected to PAHs fractionation by silica gel column chromatography and collected in separate fractions after eluting out of the column. The gradient separation of PAHs was attained by HPLC-UV analysis in reversed phase mode using a mobile phase of ACN:water (v/v) and a highly selective PAH column with a total flow rate of 1.5 mL min^{-1} (Mukhopadhyay et al., 2023). The purification method description and the instrumental analysis procedure along with the separation parameters have been elaborated in the previous chapter. Target PAHs were identified and characterized based on their RTs compared against a multi-component PAH reference standard mix. Quantitative determination of the analyzed compounds was also performed on the basis of a processing method created using the standard PAH solution. The complete procedure adopted has been diagrammatically represented in Fig. 17 and some sample chromatograms representing high PAHs yield at different MAE conditions (as obtained in HPLC) have been displayed in Fig. 18(a-i).

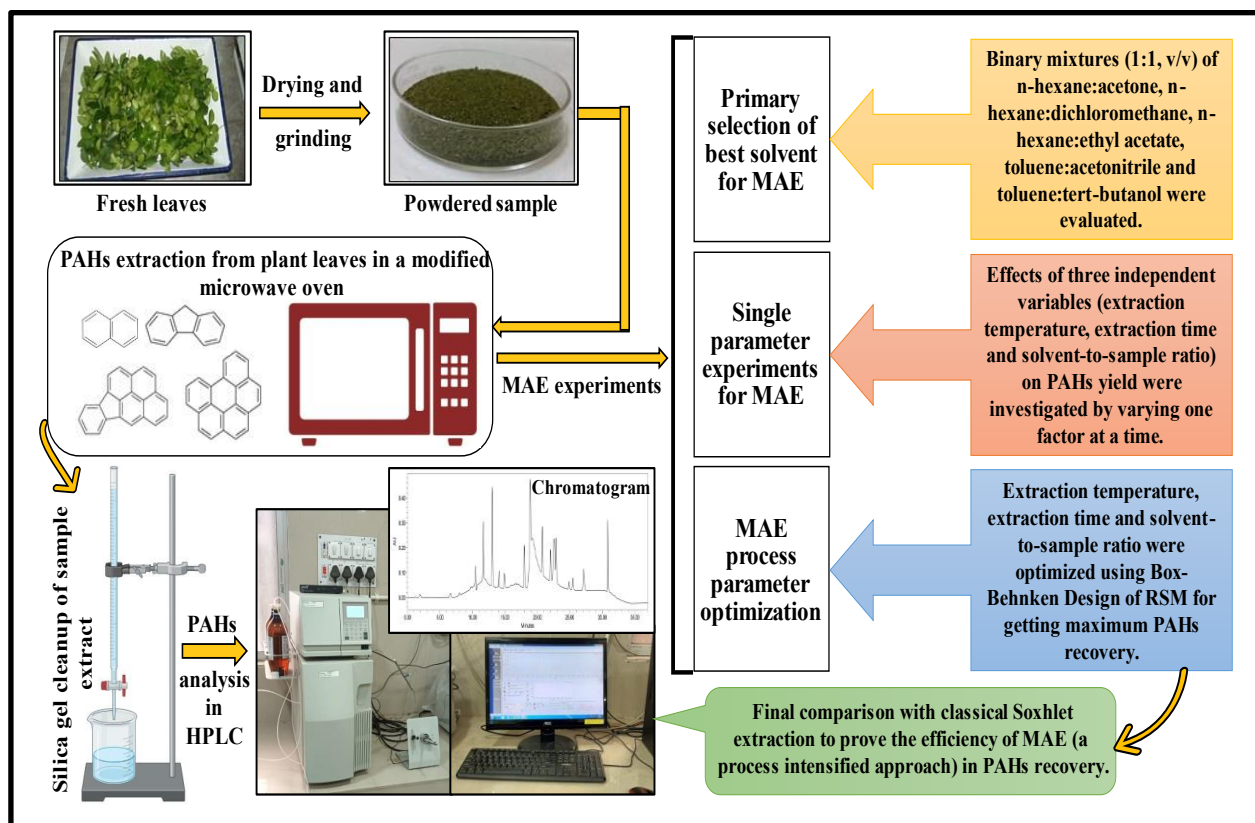
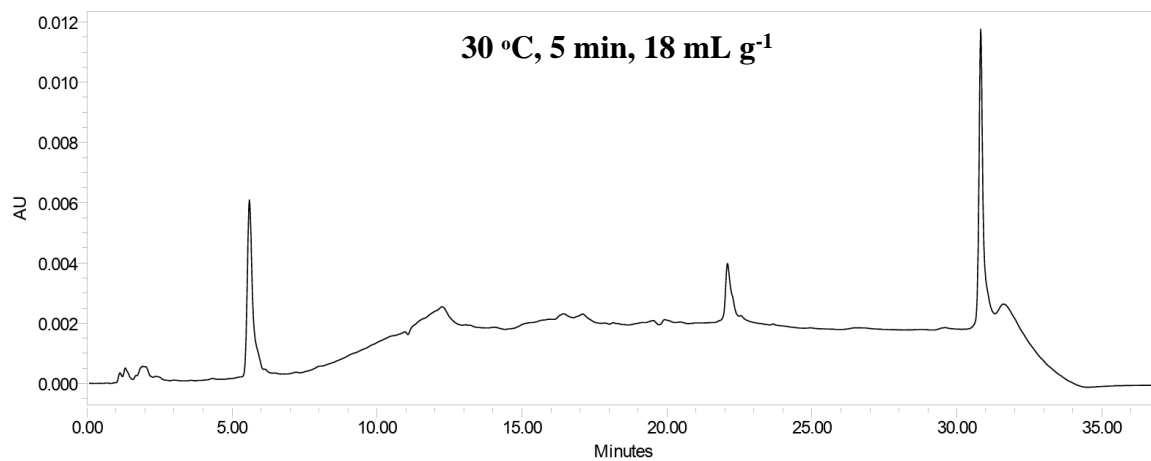
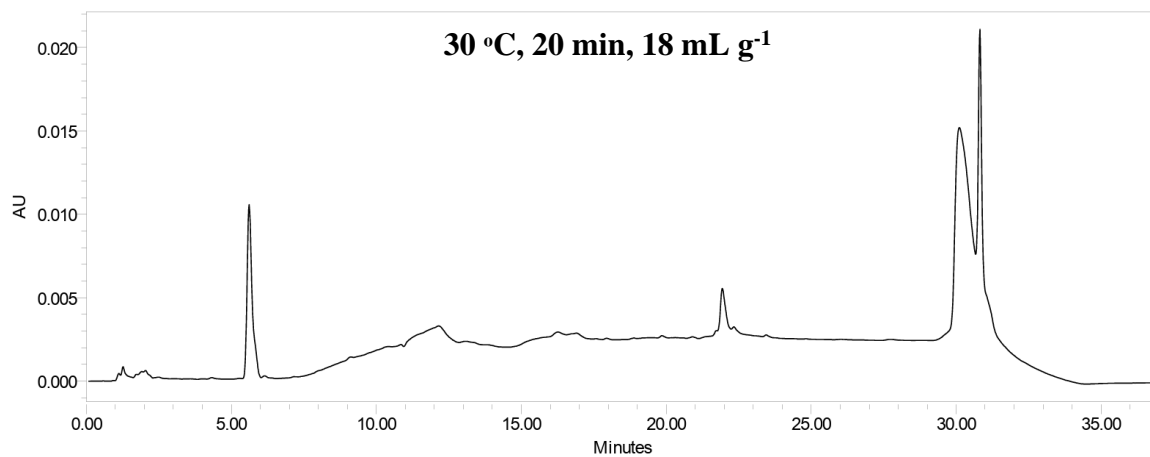


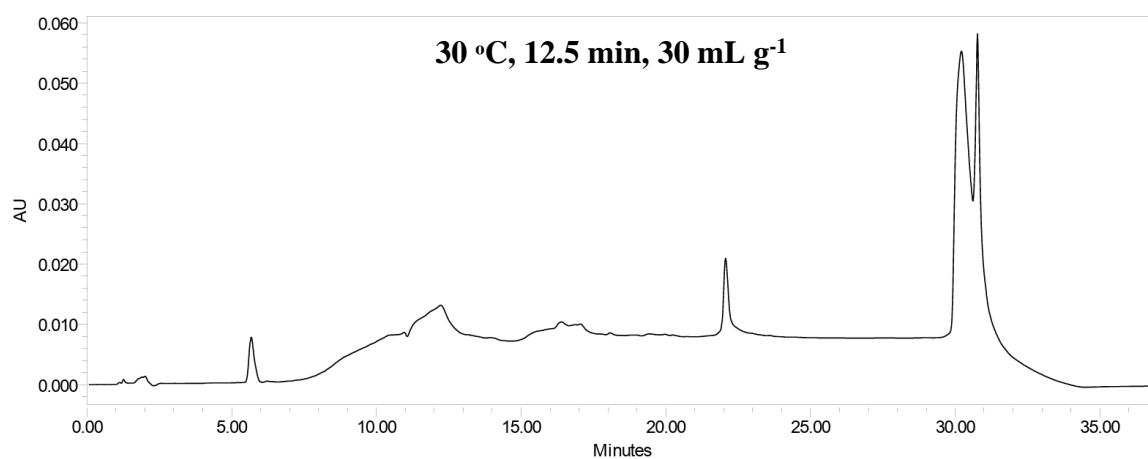
Fig. 17. Schematic depiction of the overall methodology.



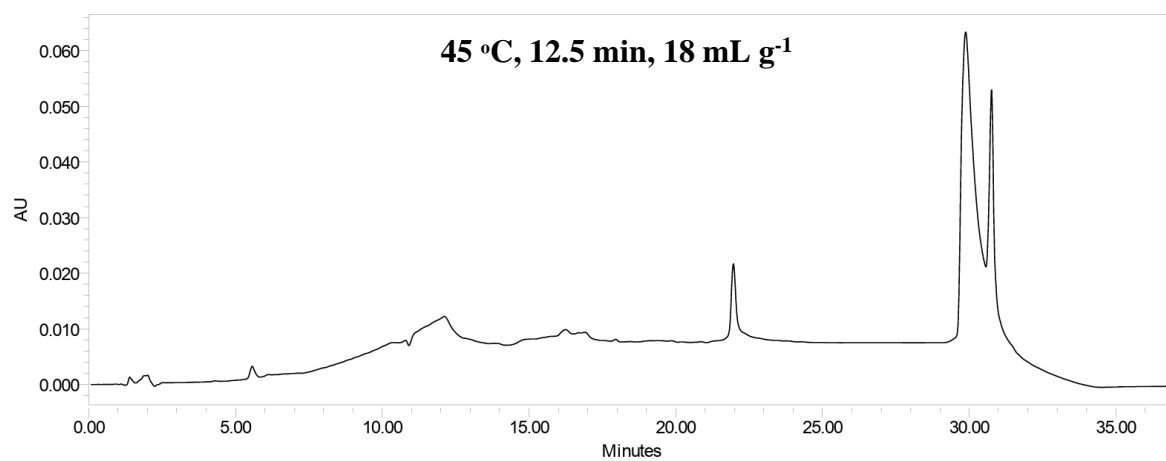
(a)



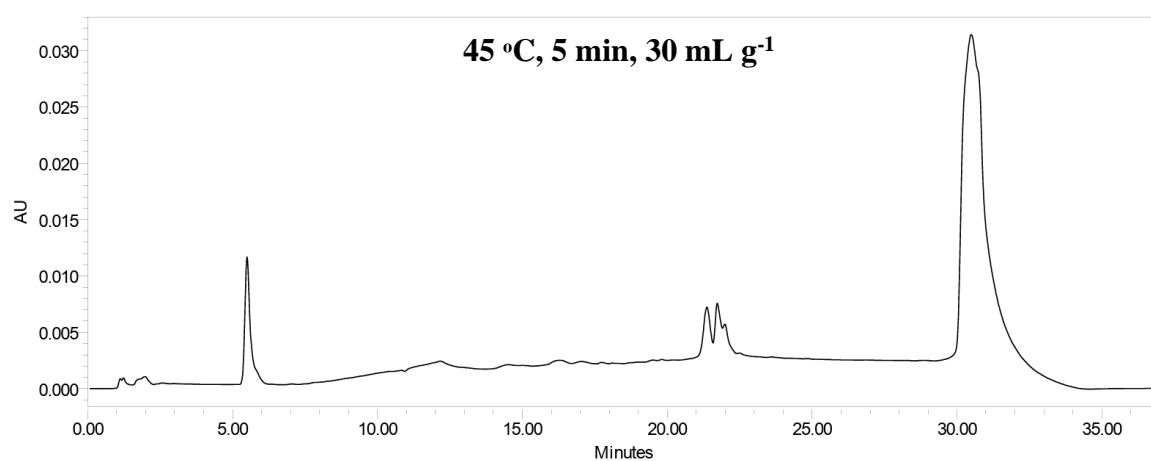
(b)



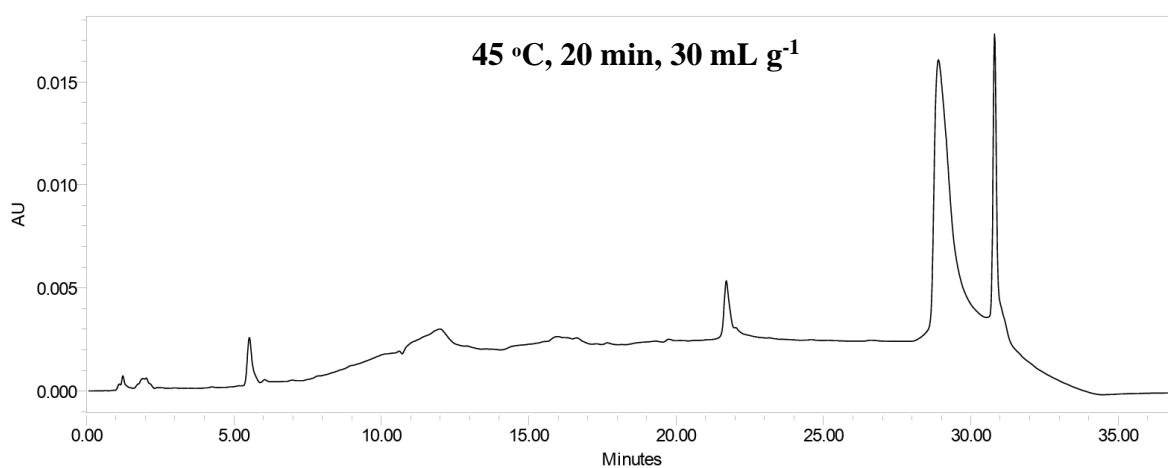
(c)



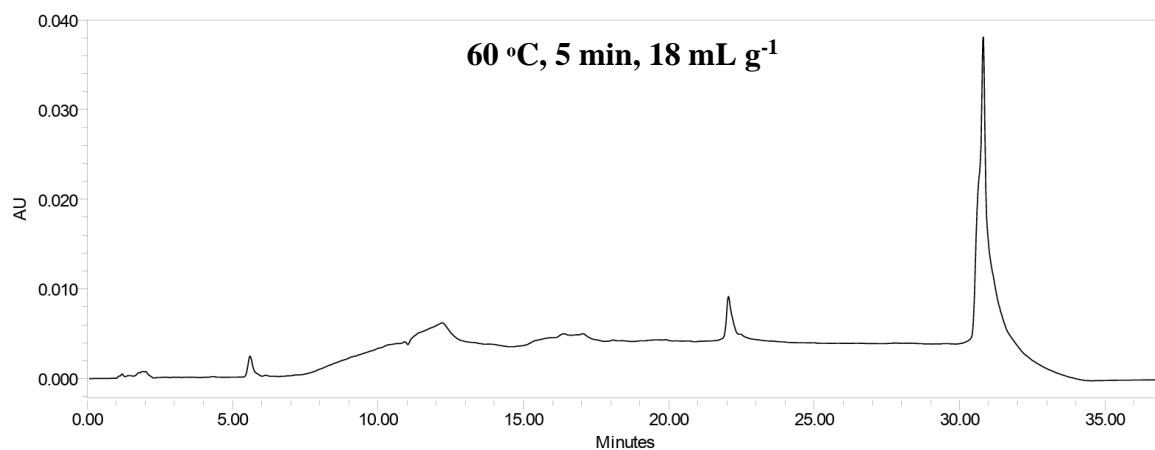
(d)



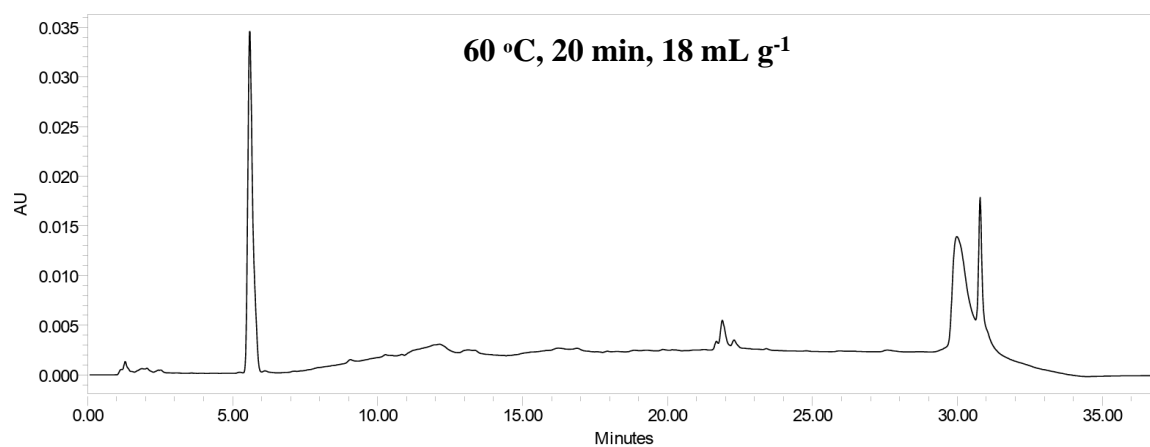
(e)



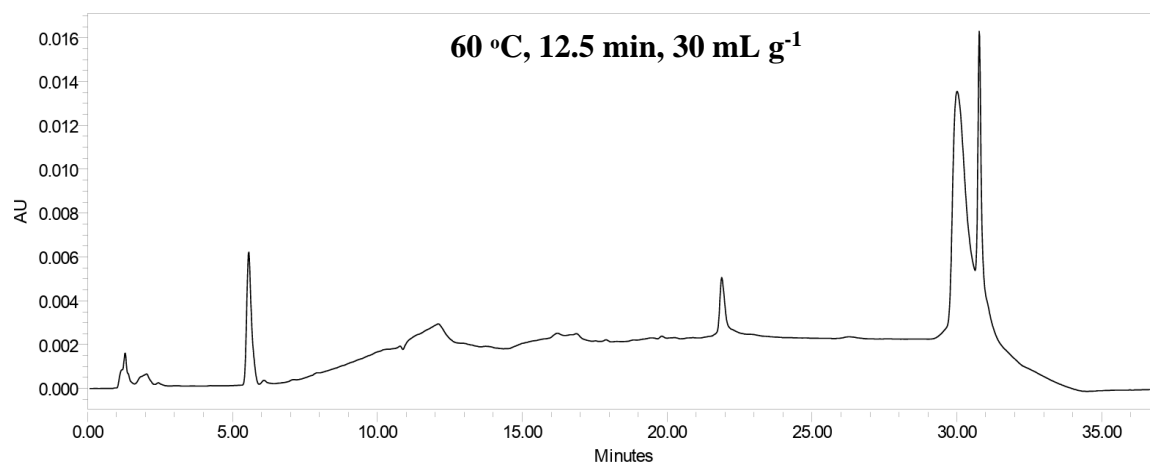
(f)



(g)



(h)



(i)

Fig. 18 (a-i). Representative chromatograms of PAHs extracted from plant leaves under varying conditions of extraction temperature (30-60 °C), extraction time (5-20 min) and solvent-to-sample ratio (6-30 mL g⁻¹) in MAE.

4.3. Results and discussion

4.3.1. Solvent suitability in MAE

Selection of an appropriate solvent is the first step in extraction application which depends on the sample matrix and target compounds (Huschek et al., 2022). Adequate or optimal recovery of PAHs can only be achieved by suitable choice of the solvent selective for the process with respect to solubility factors because of their high hydrophobicity and inherent properties. Different combinations of organic solvents (n-hexane:acetone, n-hexane:dichloromethane, n-hexane:ethyl acetate, toluene:acetonitrile and toluene:tert-butanol) were explored for the selection of the best one for maximized PAHs yield or recovery from plant leaves. The solvation ability of a solvent depends on its polarity (Zarrinmehr et al., 2022). Pure non-polar solvents, though generally give better extraction yield for non-polar PAHs based on the concept of ‘like dissolves like’ (Deshmukh et al., 2019), are not compatible to MAE because of their ineffectiveness to absorb microwaves having low dielectric constants and causing no heating effect for extraction and isolation of PAHs (Huschek et al., 2022). Therefore, in the proposed work, mixtures of polar and non-polar solvents (in the ratio of 1:1) were used to facilitate the interaction between microwaves and extractant and also to improve the extraction selectivity and rate of heating in order to enhance the analyte recoveries from respective matrix. Microwave-induced cell lysis or disruption, layer-by-layer diffusion of solvent into the leaf matrix and extraction and release of the target analytes in the extractant are the fundamental processes of MAE which result in enhanced performance in terms of yield and recovery (Araujo et al., 2021). Varying concentrations of PAHs were obtained in MAE using the solvents studied as reflected in Fig. 19 and the trend was found as follows: PAHs yield_{with toluene:acetonitrile} (283.77 $\mu\text{g g}^{-1}$) > PAHs yield_{with toluene:tert-butanol} (258.72 $\mu\text{g g}^{-1}$) > PAHs yield_{with n-hexane:acetone} (175.53 $\mu\text{g g}^{-1}$) > PAHs yield_{with n-hexane:dichloromethane} (160.14 $\mu\text{g g}^{-1}$) > PAHs yield_{with n-hexane:ethyl acetate} (129.69 $\mu\text{g g}^{-1}$). Solvent combinations of toluene with highly polar acetonitrile and tert-butanol exhibited maximum extraction yield than the binary mixtures of n-hexane with acetone, dichloromethane and ethyl acetate. This could be attributed to: a) stronger microwave absorption by acetonitrile and tert-butanol having high relative polarities (0.46 and 0.389 respectively) and dielectric constants (37.5 and 17.51 respectively), thereby leading to the attainment of desired temperature for enhanced recovery (Zarrinmehr et al., 2022) and b) the aromatic nature of toluene which renders it more effective in breaking down the PAHs-matrix (more specifically π - π) interactions and solvating desired analytes through strong dispersive electrostatic forces as compared to n-hexane which manifest weak intermolecular interactions

with PAHs (Gao et al., 2015). Hence, toluene:acetonitrile, showing highest PAHs yield, has been preferred as the optimal solvent for all the other experiments in MAE.

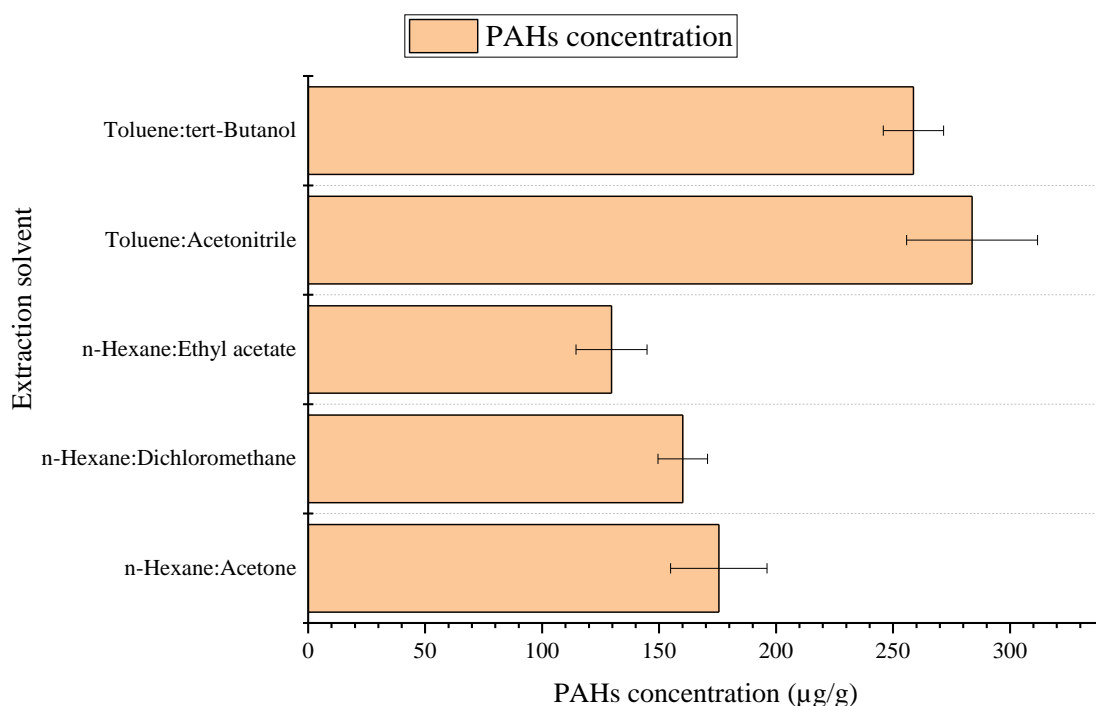


Fig. 19. Comparative study on obtained concentrations of PAHs extracted from *Murraya* leaves using different solvent mixtures.

4.3.2. Single-parameter experiments of MAE

4.3.2.1. Effect of extraction temperature on PAHs yield

As observed in Fig. 20(a), increase in temperature steadily enhanced the extraction yield and highest PAHs concentration ($292.31 \mu\text{g g}^{-1}$) was obtained at 45°C , which gradually decreased with further increase in temperature. Such observation can be related to the fact that the high temperature improves the solubility of PAHs by increasing solvent diffusivity and solvation power and by decreasing solvent viscosity and surface tension, resulting in enhanced rates of diffusion and mass transfer (Veggi et al., 2013). Thus, under these conditions, extraction rate and efficiency also get increased as elevated temperature drives rapid desorption of compounds from the biomatrix active sites. Since, temperature and microwave irradiation power are directly proportional to each other (i.e., microwave power spontaneously changes to maintain the desired temperature level) (Chen et al., 2023), only temperature effect has been studied, while the power level was maintained at 100 W. It is worth mentioning that the excessive high

temperature in MAE can lead to analyte degradation and huge solvent losses as also noticed by [Chen et al. \(2023\)](#), [Idham et al. \(2022\)](#) and [Liu et al. \(2021\)](#). Therefore, 45 °C temperature can be said to be favourable for PAHs extraction from *M. paniculata* leaves in MAE.

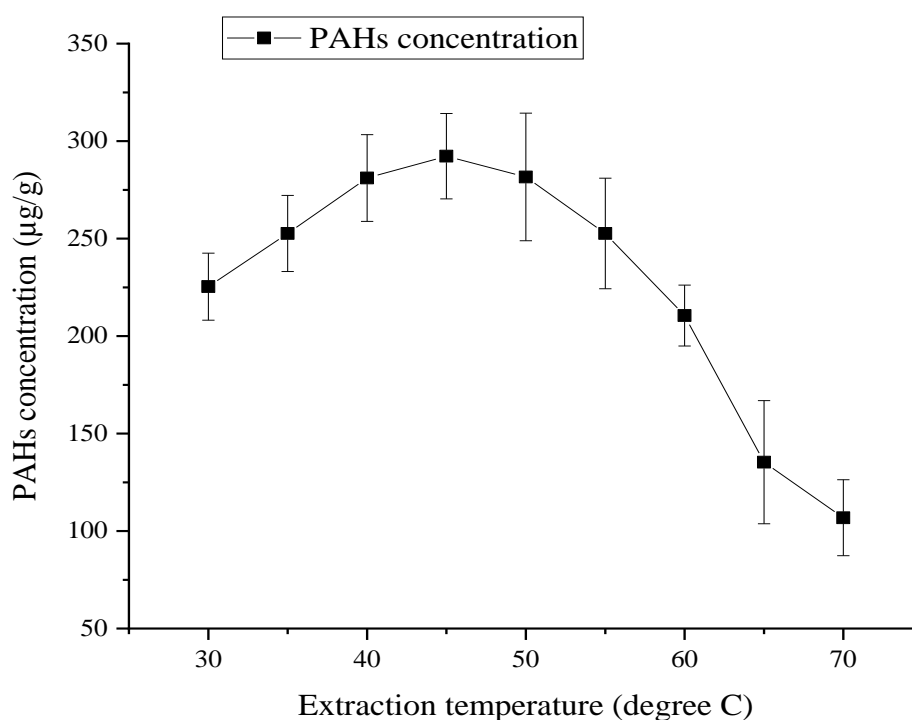
4.3.2.2. Effect of extraction time on PAHs yield

Extraction time in MAE is an important factor controlling the mass transfer of compounds from the matrix to the extractant by means of diffusion and permeation and is imperative to be optimized for the purpose of protecting the target analytes from heat generated by high temperature and curtailing the costs of energy consumption during the process ([Svarc-Gajic et al., 2013](#)). Thus, profile of PAHs concentration changes with extraction time has been examined in the present study and represented in [Fig. 20\(b\)](#). Increase in PAHs concentration from 238.98 to 292.31 $\mu\text{g g}^{-1}$ was observed with gradual increase in extraction time from 5 to 12.5 min and the concentration reached maximum value (292.31 $\mu\text{g g}^{-1}$) in 12.5 min beyond which (up to 25 min) significant drop in PAHs yield (117.35 $\mu\text{g g}^{-1}$) was detected. Long-term exposure under microwave irradiation may result in degradation or transformation products and consequently, PAHs losses in tested samples, lowering the extraction yield ([Svarc-Gajic et al., 2013](#)). Similar trends in the effect of extraction time were also observed by [Chen et al. \(2023\)](#) and [Ye et al. \(2023\)](#) regarding process optimization of anthocyanin and essential oil extraction. Hence, 12.5 min has been analyzed as the suitable extraction time for maximized yield.

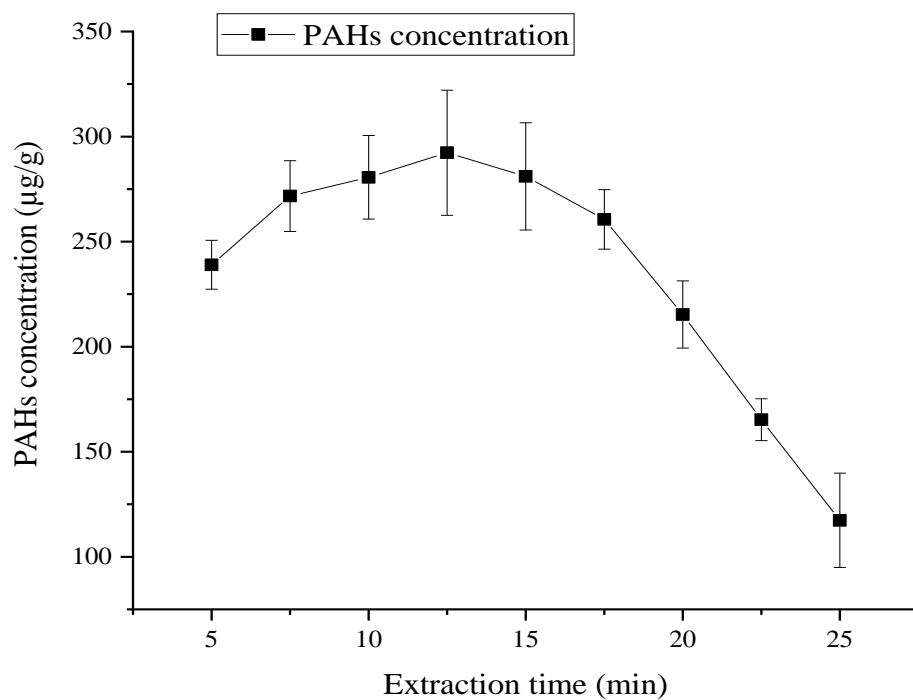
4.3.2.3. Effect of solvent-to-sample ratio on PAHs yield

The high solvent-to-sample ratio in MAE considerably enhances the extraction yield by improving the availability of adequate volume of solvent to the matrix for increased dissolution of target compounds. In the current study, higher PAHs yield with the rise in solvent-to-sample ratio from 6-21 mL g^{-1} was noticed (as also apparent from [Fig. 20\(c\)](#)) under the pre-optimized conditions of extraction temperature (45 °C) and time (12.5 min), while maximum concentration (296.25 $\mu\text{g g}^{-1}$) was determined at 21 mL g^{-1} . Steep increase in the ratio increased the surface area of contact between the solvent and solid plant matrix, allowing better solvent penetration through the matrix (due to swelling and rupture of cell walls of leaf tissue and resulting concentration gradient between the leaf sample and solvent), promoting solute-solvent interactions as well as mass diffusion of PAHs (through diminution of solvent viscosity), ultimately leading to enhanced extraction yield ([Chen et al., 2018](#)). Moreover, high solvent-to-sample ratio raised the dielectric constant of the extractant, facilitating microwave

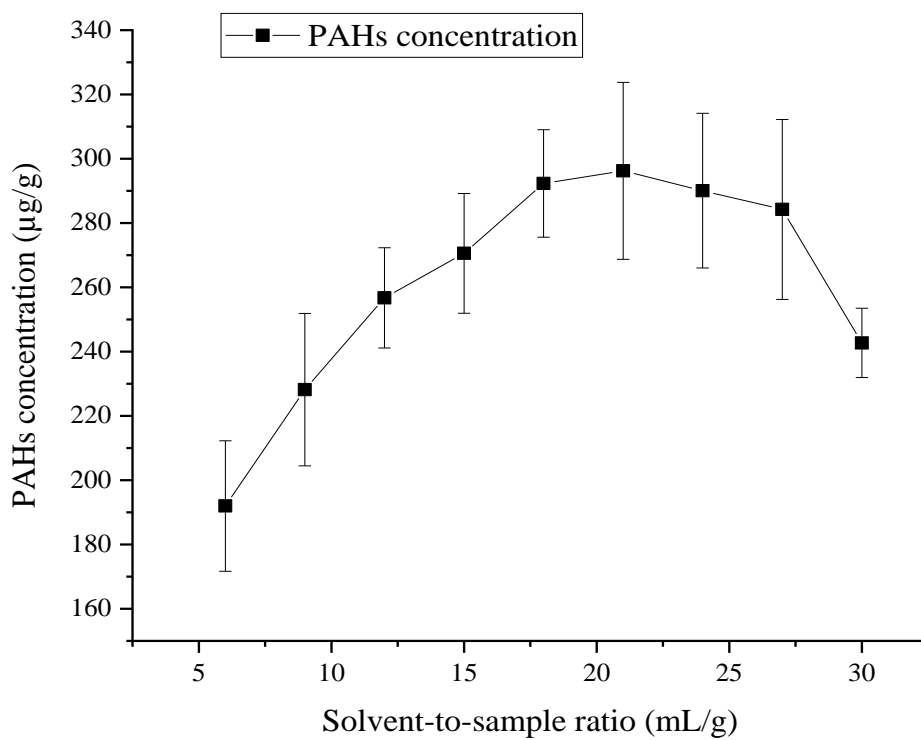
absorption which eventually caused rapid leaching of PAHs from the ruptured cells under temperature elevation. PAHs concentration ($242.71 \mu\text{g g}^{-1}$) was again found to decrease thereafter when the solvent-to-sample ratio increased from 21-30 mL g^{-1} . Usage of excess solvent can dilute the concentration of PAHs, decrease the rate of mass transfer and create diffusivity problem as a result of increased heat energy dissipation (thereby reducing the efficiency of heating and slowing down the process of extraction) with unenviable wastage of solvent (Chen et al., 2015_a; Ye et al., 2023). Conversely, PAHs yield can also be lowered by inadequate solvent volume due to intensive microwave heating of the matrix, leading to charring of the sample and hence, incomplete extraction (Samadi et al., 2017). The findings are in line with the results obtained by Mollaei et al. (2019) and Ye et al. (2023) for the extraction of essential oil from herbaceous plants. Thus, the solvent-to-sample ratio of 21 mL g^{-1} has been found to be optimum for foliar PAHs extraction.



(a)



(b)



(c)

Fig. 20. Effects of (a) extraction temperature, (b) extraction time and (c) solvent-to-sample ratio on the concentration of extracted PAHs.

4.3.3. Optimization of MAE parameters by RSM

4.3.3.1. Statistical modeling and model fitting with response surface analysis

In conformity with the above facts of single factor experiments, the MAE process for PAHs yield from *Murraya* plant leaves was further optimized using a three-factor, three-level BBD approach of RSM. The experimental and predicted responses for PAHs extraction yield with respect to concentration have been elaborated in Table 20 and no significant differences were observed between the response values as also evident from Fig. 21. A second-order quadratic polynomial regression model indicating the association between independent variables and response was developed for the process and is interpreted as the following mathematical equation (Eq. 11) in terms of actual factors:

$$\begin{aligned} \text{Extraction yield} = & -907.15403 + 36.37725 \times A + 36.19528 \times B + \\ & 14.68788 \times C - 0.37613 \times A^2 - 1.02404 \times B^2 - 0.42644 \times C^2 - \\ & 0.29167 \times (A \times B) + 0.065125 \times (A \times C) + 0.067778 \times (B \times C) \end{aligned}$$

(11)

Table 20

Design of experiments with response variable.

Run	Factor 1: A	Factor 2: B	Factor 3: C	Response: PAHs extraction yield ($\mu\text{g g}^{-1}$) (Experimental)	Response: PAHs extraction yield ($\mu\text{g g}^{-1}$) (Predicted)
1	60	12.50	6	95.62 \pm 8.41	96.39
2	45	12.50	18	290.74 \pm 12.07	290.74
3	45	5	6	145.39 \pm 10.69	150.29
4	60	5	18	197.60 \pm 8.86	191.93
5	45	20	30	210.27 \pm 18.46	205.37
6	45	12.50	18	290.74 \pm 12.07	290.74
7	45	12.50	18	290.74 \pm 12.07	290.74
8	60	12.50	30	190.82 \pm 9.84	194.57
9	30	12.50	30	170.34 \pm 19.24	169.57
10	30	5	18	125.91 \pm 17.29	124.75
11	45	5	30	210.90 \pm 12.16	212.83
12	45	20	6	120.36 \pm 17.15	118.43
13	45	12.50	18	290.74 \pm 12.07	290.74

14	30	12.50	6	122.03±17.81	118.28
15	30	20	18	165.04±10.14	170.71
16	60	20	18	105.48±4.84	106.64
17	45	12.50	18	290.74±12.07	290.74

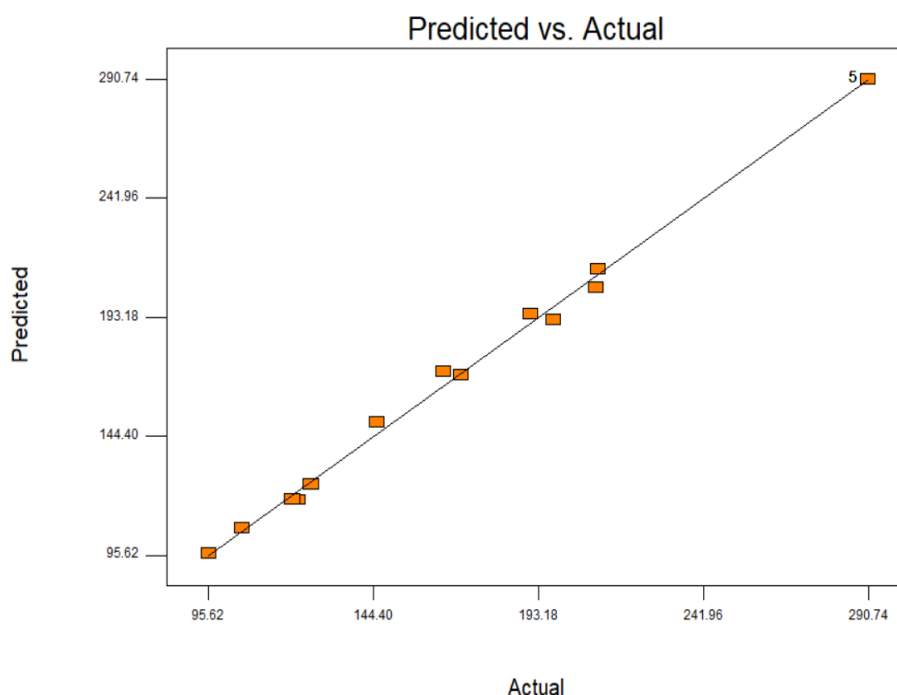


Fig. 21. Predicted vs. experimental plot of responses for PAHs extraction yield.

The ANOVA data for the response surface quadratic model are summarized in [Table 21](#) for ensuring the desired adequacy. The statistical significance of the model is well-established by the F (428.74) and p (<0.0001) values as indicated in [Table 21](#). The R^2 value ($0 \leq R^2 \leq 1$), implying the goodness of fit of a regression model, was found to be 0.9982 which signified that the experimental data set are in good agreement with the predicted values and 99.82% variabilities in PAHs extraction yield (response) can be appropriately justified by the model within the input range of factors. High values of adj. R^2 (0.9959) and pred. R^2 (0.9710) also indicated accurate and satisfactory model prediction of response, as the extent of variation between the two ought to be 0.2 to be in good agreement with each other. Coefficient of variation (C.V.) is defined as the dispersion of the experimental data from the mean values and should desirably be less than 10% ([Jovanovic et al., 2023](#)). The current study showed a C.V. value of 2.39 which is much less than the limiting value, resulting in greater accuracy, acceptability and reproducibility of the response data. Additionally, adeq. precision of 54.40

(i.e., adequate signal which is much higher than the limiting signal to noise ratio of 4) indicated strong model fitting. $p < 0.05$ suggests the significance of the model terms and hence, B, C, A^2 , B^2 , C^2 , AB, AC and BC are found to be significant.

Table 21

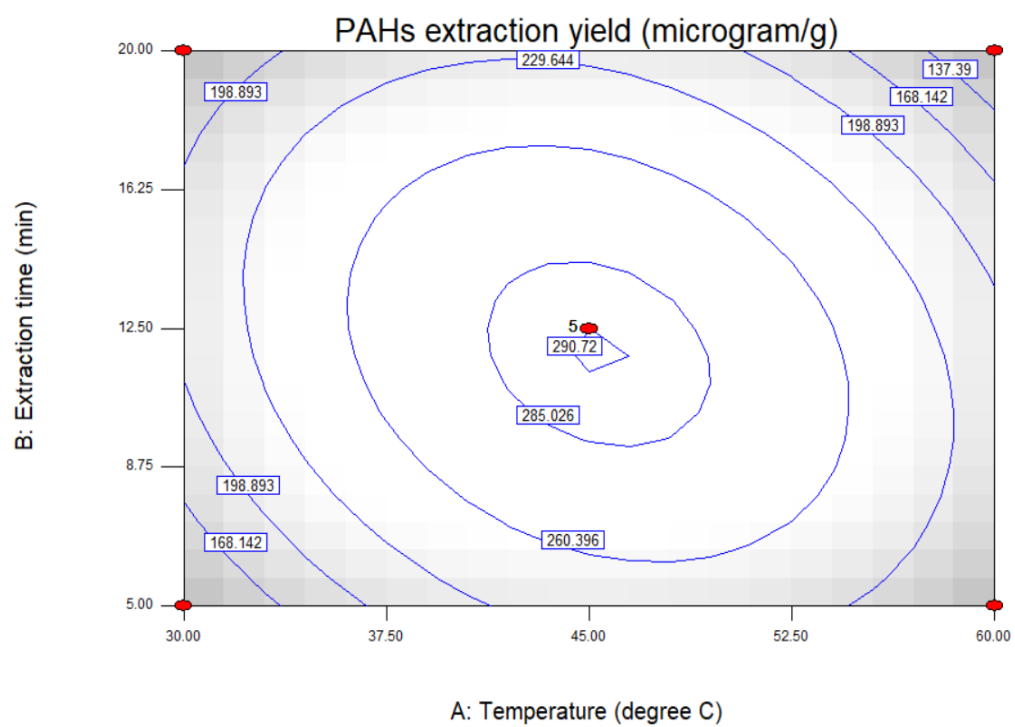
Analysis of variance for the predicted quadratic model.

Source	Sum of squares	df	Mean square	F value	p value (Prob>F)	Feasibility study of regression model	
Model	83715.21	9	9301.69	428.74	<0.0001	Std. Dev.	4.66
A	4.81	1	4.81	0.22	0.6522	Mean	194.91
B	773.23	1	773.23	35.64	0.0006	C.V.	2.39
C	11169.89	1	11169.89	514.85	<0.0001	Press	2429.88
A^2	30156.79	1	30156.79	1390.01	<0.0001	R^2	0.9982
B^2	13970.73	1	13970.73	643.95	<0.0001	Adj. R^2	0.9959
C^2	15877.39	1	15877.39	731.83	<0.0001	Pred. R^2	0.9710
AB	4306.64	1	4306.64	198.51	<0.0001	Adeq. Precision	54.404
AC	549.67	1	549.67	25.34	0.0015		
BC	148.84	1	148.84	6.86	0.0344		
Residual	151.87	7	21.70				
Lack of fit	151.87	3	50.62				
Pure error	0	4	0				
Cor. Total	83867.08	16					

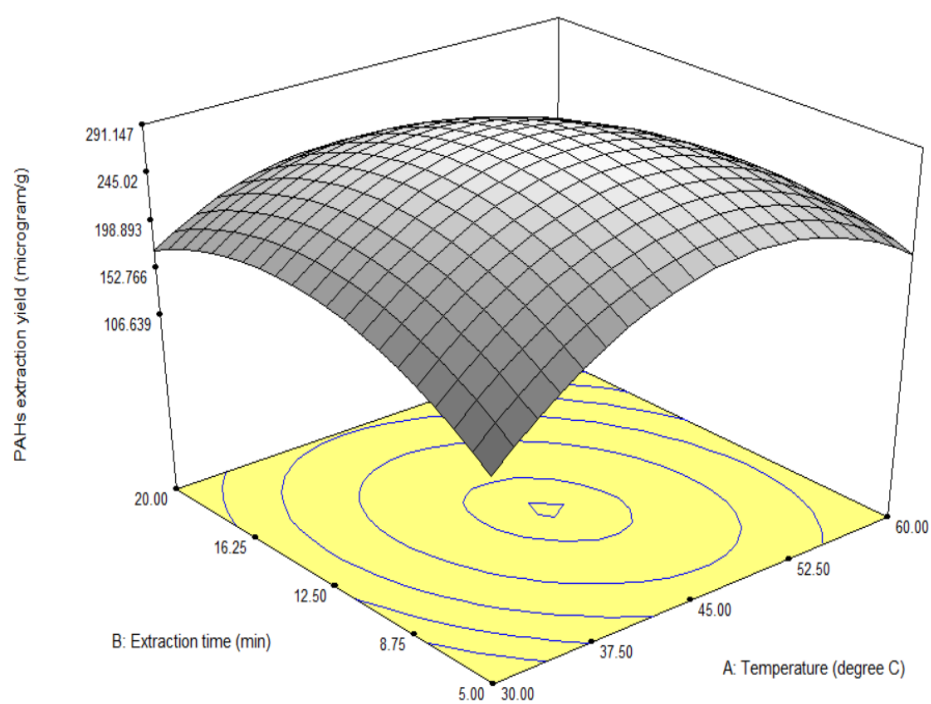
The integrated effects of extraction temperature (A), extraction time (B) and solvent-to-sample ratio (C) on extraction yield of PAHs have been illustrated with the help of two-dimensional (2D) contour and three-dimensional (3D) response surface plots in [Fig. 22\(a-c\)](#). The interaction terms AB, AC and BC were found to be positively (AC and BC) and negatively (AB) significant as also corroborated by the elliptical shapes of the contour surfaces ([Fig. 22\(a₁, b₁, c₁\)](#)), unlike circular shapes of the contour plots which depict insignificant interactions between parameters ([Gunalan et al., 2023](#)). It can also be seen from the model equation that the linear

terms including A, B, and C have positive impacts (although factor A having p value > 0.05), whereas, quadratic terms, like A^2 , B^2 and C^2 have negative impacts on the response factor.

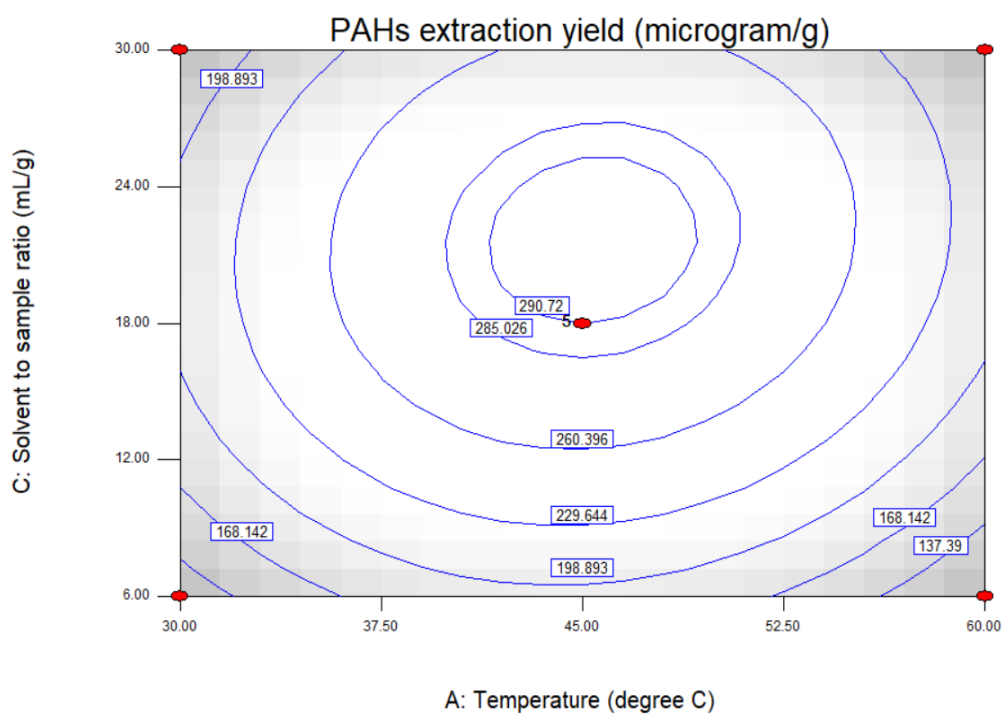
The favourable effect of high extraction temperature (in linear form) could be explained by the enhanced PAHs recovery owing to the loss of cell wall integrity and weakening of molecular interactions causing more leaching of PAHs as a result of improved mass transfer from the sample matrix due to reduced solvent viscosity. Increased temperature may also induce compound degradation and eventually reduction in extraction yield which has been represented by the negative quadratic term (A^2) (Chan et al., 2011). Similarly, increasing extraction time led to appreciable enhancement in the effective recovery of PAHs but the negative influence of the quadratic term (B^2) might be attributed to the fact that the extraction yield had already reached maximum limit (i.e., attainment of peak performance) and no further increase in yield would be achievable with further rise in extraction time (Jovanovic et al., 2023; Kaur et al., 2019). Moreover, higher solvent-to-sample ratio ensured high recovery in PAHs extraction through dilution effect which created differences in concentration of PAHs (between matrix and solvent) compelling their mass transfer from high to low concentration (Chan et al., 2011). This phenomenon continued only up to an equilibrium point beyond which no further improvement in yield was observed, as explained by the negative quadratic effect (C^2). Concerning the mutual effect between A and B (Fig. 22(a₁, a₂)), highest decrease in PAHs yield ($105.48 \mu\text{g g}^{-1}$) was observed at 60 °C in 20 min, while the yield was maximum ($290.74 \mu\text{g g}^{-1}$) at 45 °C in 12.5 min, which implied that the PAHs concentration tended to increase between 30-45 °C with varying extraction time from 5-12.5 min. Immoderate microwave exposure for long duration under elevated temperature might be the reason for lower yield. Thus, application of high temperature for shorter time period and vice versa might help achieve the increased yield, as can be understood from the negative effect of interaction (Jovanovic et al., 2023). Fig. 22(b₁, b₂) (indicating AC interaction) demonstrated an increasing trend of PAHs concentration from 30-45 °C and 6-18 mL g⁻¹ followed by a decreasing trend with further increase in extraction temperature and solvent-to-sample ratio (Darvishzadeh and Orsat, 2022). The plot of extraction time and solvent-to-sample ratio (BC) with respect to response (Fig. 22(c₁, c₂)) highlighted that the PAHs yield from plant matrix improved within 5-12.5 min and 6-18 mL g⁻¹ and peaked at 18 mL g⁻¹ in 12.5 min. Deceleration of recovery efficiency was noticed thereafter with higher extraction time and ratio (Shende et al., 2024; Wen et al., 2015).



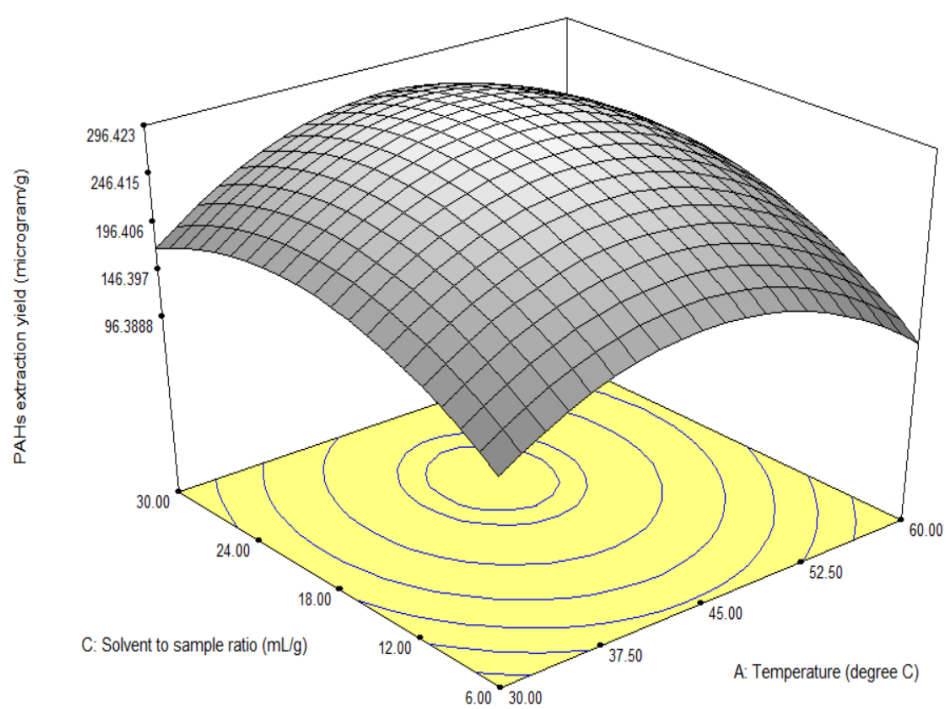
(a₁)



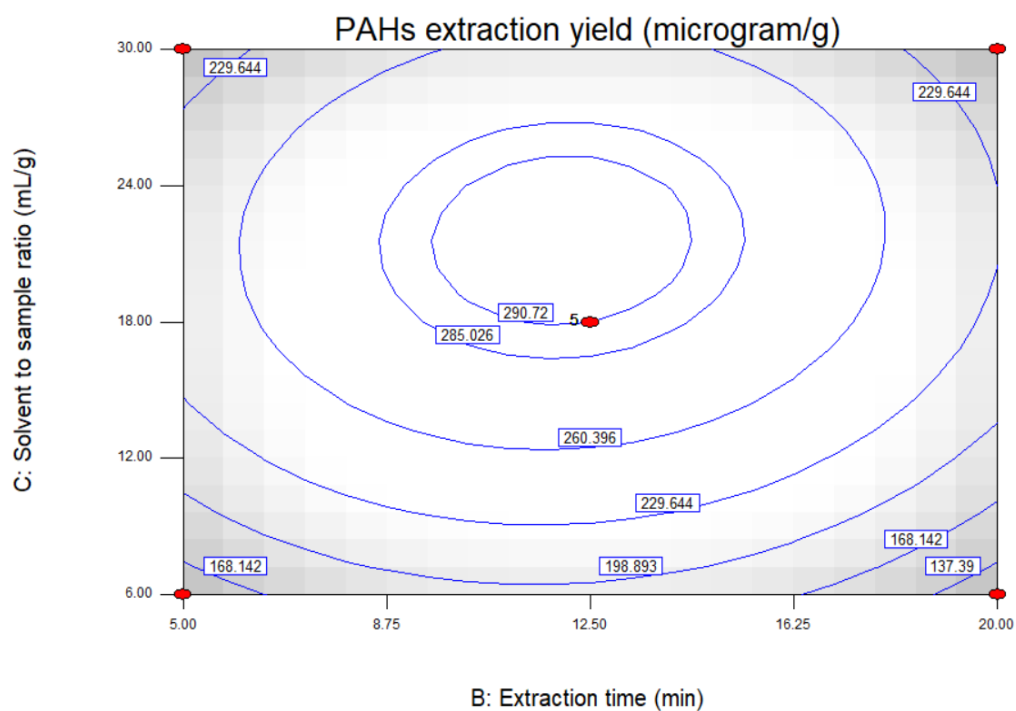
(a₂)



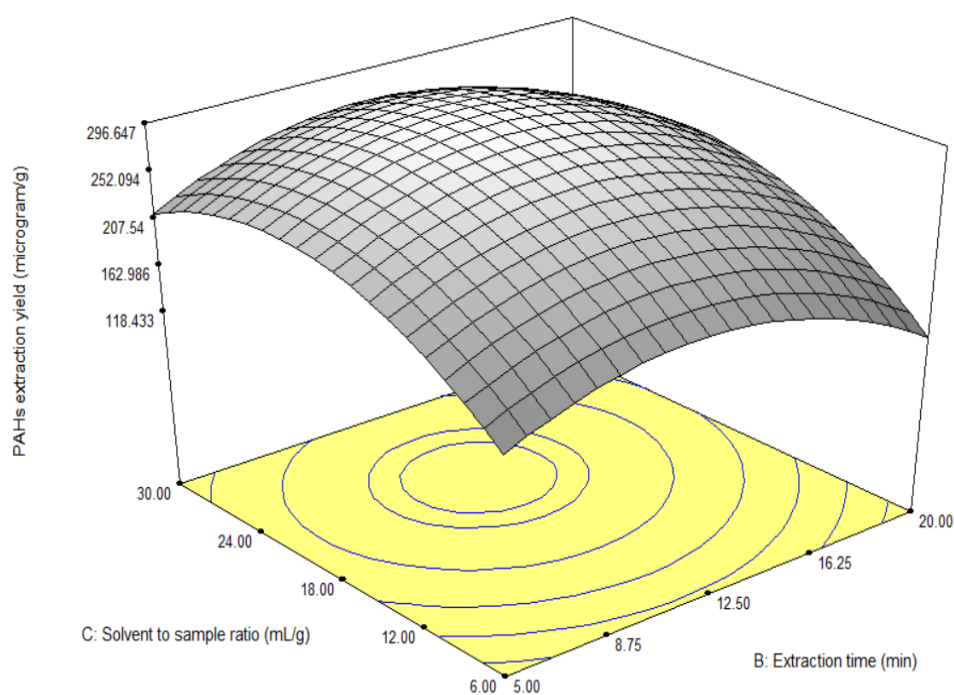
(b₁)



(b₂)



(c₁)



(c₂)

Fig. 22. 2D and 3D graphs of PAHs extraction yield against (a₁) and (a₂): extraction temperature and time, (b₁) and (b₂): extraction temperature and solvent-to-sample ratio and (c₁) and (c₂): extraction time and solvent-to-sample ratio.

4.3.3.2. Model optimization and validation

The optimum extraction parameters for highest PAHs recovery in MAE were obtained by numerical optimization process (Mali and Kumar, 2023) using Design Expert software. The optimization-driven approach presented ten solutions with the goal of keeping the input variables ‘in range’ and response at ‘maximum’. All the combinations of optimal solutions with corresponding extraction yields for PAHs having maximum desirability factor of 1 are displayed in Table 22. Among the ten predictive conditions provided for enhancing the process efficiency, the one (i.e., extraction temperature: 45.77 °C, extraction time: 11.67 min and solvent-to-sample ratio: 22.64 mL g⁻¹) associated with the highest extraction yield (296.366 µg g⁻¹) was preferred in order to validate the model reliability. Under the optimized processing conditions, experimentation was carried out with replicate measurements and the response value was determined as 290.61±13.74 µg g⁻¹ which is close to the model predicted value of PAHs extraction yield. This indicates that the model is predictive of about 98% of the actual data and nearly 2% deviation was only noticed from the predicted yield. Hence, it can be affirmed that the model is highly significant in predicting and estimating the optimum conditions of MAE for PAHs yield from plant leaf matrix with desired accuracy.

Table 22

Numerical optimization of PAHs extraction yield with desirability of 1.

Number	Extraction temperature (°C)	Extraction time (min)	Solvent-to-sample ratio (mL g ⁻¹)	Extraction yield w.r.t. concentration (µg g ⁻¹)	Desirability
1	43.32	11.20	22.43	293.46	1
2	44.34	11.70	24.45	292.508	1
3	42.86	11.29	20.69	292.92	1
4	43.23	13.95	21.24	291.706	1
5	48.44	11.76	23.14	293.257	1
6	46.57	9.77	23.19	291.356	1
7	44.91	12.51	22.91	295.707	1
8	46.97	11.23	25.13	290.942	1
9	45.40	12.90	20.02	294.63	1
10	45.77	11.67	22.64	296.366	1

4.3.4. Comparison of optimized MAE process with classical Soxhlet technique: Process intensification

After optimization, the extraction efficiency of MAE was compared with that of the traditional Soxhlet method, universally the most preferred choice for PAHs extraction but operated at boiling point temperature of extraction solvents for prolonged duration (4-48 h) (Eskilsson and Bjorklund, 2000; Giergielewicz-Mozajska et al., 2001). For the said matrix, the previously optimized extraction time for Soxhlet technique was found to be 6 h. From Table 23, it can be easily observed that the recoveries of PAHs from the same amount of sample (5 g) in both the methods are quite comparable (marginally higher in MAE), but the time requirement is about 30 times more in case of Soxhlet extraction. Moreover, the solvent consumption is 1.8 times higher for Soxhlet method. Thus, MAE showed better performance for PAHs yield when aiming to address the issues of huge solvent requirement and lengthy extraction processes.

The relative energy consumption and amount of CO₂ emission during the extraction processes are also calculated for assessing the environmental impacts using the following formulae (Eqs. 12 and 13) (Benmoussa et al., 2018; Benmoussa et al., 2023; Farhat et al., 2017):

$$E_C^* = E_C / m \quad (12)$$

$$E_{CO_2} = E_C \times 800 \quad (13)$$

where, E_C^* = Relative electric consumption (Watt-hour (Wh) / μ g of PAHs extracted),

E_C = Electric consumption (Wh),

m = mass of PAHs extracted (μ g) and

E_{CO_2} = CO₂ emission (gCO₂ / μ g of PAHs extracted).

As for energy consumption, the basic energy input for Soxhlet process was observed to be 2100 Wh (ref. Table 23) which is more than 100 times than that required for MAE (19.5 Wh). This is also true for relative energy consumption based on the total mass of extracted PAHs. Besides, it has been reported that 1 kWh of electrical energy consumed corresponds to 800 g of CO₂ emitted in the air due to burning of coal or fossil fuel (Solanki et al., 2019; Drinic et al., 2020), indicating a direct correlation between power utilization, extraction time and carbon footprint. Hence, for Soxhlet extraction, CO₂ emission (1.2 g / μ g of PAHs) was significantly higher (more than 100 times) than that of MAE, suggesting potential environmental threats. Mary Leema et al. (2022) and Vila Verde et al. (2018) also suggested MAE as an efficient method in reducing energy (by 5-6 fold) and time (by 14-15 fold) consumption as compared to

conventional processes. Again, [Benmoussa et al. \(2023\)](#) proved the superiority of microwave intensification with reduced environmental implication in terms of CO₂ ejection and wastewater generation over classical hydrodistillation techniques.

Process intensification in extraction refers to the intended advancement of the process to enhance recovery efficiency and sustainability. Safe and easy handling and reduction in time, cost and electrical energy are the key factors influencing the choice of process intensification ([Shirsath et al., 2012](#)). In the present study, microwave irradiation has been employed to intensify the process of PAHs extraction. Therefore, optimization of extraction time and solvent-to-sample ratio, distribution of heat and mass transfer (same directional flow) as well as dielectric or volumetric heating effects in MAE helped meet the energy performance requirements by lowering the energy demand or electrical energy usage and CO₂ emission along with the environmental consequences of increased energy consumption ([Benmoussa et al., 2018](#)). For all such reasons, process intensification by applying microwave heating has been proved to be a promising, cost-efficient and environmentally-safe or greener alternative to conventional Soxhlet extraction with improved extraction efficiency.

Table 23

Comparison between MAE and Soxhlet method.

Parameters	MAE	Soxhlet extraction	Comparative remarks of Soxhlet with MAE
Extraction conditions			
Sample amount (g)	5	5	–
Extraction time (h)	0.195 (11.67 min)	6 (360 min)	30 times higher
Solvent-to sample ratio (mL g ⁻¹)	22.6	40	1.8 times higher
Extraction yield (µg g ⁻¹)	290.61±13.74	279.96±24.01	1.04 times lower
Environmental implication			
Energy consumption (Wh)	19.5	2100	108 times higher
Relative Energy consumption (Wh / µg of PAHs extracted)	0.013	1.5	115 times higher
CO ₂ emission (g) / µg of PAHs extracted	0.011	1.2	109 times higher

4.4. Conclusion

In the current study, microwave-assisted Soxhlet extraction was applied as a process intensified route over conventional Soxhlet extraction for the recovery of PAHs from biomonitor plant leaves like *Murraya paniculata* (L.) Jack. The considered MAE factors which include irradiation time, solvent-to-sample ratio, microwave power, and temperature played vital roles in recovering PAHs from plant leaves. Among the solvents studied for MAE, toluene:acetonitrile revealed better extraction performance with highest PAHs yield owing to the potential of forming strong complementary molecular bonding with the compounds of interest. Single-factor experimental designs demonstrated major influences of extraction temperature, time and solvent-to-sample ratio on PAHs yield. Hence, optimization of the processing parameters of MAE was performed by combining Box-Behnken approach with RSM. The optimum conditions of 45.77 °C, 11.67 min and 22.64 mL g⁻¹ gave a maximum yield of 290.61±13.74 (observed value) µg g⁻¹ of PAHs, representing high precision when compared with the predicted value (296.366 µg g⁻¹). Therefore, it can be opined that the developed regression model is well-suited with very high predictability (98%) of the optimized yield.

The comparative study between MAE as a process intensified route of solvent extraction and conventional Soxhlet technique revealed that the MAE outperformed Soxhlet method in respect of energy requirement, extraction time and solvent volume along with less generation of CO₂, making it economic and more ecofriendly.

After protocol establishment for extraction of PAHs from biomonitor plant tissues, spatial and temporal occurrences of the pollutants were evaluated for enhanced understanding of PAHs distribution with locational and seasonal variations and discussed in Chapter 5.

Chapter 5

5. Methodology IV

*Biomonitoring of PAHs by *Murraya paniculata* (L.) Jack in South Kolkata, West Bengal, India: Spatial and temporal variations*

5.1. Background

The plant cover and green spaces are the universal attenuators of air pollution, which absorb the deadly atmospheric pollutants and protect the human population from high risks of vulnerability. PAHs may penetrate the plant leaves either by diffusion through stomatal pores (gaseous uptake) or by atmospheric deposition (in particulate phase) on leaf cuticles and their partitioning from air to outer leaf surfaces and to inner tissues is driven by environmental factors, pollutant properties and plant behavior (Lin et al., 2006). A multitude of studies has focused on PAHs determination using leaves of both deciduous and evergreen trees (*Quercus robur*, *Quercus palustris*, pine species (*Pinus pinaster*, *Pinus nigra*), Olive, *Salix matsudana* and *Murraya paniculata*) as good pollution indicators (biomonitors) of terrestrial environment and come up with multiple outcomes (De Nicola et al., 2016; Kargar et al., 2017; Karnchanasest and Satayavibul, 2005; Klingberg et al., 2022; Mukhopadhyay et al., 2021; Ray et al., 2021; Sari et al., 2021; Zhao et al., 2018). The levels of foliar PAHs undergo changes in response to spatial and temporal variations in wind flow, diurnal temperature, ambient moisture content and stability class (i.e., presence of clouds during day and night time), concentrations of tropospheric oxidants, rate of photodegradation and pollution load from

mobile or point sources of emission (Bidleman and Leone, 2004; Ohura et al., 2013; Totten et al., 2002; Wang et al., 2015). Diagnostic ratios (DRs), positive matrix factorization (PMF) and principal component analysis with multiple linear regression (PCA-MLR) are commonly employed for source apportionment studies to reveal the origin of PAHs contamination in plants and quantify the percent contribution of the components of emission (De Nicola et al., 2008; Kargar et al., 2017; Yang et al., 2017; Zhou et al., 2014). As far as air quality is concerned, better assimilation of knowledge about the interactions between the pollutants and vegetative barriers is imperative to effectively implement the biomonitoring scheme for pollution control. Paucity of related field works in and around Kolkata, India, has driven us to undertake such studies as an endeavor toward bridging the gap between scanty information and biomonitoring prospect. In this aspect, the specific objectives of the study were framed to establish the spatio-temporal patterns of PAHs concentrations in plant samples of selected contaminated zones of South Kolkata with respect to three different seasons, premonsoon, postmonsoon and winter, and apply DRs for determination of the primary sources of PAHs along with seasonal effects.

5.2. Materials and methods

5.2.1. Materials, sampling location and collection time

A field work was executed in the urban areas of South Kolkata, India, during three different seasons [premonsoon (May and June, 2019), postmonsoon (October to mid of November, 2019) and winter (January and February, 2020)], which comprised collection of waxy leaf samples of a dominant tree species, *Murraya paniculata* (L.) Jack, applying proper methodological approaches (Mukhopadhyay et al., 2021) from the roadsides of selected study sites: Jadavpur (JDV), Rash Behari Connector (RBC), Exide More (EXM) and Tollygunge (TGN). The overall considerations and representation of sampling locations are clearly delineated in Chapter 2. The choice of the above sites was mainly based on the following factors: (1) overcrowding of the areas and intense human activities, (2) huge increase in the use of motor vehicles, (3) small-scale polluting units and (4) proximity to the Central/State Pollution Control Board operated regular air quality monitoring networks.

5.2.2. Spatio-temporal variations of ambient PAHs: quantitative estimation and diagnostic ratios (DRs) for characterization of sources

The spatial and temporal trends of PAHs uptake and accumulation were examined in plant leaves of various sampling locations in urban environment under distinct climatic conditions

of premonsoon, postmonsoon and winter, depending on their concentrations, to assess the integrated exposure with time along with overall status of air quality. Differences in mean concentrations of PAHs in plant leaves were determined using two-way analysis of variance (ANOVA) in Microsoft Excel 2010 on spatial and temporal considerations (i.e., among sites and seasons). The significance level was tested at $p < 0.05$. All the data were represented as mean \pm standard deviation ($n=6$). Polluting sources of emitted PAHs in the ambient air of the urban sites were also differentiated by applying DRs (Ray et al., 2017; Tobiszewski and Namiesnik, 2012). DRs, such as $\Sigma(\text{low molecular weight PAHs})/\Sigma(\text{high molecular weight PAHs})$ (i.e., $\Sigma\text{LMW}/\Sigma\text{HMW}$), $\text{ANT}/(\text{ANT}+\text{PHE})$, $\text{FLA}/(\text{FLA}+\text{PYR})$, $\text{BaA}/(\text{BaA}+\text{CHR})$, BbF/BkF , $\text{FLU}/(\text{FLU}+\text{PYR})$, BaP/BghiP and $\text{IP}/(\text{IP}+\text{BghiP})$ (refer Table 24) were evaluated in the present study as major emission source markers on the basis of their concentrations to investigate the origin of PAHs accumulated in the plant leaves.

Table 24

Standard range of DRs applied in the study (Tobiszewski and Namiesnik, 2012).

DRs	Standard Range (with PAHs Source)
$\Sigma\text{LMW}/\Sigma\text{HMW}$	<1 (Pyrogenic)
	>1 (Petrogenic)
$\text{ANT}/(\text{ANT} + \text{PHE})$	<0.1 (Petrogenic)
	>0.1 (Pyrogenic)
	<0.4 (Petrogenic)
$\text{FLA}/(\text{FLA} + \text{PYR})$	0.4-0.5 (Fossil fuel combustion)
	>0.5 (Grass, wood, and coal combustion)
	0.2-0.35 (Coal combustion)
$\text{BaA}/(\text{BaA} + \text{CHR})$	>0.35 (Vehicular emissions)
	<0.2 (Petrogenic)
	>0.35 (Combustion)
BbF/BkF	2.5-2.9 (Aluminium smelter emissions)
	>0.5 (Diesel emissions)
$\text{FLU}/(\text{FLU} + \text{PYR})$	<0.5 (Petrol emissions)
	>0.5 (Diesel emissions)
BaP/BghiP	<0.6 (Non-traffic emissions)
	>0.6 (Traffic emissions)
	<0.2 (Petrogenic)
$\text{IP}/(\text{IP} + \text{BghiP})$	0.2-0.5 (Petroleum combustion)
	>0.5 (Grass, wood and coal combustion)

5.3. Results and discussion

5.3.1. Temporal variability in PAHs concentrations

Identification of air pollution hotspots by assessing spatial and temporal variations of pollutant concentrations is obligatory for enforcing control actions to reduce elevated risks of negative health impacts. Atmospheric concentration, transport and dispersion of PAHs, weather events, air/plant partitioning and uptake dynamics of PAHs in the plant leaves influence their content in tree foliage (De Nicola et al., 2005). Plant leaves can be considered as passive air samplers (or biomonitors) having keen propensity for differentiating even small-scale heterogeneity in the levels of urban air pollution (De Nicola et al., 2011). The temporal variabilities observed in the total concentration of foliar PAHs (TPAHs in $\mu\text{g g}^{-1}$ d.w.) among the four study points can be described in the order of: TPAHs_{winter} (278.42 ± 3.02 – 550.79 ± 10.11) > TPAHs_{postmonsoon} (210.52 ± 12.78 – 401.83 ± 13.61) > TPAHs_{premonsoon} (200.98 ± 2.72 – 329.17 ± 4.03) (Table 25). Air quality downfall as evidenced in winter months (having highest values of TPAHs) is mostly associated with air stagnation leading to clean, stable and tranquil atmosphere, restricted circulation of air masses (i.e., poor vertical mixing and horizontal dispersion) due to low velocity of the prevailing winds and night-time temperature inversion (Grundstrom et al., 2015). Non-detection of some of the HMW PAHs during winter in some sites (viz. BaP, DB[ah]A and IP at JDV; BaP at RBC and FLA at TGN) might be due to their reaction with the atmospheric oxidants under stable atmospheric stratification, generating secondary pollutants or polar PAHs derivatives (nitrated/oxygenated congeners: NPAHs/OPAHs) (Bandowe and Meusel, 2017). Percentage composition (varying between 59.01 and 87.44%) of 2-, 3- and 4-ring PAHs, namely NAP, ACY, ACE, FLU, PHE, ANT, FLA, PYR, BaA and CHR, revealed their dominance during premonsoon study of the selected sites. This can be attributed to the conversion of above-stated PAHs into gaseous phases from particulate state in presence of high temperature, enabling their easy permeation into the leaf tissues (internal diffusion by gas-phase transfer), whereas, lower levels of accumulated 5- and 6-ring PAHs may be credited to their photochemical degradation under the same condition (Ambade et al., 2022a) which led to an overall decline in TPAHs with respect to other seasons. Contrary to premonsoon, moderate temperature, relatively stable, dry and clear weather in postmonsoon period may be accountable for greater accumulation of PAHs (4.75–23.45% higher TPAHs) in *Murraya* leaves.

Table 25

Seasonal variations in total and individual concentrations ($\mu\text{g g}^{-1}$ d.w.) of PAHs measured in *Murraya paniculata* leaves of different sites.

Foliar PAHs concentrations												
	JDV			RBC			EXM			TGN		
EPA-PAHs	Premonsoon	Postmonsoon	Winter	Premonsoon	Postmonsoon	Winter	Premonsoon	Postmonsoon	Winter	Premonsoon	Postmonsoon	Winter
NAP	15.24 \pm 2.38	19.75 \pm 0.59	27.08 \pm 0.49	20.42 \pm 2.31	21.55 \pm 1.64	24.16 \pm 1.70	43.61 \pm 3.45	45.66 \pm 1.35	39.22 \pm 1.27	9.97 \pm 1.26	13.39 \pm 0.82	14.83 \pm 2.52
ACY	nd	9.56 \pm 0.67	11.28 \pm 1.56	nd	14.17 \pm 1.33	12.30 \pm 1.79	nd	53.29 \pm 1.79	55.62 \pm 2.47	5.63 \pm 0.54	6.35 \pm 0.57	9.17 \pm 1.53
ACE	25.32 \pm 2.29	nd	7.29 \pm 0.28	9.72 \pm 1.37	nd	11.86 \pm 0.37	nd	6.77 \pm 0.21	8.11 \pm 1.87	8.98 \pm 0.67	9.23 \pm 0.88	10.04 \pm 2.32
FLU	7.74 \pm 1.76	nd	7.78 \pm 0.52	9.80 \pm 3.47	10.49 \pm 1.43	5.82 \pm 0.11	13.80 \pm 2.73	11.32 \pm 0.66	7.67 \pm 1.72	10.56 \pm 3.17	nd	11.74 \pm 2.43
PHE	23.40 \pm 4.33	18.89 \pm 0.71	18.44 \pm 0.30	13.63 \pm 2.07	15.85 \pm 1.79	17.27 \pm 0.66	12.91 \pm 1.63	nd	21.32 \pm 1.57	28.62 \pm 3.77	25.86 \pm 1.77	35.57 \pm 3.36
ANT	16.44 \pm 2.94	43.70 \pm 1.62	69.11 \pm 3.10	39.02 \pm 1.45	41.58 \pm 1.46	42.83 \pm 1.35	26.29 \pm 2.46	nd	34.56 \pm 2.99	37.84 \pm 3.08	19.51 \pm 0.75	26.45 \pm 2.86
FLA	nd	39.88 \pm 1.37	23.10 \pm 0.34	40.73 \pm 2.27	46.91 \pm 2.33	59.52 \pm 2.50	nd	57.88 \pm 2.49	70.26 \pm 3.78	44.52 \pm 4.63	47.09 \pm 2.04	nd
PYR	7.93 \pm 2.26	32.20 \pm 0.89	51.25 \pm 2.79	41.52 \pm 3.14	55.27 \pm 2.69	63.09 \pm 2.19	59.66 \pm 2.67	nd	75.01 \pm 3.89	11.92 \pm 4.46	18.15 \pm 1.12	21.98 \pm 3.43
BaA	48.50 \pm 3.76	nd	81.20 \pm 2.96	33.54 \pm 1.75	37.67 \pm 1.87	50.22 \pm 1.81	65.39 \pm 3.51	78.17 \pm 2.61	86.95 \pm 2.81	nd	nd	29.47 \pm 2.22
CHR	31.90 \pm 1.68	nd	48.61 \pm 1.65	50.83 \pm 2.17	50.97 \pm 2.41	52.19 \pm 2.07	29.59 \pm 3.45	58.30 \pm 0.88	64.61 \pm 3.13	nd	nd	42.17 \pm 4.39
BbF	nd	14.57 \pm 1.25	11.60 \pm 1.34	nd	24.30 \pm 1.32	25.70 \pm 1.05	21.96 \pm 1.48	22.84 \pm 0.51	33.42 \pm 4.49	nd	20.95 \pm 1.18	36.44 \pm 4.15
BkF	10.76 \pm 2.63	22.37 \pm 0.69	25.76 \pm 0.94	nd	23.81 \pm 1.82	16.46 \pm 1.35	19.12 \pm 1.97	15.48 \pm 0.68	18.36 \pm 2.23	nd	12.72 \pm 0.50	13.96 \pm 1.26
BaP	29.47 \pm 1.99	30.92 \pm 0.69	nd	2.52 \pm 0.35	13.22 \pm 0.83	nd	2.82 \pm 0.53	4.65 \pm 0.28	9.73 \pm 0.75	3.64 \pm 0.86	11.05 \pm 1.72	11.48 \pm 1.63
DB[ah]A	59.64 \pm 2.88	62.81 \pm 1.54	nd	16.32 \pm 1.44	8.26 \pm 0.65	9.42 \pm 0.44	31.08 \pm 2.21	36.71 \pm 1.72	13.59 \pm 1.95	23.16 \pm 3.82	8.54 \pm 0.71	2.38 \pm 0.34
IP	22.69 \pm 3.66	17.53 \pm 0.52	nd	nd	1.93 \pm 0.10	5.18 \pm 0.15	2.94 \pm 0.29	3.31 \pm 0.52	4.37 \pm 0.58	13.43 \pm 2.93	17.68 \pm 0.73	10.10 \pm 1.21
B[ghi]P	nd	3.49 \pm 0.24	6.14 \pm 0.82	18.41 \pm 1.92	nd	10.12 \pm 1.01	nd	7.45 \pm 0.47	7.99 \pm 2.04	2.71 \pm 1.08	nd	2.64 \pm 0.34
Total PAHs concentration	299.03 \pm 15.18	315.67 \pm 10.33	388.64 \pm 3.94	296.46 \pm 15.52	365.98 \pm 17.46	406.14 \pm 9.38	329.17 \pm 4.03	401.83 \pm 13.61	550.79 \pm 10.11	200.98 \pm 2.72	210.52 \pm 12.78	278.42 \pm 3.02

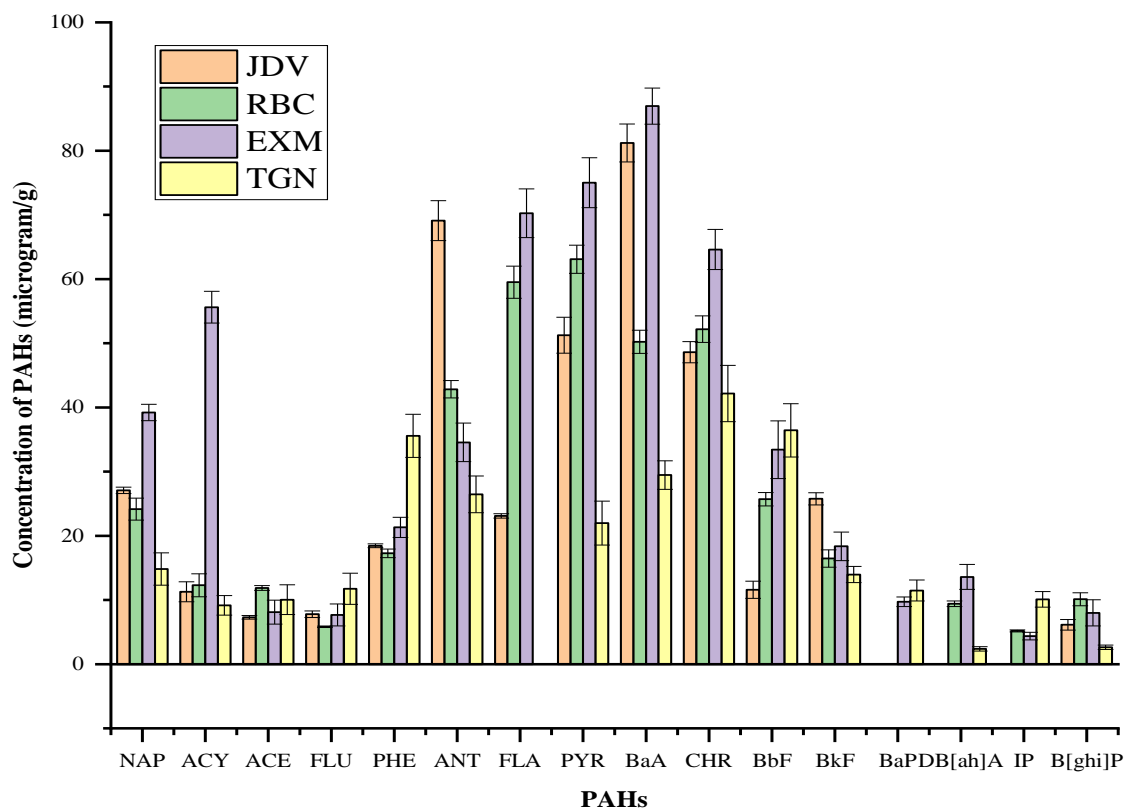
Concentration values expressed as (mean \pm S.D.)

The current findings are in line with the conclusions drawn by [De Nicola et al. \(2005\)](#), [Prajapati and Tripathi \(2008c\)](#), [Ray et al. \(2021\)](#) and [Yang et al. \(2017\)](#).

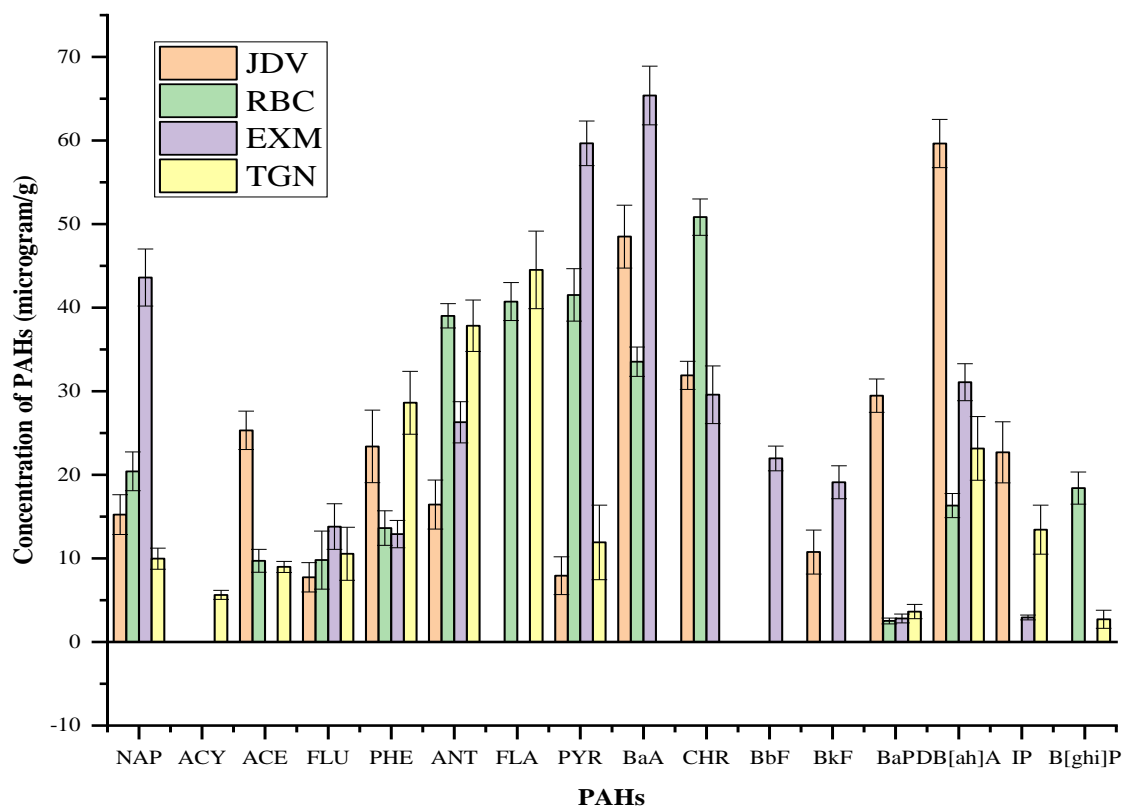
5.3.2. Spatial variability in PAHs concentrations

The significant variations in concentration of individual PAH congeners as well as total PAHs (TPAHs) were observed among the four sample locations. [Fig. 23\(a–c\)](#) illustrates the site-specific leaf PAHs concentrations in the urban locations. The highest accumulation of TPAHs ($\mu\text{g g}^{-1}$ d.w.) at EXM (329.17 ± 4.03 – 550.79 ± 10.11) than RBC (296.46 ± 15.52 – 406.14 ± 9.38), JDV (299.03 ± 15.18 – 388.64 ± 3.94) and TGN (200.98 ± 2.72 – 278.42 ± 3.02) in all the seasons may be primarily accredited to the huge vehicular emissions at the point of traffic intersection due to movement/idling of vehicles on the congested roadways. Moreover, excluding few of the PAHs, almost every PAHs congener was found to be present in highest proportions at EXM location which is supported by the availability of highest foliar dust (major carrier of PAHs) concentration in that location. Among the four locations, RBC and TGN were found to have lesser PAHs pollution burden. The spatial differences in the levels of PAHs were significantly affected by the type and intensity of local human impacts, commercial operations and traffic emissions. Therefore, the source profiles were classified in the current study through the use of distinctive characteristic ratios of PAHs (or molecular DRs: concentration ratios of particular PAHs of same molar masses and inherent properties) for minimizing uncertainties.

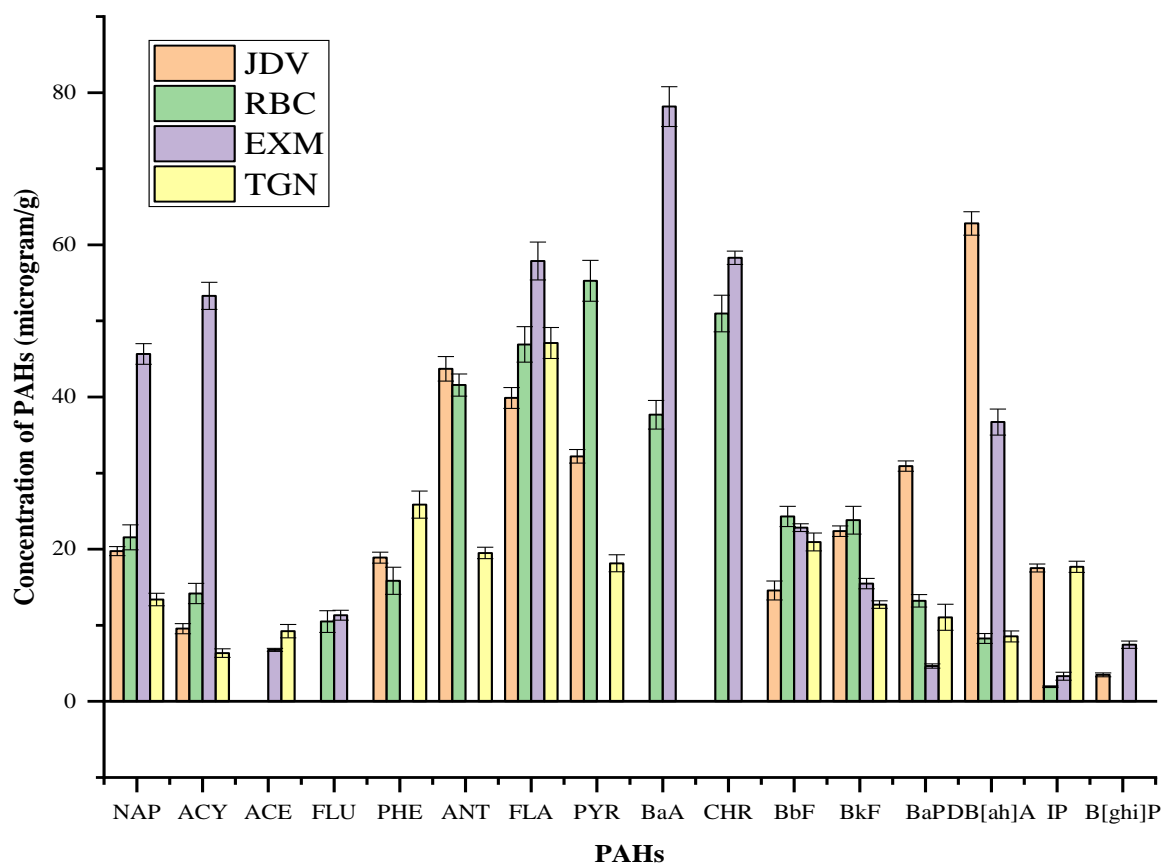
The seasonal and locational variations of the PAHs levels were significant with $p < 0.05$ ($p = 2.94 \times 10^{-11}$; 0.02) and $F > F_{\text{crit}}$ ($F = 6.76$; 2.11 and $F_{\text{crit}} = 1.73$; 1.85) as confirmed by two-way ANOVA.



(a)



(b)



(c)

Fig. 23. Locational variations in individual PAHs concentrations ($\mu\text{g g}^{-1}$ d.w.) in *Murraya paniculata* leaves with respect to three seasons (a) winter, (b) premonsoon and (c) postmonsoon.

5.3.3. Source apportionment using DRs

PAHs analysis results of ambient air samples are compared with well-described sources at the sites with reported DRs for source apportionment. The estimated values of DRs (standard ranges of which are depicted in Table 24) analyzed for discerning the heterogeneous sources of PAHs pollution in the sampling sites on seasonal basis are presented in Table 26. It may be inferred that the seasonal variability of emission sources at the sampling areas of South Kolkata had not been found to be very much prominent. $\Sigma\text{LMW}/\Sigma\text{HMW}$ and $\text{ANT}/(\text{ANT}+\text{PHE})$ ratios are usually employed to distinguish between the pyrogenic and petrogenic sources of PAHs (Pies et al., 2008; Zhang et al., 2008). As shown in Table 26, $\Sigma\text{LMW}/\Sigma\text{HMW} < 1$ and $\text{ANT}/(\text{ANT}+\text{PHE}) > 0.1$ are indicative of coal, wood and biomass combustion as well as automobile exhausts (pyrogenic origin) emitting PAHs into the atmosphere for all the sites. Moreover,

FLA, PYR, BaA, CHR, BbF, BkF, BaP, IP and B[ghi]P are categorized as combustion-derived PAHs (Bucheli et al., 2004; Hwang et al., 2003). Foliar concentrations (ref. Fig. 23(a–c)) of ACY, FLU, PHE, ANT, FLA, PYR, CHR and BkF in the sites again pointed to the release of PAHs from fly ash of open biomass and coal burning (Kakareka and Kukharchyk, 2003; Larsen and Baker, 2003; Lee et al., 2005), while, in case of TGN site, $\Sigma\text{LMW}/\Sigma\text{HMW} > 1$ during premonsoon suggested the predominance of petrogenic origin of emission. It is noteworthy that the presence of 4-, 5- and 6-ring PAHs including BaA, CHR, BbF, BkF, BaP, IP and B[ghi]P is a strong indicator of emission from petrol combustion (Dzepina et al., 2007; Ho et al., 2009; Larsen and Baker, 2003; Yunker et al., 2002). The measured DR values for FLA/(FLA+PYR), BaA/(BaA+CHR), BbF/BkF, FLU/(FLU+PYR) and BaP/BghiP had also demonstrated majorly transport-related emissions (from petrol/diesel) and presumed to be the sources for PAHs absorption by the leaves at the study sites. However, at RBC, effects of non-exhaust traffic emissions in premonsoon (BaP/BghiP < 0.6 (such as resuspension of dust particulates from road pavements, construction activities, tires and brakes, burning of solid fuels and street cafes or restaurants) and contribution from fossil fuel combustion in both pre- and post-monsoon [FLA/(FLA+PYR) \approx 0.4–0.5] were recognized as well (De La Torre-Roche et al., 2009; Katsoyiannis et al., 2007). FLA/(FLA+PYR) > 0.5 at TGN signified PAHs outflow from biomass burning during premonsoon together with vehicular activities (De La Torre-Roche et al., 2009). IP/(IP+BghiP) > 0.5 at JDV and TGN reflected mixed origin of PAHs liberated from coal or biomass burning and cooking fume emissions from chimneys of roadside restaurants (Chen et al., 2015b). The maximum variation of seasonal concentrations ($\mu\text{g g}^{-1}$ d.w.) of BaP (29.47 ± 1.99 – 30.92 ± 0.69) and DB[ah]A (59.64 ± 2.88 – 62.81 ± 1.54) at JDV confirmed the sources of oil-based cooking (grilling, smoking, frying, barbecuing and roasting, etc.) in several wayside food stalls or commercial kitchens, corroborating the above inference. Observed concentrations of DB[ah]A at EXM (13.59 ± 1.95 – $36.71 \pm 1.72 \mu\text{g g}^{-1}$ d.w.) and TGN (2.38 ± 0.34 – $23.16 \pm 3.82 \mu\text{g g}^{-1}$ d.w.) also represented the influences of cooking processes on the outdoor environment. Mainly, at RBC and EXM with IP/(IP+BghiP) lying between 0.2 and 0.5, petroleum-related PAHs pollution was observed to be widespread. Prevalence of lighter and heavier PAHs (NAP, ACY, FLU, PHE, PYR, BaA, CHR and BghiP) in high and low levels in every site is a pointer toward combustion of petroleum products and exposure to cooking oil smoke (Masih et al., 2012). Occurrence of ACE in the leaf samples due to coal combustion and diesel exhausts was recorded, but in low concentration (6.77 ± 0.21 – $25.32 \pm 2.29 \mu\text{g g}^{-1}$ d.w.) owing to its short half-life and high susceptibility for biodegradation (Chanda and Mehendale, 2005).

Table 26

Molecular DRs with their obtained values (as mean \pm S.D.) for identification of foliar PAHs origin in the sampling sites.

DRs for the plant leaves of urban areas													
PAHs ratio	Seasons	JDV			RBC			EXM			TGN		
		Value	Range	Source	Value	Range	Source	Value	Range	Source	Value	Range	Source
Σ LMW/ Σ HMW	Premonsoon	0.42 \pm 0.03	<1	Pyrogenic	0.45 \pm 0.01	<1	Pyrogenic	0.42 \pm 0.01	<1	Pyrogenic	1.02 \pm 0.26	>1	Petrogenic
	Postmonsoon	0.41 \pm 0.01	<1	Pyrogenic	0.40 \pm 0.01	<1	Pyrogenic	0.41 \pm 0.00	<1	Pyrogenic	0.55 \pm 0.00	<1	Pyrogenic
	Winter	0.57 \pm 0.02	<1	Pyrogenic	0.39 \pm 0.01	<1	Pyrogenic	0.43 \pm 0.01	<1	Pyrogenic	0.63 \pm 0.01	<1	Pyrogenic
ANT/(ANT + PHE)	Premonsoon	0.41 \pm 0.01	>0.1	Pyrogenic	0.74 \pm 0.02	>0.1	Pyrogenic	0.67 \pm 0.01	>0.1	Pyrogenic	0.57 \pm 0.01	>0.1	Pyrogenic
	Postmonsoon	0.70 \pm 0.00	>0.1	Pyrogenic	0.72 \pm 0.03	>0.1	Pyrogenic	—	—	—	0.43 \pm 0.01	>0.1	Pyrogenic
	Winter	0.79 \pm 0.01	>0.1	Pyrogenic	0.71 \pm 0.01	>0.1	Pyrogenic	0.62 \pm 0.01	>0.1	Pyrogenic	0.43 \pm 0.05	>0.1	Pyrogenic
FLA/(FLA + PYR)	Premonsoon	—	—	—	0.50 \pm 0.01	0.4-0.5	Fossil fuel combustion	—	—	—	0.79 \pm 0.06	>0.5	Grass, wood burning and diesel emission
	Postmonsoon	0.55 \pm 0.01	>0.5	Diesel emission	0.50 \pm 0.03	0.4-0.5	Fossil fuel combustion	—	—	—	0.72 \pm 0.00	>0.5	Diesel emission
	Winter	0.31 \pm 0.01	<0.5	Petrol emission	0.49 \pm 0.01	<0.5	Petrol emission	0.48 \pm 0.03	<0.5	Petrol emission	—	—	—
BaA/(BaA + CHR)	Premonsoon	0.60 \pm 0.01	>0.35	Vehicular emission or combustion	0.40 \pm 0.00	>0.35		0.69 \pm 0.04	>0.35		—	—	—
	Postmonsoon	—	—	—	0.43 \pm 0.01	>0.35	Vehicular emission or combustion	0.57 \pm 0.01	>0.35	Vehicular emission or combustion	—	—	—
	Winter	0.63 \pm 0.02	>0.35	Vehicular emission or combustion	0.49 \pm 0.02	>0.35		0.57 \pm 0.02	>0.35		0.41 \pm 0.01	>0.35	Vehicular emission or combustion
BbF/BkF	Premonsoon	—	—	—	—	—	—	1.15 \pm 0.17	>0.5	Diesel emission	—	—	—
	Postmonsoon	0.65 \pm 0.04	>0.5	Diesel emission	1.02 \pm 0.02	>0.5	Diesel emission	1.48 \pm 0.04	>0.5	Diesel emission	1.65 \pm 0.02	>0.5	Diesel emission
	Winter	0.45 \pm 0.04	na	na	1.56 \pm 0.17	>0.5	Diesel emission	1.82 \pm 0.03	>0.5	Diesel emission	2.61 \pm 0.06	>0.5	Diesel emission
FLU/(FLU + PYR)	Premonsoon	0.49 \pm 0.01	<0.5	Petrol emission	0.19 \pm 0.04	<0.5	Petrol emission	0.19 \pm 0.02	<0.5	Petrol emission	0.47 \pm 0.18	<0.5	Petrol emission

BaP/BghiP	Postmonsoon	—	—	—	0.16±0.01	<0.5	Petrol emission	—	—	—	—	—	—
	Winter	0.13±0.01	<0.5	Petrol emission	0.08±0.00	<0.5	Petrol emission	0.09±0.02	<0.5	Petrol emission	0.35±0.08	<0.5	Petrol emission
	Premonsoon	—	—	—	0.14±0.03	<0.6	Non-traffic emission	—	—	—	1.34±0.54	>0.6	Road traffic emission
	Postmonsoon	8.86±0.88	>0.6	Road traffic emission	—	—	—	0.62±0.07	>0.6	Road traffic emission	—	—	—
	Winter	—	—	—	—	—	—	1.22±0.63	>0.6	Road traffic emission	4.35±0.05	>0.6	Road traffic emission
IP/(IP + BghiP)	Premonsoon	—	—	—	—	—	—	—	—	—	0.83±0.01	>0.5	Biomass burning, coal combustion and eateries
	Postmonsoon	0.83±0.01	>0.5	Biomass burning, coal combustion and eateries	—	—	—	0.31±0.01	0.2-0.5	Combustion of petroleum fuel	—	—	—
	Winter	—	—	—	0.34±0.01	0.2-0.5	Combustion of petroleum fuel	0.35±0.11	0.2-0.5	Combustion of petroleum fuel	0.79±0.04	>0.5	Biomass burning, coal combustion and eateries

Range and sources referred from: [Akyuz and Cabuk, 2010](#); [Katsoyiannis et al., 2007](#); [Park et al., 2002](#); [Pies et al., 2008](#); [Ravindra et al., 2008_a](#); [Ravindra et al., 2008_b](#); [Shukla et al., 2022](#); [Yunker et al., 2002](#); [Zhang et al., 2008](#).

Note: ‘—’ stands for paucity of data due to non-detection of specific PAHs of the binary ratios during concentration analysis.

‘na’: Not available

5.4. Conclusion

The current work provides a detailed evaluation of PAHs concentrations with respect to seasonal distribution in air gathered from four distinct sample sites along the roads of South Kolkata in India. Plant uptake of pollutants primarily depends on the fluctuations in environmental, ecological and meteorological factors. Leaf PAHs concentrations (200.98 ± 2.72 – $550.79 \pm 10.11 \mu\text{g g}^{-1} \text{ d.w.}$) and spatial/temporal distribution pattern noticed in different sites seemed to be directly dependent on site-specific characteristics or sources. Based on seasonality, extent of leaf contamination by PAHs was extreme in winter followed by postmonsoon and then premonsoon, and the fate of pollutants being controlled by air movement, temperature, partition coefficient and boundary layer or mixing height. The isomer pair ratios (DRs) exemplified the substantial effects of pyrogenic sources of PAHs in all the sites (e.g., $\Sigma\text{LMW}/\Sigma\text{HMW} < 1$ and $\text{ANT}/(\text{ANT}+\text{PHE}) > 0.1$), and vehicular pollution and cooking exhausts were found to be the leading causes of deteriorating air quality of South Kolkata apart from combustion of solid/liquid fuels and biomass. Atmospheric condition-mediated degradation of PAHs affects proper identification/analysis of polluting sources; hence, multiple DRs have been worked upon to decipher the type of emission. Continuous monitoring (round the year) of PAHs would offer better perception into the degree of pollution and would help us to devise appropriate mitigation strategies. Thus, green belting in the vicinity of severely polluted areas using biomonitor plants such as *M. paniculata* is strongly advised for curbing the hazardous effects of air pollution and reinforcing sustainable practices for ecosystem vitality, human health and well-being. In line with the above, screening of local abundantly available different plant bioindicator species of urban roadsides of South Kolkata was undertaken in Chapter 6 based on their performance evaluation for exploitation of their potential for urban greenery planning.

Chapter 6

6. Methodology V

Assessment of different urban plant bioindicators for urban greenery planning

6.1. Background

Deteriorating air quality and increased emission rates of greenhouse gases with other criteria air pollutants in India must be tackled on war-footing to prevent the disease burden for a greener and cleaner future. Findings of continuous studies on sustainable practices by the researchers (at both government and institutional levels) for curbing air pollution have compelled the government bodies (like Central Pollution Control Board (CPCB), India) to establish a number of monitoring stations in different states of India through the National Air Monitoring Programme (NAMP) based on environmental policies and legislative actions ([Kaur and Pandey, 2021](#); [NAMP, 2023](#)). Among the major airborne pollutants, particulate matter (PM) with size specification large (aerodynamic diameter, AD: 10–100 μm), coarse (AD: 2.5–10 μm) and fine (AD: ≤ 2.5 μm) and polycyclic aromatic hydrocarbons (PAHs) including low molecular weight PAHs (LMW PAHs) and high molecular weight PAHs (HMW PAHs) critically affect human health or any other life form in the ecosphere ([Delgado-Saborit et al., 2011](#); [Venkatesan, 2016](#); [WHO, 2006](#)). Overshoot in the anthropogenic emissions, being responsible for a sharp increase in pollutants' generation, has already caused irreversible destruction to the natural environment ([Ambade et al., 2022b](#)). Remediation efforts must be identified by the scientific society to primarily address the life-threatening challenges posed by the carcinogenic or mutagenic impacts of PAHs and PM with their incidences of prevalence. Health risk evaluation of gaseous and particle-bound PAHs (in terms of benzo[a]pyrene equivalents, incremental lifetime cancer risks (ILCR) and lifetime average daily dose (LADD))

has indicated that the human exposure increases the lifetime probability of developing cancers in individuals ([Morakinyo et al., 2020](#); [Shukla et al., 2022](#)).

Traditional monitoring methods though have provision for discerning location-based real-time air quality trends in relation to actual concentrations of pollutants, they only measure the current concentration of the pollutants in the atmosphere, but never give any idea about the history of long-term accumulation of atmospheric pollutants. Such methods have limited capacity depending on the suction abilities of the installed air samplers that have to be shifted from one site to other (consuming more time) in order to have a greater picture of air quality on a regional basis with spatial gradients. They also entail huge expenses for installation and maintenance of facilities at sample locations as well as for manpower deployment for security and continuous monitoring of machineries ([Li et al., 2023](#)). From environmental perspective, urban green belts opened out as a fundamental, sustainable and lucrative solution to ambient air pollution control with greater spatio-temporal coverage ([Han et al., 2022b](#); [Liu et al., 2023](#); [Wu et al., 2021](#)). Multidimensional studies, already carried out with plant leaves, involving theoretical, experimental and computational or simulation approaches, evolved explicit perceptions of phytomonitoring and remediation of PM and PAHs along with the proper understanding of plant-air partitioning ([Borgulat and Borgulat, 2023](#); [Pleijel et al., 2022](#); [Redondo-Bermudez et al., 2021](#); [Xie et al., 2022](#)). Therefore, the growing importance of plant foliage in removing and uptaking pollutants has now become apparent relating to their epidermal formations (such as hairy layers, deep grooves, ridges, waxy cuticles, stomatal abundance), flexible characteristics, macromorphology and larger porous contact surface favourable for adherence, assimilation, internalization and distribution of pollutants in vegetal tissues ([De Nicola et al., 2017](#); [Li et al., 2021](#)). Research studies conducted at laboratory scale with optimization trials must also be validated with real-time environmental ambience loaded with manmade interventions replenishing abominably huge quantities of pollutants continuously into the atmosphere ([Ghafari et al., 2020](#)). Thus, it is essential to classify the point, non-point and mobile sources of emission for anticipating the nature and characteristics of pollutants contributing to transboundary or local air pollution ([Thunis et al., 2019](#)).

The interactions of plants with atmospheric pollutants mediate direct or indirect changes in leaf variables (e.g., chlorophyll, ascorbic acid, sugar, proline, moisture, pH, membrane permeability, wax, trichomes, surface roughness, epidermal cells, stomatal type, etc.) and phenotype which are the expressions of dynamic integrated mechanisms of plant defense against abiotic stress ([Anand et al., 2022](#); [Rai, 2016](#)). Since, environmental conditions

have profound effects on leaf parameters, analysis of such quantitative traits as biomarkers would yield valuable information on air quality. In relevance with the fact, local plant species growing in overwhelming numbers should have prime weightage for environmental purification through biomonitoring in comparison to the meagrely grown plants (Hajizadeh et al., 2019). In addition to parameter estimation for determining the combinations of plant responsive traits, assessment of species based on air pollution tolerance index (APTI) and anticipated performance index (API) ranking approaches could also assist in green belting configurations in order to improve the filtering effects of tolerant/biomonitor plants (Banerjee et al., 2019; Karmakar and Padhy, 2019). It is worth mentioning that the incorporation of some pollution sensitive plants in green landscaping fulfils the role of indicator species.

Kolkata, one of the Indian megacities most vulnerable to pollution-induced climatological hazards, has been facing tremendous unplanned growth due to overpopulation for the past few decades, causing unprecedented increase in the levels of air pollution. As a result of which, a number of respiratory airway disorders spiked among 50% of young children (<https://timesofindia.indiatimes.com/city/kolkata/50-of-city-kids-have-airway-disorder-docs-blame-pollution/articleshow/104956414.cms>). Human suffering from respiratory illness (affecting ~70% of the citizens) and reduced life expectancy (by 6.1 years) is the biggest scourge of the city (<https://timesofindia.indiatimes.com/city/kolkata/breathing-citys-toxic-air-is-like-smoking-doctors/articleshow/63423970.cms>) owing to the huge presence of aerosols. Also, there is a shortage of studies in Kolkata exploring how the mass of PM of discrete size distribution varies differently on plant leaf surfaces or in cuticular waxes and identifying structural, biochemical and physiological traits at the leaf level to predict the response of diverse plant types towards atmospheric PM and PAHs for their long-term performance in urban plantations. Research on risk factors of accumulated plant leaf PAHs is also inchoate and needs to be taken up in right earnest. Hence, the current study aimed at (1) estimating the mass fractions of surface-adsorbed and wax-retained PM (large and coarse) deposited on the leaves of eight dominant plant species (trees and shrubs) from the street canyons of Patuli in southeast Kolkata, India, to evaluate their PM retention capacities and quantifying the relationship of leaf waxes, laminar structure and surface micromorphology with particulate capture, (2) measuring the concentrations of foliar PAHs with particular focus on PAHs distribution percentage and profiling based upon ring structure with a view to studying the bioaccumulation pattern for the selected plant species highlighting the significance of specific leaf area (SLA) on total PAHs content, (3) detecting the nature of PAHs (low or high temperature-derived) at the study area

through the application of total index, (4) carrying out the toxicity risk analysis of foliar PAHs with reference to the benzo[a]pyrene equivalent concentrations and carcinogenic and mutagenic potential thereof and (5) investigating the feasibility of plant species by examining different plant leaf variables (biomarkers of air quality) with APTI and API screening for urban landscaping. The concept is pictorially elaborated in Fig. 24 below.

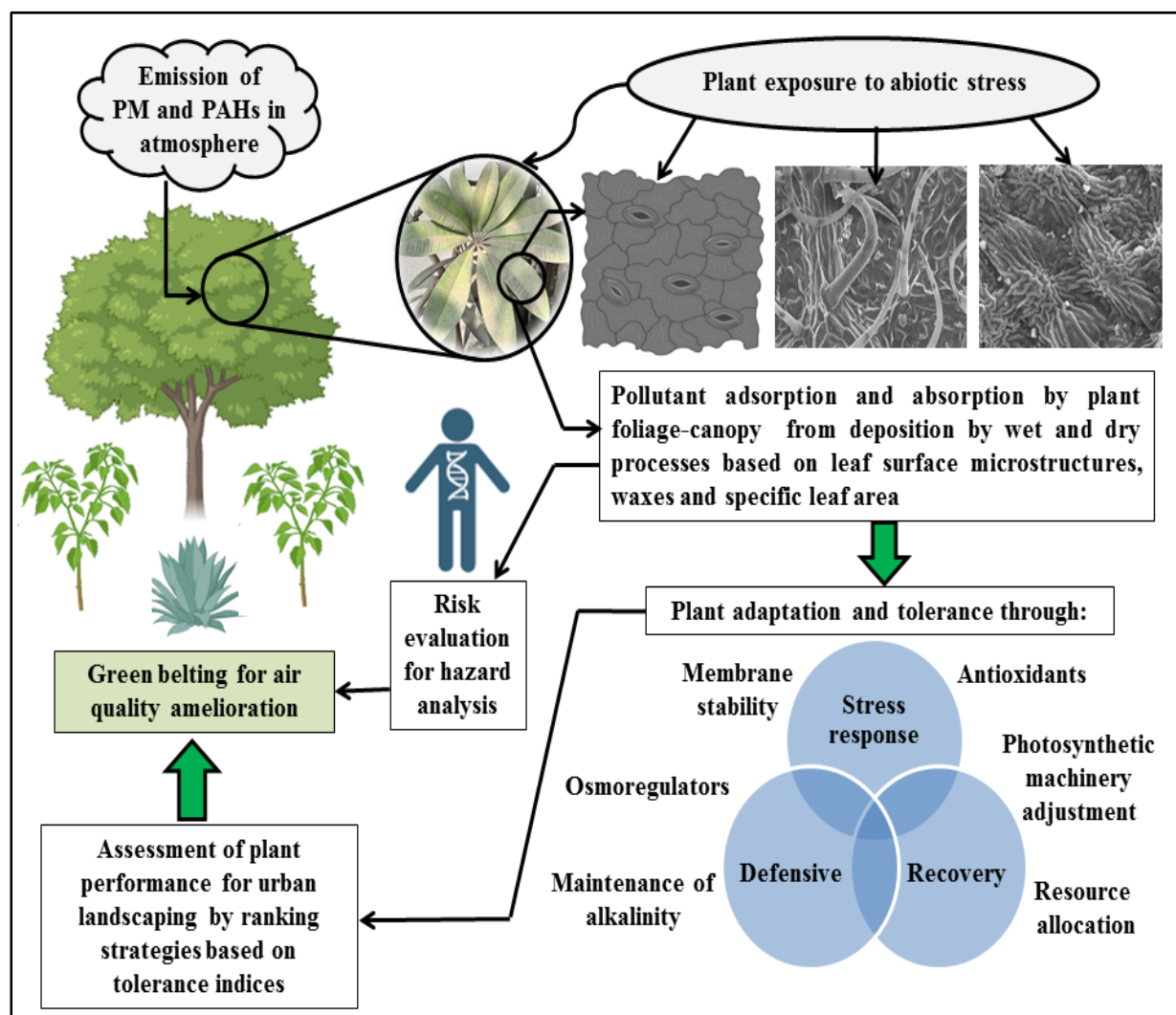


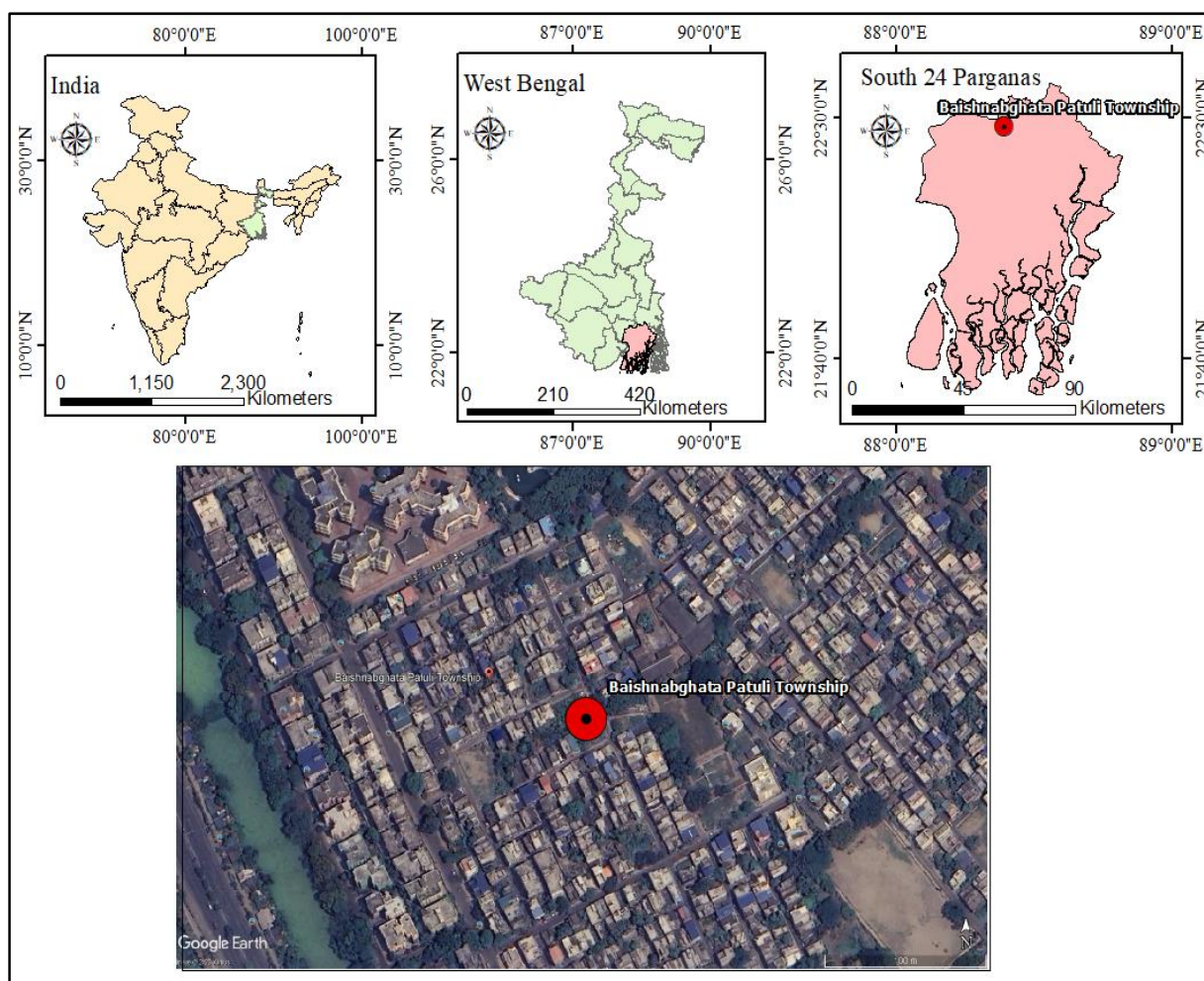
Fig. 24. Schematic view of biomonitoring of airborne PM and PAHs by plant species.

6.2. Materials and methods

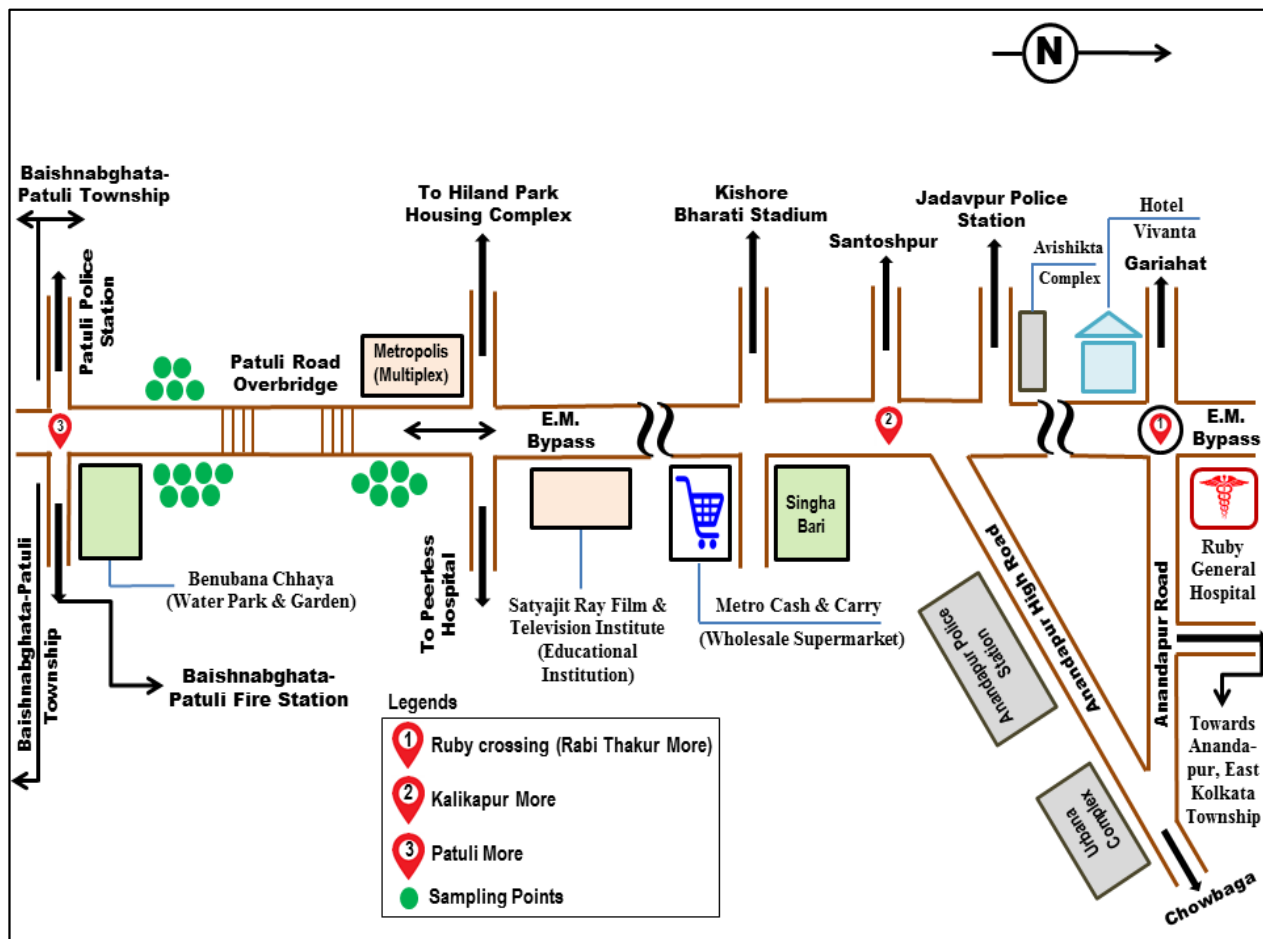
6.2.1. Location of sampling site, selection of plant species, sample collection and preservation

In the proposed work, Patuli (Baishnabghata Patuli Township (BPT): 22.4710°N, 88.3924°E) was chosen as the study area which is situated on the southern part of East Kolkata in the state

of West Bengal, India. It is well-connected to the Eastern Metropolitan (EM) Bypass (State Highway SH 1) which has very high traffic load and related commercial activities. The BPT site is under the surveillance of a semi-automatic ambient air quality monitoring station (SAAQMS) of West Bengal Pollution Control Board (WBPCB), which has prompted us to select the sampling points (near Benubana Chhaya: water park and garden, Patuli overbridge and Metropolis shopping mall) within such area due to the possibility of high load of urban pollution. The location of the study area along with a route map has been depicted in Fig. 25(a) and Fig. 25(b) highlighting the sampling spots which are adjacent to and surrounded by SH 1 (EM Bypass), super speciality hospitals, modern housing complexes, many big commercial outlets and metro train line. Moreover, air quality data given by WBPCB for three criteria pollutants, PM_{10} , SO_2 and NO_2 , across the site throughout the sampling time have been presented in Table 27 to recognize the aggravated air quality of the selected sites in Kolkata metro city.



(a)



(b)

Fig. 25. (a) Location of the study area (Baishnabghata Patuli Township, BPT) within Kolkata, West Bengal, India and (b) route map view of sampling at Patuli.

Table 27

Air quality information of BPT area based on the data of WBPCB monitoring station during the sampling period (http://emis.wbpcb.gov.in/airquality/filter_for_aqi.jsp).

Ambient air quality monitoring data						
Month	Sampling date	NO ₂ (µg m ⁻³)	SO ₂ (µg m ⁻³)	PM ₁₀ (µg m ⁻³)	Air quality index with respect to PM ₁₀ (Range)	Air quality status
	Permissible limit (24 h average)	80	80	100		
January	15/01/2021	49	9	226	184 (101–200)	Moderate
	18/01/2021	49	9	274	224 (201–300)	Poor
	24/01/2021	48	10	276	226 (201–300)	Poor
February	02/02/2021	52	10	267	217 (201–300)	Poor
	11/02/2021	45	9	172	148 (101–200)	Moderate
	17/02/2021	51	9	239	193 (101–200)	Moderate
March	03/03/2021	51	9	188	159 (101–200)	Moderate
	13/03/2021	47	9	205	170 (101–200)	Moderate
	19/03/2021	52	10	244	196 (101–200)	Moderate

The most common roadside plants of varied life forms (shrubs and trees), nature (evergreen and deciduous) and leaf types, such as *Nerium oleander* (Local name: Rakta Karabi, Family: Apocynaceae), *Tabernaemontana divaricata* (Local name: Tagar, Family: Apocynaceae), *Calotropis gigantea* (Local name: Akanda, Family: Apocynaceae), *Bauhinia acuminata* (Local name: Kanchan, Family: Fabaceae), *Polyalthia longifolia* (Local name: Debdaru, Family: Annonaceae), *Alstonia scholaris* (Local name: Chhatim, Family: Apocynaceae), *Neolamarckia cadamba* (Local name: Kadam, Family: Rubiaceae) and *Plumeria alba* (Local name: Champa, Family: Apocynaceae) were selected to examine the potential to act as vegetation barriers (with diversifying plant communities) for mitigation of air pollution (Fig. 26). Hence, in accordance with the current study, fully expanded and matured leaves were sampled using stainless steel garden scissors with proper precaution, in the peak hours at morning, from the road-facing branches of different individual plants of same species as available within 3 m height from ground level in the selected spots during January-March, 2021. The collected samples (including the replicates of each species) were then kept in polyethylene sample bags and directly taken to the laboratory for further investigation (Yang et al., 2017). The plant leaves were processed to fine powder in a mortar after rinsing with deionized water (for the removal

of extraneous materials (biological or non-biological) from foliar surfaces) and lyophilization and ultimately stored for leaf tissue analysis (De Nicola et al., 2016; Foan and Simon, 2012). Fresh leaves were also utilized for some parametric tests, like measurements of PM, RWC, membrane stability index and electrolyte leakage as well as for morphological examination.

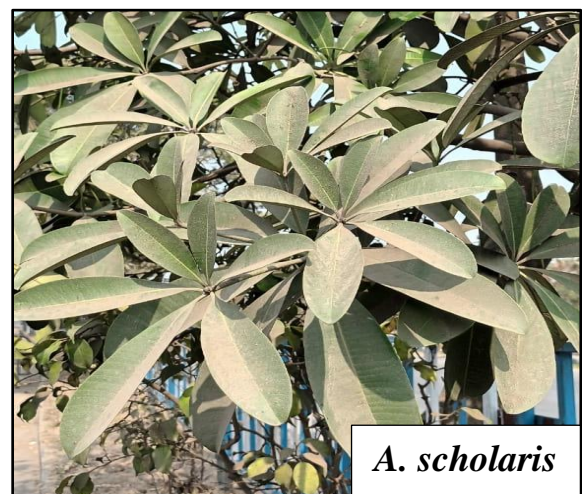
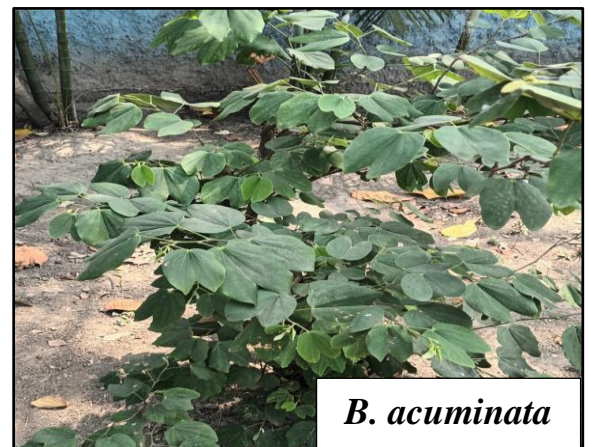




Fig. 26. Photographs of selected terrestrial urban plant species for the study.

6.2.2. Quantitative estimation of particulate matter (PM) retained on plant foliage and leaf waxes

Assessment of the contents of PM deposited on plant leaves (surface PM or sPM) and that entrapped in leaf waxes (wax PM or wPM) was accomplished in accordance with the method elaborated by [Dzierzanowski et al. \(2011\)](#). Leaf samples were kept in Erlenmeyer flasks and thoroughly washed with 250 mL of deionized water aided by agitation for 1 min to wash out the surface-adsorbed particulates. For eliminating particles of size $>100\ \mu\text{m}$, the washed-out solutions were first filtered through a metal sieve. Sequential filtration was also carried out afterwards using pre-weighed Whatman Grade 1 filter paper to collect large fraction of PM (ranging between $10\text{--}100\ \mu\text{m}$) and Whatman Grade 42 filter paper for the retention of coarse PM ($2.5\text{--}10\ \mu\text{m}$) by the help of a filtration unit with porcelain Buchner funnel fitted to a portable oil-free vacuum pump (Rivotek). Filters were again oven-dried post-filtration at $60\text{--}70\ ^\circ\text{C}$ for about 30 min and mass of each PM fraction was noted.

The plant leaves, already washed with water, were immersed in 150 mL of chloroform and shaken for 40 s to extract the wax-embedded PM for its quantification through the same filtration procedure as stated above. Total PM load was defined as the summation of sPM and wPM (i.e. summation of total large PM = large (sPM + wPM) and total coarse PM = coarse (sPM + wPM)). The resulting extracts containing dissolved waxes in chloroform were transferred to different pre-weighed vials, dried for solvent evaporation and thereafter accurately weighed as leaf waxes. Total areas of all the leaf samples were calculated using graph papers ([Prajapati and Tripathi, 2008_a](#)), which were then utilized to express the content of

PM deposited and waxes in $\mu\text{g cm}^{-2}$ of leaf area. Specific leaf areas (SLAs) were also evaluated with the estimated values of leaf area (A, cm^2) and leaf dry weight (DW, g) (Eq. 14):

$$SLA (\text{cm}^2 \text{g}^{-1}) = \frac{A}{DW} \quad (14)$$

6.2.3. Analysis of leaf core attributes to discern the biomonitoring potential of the selected plant species

6.2.3.1. Total chlorophyll, carotenoid and ascorbic acid contents

Leaf chlorophyll (Chl) and carotenoid concentrations were determined by classical spectrophotometric method, wherein, 1 g sample was extracted with 20 mL of acetone:water mixture (80:20, v/v) under stirring for 15 min at ambient temperature followed by extract filtration and refrigerated storage (Sudhakar et al., 2016). The extraction was repeated five times until complete removal of pigments from the leaf matrix was anticipated. Measurement of the filtrates was carried out with a LAMBDA 365 ultraviolet-visible (UV-Vis) spectrophotometer (PerkinElmer, USA) at 663 (for Chl a), 645 (for Chl b) and 470 (for carotenoids) nm with respect to a blank sample of 80% acetone. Chl and carotenoid contents were quantified as per the formulae (based on specific absorption coefficients) (Eqs. 15-18) proposed by Arnon (1949) and Lichtenthaler and Buschmann (2001):

$$Chl\ a (\text{mg g}^{-1}) = \frac{(12.7 \times A_{663} - 2.69 \times A_{645}) \times V}{1000 \times W} \quad (15)$$

$$Chl\ b (\text{mg g}^{-1}) = \frac{(22.9 \times A_{645} - 4.68 \times A_{663}) \times V}{1000 \times W} \quad (16)$$

$$Chl_T (\text{mg g}^{-1}) = \frac{(20.2 \times A_{645} + 8.02 \times A_{663}) \times V}{1000 \times W} \quad (17)$$

$$C_{X+C} (\text{mg g}^{-1}) = \frac{(1000 \times A_{470} - 1.82 \times Chl\ a - 85.02 \times Chl\ b) \times V}{198 \times 1000 \times W} \quad (18)$$

where, Chl a, Chl b, Chl_T and C_{X+C} = chlorophyll a, chlorophyll b, total chlorophyll and carotenoid contents, A₆₆₃, A₆₄₅ and A₄₇₀ = absorbances at 663, 645 and 470 nm, V = total volume of extract (in mL) and W = weight of leaf (g).

Plant leaves were analysed for ascorbic acid (AA) content using the standard 2,6-dichlorophenol indophenol (DCPIP, AR/ACS grade, assay: 98%; Loba Chemie, India) titration method (Hughes, 1983; Roy et al., 2020). AA was extracted from the plant leaves (2 g) in 4% oxalic acid (ACS reagent, ≥99%; Merck, Darmstadt, Germany) solution of 100 mL (titrating

medium) and the mixture was stirred for 30 min. Leaf extracts were then centrifuged (Remi laboratory centrifuge R-8M Plus) at 2800 rpm for 10 min. Subsequently, 5 mL of the supernatant and AA (extra pure 99%; Loba Chemie, India) working standard were transferred into two separate conical flasks containing 10 mL of 4% oxalic acid and titrated against the dye till the appearance of pink colour (endpoint). AA contents were calculated using the expression (Eq. 19) as follows (Roy et al., 2020):

$$AA (mg\ g^{-1}) = \frac{0.5 (mg) \times V_2 (mL) \times 100 (mL)}{V_1 (mL) \times 5 (mL) \times Sampleweight (g)} \quad (19)$$

where, V_1 = Volume of dye consumed for the working standard and V_2 = Volume of dye consumed for the sample.

6.2.3.2. Relative water content and foliar pH

Appropriate measurement of relative water content (RWC) of sampled leaf tissues was performed by the following mathematical expression (Eq. 20) (Pathak et al., 2011) considering leaf fresh weight (FW), turgid weight (TW acquired after water saturation of the leaves kept overnight in submerged condition) and dry weight (DW obtained after drying of leaves in hot air oven at 70-80 °C):

$$RWC (\%) = \frac{(FW - DW)}{(TW - DW)} \times 100 \quad (20)$$

pH of the filtered leaf extracts was monitored using a LT-23 digital pH meter (Labtronics, India) calibrated with standard buffer capsules of pH 4 and 9, after homogenization of 2 g of sample in 40 mL of double distilled water (Zhang et al., 2016).

6.2.3.3. Membrane stability index and electrolyte leakage

Fresh plant leaves of each species were cut into small circular discs which were then immersed in 20 mL of deionized water-filled glass beakers and incubated for 2-3 h at room temperature. Initial electrical conductivity (EC_1) of the solution was measured with a benchtop digital conductivity meter (Labtronics, Model: LT-23). The glass beakers were placed in boiling water bath for 15 min and again cooled down to room temperature in order to record the final electrical conductivity values (EC_2). The membrane stability index (MSI in %) (Eq. 21) and electrolyte leakage (EL in %) (Eq. 22) were evaluated in terms of conductance due to ion leakage from the foliar tissues applying the below-mentioned formulae (Mukherjee et al., 2020; Singh et al., 2007):

$$MSI (\%) = (EC_2 - \frac{EC_1}{EC_2}) \times 100 \quad (21)$$

$$EL (\%) = (\frac{EC_1}{EC_2}) \times 100 \quad (22)$$

6.2.3.4. Leaf carbon content

Carbon content of plant leaves was quantitated by loss on ignition method which is a simple, rapid and cost-effective technique widely employed for larger sample sizes (Dean, 1974; Paull et al., 2021). Initially, the leaves were oven-dried at 70-80 °C for 48 h and consequently, 1 g of dried sample was subjected to the process of dry ashing at 550 °C temperature for 3 h using a muffle furnace (Baxter et al., 2014). Content of leaf carbon was then obtained with Eq. 23:

$$LOI = \frac{DW-AW}{DW} \times 100 \quad (23)$$

where, LOI = loss on ignition (%), DW = dry weight of sample (g) and AW = ash weight of sample (g).

6.2.3.5. Protein, proline and total soluble sugar contents

Quantification of proteins in plant leaves was carried out using a colorimetric assay, i.e., Bradford method (Bradford, 1976). Primarily, leaf protein extracts were obtained after grinding of dried foliar tissues (2 g for each extraction) in 5-10 mL of extraction buffer (STET lysis buffer; SRL, India) with mortar pestle accompanied by centrifugation. For analysing the protein content of all the leaf samples, 5 mL of Bradford reagent (SRL, India) was added to 0.1 mL of each extract in separate test tubes, mixed thoroughly and incubated for 5-10 min. Absorbances of the solutions were then recorded at 595 nm by a UV/Vis spectrophotometer (PerkinElmer, USA; L365) with reference to a reagent blank (composed of 0.1 mL extraction buffer and 5 mL Bradford reagent). Protein concentrations were thus determined against a calibration curve of commercial bovine serum albumin (BSA, assay: 98%; SRL, India) prepared by a series of standards diluted from the BSA stock of 2 mg mL⁻¹ in extraction buffer and computed on a dry weight basis in mg g⁻¹.

Proline content of plant leaves was assessed according to the protocol proposed by Bates et al. (1973) using ninhydrin reagent. Leaf tissues (1 g) were first macerated in an aqueous solution (3% w/v) of sulfosalicylic acid (extrapure, 99%; SRL, India) (20 mL). After homogenization, tissue homogenates were centrifuged at 2800 rpm for 10 min. The supernatants were collected thereafter in glass vials for analysis, wherein, 2 mL of ninhydrin

reagent (extrapure AR/ACS grade, 99%; SRL, India) (prepared by dissolving 1.25 g in a solution of glacial acetic acid (ACS reagent, $\geq 99.7\%$; Merck, Darmstadt, Germany) (30 mL), deionized water (15 mL) and 85% ortho-phosphoric acid (extrapure, assay: 85%; SRL, India) (5 mL) (6:3:1) (Ncube et al., 2013)) and 2 mL of glacial acetic acid were added to different test tubes containing 2 mL of extract. The sample tubes with mixture were kept in boiling water bath for 1 h and 4 mL of toluene was then added to each tube after cooling them down to room temperature. Upon vigorous mixing, the organic (toluene or chromophore) layer was pipetted out and transferred to glass cuvettes for absorbance reading at 520 nm as against a sample blank with only toluene. A standard curve (of pure proline (99% by assay; SRL, India) with initial stock of 0.1 mg mL^{-1}) was used for calculating the unknown concentrations of proline in the test samples in mg g^{-1} DW of leaves.

To isolate and quantify total soluble sugars, ground foliar tissues (1.5 g) were subjected to sequential extractions (three times for 5 min each) using 15 mL of hot ethanol (80%). The clear extracts were recovered after centrifugation and 2 mL aliquot of the extracts transferred in each test tube was mixed with 5 mL of 5% (w/v) zinc sulphate (pure, 99%; SRL, India) and 4.7 mL of 0.3 (N) barium hydroxide (pure, 98%; SRL, India) solutions. The mixtures were vigorously shaken and again centrifuged for 10 min at 2800 rpm. 4 mL of anthrone reagent (extrapure AR, 98%; SRL, India) solution (of standard composition — 2 g dissolved in 1 L of concentrated sulphuric acid) was then added to 0.5 mL aliquot of the collected supernatant in glass tubes and heated to 90-100 °C for 10 min. The resulting solutions were allowed to cool down and consequently analysed spectrophotometrically at 630 nm in respect of a blank (1 mL distilled water and 5 mL reagent) (Sarabi and Arjmand-Ghajur, 2021; Yemm and Willis, 1954). Quantitation of total soluble sugars was performed based on a standard curve of varying concentrations of glucose (extrapure AR/ACS; SRL, India) made from the stock of 0.2 mg mL^{-1} and expressed in mg g^{-1} DW of leaves.

6.2.4. Air pollution tolerance index (APTI)

Plants' inherent ability to combat air pollution was examined through the estimation of APTI based on the formula of Singh and Rao (1983) and Singh et al. (1991) involving biochemical and physiological markers, such as Chl, AA, RWC and pH, as indicated and explained in Eq. 3 of Chapter 1.

6.2.5. Anticipated performance index (API)

Feasibility of plant species for green belting to help in ecological restoration was assessed by API which particularly depends on several biological, biochemical and socioeconomic characteristics of plants including APTI, type of plant and growth habit, arrangement of plant canopy, laminar structure and economic value (Pandey et al., 2015_a, 2015_b; Prajapati and Tripathi, 2008_b). API is based on a grading system where each plant is assigned with a grade (+) / (–) owing to its traits, totalling up to 16 positive points and leading to a percentage evaluation (% score) as given by the following formula (Eq. 24):

$$\% \text{ Score} = \frac{\text{Total grades obtained by the plant species}}{\text{Maximum possible grades for any plant species (16)}} \times 100 \quad (24)$$

API values were determined for all the plants corresponding to their respective % score, to finally ensure their category for utilization in urban landscaping.

6.2.6. Investigation of leaf surface micromorphology

The adaxial and abaxial surfaces of plant leaves were studied with the help of a scanning electron microscope (SEM, Hitachi S-3400 N) for minute observations of leaf surface microstructures and epidermal characteristics along with PM deposition. The fresh leaves were first sized into pieces, not more than 3–5 mm², and then placed into the solution of phosphate buffer (molecular biology grade; SRL, India) for 2–3 min. After buffer wash, leaf samples were fixed in methanol for 10 min and dehydrated with graded alcohol (ethanol: 30, 50, 70, 80, 90, 100% followed by t-butanol: 70, 80, 90, 100%) solutions maintaining 15 min per change (Ickert-Bond et al., 2018; Kim, 2020; Yuan et al., 2020). All the specimens were air-dried and kept under desiccation for a dry environment. The dried samples were mounted on specimen stubs using double-sided carbon adhesive tape and gold coated in a sputter coater. The SEM images (with magnification range of 35X-3000X) were finally acquired under high vacuum at an accelerating voltage of 15 kV.

6.2.7. PAHs determination in plant foliage

Prior to analysis, the process of Soxhlet extraction was employed, where 120 mL of toluene was used to extract PAHs from plant leaves (10 g for each sample) for 6 h and the specific fractions of PAHs were separated using silica gel (high purity grade, 100-200 mesh; Merck, Darmstadt, Germany) column as previously reported in Mukhopadhyay et al. (2023). The

collected fractions were almost concentrated to dryness via rotary evaporation (Rotavapor R–3, Buchi) and solvent-exchanged to analytical grade methanol for high performance liquid chromatographic (HPLC) analysis. Concentrations of 16 priority USEPA-PAHs (naphthalene (NAP), acenaphthylene (ACY), acenaphthene (ACE), fluorene (FLU), phenanthrene (PHE), anthracene (ANT), fluoranthene (FLA), pyrene (PYR), benzo[a]anthracene (BaA), chrysene (CHR), benzo[b]fluoranthene (BbF), benzo[k]fluoranthene (BkF), benzo[a]pyrene (BaP), dibenzo[a,h]anthracene (DB[ah]A), indeno[1,2,3-cd]pyrene (IP) and benzo[g,h,i]perylene (B[ghi]P)) were measured with HPLC-UV (Waters, USA) detection (2489 UV/Vis detector) method through the use of a certified standard (Sigma-Aldrich, United States) at 254 nm in gradient elution mode (with run time of 37 min, overall flow rate 1.5 mL min⁻¹ and 20 µL sample injection) using organic (acetonitrile) and aqueous (water) mobile phases. Based on the non-polar nature of analytes, Waters PAH C18 column (length: 250 mm; inner diameter: 4.6 mm; particle size: 5 µm) was used in the analysis (separation mode: reversed phase). Validation of the analytical method for PAHs quantification was performed in the context of recovery (78–99%), limit of detection (LOD: 0.001–0.003 µg g⁻¹) and limit of quantification (LOQ: 0.03–0.09 µg g⁻¹). The chromatographic test conditions followed for analysing foliar PAHs and the validity measurements through laboratory level quality assurance/control program were elaborated in an earlier work ([Mukhopadhyay et al., 2023](#)).

6.2.8. Risk factor assessment

Risks associated to PAHs were evaluated by means of carcinogenic and mutagenic equivalent concentrations (BaP_{TEQ} and BaP_{MEQ} in µg g⁻¹ respectively) relative to BaP (which is regarded as an indicator of carcinogenic PAHs). Individual toxicity (i.e. carcinogenicity and mutagenicity) of each PAH congener was calculated by multiplying the measured foliar concentration of every PAH compound (PAH_i) with its toxic equivalency factor (TEF) ([Nisbet and LaGoy, 1992](#)) and mutagenic equivalency factor (MEF) ([Durant et al., 1996](#)). Values of BaP_{TEQ} (for all the 16 PAHs) and BaP_{MEQ} (for BaA, CHR, BbF, BkF, BaP, DB[ah]A, IP and B[ghi]P) were then summed up to estimate the total carcinogenic and mutagenic potencies of PAHs present in the matrix (denoted in [Eq. 25](#) and [Eq. 26](#)) ([Ihunwo et al., 2021](#); [Verma et al., 2022](#)) with the assumption that the toxicity of all the individual PAHs would be additive ([USEPA, 2002](#); [WHO, 2000](#)). Contribution of each PAH to total risk potency was also determined in terms of carcinogenic and mutagenic potential (CP and MP in %) as represented below in [Eq. 27](#) and [Eq. 28](#) ([Błaszczuk et al., 2017](#); [Delgado-Saborit et al., 2011](#)):

$$BaP_{TEQ} = \sum_{i=1}^N PAH_i \times TEF_i \quad (25)$$

$$BaP_{MEQ} = \sum_{i=1}^N PAH_i \times MEF_i \quad (26)$$

$$CP_i = \frac{\frac{PAH_i \times TEF_i}{BaP}}{\sum_{i=1}^N \frac{PAH_i \times TEF_i}{BaP}} \times 100 \quad (27)$$

$$MP_i = \frac{\frac{PAH_i \times MEF_i}{BaP}}{\sum_{i=1}^N \frac{PAH_i \times MEF_i}{BaP}} \times 100 \quad (28)$$

6.2.9. Statistical analysis

The results have been reported in terms of standard deviation (SD) as mean \pm SD of each dataset of triplicate values. Statistical analysis was carried out using one-way and two-way ANOVA in Microsoft Excel in order to express the significance of the data variability. Correlation coefficient (r) was estimated to reveal the positive or negative linear relationships between PM and PAHs and between PM or PAHs with each of the different leaf variables (biochemical, physiological and morphological). The same was also performed between some of the leaf traits to understand their strength of relationship. The significance threshold was maintained at $p < 0.05$ for data acceptability and reliability.

6.3. Results and discussion

6.3.1. PM capturing potential of plant leaves: Impacts of environmental influence, leaf waxes and morphology

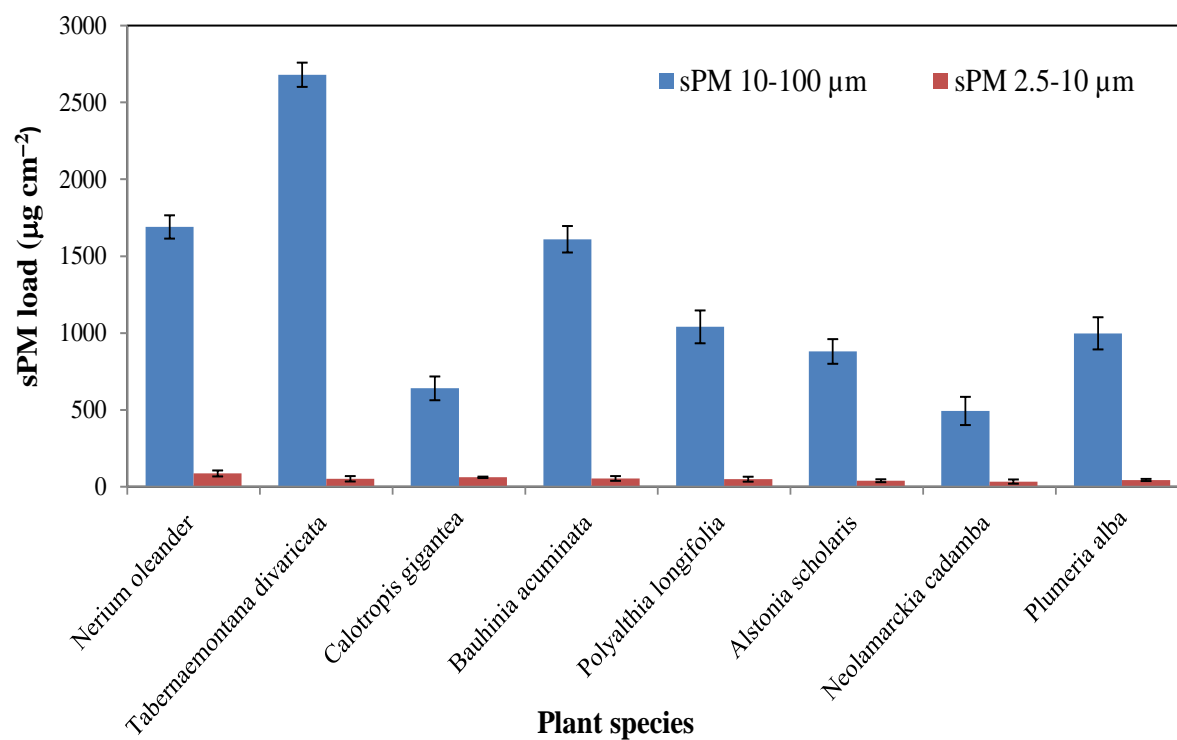
The competence of plants for particulate retention plays a pivotal role in selection of species for designing of urban green spaces, leading to sustained source of environmental comfort and protection. PM reduction by plants from the ambient air involves discrete mitigative mechanisms — diffusion, impaction, interception, sedimentation and a combination thereof and is governed by the abundance, diversity and arrangement of plant species in a vegetation cover (taking into account leaf traits, phenology, tree measurement, crown spread and plant growth characteristics), actual distance of the green zone from the original source of emissions as well as particle sizes and concentration (Beckett et al., 2000; Brantley et al., 2014; Huang et al., 2013; Janhall, 2015). Foliar micromorphology, properties of leaf cuticle and environmental factors including weather and climate change, landscape ecology and human settlements also

have considerable impacts on deposition and accumulation of PM on plant leaves (Thompson, 2018).

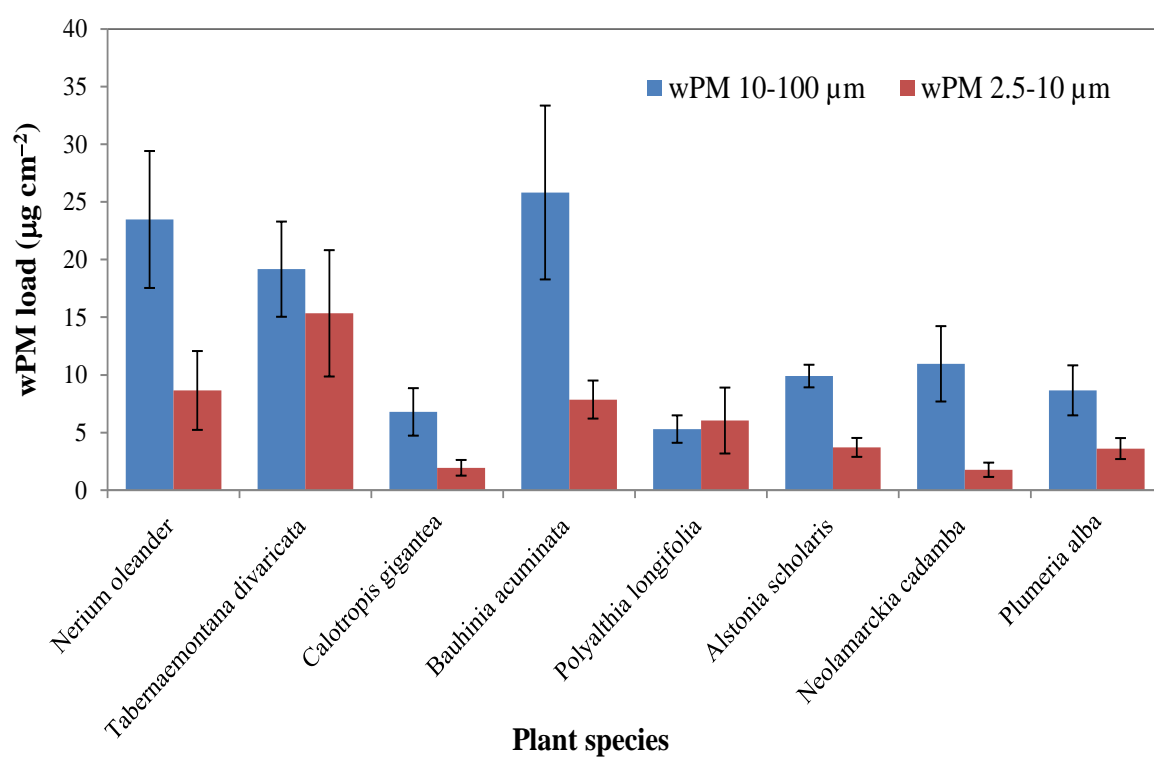
The mass of different size fractions of PM captured by the surfaces and cuticular waxes of plant leaves has been demonstrated in Fig. 27(a) and Fig. 27(b). The occurrence of high concentrations of PM in the study area is directly related to the level of pollution from atmospheric stability (most common in winter months) and anthropogenic factors, such as construction activities, heterogeneous fleet of vehicles, high traffic flow and volume, turbulences generated by motor vehicles, urban road/street design and existence of various types of roadside buildings/business establishments. Significant variability ($F > F_{crit}$ and $p < 0.05$) between the accumulation of both sPM and wPM were noticed among all the species applying one-way ANOVA along with significant differences in their total loads. It was found that the large particles (10–100 μm) were dominant ($493 \pm 91.70 - 2680 \pm 78.85 \mu\text{g cm}^{-2}$) in the deposition of PM on leaf surfaces as compared to the coarse PM (2.5–10 μm) ($33.59 \pm 13.68 - 86.51 \pm 19.45 \mu\text{g cm}^{-2}$) (ref. Fig. 27(a)) and the total sPM (large + coarse) load on the plant foliages ranged between $526.59 \pm 105.38 - 2731.76 \pm 96.39 \mu\text{g cm}^{-2}$. In cuticular/epicuticular waxes, though different PM fractions were trapped, total accumulation of large and coarse particulates (total wPM: $8.73 \pm 1.39 - 34.51 \pm 9.61 \mu\text{g cm}^{-2}$) was observed to be less with respect to surface deposition (ref. Fig. 27(b)). Also, individual concentrations of large ($5.30 \pm 1.19 - 25.82 \pm 7.54 \mu\text{g cm}^{-2}$) and coarse ($1.77 \pm 0.62 - 15.34 \pm 5.48 \mu\text{g cm}^{-2}$) PM in wax layers were much less than those of the surfaces in all the plant species examined. The probable reason could be that the immobilisation of PM in waxes is not prompt but a time-intensive process, less dependent on weather variations, unlike sPM which is strongly influenced by the impact of weather turbulences (Lu et al., 2019). For spruce, black pine and juniper species, Xu et al. (2019) reported 1.58–3.33 times higher PM retention by leaf surfaces than that of waxy layers. Przybysz et al. (2019) and Zhou et al. (2022) also obtained comparable results in case of tree species (*T. baccata* L., *P. nigra* L. and *C. betulus* L.) and evergreen shrubs (*R. pulchrum*, *O. fragrans* and *P. fraseri*) respectively. Predominantly, highest proportion of large-sized PM was recorded for all the eight species, while leaf retention accounted for lowest proportion of coarse particles. This might be due to the fact that larger particles have high propensity to settle at a faster rate under gravity, thereby facilitating foliar retention, in comparison to the coarse PM which is most likely to be transported by air before their deposition on environmental surfaces (Lu et al., 2019). Dzierzanowski et al. (2011), Konczak et al. (2021) and Przybysz et al. (2019) studied PM accumulation with plant species diversity (leafy trees, conifers, shrubs, climbers

and vines) and noticed maximum contribution of large-sized particulates to the total mass of accumulated PM.

The PM retention capacity ($\mu\text{g cm}^{-2}$) of the plants varied in the order of: *Tabernaemontana divaricata* (2766.27 ± 86.79) > *Nerium oleander* (1808.64 ± 46.99) > *Bauhinia acuminata* (1697.57 ± 95.76) > *Polyalthia longifolia* (1100.44 ± 94.77) > *Plumeria alba* (1054.27 ± 112.85) > *Alstonia scholaris* (932.61 ± 89.93) > *Calotropis gigantea* (709.91 ± 71.34) > *Neolamarckia cadamba* (539.32 ± 101.49). Many studies have reported pronounced contribution of leaf waxes on PM accumulation (Popek et al., 2015; Popek et al., 2022; Przybysz et al., 2019; Saebo et al., 2012). In the present study, quantity of waxes ranged between 23.69 ± 3.83 – $182.12 \pm 24.95 \mu\text{g cm}^{-2}$ in all the species (ref. Fig. 27(c)). It was observed that *T. divaricata* showing highest accumulation of total PM displayed maximum wax content, followed by *N. oleander*. On the other hand, *C. gigantea* and *N. cadamba* presented minimum wax contents with least PM capturing capacities. The other four species (namely, *B. acuminata*, *P. longifolia*, *P. alba* and *A. scholaris*) did not follow the similar trend. Hence, it could be inferred from above that the PM accumulation would depend not only on the foliage concentrations of waxes, but also on the chemical constituents and structure of the wax layers which determine the area of interfacial surface in addition to adhesion, uptake and translocation of particles (Corada et al., 2021; Lukowski et al., 2020; Popek et al., 2015; Saebo et al., 2012). Considering all the species together, positive correlations were obtained between wax content and total large PM ($r=0.89$, $p<0.05$), total coarse PM ($r=0.45$, $p>0.05$), total PM ($r=0.89$, $p<0.05$), total sPM ($r=0.89$, $p<0.05$) and total wPM ($r=0.68$, $p<0.05$) loads. However, it can be seen from the above results that the variation between wax content and total coarse PM is not very much significant. The current findings are in line with the previous researches, conducted by Lukowski et al. (2020) and Popek et al. (2022), where leaf wax contents were positively correlated to the PM load.



(a)



(b)

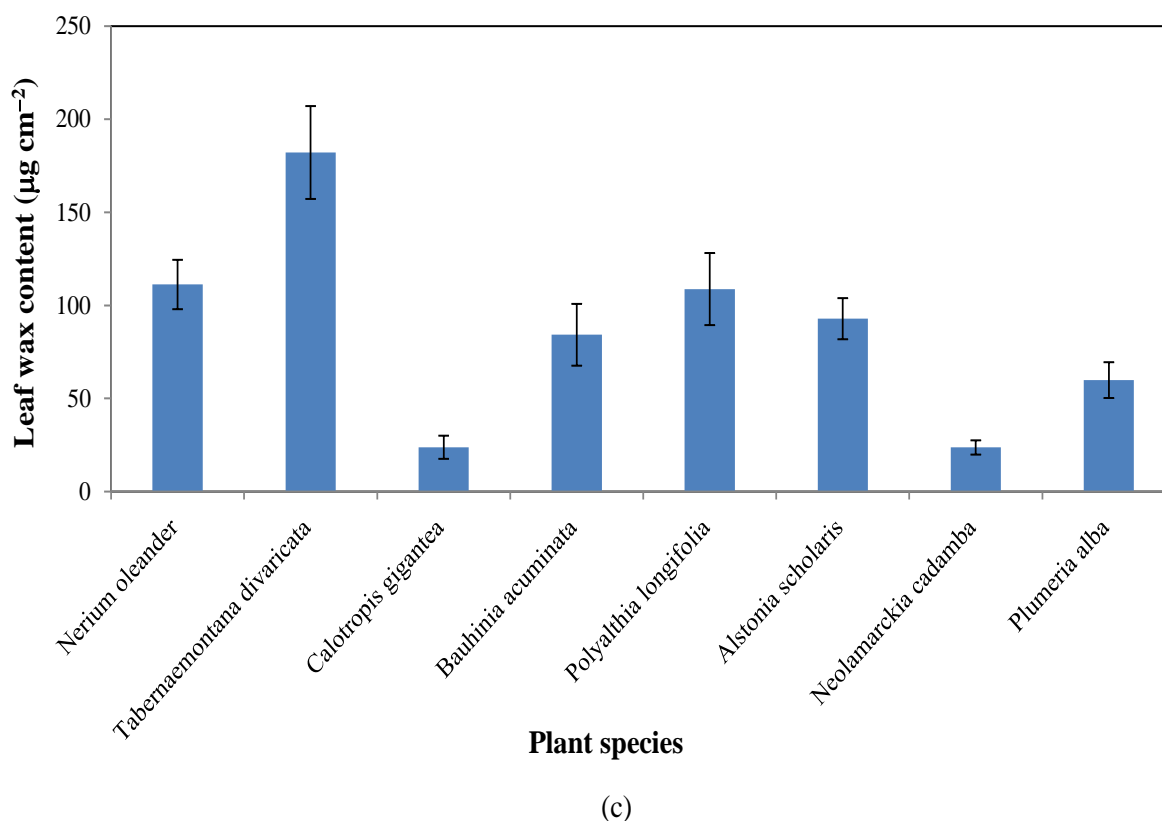


Fig. 27. Foliar contents ($\mu\text{g cm}^{-2}$) of (a) surface PM (sPM), (b) wax PM (wPM) of different size fractions and (c) waxes of selected plant species (data are presented as mean \pm SD, $n=3$).

The shape of the plant leaves also significantly controls PM accumulation (Saebo et al., 2012; Weerakkody et al., 2018b). Interaction of plant leaves having different shapes, texture and flexible porous structures with the wind generate variable drag forces on the foliages, affecting the flow regime of ambient air and cause swaying, bending and fluttering of leaves through absorption of wind momentum and dissipation of energy due to eddy shedding and formation of turbulence within the plants, resulting in deposition or dislodging of particulates (Gemba, 2007; Gillies et al., 2002). Based on the inferences given by Corada et al. (2021), Leonard et al. (2016), Popek et al. (2013), Przybysz et al. (2014), Saebo et al. (2012) and Weerakkody et al. (2018b), it has become increasingly evident that the lanceolate, ovate, obovate and lobed leaves are more capable of capturing particles. *T. divaricata*, *N. oleander* and *B. acuminata* exhibited high PM capturing potential because of their short/medium height, bushy nature and spreading crown with dense leaf arrangement; deposition being also greatly effected by their leaf shapes — lanceolate, linear-lanceolate and bilobed ovate respectively. *P. longifolia* (ovate-lanceolate leaves with wavy margin), *P. alba* (obovate leaves) and *A. scholaris* (narrowly obovate leaves) were also found to be good accumulators of PM owing to their complex leaf

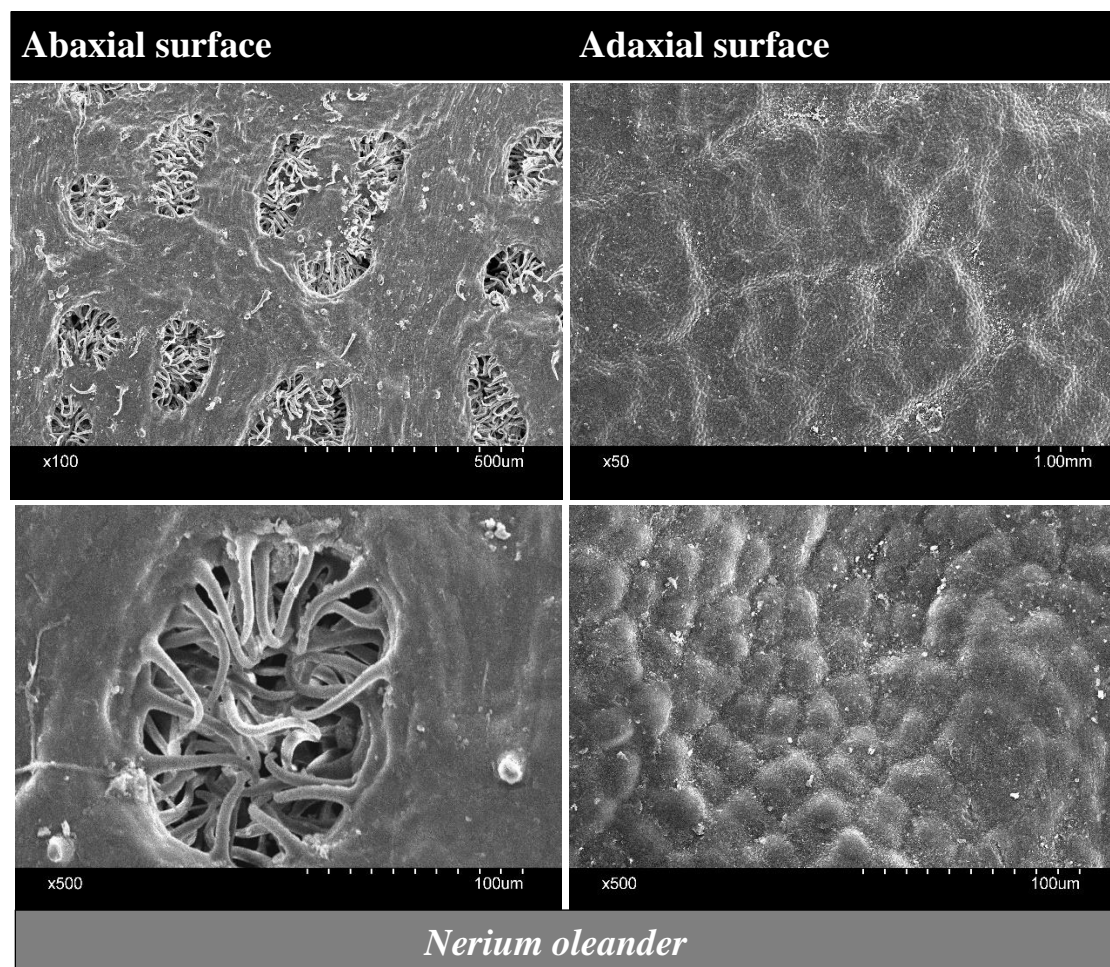
shape. *C. gigantea* (elliptic-ovate leaves), though of medium height, did not show much potential for PM capturing. *N. cadamba* (elliptic-oblong to ovate leaves) was least effective in PM retention due to its large height and branchy nature. Similarly, [Chowdhury et al. \(2022\)](#) indicated an inverse relationship between foliar deposition of PM and increased height of urban trees. Moreover, peculiar elliptical shapes of *C. gigantea* and *N. cadamba* leaves were not very much conducive to the retention of PM as already explained by [Leonard et al. \(2016\)](#) and [Weerakkody et al. \(2018b\)](#). Although noticeable PM accumulation per square cm of leaf area was not achieved for these two species in contrast to others, as a whole they can very well be used for green belts as filtering barriers against pollution and phytoaccumulators, ensuring ecological balance ([Pragasam and Ganesan, 2022](#); [Sharma and Tripathi, 2009](#)). They also have their ornamental values and economic consideration in India.

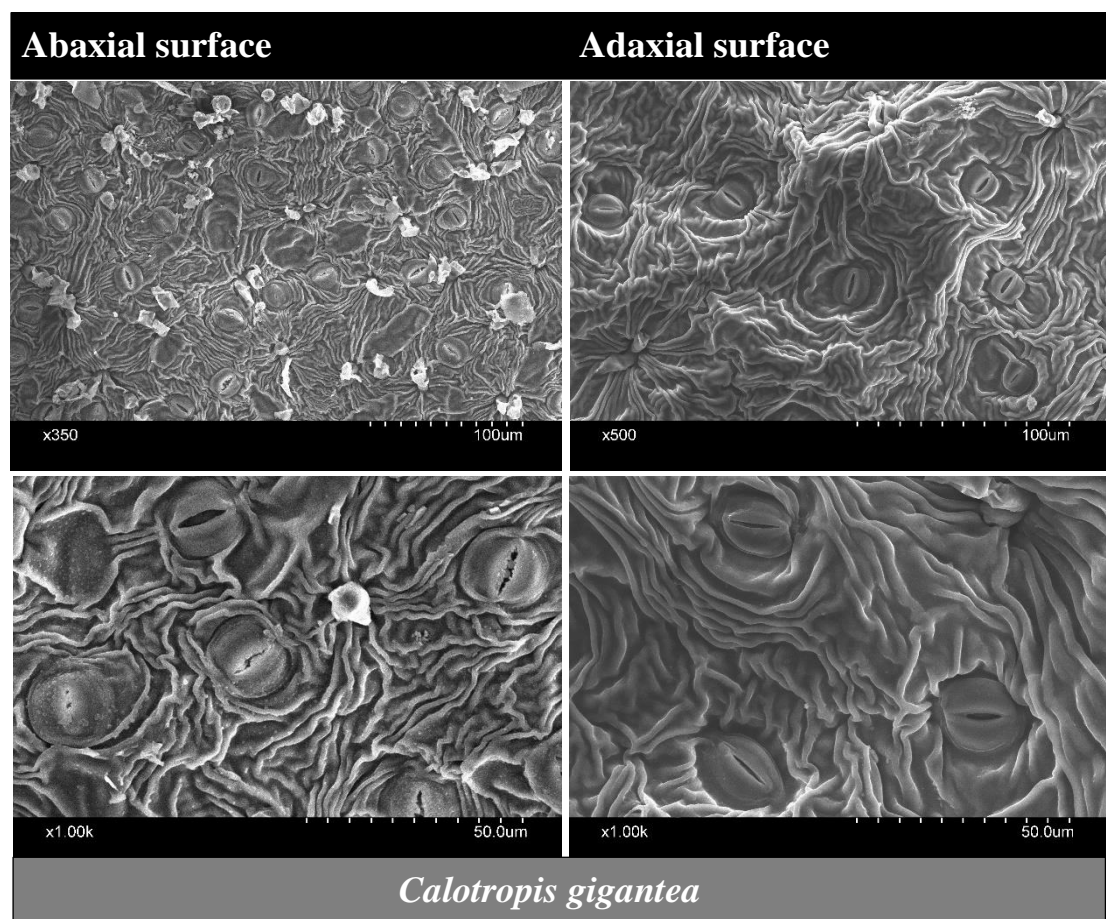
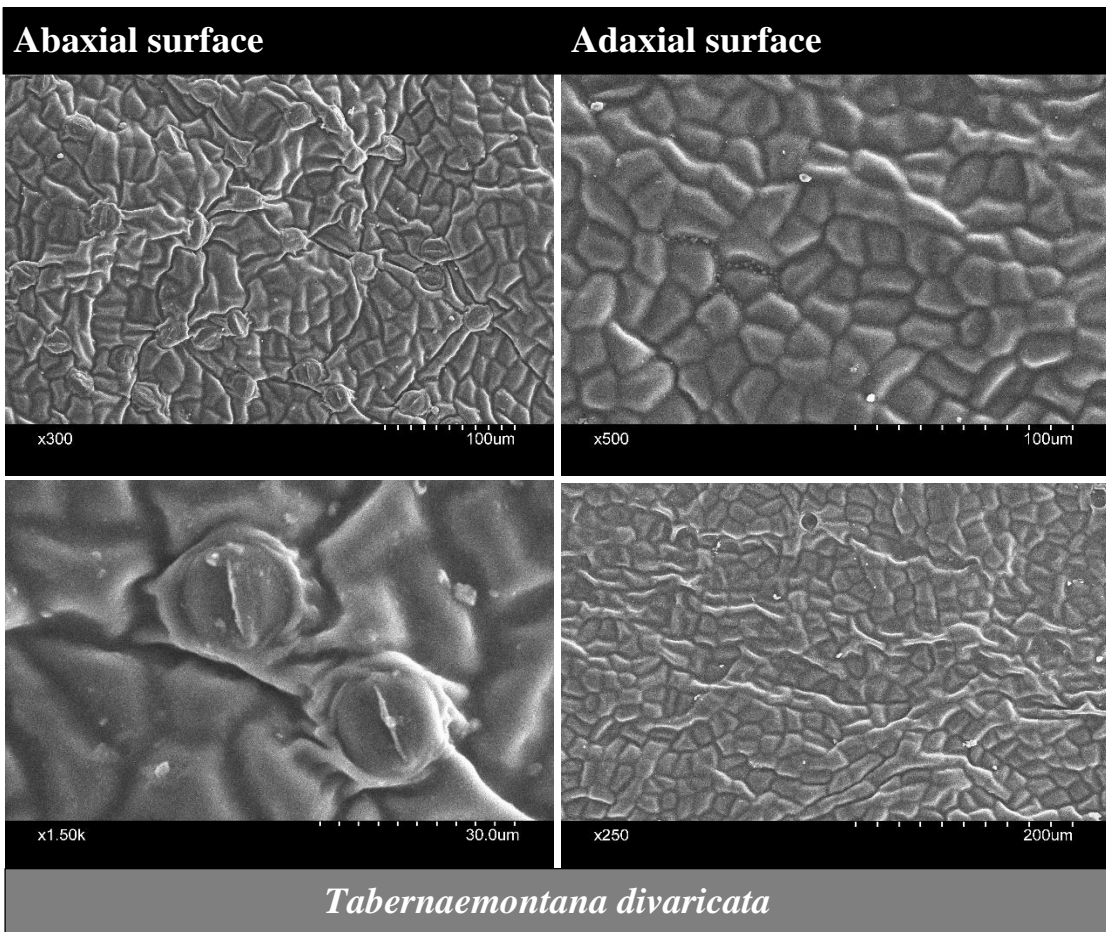
Efficacies of evergreen plants for the interception of large quantities of PM have been documented in several studies because of their strong abilities of foliage retention and typical leaf morphology ([Cai et al., 2017](#); [Corada et al., 2021](#); [Zhou et al., 2022](#)). However, in the proposed work, *B. acuminata* and *P. alba*, though deciduous species, performed desirably well to capture PM besides the other evergreen ones. Reduction in the ambient concentrations of PM by about 60% was achieved by [Pugh et al. \(2012\)](#) using deciduous trees and shrubs in the urban areas of street canyons. [Lukowski et al. \(2020\)](#) proved that the leaf surfaces of deciduous species, *B. pendula* and *Q. robur*, were highly retentive in capturing PM and *B. pendula*, being the best performer, can be effectively utilized for planting in urban environment in order to improve roadside air quality. Thus, application of deciduous plants should also be highlighted for the development of green infrastructure-based ambient air pollution control system (i.e. passive control) in combination with evergreen species.

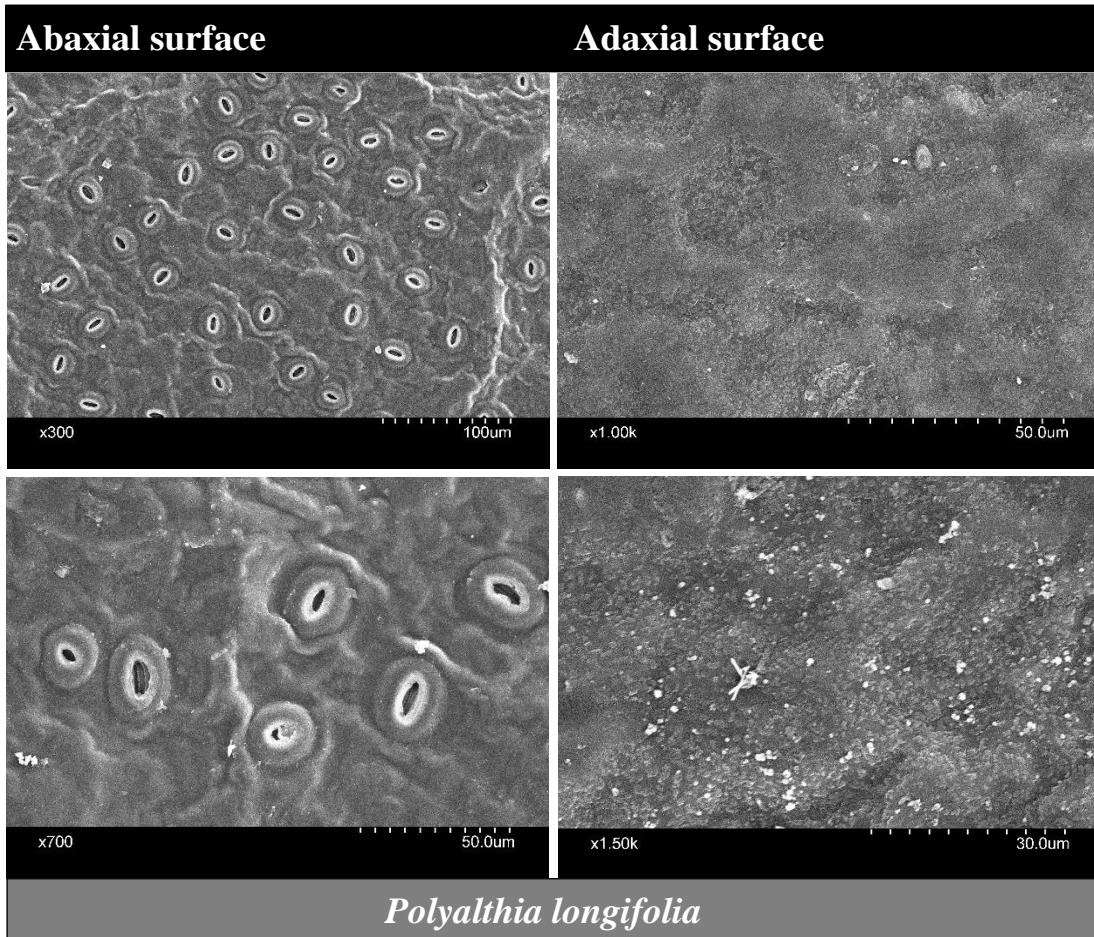
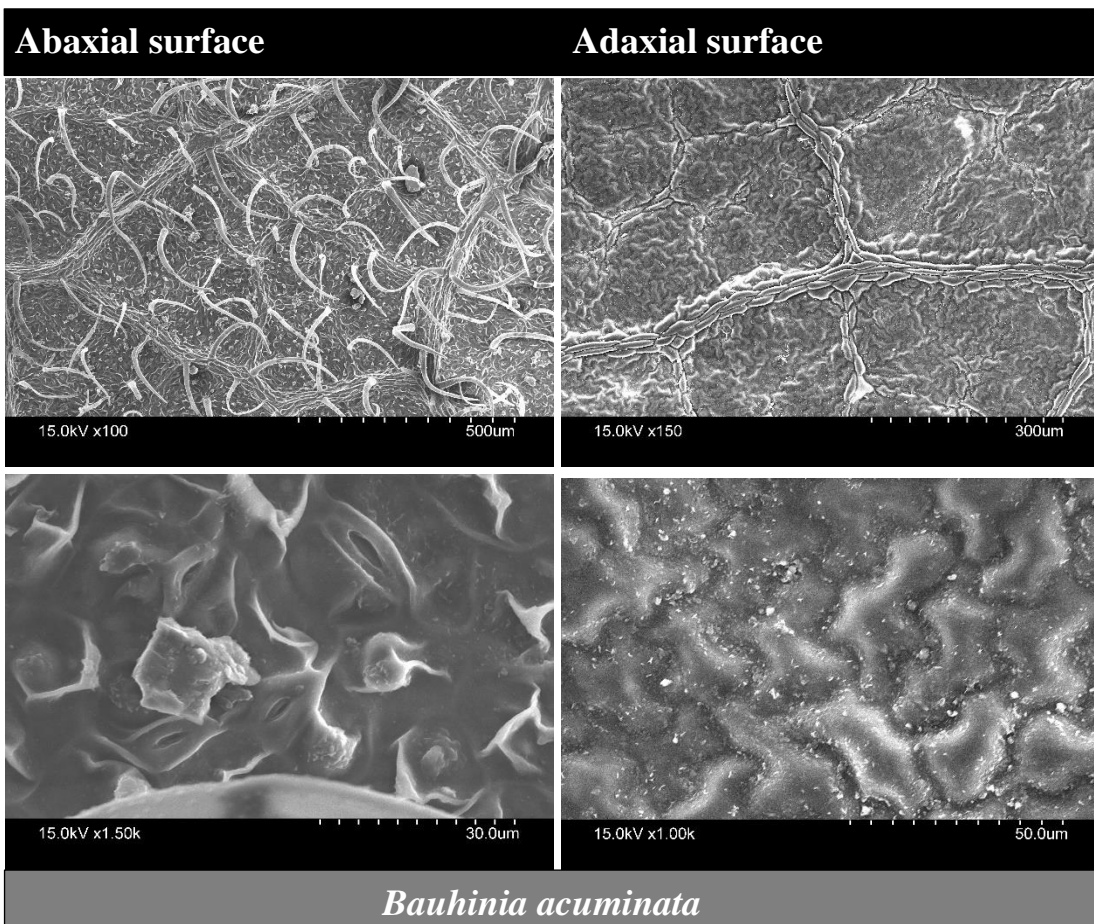
Leaf surface microstructure is one of the key factors associated with plant species' ability for adsorption or absorption of PM. The differences in the micromorphology of abaxial and adaxial surfaces of the plant leaves are apparent from [Fig. 28](#). *T. divaricata*, *C. gigantea* and *P. alba* manifested greater number of stomata on the abaxial surface than that of the adaxial side, whereas, no occurrence of stomata was noted in the adaxial surfaces of *B. acuminata*, *P. longifolia* and *N. cadamba*, but, high stomatal count was noticed in the abaxial surfaces of the same. However, open and closed stomatal distribution across the leaf epidermis caused heterogeneity in the areas of stomatal pores, influencing PM deposition through developed creases. The abaxial side of *N. oleander* was found to be characterized with highly cutinized epidermis having multiple layers and many large depressions (crypts) with prominently distributed trichomes or leaf hairs, densely covering, lining and projecting into the epidermal

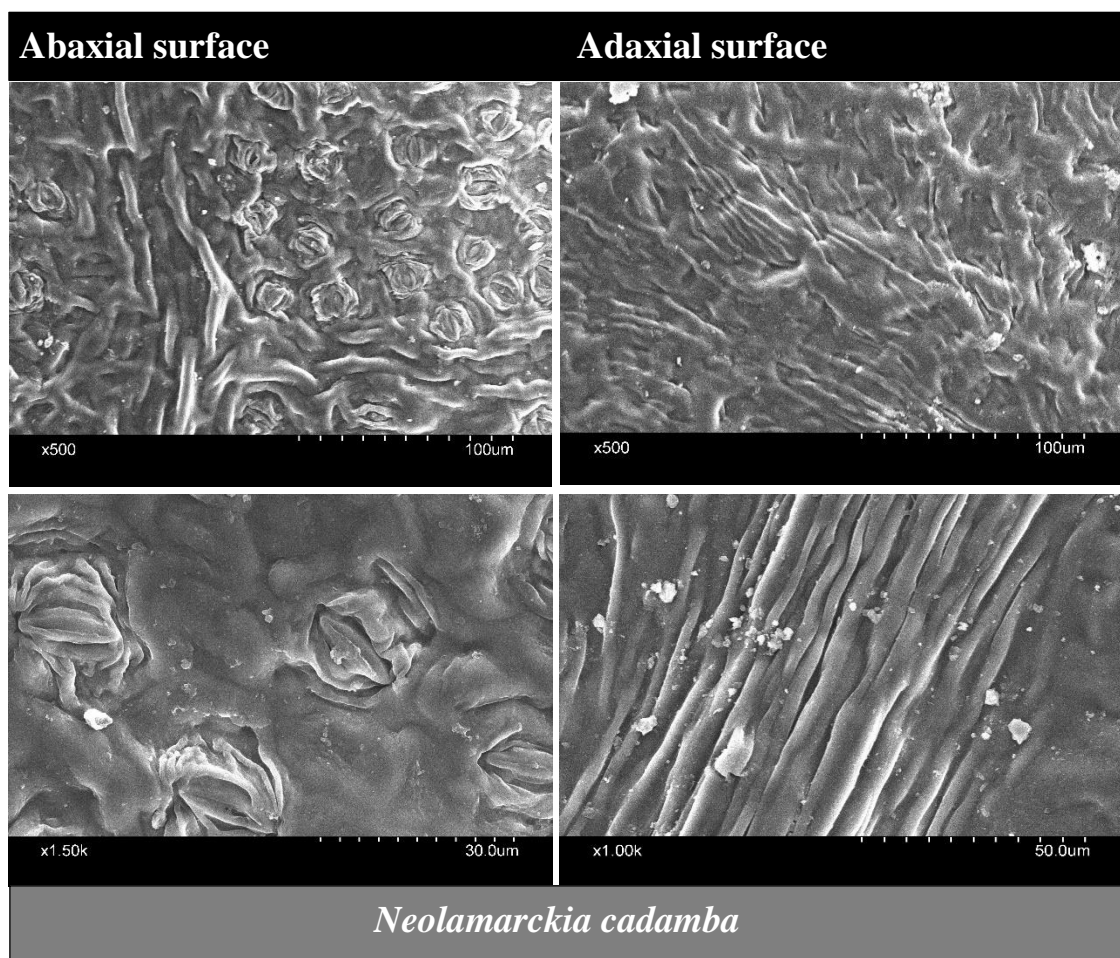
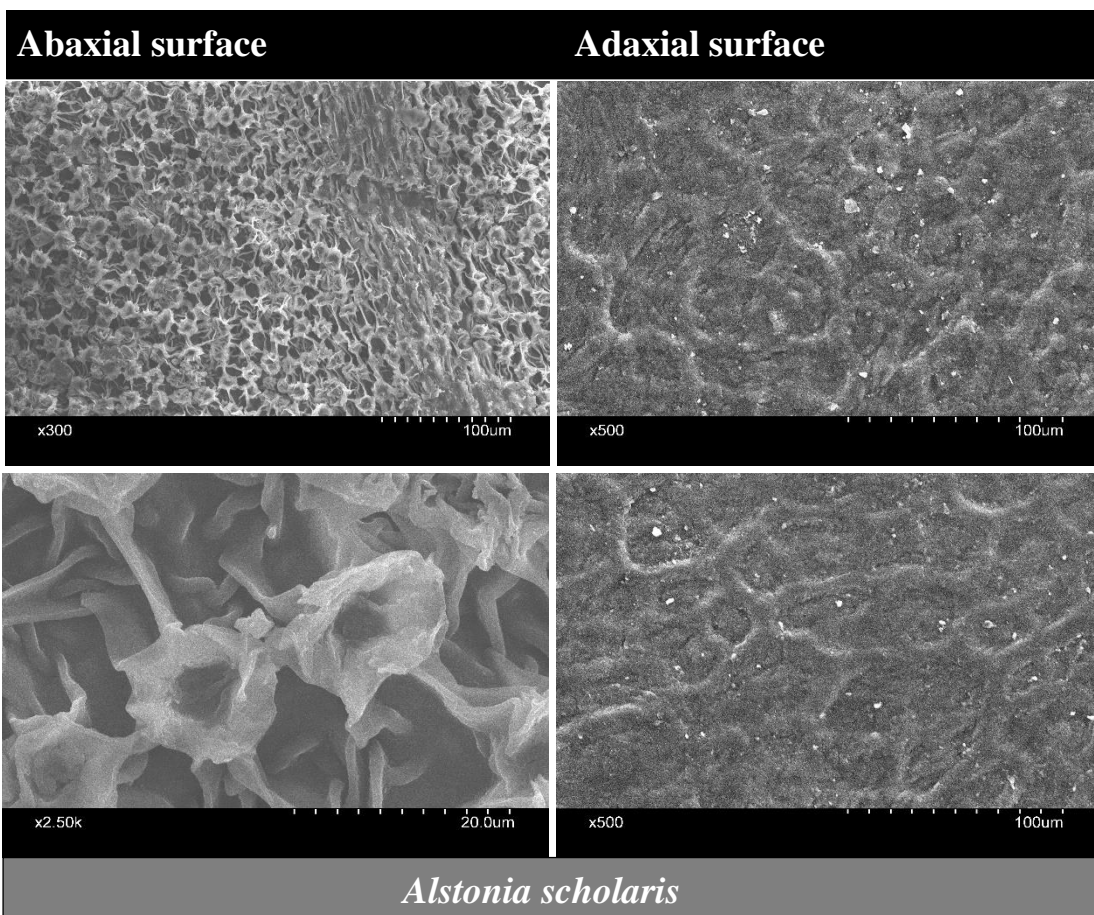
cavities and guarding the stomata within the crypts, thereby promoting PM capture (Stefi et al., 2020). Adaxial epidermis showed convex epidermal cell patterns with wax platelets forming roughness on the surfaces which helped accumulation of particulates in the grooves and furrows (Adhikari et al., 2021). The upper and lower epidermis of *T. divaricata* revealed the presence of a compact organization of epidermal cell lining combined with cuticular covering, leading to a grooved or striated surface (Seenu et al., 2019). Such intricate networks of leaf surface topography facilitated highest particle deposition. In *C. gigantea*, cuticular striations were present around the stomata, spreading out covering guard cells and epidermal cells on both upper and lower sides of the leaves, having particles sticking to the stomatal openings and the adjoining clefts, rifts or narrow grooves generated by the clustering of waxy cuticular materials (Abeyasinghe and Scharaschkin, 2022). The adaxial epidermal surface of *N. cadamba* consisted of wrinkled and striated dense cuticular protrusions or ridges, but, on the abaxial surface, the same were detected surrounding the stomata (Jamil et al., 2009). Despite the presence of uneven microstructures with ridges or grooves, foliar accumulation of PM on the leaves of *C. gigantea* and *N. cadamba* was not significantly appreciable in respect of other species. Therefore, it can be presumed that the large leaf size, elliptic shape, arrangement and field/environmental conditions may also act as limiting factors for PM capture (Leonard et al., 2016). Additionally, plant height sometimes plays an important role. The epidermis of *B. acuminata* contained large number of abaxial trichomes protruding from fibrous midrib, veins and veinlets, creating deep ridges and irregular polygonal convex shaped adaxial epidermal cells forming trenches and grooves. These particular morphological structures assisted in huge PM accumulation (Duarte-Almeida et al., 2015; Pereira et al., 2018). It is well-known that the leaf hairs reduce the rate of retained particulate resuspension and provide high surface area for capture, enhancing foliage adhesion of particles (Beckett et al., 2000; Leonard et al., 2016; Prusty et al., 2005; Qiu et al., 2009; Saebo et al., 2012). A huge number of stomata were seen in the lower epidermis of *P. longifolia* with particle deposition in and around the stomatal cavities. It has been seen in *P. longifolia* that the high stomatal conductance increases the rate of transpiration in plants, accelerating the capture of PM on the moisture layer formed due to transpiration (Jamil et al., 2009; Tong, 1991). The adaxial surface, on the other hand, also indicated particulate accumulation on the waxy film of the epidermis. In *A. scholaris*, the cuticular layer appeared to be in varicose and papillate forms with cuticular ridges interconnecting the projections on the abaxial epidermis, hiding the stomata underneath. Perhaps, such morphology might have been resulted from the species' response to biotic/abiotic stress to thrive in the polluted environment and aided the entrapment of particles in the

protrusions, inhibiting their entry into the hidden stomatal apparatus and clogging thereof. Polygonal epidermal cell outlines having striated cuticles were observed on the adaxial side with particle deposition (Singh et al., 2016_b). The upper and lower epidermal surfaces of *P. alba* leaves are composed of cuticular layer with arch like structures, paracytic stomata (embedded within cuticular arches), vein-like projections and cell lining, developing grooves and ridges which might be associated with PM retention (El-Khatib et al., 2012; Shrivastava and Mishra, 2018). Studies carried out by Li et al. (2021), Niu et al. (2020), Redondo-Bermudez et al. (2021), Shao et al. (2019) and Weerakkody et al. (2018_b) also corroborated the current observations, explicitly elaborating the importance of plant leaves with rough surfaces, microhairs, epidermal undulations due to specialized cell structure, distinct stomatal complexes, cuticular folds and waxes.









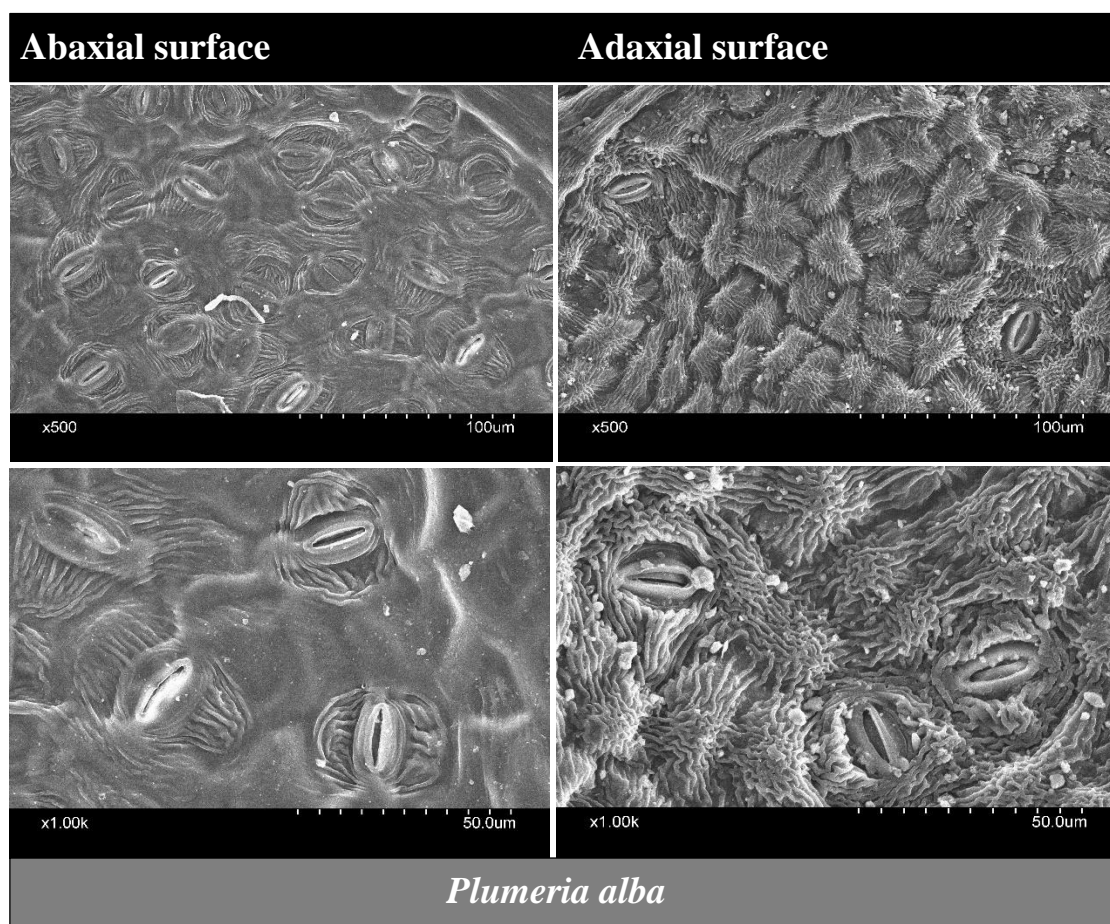


Fig. 28. SEM images of abaxial and adaxial surfaces of studied plant leaves with particulate deposition.

6.3.2. Bioaccumulation of PAHs

It is an established fact that the foliar uptake is the principal route of PAHs transfer directly from the atmosphere to the plants when exposed to airborne PAHs pollution in the outdoor environment (Lehndorff and Schwark, 2004). PAHs may either be adsorbed on waxy cuticular leaf surfaces or absorbed in the internal leaf mesophyll tissues (penetrating the membranes) via cuticular and stomatal infiltration (Desalme et al., 2013). Interspecies variations in the pattern of accumulation of PAHs in plant leaves relating to the distribution percentage of each foliar PAH congener and contribution percentage of PAHs categorized by different aromatic rings to total PAHs are evaluated based on the PAHs concentrations in the samples and represented in Fig. 29(a) and Fig. 29(b). Significant differences were found in the accumulated concentrations of PAHs among the species using two-way ANOVA ($F > F_{crit}$ and $p < 0.05$). Proportion of HMW PAHs (4-6 rings) was found to be higher with respect to LMW PAHs (2-3 rings) in *N. oleander*

(~61%), *T. divaricata* (~62%), *C. gigantea* (~53%) and *N. cadamba* (~55%), whereas in *P. alba*, the difference is marginal (LMW: ~51% and HMW: ~49%). Besides, *B. acuminata*, *P. longifolia* and *A. scholaris* showed greater potential for accumulation of LMW PAHs (~56%, ~57% and ~53% respectively). ACY, ACE, IP and B[ghi]P appeared to be the high yielding compounds in the leaves of *N. oleander*, *B. acuminata* and *P. alba* with 11.46-19.49%, 16.71-27.63%, 8.32-20.38% and 12.71-24.69% contributions respectively (ref. Fig. 29(a)). A similar distribution pattern of PAHs was observed in *C. gigantea* and *N. cadamba* exhibiting high levels of ACE, ANT, IP and B[ghi]P (~77% and 84% of total PAHs respectively). Highest proportion of BaP (a potent carcinogen) was noted in *Tabernaemontana* leaves (10.90% vs. other species: 0.54 - 5.16%) with PAHs, such as ACY, ACE, BkF and IP also having higher percentage compositions. Relative abundance of ACY and ACE followed by ANT and FLA in *P. longifolia* (18.86%, 15.13%, 14.04% and 8.34% respectively) and BkF and NAP in *A. scholaris* (11.36%, 23.63%, 9.37% and 8.77% respectively) was also evident from experimental observation. Thus, as seen from Fig. 29(b), percentage of 3-ring PAHs (~37–55%) was highest in almost all the species except *N. oleander* (~43%) and *N. cadamba* (~47%) where 6-ring PAHs were dominant. However, for the two species, percentage composition of PAHs with 3-rings was detected as ~39% and ~44% respectively. *C. gigantea* (~40%) and *P. alba* (~34%) were also able to arrest high proportion of 6-ring PAHs when compared with *T. divaricata* (~17%), *B. acuminata* (~21%), *P. longifolia* (~13%) and *A. scholaris* (~12%). 4-ring compounds accounted for ~4–18% of the total PAHs in the leaves of studied plants. Concerning 5-ring PAHs, *T. divaricata* showed highest fraction percentage (~34%) followed by *A. scholaris* (~25%) and least in *N. cadamba* (~4%). Contribution of 2-ring congener (NAP) to total PAHs was considerably low, ranging between ~0.13–9% in the plant species, which may be attributed to its high volatility and degradability. The mechanism of PAHs accumulation is mainly effected by gaseous diffusion and deposition based on equilibrium partitioning and gas-phase kinetics respectively, along with wet and dry deposition of PAHs associated with particles. Such processes are frequently controlled by man-made impacts, ambient concentration levels, meteorology, climatology, ecosystem properties and characteristics of plant surfaces (leaf hair density, roughness, texture, wettability and structural features of epidermis) (Desalme et al., 2013; Loppi et al., 2015; McLachlan, 1999). Since, leaf morphology differs greatly with plant diversity, accumulation behaviour is species-specific. All these factors caused differences in PAHs bioavailability, composition and content in the leaves of individual plant species from even proximal areas (Gerdol et al., 2002). Numerous

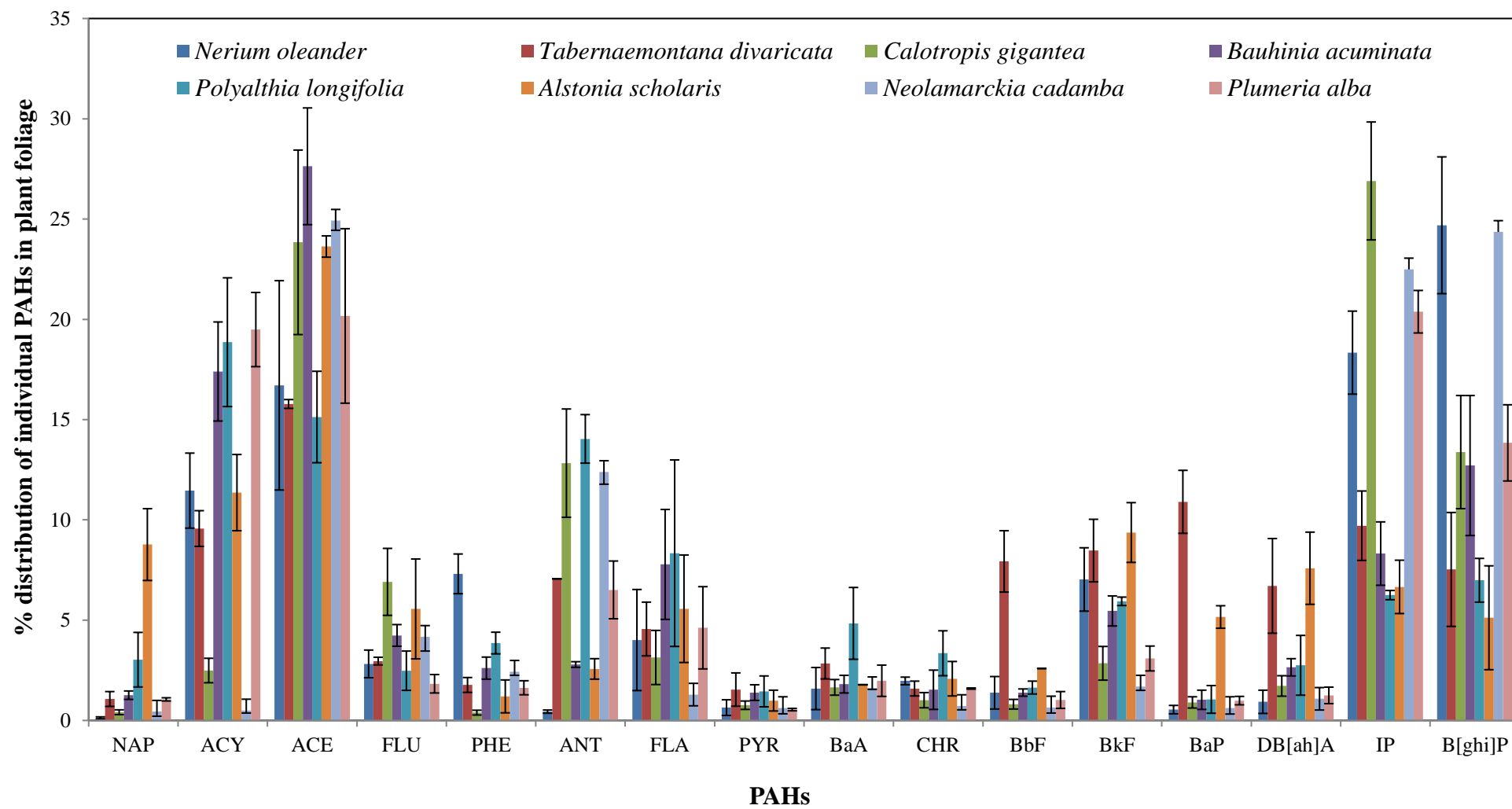
studies have investigated airborne PAHs–leaf interactions in many plants and reported differential accumulation patterns of PAHs based on the species, thereby stating it a complex phenomenon (Jia et al., 2019; Pleijel et al., 2022; Tian et al., 2019; Yang et al., 2017). In the current study, the trend of total concentration ($\mu\text{g g}^{-1}$ DW) of PAHs in the plant samples was determined as: *T. divaricata* (393.01 ± 30.34) > *P. alba* (342.28 ± 25.38) > *N. cadamba* (301.13 ± 37.31) > *N. oleander* (286.08 ± 32.65) > *C. gigantea* (267.47 ± 11.49) > *A. scholaris* (256.80 ± 32.31) > *B. acuminata* (177.22 ± 14.57) > *P. longifolia* (159.92 ± 21.23). SLA ($\text{cm}^2 \text{g}^{-1}$) of plants, which has an important bearing on the accumulation of PAHs through foliage and reflects the leaf surface area available per unit mass for the uptake of pollutants from ambient air (Nizzetto et al. (2008), varied in the following order: *T. divaricata* (376.79 ± 0.74) > *B. acuminata* (190.82 ± 0.91) > *P. longifolia* (150.82 ± 0.49) > *C. gigantea* (138.47 ± 0.21) > *P. alba* (136.45 ± 0.55) > *N. cadamba* (131.34 ± 0.29) > *A. scholaris* (122.16 ± 0.19) > *N. oleander* (71.01 ± 0.47). A positive correlation was observed between SLAs and accumulated PAHs levels ($r=0.42$, $p<0.05$), which indicated that the SLA would favour the process of foliar absorption of PAHs, depending also on other morphological factors. Positive influence of SLA on PAHs concentrations was again suggested by Terzaghi et al. (2015) and Wang et al. (2020_b). Leaf concentrations of PAHs were found to be weakly related ($r=0.35$, $p<0.05$) to total PM load, which may be due to different independent sources of emission affecting their deposition.

The concentrations of PAH compounds can be employed for the recognition of their emission source types. In this context, a total index (TI) was applied to distinguish between PAHs originated from high ($\text{TI}>4$) and low ($\text{TI}<4$) temperature processes. The TI is generally given by the following formula (Eq. 29) (Orecchio, 2010):

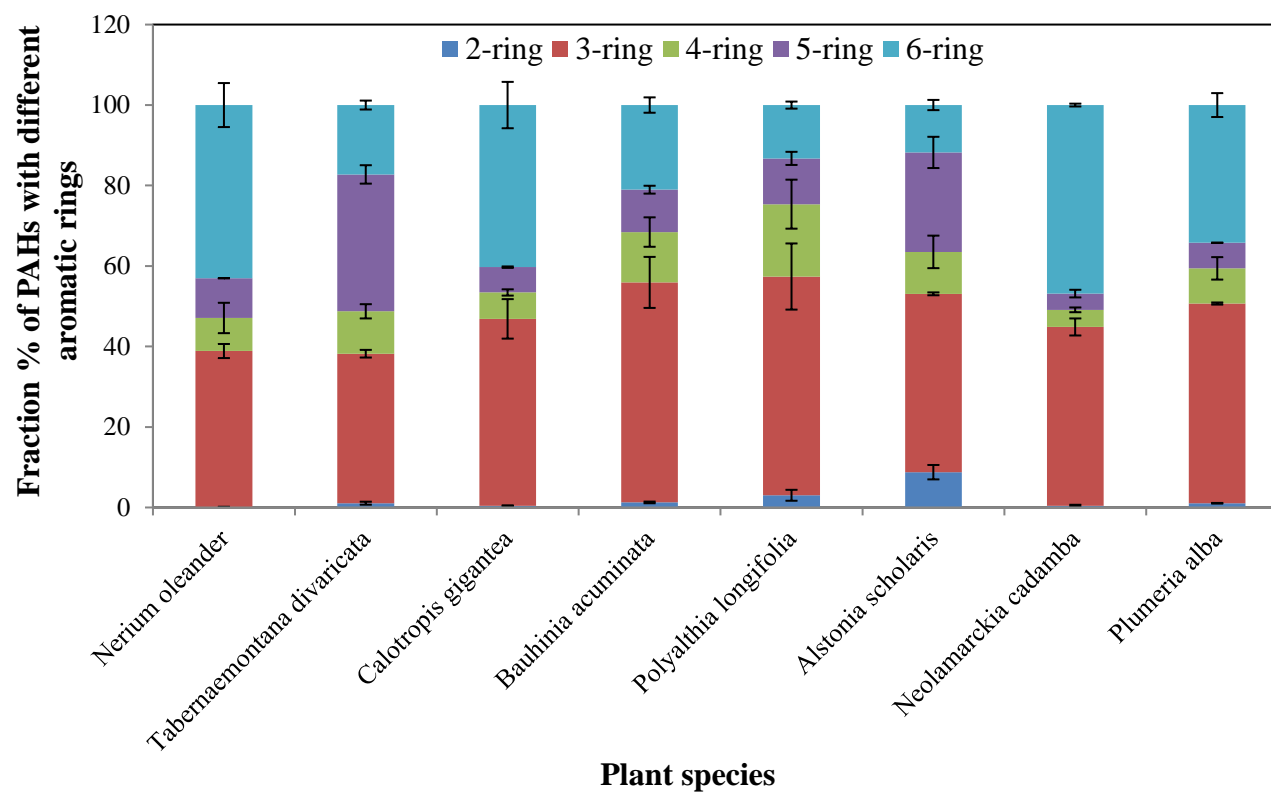
$$TI = \frac{FLA}{(FLA+PYR) \times 0.4} + \frac{ANT}{(ANT+PHE) \times 0.1} + \frac{BaA}{(BaA+CHR) \times 0.2} + \frac{IP}{(IP+B[ghi]P) \times 0.2} \quad (29)$$

TI values for all the plant samples were estimated as follows: *N. oleander* (7.08 ± 0.94), *T. divaricata* (15.89 ± 1.68), *C. gigantea* (18.16 ± 0.58), *B. acuminata* (11.97 ± 0.62), *P. longifolia* (15.29 ± 1.15), *A. scholaris* (14.07 ± 2.88), *N. cadamba* (15.90 ± 0.36) and *P. alba* (15.98 ± 0.54) and found to be more than 4, signifying vehicular emission (i.e. high temperature combustion) as the major source of PAHs in the study area. Liu et al. (2017_c), Pereira et al. (2019) and Pu et al. (2022) have used TI for identifying the sources of PAHs contamination in surface soil and subsoil layers of different depths, tree barks, total suspended particles as well as gas-phase samples and found the predominance of combustion-derived PAHs. Accretion of carcinogenic

PAHs of high molecular weight (viz. BaA, CHR, BbF, BkF, BaP, DB[ah]A and IP) as shown in the present work elucidates the importance of the selected species for biomonitoring studies. Therefore, natural vegetation with vast accumulating surfaces is crucially important in urban landscapes for scavenging or removing PAHs from the atmosphere and creates an ambience of biomonitoring of cumulative impacts of PAHs pollution using plant leaves, so vital for environmental quality assessment.



(a)



(b)

Fig. 29. Variations in leaf accumulation (mean \pm SD, n=3) of PAHs in plant species (a) % distribution of individual PAHs and (b) % fraction of PAHs of different aromatic rings with respect to total PAHs.

6.3.3. Carcinogenic and mutagenic risks of PAHs

The carcinogenicity and mutagenicity of foliar PAHs were investigated in the present study in the context of BaP equivalent concentrations (BaP_{TEQ} and BaP_{MEQ}), CP and MP to represent the toxicity of PAHs. Two-way ANOVA showed statistically significant differences ($F > F_{crit}$ and $p < 0.05$) among the concentrations, CP and MP for all the species. ΣBaP_{TEQ16} (sum total of carcinogenic or toxic equivalent concentrations of 16 PAHs) and ΣBaP_{MEQ8} (sum total of mutagenic equivalent concentrations of 8 PAHs) were found to be in the range of 9.51 ± 1.73 – 81.37 ± 5.35 and 10.60 ± 0.09 – 80.42 ± 11.44 $\mu g\ g^{-1}$ respectively for all the selected species (ref. [Table 28](#) and [Table 29](#)). Major contribution (91.54–99.12%) of seven carcinogenic PAHs having 4-, 5- and 6-rings, as mentioned earlier, was detected with the dominance of BkF, BaP, DB[ah]A and IP, which catered to the maximum toxicity in relation to ΣBaP_{TEQ16} . In case of ΣBaP_{MEQ8} , highest mutagenic threats were posed by 5- and 6-ring PAHs accounting for 93.21–98.90% among the plant species. Moreover, it can be seen from [Table 30](#) that the 4-6 ring PAHs have highest CP, whereas, 5-6 ring PAHs indicated high mutagenicity (i.e. high MP, ref. [Table 31](#)). Vehicular sources (i.e. emissions from fuel vehicles powered by petrol, diesel, natural gas or local blending of petrol with kerosene oil) might be the root cause for the release of carcinogenic and mutagenic PAHs in the sampling locations. Based on the above findings, it can be opined that the assessment and control of HMW PAHs should be given utmost priority for maintaining a clean and habitable environment and reducing possible health risks. Evaluation of potential risks of PAHs for hazard analysis due to exposure has been actively performed by many researchers ([Błaszczuk et al., 2017](#); [Fred-Ahmadu and Benson, 2019](#); [Ihunwo et al., 2021](#); [Li et al., 2014](#)) which is quite compatible with the results of the current study.

Table 28

Toxic equivalent concentrations (TEQ) of PAHs accumulated in the leaves of selected plant species.

BaP_{TEQ} (µg g⁻¹) (mean ± SD) of PAHs									
PAHs	TEF^a	<i>Nerium oleander</i>	<i>Tabernaemontana divaricata</i>	<i>Calotropis gigantea</i>	<i>Bauhinia acuminata</i>	<i>Polyalthia longifolia</i>	<i>Alstonia scholaris</i>	<i>Neolamarckia cadamba</i>	<i>Plumeria alba</i>
NAP	0.001	0.0004±0.0002	0.004±0.001	0.001±0.0003	0.002±0.0004	0.005±0.001	0.02±0.005	0.001±0.001	0.004±0.001
ACY	0.001	0.03±0.01	0.04±0.01	0.007±0.002	0.03±0.01	0.03±0.01	0.03±0.01	0.002±0.001	0.07±0.01
ACE	0.001	0.05±0.01	0.06±0.004	0.06±0.01	0.05±0.01	0.02±0.003	0.06±0.01	0.08±0.01	0.07±0.01
FLU	0.001	0.008±0.003	0.01±0.0004	0.02±0.01	0.008±0.002	0.004±0.002	0.01±0.01	0.01±0.002	0.006±0.002
PHE	0.001	0.02±0.01	0.007±0.001	0.001±0.0003	0.005±0.002	0.006±0.001	0.003±0.001	0.007±0.001	0.006±0.002
ANT	0.01	0.01±0.002	0.28±0.02	0.34±0.06	0.05±0.002	0.22±0.04	0.07±0.02	0.37±0.06	0.22±0.06
FLA	0.001	0.01±0.01	0.02±0.002	0.008±0.003	0.01±0.01	0.01±0.01	0.01±0.01	0.004±0.001	0.02±0.002
PYR	0.001	0.002±0.001	0.006±0.003	0.002±0.0004	0.002±0.001	0.002±0.001	0.003±0.0005	0.002±0.0004	0.002±0.0004
BaA	0.10	0.45±0.20	1.12±0.36	0.44±0.12	0.32±0.09	0.77±0.13	0.46±0.06	0.49±0.08	0.68±0.19
CHR	0.01	0.06±0.01	0.06±0.01	0.03±0.01	0.03±0.01	0.05±0.02	0.05±0.01	0.02±0.01	0.05±0.0001
BbF	0.10	0.39±0.15	3.12±0.78	0.22±0.05	0.25±0.01	0.26±0.07	0.67±0.09	0.19±0.05	0.35±0.10
BkF	0.10	2.01±0.61	3.33±0.81	0.76±0.24	0.97±0.04	0.95±0.15	2.41±0.62	0.51±0.11	1.06±0.27
BaP	1.00	1.55±0.30	42.84±8.80	2.42±0.59	1.82±0.61	1.68±0.66	13.25±2.84	1.86±0.52	3.42±0.93
DB[ah]A	1.00	2.66±1.09	26.36±6.24	4.61±1.08	4.69±1.06	4.40±1.35	19.50±6.27	3.26±0.98	4.28±0.95
IP	0.10	5.25±1.09	3.82±0.90	7.19±1.04	1.48±0.37	0.99±0.09	1.71±0.49	6.77±0.69	6.98±0.85
B[ghi]P	0.01	0.71±0.17	0.29±0.08	0.36±0.09	0.23±0.03	0.11±0.03	0.13±0.04	0.73±0.09	0.47±0.09
Σ BaP _{TEQ16}	—	13.21±0.13	81.37±5.35	16.47±0.28	9.95±0.85	9.51±1.73	38.39±10.36	14.31±0.49	17.69±0.96

^aList proposed by Nisbet and LaGoy (1992).

Table 29

Mutagenic equivalent concentrations (MEQ) of foliar PAHs.

PAHs	MEF ^a	BaP _{MEQ} (µg g ⁻¹) (mean ± SD) of PAHs							
		<i>Nerium oleander</i>	<i>Tabernaemontana divaricata</i>	<i>Calotropis gigantea</i>	<i>Bauhinia acuminata</i>	<i>Polyalthia longifolia</i>	<i>Alstonia scholaris</i>	<i>Neolamarckia cadamba</i>	<i>Plumeria alba</i>
BaA	0.082	0.37±0.16	0.92±0.29	0.36±0.09	0.26±0.08	0.63±0.11	0.37±0.05	0.39±0.06	0.56±0.15
CHR	0.017	0.09±0.01	0.11±0.01	0.05±0.02	0.05±0.02	0.09±0.04	0.09±0.02	0.04±0.01	0.09±0.01
BbF	0.25	0.99±0.37	7.79±1.94	0.54±0.13	0.62±0.02	0.66±0.19	1.67±0.22	0.49±0.11	0.87±0.26
BkF	0.11	2.21±0.66	3.66±0.88	0.84±0.27	1.06±0.04	1.05±0.17	2.65±0.69	0.56±0.12	1.16±0.29
BaP	1.0	1.55±0.30	42.84±8.80	2.42±0.59	1.82±0.61	1.68±0.66	13.25±2.84	1.86±0.52	3.42±0.93
DB[ah]A	0.29	0.77±0.32	7.64±1.81	1.34±0.31	1.36±0.30	1.28±0.39	5.66±1.82	0.95±0.28	1.24±0.28
IP	0.31	16.26±3.39	11.84±2.80	22.31±3.25	4.57±1.14	3.09±0.32	5.30±1.53	20.99±2.13	21.63±2.62
B[ghi]P	0.19	13.42±3.08	5.62±1.46	6.79±1.63	4.28±0.69	2.12±0.55	2.49±0.74	13.94±1.85	8.99±1.77
Σ BaP _{MEQ8}	—	35.66±5.99	80.42±11.44	34.65±4.24	14.02±0.14	10.60±0.09	31.48±6.39	39.22±3.25	37.96±4.93

^aList proposed by [Durant et al. \(1996\)](#).

Table 30

Carcinogenic potential (CP) of accumulated PAHs in the plant leaves.

PAHs	CP (in %) (mean \pm SD)							
	<i>Nerium oleander</i>	<i>Tabernaemontana divaricata</i>	<i>Calotropis gigantea</i>	<i>Bauhinia acuminata</i>	<i>Polyalthia longifolia</i>	<i>Alstonia scholaris</i>	<i>Neolamarckia cadamba</i>	<i>Plumeria alba</i>
NAP	0.002 \pm 0.001	0.01 \pm 0.002	0.01 \pm 0.005	0.02 \pm 0.002	0.05 \pm 0.003	0.06 \pm 0.003	0.01 \pm 0.002	0.02 \pm 0.002
ACY	0.23 \pm 0.05	0.05 \pm 0.01	0.04 \pm 0.01	0.31 \pm 0.04	0.32 \pm 0.12	0.08 \pm 0.002	0.01 \pm 0.003	0.38 \pm 0.04
ACE	0.35 \pm 0.07	0.08 \pm 0.005	0.39 \pm 0.04	0.49 \pm 0.05	0.25 \pm 0.09	0.16 \pm 0.03	0.52 \pm 0.08	0.39 \pm 0.07
FLU	0.06 \pm 0.02	0.01 \pm 0.002	0.11 \pm 0.03	0.08 \pm 0.01	0.04 \pm 0.02	0.04 \pm 0.03	0.09 \pm 0.03	0.04 \pm 0.01
PHE	0.12 \pm 0.01	0.01 \pm 0.001	0.01 \pm 0.005	0.05 \pm 0.01	0.06 \pm 0.02	0.01 \pm 0.01	0.05 \pm 0.01	0.03 \pm 0.01
ANT	0.10 \pm 0.001	0.34 \pm 0.004	2.08 \pm 0.28	0.5 \pm 0.02	2.35 \pm 0.71	0.17 \pm 0.004	2.61 \pm 0.49	1.26 \pm 0.29
FLA	0.08 \pm 0.04	0.02 \pm 0.01	0.05 \pm 0.02	0.14 \pm 0.05	0.14 \pm 0.02	0.04 \pm 0.03	0.03 \pm 0.003	0.09 \pm 0.04
PYR	0.01 \pm 0.01	0.01 \pm 0.002	0.01 \pm 0.004	0.02 \pm 0.01	0.02 \pm 0.01	0.01 \pm 0.004	0.01 \pm 0.01	0.01 \pm 0.001
BaA	3.40 \pm 1.59	1.37 \pm 0.38	2.67 \pm 0.74	3.22 \pm 0.77	8.10 \pm 0.05	1.19 \pm 0.26	3.39 \pm 0.62	3.83 \pm 1.38
CHR	0.47 \pm 0.11	0.08 \pm 0.01	0.16 \pm 0.06	0.27 \pm 0.18	0.56 \pm 0.26	0.14 \pm 0.11	0.15 \pm 0.05	0.31 \pm 0.004
BbF	3.05 \pm 1.13	3.83 \pm 0.77	1.32 \pm 0.27	2.49 \pm 0.32	2.75 \pm 1.03	1.73 \pm 0.39	1.37 \pm 0.25	1.97 \pm 0.76
BkF	15.14 \pm 4.45	4.09 \pm 0.79	4.63 \pm 1.52	9.75 \pm 1.36	9.96 \pm 2.71	6.27 \pm 0.13	3.56 \pm 0.85	5.98 \pm 1.29
BaP	11.74 \pm 2.45	52.65 \pm 8.11	14.69 \pm 3.28	18.32 \pm 8.71	17.61 \pm 3.05	34.51 \pm 3.10	13.00 \pm 3.06	19.34 \pm 4.54
DB[ah]A	20.18 \pm 8.54	32.40 \pm 10.79	27.98 \pm 5.95	47.22 \pm 7.61	46.12 \pm 4.73	50.79 \pm 4.24	22.77 \pm 5.76	24.21 \pm 7.22
IP	39.67 \pm 7.97	4.69 \pm 0.88	43.68 \pm 6.94	14.85 \pm 2.79	10.50 \pm 2.38	4.46 \pm 0.15	47.31 \pm 6.13	39.46 \pm 2.85
B[ghi]P	5.40 \pm 1.23	0.36 \pm 0.13	2.17 \pm 0.55	2.27 \pm 0.63	1.17 \pm 0.41	0.34 \pm 0.31	5.12 \pm 0.81	2.68 \pm 0.42

Table 31

Mutagenic potential (MP) of accumulated PAHs in the plant leaves.

PAHs	MP (in %) (mean \pm SD)							
	<i>Nerium oleander</i>	<i>Tabernaemontana divaricata</i>	<i>Calotropis gigantea</i>	<i>Bauhinia acuminata</i>	<i>Polyalthia longifolia</i>	<i>Alstonia scholaris</i>	<i>Neolamarckia cadamba</i>	<i>Plumeria alba</i>
BaA	1.04 \pm 0.81	1.06 \pm 0.08	1.05 \pm 0.18	1.82 \pm 0.46	6.03 \pm 1.07	1.26 \pm 0.01	1.00 \pm 0.07	1.44 \pm 0.76
CHR	0.26 \pm 0.03	0.11 \pm 0.06	0.14 \pm 0.02	0.26 \pm 0.23	0.79 \pm 0.38	0.29 \pm 0.08	0.10 \pm 0.01	0.27 \pm 0.001
BbF	2.78 \pm 2.00	9.56 \pm 1.10	1.54 \pm 0.68	4.42 \pm 0.17	6.20 \pm 1.72	5.45 \pm 0.53	1.23 \pm 0.46	2.25 \pm 1.25
BkF	6.21 \pm 1.09	4.78 \pm 0.71	2.44 \pm 0.60	7.66 \pm 0.35	9.84 \pm 1.45	8.38 \pm 0.66	1.42 \pm 0.21	3.07 \pm 0.49
BaP	4.35 \pm 2.07	53.13 \pm 4.28	6.98 \pm 3.11	12.99 \pm 4.55	15.87 \pm 6.54	41.89 \pm 0.40	4.74 \pm 1.95	9.02 \pm 1.56
DB[ah]A	2.13 \pm 1.69	9.56 \pm 4.56	3.84 \pm 1.71	9.74 \pm 2.22	12.06 \pm 3.73	18.01 \pm 3.09	2.42 \pm 1.05	3.25 \pm 1.41
IP	45.59 \pm 2.42	14.90 \pm 1.88	64.39 \pm 1.85	32.59 \pm 7.94	29.21 \pm 2.71	16.76 \pm 1.92	53.56 \pm 1.19	56.98 \pm 0.57
B[ghi]P	37.64 \pm 3.08	6.90 \pm 3.44	19.62 \pm 2.85	30.52 \pm 5.33	20.0 \pm 5.08	7.96 \pm 5.47	35.53 \pm 1.98	23.72 \pm 1.94

6.3.4. Analysis of biomarkers and pollution/performance indices for comparing the suitability of plant species for urban plantation

Leaf biomarkers, APTI and API, based on the characterization of plants, have been used to discern the functioning of terrestrial plants in response to prevailing pollutant changes for increasing vegetation coverage along the urban streets for uplifting the quality of ambient air. The statistical comparison of leaf characteristics and indices by two-way ANOVA revealed significant differences ($F > F_{crit}$ and $p < 0.05$) among the species.

6.3.4.1. Contents of photosynthetic pigments (chlorophyll (Chl) and carotenoids (C_{X+C}))

Chlorophyll and carotenoids are the key functional pigments of plants which control the photosynthetic capacity, favouring plant growth and yield. In response to abiotic stress, plants induce adaptive changes in their leaf traits to cope up with the environmental fluctuations. Likewise, plants are able to modulate the levels of required pigments and acclimatize to the surrounding environment for maintaining the normal process of photosynthesis (Li et al., 2018). The results demonstrated that the values of Chl_T , $Chl\ a/b$ and C_{X+C} varied from 0.90–5.13 mg g⁻¹, 1.73–4.23 mg g⁻¹ and 0.24–1.12 mg g⁻¹ respectively (ref. Table 32). It is also apparent from Table 32 that the values of $Chl\ a$ are higher than $Chl\ b$ for all the plants considered. Both Chl_T and C_{X+C} differed widely among plant species: a) shrubs: $Chl_T (T. divaricata) > Chl_T (C. gigantea) > Chl_T (P. alba) > Chl_T (B. acuminata) > Chl_T (N. oleander)$; $C_{X+C} (T. divaricata) > C_{X+C} (C. gigantea) > C_{X+C} (B. acuminata) > C_{X+C} (P. alba) > C_{X+C} (N. oleander)$ and b) trees: $Chl_T (N. cadamba) > Chl_T (P. longifolia) > Chl_T (A. scholaris)$; $C_{X+C} (P. longifolia) > C_{X+C} (N. cadamba) > C_{X+C} (A. scholaris)$. It was observed by many researchers that in presence of PM pollution, $Chl\ a/b$ ratio reduced owing to the shading of leaves by the particulate-induced decrease in the penetration of incident light (Nanos and Ilias, 2007; Shabnam et al., 2021). It is also consistent with the present study as a negative correlation ($r = -0.46$, $p < 0.05$) was obtained between total PM load and $Chl\ a/b$ ratio. The changes in the ratio might be an indication of the adaptive nature of plant leaves for maximization of the photosynthetic performance towards varying intensities of light, thereby controlling the concentration and composition of Chl molecules as well as the main functional units, photosystems I and II; the low values of $Chl\ a/b$ being responsible for enhancing the light absorption capacity under PM stress (Porra and Scheer, 2019; Shabnam et al., 2015; Shabnam et al., 2021). Moreover, C_{X+C} and Chl_T were found to be positively correlated to each other ($r = 0.83$, $p < 0.05$) which may be attributed to the antioxidant activity of carotenoids in safeguarding the chloroplasts for retaining higher chlorophyll concentration (Kacharava et al.,

2009). High levels of leaf Chl_T were noted for species *T. divaricata*, *C. gigantea*, *N. cadamba* and *P. alba*. Substantially high concentrations of chlorophyll and carotenoids can effectively be linked to the tolerance of plants against stress as already established in different studies (Enete et al., 2013; Ogunkunle et al., 2015).

6.3.4.2. Ascorbic acid (AA) content

AA, the non-enzymatic antioxidant, is an essential metabolite of plant leaves associated with the stress response to multiple interacting factors (abiotic or biotic stressors), which upregulates many metabolic functions in plants for developing their tolerance against environmental adversity (Pathak et al., 2019). Furthermore, it is able to quench or eliminate the increased levels of reactive oxygen species (ROS) generated due to pollutant exposure in the plant cells either directly or by functioning through enzymatic reactions involved in ascorbate-glutathione pathway (Noctor and Foyer, 1998). Thus, it upholds the equilibrium in between generation and mitigation of ROS (Frei et al., 2012). In the plant leaves, AA contents ranged from 3.63–18 mg g^{-1} as indicated in Table 32. Positive correlations were observed between AA contents and total PM ($r=0.64$, $p<0.05$) and PAHs ($r=0.84$, $p<0.05$) loads, justifying the presumption of the increase in leaf AA with abiotic stress. Plants having higher concentrations of AA (in this case: *T. divaricata*, *N. oleander* and *P. alba*) are said to develop more tolerance enabling them to respond quickly to pollutants for their survival and growth. However, *B. acuminata*, *P. longifolia* and *A. scholaris* exhibited lower levels of AA — this may be due to the fact that the production of AA got hampered, rendering them slow respondent towards detoxification of ROS or oxidative damage (Shah et al., 2020). The remaining two species, *C. gigantea* and *N. cadamba*, synthesized and maintained an intermediate level of AA to counter the phytotoxic effects of pollutants. The present findings revealed good congruence with recent researches (Banerjee et al., 2022; Goswami et al., 2023).

6.3.4.3. Foliar pH

Leaf extract pH serves as a stress biomarker directing pivotal functions, such as biochemical and physiological activities along with the processes of homeostatic control in plant cells (Mandal and Dhal, 2022). It has been noticed that the range of leaf pH in the collected species lies between 5.91–7.47 (Table 32). As illustrated in previous case studies (Escobedo et al., 2008; Govindaraju et al., 2012; Singh et al., 2023), plants exhibiting high foliar pH values (close to 7 or greater) are known to acquire stress tolerance to a considerable extent, which may

be linked to higher endogenous biosynthesis of AA in plants from hexose sugars imparting good resilience to fight against environmental pollution. This was corroborated by the positive correlation ($r=0.94$, $p<0.05$) as obtained between leaf pH and AA levels and also conformed to the results of [Zhang et al. \(2020\)](#). Contrariwise, air pollution sensitivity across species increases with lower pH (formed as a result of plant metabolic alterations through stomatal uptake of polluting gases (e.g. nitrogen oxides, sulphur dioxide and ozone) and organic acids) ([Latwal et al., 2023](#); [Sharma et al., 2019](#)). Further, pH was also found to be positively influenced by the concentrations of PM ($r=0.78$, $p<0.05$) and PAHs ($r=0.66$, $p<0.05$), because of its involvement in stress resistance response by increasing the content of AA in tolerant plant types with the increase in pollutants' load ([Khanoranga and Khalid, 2019](#)). Among the species considered, *T. divaricata* and *N. oleander* presented highest pH values and the lowest was recorded for *P. longifolia*.

6.3.4.4. Relative water content (RWC)

Leaf RWC is essentially required for plant photosynthesis, respiration, transpiration, growth, yield, health and tolerance ([Malav et al., 2022](#); [Singh et al., 2023](#)). In this study, RWC varied in the range of 65.16–88.93% ([Table 32](#)) among the plant types. In view of the responses of plant leaves based on water status to continuous air pollution exposure, RWC displayed a negative relationship with foliar PM load ($r=-0.61$, $p<0.05$), implying perturbations in plant cell wall permeability, water transportation and balance caused by the accumulation of particulate pollutants or aerosols on leaf canopy with a concomitant reduction in the rate of transpiration owing to clogged stomata ([Malav et al., 2022](#); [Zilaie et al., 2023](#)). On the contrary, a weak correlation ($r=0.21$, $p<0.05$) was found to exist between RWC and total PAHs. Increased tolerance of plants to atmospheric pollution with high RWC through the regulation of functional mechanisms driving plant morpho-physiology has been reported in multiple investigations ([Karmakar and Padhy, 2019](#); [Kumar et al., 2023](#)). Decline in the rate of carbon assimilation process and reduction in stomatal conductance are the known effects of lower RWC ([Lawlor, 2002](#)). In the present work, high values of RWC were seen in the leaves of *N. cadamba*, *A. scholaris*, *C. gigantea* and *P. alba*, while *P. longifolia* showed minimum leaf RWC. Similar observations of dust and heavy metal stress on leaf RWC of various plants from urban terrain were made by [Nadgorska-Socha et al. \(2017\)](#) and [Yaghmaei et al. \(2022\)](#).

6.3.4.5. Membrane stability index (MSI) and electrolyte leakage (EL): Role of proline accumulation

Cellular membranes of plants are highly susceptible to abiotic toxicants which trigger membrane damage, thereby increasing EL and cell secretion as a result of increased membrane permeability (Ma et al., 2019_b). Recurrent exposure to air pollutants stimulates excessive production of ROS in plant cells, which, in turn, catalyse the conversion of membrane lipids (phospholipids and polyunsaturated fatty acids) into lipid peroxides, causing disintegration and dysfunctioning of cell membranes, and eventually cell necrosis (accidental cell death) (Rangani et al., 2018). Thus, plants manifesting structural and functional integrity of plasma membranes (with high MSI) for cell survival are considered to be pollution tolerant species in biomonitoring (Ahmadizadeh et al., 2011). Hence, MSI and EL are better suited as pollution biomarkers for the determination of radical-induced cell membrane damage or injury (Shanazari et al., 2018; Zhang et al., 2022_b).

In accordance with the results depicted in Table 32, MSI revealed positive correlation with PM ($r=0.51$, $p<0.05$) and PAHs ($r=0.82$, $p<0.05$), whereas, EL appeared to be negatively correlated with PM ($r=-0.54$, $p<0.05$) and PAHs ($r=-0.40$, $p<0.05$). Such outcome is suggestive of the proline-mediated resistance mechanisms of plants for stress management. Proline acts as cytoplasmic osmolyte or osmoprotectant (capable of lowering osmotic potential) and ROS scavenger, which prevents disruption of cell membranes and structural collapse of biomolecules, such as proteins and DNA, promoting stress tolerance in plants through the activation of enzymatic antioxidant system (Hayat et al., 2012; Raza et al., 2023). It also modulates biochemical cascades for stress recovery, improving the performance of plants under polluted atmosphere. These inferences are again endorsed by the positive association between proline content (ref. Table 32) and abiotic stress due to PM ($r=0.44$, $p<0.05$) and PAHs ($r=0.74$, $p<0.05$). It also played a defensive role in sustaining membrane stability and reducing EL (as confirmed by the positive linear relationship ($r=0.90$, $p<0.05$) between MSI and proline and negative correlation, $r=-0.72$, $p<0.05$, between EL and proline). This study supports the previous findings of Gomes et al. (2010) and Sameena and Puthur (2021). It has been mostly seen that EL is predominantly accompanied by the efflux of potassium ions (K^+) from plant cells. Therefore, it should be emphasized that tolerant species impede the excessive release of K^+ (i.e. avoid EL) and uphold potassium homeostasis regulating plant cell physiology (Shabala and Cuin, 2008). *N. oleander* and *T. divaricata* showed highest percentages (80.52 and 88.69% respectively) of MSI and maximum proline contents (4.28 and 4.72 mg g⁻¹ respectively) with

minimum EL (0.98 and 2.31% respectively). *C. gigantea*, *N. cadamba* and *P. alba*, though exhibiting high EL % (5.60–8.26), presented higher values of MSI (60.79–78.01%) because of substantial proline content (2.44–3.56 mg g⁻¹) that may be considered to be responsible for initiation of the stress recovery process. However, minimum concentrations (0.55–1.56 mg g⁻¹) of proline as recorded in *B. acuminata*, *P. longifolia* and *A. scholaris* had initiated appreciable ion leakages (5.21–8.93%) in the foliage rendering the MSI values (47.59–55.27%) to be lowest, proving the sensitive nature of the said plants.

6.3.4.6. Leaf carbon content: Carbon allocation in stress tolerance

Plants having sessile nature are constantly exposed to environmental changes unfavourable for their survival and growth. Therefore, utilization of all the viable resources at plants' disposal would be the response of plants towards ensuring sustained growth and yield as well as combating pollution load with negation of ensuing stress injury. Among all the resources, carbon allocation may be termed as one of the most important processes of plants' defense mechanism (Hartmann and Trumbore, 2016; Hartmann et al., 2020; Xia et al., 2017). PM-induced stomatal blockage lowers the CO₂ uptake by plants and hampers photosynthesis (Saxena and Kulshrestha, 2016), thereby prompting reallocation of carbon—need throughout the plant body (Kobe et al., 2010). As a result, carbon content of plant leaves makes it an effective biomarker of plant health against pollution. Differences in the leaf carbon contents of native species are demonstrated in Table 32. Carbon content of 43.64 – 52.43% implied increased carbon allocation and synthesis of carbon compounds in the leaf tissues for stress resilience. Occurrences of positive correlations of carbon with PM ($r=0.66$, $p<0.05$) and PAHs ($r=0.72$, $p<0.05$) also prove the above contention. Foliar carbon contents were found to be highest in *T. divaricata* and *N. oleander* and lowest in *P. longifolia* (Table 32). Comparable carbon percentages (42.4%) in the overground tissues of vegetation of arid ecosystem were also noticed by Juan et al. (2014). Drake et al. (2019) and Xia et al. (2017) observed enhanced carbon distribution in the aboveground parts of the plants (leaf, wood, etc.) in comparison to belowground part for physiological processes (i.e. respiration, growth, etc.) in presence of environmental stressors such as drought, warming, high water and low light conditions. Paull et al. (2021) investigated carbon content of green wall species subjected to atmospheric pollution and inferred it to be a health response mediated by plants.

6.3.4.7. Total soluble sugar (TSS) content

TSS is usually regarded as another type of osmo-regulator (other than proline) which strengthens cell stability and turgor in plants and also triggers ROS defense machinery, protecting cellular components and controlling signaling pathways during stress (Rai, 2016). Plant sensitivity is associated with low TSS owing to the collateral effects of relatively less pollutant bioaccumulation capacity and structural impairment of leaf chlorophyll (Banerjee et al., 2021). Synergistic interactions of TSS with antioxidants at tissue and cellular levels impart stress tolerance to plants (Bolouri-Moghaddam et al., 2010). The current study also supports the above inferences (based on the results given in Table 32) as revealed by the positive correlations of TSS content with PM ($r=0.82$, $p<0.05$), PAHs ($r=0.74$, $p<0.05$), proline ($r=0.80$, $p<0.05$), AA ($r=0.91$, $p<0.05$), C_{x+c} ($r=0.15$, $p<0.05$) and Chl_T ($r=0.46$, $p<0.05$). This can be comprehended from the above correlations that the increase in pollution stress favours increased bio-synthesis and -accumulation of TSS which acts in conjunction with the enhanced levels of proline and AA, maintaining higher levels of Chl_T to counterbalance the toxicity of pollutants for sustenance and growth of plants. However, it was noted that the C_{x+c} have minimal direct impact on TSS which was, contrarily, found to have pronounced effect on leaf carbon content ($r=0.72$, $p<0.05$) as TSS might be considered as a primary carbon source for energy generation. The TSS accumulation was highest in *T. divaricata* and *N. oleander* with leaf concentrations of 24.75 and 15.05 mg g⁻¹ respectively and lowest in *P. longifolia* (5.48 mg g⁻¹) and *A. scholaris* (4.17 mg g⁻¹). Jeddi et al. (2021) and Kamble et al. (2021) also detected high concentrations of TSS in the plant leaves of polluted sites, suggesting the multifaceted roles of soluble sugars.

6.3.4.8. Protein content

Besides being principal building blocks for different aspects of plant growth such as structural growth with biomass change, expansive growth, cell production and proliferation, etc., protein molecules also govern the cellular stress responses to environmental gradients (Qazi et al., 2019). Pollution stress-mediated toxicity may act as an inducing factor for rise or decline of protein content in plant types based on their intrinsic capabilities of enduring abiotic stress (Rai, 2016). A declining trend in protein concentration (ref. Table 32) of plant leaves in response to stress was achieved in the present investigation which was affirmed by the inverse relationship of protein with PM ($r=-0.56$, $p<0.05$), PAHs ($r=-0.46$, $p<0.05$) and proline ($r=-0.71$, $p<0.05$). The catalytic presence of pollutants might be deemed to be the inhibitor of

de novo protein synthesis and also prime mover behind the proteolytic cleavage of peptide bonds degenerating protein structures into miniscule amino acids, thereby enhancing protein reduction (Iqbal et al., 2000). Protein contents of *T. divaricata* (29.75 mg g⁻¹) and *N. oleander* (30.72 mg g⁻¹) were found to be more affected by air pollutants. Likewise, decreased levels of protein content were documented for *F. benghalensis* and *T. arjuna* (sampled from industrial regions) by Banerjee et al. (2022) as well as for *D. alba* and *R. communis* growing along the congested roads with dense traffic by Khalid et al. (2019).

6.3.4.9. Air pollution induced stress tolerance of plants and considerations for green belting

One way of expressing plants' ability to combat stress is through assessment of APTI which involves Chl_T, AA, leaf pH and RWC for its evaluation. The APTI values, shown in Table 32, reflected *N. oleander*, *T. divaricata*, *C. gigantea*, *N. cadamba* and *P. alba* as tolerant species (APTI: 19.49–29.72, i.e. >17), *B. acuminata* and *A. scholaris* as intermediately tolerant (APTI: 15.29 and 14.43 respectively, i.e. lying between 10–16) and *P. longifolia* as a sensitive one (APTI: 9.65, i.e. <10). Moreover, APTI varied positively with PM ($r=0.58$, $p<0.05$) and PAHs ($r=0.90$, $p<0.05$), suggesting a direct relationship with high pollution levels. Strong positive influences of AA ($r=0.94$, $p<0.05$), pH ($r=0.84$, $p<0.05$) and Chl_T ($r=0.55$, $p<0.05$) on APTI are also considerable pertaining to the structural and functional stability of the plants against stress-causing factors. Weak correlation between RWC and APTI ($r=0.06$, $p<0.05$) defined low dependence of APTI on RWC for all the investigated species. Thus, high APTI values signify enhanced competitive abilities of stress tolerant plants for biomonitoring of urban pollution through adaptive mechanisms (Kamble et al., 2021).

Being pollution indicators, plants change their responses with varying degrees of anthropogenic contamination. Hence, strategic selection of tolerant plants for green spaces is obligatory in order to ensure urban sustainability through the obtainment of maximum area–cover served by the green zone. Concerning biomonitoring, primary selection of plants is usually based on APTI analysis, but the grade of their performance should be critically judged through the application of API which also includes the impact of APTI along with other plant traits (as discussed in section 2.5) (Bala et al., 2022). Performance factor assessment with respect to plant species gradation and API has been represented in Table 33. *N. cadamba* (93.75%), *N. oleander* (81.25%) and *P. alba* (81.25%) have highest API score and are ranked as highly competent species with best and excellent performance. *T. divaricata*, *C. gigantea* and *A. scholaris* are also screened as very good and good performers (as seen from Table 4),

although *A. scholaris* displayed intermediate tolerance on APTI scale. In addition, *B. acuminata*, though lying in the poor category as per API grade, showed better performance in PM capture because of the leaf shape with the presence of specialized appendages or trichomes on leaf surfaces (ref. section 3.1). In a recent study, [Patel et al. \(2023\)](#) proposed that the plants scoring a percentage value of less than 50% need not be considered for planting designs in urban canyons. However, in spite of being sensitive from APTI screening, *P. longifolia* proved to be a moderate performer on the basis of API gradation. This has coherence with the results showing accumulation and encapsulation of particulates due to their distinctive macro- and microscale properties with prominent topographical structures on the surfaces of the leaves (as elaborated in section 3.1). Many studies offered comprehensive descriptions on the key aspects of APTI and API with major thrust on the broader outline of green belting using native flora ([Goswami et al., 2022](#); [Patel et al., 2023](#)).

In this context, it may be argued that the plants' tolerance or adaptability does not only depend on APTI or API scale, but there are several other biochemical, physiological, morphological, environmental and topographical variables contributing to their pollution tolerance capacities ([Banerjee et al., 2022](#)). In line with the above statement, the present study focused on the multiparametric analysis highlighting the influences of pollutants (PM and PAHs), foliar morphology, leaf wax, SLA, Chl a/b, C_{X+C} , MSI, EL, proline, leaf carbon, TSS and protein apart from APTI/API and as such correlation analysis substantiated the strength of association between leaf traits and airborne pollutants. Even though RWC and protein revealed negative correlations with pollutants, Chl a/b, C_{X+C} , AA, leaf pH, MSI, EL, proline, leaf carbon and TSS had beneficial impacts on plant responses. Variability assessment of more numbers of biomarkers would throw open the options of choosing the plant types from a vast reserve of vegetation depending on their enhanced probability of positive correlation with air pollution, rendering the vista of green belting wide open with the inclusions of species-diversified plant communities. However, APTI and API may serve the purpose of quick selection of the tolerant species.

Regarding green belt formation considering building geometry and plant height combination, [Liu et al. \(2023\)](#) suggested that relatively longer building length with respect to width and alternate tree and hedge arrangement would prove more beneficial in reducing the effect of particles in urban sprawl. This may also be applicable with double rows of tree arrangement. [Wu et al. \(2021\)](#) observed that the mixed designs with small shrubs and arbour-shrub combination at maximum concentration distance would substantially lower the

exposure risks to pedestrians and pollutant concentrations in horizontal dispersion. In case of vertical dispersion, the authors found that the shrubs served the purpose of inhibition of pollutant diffusion through wind flow, resulting in faster deposition of PM within a height of 2–4 m. Conversely, [Li et al. \(2016\)](#) inferred that the low height of shrub mediated increase in the vertical movement and transportation of PM, thereby reducing ambient concentrations. Based on the above facts, it could be opined that after species selection, the following factors for planting arrangement should be considered in order to make the design effective and more conducive for maximum removal of pollutants: urban morphology/design, area under study including topography, vegetation composition and distribution, vegetation density index and coverage ratio, plant height, crown diameter, soil and water quality, aspect ratio (building width:height) and meteorological factors. Therefore, all the studied species may be surmised to be included in urban road green belt construction for alleviating somehow or other near roadway pollutant concentrations.

Table 32

Evaluation of leaf characteristics (as mean \pm SD) of selected plant species as potential biomarkers.

Parameters	Plant species							
	<i>Nerium oleander</i>	<i>Tabernaemontana divaricata</i>	<i>Calotropis gigantea</i>	<i>Bauhinia acuminata</i>	<i>Polyalthia longifolia</i>	<i>Alstonia scholaris</i>	<i>Neolamarckia cadamba</i>	<i>Plumeria alba</i>
Chl a (mg g ⁻¹ d.w.)	0.57 \pm 0.05	3.62 \pm 0.28	2.93 \pm 0.06	2.02 \pm 0.05	1.80 \pm 0.08	0.98 \pm 0.04	3.43 \pm 0.16	2.84 \pm 0.11
Chl b (mg g ⁻¹ d.w.)	0.33 \pm 0.07	1.51 \pm 0.06	1.11 \pm 0.09	0.84 \pm 0.05	0.92 \pm 0.04	0.46 \pm 0.05	0.81 \pm 0.04	1.06 \pm 0.08
Chl _T (mg g ⁻¹ d.w.)	0.90 \pm 0.03	5.13 \pm 0.34	4.04 \pm 0.15	2.86 \pm 0.10	2.72 \pm 0.11	1.44 \pm 0.07	4.24 \pm 0.20	3.90 \pm 0.18
Chl a/b	1.73 \pm 0.74	2.39 \pm 0.08	2.64 \pm 0.19	2.40 \pm 0.09	1.96 \pm 0.01	2.13 \pm 0.18	4.23 \pm 0.03	2.68 \pm 0.13
C _{X+C} (mg g ⁻¹ d.w.)	0.24 \pm 0.01	1.12 \pm 0.28	0.88 \pm 0.07	0.87 \pm 0.05	1.12 \pm 0.13	0.35 \pm 0.02	1.10 \pm 0.11	0.80 \pm 0.05
AA (mg g ⁻¹ d.w.)	15.75 \pm 0.44	18.00 \pm 0.27	10.88 \pm 0.26	7.88 \pm 0.18	3.63 \pm 0.08	7.50 \pm 0.18	9.88 \pm 0.08	11.63 \pm 0.09
Leaf extract pH	7.38 \pm 0.05	7.47 \pm 0.04	6.45 \pm 0.04	6.63 \pm 0.07	5.91 \pm 0.06	6.36 \pm 0.05	6.49 \pm 0.06	6.56 \pm 0.08
RWC (%)	76.90 \pm 0.13	70.39 \pm 0.33	84.55 \pm 0.39	78.19 \pm 0.07	65.16 \pm 0.15	85.78 \pm 0.48	88.93 \pm 0.74	81.89 \pm 0.63
MSI (%)	80.52 \pm 2.84	88.69 \pm 4.05	78.01 \pm 4.37	55.27 \pm 6.39	47.59 \pm 6.25	53.90 \pm 3.34	60.79 \pm 3.81	75.44 \pm 4.20
EL (%)	0.98 \pm 0.30	2.31 \pm 0.42	7.29 \pm 0.57	8.93 \pm 1.52	5.21 \pm 0.88	6.10 \pm 0.95	5.60 \pm 0.43	8.26 \pm 0.65
Proline content (mg g ⁻¹ d.w.)	4.28 \pm 0.59	4.72 \pm 0.18	3.56 \pm 0.73	0.55 \pm 0.13	1.56 \pm 0.49	1.27 \pm 0.37	2.54 \pm 0.66	2.44 \pm 0.58
Leaf carbon content (%)	51.50 \pm 1.24	52.43 \pm 0.95	46.77 \pm 2.45	48.96 \pm 4.54	43.64 \pm 1.24	49.32 \pm 0.89	47.80 \pm 0.23	49.74 \pm 1.29
TSS content (mg g ⁻¹ d.w.)	15.05 \pm 2.29	24.75 \pm 4.31	10.84 \pm 2.35	9.38 \pm 2.68	5.48 \pm 1.84	4.17 \pm 1.03	7.90 \pm 2.32	12.58 \pm 1.45
Protein content (mg g ⁻¹ d.w.)	30.72 \pm 3.51	29.75 \pm 2.07	33.42 \pm 3.27	34.81 \pm 2.55	33.37 \pm 4.42	40.09 \pm 3.45	34.86 \pm 4.21	31.46 \pm 2.02
APTI	20.73 \pm 2.07	29.72 \pm 3.15	19.87 \pm 1.58	15.29 \pm 0.46	9.65 \pm 0.89	14.43 \pm 1.20	19.49 \pm 0.48	20.35 \pm 1.99
Total PM load (μ g cm ⁻²)**	1808.64 \pm 46.99	2766.27 \pm 86.79	709.91 \pm 71.34	1697.57 \pm 95.76	1100.44 \pm 94.77	932.61 \pm 89.93	539.32 \pm 101.49	1054.27 \pm 112.85
Total PAHs concentration (μ g g ⁻¹)**	286.08 \pm 32.65	393.01 \pm 30.34	267.47 \pm 11.49	177.22 \pm 14.57	159.92 \pm 21.23	256.80 \pm 32.31	301.13 \pm 37.31	342.28 \pm 25.38

** Though these values are indicated in the body of the manuscript, these are again represented here for the ease of comparative/correlation study.

Table 33

Anticipated Performance Index (API) of selected plant species.

Plant species	APTI	Plant habit	Canopy structure	Type of plant	Laminar structure			Economic value	Grade allotted			Assessment Category (AC)
					Size	Texture	Hardiness		Total plus (+)	% score	API value/Grade	
<i>Nerium oleander</i>	+++++	+	+	+	++	+	+	+	13	81.25	6	Excellent
<i>Tabernaemontana divaricata</i>	+++++	+	+	+	+	+	–	++	12	75	5	Very good
<i>Calotropis gigantea</i>	++++	+	+	+	++	+	–	++	12	75	5	Very Good
<i>Bauhinia acuminata</i>	+++	–	+	–	+	+	+	+	8	50	2	Poor
<i>Polyalthia longifolia</i>	+	++	+	+	+	+	+	+	9	56.25	3	Moderate
<i>Alstonia scholaris</i>	++	++	++	+	++	+	+	–	11	68.75	4	Good
<i>Neolamarckia cadamba</i>	++++	++	++	+	++	+	+	++	15	93.75	7	Best
<i>Plumeria alba</i>	+++++	+	+	–	++	+	+	++	13	81.25	6	Excellent

Maximum grade of 16 can be scored by any plant. % Score (≤ 30) = Grade 0 (AC: Not recommended); % Score (31–40) = Grade 1 (AC: Very poor); % Score (41–50) = Grade 2 (AC: Poor); % Score (51–60) = Grade 3 (AC: Moderate); % Score (61–70) = Grade 4 (AC: Good); % Score (71–80) = Grade 5 (AC: Very good); % Score (81–90) = Grade 6 (AC: Excellent); % Score (91–100) = Grade 7 (AC: Best) (Prajapati and Tripathi, 2008_b; Pathak et al., 2011; Pandey et al., 2015_b; Kaur and Nagpal, 2017).

6.4. Conclusion

In urban areas, environmental exposures to traffic exhaust-generated PM and PAHs have led to extreme cases of morbidity and mortality. Development of green spaces fosters a better livelihood for the inhabitants. In this regard, the present study has focused on the selection of dominant locally available plant communities on the basis of their PM and PAHs retention abilities, air pollution biomarkers and tolerance. Deposition of surface PM ($493\text{--}2680\ \mu\text{g cm}^{-2}$) and wax PM ($5.30\text{--}25.82\ \mu\text{g cm}^{-2}$) of size $10\text{--}100\ \mu\text{m}$ was prominent in the leaves of all the species relative to the coarse ones, surface accumulation being recorded to be higher with all particle sizes. *T. divaricata*, *N. oleander*, *B. acuminata*, *P. longifolia* and *P. alba* were efficient PM retainers in terms of cumulative distribution. The particle accumulation by plant foliage was found to have definite correlations with intra/epicuticular wax composition and content, leaf shape and microstructural variability. PAHs concentrations were detected in the range of $159.92\text{--}393.01\ \mu\text{g g}^{-1}$ in the plant leaves, which were found to be positively effected by SLA. In, *N. oleander*, *T. divaricata*, *C. gigantea* and *N. cadamba*, HMW PAHs (53–62%) were predominant, while composition profiles of *B. acuminata*, *P. longifolia*, *A. scholaris* and *P. alba* showed the prevalence of LMW PAHs (51–57%). TI values of more than 4 implied the presence of combustion emitted PAHs, more specifically those released from traffic emissions. The toxicological risk analyses revealed carcinogenic and mutagenic hazards from mainly HMW PAHs (>90% contribution).

Plant responses to airborne pollutants for biomonitoring can easily be ascertained through the variations in the levels of different biomarkers, leading to the assessment of plant tolerance to withstand the impact of anthropogenic inputs and adverse climate in the urban areas. Parameters such as Chl a/b, C_{x+c} , AA, leaf pH, proline, leaf carbon and TSS were examined as controlling variables by correlation analysis, imparting tolerance to the plants through maintenance of Chl_T , membrane stability (viz. MSI) and ion leakage (viz. EL), under high air pollution stress severity. Abiotic stressors also triggered reduction in leaf RWC and protein content as stress symptoms.

In compliance with the results of APTI, API and leaf trait evaluations in combination with PM and PAHs capturing capabilities, *T. divaricata* and *N. oleander* proved themselves to be immensely recommendable in most aspects for green belting. Also, *N. cadamba*, *C. gigantea* and *P. alba* with high APTI and API are suitable options for air pollution mitigation, *P. alba* turning out to be superior to the first two species in PM capturing and PAHs accumulation. *B. acuminata* and *P. longifolia* may be utilized in some specific areas with dust-laden atmosphere

because of their effectiveness in high PM removal with moderate potential of PAHs biofiltration. On the other hand, PAHs filtering behaviour of *A. scholaris* with average PM retention ability makes it an obvious choice for designing urban green spaces in densely populated areas. From the above, it can be recommended that the shrubs such as *T. divaricata*, *N. oleander*, *C. gigantea*, *P. alba* and *B. acuminata* and trees like *N. cadamba*, *P. longifolia* and *A. scholaris* of native origin and fast-growing nature should be planted in combination in a staggered formation to prevent wind funnelling. The available inter-spaces between trees should also be covered with meadows (particularly dominated by grasses, herbs or non-woody plants) or hedges to form an effective barrier by lessening the gaps. Such conceptual plan for proper green landscaping must be executed in the urban regions of Kolkata with appropriately selected species with due considerations to their orientation with respect to the relative locations of industrial and housing belts having elaborate road network.

The conceptual framework along with the established results discussed so far in the current and earlier chapters has been further substantiated in Chapter 7 through the development of a mechanistic approach-based plant uptake model for PAHs across foliage-air interface.

Chapter 7

7. Methodology VI

Modeling of PAHs accumulation in biomonitors: Mechanistic approach

7.1. Background

Concerning the perilous effects of environmental pollution, plant cover is at the forefront of global transport and dispersion of persistent organic pollutants (POPs), where plant uptake and accumulation of organic chemicals through multiple routes (ref. [Fig. 30](#)) play a vital role in their alleviation. Atmospheric exchange of polycyclic aromatic hydrocarbons (PAHs) with vegetation surfaces (covering about 80% of the land) through gaseous deposition, particle deposition (wet and dry) and wet deposition controls their fate and transport in the terrestrial environment ([Cousins and Mackay, 2001](#); [Wang et al., 2015_b](#)). The environmental compartmentalization, distribution and possible fate of individual PAH congeners may diverge based on the relative differences in their molecular and bulk properties, such as vapour pressure, water solubility, partition coefficients, sorption behaviour and volatility ([Zhu et al., 2020](#)). The exchange processes are greatly facilitated by the large canopy cover of diverse plant/vegetation types. The particle-laden deposition is governed by the concentration of PAHs in particulate phase, mass size distribution of the particulate pollutants, incidence and rate of rainfall and atmospheric particulate retention capacity of plant leaves ([McLachlan, 1999](#)). Gas phase deposition includes two processes: atmosphere-vegetation partitioning of PAHs at equilibrium and gaseous deposition under kinetic-limited regime. The first step relies on temperature, gas phase concentrations of PAHs preceding sampling duration and accumulative characteristics of vegetation cover and the other step is more dependent on vapour phase concentrations of PAHs during the plant life cycle, wind flow velocity, extent of atmospheric layer stability, plant age effects, spatial arrangement of mature tree crown and leaf surface

topography (McLachlan, 1999). PAHs which are intercepted and held by leaves may undergo adsorption and/or absorption. Adsorption acts as a reversible phenomenon, but absorption causes diffusion of PAHs in mesophyll tissue via cuticle layer. Prospect of terrestrial plants with trichomes, lipophilic cuticles, vast surface area per unit volume of foliage and high stomatal density in biomonitoring of ambient pollutants has been explored to a great extent (Janhall, 2015). The overall approximate aerial plant surface area on the globe has been evaluated to be $4 \times 10^8 \text{ km}^2$ with the area of stomatal pores extending between $46\text{-}125 \text{ }\mu\text{m}^2$ (for a particular species), giving a fair idea about the leaf capturing potential for pollutants, which ultimately influences the nation's budget for pollution control (Wei et al., 2017). Periodic fluctuations in human activities are liable for varying degrees of PAHs in the ambient air. Diurnal, annual and seasonal changes in local weather patterns also determine airborne PAHs concentrations (Ravindra et al., 2006; Yang et al., 2013; Ray et al., 2017) and may even cause outflow of PAHs from leaf to the atmosphere. Quantitative evaluation of pollutant fluxes with respect to equilibrium considerations for foliar absorption or adsorption processes provides a factual basis for discerning the uptake mechanism, contribution of transport pathways and differential accumulation pattern depending on the plant-air or octanol-air or gas-particle partition coefficient (K_{PA} or K_{OA} or K_P respectively) (Mackay et al., 2006).

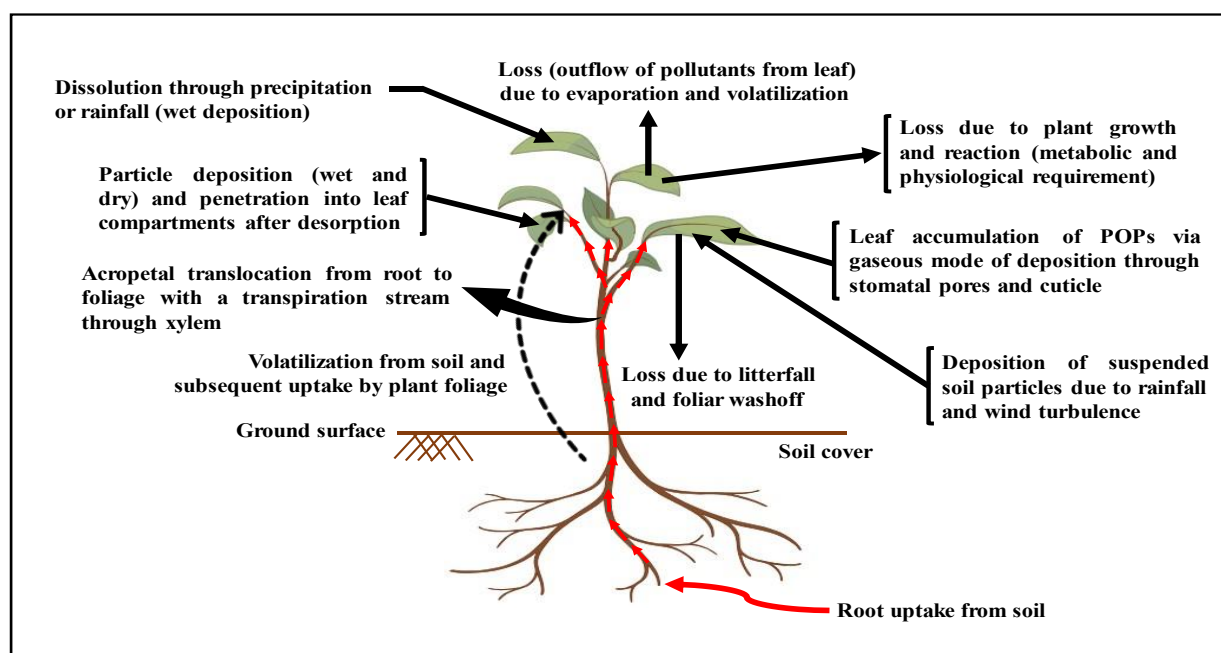


Fig. 30. Dominant routes of POP uptake, accumulation and transport in plants along with loss mechanisms (Cousins and Mackay, 2001; Collins et al., 2006).

Air-leaf system constitutes the largest boundary of biotic/abiotic mass transfer and acts as the main pathway of pollutant transport in plants of terrestrial ecosystem with different pollution gradients. Moreover, mass transfer rates of pollutants are proportional to the available contact area. Leaf accumulation and sequestration of PAHs from ambient air has been recognized as the principal means of scavenging atmospheric PAHs and are strongly influenced by the physico-chemical properties of particular PAHs, their equilibrium distribution or partitioning between plant and atmosphere (relating to K_{PA} or K_{OA} which also determines the bioconcentration of organic compounds in plant foliage) as well as plant functional traits (viz. leaf lipid, wax and water contents, surface roughness, transpiration rates, etc.) and growth characteristics (i.e., evergreen or deciduous: evergreen species are more advantageous, enabling continuous capturing of pollutants over the whole year; shedding of leaves in winter months having high air pollution levels, etc.) (Wild et al., 2006; Wang et al., 2008; De Nicola et al., 2017). K_{OA} is defined by the ratio of the chemical concentration in air and environmental surfaces (such as particulate matter, vegetation, soil and sediments) at thermodynamic equilibrium (Baskaran and Wania, 2023), while K_{PA} is represented as the ratio between equilibrium concentration of PAHs in air to that in leaves (Komp and McLachlan, 1997). Characterization studies on variabilities in the biomonitoring potential of diverse plant types (broad-leaved and conifers) employing partition coefficient measurements have been carried out in few researches (Giraldez et al., 2022; Klingberg et al., 2022). Environmental conditions, specific leaf area, leaf area index, characteristics of PAHs and atmospheric concentration largely influence the partition coefficients (Terzaghi et al., 2015). Uptake by root system and subsequent translocation (i.e., acropetal translocation) to the aerial plant parts may also contribute to the total PAHs concentrations in foliage (Collins et al., 2006).

PAHs entry into the plant leaves follows a two-step process: adsorption on cuticular surfaces (leaf cuticular compartments comprise epicuticular waxes (EW), cuticle proper (CP), and cuticular layer (CL)) by dry or wet deposition and absorption, penetration and migration or translocation into leaf tissues through stomatal uptake (Desalme et al., 2013; Li et al., 2016_a). Leaf surface cuticular adsorption of PAHs takes place via three stages: sorption to wax crystals at the surface, penetration or diffusion across the cuticular membrane and release or desorption from the membrane surface into the leaf epidermis (Li et al., 2016_b). The overall process of cuticular penetration of PAHs is usually associated to both sorption (being the driving force) and diffusion because of their concurrent occurrences (Shechter and Chefetz, 2008). Coexistence of two different paths of diffusion (lipophilic and aqueous pores or channels) in the cuticles mostly directs the pollutant penetration and hydrophobic PAHs follow the

lipophilic path of diffusion through cuticular lipids (Buchholz, 2006; Schonherr, 2006; Li and Chen, 2014). The ability of plant leaves to translocate PAHs within interior tissues determines their accumulative nature which is a prerequisite for biomonitoring (Yang et al., 2017). Once the pollutants get immobilized and trapped within those inner leaf layers, they are less affected by the weather-induced interferences and less susceptible to volatilization from foliar surfaces, thereby assuring the inherent air biofiltration capacity of plants.

Very few studies have been conducted particularizing the contributions of different pathways (gaseous and particle depositions as well as root-to-leaf translocation) to the total foliar loading of PAHs (McLachlan, 1999; Simonich and Hites, 1994_b; Bohme et al., 1999; Kaupp et al., 2000; Klingberg et al., 2022). Moreover, most of the investigations involving uptake models have been performed in laboratory or simulated conditions (hydroponic system, greenhouse/growth/closed/exposure chamber or artificially contaminated/spiked soil) (Zhu et al., 2020; Iwabuchi et al., 2020; Tani et al., 2022; Wang et al., 2023), unlike the field study without any controlled environment. Laboratory tests do not completely reflect the ambience of natural surroundings and field environment, thereby generating divergences in qualitative and quantitative results obtained from both the analyses (Wang et al., 2020_a; Fan et al., 2020). Conceptual research designs are thus required for constructive integration of laboratory and field works for the assessment of intricate mechanisms of PAHs uptake and translocation. However, route-specific accumulation of PAHs in plants may differ based on pollutant nature. Explicit interpretation of PAHs uptake mechanism through modeling approaches incorporating environmental dynamics of both abiotic and biotic factors (viz., models based on material balance, fugacity capacity, etc.) is therefore of vital importance in order to evaluate the biomonitoring potential of plant species. The resulting model would precisely help in determining the performance of species exposed to co-occurring ambient stressors. Natural phenomena like litterfall, washout effects in rainy season and natural volatilization from surfaces may contribute in getting the actual uptake by a biomonitor plant. Therefore, net uptake by the plant biomonitor is certainly different in varied plant species, which must be accounted on a case to case basis.

In view of the foregoing, the present study was undertaken using a model plant biomonitor species *Murraya paniculata* to (1) examine the partitioning of 16 EPA-PAHs from atmosphere into the particulate phase (i.e., leaf-laden particulate matter (PM)) and leaf matrix based on K_P and K_{PA} , (2) analyze the fate of ambient PAHs in plant biomonitor under real-field conditions underlining the mechanisms of foliar uptake and translocation dynamics (i.e., translocation into inner leaf compartments from foliar PM and from root to leaf), (3) identify

the PAHs scavenging or uptake pathways for *Murraya* leaves with their probable contributions, (4) evaluate the fugacity capacity of plant leaves for estimating the potential for foliar sorption and (5) predict a mechanistic model of net PAHs uptake by plant biomonitor based on real data.

7.2. Materials and methods

7.2.1. Experimental design

A modeling approach was undertaken to demonstrate the specific pathway-driven inputs of PAHs into *Murraya* leaves (i.e., bioaccumulation) on the basis of the measurements of PAHs concentrations in multiple leaf compartments and roots of *M. paniculata*, keeping in view PAHs mass transfer, partitioning and translocation behaviour as well as leaf morphology. Estimates of total leaf surface area for approximately 40 leaves (A in cm^2) were acquired with the help of graph paper (Prajapati and Tripathi, 2008a) and found as 241.75 cm^2 . Specific leaf area (SLA in $\text{cm}^2 \text{ g}^{-1}$) was calculated as 151.09 using the ratio between leaf area and dry weight. Random scaling measurements were taken for leaf thickness determination using 20-30 leaves and the average thickness was calculated as 0.025 cm for an individual leaf sample, which is quite comparable to that of the literature values (0.016-0.029 cm) (Raskin, 1983). Leaf volume (V in cm^3) was then estimated as ($A \times \text{total leaf thickness}$) and found to be 241.75 cm^3 . A process flow diagram has been comprehensively depicted in Fig. 31. Mathematical interpretation of the model and parameters has been described elaborately in the subsequent sections.

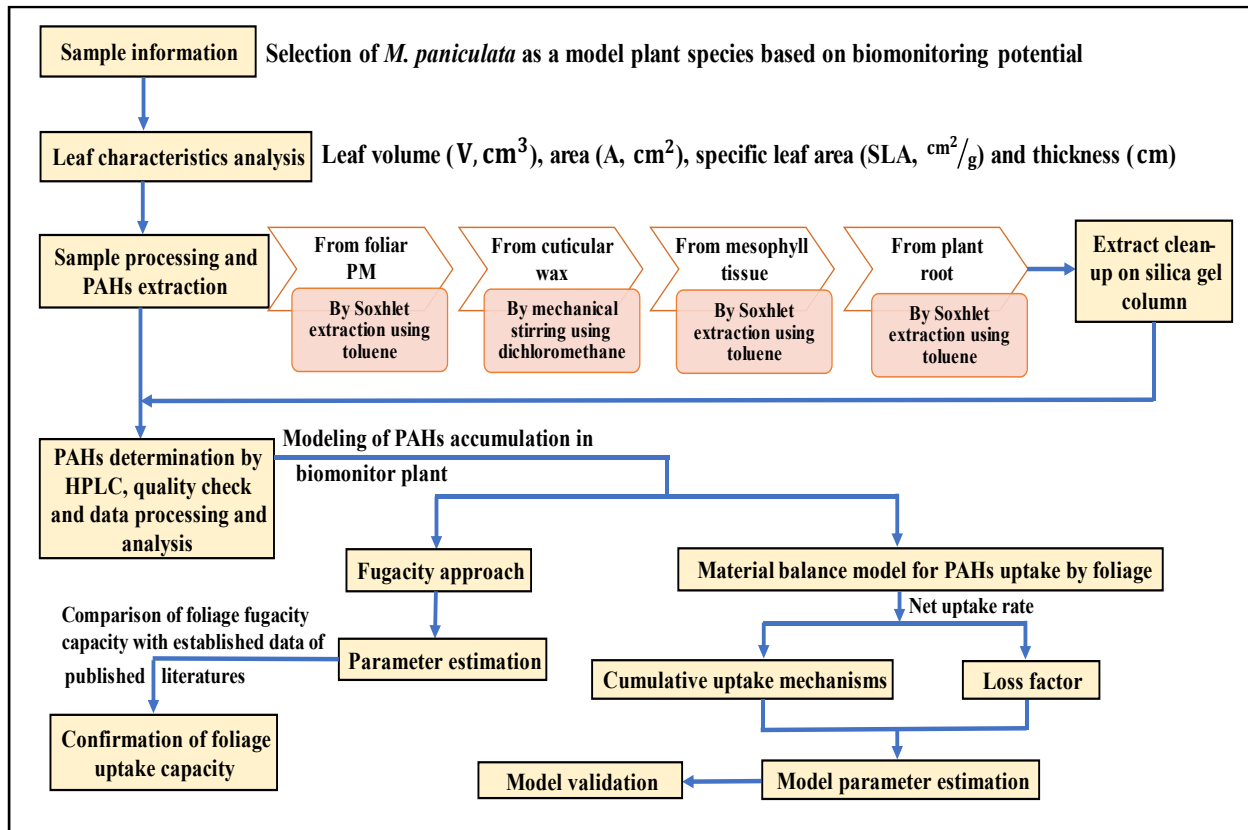


Fig. 31. Flow chart for model design.

7.2.2. Determination of plant-air partition coefficient (K_{PA})

By definition, plant-air (K_{PA}) and octanol-air (K_{OA}) partition coefficients can be mathematically expressed in Eqs. 30 and 31 (Giraldez et al., 2022; Baskaran and Wania, 2023):

$$K_{PA} = \frac{C_P}{C_A} \quad (30)$$

$$K_{OA} = \frac{C_O}{C_A} \quad (31)$$

where, C_P , C_A and C_O are the equilibrium concentrations of a chemical compound in plant leaves, air and octanol-phase respectively.

It is assumed that K_{PA} is directly proportional to K_{OA} with the consideration that the lipid-rich tissues of plant leaves acting as the storage compartment or sink for lipophilic or hydrophobic compounds like PAHs simulate the behaviour of octanol (Komp and McLachlan, 1997). Hence, in the present work, for simplicity, K_{PA} and K_{OA} have been identically used and, in some cases, K_{OA} has been substituted by K_{PA} as needed. Since, C_A is not available, therefore,

K_{OA} (or K_{PA}) (Eq. 32) was estimated using octanol-water partition coefficient (K_{OW}) (Eq. 33) (Vallero, 2014):

$$K_{OA} = \frac{K_{OW}RT}{K_H} \quad (32)$$

$$K_{OW} = \frac{C_O}{C_W} \quad (33)$$

where, K_H is the Henry's law constant ($\text{atm m}^3 \text{ mol}^{-1}$), R is the ideal gas constant ($8.21 \times 10^{-5} \text{ atm m}^3 \text{ K}^{-1} \text{ mol}^{-1}$), T is the absolute temperature (K) and C_W is the concentration of chemical compound in water-phase.

An equilibrium distribution study was conducted experimentally with the help of 'stirred flask technique' for determining the partition coefficients of PAHs (Dearden and Bresnen, 1988; Streng, 2001; Silva et al., 2021). A standard solution (5 mL) of 16 EPA-PAHs in acetonitrile (prepared by diluting a stock solution of known concentration) was initially added to the aqueous matrix of volume 10 mL following which the two matrices, i.e., water and plant leaf (sample weight: 0.5 g), were mixed together. Blank matrices devoid of target compounds were used for the partitioning experiments. Slurries were then kept under stirring condition (with moderate speed) for 6-7 days at 25 °C to allow for equilibrium partitioning (the pre-experimental results revealed that the equilibrium was achieved within the stipulated period). After equilibration time, the two phases were separated and water matrix was subjected to direct clean-up followed by HPLC analysis for PAHs quantification. Dried leaf matrix was further extracted with toluene for 6 h, purified and analyzed in HPLC for PAHs estimation. K_{OW} was then evaluated using the concentrations of individual PAHs in both leaf and water matrices and K_{OA} was finally calculated as per the aforementioned formula for each congener. C_A was also determined from the K_{PA} expression.

7.2.3. Determination of particle-gas partition coefficient (K_P)

Distribution equilibrium of PAHs between gas and leaf-laden particulate phases can be expressed by the particle-gas partition coefficient (K_P) in order to establish the adsorption potential of PM for capturing PAHs (Weschler et al., 2008). Particle-bound PAHs have been found to be associated with high K_P values (Tsapakis and Stephanou, 2005). In the current study, K_P for individual PAHs was evaluated using the following empirical equations (Eqs. 34-37) (Finizio et al., 1997; Harner, 1998; Weschler et al., 2008):

$$\log K_P = 0.79 \log K_{OA} - 10.01 \quad (34)$$

$$\log K_P = \log K_{OA} + \log f_{OM} - 11.91 \quad (35)$$

$$\log_{10} K_P = 0.829 \log_{10} K_{OA} - 10.263 \quad (36)$$

$$\log_{10} K_P = \log_{10} K_{OA} + \log_{10}(1.88 \times 10^{-12}) \quad (37)$$

where, f_{OM} is the organic matter fraction of particles (= 0.4 for urban atmosphere) (Weschler and Nazaroff, 2010). Experimentally determined $\log K_{PA}$ values were considered for calculating K_P in place of $\log K_{OA}$ to accurately predict the partitioning of PAHs into foliar PM from the ambient air.

7.2.4. Determination of PAHs mass transfer coefficients for air-leaf and root-leaf uptake

For estimating the overall air-leaf mass transfer coefficients of PAHs, an uptake model proposed by McLachlan (1999), Kobayashi et al. (2007) and Sun et al. (2016) for different systems, air to leaf, air to grain and air to crop leaf surface, was employed which can be described as follows (Eq. 38):

$$\frac{dC_L}{dt} = k_{AL} a_{AL} C_A - \frac{k_{AL} a_{AL} C_L}{BCF_{LA}} \quad (38)$$

where, C_L is the concentration of PAHs in plant leaves ($\mu\text{g g}^{-1}$), t is the time in days (d), k_{AL} is the overall air to leaf mass transfer coefficient (cm day^{-1}), a_{AL} is the volumetric leaf area (i.e., leaf surface area normalized to leaf volume) (found to be $40.02 \text{ cm}^2 \text{ cm}^{-3}$ based on experimentation), C_A is the air-phase concentration of PAHs ($\mu\text{g g}^{-1}$) and BCF_{LA} is the foliage or leaf-air bioconcentration factor defined as (C_L/C_A) . Therefore, from the plot of dC_L/dt ($\mu\text{g g}^{-1} \text{ day}^{-1}$) vs. C_L (refer **Appendix-I**), k_{AL} values were calculated for individual PAH compounds from the slope $((k_{AL} \times a_{AL})/BCF_{LA})$ of the curve.

The applicability of the above-mentioned model was further extrapolated for evaluating the root-leaf mass transfer coefficients of PAHs assuming the uptake from root compartment to foliage via transpiration stream through xylem. Thus, the model can be interpreted using Eq. 39 below:

$$\frac{dC_L}{dt} = k_{RL} a_{RL} C_R - \frac{k_{RL} a_{RL} C_L}{BCF_{LR}} \quad (39)$$

where, k_{RL} is the overall root to leaf mass transfer coefficient, a_{RL} is the contact area of root, C_R is the concentration of PAHs in root ($\mu\text{g g}^{-1}$) and BCF_{LR} is the foliage or leaf-root bioconcentration factor defined as (C_L/C_R) . The parameter $(k_{RL} \times a_{RL})$ (day^{-1}) was then

calculated for PAHs from the slope $(k_{RL} \times a_{RL}) / BCF_{LR}$ of the curve between dC_L/dt and C_L (refer **Appendix-I**) for the limitation in accurate measurement of surface area of intact root.

The rate of change of PAHs concentration in plant leaves (dC_L/dt) was estimated based on the measurement of PAHs concentration (C_L) in foliage collected (in replicates) during August-October, 2023, at a regular sampling interval of 10 days.

For determination of the root concentrations of PAHs (C_R), an uptake experiment was carried out, where root samples were initially soaked in a standard simulated PAH mix solution and samples were collected thereafter at an interval of 24 h for 10-15 days for the purpose of developing a concentration profile of PAHs in plant roots. All the leaf and root samples were extracted and the extracts were then subjected to silica gel column clean-up and chromatographic analysis for examining PAHs concentrations.

7.2.5. Estimation of bioaccumulation and translocation factors

Apart from direct uptake of PAHs from air, plant leaves collect and thereby accumulate ambient PAHs into their tissues from two main sources: PM laden PAHs and root associated PAHs. Determination of related concentrations of PAHs acquired by leaves from PM and its root is based on translocation factor (Blaine et al., 2014). The root concentration factor (RCF) (Eq. 40) and translocation factors (TF) (Eqs. 41 and 42) were assessed considering the concentrations of PAHs in plant foliage, root and surrounding medium (Lu et al., 2024).

$$RCF = C_R / C_{solution} \quad (40)$$

$$TF_{f/L} = C_L / C_f \quad (41)$$

$$[NOTE: C_L = C_W + C_M]$$

$$TF_{R/L} = C_L / C_R \quad (42)$$

where, $TF_{f/L}$ and $TF_{R/L}$ denote the translocation factors from foliar PM to leaf and root to leaf respectively, $C_{solution}$ is the concentration of PAHs in the exposure medium ($\mu\text{g mL}^{-1}$), C_f is the concentration of PAHs in foliar PM ($\mu\text{g g}^{-1}$), C_W is the concentration of PAHs in cuticular wax ($\mu\text{g g}^{-1}$) and C_M is the concentration of PAHs in leaf inner mesophyll tissue ($\mu\text{g g}^{-1}$).

7.2.6. Elucidation of plant uptake mechanism by material balance model and fugacity approach

7.2.6.1. Material balance approach (with model assumptions)

The overall foliage uptake processes of PAHs using *M. paniculata* have been presented in the proposed work. Basically, simultaneous direct-indirect uptake and direct/indirect loss of PAHs to/from leaves results in net PAHs uptake by leaves which indicates foliage air filtering capability. Though the processes are ‘unsteady state’ type individually, they result in steady rate of net uptake combinedly. Individual gain and loss components are looked into in details to have an actual net uptake (Eq. 43) of PAHs by *M. paniculata* leaves and then compared with theoretical net PAHs uptake (Eq. 44) values to confirm the validity of the predicted mechanistic PAHs uptake model.

Two compartments have majorly been considered under gain study – foliage and root. Stem has not separately been studied; however, it is obvious that the translocation process involving PAHs transfer from root tissues to plant leaves takes place through the stem via xylem. Since, the major focus was given on the quantification and percent contributions of the uptake processes of PAHs by the plant of terrestrial origin, air to leaf pathway is the dominant route of accumulation. Thus, the processes can be summarized as follows: diffusional exchange between foliage and air (depicted in the form of Eq. 45), atmospheric deposition on foliar tissues (represented as Eq. 46), uptake through wet precipitation, bulk flow, uptake and transport in plants via transpiration streams at the interface of root-stem-foliage (refer. Eq. 47) along with a loss factor (Paterson and Mackay, 1994).

Contribution of root to leaf pathway to the total foliar PAHs burden was examined neglecting the contribution from soil that may be considered to be another sink of PAHs. On the other hand, translocation of PAHs from plant leaves has been ignored as the pollutant holding capacity of foliage is much more than their abilities to translocate the chemicals into other plant parts. In case of tolerant plant types, it was reported by Perez et al. (2022) that only 2-5% of the pollutants got translocated from the leaves after absorption. Uptake through wet particle deposition and precipitation or rainfall is ignored because of their prevalence in monsoon or wet season only.

In consideration of the dynamicity of plant leaf uptake of organic contaminants, inclusion of total loss factor in material balance has been represented in terms of evaporative loss (L_{EV}) (Eq. 48) as it constitutes the major share. L_{EV} was estimated based on the kinetics of PAHs uptake by plant leaves monitored for 15 days. In brief, plant leaves were soaked in

diluted solutions of PAHs standard mix and samples were taken at a sequence of 24 h time span and analyzed for PAHs concentrations. Cumulative loss ($\mu\text{g g}^{-1}$) was determined after maximum uptake and finally expressed as rate of loss (R_L) in $\mu\text{g g}^{-1} \text{ day}^{-1}$ from which L_{EV} was evaluated and expressed in $\mu\text{g day}^{-1}$.

PAHs losses due to foliar litter and runoff have been ignored, since, these processes are observed during a specific time span of a year. Foliar PAHs transformation or degradation (representing pollutant loss) due to plant growth, metabolism and biochemical reactions is further ignored as the rate of absorption is much higher than the rate of loss in case of bio-metabolism ([Ayilara and Babalola, 2023](#)) and thus contributes minimal with respect to other factors.

The generic form of the model equation is expressed as: **Theoretical net rate of uptake of PAHs (U_{NT}) \approx Actual/calculated net rate of uptake of PAHs (U_{NC})** and is given by

$$(U_{NC}) = \left[\begin{array}{l} \text{Uptake by air – foliage gaseous exchange } (U_{ge}^{A/L}) + \\ \text{Uptake by dry particle deposition } (U_{DP}) + \\ \text{Uptake by wet particle deposition } (U_{WP}) + \\ \text{Uptake through rain dissolution } (U_R) + \\ \text{Uptake from root to foliage via transpiration stream } (U_{TS}^{R/L}) \end{array} \right] - \left[\begin{array}{l} \text{Evaporative loss } (L_{EV}) + \\ \text{Loss due to plant growth } (L_G) + \\ \text{Loss due to plant reaction } (L_{PR}) + \\ \text{Loss due to litterfall } (L_{LF}) + \text{Loss due to foliage runoff } (L_{FR}) \end{array} \right] \quad (43)$$

$$U_{NT} (\mu\text{g/day}) = \frac{V (\text{cm}^3) \times \frac{dC_L}{dt} (\mu\text{g/g.d}) \times \log K_{PA}}{SLA (\text{cm}^2/\text{g}) \times \text{Leaf thickness (cm)}} \quad (44)$$

Parameters under consideration in U_{NC}

$$(U_{ge}^{A/L}) (\mu\text{g/day}) = \frac{k_{AL} (\frac{\text{cm}}{\text{d}}) \times A (\text{cm}^2) \times C_A (\mu\text{g/g})}{SLA (\text{cm}^2/\text{g})} \quad (45)$$

$$(U_{DP}) (\mu\text{g/day}) = \left(\frac{C_f (\mu\text{g/g}) \times \text{Total mass of foliar dust (in g)} \times TF_{f/L}}{\text{days of study}} \right) \quad (46)$$

$$(U_{TS}^{R/L}) (\mu\text{g/day}) = [k_{RL} \times A_R] (1/\text{day}) \times C_R (\mu\text{g/g}) \times (TF_{R/L}) \times \text{Total mass of root sample taken (in g)} \quad (47)$$

$$L_{EV} (\mu\text{g/day}) = (R_L \text{ in } \mu\text{g/g.day}) \times \text{Total mass of leaf sample taken (in g)} \quad (48)$$

Ignored parameters

$(U_{WP}) = 0$; neglected

$(U_R) = 0$; neglected

$(L_G) = 0$; neglected

$(L_{PR}) = 0$; neglected

$(L_{LF}) = 0$; neglected

$(L_{FR}) = 0$; neglected

7.2.6.2. Fugacity approach

Fugacity capacity (Z_F , mol m⁻³ Pa⁻¹) of plant leaves was calculated using the following expressions (involving leaf-air partition coefficient (Eq. 49) and vegetation fraction resembling octanol (having hydrophobic nature) relating to partitioning characteristics (Eq. 50)) to affirm the natural filtering effect of vegetation and foliar sorptive capacities with respect to PAHs (Cousins and Mackay, 2001).

$$Z_F = K_{PA} \times Z_A \quad (49)$$

$$Z_F = v_{FO} \times Z_O \quad (50)$$

where, K_{PA} is the foliage-air partition coefficient, Z_A is the fugacity capacity of air (mol m⁻³ Pa⁻¹) and can be estimated as $1/RT$ (R = universal gas constant = 8.21×10^{-5} atm m³ K⁻¹ mol⁻¹; T = absolute temperature = 298 K), v_{FO} is the volume fraction of the octanol-like material (i.e., plant leaf lipid) in vegetation (found out to be 4.95 m³ m⁻³ based on the measurement) and Z_O is the fugacity capacity of octanol and can be given as ($Z_A \times K_{OA}$) or ($Z_W \times K_{OW}$) (Z_W (mol m⁻³ Pa⁻¹) = fugacity capacity of water = $1/K_H$; K_H = Henry's law constant in Pa m³ mol⁻¹).

7.3. Results and discussion

7.3.1. Plant-air partitioning of PAHs

Less water solubility and lower vapour pressure of HMW PAHs make them easily partitionable into organic phase, comparatively to a greater extent than LMW PAHs. The exchange and partitioning of PAHs between plant foliage and air have been evaluated by K_{PA} to discern the PAHs interception and uptake capacity of terrestrial plants. The partitioning of PAHs between foliage (i.e. octanol phase) and aqueous phases is represented in Fig. 32. Based on the results, it was observed that the concentrations of almost all the PAHs in leaf matrix were much higher

than that of the water matrix, except FLU, PHEN, FLT and CHR which exhibited high concentrations in aqueous phase and this may be attributed to the differences in their water solubilities and vapour pressures (Yu et al., 2020; Kim et al., 2019). Thus, it is interpretive that the PAHs have strong affinities to get accumulated in the foliar tissues rich in lipid fraction which is the primary phase of hydrophobic organic compound accumulation due to nonpolar absorptive nature (Gobas et al., 2018). As evident from Table 34, K_{PA} or K_{OA} values more than unity implied higher equilibrium concentrations of PAHs in octanol like plant-phase as compared to the ambient air, thereby proving the plant as a candidate biomonitor with accumulative potential. Similarly, $\log K_{PA}$ values >1 also affirmed plant leaf uptake of atmospheric PAHs. Very low air-phase equilibrium concentrations of PAHs (C_A) indicated efficient filtering capability of the chosen biomonitor species. Among the 16 PAHs, DahA having highest $\log K_{PA}$ and lowest C_A , showed strong characteristics of absorption to the biotic phase (plant foliage), whereas, filtration of FLU is lowest as apparent from highest C_A . Giraldez et al. (2022) and Klingberg et al. (2022) reported $\log K_{PA}$ values for different plant species such as *C. japonica* var. *elegans*, *Cedrus atlantica*, *Cedrus deodara*, *Cupressus arizonica*, *Quercus palustris*, etc. and confirmed plant capabilities in retaining PAHs with concomitant reduction in their ambient concentrations.

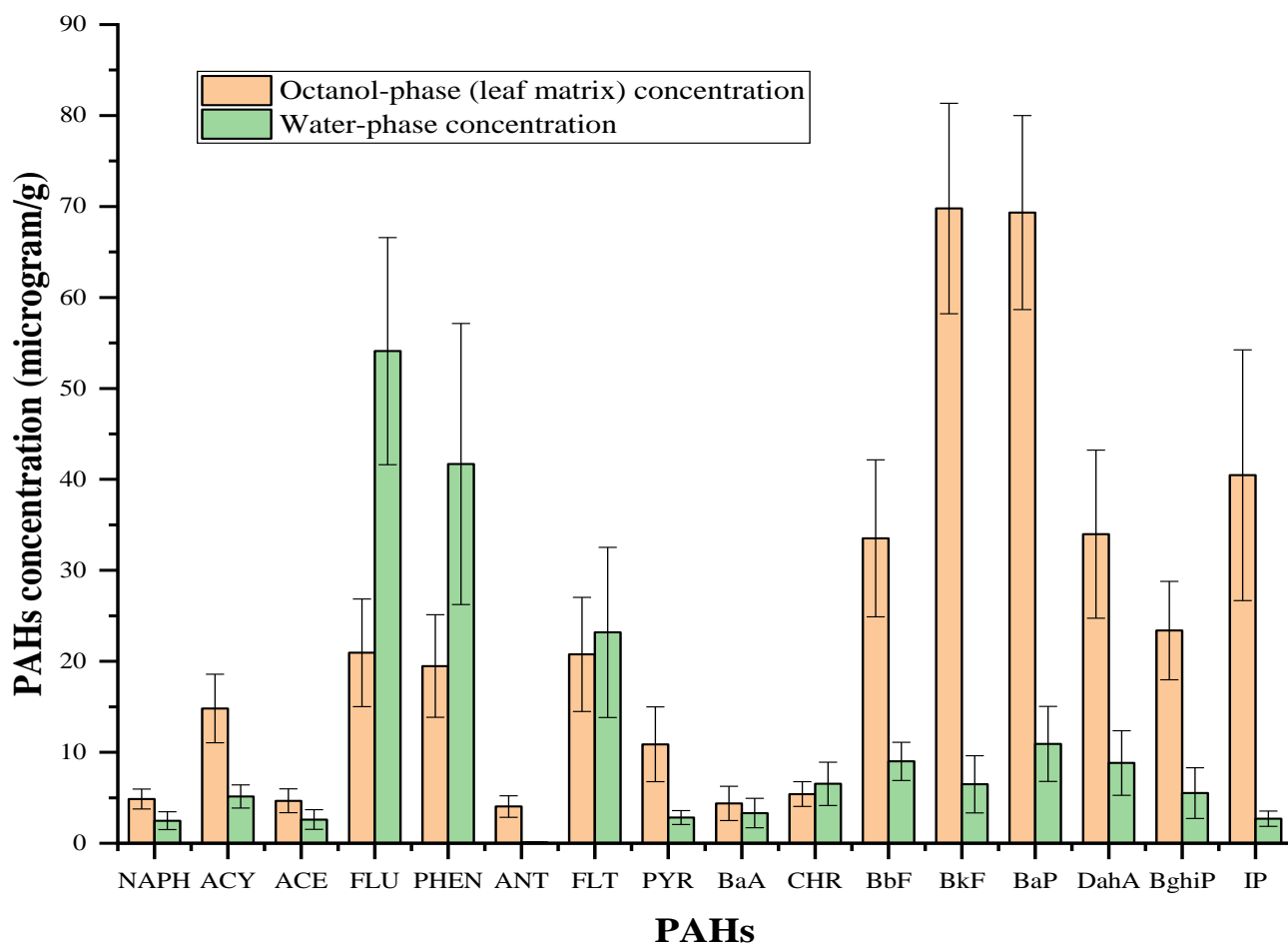


Fig. 32. Octanol (foliage)- and water- phase concentrations (mean \pm S.D.) of PAHs.

Table 34Partition coefficients and estimated air-phase concentrations (mean \pm S.D.) of PAHs.

PAHs	K_H (Atm m ³ /mol)	K_{OW}	K_{OA} / K_{PA}	Log $K_{OA} / \text{Log } K_{PA}$	$C_A = C_P / K_{PA}$ ($\mu\text{g g}^{-1}$)
NAPH	4.24×10^{-4}	1.96 \pm 0.32	113.09 \pm 40.39	2.05 \pm 0.69	0.043 \pm 0.01
ACY	8.29×10^{-5}	2.88 \pm 0.66	849.96 \pm 156.51	2.93 \pm 1.24	0.017 \pm 0.002
ACE	1.20×10^{-4}	1.79 \pm 0.19	364.95 \pm 112.45	2.56 \pm 1.63	0.013 \pm 0.003
FLU	7.77×10^{-5}	0.39 \pm 0.04	122.80 \pm 51.21	2.09 \pm 0.87	0.171 \pm 0.08
PHEN	3.20×10^{-5}	0.47 \pm 0.06	359.34 \pm 237.88	2.56 \pm 0.51	0.054 \pm 0.02
ANT	3.91×10^{-5}	40.40 \pm 2.59	25279.24 \pm 1685.75	4.40 \pm 1.89	$1.599 \times 10^{-4} \pm 1.16361\text{E-}05$
FLT	1.02×10^{-5}	0.89 \pm 0.11	2134.76 \pm 831.08	3.33 \pm 1.46	$9.724 \times 10^{-3} \pm 0.002$
PYR	9.08×10^{-6}	3.86 \pm 1.08	10400.66 \pm 3467.61	4.02 \pm 1.75	$1.046 \times 10^{-3} \pm 0.0007$
BaA	5.73×10^{-6}	1.32 \pm 0.47	5636.10 \pm 2083.24	3.75 \pm 0.94	$7.771 \times 10^{-4} \pm 0.0006$
CHR	6.41×10^{-7}	0.83 \pm 0.16	31679.59 \pm 6747.24	4.50 \pm 2.01	$1.705 \times 10^{-4} \pm 2.75777\text{E-}05$
BbF	4.26×10^{-6}	3.72 \pm 0.93	21364.50 \pm 4507.73	4.33 \pm 1.66	$1.569 \times 10^{-3} \pm 0.001$
BkF	8.27×10^{-7}	10.77 \pm 3.84	318617.49 \pm 92670.74	5.50 \pm 2.83	$2.190 \times 10^{-4} \pm 4.58352\text{E-}05$
BaP	4.54×10^{-7}	6.35 \pm 2.15	342197.86 \pm 81927.00	5.53 \pm 2.39	$2.026 \times 10^{-4} \pm 3.43813\text{E-}05$
DahA	1.47×10^{-8}	3.85 \pm 0.86	6407709.52 \pm 1012105.00	6.81 \pm 3.25	$5.303 \times 10^{-6} \pm 1.08064\text{E-}06$
BghiP	7.40×10^{-7}	4.24 \pm 1.22	140182.42 \pm 28521.51	5.15 \pm 1.99	$1.668 \times 10^{-4} \pm 4.53669\text{E-}05$
IP	1.60×10^{-6}	14.99 \pm 2.71	229213.96 \pm 29301.76	5.36 \pm 2.43	$1.765 \times 10^{-4} \pm 2.12132\text{E-}05$

The present study also assists in the development of a relationship between theoretical and experimental $\log K_{PA}$ values (Fig. 33), good predictor of terrestrial sequestration of airborne organic compounds in vegetation, on the basis of $\log K_{OA}$ (Table 35) empirically determined for individual PAHs using the expression (Eq. 51) outlined below (Xiao and Wania, 2003; Nizzetto et al., 2008) which shows the dependence of $\log K_{OA}$ on super-cooled vapour pressure of PAHs at 25 °C (P_L):

$$\log K_{OA} = -0.98784 \log P_L + 6.6914 \quad (51)$$

$$\log K_{PA} = -1.75 + 0.33 \log K_{OA} \quad (52)$$

The $\log K_{PA}$ values calculated from Eq. 52 are considered as theoretical and are given in Table 35. The experimental and theoretical values of $\log K_{PA}$ were relatively found to be in order as the R^2 value 0.795 is indicative of good fit between the data (Fig. 33). Though previously it was assumed that $\log K_{PA} \approx \log K_{OA}$, deviation was observed between them, probably due to the inclusion of the parameter P_L in the empirical equation of $\log K_{OA}$ as the standardized temperature of 25 °C might not be the actual operating condition in the laboratory.

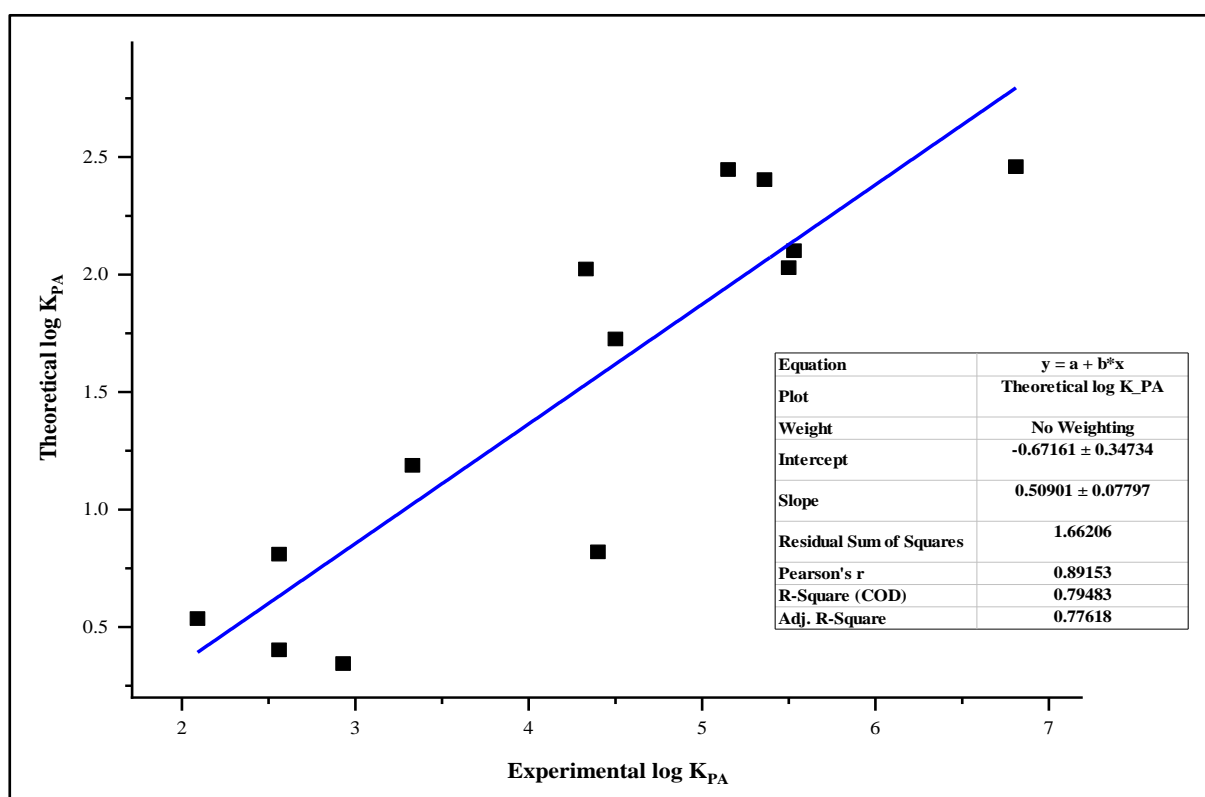


Fig. 33. Plot of theoretical and experimental $\log K_{PA}$.

Table 35Theoretical values of log K_{OA} and log K_{PA} .

PAHs	log P_L (Pa) ^a	log K_{OA} (from Eq. 51) (theoretical)	log K_{PA} (from Eq. 52) (theoretical)
NAPH	–	–	–
ACY	0.35	6.346	0.344
ACE	0.17	6.523	0.403
FLU	-0.24	6.928	0.536
PHEN	-1.08	7.758	0.810
ANT	-1.11	7.788	0.820
FLT	-2.24	8.904	1.188
PYR	–	–	–
BaA	–	–	–
CHR	-3.89	10.534	1.726
BbF	-4.80	11.433	2.023
BkF	-4.82	11.453	2.029
BaP	-5.04	11.670	2.101
DahA	-6.14	12.757	2.459
BghiP	-6.10	12.717	2.447
IP	-5.97	12.589	2.404

^a Odabasi et al. (2006)**7.3.2. Particle-gas partitioning of PAHs**

In the atmosphere, both gaseous and particulate fractions of PAHs may exist under ambient conditions. Absorption of gaseous PAHs in foliar tissues mostly takes place through stomatal pores and cuticle based on equilibrium partitioning between gas phase and vegetation, while on the contrary, the airborne particles may undergo long-distance dispersal and get accumulated and adsorbed on vegetation surfaces through atmospheric deposition and act as a probable sink for PAHs sorption (Yaffe et al., 2008). From the log K_P values depicted in Table 36, partitioning of PAHs into foliar-adsorbed PM from the ambient air was predicted and the values for individual PAHs showed coherence with that of the literature values (Lohmann and Lammel, 2004), suggesting that the PM also acts as a potential medium to capture PAHs and thus, PAHs

have a high tendency to get adsorbed on foliar PM. The plot of $\log K_P$ vs. $\log K_{OA}$ (Fig. 34) presented a good correlation ($R^2 = 0.795$), specifying PAHs partitioning into particulate organic matter, since, octanol is considered as a good representative of organic matter for anticipating the distribution of organic compounds in different phases (Baskaran and Wania, 2023; Demircioglu et al., 2011). Different K_P values for different PAHs indicated that the ambient particles exhibit discrete sorbing propensities for LMW and HMW PAHs (Demircioglu et al., 2011). It can be further observed from Table 36 that most of the 5 and 6 ring PAHs have high values of $\log K_P$ which is perfectly corroborating the fact that the HMW PAHs tend to get more associated with fine PM, having high particle-phase concentrations.

Table 36

Particle-gas partition coefficient (K_P) (mean \pm S.D.) of PAHs.

PAHs	$\log K_P$ (from Eq. 34)	$\log K_P$ (from Eq. 35)	$\log K_P$ (from Eq. 36)	$\log K_P$ (from Eq. 37)
NAPH	-8.39 \pm 0.04	-10.25 \pm 0.13	-8.56 \pm 0.11	-9.68 \pm 0.13
ACY	-7.69 \pm 0.01	-9.38 \pm 0.08	-7.83 \pm 0.06	-8.8 \pm 0.07
ACE	-7.99 \pm 0.03	-9.75 \pm 0.12	-8.14 \pm 0.09	-9.17 \pm 0.11
FLU	-8.36 \pm 0.28	-10.22 \pm 0.27	-8.53 \pm 0.23	-9.64 \pm 0.27
PHEN	-7.99 \pm 0.10	-9.75 \pm 0.21	-8.14 \pm 0.17	-9.17 \pm 0.20
ANT	-6.53 \pm 0.09	-7.91 \pm 0.02	-6.62 \pm 0.02	-7.33 \pm 0.03
FLT	-7.38 \pm 0.04	-8.98 \pm 0.14	-7.50 \pm 0.11	-8.4 \pm 0.13
PYR	-6.84 \pm 0.22	-8.29 \pm 0.19	-6.93 \pm 0.16	-7.71 \pm 0.20
BaA	-7.05 \pm 0.24	-8.56 \pm 0.22	-7.15 \pm 0.19	-7.98 \pm 0.23
CHR	-6.45 \pm 0.003	-7.81 \pm 0.09	-6.53 \pm 0.07	-7.23 \pm 0.08
BbF	-6.59 \pm 0.15	-7.98 \pm 0.10	-6.67 \pm 0.09	-7.4 \pm 0.11
BkF	-5.66 \pm 0.02	-6.80 \pm 0.11	-5.70 \pm 0.09	-6.23 \pm 0.11
BaP	-5.64 \pm 0.01	-6.77 \pm 0.09	-5.68 \pm 0.08	-6.2 \pm 0.09
DahA	-4.63 \pm 0.13	-5.50 \pm 0.07	-4.62 \pm 0.07	-4.92 \pm 0.08
BghiP	-5.94 \pm 0.15	-7.16 \pm 0.10	-5.99 \pm 0.09	-6.58 \pm 0.11
IP	-5.78 \pm 0.02	-6.95 \pm 0.06	-5.82 \pm 0.04	-6.37 \pm 0.05

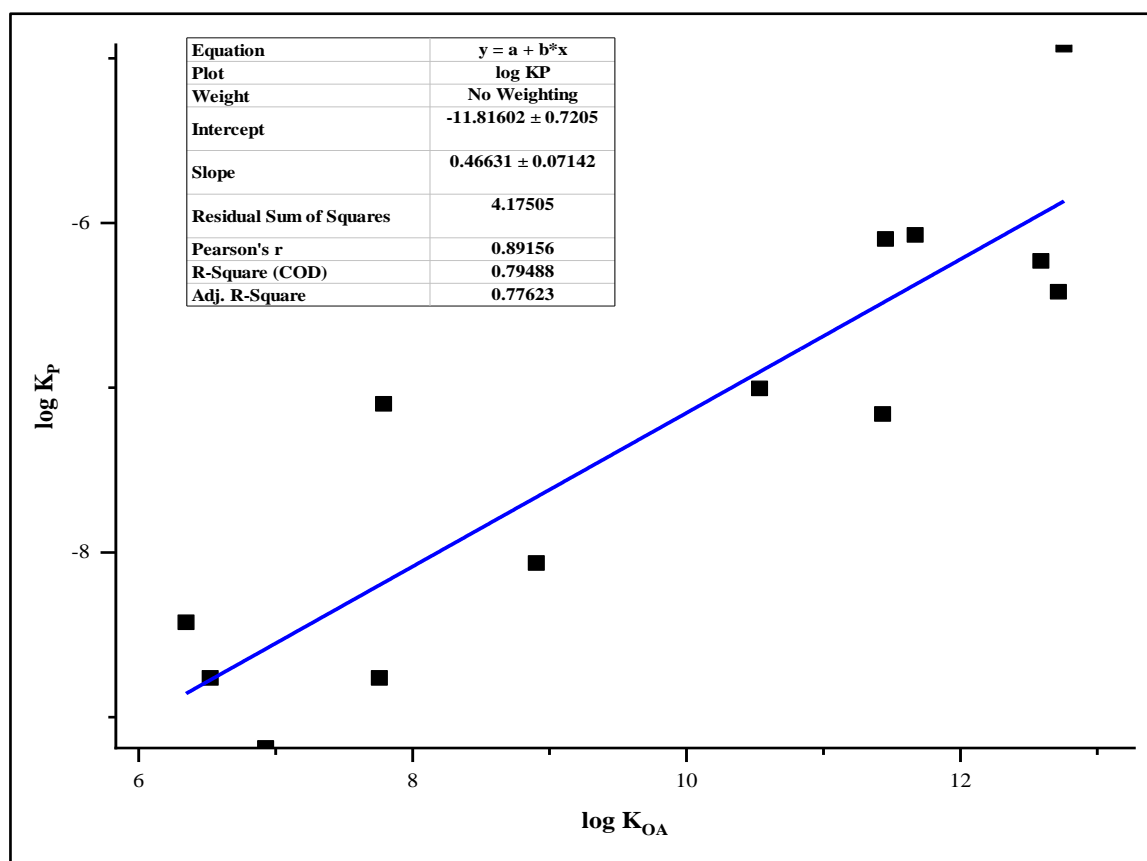


Fig. 34. Plot between log K_P and log K_{OA} .

7.3.3. Bioaccumulation of PAHs in plant leaves

7.3.3.1. PAHs translocation into leaf layers from foliar PM

After investigation of the particle-gas partitioning behaviour of PAHs, the mechanism of their translocation from foliar PM into leaf tissues was evaluated. Fig. 35 depicts the individual concentrations of 16 PAH congeners in foliar PM ($\sum C_f = 273.58 \mu\text{g g}^{-1}$), leaf cuticular wax ($\sum C_w = 247.44 \mu\text{g g}^{-1}$) and mesophyll tissues ($\sum C_m = 250.74 \mu\text{g g}^{-1}$). It can be suggested that some PAHs are susceptible to cuticular sorption ($C_w > C_m$) and some are absorbed to inner tissues ($C_m > C_w$) after desorption from foliar PM. The sorption characteristics of cuticles, the exterior foliage layer forming the first interface between plant and atmosphere, are imparted by their lipophilicity due to the presence of complex structures containing cutin and waxes (Chen et al., 2005; Wang et al., 2005; Ossola and Farmer, 2024). Moreover, it was found that most of the HMW PAHs (FLT, BbF, BaP, DahA, BghiP and IP) exhibited high cuticle-phase concentrations (i.e., retained in cuticular waxes), indicating hindered migration to inner leaf

layers owing to their high molecular mass (Ossola and Farmer, 2024). However, exceptions were seen for few LMW (ACE, FLU and ANT showing cuticular sorption) and HMW (PYR, BaA, CHR and BkF manifesting inner tissue absorption) PAHs which may be attributed to their physico-chemical properties and characteristics of foliage and surrounding environment (Yang et al., 2017).

Estimation of translocation factor ($TF_{f/L}$) > 1 (higher the TF, more is the translocation capacity (Yang et al., 2017)) based on C_f and total foliage concentration of PAHs (C_L) (refer Table 37) signified that the PAHs captured on PM (because of high particle-gas partition coefficient) got transported into the biomonitor tissues from particulates. The vital determining factors for PAHs-specific uptake include absorption into leaves and adsorption into particles followed by desorption and translocation into foliar tissues. So, a two-step air filtration mechanism is primarily taking place in the studied biomonitor species – directly by plant leaves and indirectly via particulate deposition. Hence, both adsorption and absorption are found to be the dominant mechanisms of PAHs uptake by plant leaves from the ambient atmosphere in biomonitors. All the findings reflected the accumulative nature of plant leaves and also the pollutant filtering capability of *M. paniculata* through foliage canopy is ensured.

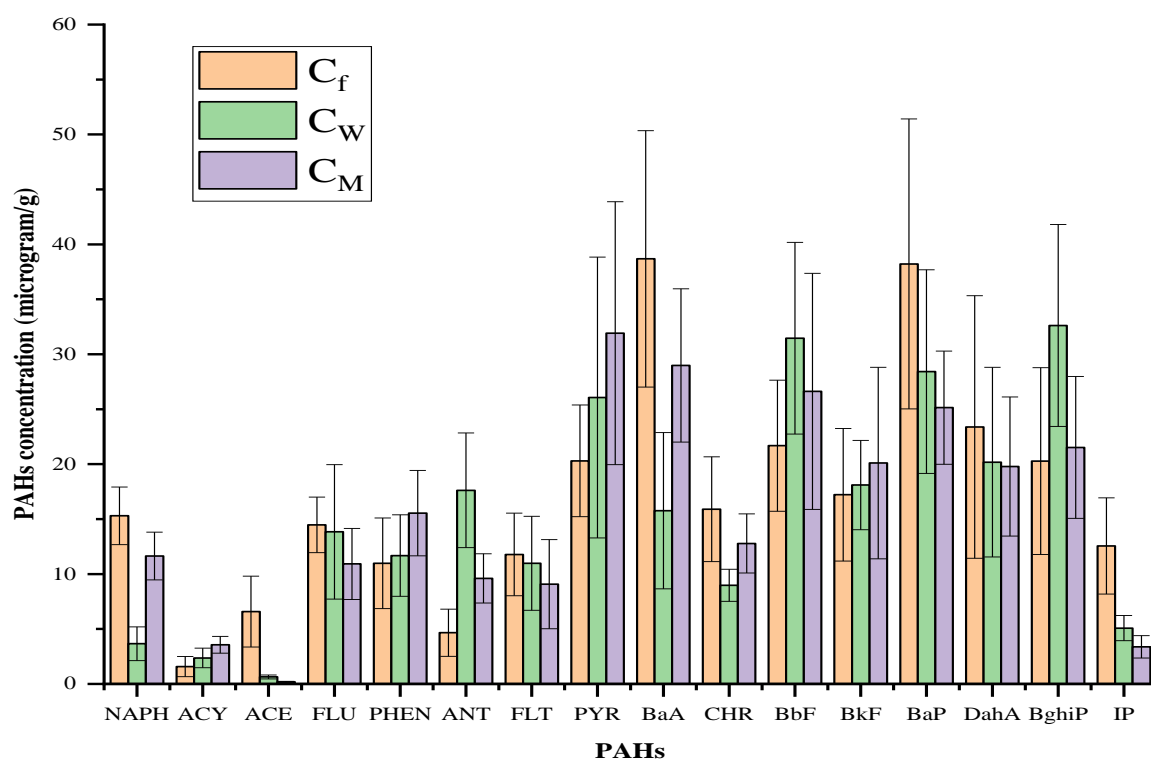


Fig. 35. Concentrations (mean \pm S.D.) of PAHs in foliar PM, leaf cuticular wax and inner mesophyll tissue.

Table 37

Overall PAHs concentration and translocation (mean \pm S.D.) in plant foliage.

PAHs	Total PAHs concentration in leaf (C _L) ($\mu\text{g g}^{-1}$)	TF _{f/L}
NAPH	15.3 \pm 2.12	1.00 \pm 0.02
ACY	5.92 \pm 1.54	3.75 \pm 0.46
ACE	0.82 \pm 0.25	0.12 \pm 0.03
FLU	24.76 \pm 9.07	1.71 \pm 0.16
PHEN	27.22 \pm 11.76	2.48 \pm 0.34
ANT	27.22 \pm 4.43	5.84 \pm 1.53
FLT	20.06 \pm 6.43	1.70 \pm 0.34
PYR	57.98 \pm 15.95	2.86 \pm 0.53
BaA	44.74 \pm 8.70	1.16 \pm 0.07
CHR	21.76 \pm 5.82	1.37 \pm 0.24
BbF	58.08 \pm 11.51	2.68 \pm 0.82
BkF	38.20 \pm 7.22	2.22 \pm 0.36
BaP	53.56 \pm 8.08	1.40 \pm 0.61
DahA	39.96 \pm 3.68	1.71 \pm 0.37
BghiP	54.14 \pm 10.94	2.67 \pm 0.96
IP	8.46 \pm 1.07	0.67 \pm 0.22
Σ	498.18 \pm 50.59	33.34 \pm 5.08

7.3.3.2. PAHs translocation into leaf from plant root

Root uptake of organic compounds is generally controlled by two pathways: apoplastic and symplastic. Transfer of compounds through cell walls and intercellular spaces is mediated by apoplastic pathway, whereas, symplastic pathway regulates the transport through plasmodesmata (Ju et al., 2020). Accumulation of organic compounds via plant root system drives their transport and translocation into plant tissues depending on the physico-chemical attributes of the chemicals and environmental conditions (Lu et al., 2023; Liang et al., 2021). To elucidate the mechanisms of root uptake and translocation to foliage, studies were carried

out with four representative PAHs (including both LMW and HMW PAHs such as NAPH, ACE, ANT and PYR), root concentrations of which are portrayed in Fig. 36. Firstly, the accumulative capacity of plant root was examined through RCF and the values are given in Table 38. RCF values of 0.72-1.12 advocated the potential of root tissue to accumulate PAHs. Similar range of RCFs was also obtained by Lu et al. (2024) for contaminants like pyrrolizidine alkaloids and their N-oxides. Cheng et al. (2020) and Pullagurala et al. (2018) also stated that the compounds having high hydrophobicity are more readily taken up by the plant roots from the surrounding medium. This has congruence with the results of the present study where appreciable concentrations of PAHs were obtained from root samples and it may be said to be driven by the root lipid content (found to be as high as $100 \pm 5.97 \text{ mg g}^{-1}$) considered as a major pool of organic pollutants.

It can now be surmised that the root accumulated PAHs could be transported to the plant foliage and thus, the PAHs translocation ability of *Murraya* root tissue was quantified by means of root-leaf translocation factor ($\text{TF}_{\text{R/L}}$). Lower $\text{TF}_{\text{R/L}}$ values (refer Table 38) imply weaker translocation from roots to leaves. Therefore, it is assumed that the PAHs showed higher tendency of bioaccumulation in roots than to be transported to the above-ground parts via transpiration pull as also evidenced by Lu et al. (2024). It may be opined here that the contribution of foliage accumulation due to transfer of PAHs from root is insignificant because of the strong adherence of PAHs with root epidermis, thereby greatly reducing the entry of PAHs into the inner root tissues with consequential reduction in their translocation into the leaf (Li et al., 2019; Miller et al., 2016; Zhang et al., 2017a, 2017b).

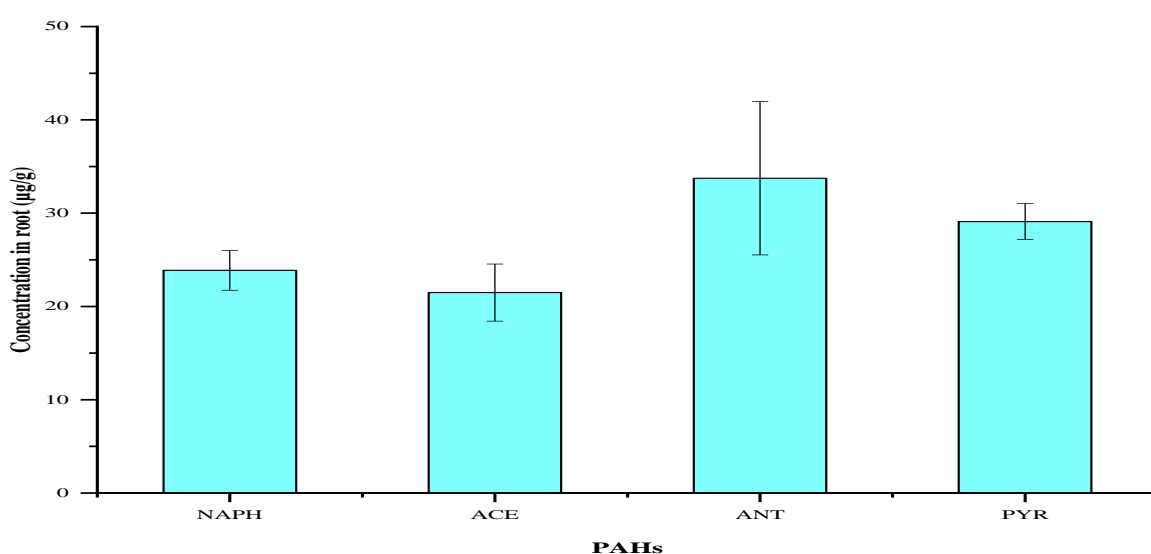


Fig. 36. Concentrations (mean \pm S.D.) of PAHs in plant root obtained from equilibrium uptake study.

Table 38

Root concentration and root-leaf translocation factors (mean \pm S.D.) of PAHs.

PAHs	RCF	TF _{R/L}
NAPH	0.80 \pm 0.07	0.64 \pm 0.02
ACE	0.72 \pm 0.14	0.04 \pm 0.001
ANT	1.12 \pm 0.22	0.81 \pm 0.17
PYR	0.97 \pm 0.30	1.99 \pm 0.25

7.3.4. Mass transfer coefficients of PAHs

7.3.4.1. Mass transfer from air to plant foliage

The overall air to leaf mass transfer coefficient (k_{AL}) (Table 39) has been used as a critical parameter for evaluating the rate of uptake of PAHs by plant leaves. The average k_{AL} value for mixed PAHs was estimated as 2039.96 cm day⁻¹, i.e., 84.99 \approx 85 cm h⁻¹, which confirms the uptake capacity as also verified from high BCF_{LA} values. Among the 16 PAHs, DahA exhibited highest k_{AL} value and the interchemical variability in k_{AL} is viewed as: DahA > BaP > IP > BkF > BghiP > CHR > BbF > PYR > ANT > BaA > FLT > ACY > ACE > FLU > PHEN > NAPH. The reported ranges of k_{AL} were found to be 168-513 cm h⁻¹ for soybean and corn leaves, 180-440 cm h⁻¹ for bell pepper leaves and 900 cm h⁻¹ for cornel and maple leaves (Sun et al., 2016; Maddalena et al., 2002; Terzaghi et al., 2015). Variations in the k_{AL} values of PAHs for *Murraya* leaves from other plant foliages can be ascribed to the fact that k_{AL} varies with plant species having variable leaf wax and lipid contents, leaf surface roughness and specific leaf area (Sun et al., 2013; Franzaring and van der Eerden, 2000). Researches have shown that the simultaneous occurrence of different PAHs in the ambient atmosphere may restrict the individual foliar PAHs uptake capacity, but increases the total PAHs adsorption (Sun et al., 2016).

Table 39

Individual air-leaf mass transfer coefficients (mean \pm S.D.) of 16 PAHs.

PAHS	Regression equation of the plot dC_L/dt ($\mu\text{g g}^{-1} \text{d}^{-1}$) vs. C_L ($\mu\text{g g}^{-1}$)	R ² value	BCF _{LA} ($=C_L/C_A$)	k_{AL} (cm day ⁻¹) = (Slope of Eq. 38 \times BCF)/ a_{AL}
NAPH	$y = -0.058x + 2.2042$	0.983	113.02326 \pm 40.44	0.16 \pm 0.06
ACY	$y = -0.1068x + 2.0865$	0.6316	871.76471 \pm 141.09	2.33 \pm 0.37

ACE	$y=-0.1236x+4.4113$	0.9837	358.46154 ± 117.04	1.11 ± 0.36
FLU	$y=-0.183x+6.1854$	0.7843	122.45614 ± 50.97	0.56 ± 0.23
PHEN	$y=-0.0378x+1.6953$	0.6873	360.74074 ± 236.89	0.34 ± 0.22
ANT	$y=-0.0876x+3.4249$	0.8646	25265.79 ± 1676.24	55.30 ± 3.67
FLT	$y=-0.2032x+7.5175$	0.9581	2134.92 ± 830.96	10.84 ± 4.22
PYR	$y=-0.2339x+9.1721$	0.9569	10401.53 ± 3468.22	60.79 ± 20.27
BaA	$y=-0.1572x+5.791$	0.7742	5636.34 ± 2083.41	22.14 ± 8.18
CHR	$y=-0.1371x+5.4174$	0.8205	31671.55 ± 6752.93	108.49 ± 23.14
BbF	$y=-0.169x+6.2494$	0.8652	21363.93 ± 4507.33	90.22 ± 19.04
BkF	$y=-0.1228x+4.7819$	0.894	318630.14 ± 92661.80	977.71 ± 284.33
BaP	$y=-0.1911x+7.3164$	0.9536	342250.74 ± 81889.60	1634.29 ± 391.03
DahA	$y=-0.175x+6.7426$	0.8849	6407693.8 ± 1012094	28019.65 ± 4425.69
BghiP	$y=-0.1611x+6.429$	0.9123	140167.87 ± 28511.22	564.24 ± 114.77
IP	$y=-0.1905x+7.4218$	0.9695	229235.13 ± 29286.79	1091.19 ± 139.41

7.3.4.2. Diffusion from roots to plant foliage

It is usually believed that the organic contaminants come in contact with the root tissues through the process of diffusion and subsequently get transported in the shoots via xylem stream (Tripathi et al., 2020). In the current work, values of leaf-root bioconcentration factor (BCF_{LR}), as can be seen from Table 40, ranged between 0.04-1.99 for the four surrogate PAHs, indicating weak ($0.01 < BCF < 0.1$) to intermediate ($0.1 < BCF < 1$) absorption for NAPH, ACE and ANT and strong ($1 < BCF < 10$) absorption for PYR (Haghnazar et al., 2023). Parameter estimation of $(k_{RL} \times a_{RL})$ (day^{-1}) (representing low values) is again implicative of less mass transfer from roots to leaves (in line with low TF_{RL}) as compared to air-foliage transfer, which has been used in the material balance model to ascertain its validity.

Table 40

Parameter estimation for overall root-leaf mass transfer (mean \pm S.D.) of PAHs.

PAHs	$BCF_{LR} (=C_L/C_R)$	$(k_{RL} \times a_{RL})$ (day^{-1}) = (Slope of Eq. 39 $\times BCF$)
NAPH	0.64 ± 0.02	0.04 ± 0.02
ACE	0.04 ± 0.001	0.005 ± 0.002
ANT	0.81 ± 0.17	0.07 ± 0.01
PYR	1.99 ± 0.25	0.47 ± 0.04

7.3.5. Determination of dC_L/dt as a model parameter of theoretical net uptake of PAHs

Mean values of dC_L/dt as calculated with respect to change in PAHs concentration of plant leaves over time considering air to leaf transport are presented in Table 41 and have been used for the validation of the predicted uptake model.

Table 41

Calculated values (mean \pm S.D.) of dC_L/dt .

PAHs	$\frac{dC_L}{dt}$ ($\mu\text{g g}^{-1} \text{day}^{-1}$)
NAPH	0.77 \pm 0.04
ACY	0.38 \pm 0.06
ACE	1.04 \pm 0.19
FLU	1.19 \pm 0.09
PHEN	0.59 \pm 0.11
ANT	0.39 \pm 0.07
FLT	0.74 \pm 0.05
PYR	0.39 \pm 0.04
BaA	0.97 \pm 0.26
CHR	0.84 \pm 0.21
BbF	1.43 \pm 0.36
BkF	0.88 \pm 0.06
BaP	1.12 \pm 0.24
DahA	0.85 \pm 0.32
BghiP	1.24 \pm 0.48
IP	0.68 \pm 0.11
Σ	13.50 \pm 1.83

7.3.6. Determination of evaporative loss (L_{EV}) from PAHs uptake kinetics

From the kinetics study, maximum uptake of PAHs by plant leaves was observed on 6th day, beyond which the rate was found to decline gradually (Fig. 37). The uptake concentration for each time period reached a plateau after 15 days. Hence, cumulative loss was calculated afterwards from 7th day of soaking till 15th day with reference to the concentration profile considering evaporation as the only loss factor (Fig. 38). Thus, R_L was estimated as 16.29 $\mu\text{g g}^{-1} \text{day}^{-1}$.

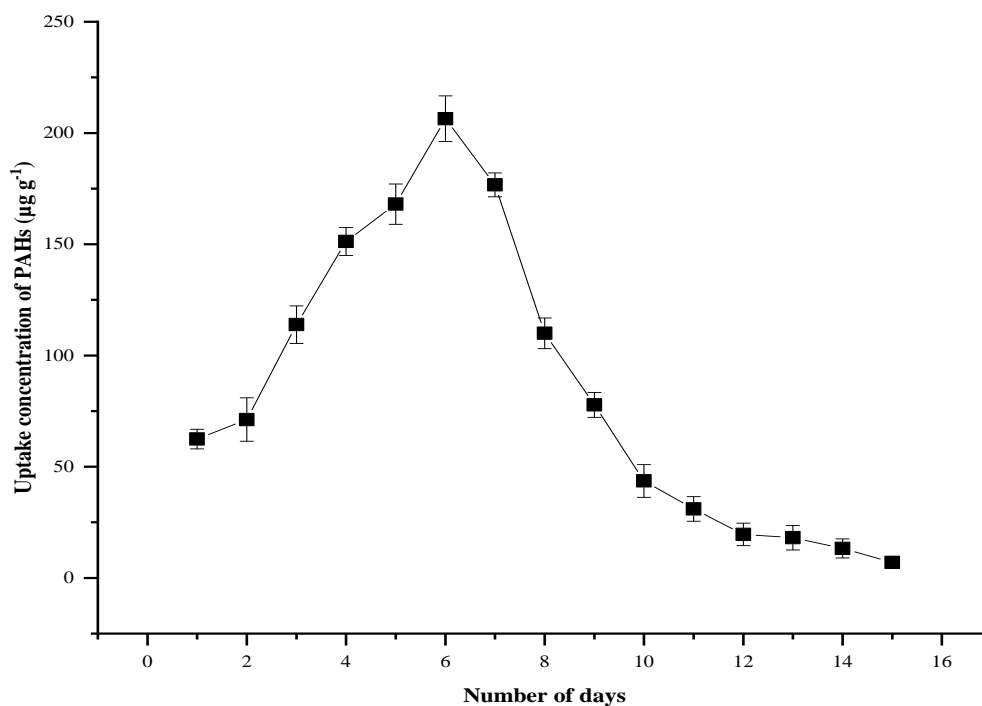


Fig. 37. Variation in leaf uptake concentration (mean \pm S.D.) of PAHs over time.

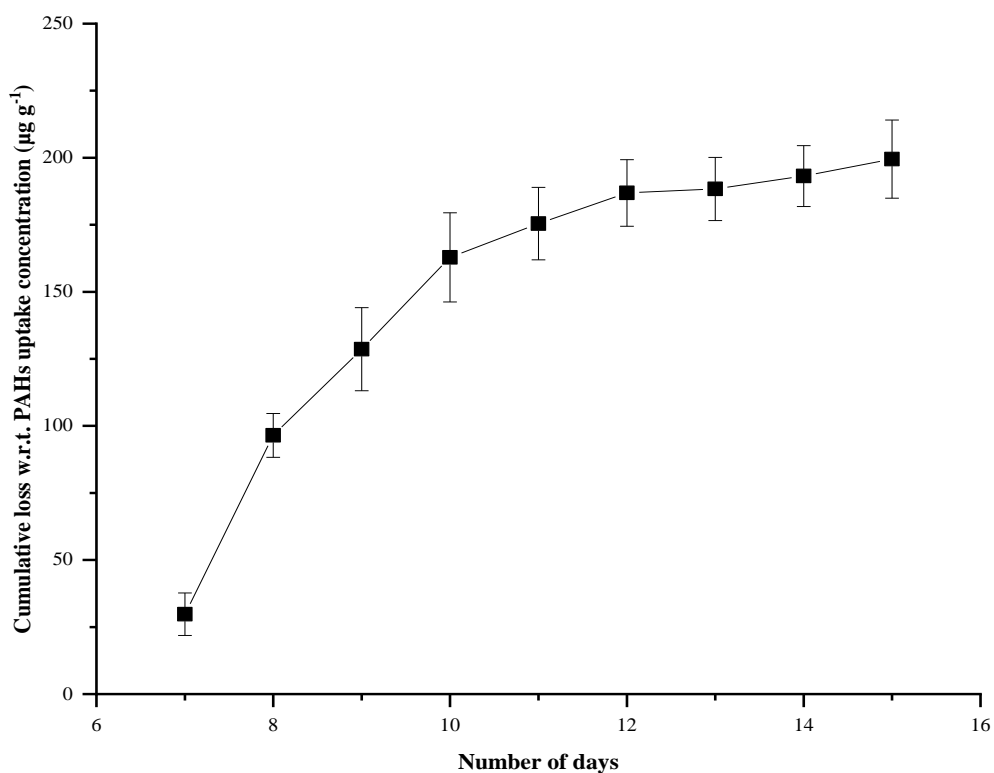


Fig. 38. Profile of cumulative loss (mean \pm S.D.) in uptake concentration of PAHs over time.

7.3.7. PAHs uptake model validation: Material balance

The present study has focused on analyzing the contributions of gaseous absorption and particle deposition to the foliage uptake of PAHs along with the assessment of the probability of PAHs translocation (acropetal) to plant leaves from root tissues through transpiration pull generated inside the xylem tissue using a material balance model. The theoretical net uptake (U_{NT}) of PAHs by the leaves is equated with calculated net uptake (U_{NC}) based on predictive gain and loss modes of PAHs. The predicted model can be simplified as follows (Eq. 53):

$$U_{NC} = (U_{ge}^{A/L} + U_{DP} + U_{TS}^{R/L}) - (L_{EV}) \quad (53)$$

The calculation of individual terms has been done as follows to validate the predictive mechanistic PAHs uptake model by the chosen biomonitor:

$$U_{NT} (\mu\text{g/day}) = \frac{V (\text{cm}^3) \times \frac{dC_L}{dt} (\mu\text{g/g.d}) \times \log K_{PA}}{SLA (\text{cm}^2/\text{g}) \times \text{Leaf thickness (cm)}} = \frac{241.75 \times 13.51 \times 64.87}{151.09 \times 1} = 1402.26 \mu\text{g/day}$$

$$(U_{ge}^{A/L}) (\mu\text{g/day}) = \frac{k_{AL} (\frac{\text{cm}}{\text{d}}) \times A (\text{cm}^2) \times C_A (\mu\text{g/g})}{SLA (\text{cm}^2/\text{g}) \times \text{Leaf thickness (cm)}} = \frac{2039.96 \times 241.75 \times 0.31}{151.09 \times 1} = 1011.85 \mu\text{g/day}$$

$$(U_{DP}) (\mu\text{g/day}) = \left(\frac{C_f (\mu\text{g/g}) \times \text{Total mass of foliar dust (g)} \times TF_{f/L}}{\text{days of study}} \right) = \frac{273.58 \times 0.5 \times 33.34}{10} = 456.06 \mu\text{g/day}$$

$$(U_{TS}^{R/L}) (\mu\text{g/day}) = [k_{RL} \times A_R] \left(\frac{1}{\text{days of study}} \right) \times C_R (\mu\text{g/g}) \times TF_{R/L} \times \text{mass of root sample taken (g)}$$

For calculating $(U_{TS}^{R/L})$, average data of four representative PAHs has been used as follows:

$$\begin{aligned} (U_{TS}^{R/L})_{\text{Average}} (\mu\text{g/day}) &= \left(\frac{[k_{RL} \times A_R] \times C_R \times TF_{R/L} \times \text{sample mass}_{NAPH} + [k_{RL} \times A_R] \times C_R \times TF_{R/L} \times \text{sample mass}_{ACE}}{+ [k_{RL} \times A_R] \times C_R \times TF_{R/L} \times \text{sample mass}_{ANT} + [k_{RL} \times A_R] \times C_R \times TF_{R/L} \times \text{sample mass}_{PYR}} \right) / 4 \\ &= ([0.04 \times 23.87 \times 0.64 \times 0.5]_{NAPH} + [0.005 \times 21.49 \times 0.04 \times 0.5]_{ACE} + [0.07 \times 33.74 \times 0.81 \times 0.5]_{ANT} + [0.47 \times 29.1 \times 1.99 \times 0.5]_{PYR}) / 4 \\ &= ([0.31]_{NAPH} + [0.002]_{ACE} + [0.96]_{ANT} + [13.61]_{PYR}) / 4 = 3.72 \mu\text{g/day} \end{aligned}$$

$$\text{Hence, uptake rate for 16 PAHs} = (U_{TS}^{R/L})_{16 \text{ PAHs}} (\mu\text{g/day}) = (U_{TS}^{R/L})_{\text{Average}} \times 16 = 3.72 \times 16 = 59.92 \mu\text{g/day}$$

$$L_{EV} (\mu\text{g/day}) = R_L (\mu\text{g/g. day}) \times \text{Total mass of leaf sample taken (g)} = 16.29 \times 5 = 81.45 \mu\text{g/day}$$

$$\text{Therefore, } U_{NC} (\mu\text{g/day}) = (1011.85 + 456.06 + 59.52 - 81.45) \mu\text{g/day} = 1445.98 \mu\text{g/day}$$

It can be concluded that U_{NT} and U_{NC} are closely matched with only 3% deviation. This suggests the validity of the predictive mechanistic model for uptake of PAHs from air by plant biomonitor like *Murraya paniculata*. The deviation can be linked to the factors ignored for model simplicity.

The findings confirmed that the gaseous uptake ($U_{ge}^{A/L}$) mechanism (i.e., absorption in cuticular wax and inner mesophyll tissue lipid) through molecular and eddy diffusion is the principal route (~ 70%). In addition, PAHs uptake through particle adsorption and deposition (U_{DP}) also showed an appreciable contribution (~31% of total uptake) to strengthening the filtering ability of the biomonitor. Vapour pressure and K_{OA} or K_{PA} of PAHs determine their distribution between gas and particulate phases, thereby impacting the process of foliar uptake (Wang et al., 2023). It has been demonstrated that the compounds having $\log K_{OA} \leq 8.5$ are more likely to undergo gaseous foliar absorption (McLachlan, 1999). Consistent results were also found in the present study with maximum uptake (as high as $1011.85 \mu\text{g day}^{-1}$) of PAHs, having $\log K_{PA}$ (assumed to be equivalent to $\log K_{OA}$) between 2.05-6.81, through gaseous exchange. However, different opinions exist for the particle-bound deposition. Collins et al. (2006) stated that the particulate adsorption is more prominent for organic compounds, having $\log K_{OA} > 11$, which then get distributed in the leaf tissues after desorption from particles. Conversely, Zhu et al. (2020) found higher leaf accumulation of polybrominated biphenyl ethers (PBDEs) with $\log K_{OA}$ of 6.55-9.66 from particle-bound deposition. Similarly, in the proposed work, significant uptake (though lesser than gaseous exchange) of PAHs with $\log K_{PA} < 11$ via dry particle deposition was evidenced. Therefore, variabilities in the rates of uptake through both the pathways may be related to plant biochemical composition and distinct mechanisms of PAHs accretion (Wang et al., 2023).

From the perspective of foliage accumulation, uptake through root ($U_{TS}^{R/L}$) has been found to be inconsiderable (~4% of total uptake), emphasizing species-dependent mechanism affected by environmental conditions and degree of pollution (Liu et al., 2019). Similar findings were found in the studies involving crop plants (rice and wheat), where foliar uptake mainly resulted in 80-90% of accumulation of PBDEs in the plant leaves as compared to the uptake pathway via root (0.34-18.70%) (Wang et al., 2015_b; Zhu et al., 2020; Wang et al., 2023). Hydrophobic compounds are absorbed in the lipid components of plant roots after binding with carrier root membrane proteins facilitating their movement and are difficult to be transported to the plant shoot system (Liu et al., 2019). Uptake and penetration of the chemicals from outer to the interior of root tissue (from epidermis through cortex, endodermis, pericycle and finally into the xylem) along with their translocation are governed by their solubilities in both water and cellular membrane consisting of lipid molecules (Trapp and McFarlane, 1994).

Concerning PAHs losses, measurements for estimation of loss factor should be more precise and accurate for reliable determination of uptake by any plant biomonitor. The current study is limited to the assessment of only evaporative loss ($81.45 \mu\text{g day}^{-1}$) as the total loss factor, i.e., volatilization from plant leaves into the atmosphere. It is evident that in tropical wet-dry climate like Kolkata city (India), chances of evaporative loss of volatile or semi-volatile PAHs will be significant. However, processes including growth dilution (L_G) (where plant growth rate or storage is much higher than the rate of uptake), photodegradation, photochemical transformation and plant metabolism (combinedly L_{PR}) should also be taken into account, which might reduce or affect the pollutant concentrations in plant foliage (Collins et al., 2006). Contribution of natural phenomena like litterfall loss (L_{LF}) and foliage runoff loss (L_{FR}) are also not included in loss of PAHs from foliage calculation. Moreover, uptake of PAHs through wet particle deposition (U_{WP}) and rain dissolution (U_R) may cause discrepancies in validation. Thus, it can be affirmed that the large foliar interface of *M. paniculata*, rich in lipids and waxes, facilitated the plant-atmosphere interaction of PAHs through their efficient accumulation mechanism and hence, offered air quality-based ecosystem services of air pollution mitigation and air quality improvement. Therefore, the chosen plant species behaves as a superior biomonitor of a contaminated environment.

7.3.8. Reconfirmation of foliar capturing capacity by fugacity approach

Fugacity represents the capability of plant leaves to hold or retain chemical compounds and plays an important role in predicting and characterizing bioaccumulation of organic

contaminants (Bolinus et al., 2016). PAHs absorption or adsorption is regulated by the fugacity gradient across the air-plant interface, facilitating the net mass flux of PAHs from abiotic to biotic phase, i.e., bioconcentration, causing more accumulation of contaminants in the vegetation with the increase in lipid content. Fugacity capacities of plant leaves (Table 42) were found to be consistent with the literature values $40\text{--}8.1\times 10^4 \text{ mol m}^{-3} \text{ Pa}^{-1}$ for *Rhododendron* leaves (*R. ponticum* L.) (Bolinus et al., 2016). The results thus support the previous findings proving plant uptake, retention and accumulative capacities for PAHs. It is also established that the leaf lipids and waxes (bearing resemblance to octanol) are the major stores of PAHs and partitioning of PAHs into leaf cuticles from the atmosphere can be based on either absorption into lipids or adsorption (surface process) or combination of both (Cousins and Mackay, 2001).

Table 42

Fugacity capacities (mean \pm S.D.) of *Murraya* leaves.

PAHs	$K_H (\text{Pa m}^3 \text{mol}^{-1})^*$	$Z_F (\text{mol m}^{-3} \text{Pa}^{-1})$ (from Eq. 49)	$Z_F (\text{mol m}^{-3} \text{Pa}^{-1})$ (from Eq. 50)
NAPH	43.01	0.045 ± 0.02	0.23 ± 0.06
ACY	8.40	0.34 ± 0.06	1.69 ± 0.52
ACE	12.17	0.15 ± 0.04	0.73 ± 0.17
FLU	7.87	0.049 ± 0.02	0.25 ± 0.04
PHEN	3.24	0.144 ± 0.09	0.72 ± 0.18
ANT	3.96	10.11 ± 0.67	50.50 ± 5.33
FLT	1.04	0.85 ± 0.39	4.24 ± 1.76
PYR	0.92	4.16 ± 1.39	20.77 ± 4.65
BaA	0.581	2.25 ± 0.83	11.25 ± 3.84
CHR	6.50×10^{-2}	12.67 ± 2.70	63.21 ± 10.18
BbF	0.43	8.55 ± 1.81	42.82 ± 8.24
BkF	8.40×10^{-2}	127.45 ± 37.10	634.66 ± 120.56
BaP	4.60×10^{-2}	136.88 ± 32.80	683.32 ± 138.96

DahA	1.49×10^{-3}	2563.08±404.84	12790.27±1248.95
BghiP	7.50×10^{-2}	56.07±11.41	279.84±45.73
IP	0.162	91.69±11.72	458.03±63.28

*Earl et al. (2003)

7.4. Conclusion

Generally, ambient dispersion of PAHs gets intercepted via three matrices in the environment: water, soil and vegetation. It is noteworthy that poor solubility of PAHs in water makes them available mainly in soil-sediments and vegetation. Due to the presence of lipid reservoir in different parts of plants, soil-PAHs get transported to the adjacent plant roots and they undergo translocation towards plant foliage due to their distribution characteristics. On the other hand, foliage receives air-dispersed PAHs directly by two major routes: uptake through stomata to mesophyll tissue and uptake from adsorbed phase carried by PM and cuticle-wax layer. Despite the previously mentioned simplifications, the proposed mechanistic model of PAHs uptake by *Murraya paniculata* enables the prediction of the described pathways of net uptake and distribution. Based on the analysis of PAHs concentration in different matrices, the major key pathways involved in foliar uptake have been delineated in this study considering strong relationship among the predictive variables for material balance modeling of PAHs in the plant leaves. Absorption of PAHs into plant leaves, i.e., direct entry via stomata and infiltration through cuticular surface, and indirect entry through foliar PM adsorption-desorption pathway have been identified as the predominant uptake mechanisms for *Murraya paniculata* with respect to their partitioning in plant foliage and foliar particulates and enhanced mass transfer. Restricted translocation of PAHs (with reduced mass transfer) to leaf via root was further noticed due to the strong effects of impediment of root lipids. Sorptive ability of plant leaves was also validated through estimation of their fugacity capacity. Finally, it can be stated that we could quantify the pathway contributions of foliar PAHs uptake, favourably close to the reality, using the constructed model shedding light on actual uptake mechanisms by foliage, where exchange between plant and air is often encountered in a polluted environment. Therefore, the presented model offered itself to be suitable for measuring uptake mechanisms from air to leaves, depending on plant species chosen, physical and chemical characteristics of PAHs, concentration of PAHs in air as well as weather conditions. However, it can be opined that the model works satisfactorily.

Chapter 8

Summary of results, Concluding remarks and Recommendations for future work

In this Chapter we will summarize the entire research work carried out, conclude with the important outcomes of each part of research and provide recommendations for the future direction of research that should continue.

8.1. Summary of results and concluding remarks

Over the last few decades, poor air quality has initiated challenges and complexities in the livelihood of inhabitants and also threatened the existence of biodiversity. It is therefore very much imperative that a perennial green vegetation cover (having the abilities of monitoring and filtering air pollutants) around human settlements shall be created, maintained and sustained to ensure ecological benefits of reducing environmental stress adversity. To this end, the study mainly covered the urban fringes of South Kolkata in West Bengal, India, and primarily recognized dominant roadside plant species with high air pollution tolerance, biomonitoring potential and airborne dust retention capacity with long-term sustainability even under high urban pollution load.

- ❖ *Assessment of biomonitoring potential of *Murraya paniculata* (L.) Jack (terrestrial plant) along major roads of South Kolkata, India*
- Distribution pattern of foliar dust (mg cm^{-2}) among the selected study sites was found as: foliar dust load_{EXM} (2.26 ± 0.02) > foliar dust load_{TGN} (1.05 ± 0.02) > foliar dust load_{JDV} (0.95 ± 0.02) > foliar dust load_{RBC} (0.85 ± 0.04). Maximum load of foliar dust at EXM can be attributed to the existence of a road crossing and continuous vehicular movement in huge number with unavoidable traffic clogging. On the contrary, CMD showed lowest foliar accumulation of dust ($0.025 \pm 0.01 \text{ mg cm}^{-2}$) because of its remote location, far away from traffic congestion.

- APTI values were then obtained for *M. paniculata*, which ranged from 19.78 ± 1.20 to 31.12 ± 0.72 among the sampling sites and varied with the level of pollution. Therefore, it is evident that *M. paniculata* plant behaves as a candidate biomonitor. It is also seen that APTI values varied linearly ($R^2 = 0.97$) with PM and other pollution burden (Fig. 39). Therefore, it can be concluded that APTI increased with the pollution load for *M. paniculata*.

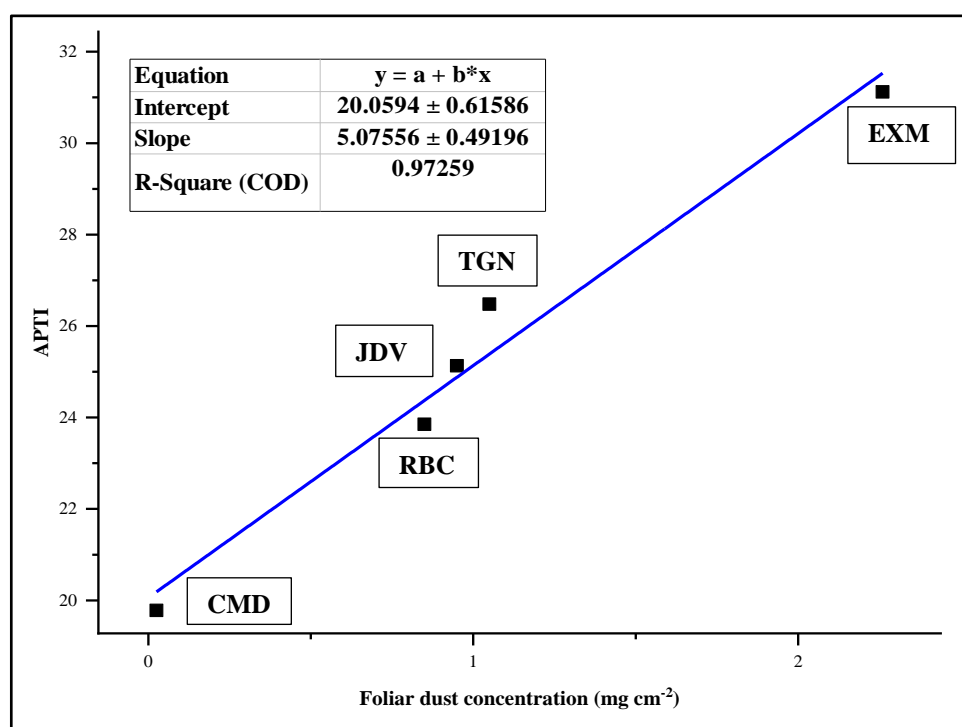


Fig. 39. Variation of APTI of *Murraya paniculata* with foliar dust concentration.

- Abiotic stress generated from highest load of road dust at EXM caused extreme damage to the leaf carotenoids, leading to minimum concentration ($0.42 \pm 0.09 \text{ mg g}^{-1}$) as compared to the other urban sites. Reduction in carotenoid levels with the increase in foliar dust was also observed at JDV and TGN. Carotenoid content ($0.62 \pm 0.03 \text{ mg g}^{-1}$) deviated from the trend at RBC and showed slightly higher concentration in comparison to the control site ($0.60 \pm 0.02 \text{ mg g}^{-1}$).
- Foliar lipid contents varied between 26.19 ± 1.16 to $128.92 \pm 2.46 \text{ mg g}^{-1}$ at the pollution sites which allowed PAHs absorption.
- Stomal blockage and guard cell deformation, rough leaf surfaces, degradation of crystal structures of epicuticular waxes around the stomata and entrapment of dust particles were also detected through SEM observation with energy-dispersive X-ray microanalysis.

- Appreciable accumulation of PAHs in leaf lipids was observed, which signifies the plant species as a member of plant biomonitor group.

❖ *Extraction and analysis of PAHs from bioindicators*

Progressing towards the first step of biomonitoring scheme with respect to PAHs which involves standardized measurement of pollutant concentrations in biomonitor tissues, quantification of PAHs levels in the leaves of *M. paniculata* was attempted based on the route of solvent extraction assisted with extract purification and PAHs analysis by GC-MS (qualitative) and HPLC (quantitative). For reliable quantitation of PAHs in HPLC, method validation was performed in terms of recovery percentage (78-99%), LOD (0.001-0.003 $\mu\text{g g}^{-1}$) and LOQ (0.03-0.09 $\mu\text{g g}^{-1}$).

- Conventional Soxhlet extraction method displayed better performance among the other extraction methods (mechanical stirring, sonication, MAE) and showed an extraction yield of 272.07 $\mu\text{g g}^{-1}$ which is almost at par with that of the yield (280.17 $\mu\text{g g}^{-1}$) obtained through MAE, proving comparable efficiencies of extraction.
- Focusing on the conventional route, optimization of Soxhlet method (to check the dependency of method efficiency on extraction solvent and extraction time) using one-factor-at-a-time approach demonstrated maximum PAHs recovery during 6 h of extraction with extracting solvent toluene.
- Efficient extraction followed by purification-instrumental analysis (using GC-MS and HPLC) is devised as a biomonitoring protocol.

❖ *Microwave-assisted Soxhlet extraction (MAE) method for PAHs isolation from *Murraya paniculata* (L.) Jack: Process optimization using response surface methodology as process intensification*

It is worth mentioning here that in a very short time MAE achieved extraction yield similar to that of Soxhlet operated for long duration. Hence, for high PAHs recoveries in short extraction time with minimal use of solvent, MAE has been adopted for intensification of the extraction process to isolate PAHs from *Murraya* leaves.

- The order of PAHs extraction yield using microwave-induced cell lysis with different solvents was obtained as follows: PAHs_{yield} with toluene:acetonitrile (283.77 $\mu\text{g g}^{-1}$) > PAHs_{yield} with toluene:tert-butanol (258.72 $\mu\text{g g}^{-1}$) > PAHs_{yield} with n-hexane:acetone (175.53 $\mu\text{g g}^{-1}$) > PAHs_{yield} with n-hexane:dichloromethane (160.14 $\mu\text{g g}^{-1}$) > PAHs_{yield} with n-hexane:ethyl acetate (129.69 $\mu\text{g g}^{-1}$). Toluene:acetonitrile and toluene:tert-butanol solvent mixtures showed maximum

extraction yield than the solvent blends of n-hexane: acetone, n-hexane: dichloromethane and n-hexane: ethyl acetate.

- Optimization of MAE process parameters (extraction temperature, extraction time and solvent-to-sample ratio) by one-factor-at-a-time approach and RSM-BBD using pre-optimized solvent combination of toluene:acetonitrile revealed their significant effects (both independent (or main) and interactive) on PAHs extraction yield (response factor).
- The developed response prediction model of extraction yield was substantiated by ANOVA and the model R^2 value was found to be 0.9982, verifying enhanced model efficacy in predicting the output (98% prediction accuracy with acceptable range of deviation). The optimum extraction temperature of 45.77 °C, extraction time of 11.67 min and solvent-to-sample ratio of 22.64 mL g⁻¹ were achieved to maximize MAE performance generating highest yield.
- Additionally, superior performance efficiency of MAE relating to improved extraction conditions and less environmental implications of energy use and CO₂ ejection over Soxhlet method has been ensured, satisfying the basic principles of process intensification.

❖ *Biomonitoring of PAHs by *Murraya paniculata* (L.) Jack in South Kolkata, West Bengal, India: Spatial and temporal variations*

Concerning analysis of PAHs origin as well as temporal and spatial occurrences as crucial aspects of biomonitoring, the results showed strong impacts of seasons and locations on distribution of pollutant concentrations.

- Temporal pattern of PAHs contamination in the foliage of *M. paniculata* reflected the level of variability as highest in winter (278.42-550.79 µg g⁻¹) than postmonsoon (210.52-401.83 µg g⁻¹) and premonsoon (200.98-329.17 µg g⁻¹), implying the interrelationship of meteorological variables with the degree of variation.
- Profound influences of location-specific intensive anthropogenic activities on PAHs concentrations (indicating EXM as the most polluted site with highest levels (329.17-550.79 µg g⁻¹) of PAHs) were also evidenced with negligible seasonal variation of pollutant sources.
- Site-based DR analysis (Σ LMW/ Σ HMW: 0.39-1.02; ANT/(ANT + PHE): 0.41-0.79; FLA/(FLA + PYR): 0.31-0.79; BaA/(BaA + CHR): 0.40-0.69; BbF/BkF: 0.45-2.61; FLU/(FLU + PYR): 0.08-0.47; BaP/BghiP: 0.14-8.86 and IP/(IP + BghiP): 0.31-0.83) revealed abundance of pyrogenic PAHs from vehicular sources and combustion of coal, biomass and liquid fuels (petrol, diesel, kerosene, cooking oil).

- Thus, green belting along toxic hotspots with biomonitor plants such as *M. paniculata* is greatly recommended for alleviating the pernicious impacts of air pollutants, thereby stepping towards environmental sustainability.
- ❖ *Assessment of different urban plant bioindicators for urban greenery planning*
 From the study of greenery planning, biomarker (morphological, biochemical and physiological) assessment was confirmed as a vital step towards screening of plant species for biomonitoring of PM and PAHs in order to conserve, restore and govern the functions of ecosystem.
- Eight urban roadside plant species were selected, namely *Nerium oleander*, *Tabernaemontana divaricata*, *Calotropis gigantea*, *Bauhinia acuminata*, *Polyalthia longifolia*, *Alstonia scholaris*, *Neolamarckia cadamba* and *Plumeria alba*, for scrutinizing their biomonitoring potential. Their PM capturing capabilities ($539.32\text{--}2766.27\ \mu\text{g cm}^{-2}$) and PAHs uptake capacities ($159.92\text{--}393.01\ \mu\text{g g}^{-1}$) were studied and compared.
- Variations found in the PM retention capacities ($\mu\text{g cm}^{-2}$) of the plants are as follows: *T. divaricata* (2766.27 ± 86.79) > *N. oleander* (1808.64 ± 46.99) > *B. acuminata* (1697.57 ± 95.76) > *P. longifolia* (1100.44 ± 94.77) > *P. alba* (1054.27 ± 112.85) > *A. scholaris* (932.61 ± 89.93) > *C. gigantea* (709.91 ± 71.34) > *N. cadamba* (539.32 ± 101.49).
- The differences in the micromorphology of abaxial and adaxial surfaces of the plant leaves are also presented in details.
- The accumulation ($\mu\text{g g}^{-1}$) pattern of PAHs through foliage, reflecting its dependence on the leaf surface area available per unit mass for the uptake of pollutants from ambient air, differed as follows: *T. divaricata* (393.01 ± 30.34) > *P. alba* (342.28 ± 25.38) > *N. cadamba* (301.13 ± 37.31) > *N. oleander* (286.08 ± 32.65) > *C. gigantea* (267.47 ± 11.49) > *A. scholaris* (256.80 ± 32.31) > *B. acuminata* (177.22 ± 14.57) > *P. longifolia* (159.92 ± 21.23).
- All the plants exhibited higher values of Chl a than Chl b. Interspecies differences of Chl_T and C_{X+C} are found as: a) shrubs: Chl_T (*T. divaricata*) > Chl_T (*C. gigantea*) > Chl_T (*P. alba*) > Chl_T (*B. acuminata*) > Chl_T (*N. oleander*); C_{X+C} (*T. divaricata*) > C_{X+C} (*C. gigantea*) > C_{X+C} (*B. acuminata*) > C_{X+C} (*P. alba*) > C_{X+C} (*N. oleander*) and b) trees: Chl_T (*N. cadamba*) > Chl_T (*P. longifolia*) > Chl_T (*A. scholaris*); C_{X+C} (*P. longifolia*) > C_{X+C} (*N. cadamba*) > C_{X+C} (*A. scholaris*).
- Increased cellular levels of leaf AA and foliar pH were observed in *T. divaricata* (AA: $18.00\ \mu\text{g g}^{-1}$, pH: 7.47) and *N. oleander* (AA: $15.75\ \mu\text{g g}^{-1}$, pH: 7.38), proving their inherent defense mechanism and adaptation.

- Leaves of *N. cadamba*, *A. scholaris*, *C. gigantea* and *P. alba* manifested high RWC (81.89–88.93%), while on the contrary, minimum value of RWC (65.16%) was found in *P. longifolia*.
- Highest MSI with maximum proline contents and minimum EL was noticed in *N. oleander* (80.52%, 4.28 mg g⁻¹ and 0.98% respectively) and *T. divaricata* (88.69%, 4.72 mg g⁻¹ and 2.31% respectively). However, with high EL% (5.60–8.26), *C. gigantea*, *N. cadamba* and *P. alba* represented high MSI (60.79–78.01%) which can be related to their significant proline content (2.44–3.56 mg g⁻¹) playing a role in balancing the induced stress.
- Carbon contents of selected leaves were measured (43.64 – 52.43%), signifying enhanced allocation of carbon which has been further proved to be directly related to plant mechanisms of adaptation.
- It is revealed that there are positive correlations of TSS content with PM and PAHs.
- Protein concentration decreased with the increase in abiotic stress as observed from the inverse relationship of protein with PM and PAHs.
- The studied plants exhibited distinct levels of tolerance (with APTI ranging between 9.65–29.72) and multifunctional performance assessment based on API scores (50–93.75%) affirmed their implementation in green infrastructure designing.

❖ *Modeling of PAHs accumulation in biomonitors: Mechanistic approach*

Further, to get a deeper insight into the foliage accumulation of PAHs, a mechanistic model of material balance has been demonstrated defining the rate of PAHs uptake in a biomonitor plant compartments of *M. paniculata* as a function of time. The model elucidated a perceptible conception of PAHs uptake mechanisms, plant bioaccumulation and translocation.

- Air to leaf distribution characteristics were studied to get the idea of partitioning behaviour of PAHs.
- Material balance-based mechanistic model of PAHs uptake has been considered.
- It can be concluded that the lipid reservoirs present in different plant parts facilitated the transport of soil-PAHs to the adjacent plant roots and distribution characteristics of PAHs favoured their translocation towards plant foliage but to a lower extent. On the other hand, foliage directly acquires air-dispersed PAHs through two major pathways: uptake through stomata to mesophyll tissue and uptake from adsorbed phase carried by PM and cuticle-wax layer.

➤ The final predictive model looks as follows:

$$\begin{aligned}
 U_{NC} &= \left[\text{Uptake by air – foliage gaseous exchange } (U_{ge}^{A/L}) \right. \\
 &+ \text{Uptake by dry particle deposition } (U_{DP}) \\
 &+ \text{Uptake from root to foliage via transpiration stream } (U_{TS}^{R/L}) \left. \right] \\
 &- [\text{Evaporative loss } (L_{EV})]
 \end{aligned}$$

8.2. Recommendations for future work

On the basis of the concluding remarks, the research study has opened up new dimensions for future work.

8.2.1. Designing of advanced and efficient extraction method of PAHs from plant matrix as improved biomonitoring protocol

Technology advancement in the process of extraction of PAHs from plant tissues should ensure high recovery efficiency, enhanced extraction rate and yield, low cost and sustainability. The burgeoning demand for reducing solvent volume, extraction time and sample amount has raised the need for developing novel extraction techniques for PAHs isolation. ASE/PLE, SFE, DSASE, pulsed electric field-assisted extraction (PEF), cold atmospheric plasma extraction (CAPE), high hydrostatic pressure-assisted extraction (HHP) and enzyme-assisted extraction (EAE) are the superior choices over conventional technologies other than MAE (used in the present study), which have not been yet extensively studied. These non-conventional methods come under the category of ‘Greener approaches’ because of their useful application with deep eutectic and ionic solvents (inorganic) (i.e., limited use of organic solvents warranting health and safety measures), reduced extraction time and energy consumption. Despite their advantages, the rising costs of state-of-the-art techniques are the main obstacles to their employment which must be addressed before use. Hence, critical selection and standardization of the green extraction techniques are the prerequisites towards improved biomonitoring approaches and selectivity of such extraction methods depends on the extraction solvent, type of plant matrix, duration of sampling of plant materials, sample pretreatment, particle size of dried plant tissues and operating temperature. Notable progress in biomonitoring framework can therefore be possible through successful integration of advanced extraction techniques in the pollution assessment scheme for environmental application.

8.2.2. Exploitation of efficient members of plant biomonitor: Use of lower plants like lichen and bryophytes as biomonitors

Apart from further researches on new plant cultivars, future experimentations on lower plants, in particular bryophytes (i.e., mosses) and lichens, should be orchestrated on account of their structures and high particle capturing capacities for improved biomonitoring of ambient air with variable pollution intensities. Lichens (association of algae and fungi) and mosses because of their unique morphological features without any root structure, protective cuticular covering, functional absorbing organ or biofiltration machinery, but having large surface-to-volume ratio for maximizing pollutant capture, can favourably be used as biomonitoring agents across anthropic activity-induced pollution gradients. Devastating pollution effects may sometimes cause disappearance or extinction of lichen or moss colonies. Exercise of transplant methods (i.e., translocation from a control site to contaminated areas) using lichens or mosses for air pollution assessment has therefore been suggested for greater insight into pollutant distribution. Despite their potential, scope of areas involving exploitation of lower plants for biomonitoring of air pollution heterogeneity due to the presence of wide array of pollutants under diverse conditions including urban, peri-urban, industrial and rural locations is under-researched in India. To support the above-stated facts, the potential of one of the efficient members of plant biomonitors, lichen (Fig. 40), was investigated in the present work through preliminary examination of two of the most widely regulated criteria air pollutants (PAHs and heavy metals (HMs)) (Fig. 41 and Fig. 42) and the results substantiating their accumulative behaviour enable the areas wide open for extended research on non-vascular lower plants. It is very much relevant to mention here that the sample collection, pretreatment and preparation methods for analysis of pollutant concentrations should be handled with utmost care, concern and sensitivity owing to their scarce availability at the study sites and strong adherence to the bark tissues.



Fig. 40. Photographs of epiphytic lichen species sampled from Kolkata, India.

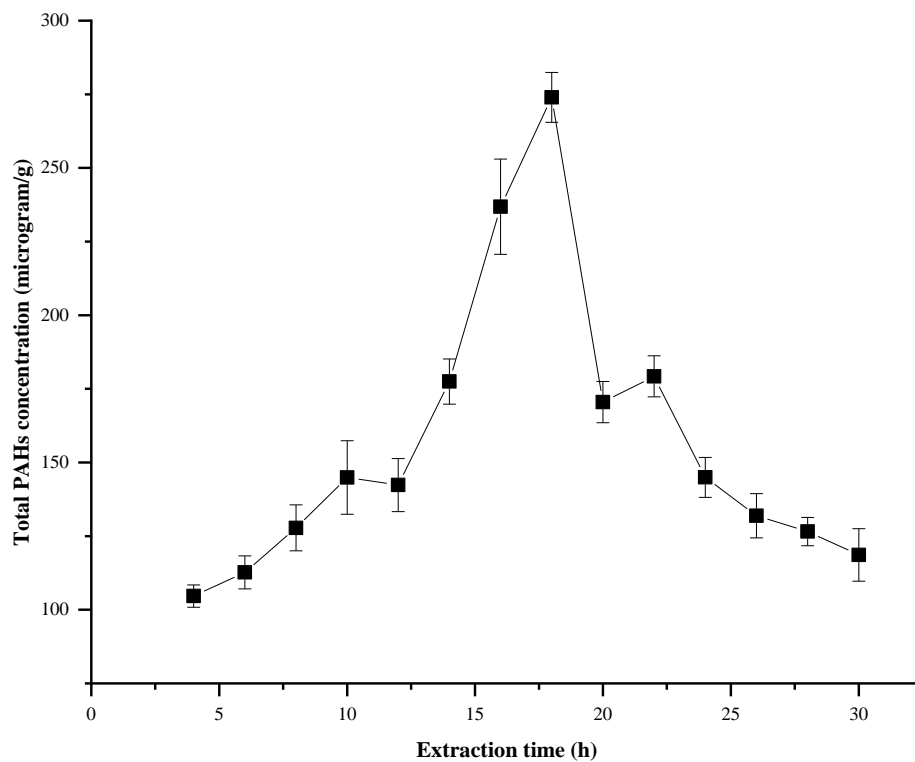


Fig. 41. Variation in concentrations of PAHs isolated from lichen species with extraction time.

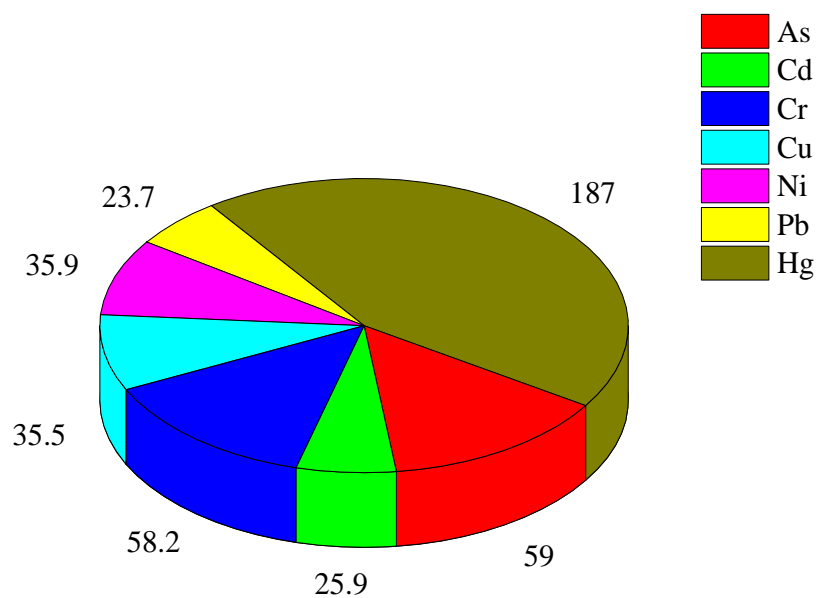
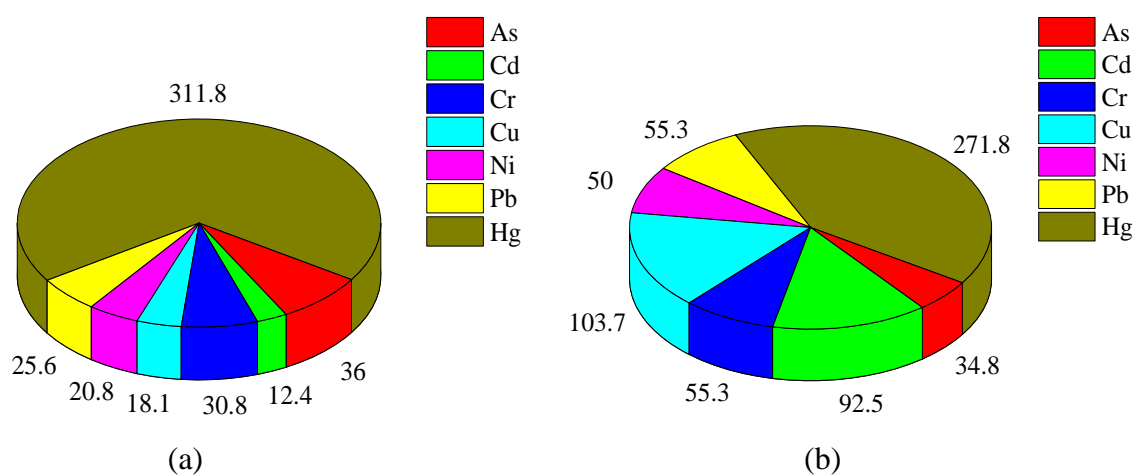


Fig. 42. Heavy metal distribution (with respect to concentration in mg kg⁻¹) in lichen species.

8.2.3. Biomonitoring of heavy metals (priority air pollutant) using terrestrial plant foliages

In recent decades, high rise in anthropogenic emissions has increased the background concentrations of HMs at an alarming scale that continue to menace the whole environment along with the inhabitants. Because of their existence in mainly ionic state (i.e., inorganic form), HMs are very difficult to decompose and thus, exhibits long-term environmental persistence with intolerable toxicity whether present in high or low levels. Hence, assessment of atmospheric HMs using foliages of higher terrestrial plants in a cost-effective way is of practical relevance concerning biomonitoring. Besides, foliar particulates (i.e., PMs that have been intercepted by plant leaves) can also serve as effective indicators of HMs, representing their ambient composition. Thus, total capacity of foliar uptake of HMs is determined through direct leaf absorption and foliar PM adsorption followed by internalization and penetration into leaf tissues. Corroborating the above, analysis of environmentally hazardous HMs (As, Cd, Cr, Cu, Ni, Pb and Hg) in plant leaves as well as leaf-laden particulates has been attempted in the proposed work employing some of the higher plants used in our previous studies, namely *T. divaricata*, *C. gigantea*, *N. cadamba* and *A. scholaris*, in order to provide a fair idea of the potential of terrestrial species in the context of HM biomonitoring. Patterns of HM distribution across various plant species are depicted in Fig. 43 which can serve as a baseline data for future work in this field. From the distribution pattern, it is observed that the levels of Hg in the plant tissues are much higher as compared to other HMs. Therefore, stress should be given on detailed monitoring of Hg along with others, which could otherwise lead to tremendous health hazards.

A brief summary of the scope of future research has been outlined in a flowchart in Fig. 44.



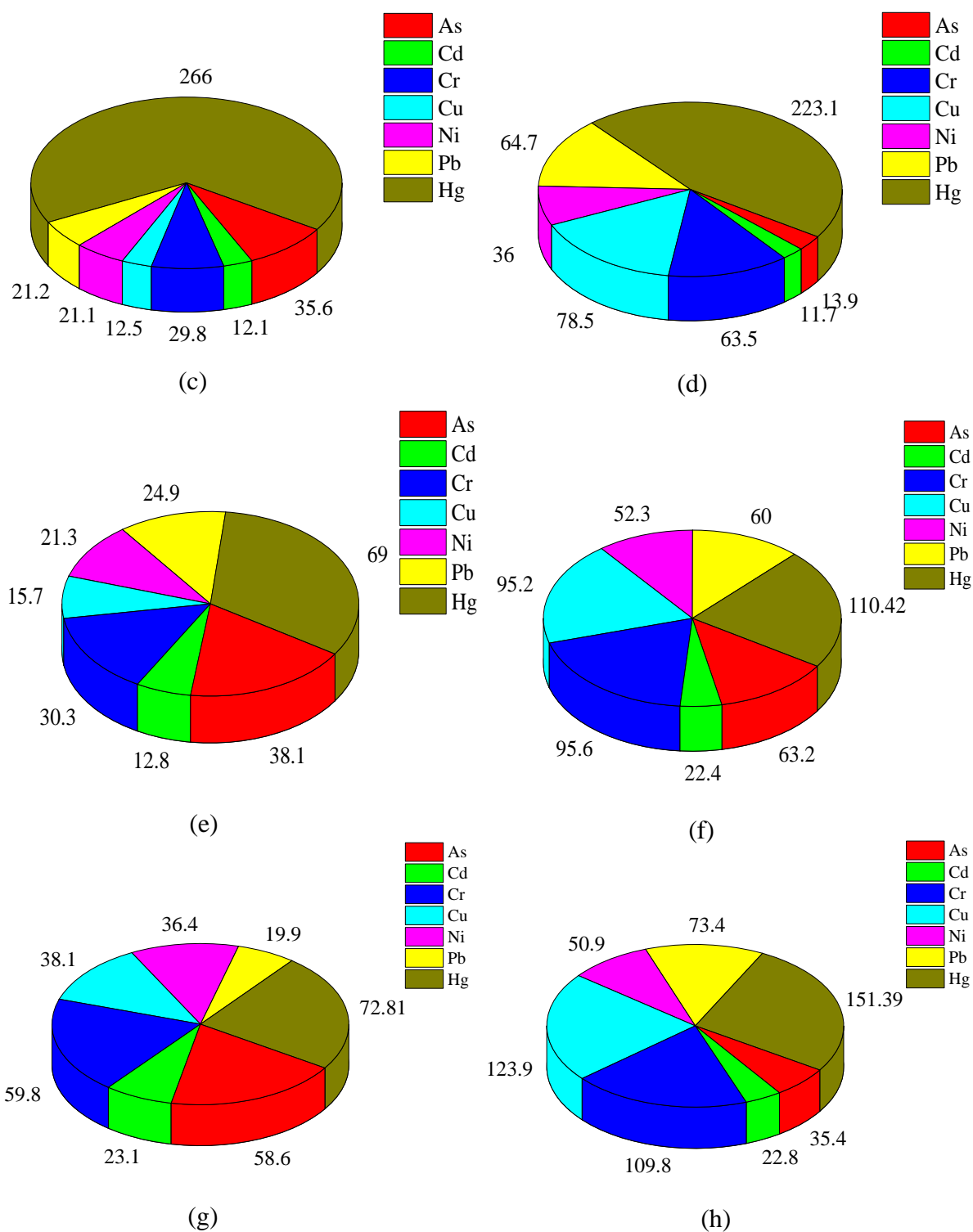


Fig. 43. Heavy metal distribution (with respect to concentration in mg kg⁻¹) in some higher terrestrial plants (a, b) leaves and foliar adsorbed dust particulates of *T. divaricata*, (c, d) leaves and foliar adsorbed dust particulates of *C. gigantea*, (e, f) leaves and foliar adsorbed dust particulates of *N. cadamba* and (g, h) leaves and foliar adsorbed dust particulates of *A. scholaris*.

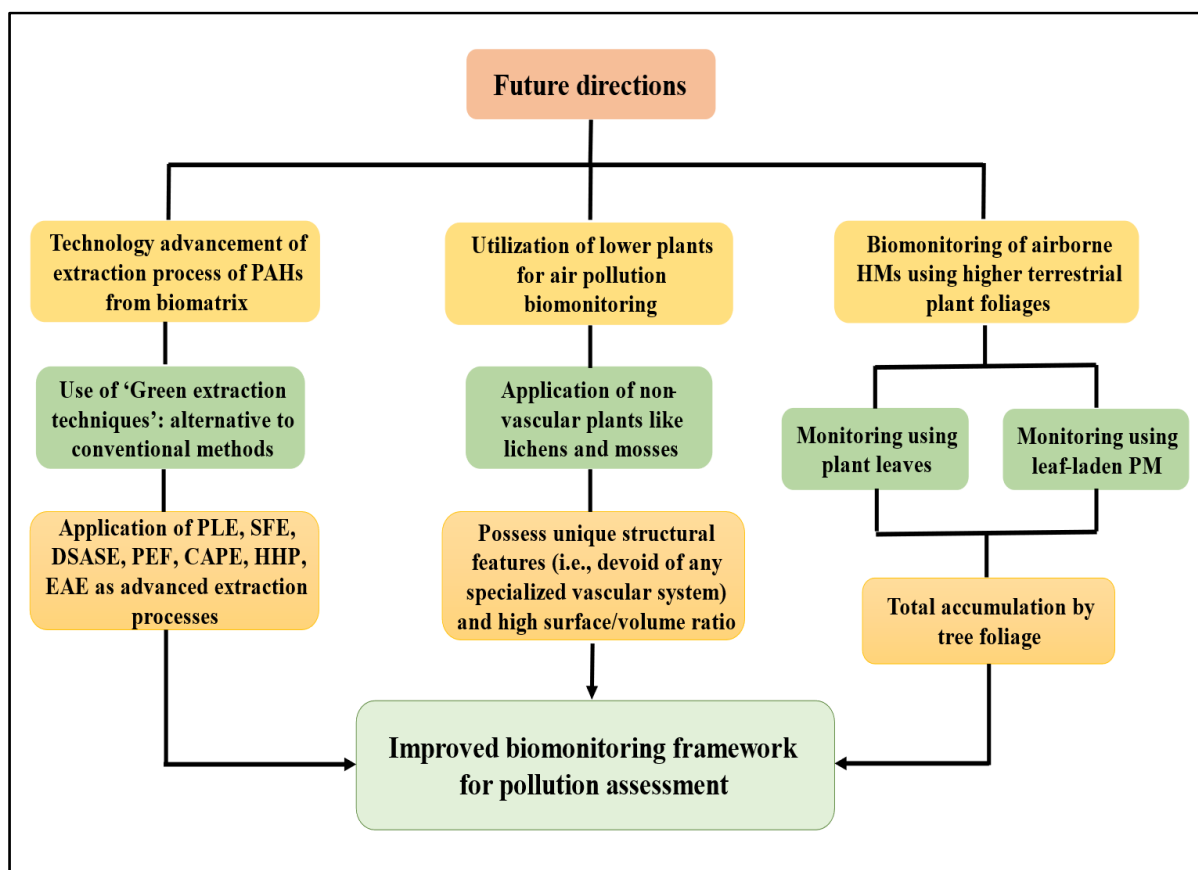


Fig. 44. Future scope of the methodology in a nutshell.

References

- Abayi, J.J.M., Gore, C.T. , Nagawa, C. , Bandowe, B.A.M., Matovu, H., Mubiru, E., Ngeno, E.C., Odongo, S., Sillanpaa, M., Ssebugere, P., 2021. Polycyclic aromatic hydrocarbons in sediments and fish species from the White Nile, East Africa: bioaccumulation potential, source apportionment, ecological and health risk assessment. *Environ. Pollut.* 278, 116855.
- Abdel-Shafy, H.I., Mansour, M.S.M., 2016. A review on polycyclic aromatic hydrocarbons: Source, environmental impact, effect on human health and remediation. *Egypt. J. Petrol.* 25, 107–123.
- Abeyasinghe, P.D., Scharaschkin, T., 2022. Comparative anatomy of two forms of Sri Lankan *Calotropis gigantea* (L.) R. Br. (Family Apocynaceae s.l. – Subfamily Asclepiadoideae) - Taxonomic implications. *Ceylon J. Sci.* 51, 307-318.
- Aboal, J.R., Concha-Grana, E., De Nicola, F., Muniategui-Lorenzo, S., et al., 2020. Testing a novel biotechnological passive sampler for monitoring atmospheric PAH pollution. *J. Hazard. Mater.* 381, 120949.
- ACGIH (American Conference of Governmental Industrial Hygienists), 2005. Polycyclic aromatic hydrocarbons (PAHs) biologic exposure indices (BEI) Cincinnati. OH: American Conference of Governmental Industrial Hygienists.
- Achakzai, K., Khalid, S., Adrees, M., Bibi, A., Ali, S., Nawaz, R., Rizwan, M., 2017. Air pollution tolerance index of plants around brick kilns in Rawalpindi, Pakistan. *J. Environ. Manag.* 190, 252–258.
- Adeleye, A.O., Jin, H., Di, Y., Li, D., Chen, J., Ye, Y., 2016. Distribution and ecological risk of organic pollutants in the sediments and seafood of Yangtze Estuary and Hangzhou Bay, East China Sea. *Sci. Total Environ.* 541, 1540-1548.
- Adhikari, S., Siebert, S.J., Jordaan, A., 2021. Evidence of chromium dust pollution on the leaves of food and medicinal plants from mining areas of Sekhukhuneland, South Africa. *S. Afr. J. Bot.* 143, 226–237.
- Agarwal, S., Tiwari, S.L., 1997. Susceptibility level of plants on the basis of air pollution tolerance index. *Indian For.* 123, 319–322.
- Agency for Toxic Substances and Disease Registry [ATSDR], 1995. Toxicological profile for polycyclic aromatic hydrocarbons. U.S. Department of Health and Human Services, Public

- Health Service: Atlanta, GA. <http://www.atsdr.cdc.gov/toxprofiles/tp69.pdf>. (Accessed 22 January 2019)
- Agus, B.A.P., Rajentran, K., Selamat, J., Lestari, S.D., Umar, N.B., Hussain, N., 2023. Determination of 16 EPA PAHs in food using gas and liquid chromatography. *J. Food Compos. Anal.* 116, 105038.
- Ahmadizadeh, M., Nori, A., Shahbazi, H., Habibpour, M., 2011. Effects of drought stress on some agronomic and morphological traits of durum wheat (*Triticum durum* Desf.) landraces under greenhouse condition. *Afr. J. Biotechnol.* 10, 14097–14107.
- Akram, N.A., Shafiq, F., Ashraf, M., 2017. Ascorbic acid-A potential oxidant scavenger and its role in plant development and abiotic stress tolerance. *Front. Plant Sci.* 8, 1-17.
- Akyuz, M., Cabuk, H., 2010. Gas-particle partitioning and seasonal variation of polycyclic aromatic hydrocarbons in the atmosphere of Zonguldak, Turkey. *Sci. Total Environ.* 408, 5550–5558.
- Al-Alam, J., Fajloun, Z., Chbani, A., Millet, M., 2017. The use of conifer needles as biomonitor candidates for the study of temporal air pollution variation in the Strasbourg region. *Chemosphere* 168, 1411-1421.
- Ali-Taleshi, M.S., Squizzato, S., Bakhtiari, A.R., Moeinaddini, M., Masiol, M., 2021. Using a hybrid approach to apportion potential source locations contributing to excess cancer risk of PM_{2.5}-bound PAHs during heating and non-heating periods in a megacity in the Middle East. *Environ. Res.* 201, 111617.
- Ambade, B., Kumar, A., Kumar, A., Sahu, L.K., 2022a. Temporal variability of atmospheric particulate-bound polycyclic aromatic hydrocarbons (PAHs) over central east India: Sources and carcinogenic risk assessment. *Air Qual. Atmos. Health* 15, 115–130.
- Ambade, B., Sethi, S.S., Kurwadkar, S., Mishra, P., Tripathee, L., 2022b. Accumulation of polycyclic aromatic hydrocarbons (PAHs) in surface sediment residues of Mahanadi River Estuary: Abundance, source, and risk assessment. *Mar. Pollut. Bull.* 183, 114073.
- Ambade, B., Sethi, S.S., Kurwadkar, S., Kumar, A., Sankar, T.K., 2021. Toxicity and health risk assessment of polycyclic aromatic hydrocarbons in surface water, sediments and groundwater vulnerability in Damodar River Basin. *Groundw. Sustain. Dev.* 13, 100553.
- Amellal, N., Portal, J.M., Berthelin, J., 2001. Effect of soil structure on the bioavailability of polycyclic aromatic hydrocarbons within aggregates of a contaminated soil. *Appl. Geochem.* 16, 1611–1619.
- Anand, P., Mina, U., Khare, M., Kumar, P., Kota, S.H., 2022. Air pollution and plant health response-current status and future directions. *Atmos. Pollut. Res.* 13, 101508.

- Andersson, T., 2007. Parameters Affecting the Extraction of Polycyclic Aromatic Hydrocarbons with Pressurised Hot Water. PhD-Thesis, University of Helsinki, Department of Chemistry, Laboratory of Analytical Chemistry, Finland.
- Anna, K.I., Emanuel, G., Anna, S.R., Blonska, E., Lasota, J., Lagan, S., 2018. Linking the contents of hydrophobic PAHs with the canopy water storage capacity of coniferous trees. *Environ. Pollut.* 242, 1176-1184.
- Araujo, R.G., Rodriguez-Jasso, R.M., Ruiz, H.A., Govea-Salas, M., Pintado, M., Aguilar, C.N., 2021. Recovery of bioactive components from avocado peels using microwave-assisted extraction. *Food Bioprod. Process.* 127, 152–161.
- Archanaa, S., Moise, S., Suraishkumar, G.K., 2012. Chlorophyll interference in microalgal lipid quantification through the Bligh and Dyer method. *Biomass and Bioenergy* 46, 805-808.
- Ares, A., Aboal, J.R., Fernandez, J.A., Real, C., Carballeira, A., 2009. Use of the terrestrial moss *Pseudoscleropodium purum* to detect sources of small scale contamination by PAHs. *Atmos. Environ.* 43, 5501–5509.
- Ares, A., Fernandez, J.A., Aboal, J.R., Carballeira, A., 2011. Study of the air quality in industrial areas of Santa Cruz de Tenerife (Spain) by active biomonitoring with *Pseudoscleropodium purum*. *Ecotox. Environ. Safe.* 74, 533-541.
- Arndt, S.K., Irawan, A., Sanders, G.J., 2015. Apoplastic water fraction and rehydration techniques introduce significant errors in measurements of relative water content and osmotic potential in plant leaves. *Physiol. Plant.* 155, 355-368.
- Arnon, D.I., 1949. Copper enzymes in isolated chloroplasts. Polyphenoloxidase in *Beta vulgaris*. *Plant Physiol.* 24, 1–15.
- Arya, N., Kaur, J., Verma, A., Jyotsna Dhanik, J., Vivekanand, 2017. Chemical composition of leaf essential oil of wild and domestic genotypes of *Murraya paniculata* L. J. *Essent. Oil-Bear. Plants* 20, 468-473.
- Ashayeri, N.Y., Keshavarzi, B., Moore, F., Kersten, M., Yazdi, M., Lahijanzadeh, A.R., 2018. Presence of polycyclic aromatic hydrocarbons in sediments and surface water from Shadegan wetland–Iran: a focus on source apportionment, human and ecological risk assessment and sediment-water exchange. *Ecotoxicol. Environ. Saf.* 148, 1054-1066.
- ATSDR (Agency for Toxic Substances and Disease Registry), 1995. Toxicological profile for polycyclic aromatic hydrocarbons. U.S. Department of Health and Human Services, Public Health Service: Atlanta, GA. <http://www.atsdr.cdc.gov/toxprofiles/tp69.pdf> (accessed 22 January 2019).

- Augusto, S., Maguas, C., Matos, J., Pereira, M.J., Branquinho, C., 2010. Lichens as an integrating tool for monitoring PAH atmospheric deposition: A comparison with soil, air and pine needles. *Environ. Pollut.* 158, 483–489.
- Ayen, R.J., Palmer, C.R., Swanstrom, C.P., 1994. Thermal desorption, in: Wilson, D.J., Clarke, A.N. (Eds.), *Hazardous waste site soil remediation: Theory and application of innovative technologies*. Marcel Dekker Inc., New York, pp. 265-310.
- Ayilara, M.S., Babalola, O.O., 2023. Bioremediation of environmental wastes: the role of microorganisms. *Front. Agron.* 5, 1-15.
- Bacon, M.A., Wilkinson, S., Davies, W.J., 1998. pH-regulated leaf cell expansion in droughted plants is abscisic acid dependent. *Plant Physiol.* 118, 1507–1515.
- Badamasi, H., 2022. Urban roadside trees as eco-sustainable filters of atmospheric pollution: A review of recent evidence from atmospheric trace elements deposition. In: Tiwari, S., Agrawal, S. (Eds.), *New Paradigms in Environmental Biomonitoring Using Plants*. Elsevier, pp. 73-94.
- Baek, S.O., Goldstone, M.E., Kirk, P.W.W., Lester, J.N., Perry, R., 1991. Concentrations of particulate and gaseous polycyclic aromatic hydrocarbons in London air following a reduction in the lead content of petrol in the United Kingdom. *Sci. Total Environ.* 111, 169–199.
- Bahndral, A., Shams, R., Dash, K.K., Ali, N.A., Shaikh, A.M., Kovacs, B., 2024. Microwave assisted extraction of cellulose from lemon grass: Effect on techno-functional and microstructural properties. *J. Agric. Food Res.* 16, 101170.
- Bala, N., Pakade, Y.B., Katnoria, J.K., 2022. Assessment of air pollution tolerance index and anticipated performance index of a few local plant species available at the roadside for mitigation of air pollution and green belt development. *Air Qual. Atmos. Health* 15, 2269–2281.
- Balampanis, D.E., Coulon, F., Simms, N., Longhurst, P., Pollard, S.J.T., Fenech, C., Villa, R., 2017. An assessment of different extraction and quantification methods of penta- and hexachlorobenzene from SRF fly-ash. *Anal. Chem. Res.* 12, 28-33.
- Baldocchi, D.D., Hicks, B.B., Camara, P., 1987. A canopy stomatal resistance model for gaseous deposition to vegetated surfaces. *Atmos. Environ.* 21, 91-101.
- Balogh, G., Peter, M., Glatz, A., Gombos, I., Torok, Z., Horvath, I., Harwood, J.L., Vigh, L., 2013. Key role of lipids in heat stress management. *FEBS Lett.* 587, 1970–1980.
- Bandowe, B.A.M., Meusel, H., 2017. Nitrated polycyclic aromatic hydrocarbons (nitro-PAHs) in the environment—A review. *Sci. Total Environ.* 581–582, 237–257.

- Banerjee, S., Banerjee, A., Palit, D., 2022. Morphological and biochemical study of plant species-a quick tool for assessing the impact of air pollution. *J. Clean. Prod.* 339, 130647.
- Banerjee, S., Banerjee, A., Palit, D., Roy, R., 2019. Assessment of vegetation under air pollution stress in urban industrial area for greenbelt development. *Int. J. Environ. Sci. Technol.* 16, 5857–5870.
- Banerjee, S., Palit, D., Banerjee, A., 2021. Variation of tree biochemical and physiological characters under different air pollution stresses. *Environ. Sci. Pollut. Res.* 28, 17960–17980.
- Bangkedphol, S., Sakultantimetha, A., Keenan, H.E., Songsasen, A., 2006. Optimization of microwave-assisted extraction of polycyclic aromatic hydrocarbons from sediments. *J. Environ. Sci. Health A Tox. Hazard Subst. Environ. Eng.* 41, 1105–16.
- Bansod, S.P., Parikh, J.K., Sarangi, P.K., 2023. Pineapple peel waste valorization for extraction of bio-active compounds and protein: Microwave assisted method and Box Behnken design optimization. *Environ. Res.* 221, 115237.
- Barreca, S., Mazzola, A., Orecchio, S., Tuzzolino, N., 2014. Polychlorinated biphenyls in sediments from Sicilian coastal area (Scoglitti) using automated soxhlet, GC-MS, and principal component analysis. *Polycycl. Aromat. Comp.* 34, 237–262.
- Barri, T., Jonsson, J.A., 2008. Advances and developments in membrane extraction for gas chromatography: techniques and applications. *J. Chromatogr. A* 1186, 16–38.
- Baskar, G., Kalavathy, G., Aiswarya, R., Selvakumari, I.A., 2019. Advances in bio-oil extraction from nonedible oil seeds and algal biomass. In: Azad, K. (Ed.), *Advances in Eco-fuels for a Sustainable Environment*. Woodhead Publishing, pp. 187–210.
- Baskaran, S., Wania, F., 2023. Applications of the octanol–air partitioning ratio: a critical review. *Environ. Sci.: Atmos.* 3, 1045–1065.
- Bates, L.S., Waldren, R.P., Teare, I.D., 1973. Rapid determination of free proline for water-stress studies. *Plant Soil* 39, 205–207.
- Baxter, X.C., Darvell, L.I., Jones, J.M., Barraclough, T., Yates, N.E., Shield, I., 2014. *Miscanthus* combustion properties and variations with *Miscanthus* agronomy. *Fuel* 117, 851–869.
- Beckett, K.P., Freer-Smith, P.H., Taylor, G., 2000. Particulate pollution capture by urban trees: effect of species and wind speed. *Global Change Biol.* 6, 995–1003.
- Benmoussa, H., Bechohra, I., He, S., Elfalleh, W., Chawech, R., 2023. Optimization of sonohydrodistillation and microwave assisted hydrodistillation by response surface

- methodology for extraction of essential oils from *Cinnamomum cassia* barks. Ind. Crops Prod. 192, 115995.
- Benmoussa, H., Elfalleh, W., Shudong, H., Romdhane, M., Benhamou, A., Chawech, R., 2018. Microwave hydrodiffusion and gravity for rapid extraction of essential oil from Tunisian cumin (*Cuminum cyminum* L.) seeds: Optimization by response surface methodology. Ind. Crops Prod. 124, 633–642.
- Benson, N.U., Fred-Ahmadu, O.H., Olugbuyiro, J.A.O., Anake, W.U., Adedapo, A.E., Olajire, A.A., 2018. Concentrations, sources and risk characterisation of polycyclic aromatic hydrocarbons (PAHs) in green, herbal and black tea products in Nigeria. J. Food Compos. Anal. 66, 13–22.
- Berset, J.D., Ejem, M., Holzer, R., Lischer, P., 1999. Comparison of different drying, extraction and detection techniques for the determination of priority polycyclic aromatic hydrocarbons in background contaminated soil samples. Anal. Chim. Acta 383, 263–275.
- Bharali, B., Bates, J.W., 2006. Detoxification of dissolved SO₂ (bisulfite) by terricolous mosses. Ann. Bot. 97, 257–263.
- Bharti, S.K., Trivedi, A., Kumar, N., 2018. Air pollution tolerance index of plants growing near an industrial site. Urban Clim. 24, 820–829.
- Bi, Y.F., Guo, F.Y., Yang, L., Zhong, H., Wang, A.K., Wang, Y.K., Wu, Z.Z., Du, X.H., 2018. *Phyllostachys edulis* forest reduces atmospheric PM_{2.5} and PAHs on hazy days at suburban area. Sci. Rep. 8, 1–11.
- Bidleman, T.E., Leone, A., 2004. Soil–air relationships for toxaphene in the southern United States. Environ. Toxicol. Chem. 23, 2337–2342.
- Bidleman, T.F., 1988. Atmospheric processes: Wet and dry depositions of organic compounds are controlled by their vapour-particle partitioning. Environ. Sci. Technol. 22, 361–367.
- Birgul, A., Tasdemir, Y., Cindoruk, S.S., 2011. Atmospheric wet and dry deposition of polycyclic aromatic hydrocarbons (PAHs) determined using a modified sampler. Atmos. Res. 101, 341–353.
- Birke, M., Rauch, U., Hofmann, F., 2018. Tree bark as a bioindicator of air pollution in the city of Stassfurt, Saxony-Anhalt, Germany. J. Geochem. Explor. 187, 97–117.
- Blaine, A.C., Rich, C.D., Sedlacko, E.M., Hundal, L.S., Kumar, K., Lau, C., Mills, M.A., Harris, K.M., Higgins, C.P., 2014. Perfluoroalkyl acid distribution in various plant compartments of edible crops grown in biosolids-amended soils. Environ. Sci. Technol. 48, 7858–7865.

- Blasco, M., Domeno, C., Bentayeb, K., Nerin, C., 2007. Solid-phase extraction clean-up procedure for the analysis of PAHs in lichens. *Int. J. Environ. Anal. Chem.* 87, 833–846.
- Blasco, M., Domeno, C., Lopez, P., Nerin, C., 2011. Behaviour of different lichen species as biomonitors of air pollution by PAHs in natural ecosystems. *J. Environ. Monit.* 13, 2588–2596.
- Blasco, M., Domeno, C., Nerin, C., 2006. Use of lichens as pollution biomonitors in remote areas: Comparison of PAHs extracted from lichens and atmospheric particles sampled in and around the Somport Tunnel (Pyrenees). *Environ. Sci. Technol.* 40, 6384–6391.
- Blasco, M., Domeno, C., Nerin, C., 2008. Lichens biomonitoring as feasible methodology to assess air pollution in natural ecosystems: Combined study of quantitative PAHs analyses and lichen biodiversity in the Pyrenees Mountains. *Anal. Bioanal. Chem.* 391, 759–771.
- Blaszczyk, E., Rogula-Kozłowska, W., Klejnowski, K., Fulara, I., Mielzynska-Svach, D., 2017. Polycyclic aromatic hydrocarbons bound to outdoor and indoor airborne particles (PM_{2.5}) and their mutagenicity and carcinogenicity in Silesian kindergartens, Poland. *Air Qual. Atmos. Health* 10, 389–400.
- Bligh, E.G., Dyer, W.J., 1959. A rapid method of total lipid extraction and purification. *Can. J. Biochem. Physiol.* 37, 911–7.
- Bligny, R., Gout, E., Kaiser, W., Heber, U., et al., 1997. pH regulation in acid-stressed leaves of pea plants grown in the presence of nitrate or ammonium salts: studies involving ³¹P-NMR spectroscopy and chlorophyll fluorescence. *Biochim. Biophys. Acta* 1320, 142–152.
- Bogdanovic, T., Pleadin, J., Petricevic, S., Listes, E., Sokolic, D., Markovic, K., Ozogul, F., Simat, V., 2019. The occurrence of polycyclic aromatic hydrocarbons in fish and meat products of Croatia and dietary exposure. *J. Food Compos. Anal.* 75, 49–60.
- Bohme, F., Welsch-Pausch, K., McLachlan, M.S., 1999. Uptake of airborne semivolatile organic compounds in agricultural plants: field measurements of interspecies variability. *Environ. Sci. Technol.* 33, 1805–1813.
- Bolinius, D.J., MacLeod, M., McLachlan, M.S., Mayer, P., Jahnke, A., 2016. A passive dosing method to determine fugacity capacities and partitioning properties of leaves. *Environ. Sci.: Processes Impacts* 18, 1325–1332.
- Bolouri-Moghaddam, M.R., Roy, K.L., Xiang, L., Rolland, F., Van den Ende, W., 2010. Sugar signalling and antioxidant network connections in plant cells. *FEBS J.* 277, 2022–2037.
- Bonventre, J.A., 2014. Solvents. In: Wexler, P. (Ed.), *Encyclopedia of Toxicology* (3rd edition). Academic Press, pp. 356–357.

- Borgulat, J., Borgulat, A., 2023. Biomonitoring of atmospheric PAHs using fir and spruce needles in forests in the vicinity of mountain villages. *Environ. Pollut.* 330, 121814.
- Bostrom, C.E., Gerde, P., Hanberg, A., Jernstrom, B., Johansson, C., Kyrklund, T., Rannug, A., Tornqvist, M., Victorin, K., Westerholm, R., 2002. Cancer risk assessment, indicators, and guidelines for polycyclic aromatic hydrocarbons in the ambient air. *Environ. Health Perspect.* 110, 451–488.
- Bradford, M.M., 1976. A rapid and sensitive method for the quantitation of micro-gram quantities of protein utilizing the principle of protein-dye binding. *Anal. Biochem.* 72, 248–254.
- Brantley, H.L., Hagler, G.S.W., Deshmukh, P.J., Baldauf, R.W., 2014. Field assessment of the effects of roadside vegetation on near-road black carbon and particulate matter. *Sci. Total Environ.* 468, 120–129.
- Bucheli, T.D., Blum, F., Desaulles, A., Gustafsson, O., 2004. Polycyclic aromatic hydrocarbons, black carbon, and molecular markers in soils of Switzerland. *Chemosphere* 56, 1061–1076.
- Buchholz, A., 2006. Characterization of the diffusion of non-electrolytes across plant cuticles: properties of the lipophilic pathway. *J. Exp. Bot.* 57, 2501–2513.
- Budzinski, H., Jones, I., Bellocq, J., Pierard, C., Garrigues, P., 1997. Evaluation of sediment contamination by polycyclic aromatic hydrocarbons in the Gironde estuary. *Mar. Chem.* 58, 85-97.
- Caballero-Casero, N., Cabuk, H., Martínez-Sagarra, G., Devesa, J.A., Rubio, S., 2015. Nanostructured alkyl carboxylic acid-based restricted access solvents: Application to the combined microextraction and cleanup of polycyclic aromatic hydrocarbons in mosses. *Anal. Chim. Acta* 890, 124-133.
- Cai, M., Xin, Z., Yu, X., 2017. Spatio-temporal variations in PM leaf deposition: a metaanalysis. *Environ. Pollut.* 231, 207–218.
- Callen, M., Lopez, J., Iturmendi, A., Mastral, A.M., 2013. Nature and sources of particle associated polycyclic aromatic hydrocarbons (PAH) in the atmospheric environment of an urban area. *Environ. Pollut.* 183, 166-174.
- Callen, M.S., Iturmendi, A., Lopez, J.M., Mastral, A.M., 2014. Source apportionment of the carcinogenic potential of polycyclic aromatic hydrocarbons (PAH) associated to airborne PM₁₀ by a PMF model. *Environ. Sci. Pollut. Res.* 21, 2064-2076.

- Camel, V., 2000. Microwave-assisted solvent extraction of environmental samples. *TrAC Trend. Anal. Chem.* 19, 229-248.
- Camel, V., 2001. Recent extraction techniques for solid matrices—supercritical fluid extraction, pressurized fluid extraction and microwave-assisted extraction: their potential and pitfalls. *Analyst* 126, 1182-1193.
- Cao, D., Qiao, X., Guo, Y., Liu, P., 2024. Valorization of pawpaw (*Carica papaya* L.) leaves as a source of polyphenols by ionic liquid-based microwave-assisted extraction: Comparison with other extraction methods and bioactivity evaluation. *Food Chem. X* 22, 101500.
- Capozzi, F., Giordano, S., Aboal, J.R., Adamo, P., Bargagli, R., Boquete, T., Di Palma, A., Real, C., Reski, R., Spagnuolo, V., Steinbauer, K., Tretiach, M., Varela, Z., Zechmeister, H., Fernandez, J.A., 2016. Best options for the exposure of traditional and innovative moss bags: A systematic evaluation in three European countries. *Environ. Pollut.* 214, 362–373.
- Capozzi, F., Palma, A.D., Adamo, P., Spagnuolo, V., Giordano, S., 2017. Monitoring chronic and acute PAH atmospheric pollution using transplants of the moss *Hypnum cupressiforme* and *Robinia pseudacacia* leaves. *Atmos. Environ.* 150, 45-54.
- Caricchia, A.M., Chiavarini, S., Pezza, M., 1999. Polycyclic aromatic hydrocarbons in the urban atmospheric particulate matter in the City of Naples (Italy). *Atmos. Environ.* 33, 3731–3738.
- Cecconi, E., Fortuna, L., Pellegrini, E., Bertuzzi, S., Lorenzini, G., Nali, C., Tretiach, M., 2019. Beyond ozone-tolerance: Effects of ozone fumigation on trace element and PAH enriched thalli of the lichen biomonitor *Pseudevernia furfuracea*. *Atmos. Environ.* 210, 132–142.
- Central Pollution Control Board (CPCB), 2003. Guidelines for Ambient Air Quality Monitoring. National Ambient Air Quality Monitoring Series: NAAQMS/ ... /2003-04. pp. 155.
- Chan, C.-H., Yusoff, R., Ngoh, G.-C., Kung, F.W.-L., 2011. Microwave-assisted extractions of active ingredients from plants. *J. Chromatogr. A* 1218, 6213–6225.
- Chanda, S., Mehendale, H.M., 2005. Acenaphthene. In: Wexler, P. (Ed.), *Encyclopedia of Toxicology*. Academic Press, pp. 11–13.
- Chaudhary, I.J., Rathore, D., 2018. Suspended particulate matter deposition and its impact on urban trees. *Atmos. Pollut. Res.* 9, 1072–1082.
- Chaudhary, N., 2022. Pollution biomarkers in environmental biomonitoring: An insight into air pollution. In: Tiwari, S., Agrawal, S. (Eds.), *New Paradigms in Environmental Biomonitoring Using Plants*. Elsevier, pp. 165-180.

- Chen, F.L., Du, X.Q., Zu, Y.G., Yang, L., 2015a. A new approach for preparation of essential oil, followed by chlorogenic acid and hyperoside with microwave-assisted simultaneous distillation and dual extraction (MSDDE) from *Vaccinium uliginosum* leaves. *Ind. Crops Prod.* 77, 809–826.
- Chen, P., Kang, S., Li, C., Rupakheti, M., Yan, F., Li, Q., Ji, Z., Zhang, Q., Luo, W., Sillanpaa, M., 2015b. Characteristics and sources of polycyclic aromatic hydrocarbons in atmospheric aerosols in the Kathmandu Valley Nepal. *Sci. Total Environ.* 538, 86–92.
- Chen, F.L., Jia, J., Zhang, Q., Yang, L., Gu, H.Y., 2018. Isolation of essential oil from the leaves of *Polygonum viscosum* Buch-ham. using microwave-assisted enzyme pretreatment followed by microwave hydrodistillation concatenated with liquid–liquid extraction. *Ind. Crops Prod.* 112, 327–341.
- Chen, J., Xia, X., Wang, H., Zhai, Y., Xi, N., Lin, H., Wen, W., 2019. Uptake pathway and accumulation of polycyclic aromatic hydrocarbons in spinach affected by warming in enclosed soil/water-air-plant microcosms. *J. Hazard. Mater.* 379, 120831.
- Chen, L., Song, D., Tian, Y., Ding, L., Yu, A., Zhang, H., 2008. Application of on-line microwave sample-preparation techniques. *Trends Anal. Chem.* 27, 151–159.
- Chen, L., Yin, L., Song, F., Liu, Z., Zheng, Z., Xing, J., Liu, S., 2013. Determination of pesticide residues in ginseng by dispersive liquid–liquid microextraction and ultra high performance liquid chromatography–tandem mass spectrometry. *J. Chromatogr. B* 917–918, 71–77.
- Chen, L., Yong, R., Xing, B., Mai, B., He, J., Wei, X., Fu, J., Sheng, G., 2005. Contents and sources of polycyclic aromatic hydrocarbons and organochlorine pesticides in vegetable soils of Guangzhou, China. *Chemosphere* 60, 879–890.
- Chen, L., Zhong, J., Lin, Y., Yuan, T., Huang, J., Gan, L., Wang, L., Lin, C., Fan, H., 2023. Microwave and enzyme co-assisted extraction of anthocyanins from Purple-heart Radish: Process optimization, composition analysis and antioxidant activity. *Lwt* 187, 115312.
- Cheng, K., Li, J.Y., Wang, Y., Ji, W.W., Cao, Y., 2022. Characterization and risk assessment of airborne polycyclic aromatic hydrocarbons from open burning of municipal solid waste. *Front. Environ. Sci.* 10, 861770.
- Cheng, Z., Yao, Y., Sun, H., 2020. Comparative uptake, translocation and subcellular distribution of phthalate esters and their primary monoester metabolites in Chinese cabbage (*Brassica rapa* var. *chinensis*). *Sci. Total Environ.* 742, 140550

- Choi, S.D., 2014. Time trends in the levels and patterns of polycyclic aromatic hydrocarbons (PAHs) in pine bark, litter, and soil after a forest fire. *Sci. Total Environ.* 470–471, 1441–1449.
- Chowdhury, A.S., Uddin, M.J., Baul, T.K., Akhter, J., Nandi, R., Karmakar, S., Nath, T.K., 2022. Quantifying the potential contribution of urban trees to particulate matters removal: A study in Chattogram city, Bangladesh. *J. Clean. Prod.* 380, 135015.
- Chrabaszcz, M., Mroz, L., 2017. Tree Bark, a valuable source of information on air quality. *Pol. J. Environ. Stud.* 26, 453–466.
- Christou, A., Stavrou, I.J., Kapnissi-Christodoulou, C.P., 2021. Continuous and pulsed ultrasound-assisted extraction of carob's antioxidants: Processing parameters optimization and identification of polyphenolic composition. *Ultrason. Sonochem.* 76, 105630.
- Chropenova, M., Greguskova, E.K., Karaskova, P., Pribylova, P., Kukucka, P., Barakova, D., Cupr, P., 2016. Pine needles and pollen grains of *Pinus mugo* Turra – A biomonitoring tool in high mountain habitats identifying environmental contamination. *Ecol. Indic.* 66, 132–142.
- Chrysikou, L., Gemenetzi, P., Kouras, A., Manoli, E., Terzi, E., Samara, C., 2008. Distribution of persistent organic pollutants, polycyclic aromatic hydrocarbons and trace elements in soil and vegetation following a large scale landfill fire in northern Greece. *Environ. Int.* 34, 210–225.
- Chun, M.Y., 2011. Relationship between PAHs concentrations in ambient air and deposited on Pine needles. *Environ. Health Toxicol.* 26, 1–6.
- Cicero, A.M., Pietrantonio, E., Romanelli, G., Di Muccio, A., 2000. Comparison of Soxhlet, shaking, and microwave assisted extraction techniques for determination of PCB congeners in a marine sediment. *Bull. Environ. Contam. Toxicol.* 65, 307–313.
- Ciecierska, M., Obiedzinski, M.W., 2013. Polycyclic aromatic hydrocarbons in the bakery chain. *Food Chem.* 141, 1–9.
- Codina, G., Vaquero, M.T., Comellas, L., Broto-Puig, F., 1994. Comparison of various extraction and clean-up methods for the determination of polycyclic aromatic hydrocarbons in sewage sludge-amended soils. *J. Chromatogr. A* 673, 21–29.
- Colabuono, F.I., Taniguchi, S., Cipro, C.V.Z., da Silva, J., Bicego, M.C., Montone, R.C., 2015. Persistent organic pollutants and polycyclic aromatic hydrocarbons in mosses after fire at the Brazilian Antarctic Station. *Mar. Pollut. Bull.* 93, 266–269.
- Collins, C., Fryer, M., Grosso, A., 2006. Plant uptake of non-ionic organic chemicals. *Environ. Sci. Technol.* 40, 45–52.

- Concha-Grana, E., Pineiro-Iglesias, M., Muniategui-Lorenzo, S., Lopez-Mahia, P., Prada-Rodríguez, D., 2015a. Proposal of a procedure for the analysis of atmospheric polycyclic aromatic hydrocarbons in mosses. *Talanta* 134, 239-246.
- Concha-Grana, E., Muniategui-Lorenzo, S., De Nicola, F., Aboal, J.R., Rey-Asensio, A.I., Giordano, S., Reski, R., Lopez-Mahia, P., Prada-Rodríguez, D., 2015b. Matrix solid phase dispersion method for determination of polycyclic aromatic hydrocarbons in moss. *J. Chromatogr. A* 1406, 19-26.
- Connel, D.W., Hawker, D.W., Warne, M.J., Vowles, P.P., 1997. Polycyclic aromatic hydrocarbons (PAHs). In: McCombs, K., Starkweather, A.W. (Eds.), *Introduction into environmental chemistry*. CRC Press LLC, Boca Raton, pp. 205–217.
- Conti, M.E., Cecchetti, G., 2001. Biological monitoring: lichens as bioindicators of air pollution assessment- a review. *Environ. Pollut.* 114, 471-492.
- Corada, K., Woodward, H., Alaraj, H., Collins, C.M., de Nazelle, A., 2021. A systematic review of the leaf traits considered to contribute to removal of airborne particulate matter pollution in urban areas. *Environ. Pollut.* 269, 116104.
- CoSeteng, M.Y., et al., 1989. Influence of titratable acidity and pH on intensity of sourness of citric, malic, tartaric, lactic and acetic acid solutions and on the overall acceptability of imitation apple juice. *Can. Inst. Food Sci. Technol. J.* 22, 46-51.
- Cousins, I.T., Mackay, D., 2001. Strategies for including vegetation compartments in multimedia models. *Chemosphere* 44, 643-654.
- Cresswell, S.L., Haswell, S.J., 1999. Evaluation of on-line methodology for microwave-assisted extraction of polycyclic aromatic hydrocarbons (PAHs) from sediment samples. *Analyst* 124, 1361-1366.
- Curren, M.S.S., King, J.W., 2001. Solubility of triazine pesticides in pure and modified subcritical water. *Anal. Chem.* 73, 740-745.
- Currie, B.A., Bass, B., 2008. Estimates of air pollution mitigation with green plants and green roofs using the UFORE model. *Urban Ecosyst.* 11, 409-422.
- Cuyppers, C., 2001. Bioavailability of polycyclic aromatic hydrocarbons in soils and sediments: Prediction of bioavailability and characterization of organic matter domains. PhD-thesis, Wageningen University, The Netherlands.
- Dadkhah, A.A., Akgerman, A., 2002. Hot water extraction with in situ wet oxidation: PAHs removal from soil. *J. Hazard. Mater.* 93, 307–320.

- Darvishzadeh, P., Orsat, V., 2022. Microwave-assisted extraction of antioxidant compounds from Russian olive leaves and flowers: Optimization, HPLC characterization and comparison with other methods. *J. Appl. Res. Med. Aromat. Plants* 27, 100368.
- Das, K., Roychoudhury, A., 2014. Reactive oxygen species (ROS) and response of antioxidants as ROS-scavengers during environmental stress in plants. *Front. Environ. Sci.* 2, 1-13.
- Davoodi-nasab, P., Rahbar-kelishami, A., Safdari, J., Abolghasemi, H., 2017. Performance study of neodymium extraction by carbon nanotubes assisted emulsion liquid membrane using response surface methodology. *Int. J. Chem. Mol. Eng.* 11, 168–172.
- Davoudi, M., Esmaili-Sari, A., Bahramifar, N., Moeinaddini, M., 2021. Spatio-temporal variation and risk assessment of polycyclic aromatic hydrocarbons (PAHs) in surface dust of Qom metropolis, Iran. *Environ. Sci. Pollut. Res.* 28, 9276-9289.
- de Castro, M.D.L., Ayuso, L.E.G., 2000. Environmental applications | Soxhlet extraction. In: Wilson, I.D. (Ed.), *Encyclopedia of Separation Science*. Academic Press, pp. 2701–2709.
- de Koning, S., Janssen, H.-G., Brinkman, U.A.T., 2009. Modern methods of sample preparation for GC analysis. *Chromatographia Supplement* 69, S33-S78.
- De La Torre-Roche, R.J., Lee, W.-Y., Campos-Diaz, S.I., 2009. Soil-borne polycyclic aromatic hydrocarbons in El Paso, Texas: Analysis of a potential problem in the United States/Mexico border region. *J. Hazard. Mater.* 163, 946–958.
- De Nicola, F., Claudia, L., MariaVittoria, P., Giulia, M., Anna, A., 2011. Biomonitoring of PAHs by using *Quercus ilex* leaves: Source diagnostic and toxicity assessment. *Atmos. Environ.* 45, 1428 1433.
- De Nicola, F., Concha Grana, E., Lopez Mahia, P., Muniategui Lorenzo, S., Prada Rodriguez, D., Retuerto, R., Carballeira, A., Aboal, J.R., Fernandez, J.A., 2017. Evergreen or deciduous trees for capturing PAHs from ambient air? A case study. *Environ. Pollut.* 221, 276–284.
- De Nicola, F., Grana, E.C., Aboal, J.R., Carballeira, A., Fernandez, J.A., Mahia, P.L., Rodriguez, D.P., Lorenzo, S.M., 2016. PAH detection in *Quercus robur* leaves and *Pinus pinaster* needles: A fast method for biomonitoring purpose. *Talanta* 153, 130–137.
- De Nicola, F., Maisto, G., Prati, M.V., Alfani, A., 2005. Temporal variations in PAH concentrations in *Quercus ilex* L. (holm oak) leaves in an urban area. *Chemosphere* 61, 432-440.
- De Nicola, F., Maisto, G., Prati, M.V., Alfani, A., 2008. Leaf accumulation of trace elements and polycyclic aromatic hydrocarbons (PAHs) in *Quercus ilex* L. *Environ. Pollut.* 153, 376–383.

- De Nicola, F., Spagnuolo, V., Baldantoni, D., Sessa, L., Alfani, A., Bargagli, R., Monaci, F., Terracciano, S., Giordano, S., 2013. Improved biomonitoring of airborne contaminants by combined use of holm oak leaves and epiphytic moss. *Chemosphere* 92, 1224-1230.
- Dean Jr., W.E., 1974. Determination of carbonate and organic matter in calcareous sediments and sedimentary rocks by loss on ignition: comparison with other methods. *J. Sediment. Petrol.* 44, 242–248.
- Dean, J.R., Xiong, G., 2000. Extraction of organic pollutants from environmental matrices: selection of extraction technique. *Trends Anal. Chem.* 19, 553– 564.
- Dearden, J.C., Bresnen, G.M., 1988. The measurement of partition coefficients. *Quantitative Structure-Activity Relationships* 7, 133-144.
- Delacour, C., Lutz, C., Kuhn, S., 2019. Pulsed ultrasound for temperature control and clogging prevention in micro-reactors. *Ultrason. Sonochem.* 55, 67–74.
- Delgado-Saborit, J.M., Stark, C., Harrison, R.M., 2011. Carcinogenic potential, levels and sources of polycyclic aromatic hydrocarbon mixtures in indoor and outdoor environments and their implications for air quality standards. *Environ. Int.* 37, 383–392.
- Delhaes, P., Drillon, M., 1987. *Organic and Inorganic Low-Dimensional Crystalline Materials*. Plenum, New York.
- Delhomme, O., Rieb, E., Millet, M., 2007. Solid-phase extraction and LC with fluorescence detection for analysis of PAHs in rainwater. *Chromatographia* 65, 163-171.
- Demircioglu, E., Sofuoglu, A., Odabasi, M., 2011. Atmospheric concentrations and phase partitioning of polycyclic aromatic hydrocarbons in Izmir, Turkey. *Clean–Soil, Air, Water* 39, 319-327.
- Dent, M., Dragovic-Uzelac, V., Penic, M., Brncic, M., Bosiljkov, T., Levaj, B., 2013. The effect of extraction solvents, temperature and time on the composition and mass fraction of polyphenols in Dalmatian Wild Sage (*Salvia officinalis* L.) extracts. *Food Technol. Biotechnol.* 51, 84–91.
- Deokar, D.S., Pagare, I.S., Naseem, A.M., Kshirsagar, S., Shindhe, L., 2016. Chemical derivatization UV spectrophotometric method for detection of P-aminophenol and energy of activation approach to set degradation protocol for forced degradation studies. *Int. J. Pharm. Res. Rev.* 5, 1–12.
- Desalme, D., Binet, P., Chiapusio, G., 2013. Challenges in tracing the fate and effects of atmospheric polycyclic aromatic hydrocarbon deposition in vascular plants. *Environ. Sci. Technol.* 47, 3967–3981.

- Deshmukh, S., Kumar, R., Bala, K., 2019. Microalgae biodiesel: A review on oil extraction, fatty acid composition, properties and effect on engine performance and emissions. *Fuel Process. Technol.* 191, 232–247.
- Detmar, J., Jurisicova, A., 2010. Embryonic resorption and polycyclic aromatic hydrocarbons: putative immune-mediated mechanisms. *Syst. Biol. Reprod. Med.* 56, 3–17.
- Dolegowska, S., Migaszewski, Z.M., 2011. PAH concentrations in the moss species *Hylocomium splendens* (Hedw.) B.S.G. and *Pleurozium schreberi* (Brid.) Mitt. from the Kielce area (south-central Poland). *Ecotox. Environ. Safe.* 74, 1636–1644.
- Domeno, C., Blasco, M., Sanchez, C., Nerin, C., 2006. A fast extraction technique for extracting polycyclic aromatic hydrocarbons (PAHs) from lichens samples used as biomonitors of air pollution: Dynamic sonication versus other methods. *Anal. Chim. Acta* 569, 103–112.
- Domeno, C., Canellas, E., Alfaro, P., Rodriguez-Lafuente, A., Nerin, C., 2012. Atmospheric pressure gas chromatography with quadrupole time of flight mass spectrometry for simultaneous detection and quantification of polycyclic aromatic hydrocarbons and nitro-polycyclic aromatic hydrocarbons in mosses. *J. Chromatogr. A.* 1252, 146–154.
- Domingos, M., Bulbovas, P., Camargo, C.Z., Aguiar-Silva, C., Brandao, S.E., Dafre-Martinelli, M., Dias, A.P., Engela, M., Gagliano, J., Moura, B.B., Alves, E.S., Rinaldi, M.C., Gomes, E.P., Furlan, C.M., Figueiredo, A.M., 2015. Searching for native tree species and respective potential biomarkers for future assessment of pollution effects on the highly diverse Atlantic Forest in SE-Brazil. *Environ. Pollut.* 202, 85–95.
- Dong, C.D., Chen, C.F., Chen, C.W., 2012. Determination of polycyclic aromatic hydrocarbons in industrial harbor sediments by GC-MS. *Int. J. Environ. Res. Public Health* 9, 2175–2188.
- dos Santos, R.R., de, Z., Cardeal, L., Menezes, H.C., 2020. Phase distribution of polycyclic aromatic hydrocarbons and their oxygenated and nitrated derivatives in the ambient air of a Brazilian urban area. *Chemosphere* 250, 126223.
- Dosoky, N.S., Satyal, P., Gautam, T.P., Setzer, W.N., 2016. Composition and biological activities of *Murraya paniculata* (L.) Jack essential oil from Nepal. *Medicines* 3, 1–10.
- Drake, J.E., Tjoelker, M.G., Aspinwall, M.J., Reich, P.B., Pfautsch, S., Barton, C.V.M., 2019. The partitioning of gross primary production for young *Eucalyptus tereticornis* trees under experimental warming and altered water availability. *New Phytol.* 222, 1298–1312.
- Drinic, Z., Pljevljakusic, D., Zivkovic, J., Bigovic, D., Savikin, K., 2020. Microwave-assisted extraction of *O. vulgare* L. spp. *hirtum* essential oil: Comparison with conventional hydro-distillation. *Food Bioprod. Process* 120, 158–165.

- Duarte-Almeida, J.M., Clemente, M.S., Arruda, R.C.O., Vaz, A.M.S.F., Salatino, A., 2015. Glands on the foliar surfaces of tribe Cercideae (Caesapiniodeae, Leguminosae): distribution and taxonomic significance. *An. Acad. Bras. Cienc.* 87, 787–796.
- Dudhagara, D.R., Rajpara, R.K., Bhatt, J.K., Gosai, H.B., Sachaniya, B.K., Dave, B.P., 2016. Distribution, sources and ecological risk assessment of PAHs in historically contaminated surface sediments at Bhavnagar coast, Gujarat, India. *Environ. Pollut.* 213, 338–346.
- Duong, T.T.T., Lee, B.K., 2011. Determining contamination level of heavy metals in road dust from busy traffic areas with different characteristics. *J. Environ. Manage.* 92, 554–562.
- Durant, J., Busby, W., Lafleur, A., Penman, B., Crespi, C., 1996. Human cell mutagenicity of oxygenated, nitrated and unsubstituted polycyclic aromatic hydrocarbons associated with urban aerosols. *Mutat. Res.-Genet. Tox.* 371, 123–157.
- Dwyer, J.M., Hobbs, R.J., Mayfield, M.M., 2014. Specific leaf area responses to environmental gradients through space and time. *Ecology* 95, 399–410.
- Environmental Protection Agency (EPA), 1984. Methods for Organic Chemical Analysis of Municipal and Industrial Wastewater. Appendix A to Part 136. Method 610-Polynuclear Aromatic Hydrocarbons.
- Dzepina, K., Arey, J., Marr, L.C., Worsnop, D.R., Salcedo, D., Zhang, Q., Onasch, T.B., Molina, L.T., Molina, M.J., Jimenez, J.L., 2007. Detection of particle-phase polycyclic aromatic hydrocarbons in Mexico City using an aerosol mass spectrometer. *Int. J. Mass Spectrom.* 263, 152–170.
- Dzierzanowski, K., Popek, R., Gawronska, H., Saebo, A., Gawronski, S.W., 2011. Deposition of particulate matter of different size fractions on leaf surfaces and in waxes of urban forest species. *Int. J. Phytoremediation* 13, 1037–1046.
- Earl, N., Cartwright, C.D., Horrocks, S.J., Worboys, M., Swift, S., Kirton, J.A., Askan, A.U., Kelleher, H., Nancarrow, D.J., 2003. Review of the Fate and Transport of Selected Contaminants in the Soil Environment. Environment Agency R&D, Bristol, UK. Technical Report P5-079/TR1.
- Edokpayi, J.N., Odiyo, J.O., Popoola, O.E., Msagati, T.A.M., 2016. Determination and distribution of polycyclic aromatic hydrocarbons in rivers, sediments and wastewater effluents in Vhembe District, South Africa. *Int. J. Environ. Res. Public Health* 13, 1–12.
- El-Khatib, A.A., El-Rahman, A.M.A., El-Sheikh, O.M., 2012. Biomagnetic monitoring of air pollution using dust particles of urban tree leaves at upper Egypt. *Assiut Univ. J. Bot.* 41, 111–130.

- Enete, I.C., Chukwudeluzu, V.U., Okolie, A.O., 2013. Evaluation of air pollution tolerance index of plants and ornamental shrubs in Enugu City: Implications for urban heat island effect. *World Environ.* 3, 108–115.
- Environmental Protection Agency (EPA), 1984. Methods for Organic Chemical Analysis of Municipal and Industrial Wastewater. Appendix A to Part 136. Method 610—Polynuclear Aromatic Hydrocarbons.
- Environmental Protection Agency (EPA), 1999. Determination of Polycyclic Aromatic Hydrocarbons (PAHs) in Ambient Air using Gas Chromatography/Mass Spectrometry (GC/MS). Second ed. Compendium Method TO-13A.
- Eriksson, M., Faldt, J., Dalhammar, G., Borg-Karlson, A.K., 2001. Determination of hydrocarbons in old creosote contaminated soil using headspace solid phase microextraction and GC-MS. *Chemosphere* 44, 1641–1648.
- Escobedo, F.J., Wagner, J.E., Nowak, D.J., De la Maza, C.L., Rodriguez, M., Crane, D.E., 2008. Analyzing the cost effectiveness of Santiago, Chile's policy of using urban forests to improve air quality. *J. Environ. Manag.* 86, 148–157.
- Esilsson, C.S., Bjorklund, E., 2000. Analytical-scale microwave-assisted extraction. *J. Chromatogr. A* 902, 227-250.
- Espenshade, J., Thijs, S., Gawronski, S., Bove, H., Weyens, N., Vangronsveld, J., 2019. Influence of urbanization on epiphytic bacterial communities of the *Platanus x hispanica* tree leaves in a biennial study. *Front. Microbiol.* 10, 1-14.
- EU, 2011. Commission Regulation (EU) No 835/2011 of 19 August 2011 amending Regulation (EC) No 1881/2006 as regards maximum levels for polycyclic aromatic hydrocarbons in foodstuffs. *Official Journal of European Union* L215, 4–8.
- European Communities (Drinking Water) Regulations, 2007. A handbook on implementation for Water Services Authorities for Public Water Supplies (S.I. 278 of 2007). Section 2, pp. 1–12.
- Fabure, J., Meyer, C., Denayer, F., Gaudry, A., Gilbert, D., Bernard, N., 2010. Accumulation capacities of particulate matter in an acrocarpous and a pleurocarpous moss exposed at three differently polluted sites (industrial, urban and rural). *Water Air Soil Pollut.* 212, 205–217.
- Fan, Y., Chen, S.J., Li, Q.Q., Zeng, Y., Yan, X., Ma, B.X., 2020. Uptake of halogenated organic compounds (HOCs) into peanut and corn during the whole life cycle grown in an agricultural field. *Environ. Pollut.* 263, 114400.
- Farhat, A., Benmoussa, H., Bachoual, R., Nasfi, Z., Elfalleh, W., Romdhane, M., Bouajila, J., 2017. Efficiency of the optimized microwave assisted extractions on the yield, chemical

- composition and biological activities of Tunisian *Rosmarinus officinalis* L. essential oil. Food Bioprod. Process. 105, 224–233.
- Fazeli, F., Ardabili, S.M.S., Piravivanak, Z., Honarvar, M., Mooraki, N., 2020. Optimization of extraction conditions for polycyclic aromatic hydrocarbons determination in smoked rice using the high performance liquid chromatography-fluorescence detection. J. Food Meas. Charact. 14, 1236–1248.
- Fellet, G., Poscic, F., Licen, S., Marchiol, L., Musetti, R., Tolloi, A., Barbieri, P., Zerbi, G., 2016. PAHs accumulation on leaves of six evergreen urban shrubs: a field experiment. Atmos. Pollut. Res. 7, 915-924.
- Fenton, A.F., 1964. Atmospheric pollution of Belfast and its relationship to the lichen flora. Irish Nat. J. 14, 237-245.
- Finizio, A., Mackay, D., Bidleman, T., Harner, T., 1997. Octanol-air partition coefficient as a predictor of partitioning of semi-volatile organic chemicals to aerosols. Atmos. Environ. 31, 2289-2296.
- Florencia, T.M., Iván, T.B., Alejandra, C.H., 2022. Health risk assessment of exposure to polycyclic aromatic hydrocarbons in household indoor environments. Environ. Adv. 7, 100159.
- Flotron, V., Houessou, J., Bosio, A., et al., 2003. Rapid determination of polycyclic aromatic hydrocarbons in sewage sludges using microwave-assisted solvent extraction: comparison with other extraction methods. J. Chromatogr. A 999, 175–184.
- Foan, L., Domercq, M., Bermejo, R., Santamaria, J.M., Simon, V., 2015. Mosses as an integrating tool for monitoring PAH atmospheric deposition: Comparison with total deposition and evaluation of bioconcentration factors. A year-long case-study. Chemosphere 119, 452-458.
- Foan, L., Leblond, S., Thoni, L., Raynaud, C., Santamaria, J.M., Sebilo, M., Simon, V., 2014. Spatial distribution of PAH concentrations and stable isotope signatures ($\delta^{13}\text{C}$, $\delta^{15}\text{N}$) in mosses from three European areas - Characterization by multivariate analysis. Environ. Pollut. 184, 113-122.
- Foan, L., Sablayrolles, C., Elustondo, D., Lasheras, E., Gonzalez, L., Ederri, A., Simon, V., Santamaria, J.M., 2010. Reconstructing historical trends of polycyclic aromatic hydrocarbon deposition in a remote area of Spain using herbarium moss material. Atmos. Environ. 44, 3207-3214.

- Foan, L., Simon, V., 2012. Optimization of pressurized liquid extraction using a multivariate chemometric approach and comparison of solid-phase extraction cleanup steps for the determination of polycyclic aromatic hydrocarbons in mosses. *J. Chromatogr. A.* 1256, 22-31.
- Franzaring, J., van der Eerden, L.J.M., 2000. Accumulation of airborne persistent organic pollutants (POPs) in plants. *Basic Appl. Ecol.* 1, 25-30.
- Fred-Ahmadu, O.H., Benson, N.U., 2019. Polycyclic aromatic hydrocarbons (PAHs) occurrence and toxicity in *Camellia sinensis* and Herbal Tea. *Polycycl. Aromat. Compd.* 39, 383–393.
- Frei, M., Wissuwa, M., Pariasca-Tanaka, J., Chen, C.P., Sudekum, K.H., Kohno, Y., 2012. Leaf ascorbic acid level — Is it really important for ozone tolerance in rice? *Plant Physiol. Biochem.* 59, 63–70.
- Frempong, T.F., Boadi, N.O., Badu, M., 2021. Optimization of extraction conditions for polyphenols from the stem bark of *Funtumia elastica* (Funtum) utilizing response surface methodology. *AAS Open Res.* 4, 1–23.
- Fujiwara, F., Guinez, M., Cerutti, S., Smichowski, P., 2014. UHPLC-(+)APCI-MS/MS determination of oxygenated and nitrated polycyclic aromatic hydrocarbons in airborne particulate matter and tree barks collected in Buenos Aires city. *Microchem. J.* 116, 118-124.
- Galuszka, A., 2007. Distribution patterns of PAHs and trace elements in mosses *Hylocomium splendens* (Hedw.) B.S.G. and *Pleurozium schreberi* (Brid.) Mitt. from different forest communities: a case study, south-central Poland. *Chemosphere* 67, 1415-22.
- Gao, B., Guo, H., Wang, X.M., Zhao, X.Y., Ling, Z.H., Zhang, Z., Liu, T.Y., 2013. Tracer-based source apportionment of polycyclic aromatic hydrocarbons in PM_{2.5} in Guangzhou, southern China, using positive matrix factorization (PMF). *Environ. Sci. Pollut. Res.* 20, 2398-2409.
- Gao, Q., Haglund, P., Pommer, L., Jansson, S., 2015. Evaluation of solvent for pressurized liquid extraction of PCDD, PCDF, PCN, PCBz, PCPh and PAH in torrefied woody biomass. *Fuel* 154, 52-58.
- Garban, B., Blanchoud, H., Motelay-Massei, A., Chevreuil, M., Ollivon, D., 2002. Atmospheric bulk deposition of PAHs onto France: trends from urban to remote sites. *Atmos. Environ.* 36, 5395–5403.

- Garcia, M.R., Martins, C.C., 2021. A systematic evaluation of polycyclic aromatic hydrocarbons in South Atlantic subtropical mangrove wetlands under a coastal zone development scenario. *J Environ. Manage.* 277, 111421.
- Garty, J., 2001. Biomonitoring atmospheric heavy metals with lichens: theory and application. *Crit. Rev. Plant. Sci.* 20, 309-371.
- Gaur, P.K., Mishra, S., Kumar, A., Panda, B.P., 2014. Development and optimization of gastroretentive mucoadhesive microspheres of gabapentin by Box–Behnken design. *Artif. Cells Nanomed. Biotechnol.* 42, 167–77.
- Gemba, K., 2007. Shape Effects on Drag. Department of Aerospace Engineering, California State University (Accessed online on 17-04-2023).
- Gerdol, R., Bragazza, L., Marchesini, R., Medici, A., Pedrini, P., Benedetti, S., Bovolenta, A., Coppi, S., 2002. Use of moss (*Tortula muralis* Hedw.) for monitoring organic and inorganic air pollution in urban and rural sites in northern Italy. *Atmos. Environ.* 20, 4069–4075.
- German-Hernandez, M., Pino, V., Anderson, J.L., Afonso, A.M., 2011. Use of ionic liquid aggregates of 1-hexadecyl-3-butyl imidazolium bromide in a focused-microwave assisted extraction method followed by high-performance liquid chromatography with ultraviolet and fluorescence detection to determine the 15 + 1 EU priority PAHs in toasted cereals (“gofios”). *Talanta* 85, 1199-1206.
- Gerssen, A., McElhinney, M.A., Mulder, P.P.J., Bire, R., Hess, P., de Boer, J., 2009. Solid phase extraction for removal of matrix effects in lipophilic marine toxin analysis by liquid chromatography-tandem mass spectrometry. *Anal. Bioanal. Chem.* 394, 1213–1226.
- Ghafari, S., Kaviani, B., Sedaghatpour, S., Allahyari, M.S., 2020. Ecological potentials of trees, shrubs and hedge species for urban green spaces by multi criteria decision making. *Urban For. Urban Green.* 55, 126824.
- Ghosal, D., Ghosh, S., Dutta, T.K., Ahn, Y., 2016. Current state of knowledge in microbial degradation of polycyclic aromatic hydrocarbons (PAHs): A review. *Front. Microbiol.* 7, 1-27.
- Giergielewicz-Mozajska, H., Dabrowski, L., Namiesnik, J., 2001. Accelerated solvent extraction (ASE) in the analysis of environmental solid samples and some aspects of theory and practice. *Crit. Rev. Anal. Chem.* 31, 149-165.
- Gilbert, O.L., 1970. Further studies on the effect of sulphur dioxide on lichens and bryophytes. *New Phytol.* 69, 605–627.
- Gillies, J.A., Nickling, W.G., King, J., 2002. Drag coefficient and plant form response to wind speed in three plant species: burning bush (*Euonymus alatus*), Colorado Blue Spruce (*Picea*

- pungens glauca*), and Fountain Grass (*Pennisetum setaceum*). J. Geophys. Res. Atmos. 107, 1–15.
- Giraldez, P., Aboal, J.R., Fernandez, J.A., Di Guardo, A., Terzaghi, E., 2022. Plant-air partition coefficients for thirteen urban conifer tree species: Estimating the best gas and particulate matter associated PAH removers. Environ. Pollut. 315, 120409.
- Gobas, F.A.P.C., Mayer, P., Parkerton, T.F., Burgess, R.M., van de Meent, D., Gouin, T., 2018. A chemical activity approach to exposure and risk assessment of chemicals. Environ. Toxicol. Chem. 37, 1235–1251.
- Gocht, T., Klemm, O., Grathwohl, P., 2007. Long-term atmospheric bulk deposition of polycyclic aromatic hydrocarbons (PAHs) in rural areas of southern Germany. Atmos. Environ. 41, 1315–1327.
- Gomes, F.P., Oliva, M.A., Mielke, M.S., Almeida, A.A.F., Aquino, L.A., 2010. Osmotic adjustment, proline accumulation and cell membrane stability in leaves of *Cocos nucifera* submitted to drought stress. Sci. Hortic. 126, 379–384.
- Goswami, M., Kumar, V., Kumar, P., Singh, N., 2022. Prediction models for evaluating the impacts of ambient air pollutants on the biochemical response of selected tree species of Haridwar, India. Environ. Monit. Assess. 194, 1–16.
- Goswami, M., Kumar, V., Singh, N., Kumar, P., 2023. A biochemical and morphological study with multiple linear regression modeling–based impact prediction of ambient air pollutants on some native tree species of Haldwani City of Kumaun Himalaya, Uttarakhand, India. Environ. Sci. Pollut. Res. 30, 74900–74915.
- Goswami, P., Ohura, T., Guruge, K.S., Yoshioka, M., Yamanaka, N., Akiba, M., Munuswamy, N., 2016. Spatio-temporal distribution, source, and genotoxic potential of polycyclic aromatic hydrocarbons in estuarine and riverine sediments from southern India. Ecotoxicol. Environ. Saf. 130, 113–123.
- Govindaraju, M., Ganeshkumar, R.S., Muthukumaran, V.R., Visvanathan, P., 2012. Identification and evaluation of air-pollution tolerant plants around lignite-based thermal power station for greenbelt development. Environ. Sci. Pollut. Res. 19, 1210–1223.
- Graham, M.C., Allan, R., Fallick, A.E., Farmer, J.G., 2006. Investigation of extraction and clean-up procedures used in the quantification and stable isotopic characterisation of PAHs in contaminated urban soils. Sci. Total Environ. 360, 81–89.
- Graney, J.R., Landis, M.S., Puckett, K.J., Studabaker, W.B., Edgerton, E.S., Legge, A.H., Percy, K.E., 2017. Differential accumulation of PAHs, elements, and Pb isotopes by five

- lichen species from the Athabasca Oil Sands Region in Alberta, Canada. *Chemosphere* 184, 700-710.
- Gries, C., 1996. Lichens as Indicators of Air Pollution, in: Nash III, T.H. (Ed.), *Lichen Biology*. Cambridge University Press, Cambridge, pp. 240-254.
- Grosso, C., Ferreres, F., Gil-Izquierdo, A., Valentao, P., Sampaio, M., Lima, J., Andrade, P.B., 2014. Box–Behnken factorial design to obtain a phenolic-rich extract from the aerial parts of *Chelidonium majus* L. *Talanta* 130, 128-136.
- Grundstrom, M., Tang, L., Hallquist, M., Nguyen, H., Chen, D., Pleijel, H., 2015. Influence of atmospheric circulation patterns on urban air quality during the winter. *Atmos. Pollut. Res.* 6, 278–285.
- Guidotti, M., Stella, D., Owczarek, M., De Marco, A., De Simone, C., 2003. Lichens as polycyclic aromatic hydrocarbons bioaccumulators used in atmospheric pollution studies. *J. Chromatogr. A* 985, 185-90.
- Guiffard, I., Geny, T., Veyrand, B., Marchand, P., Pellouin-Grouhel, A., Le Bizec, B., Bichon, E., 2020. Quantification of light polycyclic aromatic hydrocarbons in seafood samples using on-line dynamic headspace extraction, thermodesorption, gas chromatography tandem mass spectrometry, based on an isotope dilution approach. *J. Chromatogr. A* 1619, 460906.
- Gunalan, S., Thangaiah, A., Rathnasamy, V.K., Janaki, J.G., Thiyagarajan, A., Kuppusamy, S., Arunachalam, L., 2023. Microwave-assisted extraction of biomolecules from moringa (*Moringa oleifera* Lam.) leaves var. PKM 1: A optimization study by response surface methodology (RSM). *Kuwait J. Sci.* 50, 339-344.
- Gupta, G.P., Kumar, B., Kulshrestha, U.C., 2016. Impact and pollution indices of urban dust on selected plant species for green belt development: mitigation of the air pollution in NCR Delhi, India. *Arab. J. Geosci.* 9, 136.
- Haghnazar, H., Sabbagh, K., Johannesson, K.H., Pourakbar, M., Aghayani, E., 2023. Phytoremediation capability of *Typha latifolia* L. to uptake sediment toxic elements in the largest coastal wetland of the Persian Gulf. *Mar. Pollut. Bull.* 188, 114699.
- Haiba, N.S.A., 2019. Polycyclic aromatic hydrocarbons (PAHs) in the River Nile, Egypt: occurrence and distribution. *Polycycl. Aromat. Comp.* 39, 425-433.
- Hajizadeh, Y., Mokhtari, M., Faraji, M., Abdollahnejad, A., Mohammadi, A., 2019. Biomonitoring of airborne metals using tree leaves: Protocol for biomonitor selection and spatial trend. *MethodsX* 6, 1694–1700.

- Haleyur, N., Shahsavari, E., Mansur, A.A., Koshlaf, E., Morrison, P.D., Osborn, A.M., Ball, A.S., 2016. Comparison of rapid solvent extraction systems for the GC–MS/MS characterization of polycyclic aromatic hydrocarbons in aged, contaminated soil. *MethodsX* 3, 364–370.
- Hall, D.G., Ammar, E.-D., Bowman, K.D., Stover, E., 2018. Epifluorescence and Stereomicroscopy of Trichomes Associated with Resistant and Susceptible Host Plant Genotypes of the Asian Citrus Psyllid (Hemiptera: Liviidae), Vector of Citrus Greening Disease Bacterium. *J. Microsc. Ultrastruct.* 6, 56–63.
- Han, D., Row, K.H., 2010. Recent applications of ionic liquids in separation technology. *Molecules* 15, 2405-2426.
- Han, Y., Lee, J., Haiping, G., Kim, K.H., Wanxi, P., Bhardwaj, N., Oh, J.M., Brown, R.J.C., 2022a. Plant-based remediation of air pollution: A review. *J. Environ. Manage.* 301, 113860.
- Han, F., Kota, S.H., Sharma, S., Zhang, J., Ying, Q., Zhang, H., 2022b. Modeling polycyclic aromatic hydrocarbons in India: Seasonal variations, sources and associated health risks. *Environ. Res.* 212, 113466.
- Haque, M.S., Singh, R.B., 2017. Air pollution and human health in Kolkata, India: A case study. *Climate* 5, 1-16.
- Haritash, A.K., Kaushik, C.P., 2009. Biodegradation aspects of polycyclic aromatic hydrocarbons (PAHs): A review. *J. Hazard Mater* 169, 1–15.
- Harmens, H., Foan, L., Simon, V., Mills, G., 2013. Terrestrial mosses as biomonitors of atmospheric POPs pollution: A review. *Environ. Pollut.* 173, 245-254.
- Harner, T., 1998. Octanol-air partition coefficient for describing particle/gas partitioning of aromatic compounds in urban air. *Environ. Sci. Technol.* 32, 1494-1502.
- Hartmann, H., Bahn, M., Carbone, M., Richardson, A.D., 2020. Plant carbon allocation in a changing world – challenges and progress: introduction to a Virtual Issue on carbon allocation. *New Phytol.* 227, 981–988.
- Hartmann, H., Trumbore, S., 2016. Understanding the roles of nonstructural carbohydrates in forest trees – from what we can measure to what we want to know. *New Phytol.* 211, 386–403.
- Hatzinger, P.B., Alexander, M., 1995. Effect of aging of chemicals in soil on their biodegradability and extractability. *Environ. Sci. Technol.* 29, 537–545.

- Hauser, B., Popp, P., 2001. Membrane-assisted solvent extraction of organochlorine compounds in combination with large-volume injection/gas chromatography-electron capture detection. *J. Sep. Sci.* 24, 551-560.
- Havaux, M., 2013. Carotenoid oxidation products as stress signals in plants. *Plant J.* 79, 597–606.
- Hawthorne, S.B., Grabanski, C.B., Martin, E., Miller, D.J., 2000. Comparisons of Soxhlet extraction, pressurized liquid extraction, supercritical fluid extraction and subcritical water extraction for environmental solids: recovery, selectivity and effects on sample matrix. *J. Chromatogr. A* 892, 421–433.
- Hawthorne, S.B., Grabanski, C.B., 2000. Correlating selective supercritical fluid extraction with bioremediation behaviour of PAHs in a field treatment plot. *Environ. Sci. Technol.* 34, 4103–4110.
- Hayat, S., Hayat, Q., Alyemeni, M.N., Wani, A.S., Pichtel, J., Ahmad, A., 2012. Role of proline under changing environments. *Plant Signal. Behav.* 7, 1456–1466.
- Henson, I.E., Mahalakshmi, V., Bidinger, F.R., Alagarswamy, G., 1981. Genotypic variation in pearl miller (*Pennisetum americanum* (L.) Leeke) in the ability to accumulate abscisic acid in response to water stress. *J. Exp. Bot.* 32, 899-910.
- Herbert, P., Silva, A.L., Joao, M.J., Santos, L., Alves, A., 2006. Determination of semi-volatile priority pollutants in landfill leachates and sediments using microwave-assisted headspace solid-phase microextraction. *Anal. Bioanal. Chem.* 386, 324–331.
- Herrera-Pool, E., Ramos-Diaz, A.L., Lizardi-Jimenez, M.A., Pech-Cohuo, S., Ayora-Talavera, T., Cuevas-Bernardino, J.C., Garcia-Cruz, U., Pacheco, N., 2021. Effect of solvent polarity on the ultrasound assisted extraction and antioxidant activity of phenolic compounds from habanero pepper leaves (*Capsicum chinense*) and its identification by UPLC-PDA-ESI-MS/MS. *Ultrason. Sonochem.* 76, 105658.
- Hiller, E., Bartal, M., 2006. Geochemical behaviour of naphthalene, phenanthrene and pyrene in soil: Kinetic and equilibrium sorption studies. *Slovak Geol. Mag.* 12, 3–9.
- Ho, K.F., Ho, S.S. H., Lee, S.C., Cheng, Y., Chow, J.C., Watson, J.G., Louie, P.K.K., Tian, L., 2009. Emissions of gas- and particle-phase polycyclic aromatic hydrocarbons (PAHs) in the Shing Mun tunnel Hong Kong. *Atmos. Environ.* 43, 6343–6351.
- Holoubek, I., Korinek, P., Seda, Z., Schneiderova, E., Holoubkova, I., Pacl, A., Triska, J., Cudlin, P., Caslavsky, J., 2000. The use of mosses and pine needles to detect persistent organic pollutants at local and regional scales. *Environ. Pollut.* 109, 283-92.

- Holt, E.A., Miller, S.W., 2011. Bioindicators: Using organisms to measure environmental impacts. *Nature Education Knowledge* 2, 1-10.
- Hossain, M.A., Hossain, M.D., Rohman, M.M., da Silva, J.A.T., Fujita, M., 2012. Onion major compounds (flavonoids, organosulfurs) and highly expressed glutathione-related enzymes: possible physiological interaction, gene cloning and stress response. In: Aguirre, C.B., Jaramillo, L.M. (Eds.), *Onion Consumption and Health*. Nova Publishers, New York, USA, pp. 49-90.
- Howsam, M., Jones, K.C., Ineson, P., 2000. PAHs associated with the leaves of three deciduous tree species. I — Concentrations and profiles. *Environ. Pollut.* 108, 413-424.
- Howsam, M., Jones, K.C., Ineson, P., 2001. PAHs associated with the leaves of three deciduous tree species. II: uptake during a growing season. *Chemosphere* 44, 155-164.
- Hsieh, Y.Z., Chang, A.C., 1997. Effects of analyte-matrix interactions on supercritical fluid extraction efficiencies of polycyclic aromatic hydrocarbons. *Anal. Chim. Acta* 342, 41-50.
- <http://emis.wbpcb.gov.in/airquality/citizenreport.do> (accessed on 11 July, 2021).
- <https://app.cpcbcr.com/ccr/#/caaqm-dashboard-all/caaqm-landing> (accessed on 11 July, 2021).
- https://cpbenvvis.nic.in/envis_newsletter/Air%20Quality%20of%20Delhi.pdf
- <https://in.usembassy.gov/embassy-consulates/kolkata/air-quality-data/>
- <https://monographs.iarc.fr/wp-content/uploads/2018/06/mono32.pdf>
- <https://news.un.org/en/story/2023/05/1136832>
- <https://timesofindia.indiatimes.com/city/kolkata/50-of-city-kids-have-airway-disorder-docs-blame-pollution/articleshow/104956414.cms>
- <https://timesofindia.indiatimes.com/city/kolkata/breathing-citys-toxic-air-is-like-smoking-doctors/articleshow/63423970.cms>
- <https://wrri.ncsu.edu/docs/partnerships/bmc/PAHFactSheet.pdf>
- <https://www.who.int/data/gho/data/themes/air-pollution>
- <https://www.who.int/data/gho/data/themes/topics/topic-details/GHO/ncd-mortality>
- Hu, T., Mao, Y., Ke, Y., Liu, W., Cheng, C., Shi, M., Zhang, Z., Zhang, J., Qi, S., Xing, X., 2021. Spatial and seasonal variations of PAHs in soil, air, and atmospheric bulk deposition along the plain to mountain transect in Hubei province, central China: air-soil exchange and long-range atmospheric transport. *Environ. Pollut.* 291, 118139.
- Huang, C.W., Lin, M.Y., Khlystov, A., Katul, G., 2013. The effects of leaf area density variation on the particle collection efficiency in the size range of ultrafine particles (UFP). *Environ. Sci. Technol.* 47, 11607–11615.

- Huang, X.F., Xue, L., He, L.Y., 2010. On-line measurement of organic aerosol elemental composition based on high resolution aerosol mass spectrometry (in Chinese). *Chin. Sci. Bull.* 55, 3391-3396.
- Hubert, A., Popp, P., Wenzel, K.-D., Engewald, W., Schuurmann, G., 2003. One-step cleanup for PAH residue analysis in plant matrices using size-exclusion chromatography. *Anal. Bioanal. Chem.* 376, 53–60.
- Hughes, D.E., 1983. Titrimetric determination of ascorbic acid with 2, 6-Dichlorophenol Indophenol in commercial liquid diets. *J. Pharm. Sci.* 72, 126–129.
- Huschek, G., Rawel, H.M., Schweikert, T., Henkel-Oberlander, J., Sagu, S.T., 2022. Characterization and optimization of microwave-assisted extraction of B-phycoerythrin from *Porphyridium purpureum* using response surface methodology and Doehlert design. *Bioresour. Technol. Rep.* 19, 101212.
- Hussain, K., Hoque, R.R., 2015. Seasonal attributes of urban soil PAHs of the Brahmaputra Valley. *Chemosphere* 119, 794–802.
- Hussain, K., Hoque, R.R., Balachandran, S., Medhi, S., Idris, M.G., Rahman, M., Hussain, F.L., 2018. Monitoring and risk analysis of PAHs in the environment. In: Hussain, C.M. (Ed.), *Handbook of Environmental Materials Management*. Springer International Publishing AG, pp. 1-35.
- Hussain, K., Rahman, M., Prakash, A., Sarma, K.P., Hoque, R.R., 2016. Atmospheric bulk deposition of PAHs over Brahmaputra Valley: characteristics and influence of meteorology. *Aerosol Air Qual. Res.* 16, 1675–1689.
- Hwang, H.M., Wade, T.L., 2008. Aerial distribution, temperature-dependent seasonal variation, and sources of polycyclic aromatic hydrocarbons in pine needles from the Houston metropolitan area, Texas, USA. *J. Environ. Sci. Health A* 43, 1243-1251.
- Hwang, H.-M., Wade, T.L., Sericano, J.L., 2003. Concentrations and source characterization of polycyclic aromatic hydrocarbons in pine needles from Korea, Mexico, and United States. *Atmos. Environ.* 37, 2259–2267.
- Hwang, S., Cutright, T.J., 2002. The impact of contact time on pyrene sorptive behavior by a sandy-loam soil. *Environ. Pollut.* 117, 371–378.
- Hyotylainen, T., Riekkola, M.L., 2008. Sorbent- and liquid-phase microextraction techniques and membrane-assisted extraction in combination with gas chromatographic analysis: a review. *Anal. Chim. Acta* 614, 27–37.
- IARC (International Agency for Research on Cancer), 1983. Polynuclear aromatic compounds, Part 1: Chemical, environmental and experimental data. IARC monographs on evaluation

- of the carcinogenic risk of chemicals to humans, World Health Organization, IARC, Lyon, France, Vol. 32, pp. 1–453.
- IARC, 2013. Outdoor air pollution a leading environmental cause of cancer deaths. Press release 221, Lyon/Geneva, pp. 1-4. (Retrieved from https://www.iarc.fr/wp-content/uploads/2018/07/pr221_E.pdf) (Accessed 12 December 2020).
- Ickert-Bond, S.M., Harris, A.J., Lutz, S., Wen, J., 2018. A detailed study of leaf micromorphology and anatomy of New World *Vitis* L. subgenus *Vitis* within a phylogenetic and ecological framework reveals evolutionary convergence. *J. Syst. Evol.* 56, 309–330.
- Idham, Z., Putra, N.R., Aziz, A.H.A., Zaini, A.S., Rasidek, N.A.M., Mili, N., Yunus, M.A.C., 2022. Improvement of extraction and stability of anthocyanins, the natural red pigment from roselle calyces using supercritical carbon dioxide extraction. *J. CO₂ Util.* 56, 101839.
- Ihunwo, O.C., Ibezim-Ezeani, M.U., DelValls, T.A., 2021. Human health and ecological risk of polycyclic aromatic hydrocarbons (PAHs) in sediment of Woji creek in the Niger Delta region of Nigeria. *Mar. Pollut. Bull.* 162, 111903
- IPCS (International Programme on Chemical Safety), 1998. Selected non-heterocyclic polycyclic aromatic hydrocarbons. <http://www.inchem.org/documents/ehc/ehc/ehc202.htm> (accessed 22 January 2019).
- Iqbal, M., Jura-Morawiec, J., Wloch, W., Mahmooduzzafar, 2010a. Foliar characteristics, cambial activity and wood formation in *Azadirachta indica* A. Juss. as affected by coal–smoke pollution. *Flora* 205, 61–71.
- Iqbal, M., Mahmooduzzafar, Nighat, F., Khan, P.R., 2010b. Photosynthetic, metabolic and growth responses of *Triumfetta rhomboidea* to coal-smoke pollution at different stages of plant ontogeny. *J. Plant Interact.* 5, 11–19.
- Iqbal, M., Srivastava, P.S., Siddiqi, T.O., 2000. Anthropogenic stresses in the environment and their consequences. In: Iqbal, M., et al. (Eds.), *Environmental Hazards, Plants and People*. CBS Publishers, New Delhi, pp. 1–40.
- Iwabuchi, A., Katte, N., Suwa, M., Goto, J., Inui, H., 2020. Factors regulating the differential uptake of persistent organic pollutants in cucurbits and non-cucurbits. *J. Plant Physiol.* 245, 153094.
- Jakubowska, N., Polkowska, Z., Namiesnik, J., Przyjazny, A., 2005. Analytical applications of membrane extraction for biomedical and environmental liquid sample preparation, *Crit. Rev. Anal. Chem.* 35, 217–235.

- Jamil, S., Abhilash, P.C., Singh, A., Singh, N., Behl, H.M., 2009. Fly ash trapping and metal accumulating capacity of plants: Implication for green belt around thermal power plants. *Landsc. Urban. Plan.* 92, 136–147.
- Jang, E., Alam, M.S., & Harrison, R.M., 2013. Source apportionment of polycyclic aromatic hydrocarbons in urban air using positive matrix factorization and spatial distribution analysis. *Atmos. Environ.* 79, 271–285.
- Janhall, S., 2015. Review on urban vegetation and particle air pollution — deposition and dispersion. *Atmos. Environ.* 105, 130–137.
- Janska, M., Tomaniova, M., Hajslova, J., Kocourek, V., 2004. Appraisal of “classic” and “novel” extraction procedure efficiencies for the isolation of polycyclic aromatic hydrocarbons and their derivatives from biotic matrices. *Anal. Chim. Acta* 520, 93–103.
- Jayalal, U., Oh, S.O., Park, J.S., Sung, J.H., Kim, S.H., Hur, J.S., 2016. Evaluation of air quality using lichens in three different types of forest in Korea. *Forest Sci. Technol.* 12, 1–8.
- Jeddi, K., Siddique, K.H.M., Chaieb, M., Hessini, K., 2021. Physiological and biochemical responses of *Lawsonia inermis* L. to heavy metal pollution in arid environments. *S. Afr. J. Bot.* 143, 7–16.
- Ji, X., Abakumov, E., 1, Polyako, V., Xie, X., Dongyang, W., 2019. The ecological impact of mineral exploitation in the Russian Arctic: A field-scale study of polycyclic aromatic hydrocarbons (PAHs) in permafrost-affected soils and lichens of the Yamal-Nenets autonomous region. *Environ. Pollut.* 255, 113239.
- Jia, J., Bi, C., Zhang, J., Chen, Z., 2019. Atmospheric deposition and vegetable uptake of polycyclic aromatic hydrocarbons (PAHs) based on experimental and computational simulations. *Atmos. Environ.* 204, 135–141.
- Jia, W., Davies, W.J., 2007. Modification of leaf apoplastic pH in relation to stomatal sensitivity to root-sourced abscisic acid signals. *Plant Physiol.* 143, 68–77.
- Jiang, G., Song, X., Xie, J., Shi, T., & Yang, Q., 2023. Polycyclic aromatic hydrocarbons (PAHs) in ambient air of Guangzhou city: Exposure levels, health effects and cytotoxicity. *Ecotoxicol. Environ. Saf.* 262, 115308.
- Jiang, Y., Fan, M., Hu, R., Zhao, J., Wu, Y., 2018. Mosses are better than leaves of vascular plants in monitoring atmospheric heavy metal pollution in urban areas. *Int. J. Environ. Res. Public Health* 15, 1–13.
- Jiao, X.C., Zuo, Q., Cao, J., Wu, S.P., Wang, Y.G., Tao, S., 2004. PAHs in foliar dust from Beijing urban area. *Environ. Sci.* 25, 162–165.

- Jin, R., Bandowe, B.A.M., Zheng, M., Liu, G., Nezikova, B., Prokes, R., Cupr, P., Klanova, J., Lammel, G., 2021. Atmospheric deposition of chlorinated and brominated polycyclic aromatic hydrocarbons in central Europe analyzed by GC-MS/MS. *Environ. Sci. Pollut. Res.* 28, 61360–61368.
- Jovanovic, M., Mudric, J., Drinic, Z., Matejic, J., Kitic, D., Bigovic, D., Savikin, K., 2022. Optimization of ultrasound-assisted extraction of bitter compounds and polyphenols from willow gentian underground parts. *Sep. Purif. Technol.* 281, 119868.
- Jovanovic, M.S., Milutinovic, M., Lazarevic, Z., Mudric, J., Matejic, J., Kitic, D., Savikin, K., 2023. Heat-and microwave-assisted extraction of bioactive compounds from *Gentiana asclepiadea* L. underground parts: Optimization and comparative assessment using response surface methodology. *J. Appl. Res. Med. Aromat. Plants* 34, 100483.
- Ju, C., Zhang, H.C., Wu, R.L., Dong, S.X., Yao, S.J., Wang, F.Y., Cao, D.T., Xu, S.J., Fang, H., Yu, Y.L., 2020. Upward translocation of acetochlor and atrazine in wheat plants depends on their distribution in roots. *Sci. Total Environ.* 703, 135636.
- Juan, Z., Xiu-jun, W., Jia-ping, W., Wei-xia, W., 2014. Carbon and nitrogen contents in typical plants and soil profiles in Yanqi Basin of Northwest China. *J. Integr. Agric.* 13, 648–656.
- Jung, K.H., Kim, J.K., Noh, J.H., Eun, J.W., Bae, H.J., Kim, M.G., et al., 2013. Characteristic molecular signature for the early detection and prediction of polycyclic aromatic hydrocarbons in rat liver. *Toxicol. Lett.* 216, 1–8.
- Kacharava, N., Chanishvili, S., Badridze, G., Chkhubianishvili, E., Janukashvili, N., 2009. Effect of seed irradiation on the content of antioxidants in leaves of Kidney bean, Cabbage and Beet cultivars. *Aust. J. Crop. Sci.* 3, 137–145.
- Kakareka, S.V., Kukharchyk, T.I., 2003. PAH emission from the open burning of agricultural debris. *Sci. Total Environ.* 308, 257–261.
- Kakareka, S.V., Kukharchyk, T.I., Khomich, V.S., 2005. Study of PAH emission from the solid fuels combustion in residential furnaces. *Environ. Pollut.* 133, 383–387.
- Kalbe, U., Berger, W., Eckardt, J., Simon, F.G., 2008. Evaluation of leaching and extraction procedures for soil and waste. *Waste Manag* 28, 1027–1038.
- Kamankesh, M., Mohammadi, A., Hosseini, H., Modarres Tehrani, Z., 2015. Rapid determination of polycyclic aromatic hydrocarbons in grilled meat using microwave-assisted extraction and dispersive liquid–liquid microextraction coupled to gas chromatography–mass spectrometry. *Meat Sci.* 103, 61–67.

- Kamarudin, N.A., Muhamad, N., Salleh, N.N.H.N., Tan, S.C., 2021. Impact of solvent selection on phytochemical content, recovery of tannin and antioxidant activity of *Quercus infectoria* Galls. *Pharmacogn. J.* 13, 1195–1204.
- Kamble, P., Bodhane, P.S., Beig, G., Awale, M., Mukkannawar, U., Mane, A.V., Mujumdar, M., Kuchekar, S.R., Patil, V.N., 2021. Impact of transport sector emissions on biochemical characteristics of plants and mitigation strategy in Pune, India. *Environ. Chall.* 4, 100081.
- Kameda, T., 2011. Atmospheric chemistry of polycyclic aromatic hydrocarbons and related compounds. *J. Health Sci.* 57, 504–11.
- Kameda, Y., Shirai, J., Komai, T., Nakanishi, J., Masunaga, S., 2005. Atmospheric polycyclic aromatic hydrocarbons: size distribution, estimation of their risk and their depositions to human respiratory tract. *Sci. Total Environ.* 340, 71–80.
- Kang, D.H., Rothman, N., Poirier, M.C., Greenberg, A., Hsu, C.H., Schwartz, B.S., Baser, M.E., Groopman, J.D., Weston, A., Strickland, P.T., 1995. Interindividual differences in the concentration of 1-hydroxypyrene-glucuronide in urine and polycyclic aromatic hydrocarbon-DNA adducts in peripheral white blood cells after charbroiled beef consumption. *Carcinogenesis* 16, 1079–85.
- Kargar, N., Matin, G., Matin, A.A., Buyukisik, H.B., 2017. Biomonitoring, status and source risk assessment of polycyclic aromatic hydrocarbons (PAHs) using honeybees, pine tree leaves, and propolis. *Chemosphere* 186, 140-150.
- Karmakar, D., Deb, K., Padhy, P.K., 2021. Ecophysiological responses of tree species due to air pollution for biomonitoring of environmental health in urban area. *Urban Clim.* 35, 1-11.
- Karmakar, D., Padhy, P.K., 2019. Air pollution tolerance, anticipated performance, and metal accumulation indices of plant species for greenbelt development in urban industrial area. *Chemosphere* 237, 124522.
- Karnchanasest, B., Satayavibul, A., 2005. Orange jasmine leaves as an indicator of atmospheric polycyclic aromatic hydrocarbons. *Songklanakarin J. Sci. Technol.* 27, 877-888.
- Katoch, K., Nazir, R., Khamparia, A., Pandey, B., Dey, A., Pandey, D.K., 2023. Optimization of microwave-assisted extraction of plumbagin from *Plumbago zeylanica* by response surface methodology and adaptive neuro-fuzzy inference system modelling. *Ind Crops Prod* 203, 117107.
- Katsoyiannis, A., Terzi, E., Cai, Q.-Y., 2007. On the use of PAH molecular diagnostic ratios in sewage sludge for the understanding of the PAH sources. Is this use appropriate? *Chemosphere* 69, 1337–1339.

- Kaupp, H., Blumenstock, M., McLachlan, M.S., 2000. Retention and mobility of atmospheric particle-associated organic pollutant PCDD/Fs and PAHs in maize leaves. *New Phytol.* 148, 473-480.
- Kaur, M., Nagpal, A.K., 2017. Evaluation of air pollution tolerance index and anticipated performance index of plants and their application in development of green space along the urban areas. *Environ. Sci. Pollut. Res.* 24, 18881–18895.
- Kaur, P., Kumar Pandey, D., Gupta, R.C., Dey, A., 2019. Simultaneous microwave assisted extraction and HPTLC quantification of mangiferin, amarogentin, and swertiamarin in *Swertia* species from Western Himalayas. *Ind. Crops Prod.* 132, 449–459.
- Kaur, R., Pandey, P., 2021. Air pollution, climate change, and human health in Indian cities: A brief review. *Front. Sustain. Cities* 3, 1–18.
- Khalid, N., Masood, A., Noman, A., Aqeel, M., Qasim, M., 2019. Study of the responses of two biomonitor plant species (*Datura alba* & *Ricinus communis*) to roadside air pollution. *Chemosphere* 235, 832–841.
- Khan, M., Ahmad, R., Khan, M.D., Rizwan, M., et al., 2018. Trace elements in abiotic stress tolerance. In: Hasanuzzaman, M., Fujita, M., Oku, H., Nahar, K., Hawrylak-Nowak, B. (Eds.), *Plant Nutrients and Abiotic Stress Tolerance*. Springer, Singapore, pp. 137-151.
- Khan, M.F., Latif, M.T., Lim, C.H., Amil, N., Jaafar, S.A., Dominick, D., Nadzir, M.S.M., Sahani, M., Tahir, N.M., 2015. Seasonal effect and source apportionment of polycyclic aromatic hydrocarbons in PM_{2.5}. *Atmos. Environ.* 106, 178-190.
- Khan, Z., Troquet, J., Vachelard, C., 2005. Sample preparation and analytical techniques for determination of polyaromatic hydrocarbons in soils. *Int. J. Environ. Sci. Tech.* 2, 275-286.
- Khanoranga, Khalid, S., 2019. Phytomonitoring of air pollution around brick kilns in Balochistan province Pakistan through air pollution index and metal accumulation index. *J. Clean. Prod.* 229, 727–738.
- Khuman, S.N., Chakraborty, P., Cincinelli, A., Snow, D., Kumar, B., 2018. Polycyclic aromatic hydrocarbons in surface waters and riverine sediments of the Hooghly and Brahmaputra Rivers in the Eastern and Northeastern India. *Sci. Total Environ.* 636, 751-760.
- Kim, K.H., Jahan, S.A., Kabir, E., Brown, R.J.C., 2013. A review of airborne polycyclic aromatic hydrocarbons (PAHs) and their human health effects. *Environ. Int.* 60, 71–80.
- Kim, K.W., 2020. Methanol fixation for scanning electron microscopy of plants. *Appl. Microsc.* 50, 1–6.

- Kim, L., Jeon, H.-J., Kim, Y.-C., Yang, S.-H., Choi, H., Kim, T.-O., Lee, S.-E., 2019. Monitoring polycyclic aromatic hydrocarbon concentrations and distributions in rice paddy soils from Gyeonggi-do, Ulsan, and Pohang. *Appl. Biol. Chem.* 62, 1-8.
- Kimbrough, K.L., Dickhut, R.M., 2006. Assessment of polycyclic aromatic hydrocarbon input to urban wetlands in relation to adjacent land use. *Mar. Pollut. Bull.* 52, 1355-1363.
- Klamerus-Iwan, A., Blonska, E., Lasota, J., Waligorski, P., Kalandyk, A., 2018. Seasonal variability of leaf water capacity and wettability under the influence of pollution in different city zones. *Atmos. Pollut. Res.* 9, 455-463.
- Klingberg, J., Strandberg, B., Sjöman, H., Taube, M., Wallin, G., Pleijel, H., 2022. Polycyclic aromatic hydrocarbon (PAH) accumulation in *Quercus palustris* and *Pinus nigra* in the urban landscape of Gothenburg Sweden. *Sci. Total Environ.* 805, 150163.
- Kobayashi, R., Cahill, T.M., Okamoto, R.A., Maddalena, R.L., Kado, N.Y., 2007. Controlled exposure chamber study of uptake and clearance of airborne polycyclic aromatic hydrocarbons by wheat grain. *Environ. Sci. Technol.* 41, 7934-7940.
- Kobe, R.K., Iyer, M., Walters, M.B., 2010. Optimal partitioning theory revisited: nonstructural carbohydrates dominate root mass responses to nitrogen. *Ecology* 91, 166–179.
- Kodnik, D., Carniel, F.C., Lichen, S., Tolloi, A., Barbieri, P., Tretiach, M., 2015. Seasonal variations of PAHs content and distribution patterns in a mixed land use area: A case study in NE Italy with the transplanted lichen *Pseudevernia furfuracea*. *Atmos. Environ.* 113, 255-263.
- Komp, P., McLachlan, M.S., 1997. Interspecies variability of the plant/air partitioning of polychlorinated biphenyls. *Environ. Sci. Technol.* 31, 2944–2948.
- Konczak, B., Cempa, M., Pierzchała, L., Deska, M., 2021. Assessment of the ability of roadside vegetation to remove particulate matter from the urban air. *Environ. Pollut.* 268, 115465.
- Kootstra, P.R., Straub, M.H.C., Stil, G.H., van der Velde, E.G., Hesselink, W., Land, C.C.J., 1995. Solid-phase extraction of polycyclic aromatic hydrocarbons from soil samples. *J. Chromatogr. A* 697, 123–129.
- Krauss, M., Wilcke, W., Martius, C., Bandeira, A.G., Garcia, M.V.B., Amelung, W., 2005. Atmospheric versus biological sources of polycyclic aromatic hydrocarbons (PAHs) in a tropical rain forest environment. *Environ. Pollut.* 135, 143-154.
- Krommer, V., Zechmeister, H.G., Roder, I., Scharf, S., Hanus-İllnar, A., 2007. Monitoring atmospheric pollutants in the biosphere reserve Wienerwald by a combined approach of biomonitoring methods and technical measurements. *Chemosphere* 67, 1956–1966.

- Kuang, Y.W., Li, J., Hou, E.Q., 2015. Lipid-content-normalized polycyclic aromatic hydrocarbons (PAHs) in the xylem of conifers can indicate historical changes in regional airborne PAHs. *Environ. Pollut.* 196, 53-59.
- Kuiper, P.J.C., 1985. Environmental changes and lipid metabolism of higher plants. *Physiol. Plant.* 64, 118-122.
- Kumar, S., Negi, S., Maiti, P., 2017. Biological and analytical techniques used for detection of polyaromatic hydrocarbons. *Environ. Sci. Pollut. Res.* 24, 25810–25827.
- Kumar, Y., Mina, U., Rajput, V.D., Minkina, T., Kumar, S.N., Harit, R.C., Garg, M.C., 2023. Investigating the biochemical responses in wheat cultivars exposed to thermal power plant emission. *Bull. Environ. Contam. Toxicol.* 110, 1–8.
- Kumari, R., Chaturvedi, P., Ansari, N.G., Murthy, R.C., Patel, D.K., 2012. Optimization and validation of an extraction method for the analysis of polycyclic aromatic hydrocarbons in chocolate candies. *J. Food Sci.* 77, T34–T40.
- Kuo, C.Y., Hsu, Y.W., Lee, H.S., 2003. Study of human exposure to particulate PAHs using personal air samplers. *Arch. Environ. Contam. Toxicol.* 44, 454–9.
- Landis, M.S., Studabaker, W.B., Pancras, J.P., Graney, J.R., Puckett, K., White, E.M., Edgerton, E.S., 2019. Source apportionment of an epiphytic lichen biomonitor to elucidate the sources and spatial distribution of polycyclic aromatic hydrocarbons in the Athabasca Oil Sands Region, Alberta, Canada. *Sci. Total Environ.* 654, 1241-1257.
- Larsen, R.K., Baker, J.E., 2003. Source apportionment of polycyclic aromatic hydrocarbons in the urban atmosphere: A comparison of three methods. *Environ. Sci. Tech.* 37, 1873–1881.
- Latwal, M., Sharma, S., Kaur, I., Nagpal, A.K., 2023. Global assessment of air pollution indices of trees and shrubs for biomonitoring and green belt development – A tabulated review. *Water Air Soil Pollut.* 234, 205.
- Lau, E.V., Gan, S., Ng, H.K., 2010. Extraction techniques for polycyclic aromatic hydrocarbons in soils. *Int. J. Anal. Chem.* 1-9 (Article ID 398381).
- Lau, E.V., Gan, S., Ng, H.K., Poh, P.E., 2014. Extraction agents for the removal of polycyclic aromatic hydrocarbons (PAHs) from soil in soil washing technologies. *Environ. Pollut.* 184, 640–649.
- Lawal, A.T., 2017. Polycyclic aromatic hydrocarbons. A review. *Cogent Environ. Sci.* 3, 1-89.
- Lawlor, D.W., 2002. Limitation to photosynthesis in water-stressed leaves: stomata vs. metabolism and the role of ATP. *Ann. Bot.* 89, 871–885.

- Lee, B.C., Shimizu, Y., Matsuda, T., Matsui, S., 2005. Characterization of polycyclic aromatic hydrocarbons (PAHs) in different size fractions in deposited road particles (DRPs) from Lake Biwa Area Japan. *Environ. Sci. Tech.* 39, 7402–7409.
- Lehndorff, E., Schwark, L., 2004. Biomonitoring of air quality in the Cologne Conurbation using pine needles as a passive sampler — Part II: Polycyclic aromatic hydrocarbons (PAH). *Atmos. Environ.* 38, 3793–3808.
- Lehndorff, E., Schwark, L., 2010. Biomonitoring of air quality in the Cologne Conurbation using pine needles as a passive sampler – Part III: Major and trace elements. *Atmos. Environ.* 44, 2822–2829.
- Leonard, R.J., McArthur, C., Hochuli, D.F., 2016. Particulate matter deposition on roadside plants and the importance of leaf trait combinations. *Urban For. Urban Green.* 20, 249–253.
- Letellier, M., Budzinski, H., Bellocq, J., Connan, J., 1999. Focused microwave-assisted extraction of polycyclic aromatic hydrocarbons and alkanes from sediments and source rocks. *Org. Geochem.* 30, 1353–1365.
- Li, C., Ji, J., Wang, G., Li, Z., Wang, Y., Fan, Y., 2020. Over-expression of LcPDS, LcZDS, and LcCRTISO, genes from Wolfberry for carotenoid biosynthesis, enhanced carotenoid accumulation, and salt tolerance in Tobacco. *Front. Plant Sci.* 11, 1–12.
- Li, G.L., Lang, Y.H., Gao, M.S., Yang, W., Peng, P., Wang, X.M., 2014. Carcinogenic and mutagenic potencies for different PAHs sources in coastal sediments of Shandong Peninsula. *Mar. Pollut. Bull.* 84, 418–423.
- Li, Q., Chen, B., 2014. Organic pollutant clustered in the plant cuticular membranes: visualizing the distribution of phenanthrene in leaf cuticle using two-photon confocal scanning laser microscopy. *Environ. Sci. Technol.* 48, 4774–4781.
- Li, Q., Li, Y., Zhu, L., Xing, B., Chen, B., 2017. Dependence of plant uptake and diffusion of polycyclic aromatic hydrocarbons on the leaf surface morphology and micro-structures of cuticular waxes. *Sci. Rep.* 7, 1–11.
- Li, X., Zhang, T., Sun, F., Song, X., Zhang, Y., Huang, F., Yuan, C., Yu, H., Zhang, G., Qi, F., Shao, F., 2021. The relationship between particulate matter retention capacity and leaf surface micromorphology of ten tree species in Hangzhou, China. *Sci. Total Environ.* 771, 144812.
- Li, Y., Li, Q., Chen, B., 2016a. Organic pollutant penetration through fruit polyester skin: a modified three-compartment diffusion model. *Sci. Rep.* 6, 1–14.

- Li, X.B., Lu, Q.C., Lu, S.J., He, H.D., Peng, Z.R., Gao, Y., Wang, Z.Y., 2016b. The impacts of roadside vegetation barriers on the dispersion of gaseous traffic pollution in urban street canyons. *Urban For. Urban Green.* 17, 80–91.
- Li, Y., Chen, B., Zhu, L., 2010. Single-solute and bi-solute sorption of phenanthrene and pyrene onto pine needle cuticular fractions. *Environ. Pollut.* 158, 2478–2484.
- Li, Y., He, N., Hou, J., Xu, L., Liu, C., Zhang, J., Wang, Q., Zhang, X., Wu, X., 2018. Factors influencing leaf chlorophyll content in natural forests at the biome scale. *Front. Ecol. Evol.* 6, 1–10.
- Li, Y., Hoi, K.I., Mok, K.M., Yuen, K.V., 2023. Emerging air quality monitoring methods. In: Li, Y., Hoi, K.I., Mok, K.M., Yuen, K.V. (Eds.), *Air Quality Monitoring and Advanced Bayesian Modeling*. Elsevier, pp. 105–172.
- Li, Y., Sallach, J.B., Zhang, W., Boyd, S.A., Li, H., 2019. Insight into the distribution of pharmaceuticals in soil-water-plant systems. *Water Res.* 152, 38–46.
- Liang, J., Fang, H.L., Zhang, T.L., Wang, X.X., Liu, Y.D., 2017. Heavy metal in leaves of twelve plant species from seven different areas in Shanghai, China. *Urban For. Urban Green.* 27, 390–398.
- Liang, Y., Zhou, L., Zhang, X., Yu, H., Guo, M., Yu, J., Wang, X., Yang, M., Lou, Z., Luo, F., Sun, H., Chen, Z., 2021. Uptake, accumulation, translocation, and subcellular distribution of perchlorate in tea (*Camellia sinensis* L.) plants. *J. Agric. Food Chem.* 69, 4655–4662.
- Li-bin, L., Yan, L., Jin-ming, L., Ning, T., Kazuichi, H., Tsuneaki, M., 2007. Development of analytical methods for polycyclic aromatic hydrocarbons (PAHs) in airborne particulates: A review. *J. Environ. Sci.* 19, 1–11.
- Lichtenthaler, H.K., 1987. Chlorophylls and carotenoids: Pigments of photosynthetic biomembranes. In: Douce, R., Packer, L. (Eds.), *Methods in Enzymology*. Academic Press Inc., New York, 148, pp. 350–382.
- Lichtenthaler, H.K., Buschmann, C., 2001. Chlorophylls and carotenoids: Measurement and characterization by UV-Vis spectroscopy. *Current Protocols in Food Analytical Chemistry* 1, F4.3.1–F4.3.8.
- Lichtenthaler, H.K., Wellburn, A.R., 1983. Determinations of total carotenoids and chlorophylls a and b of leaf extracts in different solvents. *Biochem. Soc. Trans.* 11, 591–592.

- Ligaray, M., Baek, S.S., Kwon, H.O., Choi, S.D., Cho, K.H., 2016. Watershed-scale modeling on the fate and transport of polycyclic aromatic hydrocarbons (PAHs). *J. Hazard. Mater.* 320, 442–457.
- Liguori, L., Heggstad, K., Hove, H.T., Julshamn, K., 2006. An automated extraction approach for isolation of 24 polyaromatic hydrocarbons (PAHs) from various marine matrixes. *Anal. Chim. Acta* 573–574, 181–188.
- Lin, C.C., Chen, S.J., Huang, K.L., Hwang, W.I., Chang-Chien, G.P., Lin, W.Y., 2005. Characteristics of metals in nano/ultrafine/fine/coarse particles collected beside a heavily trafficked road. *Environ. Sci. Technol.* 39, 8113–8122.
- Lin, D., Zhu, L., He, W., Tu, Y., 2006. Tea plant uptake and translocation of polycyclic aromatic hydrocarbons from water and around air. *J. Agric. Food Chem.* 54, 3658–3662.
- Liu, D., Lin, T., Syed, J.H., Cheng, Z., Xu, Y., Li, K., Zhang, G., Li, J., 2017a. Concentration, source identification, and exposure risk assessment of PM_{2.5}-bound parent PAHs and nitro-PAHs in atmosphere from typical Chinese cities. *Sci. rep.* 7, 10398.
- Liu, M., Wang, Z., Li, S., Lu, X., et al., 2017b. Changes in specific leaf area of dominant plants in temperate grasslands along a 2500-km transect in northern China. *Sci. Rep.* 7, 1–9.
- Liu, X., Bai, Z., Yu, Q., Cao, Y., Zhou, W., 2017c. Polycyclic aromatic hydrocarbons in the soil profiles (0–100 cm) from the industrial district of a large open-pit coal mine, China. *RSC Adv.* 7, 28029–28037.
- Liu, K., Han, W., Pan, W.P., Riley, J.T., 2001. Polycyclic aromatic hydrocarbon (PAH) emissions from a coal-fired pilot FBC system. *J. Hazard Mater* 84, 175–188.
- Liu, Q., He, W.Q., Aguedo, M., Xia, X., Bai, W.B., Dong, Y.Y., Song, J.Q., Richel, A., Goffin, D., 2021. Microwave-assisted alkali hydrolysis for cellulose isolation from wheat straw: Influence of reaction conditions and non-thermal effects of microwave. *Carbohydr. Polym.* 253, 117170.
- Liu, Q., Sun, Y., Hu, B., Liu, Z.R., Akio, S., Wang, Y.S., 2012. In situ measurement of PM₁ organic aerosol in Beijing winter using a high-resolution aerosol mass spectrometer (in Chinese). *Chin. Sci. Bull.* 57, 819–826.
- Liu, Q., Wang, X., Yang, R., Yang, L., Sun, B., Zhu, L., 2019. Uptake kinetics, accumulation, and long-distance transport of organophosphate esters in plants: impacts of chemical and plant properties. *Environ. Sci. Technol.* 53, 4940–4947.
- Liu, X., Shi, X.Q., Peng, Z.R., He, H.D., 2023. Quantifying the effects of urban fabric and vegetation combination pattern to mitigate particle pollution in near-road areas using machine learning. *Sustain. Cities Soc.* 93, 104524.

- Lloyd, S.W., Tucker, C.S., 1988. Comparison of three solvent systems for extraction of chlorophyll a from fish pond phytoplankton communities. *J. World Aquacult. Soc.* 19, 36-40.
- Lohmann, R., Lammel, G., 2004. Adsorptive and absorptive contributions to the gas-particle partitioning of polycyclic aromatic hydrocarbons: State of knowledge and recommended parametrization for modeling. *Environ. Sci. Technol.* 38, 3793-3803.
- Lopez-Avila, V., Benedicto, J., Bauer, K.M., 1998. Stability of organochlorine and organophosphorus pesticides when extracted from solid matrixes with microwave energy. *J. AOAC. Int.* 81, 1224-1232.
- Loppi, S., Pozo, K., Estellano, V.H., Corsolini, S., Sardella, G., Paoli, L., 2015. Accumulation of polycyclic aromatic hydrocarbons by lichen transplants: comparison with gas-phase passive air samplers. *Chemosphere* 134, 39–43.
- Lu, T., Lin, X., Chen, J., Huang, D., Li, M., 2019. Atmospheric particle retention capacity and photosynthetic responses of three common greening plant species under different pollution levels in Hangzhou. *Glob. Ecol. Conserv.* 20, e00783.
- Lu, Y., Han, H., Huang, X., Yi, Y., Wang, Z., Chai, Y., Zhang, X., Lu, C., Wang, C., Chen, H., 2023. Uptake and translocation of organic pollutants in *Camellia sinensis* (L.): a review. *Environ. Sci. Pollut. Res.* 30, 118133–118148.
- Lu, Y., Han, H., Jiang, C., Liu, H., Wang, Z., Chai, Y., Zhang, X., Qiu, J., Chen, H., 2024. Uptake, accumulation, translocation and transformation of seneciophylline (Sp) and seneciophylline-N-oxide (SpNO) by *Camellia sinensis* L. *Environ. Int.* 188, 108765.
- Lukowski, A., Popek, R., Karolewski, P., 2020. Particulate matter on foliage of *Betula pendula*, *Quercus robur*, and *Tilia cordata*: deposition and ecophysiology. *Environ. Sci. Pollut. Res.* 27, 10296–11030.
- Luo, Y., Sun, J., Wang, P., Li, Y., Li, H., Xiao, K., Yang, R., Zhang, Q., Jiang, G., 2020. Age dependence accumulation of organochlorine pesticides and PAHs in needles with different forest types, southeast Tibetan Plateau. *Sci. Total Environ.* 716, 137176.
- Luque-Garcia, J.L., Luque de Castro, M.D., 2003. Where is microwave based analytical treatment for solid sample pre-treatment going?. *Trends Anal. Chem.* 22, 90-99.
- Ma, C., Ye, S., Lin, T., Ding, X., Yuan, H., Guo, Z., 2014. Source apportionment of polycyclic aromatic hydrocarbons in soils of wetlands in the Liao River Delta, Northeast China. *Mar. Pollut. Bull.* 80, 160-167.

- Ma, X., Huang, P., Dang, X., Ai, Y., Zheng, D., Chen, H., 2019a. MWCNTs/MnO₂ nanocomposite-based polythiophene coating for solid-phase microextraction and determination of polycyclic aromatic hydrocarbons in soil. *Microchem. J.* 146, 1026–1032.
- Ma, Y., Wang, B., Zhang, R., Gao, Y., Zhang, X., Li, Y., Zuo, Z., 2019b. Initial simulated acid rain impacts reactive oxygen species metabolism and photosynthetic abilities in *Cinnamomum camphora* undergoing high temperature. *Ind. Crop. Prod.* 135, 352–361.
- Mackay, D., Foster, K.L., Patwa, Z., Webster, E., 2006. Chemical partitioning to foliage: the contribution and legacy of Davide Calamari. *Environ. Sci. Pollut. Res.* 13, 2-8.
- Maddalena, R.L., McKone, T.E., Kado, N.Y., 2002. Exposure chamber measurements of mass transfer and partitioning at the plant/air interface. *Environ. Sci. Technol.* 36, 3577-3585.
- Madej, K., 2009. Microwave-assisted and cloud-point extraction in determination of drugs and other bioactive compounds. *TrAC Trend. Anal. Chem.* 28, 436-446.
- Madheshiya, P., Gupta, G.S., Sahoo, A., Tiwari, S., 2022. Biomonitoring tools and bioprogramming: An overview. In: Tiwari, S., Agrawal, S. (Eds.), *New Paradigms in Environmental Biomonitoring Using Plants*. Elsevier, pp. 341-366.
- Majd, M., Nojavan, S., 2021. Determination of polycyclic aromatic hydrocarbons in soil, tree leaves, and water samples by magnetic dispersive solid-phase extraction based on β -cyclodextrin functionalized graphene oxide followed by GC-FID. *Microchem. J.* 171, 106852.
- Malav, L.C., Kumar, S., Islam, S., Chaudhary, P., Khan, S.A., 2022. Assessing the environmental impact of air pollution on crops by monitoring air pollution tolerance index (APTI) and anticipated performance index (API). *Environ. Sci. Pollut. Res.* 29, 50427–50442.
- Mali, P.S., Kumar, P., 2023. Optimization of microwave assisted extraction of bioactive compounds from black bean waste and evaluation of its antioxidant and antidiabetic potential in vitro. *Food Chem. Adv.* 3, 100543.
- Malik, J., Mandal, S.C., 2022. Extraction of herbal biomolecules. In: Mandal, S.C., Nayak, A.K., Dhara, A.K. (Eds.), *Herbal Biomolecules in Healthcare Applications*. Academic Press, pp. 21–46.
- Mallah, M.A., Changxing, L., Mallah, M.A., Noreen, S., Liu, Y., Saeed, M., Xi, H., Ahmed, B., Feng, F., Mirjat, A.A., Wang, W., Jabar, A., Naveed, M., Li, J.H., Zhang, Q., 2022. Polycyclic aromatic hydrocarbon and its effects on human health: An overview. *Chemosphere* 296, 133948.

- Manahan, S.E., 2005. Environmental Chemistry, eighth ed. CRC Press LLC, Boca Raton, Florida, USA.
- Mandal, K., Dhal, N.K., 2022. Pollution resistance assessment of plants around chromite mine based on anticipated performance index, dust capturing capacity and metal accumulation index. *Environ. Sci. Pollut. Res.* 29, 63357–63368.
- Manoli, E., Samara, C., 1999. Polycyclic aromatic hydrocarbons in natural waters: sources, occurrence and analysis. *Trends Anal. Chem.* 18, 717–428.
- Manzetti, S., 2013. Polycyclic aromatic hydrocarbons in the environment: Environmental fate and transformation. *J. Polycycl. Aromat. Comp.* 33, 311–330.
- Martinez-Ramos, T., Benedito-Fort, J., Watson, N.J., Ruiz-Lopez, I.I., Che-Galicia, G., Corona-Jimenez, E., 2020. Effect of solvent composition and its interaction with ultrasonic energy on the ultrasound-assisted extraction of phenolic compounds from mango peels (*Mangifera indica* L.). *Food Bioprod. Process.* 122, 41–54.
- Mary Leema, J.T., Persia Jothy, T., Dharani, G., 2022. Rapid green microwave assisted extraction of lutein from *Chlorella sorokiniana* (NIOT-2)—process optimization. *Food Chem.* 372, 131151.
- Masih, J., Dyavarchetty, S., Nair, A., Taneja, A., Singhvi, R., 2019. Concentration and sources of fine particulate associated polycyclic aromatic hydrocarbons at two locations in the western coast of India. *Environ. Technol. Innov.* 13, 179–188.
- Masih, J., Singhvi, R., Kumar, K., Jain, V.K., Taneja, A., 2012. Seasonal variation and sources of polycyclic aromatic hydrocarbons (PAHs) in indoor and outdoor air in a semi arid tract of northern India. *Aerosol Air Qual. Res.* 12, 515–525.
- Masiol, M., Hofer, A., Squizzato, S., Piazza, R., Rampazzo, G., Pavoni, B., 2012. Carcinogenic and mutagenic risk associated to airborne particle-phase polycyclic aromatic hydrocarbons: a source apportionment. *Atmos. Environ.* 60, 375–382.
- Mason, T.J., Chemat, F., Vinatoru, M., 2011. The extraction of natural products using ultrasound or microwaves. *Curr. Org. Chem.* 15, 237–247.
- McLachlan, M.S., 1999. Framework for the interpretation of measurements of SOC_s in plants. *Environ. Sci. Technol.* 33, 1799–1804.
- Mehmood, T., Zhu, T., Ahmad, I., Li, X., 2020. Ambient PM_{2.5} and PM₁₀ bound PAHs in Islamabad, Pakistan: Concentration, source and health risk assessment. *Chemosphere* 257, 127187.

- Metrak, M., Aneta, E., Wilkomirski, B., Staszewski, T., Suska-Malawska, M., 2016. Interspecific differences in foliar 1 PAHs load between Scots pine, birch, and wild rosemary from three polish peat bogs. *Environ. Monit. Assess.* 188, 1-13.
- Meylan, W.M., Howard, P.H., 2005. Estimating octanol–air partition coefficients with octanol–water partition coefficients and Henry’s law constants. *Chemosphere*, 61, 640-644.
- Mibei, E.K., Ambuko, J., Giovannoni, J.J., Onyango, A.N., Owino, W.O., 2017. Carotenoid profiling of the leaves of selected African eggplant accessions subjected to drought stress. *Food Sci. Nutr.* 5, 113–122.
- Migaszewski, Z.M., Galuszka, A., Crock, J.G., Lamothe, P.J., Dolegowska, S., 2009. Interspecies and interregional comparisons of the chemistry of PAHs and trace elements in mosses *Hylocomium splendens* (Hedw.) B.S.G. and *Pleurozium schreberi* (Brid.) Mitt. from Poland and Alaska. *Atmos. Environ.* 43, 1464–1473.
- Migaszewski, Z.M., Galuszka, A., Paslawski, P., 2002. Polynuclear aromatic hydrocarbons, phenols, and trace metals in selected soil profiles and plant bioindicators in the Holy Cross Mountains, South-Central Poland. *Environ. Int.* 28, 303-313.
- Miller, E.L., Nason, S.L., Karthikeyan, K.G., Pedersen, J.A., 2016. Root uptake of pharmaceuticals and personal care product ingredients. *Environ. Sci. Tech.* 50, 525–541.
- Mina, U., Chandrashekara, T.K., Kumar, S.N., Meena, M.C., et al., 2018. Impact of particulate matter on basmati rice varieties grown in Indo-Gangetic Plains of India: Growth, biochemical, physiological and yield attributes. *Atmos. Environ.* 188, 174–184.
- Mishra, N., Ayoko, G.A., Morawska, L., 2016. Atmospheric polycyclic aromatic hydrocarbons in the urban environment: Occurrence, toxicity and source apportionment. *Environ. Pollut.* 208, 110-117.
- Mishra, S., Aeri, V., 2016. Optimization of microwave-assisted extraction conditions for preparing lignan-rich extract from *Saraca asoca* bark using Box–Behnken design. *Pharm. Biol.* 54, 1255-1262.
- Mohamed, A.H., M’hamed, M., Fatma, M., Hichem, B.M., 2016. Air Pollution Mapping with Bio-Indicators in Urban Areas, in: Sallis, P. (Ed.), *Air Quality*. IntechOpen, Rijeka, pp. 163-181.
- Mokrani, A., Madani, K., 2016. Effect of solvent, time and temperature on the extraction of phenolic compounds and antioxidant capacity of peach (*Prunus persica* L.) fruit. *Sep. Purif. Technol.* 162, 68–76.

- Mollaei, S., Sedighi, F., Habibi, B., Hazrati, S., Asgharian, P., 2019. Extraction of essential oils of *Ferulago angulata* with microwave-assisted hydrodistillation. *Ind. Crops Prod.* 137, 43–51.
- Moradi, P., Mahdavi, A., Khoshkam, M., Iriti, M., 2017. Lipidomics unravels the role of leaf lipids in Thyme plant response to drought stress. *Int. J. Mol. Sci.* 18, 1-15.
- Morakinyo, O.M., Mukhola, M.S., Mokgobu, M.I., 2020. Concentration levels and carcinogenic and mutagenic risks of PM_{2.5}-bound polycyclic aromatic hydrocarbons in an urban–industrial area in South Africa. *Environ. Geochem. Health* 42, 2163–2178.
- Mueller, A., Ulrich, N., Hollmann, J., Zapata Sanchez, C.E., Rolle-Kampczyk, U.E., von Bergen, M., 2019. Characterization of a multianalyte GC-MS/MS procedure for detecting and quantifying polycyclic aromatic hydrocarbons (PAHs) and PAH derivatives from air particulate matter for an improved risk assessment. *Environ. Pollut.* 255, 112967.
- Mukherjee, A., Agrawal, S.B., Agrawal, M., 2020. Responses of tropical tree species to urban air pollutants: ROS/RNS formation and scavenging. *Sci. Total Environ.* 710, 1-14.
- Mukhopadhyay, S., Dutta, R., Das, P., 2020. A critical review on plant biomonitors for determination of polycyclic aromatic hydrocarbons (PAHs) in air through solvent extraction techniques. *Chemosphere* 251, 1-21.
- Mukhopadhyay, S., Dutta, R., Dhara, A., 2021. Assessment of air pollution tolerance index of *Murraya paniculata* (L.) Jack in Kolkata metro city, West Bengal India. *Urban Clim.* 39, 100977.
- Mukhopadhyay, S., Dutta, R., Dhara, A., Das, P., 2023. Biomonitoring of polycyclic aromatic hydrocarbons (PAHs) by *Murraya paniculata* (L.) Jack in South Kolkata, West Bengal, India: spatial and temporal variations. *Environ. Geochem. Health* 45, 5761-5781.
- Muller, J.F., Hawker, D.W., McLachlan, M.S., Connell, D.W., 2001. PAHs, PCDD/Fs, PCBs and HCB in leaves from Brisbane, Australia. *Chemosphere* 43, 507-515.
- Munyeza, C.F., Rohwer, E.R., Forbes, P.B.C., 2019. A review of monitoring of airborne polycyclic aromatic hydrocarbons: An African perspective. *Trends Environ. Anal. Chem.* 24, e00070.
- Murakami, M., Abe, M., Kakumoto, Y., Kawano, H., Fukasawa, H., Saha, M., Takada, H., 2012. Evaluation of ginkgo as a bimonitor of airborne polycyclic aromatic hydrocarbons. *Atmos. Environ.* 54, 9-17.
- Nadali, A., Leili, M., Bahrami, A., Karami, M., & Afkhami, A., 2021. Phase distribution and risk assessment of PAHs in ambient air of Hamadan, Iran. *Ecotoxicol Environ Saf* 209, 111807.

- Nadgorska-Socha, A., Kandziora-Ciupa, M., Trzesicki, M., Barczyk, G., 2017. Air pollution tolerance index and heavy metal bioaccumulation in selected plant species from urban biotopes. *Chemosphere* 183, 471-482.
- Nakazato, R.K., Esposito, M.P., Cardoso-Gustavson, P., Bulbovas, P., Pedroso, A.N.V., Silveira de Assis, P.I.L., Domingos, M., 2018. Efficiency of biomonitoring methods applying tropical bioindicator plants for assessing the phytotoxicity of the air pollutants in SE, Brazil. *Environ. Sci. Pollut. Res.* 25, 19323–19337.
- NAMP, 2023. National air quality monitoring program. URL: https://cpcb.nic.in/about_namp/.
- Nanos, G.D., Ilias, I.F., 2007. Effects of inert dust on olive (*Olea europaea* L.) leaf physiological parameters. *Environ. Sci. Pollut. Res.* 14, 212–214.
- Nascimbene, J., Tretiach, M., Corana, F., Schiavo, F.L., Kodnik, D., Dainese, M., Mannucci, B., 2014. Patterns of traffic polycyclic aromatic hydrocarbon pollution in mountain areas can be revealed by lichen biomonitoring: A case study in the Dolomites (Eastern Italian Alps). *Sci. Total Environ.* 475, 90-96.
- National Atmospheric Emissions Inventory (NAEI), 2013. Overview of Air Pollutants. <http://naei.defra.gov.uk/overview/ap-overview> (accessed 21 January 2019).
- National Research Council, 1983. Polycyclic Aromatic Hydrocarbons: Evaluation of Sources and Effects. The National Academies Press, Washington, DC, p. 476.
- Ncube, B., Finnie, J.F., Van Staden, J., 2013. Dissecting the stress metabolic alterations in in vitro *Cyrtanthus* regenerants. *Plant Physiol. Biochem.* 65, 102–110.
- Ncube, S., Poliwoda, A., Tutu, H., Wieczorek, P., Chimuka, L., 2016. Multivariate optimization of the hollow fibre liquid phase microextraction of muscimol in human urine samples. *J Chromatogr B Analyt Technol Biomed Life Sci.* 1033–1034, 372-381.
- Ncube, S., Tavengwa, N., Soqaka, A., Cukrowska, E., Chimuka, L., 2018. Development of a single format membrane assisted solvent extraction-molecularly imprinted polymer technique for extraction of polycyclic aromatic hydrocarbons in wastewater followed by gas chromatography mass spectrometry determination. *J. Chromatogr. A* 1569, 36–43.
- Ngamkhae, N., Monthakantirat, O., Chulikhit, Y., Boonyarat, C., Boonyarat, C., Maneenet, J., Khamphukdee, C., Kwankhao, P., Pitiporn, S., Daodee, S., 2022. Optimization of extraction method for Kleeb Bua Daeng formula and comparison between ultrasound-assisted and microwave-assisted extraction. *J. Appl. Res. Med. Aromat. Plants* 28, 100369.
- Nieuwoudt, C., Pieters, R., Quinn, L.P., Kylin, H., Borgen, A.R., Bouwman, H., 2011. Polycyclic aromatic hydrocarbons (PAHs) in soil and sediment from industrial, residential,

- and agricultural areas in Central South Africa: An initial assessment. *J. Soil Sediment Contam.* 20, 188-204.
- Nikolaou, K., Masclet, P., Mouvier, G., 1984. Sources and chemical reactivity of polynuclear aromatic hydrocarbons in the atmosphere—A critical review. *Sci. Total Environ.* 32, 103-132.
- Nisbet, I.C.T., Lagoy, P.K., 1992. Toxic equivalency factors (TEFs) for polycyclic aromatic hydrocarbons (PAHs). *Regul. Toxicol. Pharmacol.* 16, 290-300.
- Niu, L., Zhou, Y., Xu, C., Zhang, C., Zhou, J., Zhang, X., Liu, W., 2019a. Solid fuel combustion as a major contributor of polycyclic aromatic hydrocarbons in rural China: Evidence from emission inventory and congener profiles in tree bark. *Environ. Pollut.* 246, 621-629.
- Niu, L., Xu, C., Zhou, Y., Liu, W., 2019b. Tree bark as a biomonitor for assessing the atmospheric pollution and associated human inhalation exposure risks of polycyclic aromatic hydrocarbons in rural China. *Environ. Pollut.* 246, 398-407.
- Niu, X., Wang, B., Wei, W., 2020. Response of the particulate matter capture ability to leaf age and pollution intensity. *Environ. Sci. Pollut. Res.* 27, 34258–34269.
- Nizzetto, L., Pastore, C., Liu, X., Camporini, P., Stroppiana, D., Herbert, B., Boschetti, M., Zhang, G., Brivio, P.A., Jones, K.C., Di Guardo, A., 2008. Accumulation parameters and seasonal trend for PCBs in temperate and boreal forest plant species. *Environ. Sci. Technol.* 42, 5911–5916.
- Nobel, W., Beismann, H., Franzaring, J., Kostka-Rick, R., Wagner, G., Erhardt, W., 2005. Standardised biological measurement procedures to determine and evaluate the effect of air pollution on plants (biomonitoring) in Germany- Status and perspectives. *Gefahrstoffe Reinhaltung der Luft* 65, 478-484.
- Nobrega, J.A., Trevizan, L.C., Araujo, G.C.L., Nogueira, A.R.A., 2002. Focused-microwave-assisted strategies for sample preparation. *Spectrochim. Acta B* 57, 1855-1876.
- Noctor, G., Foyer, C.H., 1998. Ascorbate and glutathione: keeping active oxygen under control. *Annu. Rev. Plant Physiol. Plant Mol. Biol.* 49, 249–279.
- Northcott, G.L., Jones, K.C., 2000. A review of experimental methodologies and analytical techniques for the characterisation of organic compound bound residues in soil and sediment. *Environ. Pollut.* 108, 19-43.
- Nowak, D.J., Crane, D.E., Stevens, J.C., 2006. Air pollution removal by urban trees and shrubs in the United States. *Urban For. Urban Green.* 4, 115-123.

- Nylander, W., 1866. Les lichens du Jardin de Luxembourg. Bull. Soc. Bot. Fr. 13, 364-372.
- Obayori, O.S., Ilori, M.O., Amund, O.O., 2013. Bacterial metabolism of pyrene, in: Ruzicka, P., Pyrene, Kral T. (Eds.), Pyrene: Chemical Properties, Biochemistry, Applications and Toxic Effects. Nova Science Publishers, New York, pp. 79–108.
- Obrist, D., Zielinska, B., Perlinger, J.A., 2015. Accumulation of polycyclic aromatic hydrocarbons (PAHs) and oxygenated PAHs (OPAHs) in organic and mineral soil horizons from four U.S. remote forests. Chemosphere 134, 98–105.
- Odabasi, M., Cetin, E., Sofuoglu, A., 2006. Determination of octanol–air partition coefficients and supercooled liquid vapor pressures of PAHs as a function of temperature: Application to gas–particle partitioning in an urban atmosphere. Atmos. Environ. 40, 6615–6625.
- Ogunkunle, C.O., Suleiman, L.B., Oyediji, S., Awotoye, O.O., Fatoba, P.O., 2015. Assessing the air pollution tolerance index and anticipated performance index of some tree species for biomonitoring environmental health. Agrofor. Syst. 89, 447–454.
- Ohura, T., Amagai, T., Fusaya, M., Matsushita, H., 2004. Polycyclic aromatic hydrocarbons in indoor and outdoor environments and factors affecting their concentrations. Environ. Sci. Technol. 38, 77–83.
- Ohura, T., Horii, Y., Kojima, M., Kamiya, Y., 2013. Diurnal variability of chlorinated polycyclic aromatic hydrocarbons in urban air, Japan. Atmos. Environ. 81, 84–91.
- Oishi, Y., 2018. Comparison of moss and pine needles as bioindicators of transboundary polycyclic aromatic hydrocarbon pollution in central Japan. Environ. Pollut. 234, 330-338.
- Oksanen, I., 2006. Ecological and biotechnological aspects of lichens. Appl. Microbiol. Biotechnol. 73, 723-734.
- Onete, M., Pop, O.G., Gruia, R., 2010. Plants as indicators of environmental conditions of urban spaces from central parks of Bucharest. Environ. Eng. Manag. J. 9, 1637-1645.
- Orecchio, S., 2007. PAHs associated with the leaves of *Quercus ilex* L.: Extraction, GC–MS analysis, distribution and sources: Assessment of air quality in the Palermo (Italy) area. Atmos. Environ. 41, 8669-8680.
- Orecchio, S., 2010. Assessment of polycyclic aromatic hydrocarbons (PAHs) in soil of a Natural Reserve (Isola delle Femmine) (Italy) located in front of a plant for the production of cement. J. Hazard. Mater. 173, 358–368.
- Orecchio, S., Gianguzza, A., Culotta, L., 2008. Absorption of polycyclic aromatic hydrocarbons by *Pinus* bark: Analytical method and use for environmental pollution monitoring in the Palermo area (Sicily, Italy). Environ. Res 107, 371-379.

- Orsi, M., Sanderson, W.E., Essex, J.W., 2009. Permeability of small molecules through a lipid bilayer: A multiscale simulation study. *J. Phys. Chem. B* 113, 12019–12029.
- Ossola, R., Farmer, D., 2024. The chemical landscape of leaf surfaces and its interaction with the atmosphere. *Chem. Rev.* 124, 5764–5794.
- Otvos, E., Kozak, I.O., Fekete, J., Sharma, V.K., Tuba, Z., 2004. Atmospheric deposition of polycyclic aromatic hydrocarbons (PAHs) in mosses (*Hypnum cupressiforme*) in Hungary. *Sci. Total Environ.* 330, 89–99.
- Pabby, K.A., Swain, B., Maria, A., 2017. Recent advances in smart integrated membrane assisted liquid extraction technology. *Chem. Eng. Process.: Process Intensif.* 120, 27–56.
- Pandey, A.K., Pandey, M., Tripathi, B.D., 2015a. Air pollution tolerance index of climber plant species to develop vertical greenery systems in a polluted tropical city. *Landsc. Urban Plan.* 144, 119–127.
- Pandey, A.K., Pandey, M., Mishra, A., Tiwary, S.M., Tripathi, B.D., 2015b. Air pollution tolerance index and anticipated performance index of some plant species for development of urban forest. *Urban For. Urban Green.* 14, 866–871.
- Pandey, A.K., Pandey, M., Tripathi, B.D., 2016. Assessment of Air Pollution Tolerance Index of some plants to develop vertical gardens near street canyons of a polluted tropical city. *Ecotoxicol. Environ. Saf.* 134, 358–364.
- Pandey, S.K., Kim, K.-H., Brown, R.J., 2011. A review of techniques for the determination of polycyclic aromatic hydrocarbons in air. *TrAC Trends Anal. Chem.* 30, 1716–1739.
- Papa, S., Bartoli, G., Nacca, F., D’Abrosca, B., Cembrola, E., Pellegrino, A., Fiorentino, A., Fuggi, A., Fioretto, A., 2012. Trace metals, peroxidase activity, PAHs contents and ecophysiological changes in *Quercus ilex* leaves in the urban area of Caserta (Italy). *J. Environ. Manag.* 113, 501–509.
- Park, J.S., Wade, T.L., Sweet, S., 2001. Atmospheric distribution of polycyclic aromatic hydrocarbons and deposition to Galveston Bay, Texas, USA. *Atmos. Environ.* 35, 3241–3249.
- Park, S.S., Kim, Y.J., Kang, C.H., 2002. Atmospheric polycyclic aromatic hydrocarbons in Seoul Korea. *Atmos. Environ.* 36, 2917–2924.
- Parmar, T.K., Rawtani, D., Agrawal, Y.K., 2016. Bioindicators: the natural indicator of environmental pollution. *Front. Life Sci.* 9, 110–118.
- Patel, A.B., Shaikh, S., Jain, K.R., Desai, C., Madamwar, D., 2020. Polycyclic aromatic hydrocarbons: Sources, toxicity, and remediation approaches. *Front. Microbiol.* 11, 1–23.

- Patel, K., Chaurasia, M., Rao, K.S., 2023. Urban dust pollution tolerance indices of selected plant species for development of urban greenery in Delhi. *Environ. Monit. Assess.* 195, 1–21.
- Paterson, S., Mackay, D., 1994. A model of organic chemical uptake by plants from soil and the atmosphere. *Environ. Sci. Technol.* 28, 2259–2266.
- Pathak, J., Rajneesh, Ahmed H., Singh, D.K., Singh, P.R., Kumar, D., Kannaujiya, V.K., Singh, S.P., Sinha, R.P., 2019. Oxidative stress and antioxidant defense in plants exposed to ultraviolet radiation. In: Hasanuzzaman, M., Fotopoulos, V., Nahar, K., Fujita, M. (Eds.), *Reactive Oxygen, Nitrogen and Sulfur Species in Plants: Production, Metabolism, Signaling and Defense Mechanisms*. John Wiley & Sons, Inc., pp. 371–420.
- Pathak, V., Tripathi, B., Mishra, V., 2011. Evaluation of Anticipated Performance Index of some tree species for green belt development to mitigate traffic generated noise. *Urban For. Urban Green.* 10, 61–66.
- Pathan, A.K., Bond, J., Gaskin, R.E., 2008. Sample preparation for scanning electron microscopy of plant surfaces--horses for courses. *Micron* 39, 1049–61.
- Patnaik, P., 2007. A comprehensive guide to the hazardous properties of chemical substances (3rd Ed.). Hoboken: John Wiley & Sons, pp.1059.
- Paull, N.J., Krix, D., Irga, P.J., Torpy, F.R., 2021. Green wall plant tolerance to ambient urban air pollution. *Urban For. Urban Green.* 63, 127201.
- Peng, R.H., Xiong, A. S., Xue, Y., Fu, X.Y., Gao, F., Zhao, W., Tian Y.S., Yao, Q.H., 2008. Microbial biodegradation of polyaromatic hydrocarbons. *FEMS Microbiol. Rev.* 32, 927–955.
- Peng, Y.Y., Liao, L.L., Liu, S., Nie, M.M., et al., 2019. Magnesium deficiency triggers SGR-mediated chlorophyll degradation for magnesium remobilization. *Plant Physiol.* 181, 262–275.
- Pereira Netto, A.D., Barreto, R.P., Moreira, J.C., Arbilla, G., 2007. Spatial distribution of polycyclic aromatic hydrocarbons in *Terminalia catappa* L. (Combretaceae) bark from a selected heavy road traffic area of Rio de Janeiro City, Brazil. *J. Hazard. Mater.* 142, 389–96.
- Pereira, G.M., da Silva Caumo, S.E., do Nascimento, E.Q.M., Parra, Y.J., de Castro Vasconcellos, P., 2019. Polycyclic aromatic hydrocarbons in tree barks, gaseous and particulate phase samples collected near an industrial complex in Sao Paulo (Brazil). *Chemosphere* 237, 124499.

- Pereira, L.B.S., Costa-Silva, R., Felix, L.P., Agra, M.F., 2018. Leaf morphoanatomy of “mororo” (*Bauhinia* and *Schnella*, Fabaceae). *Rev. Bras. Farmacogn.* 28, 383–392.
- Perera, F., Herbstman, J., 2011. Prenatal environmental exposures, epigenetics, and disease. *Reprod. Toxicol.* 31, 363–73.
- Perez, L.M., Yue, Z., Saha, S., Dean, J.F.D., Jenkins, J.N., Stelly, D.M., Tseng, T.-M., 2022. Absorption and translocation of [^{14}C]2, 4-dichlorophenoxyacetic acid in herbicide-tolerant chromosome substitution lines of *Gossypium hirsutum* L. *Front. Agron.* 4, 1-10.
- Petkovsek, S.A.S., Batic, F., Lasnik, C.R., 2007. Norway spruce needles as bioindicator of air pollution in the area of influence of the Sostanj Thermal Power Plant, Slovenia. *Environ. Pollut.* 151, 287–291.
- Pies, C., Hoffmann, B., Petrowsky, J., Yang, Y., Ternes, T.A., Hofmann, T., 2008. Characterization and source identification of polycyclic aromatic hydrocarbons (PAHs) in river bank soils. *Chemosphere* 72, 1594–1601.
- Pinelo, M., Sineiro, J., Nunez, M.J., 2006. Mass transfer during continuous solid–liquid extraction of antioxidants from grape byproducts. *J. Food Eng.* 77, 57–63.
- Pleijel, H., Klingberg, J., Strandberg, B., Sjoman, H., Tarvainen, L., Wallin, G., 2022. Differences in accumulation of polycyclic aromatic compounds (PACs) among eleven broadleaved and conifer tree species. *Ecol. Indic.* 145, 109681.
- Pongpiachan, S., 2015. Impacts of agricultural waste burning on the enhancement of PM 2.5-bound polycyclic aromatic hydrocarbons in northern Thailand. *WIT Trans Ecol Envir* 198, 3–14.
- Poole, C.F., 2004. Chromatographic and spectroscopic methods for the determination of solvent properties of room temperature ionic liquids. *J. Chromatogr. A* 1037, 49-82.
- Popek, R., Gawronska, H., Gawronski, S.W., 2015. The level of particulate matter on foliage depends on the distance from the source of emission. *Int. J. Phytoremediation* 17, 1262–1268.
- Popek, R., Gawronska, H., Wrochna, M., Gawronski, S.W., Saebo, A., 2013. Particulate matter on foliage of 13 woody species: deposition on surfaces and phytostabilisation in waxes—a 3-year study. *Int. J. Phytoremediation* 15, 245–256.
- Popek, R., Mahawar, L., Shekhawat, G.S., Przybysz, A., 2022. Phyto-cleaning of particulate matter from polluted air by woody plant species in the near-desert city of Jodhpur (India) and the role of heme oxygenase in their response to PM stress conditions. *Environ. Sci. Pollut. Res.* 29, 70228–70241.

- Porra, R.J., Scheer, H., 2019. Towards a more accurate future for chlorophyll a and b determinations: the inaccuracies of Daniel Arnon's assay. *Photosynth. Res.* 140, 215–219.
- Povinec, P.P., Hirose, K., Aoyama, M., Tateda, Y., 2021. Radioactivity impact on Japan. In: Povinec, P.P., Hirose, K., Aoyama, M., Tateda, Y. (Eds.), *Fukushima Accident (Second Edition)*. Elsevier B.V., pp. 245–384.
- Pragasam, L.A., Ganesan, A., 2022. Assessment of air pollutants and pollution tolerant tree species for the development of Greenbelt at Narasapura Industrial Estate, India. *Geol. Ecol. Landsc.* 1–9.
- Prajapati, S., Tripathi, B., 2008a. Seasonal variation of leaf dust accumulation and pigment content in plant species exposed to urban particulates pollution. *J. Environ. Qual.* 37, 865–870.
- Prajapati, S.K., Tripathi, B.D., 2008b. Anticipated Performance Index of some tree species considered for green belt development in and around an urban area: A case study of Varanasi city, India. *J. Environ. Manage.* 88, 1343–1349.
- Prajapati, S.K., Tripathi, B.D., 2008c. Biomonitoring seasonal variation of urban air polycyclic aromatic hydrocarbons (PAHs) using *Ficus benghalensis* leaves. *Environ. Pollut.* 151, 543–548.
- Prajapati, S.K., 2012. Ecological effect of airborne particulate matter on plants. *Environ. Skept. Crit.* 1, 12–22.
- Prasad, B.J., Rao, D.N., 1982. Relative sensitivity of a leguminous and a cereal crop to sulphur dioxide pollution. *Environ. Pollut.* 29, 57–70.
- Prevot, A.B., Gulmini, M., Zelano, V., & Pramauro, E., 2001. Microwave-assisted extraction of polycyclic aromatic hydrocarbons from marine sediments using nonionic surfactant solutions. *Anal. Chem.* 73, 3790–3795.
- Prieto, A., Telleria, O., Etxebarria, N., Fernandez, L.A., Usobiaga, A., Zuloaga, O., 2008. Simultaneous preconcentration of a wide variety of organic pollutants in water samples. Comparison of stir bar sorptive extraction and membrane-assisted solvent extraction. *J. Chromatogr. A* 1214, 1–10.
- Prusty, B.A.K., Mishra, P.C., Azeez, P.A., 2005. Dust accumulation and leaf pigment content in vegetation near the national highway at Sambalpur, Orissa, India. *Ecotoxicol. Environ. Saf.* 60, 228–235.
- Przybysz, A., Nersisyan, G., Gawronski, S.W., 2019. Removal of particulate matter and trace elements from ambient air by urban greenery in the winter season. *Environ. Sci. Pollut. Res.* 26, 473–482.

- Przybysz, A., Saebo, A., Hanslin, H.M., Gawronski, S.W., 2014. Accumulation of particulate matter and trace elements on vegetation as affected by pollution level, rainfall and the passage of time. *Sci. Total Environ.* 481, 360–369.
- Pu, C., Xiong, J., Zhao, R., Fang, J., Liao, Y., Song, Q., Zhang, J., Zhang, Y., Liu, H., Liu, W., Chen, W., Zhou, H., Qi, S., 2022. Levels, sources, and risk assessment of polycyclic aromatic hydrocarbons (PAHs) in soils of karst trough zone, Central China. *J. Hydrol.* 614, 128568.
- Pugh, T.A.M., MacKenzie, A.R., Whyatt, J.D., Hewitt, C.N., 2012. Effectiveness of green infrastructure for improvement of air quality in urban street canyons. *Environ. Sci. Technol.* 46, 7692–7699.
- Pullagurala, V.L.R., Rawat, S., Adisa, I.O., Hernandez-Viezcas, J.A., Peralta-Videa, J.R., Gardea-Torresdey, J.L., 2018. Plant uptake and translocation of contaminants of emerging concern in soil. *Sci. Total Environ.* 636, 1585–1596.
- Putra, I.G.A.M., Permana, I.D.G.M., Suhendra, L., 2021. Optimization of dielectric constant and ratio material to solvent using response surface methodology on antioxidant activity Teter leaves extract (*Solanum erianthum*). *Int. J. Curr. Microbiol. Appl. Sci.* 10, 376–392.
- Puy-Alquiza, M.J., Reyes, V., Wrobel, K., Wrobel, K., Elguera, J.C.T., Miranda-Aviles, R., 2016. Polycyclic aromatic hydrocarbons in urban tunnels of Guanajuato city (Mexico) measured in deposited dust particles and in transplanted lichen *Xanthoparmelia mexicana* (Gyeln.) Hale. *Environ. Sci. Pollut. Res.* 23, 11947–11956.
- Qazi, H.L., Jan, N., Ramazan, S., John, R., 2019. Protein modification in plants in response to abiotic stress. In: Dar, T.A., Singh, L.R. (Eds.), *Protein Modificomics*. Academic Press, pp. 171–201.
- Qi, A., Wang, P., Lv, J., Zhao, T., Huang, Q., Wang, Y., Zhang, X., Wang, M., Xiao, Y., Yang, L., Ji, Y., Wang, W., 2023. Distributions of PAHs, NPAHs, OPAHs, BrPAHs, and ClPAHs in air, bulk deposition, soil, and water in the Shandong Peninsula, China: Urban-rural gradient, interface exchange, and long-range transport. *Ecotoxicol. Environ. Saf.* 265, 115494.
- Qiu, Y., Guan, D., Song, W., Huang, K., 2009. Capture of heavy metals and sulfur by foliar dust in urban Huizhou, Guangdong Province, China. *Chemosphere* 75, 447–452.
- Qiu, Y.Y., Gong, Y.X., Ni, H.G., 2019. Contribution of soil erosion to PAHs in surface water in China. *Sci. Total Environ.* 686, 497–504.

- Quintana, S.E., Salas, S., Garcia-Zapateiro, L.A., 2021. Bioactive compounds of mango (*Mangifera indica*): A review of extraction technologies and chemical constituents. *J. Sci. Food Agric.* 101, 6186–6192.
- Rai, P.K., 2016. Impacts of particulate matter pollution on plants: implications for environmental biomonitoring. *Ecotoxicol. Environ. Saf.* 129, 120–136.
- Rajput, M., Agrawal, M., 2005. Biomonitoring of air pollution in a seasonally dry tropical suburban area using wheat transplants. *Environ. Monit. Assess.* 101, 39–53.
- Ramirez-Brewer, D., Quintana, S.E., Garcia-Zapateiro, L.A., 2024. Modeling and optimization of microwave-assisted extraction of total phenolics content from mango (*Mangifera indica*) peel using response surface methodology (RSM) and artificial neural networks (ANN). *Food Chem.* X 22, 101420.
- Rangani, J., Panda, A., Patel, M., Parida, A.K., 2018. Regulation of ROS through proficient modulations of antioxidative defense system maintains the structural and functional integrity of photosynthetic apparatus and confers drought tolerance in the facultative halophyte *Salvadora persica* L. *J. Photochem. Photobiol. B* 189, 214–233.
- Raskin, I., 1983. A method for measuring leaf volume, density, thickness, and internal gas volume. *HortScience*, 18, 698-699.
- Ratola, N., Amigo, J.M., Alves, A., 2010. Comprehensive assessment of pine needles as bioindicators of PAHs using multivariate analysis. The importance of temporal trends. *Chemosphere* 81, 1517-1525.
- Ratola, N., Amigo, J.M., Oliveira, M.S.N., Araujo, R., Silva, J.A., Alves, A., 2011. Differences between *Pinus pinea* and *Pinus pinaster* as bioindicators of polycyclic aromatic hydrocarbons. *Environ. Exp. Bot.* 72, 339-347.
- Ratola, N., Herbert, P., Alves, A., 2012. Microwave-assisted headspace solid-phase microextraction to quantify polycyclic aromatic hydrocarbons in pine trees. *Anal. Bioanal. Chem.* 403, 1761–1769.
- Ratola, N., Lacorte, S., Barcelo, D., Alves, A., 2009. Microwave-assisted extraction and ultrasonic extraction to determine polycyclic aromatic hydrocarbons in needles and bark of *Pinus pinaster* Ait. and *Pinus pinea* L. by GC–MS. *Talanta* 77, 1120-1128.
- Ravindra, K., Bencs, L., Wauters, E., de Hoog, J., Deutsch, F., Roekens, E., Bleux, N., Berghmans, P., Van Grieken, R., 2006. Seasonal and site-specific variation in vapour and aerosol phase PAHs over Flanders (Belgium) and their relation with anthropogenic activities. *Atmos. Environ.* 40, 771–785.

- Ravindra, K., Sokhi, R., Van Grieken, R., 2008a. Atmospheric polycyclic aromatic hydrocarbons: Source attribution, emission factors and regulation. *Atmos. Environ.* 42, 2895–2921.
- Ravindra, K., Wauters, E., Van Grieken, R., 2008b. Variation in particulate PAHs levels and their relation with the transboundary movement of the air masses. *Sci. Total Environ.* 396, 100–110.
- Ray, D., Chatterjee, A., Majumdar, D., Ghosh, S.K., Raha, S., 2017. Polycyclic aromatic hydrocarbons over a tropical urban and a high altitude Himalayan Station in India: Temporal variation and source apportionment. *Atmos. Res.* 197, 331–341.
- Ray, D., Ghosh, A., Chatterjee, A., Ghosh, S.K., Raha, S., 2019. Size-specific PAHs and associated health risks over a tropical urban metropolis: Role of long-range transport and meteorology. *Aerosol Air Qual. Res.* 19, 2446–2463.
- Ray, D., Ghosh, S.K., Raha, S., 2021. Seasonal foliar uptake of atmospheric polycyclic aromatic hydrocarbons by some local plants in a tropical metropolis in India. *Atmos. Pollut. Res.* 12, 104–112.
- Raza, A., Charagh, S., Abbas, S., Hassan, M.U., Saeed, F., Haider, S., Sharif, R., Anand, A., Corpas, F.J., Jin, W., Varshney, R.K., 2023. Assessment of proline function in higher plants under extreme temperatures. *Plant Biol.* 25, 379–395.
- Redondo-Bermudez, M.D.C., Gulenc, I.T., Cameron, R.W., Inkson, B.J., 2021. ‘Green barriers’ for air pollutant capture: Leaf micromorphology as a mechanism to explain plants capacity to capture particulate matter. *Environ. Pollut.* 288, 117809.
- Reichardt, C., Welton, T., 2010. *Solvents and Solvent Effects in Organic Chemistry* (4th edition). Wiley, p. 718.
- Renoldi, F., Lietti, L., Saponaro, S., Bonomo, L., Forzatti, P., 2003. Thermal desorption of a PAH-contaminated soil: a case study. *WIT Trans. Ecol. Environ.* 64, 1123–1132.
- Riccardi, C., Filippo, P.D., Pomata, D., Basilio, M.D., Spicaglia, S., Buiarelli, F., 2013. Identification of hydrocarbon sources in contaminated soils of three industrial areas. *Sci. Total Environ.* 450–451, 13–21.
- Richter, B.E., Jones, B.A., Ezzell, J.L., Porter, N.L., 1996. Accelerated solvent extraction: A technique for sample preparation. *Anal. Chem.* 68, 1033–1039.
- Rinaldi, M.C.S., Domingos, M., Dias, A.P.L., Esposito, J.B.N., Pagliuso, J.D., 2012. Leaves of *Lolium multiflorum* ‘Lema’ and tropical tree species as biomonitors of polycyclic aromatic hydrocarbons. *Ecotoxicol. Environ. Saf.* 79, 139–147.

- Rodil, R., Schellin, M., Popp, P., 2007. Analysis of polycyclic aromatic hydrocarbons in water and beverages using membrane-assisted solvent extraction in combination with large volume injection-gas chromatography-mass spectrometric detection. *J. Chromatogr. A* 1163, 288–297.
- Rodriguez, J.H., Pignata, M.L., Fangmeier, A., Klumpp, A., 2010. Accumulation of polycyclic aromatic hydrocarbons and trace elements in the bioindicator plants *Tillandsia capillaris* and *Lolium multiflorum* exposed at PM₁₀ monitoring stations in Stuttgart (Germany). *Chemosphere* 80, 208-215.
- Rodriguez, J.H., Wannaz, E.D., Franzaring, J., Klumpp, A., Fangmeier, A., Pignata, M.L., 2015. Biomonitoring of airborne fluoride and polycyclic aromatic hydrocarbons in industrial areas of Cordoba, Argentina, using standardized grass cultures of *Lolium multiflorum*. *Atmos. Pollut. Res.* 6, 444-453.
- Rodriguez, J.H., Wannaz, E.D., Salazar, M.J., Pignata, M.L., Fangmeier, A., Franzaring, J., 2012. Accumulation of polycyclic aromatic hydrocarbons and heavy metals in the tree foliage of *Eucalyptus rostrata*, *Pinus radiata* and *Populus hybridus* in the vicinity of a large aluminium smelter in Argentina. *Atmos. Environ.* 55, 35-42.
- Roy, A., Bhattacharya, T., Kumari, M., 2020. Air pollution tolerance, metal accumulation and dust capturing capacity of common tropical trees in commercial and industrial sites. *Sci. Total Environ.* 722, 137622.
- Saadati, N., Abdullah, M.P., Zakaria, Z., Sany, S.B.T., Rezayi, M., Hassonizadeh, H., 2013. Limit of detection and limit of quantification development procedures for organochlorine pesticides analysis in water and sediment matrices. *Chem. Cent. J.* 7, 1–10.
- Sadowska-Rociek, A., Cieslik, E., Sieja, K., 2015. Determination of polycyclic aromatic hydrocarbons in chocolate using the combination of Quick Easy Cheap Effective Rugged Safe method and dispersive liquid-liquid microextraction. *J. Food Nutr. Res.* 1-9.
- Saebo, A., Popek, R., Nawrot, B., Hanslin, H.M., Gawronska, H., Gawronski, S.W., 2012. Plant species differences in particulate matter accumulation on leaf surfaces. *Sci. Total Environ.* 427-428, 347–354.
- Samadi, M., Abidin, Z.Z., Yunus, R., Awang Biak, D.R., Yoshida, H., Lok, E.H., 2017. Assessing the kinetic model of hydro-distillation and chemical composition of *Aquilaria malaccensis* leaves essential oil. *Chin. J. Chem. Eng.* 25, 216–222.
- Sameena, P.P., Puthur, J.T., 2021. Differential modulation of photosynthesis and defense strategies towards copper toxicity in primary and cotyledonary leaves of *Ricinus communis* L. *J. Photochem. Photobiol.* 8, 100059.

- Sanchez-Prado, L., Garcia-Jares, C., Llompart, M., 2010. Microwave-assisted extraction: Application to the determination of emerging pollutants in solid samples. *J. Chromatogr. A* 1217, 2390–2414.
- Sarabi, V., Arjmand-Ghajur, E., 2021. Exogenous plant growth regulators/plant growth promoting bacteria roles in mitigating water-deficit stress on chicory (*Cichorium pumilum* Jacq.) at a physiological level. *Agric. Water Manag.* 245, 106439.
- Sari, M.F., Esen, F., Tasdemir, Y., 2021. Characterization, source apportionment, air/plant partitioning and cancer risk assessment of atmospheric PAHs measured with tree components and passive air sampler. *Environ. Res.* 194, 110508.
- Sarria-Villa, R., Ocampo-Duque, W., Paez, M., Schuhmacher, M., 2016. Presence of PAHs in water and sediments of the Colombian Cauca River during heavy rain episodes, and implications for risk assessment. *Sci. Total Environ.* 540, 455–465.
- Sartori, F., Wade, T.L., Sericano, J.L., Mohanty, B.P., Smith, K.A., 2010. Polycyclic aromatic hydrocarbons in soil of the Canadian River floodplain in Oklahoma. *J. Environ. Qual.* 39, 568–579.
- Saxena, P., Kulshrestha, U., 2016. Biochemical effects of air pollutants on plants. In: Kulshrestha, U., Saxena, P. (Eds.), *Plant Responses to Air Pollution*. Springer, Singapore, pp. 59–70.
- Scaramboni, C., Neris, J.B., do Nascimento, R.D.K.S., Chiaranda da Rosa, N.L., Carvalho, J.S., Grosseli, G.M., Campos, M.L.A.M., Fadini, P.S., Urban, R.C., 2021. Optimization of a low volume extraction method to determine polycyclic aromatic hydrocarbons in aerosol samples. *Front. Environ. Sci.* 9, 1–11.
- Schönherr, J., 2006. Characterization of aqueous pores in plant cuticles and permeation of ionic solutes. *J. Exp. Bot.* 57, 2471–2491.
- Schrlau, J.E., Geiser, L., Hageman, K.J., Landers, D.H., Simonich, S.M., 2011. Comparison of lichen, conifer needles, passive air sampling devices, and snowpack as passive sampling media to measure semi-volatile organic compounds in remote atmospheres. *Environ. Sci. Technol.* 45, 10354–10361.
- Schulz, H., Popp, P., Huhn, G., Stark, H.-J., Schuurmann, G., 1999. Biomonitoring of airborne inorganic and organic pollutants by means of pine tree barks. I. Temporal and spatial variations. *Sci. Total Environ.* 232, 49–58.
- See, S.W., Karthikeyan, S., Balasubramanian, R., 2006. Health risk assessment of occupational exposure to particulate-phase polycyclic aromatic hydrocarbons associated with Chinese, Malay and Indian cooking. *J. Environ. Monit.* 8, 369–76.

- Seenu, Y., Ravichandran, K.R., Sivadas, A., Mayakrishnan, B., Thangavelu, M., 2019. Vegetative anatomy of *Tabernaemontana alternifolia* L. (Apocynaceae) endemic to southern Western Ghats, India. *Acta Biol. Szeged.* 63, 185-193.
- Sen, A., Khan, I., Kundu, D., Das, K., Datta, J.K., 2017. Ecophysiological evaluation of tree species for biomonitoring of air quality and identification of air pollution-tolerant species. *Environ. Monit. Assess.* 189, 1-15.
- Senser, M., Kloos, M., Lutz, C., 1990. Influence of soil substrate and ozone plus acid mist on the pigment content and composition of needles from young spruce trees. *Environ. Pollut.* 64, 295.
- Serenjeh, F.N., Hashemi, P., Ghiasvand, A.R., Rasolzadeh, F., Heydari, N., Badiei, A., 2020. Cooling assisted headspace microextraction by packed sorbent coupled to HPLC for the determination of volatile polycyclic aromatic hydrocarbons in soil. *Anal. Chim. Acta* 1125, 128-134.
- Sett, R., 2017. Responses in plants exposed to dust pollution. *Horticult. Int. J.* 1, 53–56.
- Shabala, S., Cuin, T.A., 2008. Potassium transport and plant salt tolerance. *Physiol. Plant.* 133, 651–669.
- Shabnam, N., Oh, J., Park, S., Kim, H., 2021. Impact of particulate matter on primary leaves of *Vigna radiata* (L.) R. Wilczek. *Ecotoxicol. Environ. Saf.* 212, 111965.
- Shabnam, N., Sharmila, P., Sharma, A., Strasser, R.J., Pardha-Saradhi, P., 2015. Mitochondrial electron transport protects floating leaves of long leaf pondweed (*Potamogeton nodosus* Poir) against photoinhibition: comparison with submerged leaves. *Photosynth. Res.* 125, 305–319.
- Shah, K., Amin, N.u., Ahmad, I., Ara, G., Ren, X., Xing, L., 2019. Effects of chronic dust load on leaf pigments of the landscape plant *Murraya paniculata*. *Gesunde Pflanzen* 71, 249–258.
- Shah, K., An, N., Ma, W., Ara, G., Ali, K., Kamanova, S., Zuo, X., Han, M., Ren, X., Xing, L., 2020. Chronic cement dust load induce novel damages in foliage and buds of *Malus domestica*. *Sci. Rep.* 10, 1–12.
- Shamsuri, A.A., Abdullah, D.K., 2010. Ionic liquids: preparations and limitations. *Makara, Sains* 14, 101-106.
- Shanazari, M., Golkar, P., Mirmohammady Maibody, A.M., 2018. Effects of drought stress on some agronomic and bio-physiological traits of *Triticum aestivum*, *Triticale*, and *Tritipyrum* genotypes. *Arch. Agron. Soil Sci.* 64, 2005–2018.

- Shao, F., Wang, L., Sun, F., Li, G., Yu, L., Wang, Y., Zeng, X., Yan, H., Dong, L., Bao, Z., 2019. Study on different particulate matter retention capacities of the leaf surfaces of eight common garden plants in Hangzhou, China. *Sci. Total Environ.* 652, 939–951.
- Sharma, A.P., Tripathi, B.D., 2009. Assessment of atmospheric PAHs profile through *Calotropis gigantea* R.Br. leaves in the vicinity of an Indian coal-fired power plant. *Environ. Monit. Assess.* 149, 477–482.
- Sharma, B., Bhardwaj, S.K., Sharma, S., Nautiyal, R., Kaur, L., Alam, N.M., 2019. Pollution tolerance assessment of temperate woody vegetation growing along the National Highway-5 in Himachal Pradesh, India. *Environ. Monit. Assess.* 191, 1–14.
- Sharma, B.M., Melymuk, L., Bharat, G.K., Pribylova, P., Sanka, O., Klanova, J., Nizzetto, L., 2018. Spatial gradients of polycyclic aromatic hydrocarbons (PAHs) in air, atmospheric deposition, and surface water of the Ganges River basin. *Sci. Total Environ.* 627, 1495–1504.
- Shechter, M. & Chefetz, B., 2008. Insights into the sorption properties of cutin and cutan biopolymers. *Environ. Sci. Technol.* 42, 1165–1171.
- Shende, A.S., Joshi, J., Rao, P.S., 2024. Process optimization of microwave-assisted aqueous extraction of tannins and saponins from Malabar Spinach (*Basella alba*) leaves using ANN-GA and RSM methodology. *Measurement: Food* 13, 100117.
- Shi, S., Wu, Z., Liu, F., Fan, W., 2016. Retention of atmospheric particles by local plant leaves in the Mount Wutai Scenic Area, China. *Atmosphere* 7, 1–12.
- Shin, S.M., Lee, J.Y., Shin, H.J., Kim, Y.P., 2022. Seasonal variation and source apportionment of Oxygenated Polycyclic Aromatic Hydrocarbons (OPAHs) and Polycyclic Aromatic Hydrocarbons (PAHs) in PM_{2.5} in Seoul, Korea. *Atmos. Environ.* 272, 118937.
- Shinoda, W., 2016. Permeability across lipid membranes. *BBA-Biomembranes* 1858, 2254–2265.
- Shirsath, S.R., Sonawane, S.H., Gogate, P.R., 2012. Intensification of extraction of natural products using ultrasonic irradiations—A review of current status. *Chem. Eng. Process.: Process Intensif.* 53, 10–23.
- Shrivastava, R., Mishra, A., 2018. Air pollution induced changes in foliar micro-morphology of roadside shrub species, *Thevetia peruviana* and *Plumeria alba* in Rewa City, MP, India. *Int. Res. J. Environmental Sci.* 7, 1–7.
- Shu, Y.Y., Lai, T.L., 2001. Effect of moisture on the extraction efficiency of polycyclic aromatic hydrocarbons from soils under atmospheric pressure by focused microwave-assisted extraction. *J. Chromatogr. A* 927, 131–141.

- Shukla, S., Khan, R., Bhattacharya, P., Devanesan, S., AlSalhi, M.S., 2022. Concentration, source apportionment and potential carcinogenic risks of polycyclic aromatic hydrocarbons (PAHs) in roadside soils. *Chemosphere* 292, 133413.
- Shukla, V., Upreti, D.K., 2009. Polycyclic aromatic hydrocarbon (PAH) accumulation in lichen, *Phaeophyscia hispidula* of DehraDun City, Garhwal Himalayas. *Environ. Monit. Assess.* 149, 1–7.
- Sibiya, P., Potgieter, M., Cukrowska, E., Jonsson, J.A., Chimuka, L., 2012. Development and application of solid phase extraction method for polycyclic aromatic hydrocarbons in water samples in Johannesburg Area, South Africa. *S. Afr. J. Chem.* 65, 206–213.
- Sifermann-Harms, D., 1987. The light harvesting and protective functions of carotenoids in photosynthetic membranes. *Physiol. Plant.* 69, 561–568.
- Silva, M., Stray, H., Metidji, M.O., Bjornstad, T., 2021. Variation of the partition coefficient of phase-partitioning compounds between hydrocarbon and aqueous phases: an experimental study. *Fuel* 300, 120915.
- Simonich, S.L., Hites, R., 1994a. Importance of vegetation in removing polycyclic hydrocarbons from the atmosphere. *Nature* 370, 49–51.
- Simonich, S.L., Hites, R.A., 1994b. Vegetation-atmosphere partitioning of polycyclic aromatic hydrocarbons. *Environ. Sci. Technol.* 28, 939–943.
- Singh, A.K., Kumar, M., Bauddh, K., Singh, A., Singh, P., Madhav, S., Shukla, S.K., 2023. Environmental impacts of air pollution and its abatement by plant species: A comprehensive review. *Environ. Sci. Pollut. Res.* 30, 79587–79616.
- Singh, H.P., Batish, D.R., Kohli, R.K., Arora, K., 2007. Arsenic-induced root growth inhibition in mung bean (*Phaseolus aureus* Roxb.) is due to oxidative stress resulting from enhanced lipid peroxidation. *Plant Growth Regul.* 53, 65–73.
- Singh, S., Parihar, P., Singh, R., Singh, V.P., Prasad, S.M., 2016a. Heavy metal tolerance in plants: Role of transcriptomics, proteomics, metabolomics, and ionomics. *Front. Plant Sci.* 6, 1–36.
- Singh, S., Gupta, N.C., Bhattacharya, P., 2016b. Morphological study of leaf epidermis for *Alstonia scholaris* (L.) R. Br at institutional site of urban Delhi. In: Kumar, S., Beg, M.A., Sayeed, M.T. (Eds.), *Environmental concerns of 21st century: Indian and global context*. Book Age Publications, Delhi, India, pp. 235–246.
- Singh, S.K., Rao, D.N., 1983. Evaluation of the Plants for their Tolerance to Air Pollution, *Proceedings Symposium on Air Pollution Control held at IIT-Delhi*. pp. 218–224.

- Singh, S.K., Rao, D.N., Agrawal, M., Pandey, J., Naryan, D., 1991. Air pollution tolerance index of plants. *J. Environ. Manage.* 32, 45-55.
- Siudek, P., 2023. Polycyclic aromatic hydrocarbons in coarse particles (PM₁₀) over the coastal urban region in Poland: Distribution, source analysis and human health risk implications. *Chemosphere* 311, 137130.
- Skert, N., Falomo, J., Giorgini, L., Acquavita, A., Capriglia, L., Grahonja, R., Miani, N., 2010. Biological and artificial matrixes as PAH accumulators: An experimental comparative study. *Water Air Soil Pollut.* 206, 95–103.
- Skrynetska, I., Karcz, J., Barczyk, G., Kandziora-Ciupa, M., Ciepal, R., Nadgorska-Socha, A., 2019. Using *Plantago major* and *Plantago lanceolata* in environmental pollution research in an urban area of Southern Poland. *Environ. Sci. Pollut. Res.* 26, 23359-23371.
- Slaski, J.J., Archambault, D.J., Li, X., 2000. Evaluation of Polycyclic Aromatic Hydrocarbon (PAH) Accumulation in Plants. The Potential Use of PAH Accumulation as a Marker of Exposure to Air Emissions from Oil and Gas Flares. Report prepared for the Air Research Users Group. Alberta Environment, Edmonton, Alberta, ISBN 0-7785-1228-2.
- Smith, K.E.C., Northcott, G.L., Jones, K.C., 2006. Influence of the extraction methodology on the analysis of polycyclic aromatic hydrocarbons in pasture vegetation. *J. Chromatogr. A* 1116, 20–30.
- Sobus, J.R., McClean, M.D., Herrick, R.F., Waidyanatha, S., Nylander-French, L.A., Kupper, L.L., Rappaport, S.M., 2009. Comparing urinary biomarkers of airborne and dermal exposure to polycyclic aromatic compounds in asphalt-exposed workers. *Ann. Occup. Hyg.* 53, 561–71.
- Sojinu, O.S., Sonibare, O.O., Ekundayo, O., Zeng, E.Y., 2010. Biomonitoring potentials of polycyclic aromatic hydrocarbons (PAHs) by higher plants from an oil exploration site, Nigeria. *J. Hazard. Mater.* 184, 759-64.
- Solanki, K.P., Desai, M.A., Parikh, J.K., 2019. Microwave intensified extraction: a holistic approach for extraction of citronella oil and phenolic compounds. *Chem. Eng. Process.: Process Intensif.* 146, 107694.
- Soursou, V., Campo, J., Pico, Y., 2023. Revisiting the analytical determination of PAHs in environmental samples: An update on recent advances. *Trends Environ. Anal. Chem.* 37, e00195.
- Sporring, S., Bowadt, S., Svensmark, B., Bjorklund, E., 2005. Comprehensive comparison of classic Soxhlet extraction with Soxtec extraction, ultrasonication extraction, supercritical

- fluid extraction, microwave assisted extraction and accelerated solvent extraction for the determination of polychlorinated biphenyls in soil. *J Chromatogr A* 1090, 1–9.
- Srogi, K., 2007. Monitoring of environmental exposure to polycyclic aromatic hydrocarbons: a review. *Environ. Chem. Lett.* 5, 169–95.
- Stefi, A.L., Mitsigiorgi, K., Vassilacopoulou, D., Christodoulakis, N.S., 2020. Response of young *Nerium oleander* plants to long-term non-ionizing radiation. *Planta* 251, 1–17.
- Steiner, D., Krska, R., Malachova, A., Taschl, I., Sulyok, M., 2020. Evaluation of matrix effects and extraction efficiencies of LC–MS/MS methods as the essential part for proper validation of multiclass contaminants in complex feed. *J. Agric. Food Chem.* 68, 3868–3880.
- Stephens Jr., D.L., McFadden, T., Heath, O.D., Mauldin, R.F., 1994. The effect of sonication on the recovery of polycyclic aromatic hydrocarbons from coal stack ash surfaces. *Chemosphere* 28, 1741–1747.
- Streng, W.H., 2001. Partitioning: Experimental Procedures and Examples. In: *Characterization of Compounds in Solution*. Springer, Boston, MA, pp. 161-180.
- Studabaker, W.B., Puckett, K.J., Percy, K.E., Landis., M.S., 2017. Determination of polycyclic aromatic hydrocarbons, dibenzothiophene, and alkylated homologs in the lichen *Hypogymnia physodes* by gas chromatography using single quadrupole mass spectrometry and time-of-flight mass spectrometry. *J. Chromatogr. A* 1492, 106-116.
- Sucharova, J., Hola, M., 2014. PAH and PCB determination of the concentration gradient in moss *Pleurozium schreberi* near a highway and seasonal variability at the background reference site. *Intern. J. Environ. Anal. Chem.* 94, 712-727.
- Sudhakar, P., Latha, P., Reddy, P.V., 2016. *Phenotyping Crop Plants for Physiological and Biochemical Traits*. Academic Press, pp. 194.
- Suman, 2021. Air quality indices: A review of methods to interpret air quality status. *Mater. Today: Proc.* 34, 863-868.
- Sun, F., Littlejohn, D., Gibson, M.D., 1998. Ultrasonication extraction and solid phase extraction clean-up for determination of US EPA 16 priority pollutant polycyclic aromatic hydrocarbons in soils by reversed-phase liquid chromatography with ultraviolet absorption detection. *Anal. Chim. Acta* 364, 1–11.
- Sun, F., Wen, D., Kuang, Y., Li, J., Li, J., Zuo, W., 2010. Concentrations of heavy metals and polycyclic aromatic hydrocarbons in needles of Masson pine (*Pinus massoniana* L.) growing nearby different industrial sources. *J. Environ. Sci.* 22, 1006-1013.

- Sun, H., Guo, S., Nan, Y., Ma, R., 2018. Direct determination of surfactant effects on the uptake of gaseous parent and alkylated PAHs by crop leaf surfaces. *Ecotoxicol. Environ. Saf.* 154, 206-213.
- Sun, H., Guo, S., Zhu, N., Sang, N., Chen, Z., 2016. In situ determination of multiple polycyclic aromatic hydrocarbons uptake by crop leaf surfaces using multi-way models. *Environ. Pollut.* 218, 523-529.
- Sun, H.F., Yang, Y.N., Zhu, Y.X., Zhang, Y., 2013. In situ investigation of the depuration of fluoranthene adsorbed on the leaf surface of living mangrove seedlings. *Talanta* 116, 441-447.
- Svarc-Gajic, J., Stojanovic, Z., Carretero, A.S., Roman, D.A., Borrás, I., Vasiljevic, I., 2013. Development of a microwave-assisted extraction for the analysis of phenolic compounds from *Rosmarinus officinalis*. *J. Food Eng.* 119, 525-532.
- Swami, A., Bhatt, D., Joshi, P.C., 2004. Effects of automobile pollution on sal (*Shorea robusta*) and rohini (*Mallotus philippinensis*) at Asarori, Dehradun. *Himal. J. Environ. Zool.* 18, 57–61.
- Swisłowski, P., Hrabak, P., Waclawek, S., Liskova, K., Antos, V., Rajfur, M., Zabkowska-Waclawek, M., 2021. The application of active biomonitoring with the use of mosses to identify polycyclic aromatic hydrocarbons in an atmospheric aerosol. *Molecules* 26, 1–11.
- Szulejko, J.E., Kim, K.H., Brown, R.J.C., Bae, M.S., 2014. Review of progress in solvent extraction techniques for the determination of polyaromatic hydrocarbons as airborne pollutants. *TrAC - Trends Anal. Chem.* 61, 40–48.
- Tani, A., Koike, M., Mochizuki, T., Yamane, M., 2022. Leaf uptake of atmospheric monocyclic aromatic hydrocarbons depends on plant species and compounds. *Ecotoxicol. Environ. Saf.* 236, 113433.
- Tao, S., Cao, H., Liu, W., Li, B., Cao, J., Xu, F., Wang, X., Coveney, R.M., Shen, W., Qin, B., Sun, R., 2003. Fate modeling of phenanthrene with regional variation in Tianjin, China. *Environ. Sci. Technol.* 37, 2453–2459.
- Tatke, P., Jaiswal, Y., 2011. An overview of microwave assisted extraction and its applications in herbal drug research. *Res. J. Med. Plant* 5, 21-31.
- Teixeira, E.C., Agudelo-Castaneda, D.M., Fachel, J.M.G., Leal, K.A., Garcia, K. de O., Wiegand, F., 2012. Source identification and seasonal variation of polycyclic aromatic hydrocarbons associated with atmospheric fine and coarse particles in the Metropolitan Area of Porto Alegre, RS, Brazil. *Atmos. Res.* 118, 390-403.

- Terzaghi, E., Zacchello, G., Scacchi, M., Raspa, G., Jones, K.C., Cerabolini, B., Di Guardo, A., 2015. Towards more ecologically realistic scenarios of plant uptake modelling for chemicals: PAHs in a small forest. *Sci. Total Environ.* 505, 329-37.
- Teslic, N., Bojanic, N., Rakic, D., Takaci, A., Zekovic, Z., Fistes, A., Bodroza-Solarov, M., Pavlic, B., 2019. Defatted wheat germ as source of polyphenols - Optimization of microwave-assisted extraction by RSM and ANN approach. *Chem. Eng. Process.: Process Intensif.* 143, 107634.
- Thawale, P.R., Babu, S.S., Wakode, R.R., Singh, S.K., Kumar, S., Juwarkar, A.A, 2011. Biochemical changes in plant leaves as a biomarker of pollution due to anthropogenic activity. *Environ. Monit. Assess.* 177, 527–535.
- Thompson, J.E., 2018. Airborne particulate matter: human exposure & health effects. *J. Occup. Environ. Med.* 60, 392–423.
- Thunis, P., Clappier, A., Tarrason, L., Cuvelier, C., Monteiro, A., Pisoni, E., Wesseling, J., Belis, C.A., Pirovano, G., Janssen, S., Guerreiro, C., Peduzzi, E., 2019. Source apportionment to support air quality planning: Strengths and weaknesses of existing approaches. *Environ. Int.* 130, 104825.
- Tian, L., Yin, S., Ma, Y., Kang, H., Zhang, X., Tan, H., Meng, H., Liu, C., 2019. Impact factor assessment of the uptake and accumulation of polycyclic aromatic hydrocarbons by plant leaves: Morphological characteristics have the greatest impact. *Sci. Total Environ.* 652, 1149-1155.
- Tiwari, S., Agrawal, M., Marshall, F.M., 2006. Evaluation of ambient air pollution impact on carrot plants at a sub urban site using open top chambers. *Environ. Monit. Assess.* 119, 15–30.
- Tobiszewski, M., Namiesnik, J., 2012. PAH diagnostic ratios for the identification of pollution emission sources. *Environ. Pollut.* 162, 110–119.
- Tomasi, I.T., Santos, S.C.R., Boaventura, R.A.R., Botelho, C.M.S., 2023. Optimization of microwave-assisted extraction of phenolic compounds from chestnut processing waste using response surface methodology. *J. Clean. Prod.* 395, 136452.
- Tong, S.T.Y., 1991. The retention of copper and lead particulate matter in plant foliage and forest soil. *Environ. Int.* 17, 31–37.
- Tongo, I., Ogbeide, O., Ezemonye, L., 2017. Human health risk assessment of polycyclic aromatic hydrocarbons (PAHs) in smoked fish species from markets in Southern Nigeria. *Toxicol. Rep.* 4, 55-61.

- Totten, L.A., Eisenreich, S.J., Brunciak, P.A., 2002. Evidence for destruction of PCBs by the OH radical in urban atmospheres. *Chemosphere* 47, 735–746.
- Trapp, S., McFarlane, C., 1994. Plant contamination. *Environ. Sci. Pollut. Res.* 1, 252.
- Traven, L., 2013. Sources, trends and ecotoxicological risks of PAH pollution in surface sediments from the northern Adriatic Sea (Croatia). *Mar. Pollut. Bull.* 77, 445-450.
- Tripathi, S., Singh, V.K., Srivastava, P., Singh, R., Devi, R.S., Kumar, A., Bhadouria, R., 2020. Phytoremediation of organic pollutants: current status and future directions. In: *Abatement of environmental pollutants*. Elsevier, pp. 81-105.
- Trivedi, A.K., Sati, J., 2013. Impact of air pollution on plant metabolism. In: Hemantaranjan, A. (Ed.), *Advances in Plant Physiology (An International Treatise Series, Vol. 14)*. Scientific Publishers, India, pp. 547-557.
- Truscott, T.G., 1990. New trends in photobiology: The photophysics and photochemistry of the carotenoids. *J. Photochem. Photobiol. B. Biol.* 6, 359–371.
- Tsapakis, M., Stephanou, E.G., 2005. Occurrence of gaseous and particulate polycyclic aromatic hydrocarbons in the urban atmosphere: study of sources and ambient temperature effect on the gas/particle concentration and distribution. *Environ. Pollut.* 133, 147–156.
- Ugwu, K.E., Ukoha, P.O., 2016. Impacts of extraction methods and solvent systems in the assessment of toxic organic compounds in a solid matrix. *AJCPS* 1, 23-28.
- Unwin, J., Cocker, J., Scobbie, E., Chambers, H., 2006. An assessment of occupational exposure to polycyclic aromatic hydrocarbons in the UK. *Ann. Occup. Hyg.* 50, 395–403.
- USEPA, 2002. Peer consultation workshop on approaches to polycyclic aromatic hydrocarbon (PAH) health assessment. U.S. Environmental Protection Agency, Office of Research and Development, National Center for Environmental Assessment, Washington Office, Washington, DC, EPA/635/R-02/005.
- <https://cfpub.epa.gov/ncea/risk/recordisplay.cfm?deid=54787>
- Vagi, M.C., Kostopoulou, M.N., Petsas, A.S., Lalousi, M.E., Rasouli, C., Lekkas, T.D., 2005. Toxicity of organophosphorous pesticides to the marine alga *Tetraselmis suecica*. *Global NEST J.* 7, 222–227.
- Vallero, D., 2014. Air pollutant kinetics and equilibrium. In: *Fundamentals of Air Pollution (fifth Ed.)*. Academic Press, NY, pp. 437–474.
- Van der Wat, L., Forbes, P.B.C., 2015. Lichens as biomonitors for organic air pollutants. *Trends Anal. Chem* 64, 165–172.

- Van der Wat, L., Forbes, P.B.C., 2019. Comparison of extraction techniques for polycyclic aromatic hydrocarbons from lichen biomonitors. *Environ. Sci. Pollut. Res.* 26, 11179-11190.
- van Heerden, P.D.R., Kruger, G.H.J., Louw, M.K., 2007. Dynamic responses of photosystem II in the Namib Desert shrub, *Zygophyllum prismatocarpum*, during and after foliar deposition of limestone dust. *Environ. Pollut.* 146, 34–45.
- Veggi, P.C., Martinez, J., Meireles, M.A.A., 2013. Fundamentals of microwave extraction. In: Chemat, F., Cravotto, G. (Eds.), *Microwave-Assisted Extraction for Bioactive Compounds*. Food Engineering Series. Springer, pp. 15–52.
- Venkatesan, P., 2016. WHO report: air pollution is a major threat to health. *Lancet Respir. Med.* 4, 351.
- Verma, P.K., Sah, D., Satish, R., Rastogi, N., Kumari, K.M., Lakhani, A., 2022. Atmospheric chemistry and cancer risk assessment of polycyclic aromatic hydrocarbons (PAHs) and nitro-PAHs over a semi-arid site in the Indo-Gangetic plain. *J. Environ. Manag.* 317, 115456.
- Vestenius, M., Leppanen, S., Anttila, P., Kyllonen, K., Hatakka, J., Hellen, H., Hyvarinen, A.P., Hakola, H., 2011. Background concentrations and source apportionment of polycyclic aromatic hydrocarbons in south-eastern Finland. *Atmos. Environ.* 45, 3391-3399.
- Vila Verde, G.M., Barros, D.A., Oliveira, M.S., Aquino, G.L.B., Santos, D.M., De Paula, J.R., Dias, L.D., Pineiro, M., Pereira, M.M., 2018. A Green protocol for microwave-assisted extraction of volatile oil terpenes from *Pterodon emarginatus* Vogel. (Fabaceae). *Molecules* 23, 1-12.
- Viner, B., 2023. Coming and going: Transport and tracking. In: Hiscox, A.L. (Ed.), *Conceptual Boundary Layer Meteorology*. Academic Press, pp. 217-241.
- Viskari, E.L., Rekila, R., Roy, S., Lehto, O., Ruuskanen, J., Karenlampi, L., 1997. Airborne pollutants along a roadside: Assessment using snow analyses and moss bags. *Environ. Pollut.* 97, 153-160.
- Vitali, M., Antonucci, A., Owczarek, M., Guidotti, M., Astolfi, M.L., Manigrasso, M., Avino, P., Bhattacharya, B., Protano, C., 2019. Air quality assessment in different environmental scenarios by the determination of typical heavy metals and Persistent Organic Pollutants in native lichen *Xanthoria parietina*. *Environ. Pollut.* 254, 113013.
- Vukovic, G., Urosevic, M.A., Goryainova, Z., Pergal, M., Skrivanj, S., Samson, R., Popovic, A., 2015. Active moss biomonitoring for extensive screening of urban air pollution: Magnetic and chemical analyses. *Sci. Total Environ.* 521-522, 200-10.

- Wagrowski, D.M., Hites, R.A., 1996. Polycyclic aromatic hydrocarbon accumulation in urban, suburban, and rural vegetation. *Environ. Sci. Technol.* 31, 279–282.
- Wandan, E.N., Elleingand, E.F., Ndouba, A.M., 2011. A screening for benzo[a]pyrene in cocoa beans subjected to different drying methods during on farm processing. *Int. J. Eng. Sci. Technol.* 3, 3621–3630.
- Wang, D., Chen, J., Xu, Z., Qiao, X., Huang, L., 2005. Disappearance of polycyclic aromatic hydrocarbons sorbed on surfaces of pine *Pinus thunbergii* needles under irradiation of sunlight: volatilization and photolysis. *Atmos. Environ.* 39, 4583–4591.
- Wang, F., Lin, T., Feng, J., Fua, H., Guo, Z., 2015a. Source apportionment of polycyclic aromatic hydrocarbons in PM_{2.5} using positive matrix factorization modeling in Shanghai, China. *Environ. Sci.: Processes Impacts* 17, 197–205.
- Wang, Y., Wang, S., Xu, Y., Luo, C., Li, J., Zhang, G., 2015b. Characterization of the exchange of PBDEs in a subtropical paddy field of China: A significant inputs of PBDEs via air–foliage exchange. *Environ. Pollut.* 205, 1–7.
- Wang, G., Liu, Y., Jiang, N., Liu, Y., Zhao, X., Tao, W., Lou, Y., Li, N., Wang, H., 2020a. Field study on bioaccumulation and translocation of polybrominated diphenyl ethers in the sediment-plant system of a national nature reserve, North China. *Chemosphere* 261, 127740.
- Wang, J., Bao, H., Zhang, H., Li, J., Hong, H., Wu, F., 2020b. Effects of cuticular wax content and specific leaf area on accumulation and partition of PAHs in different tissues of wheat leaf. *Environ. Sci. Pollut. Res.* 27, 18793–18802.
- Wang, Q., Zhao, Y., Yan, D., Yang, L., Li, Z., Huang, B., 2004. Historical records of airborne polycyclic aromatic hydrocarbons by analyzing dated corks of the bark pocket in a Longpetiole Beech Tree. *Environ. Sci. Technol.* 38, 4739–4744.
- Wang, W., Meng, B., Lu, X., Liu, Y., Tao, S., 2007. Extraction of polycyclic aromatic hydrocarbons and organochlorine pesticides from soils: a comparison between Soxhlet extraction, microwave-assisted extraction and accelerated solvent extraction techniques. *Anal. Chim. Acta* 602, 211–222.
- Wang, Y., Tian, Z., Zhu, H., Cheng, Z., Kang, M., Luo, C., Li, J., Zhang, G., 2012. Polycyclic aromatic hydrocarbons (PAHs) in soils and vegetation near an e-waste recycling site in South China: concentration, distribution, source, and risk assessment. *Sci. Total Environ.* 439, 187–193.
- Wang, Y., Zhang, Z., Xu, Y., Rodgers, T.F.M., Ablimit, M., Li, J., Tan, F., 2023. Identifying the contributions of root and foliage gaseous/particle uptakes to indoor plants for phthalates, OPFRs and PAHs. *Sci. Total Environ.* 883, 163644.

- Wang, Y.Q., Tao, S., Jiao, X.C., Coveney, R.M., Wu, S.P., Xing, B.S., 2008. Polycyclic aromatic hydrocarbons in leaf cuticles and inner tissues of six species of trees in urban Beijing. *Environ. Pollut.* 151, 158–164.
- Wang, Z., Ren, P., Sun, Y., Ma, X., Liu, X., Na, G., Yao, Z., 2013. Gas/particle partitioning of polycyclic aromatic hydrocarbons in coastal atmosphere of the north Yellow Sea, China. *Environ. Sci. Pollut. Res* 20, 5753–63.
- Wannaz, E.D., Abril, G.A., Rodriguez, J.H., Pignata, M.L., 2013. Assessment of polycyclic aromatic hydrocarbons in industrial and urban areas using passive air samplers and leaves of *Tillandsia capillaris*. *J. Environ. Chem. Eng.* 1, 1028-1035.
- Waters Corporation, 2008. EPA Method 550.1 Determination of Polycyclic Aromatic Hydrocarbons in Drinking Water by Liquid–Solid Extraction and High Performance Liquid Chromatography with Ultraviolet Detection (Application Note). pp. 14–15.
- Weerakkody, U., Dover, J.W., Mitchell, P., Reiling, K., 2018a. Quantification of the traffic-generated particulate matter capture by plant species in a living wall and evaluation of the important leaf characteristics. *Sci. Total Environ.* 635, 1012-1024.
- Weerakkody, U., Dover, J.W., Mitchell, P., Reiling, K., 2018b. Evaluating the impact of individual leaf traits on atmospheric particulate matter accumulation using natural and synthetic leaves. *Urban For. Urban Green.* 30, 98–107.
- Wei, X., Lyu, S., Yu, Y., Wang, Z., Liu, H., Pan, D., Chen, J., 2017. Phylloremediation of air pollutants: Exploiting the potential of plant leaves and leaf-associated microbes. *Front. Plant Sci.* 8, 1-23.
- Weidemann, E., Buss, W., Edo, M., Masek, O., Jansson, S., 2018. Influence of pyrolysis temperature and production unit on formation of selected PAHs, oxy-PAHs, N-PACs, PCDDs, and PCDFs in biochar—a screening study. *Environ. Sci. Pollut. Res.* 25, 3933–3940.
- Wellburn, A.R., Majernik, O., Wellburn, F.A.M., 1972. Effects of SO₂ and NO₂ polluted air upon the ultrastructure of chloroplasts. *Environ. Pollut.* 3, 37–49.
- Wen, Y., Chen, H., Zhou, X., Deng, Q., Zhao, Y., Zhao, C., Gong, X., 2015. Optimization of the microwave-assisted extraction and antioxidant activities of anthocyanins from blackberry using a response surface methodology. *RSC Adv.* 5, 19686-19695.
- Weschler, C.J., Nazaroff, W.W., 2010. SVOC partitioning between the gas phase and settled dust indoors. *Atmos. Environ.* 44, 3609-3620.

- Weschler, C.J., Salthammer, T., Fromme, H., 2008. Partitioning of phthalates among the gas phase, airborne particles and settled dust in indoor environments. *Atmos. Environ.* 42, 1449-1460.
- WHO, 2000. Air Quality Guidelines for Europe. Polycyclic aromatic hydrocarbons. European Series No 91, World Health Organization. WHO Regional Publications, Geneva.
- WHO, Regional Office for Europe & Joint WHO/Convention Task Force on the Health Aspects of Air Pollution, 2006. Health risks of particulate matter from long-range transboundary air pollution. Copenhagen: WHO Regional Office for Europe, p. 99.
<https://apps.who.int/iris/handle/10665/107691>
- Wieczorek, J., Sienkiewicz, S., Pietrzak, M., Wieczorek, Z., 2015. Uptake and phytotoxicity of anthracene and benzo[k]fluoranthene applied to the leaves of celery plants (*Apium graveolens* var. *secalinum* L.). *Ecotoxicol. Environ. Saf.* 115, 19-25.
- Wik, A., Dave, G., 2009. Occurrence and effects of tire wear particles in the environment – A critical review and an initial risk assessment. *Environ. Pollut.* 157, 1-11.
- Wild, E., Dent, J., Thomas, O.G., Jones, K.C., 2006. Visualizing the air-to-leaf transfer and within-leaf movement and distribution of phenanthrene: further studies utilizing two-photon excitation microscopy. *Environ. Sci. Technol.* 40, 907–916.
- Wong, Y.H., Lau, H.W., Tan, C.P., Long, K., Nyam, K.L., 2014. Binary solvent extraction system and extraction time effects on phenolic antioxidants from Kenaf Seeds (*Hibiscus cannabinus* L.) extracted by a pulsed ultrasonic-assisted extraction. *Sci. World J.* 1-7 (Article ID 789346).
- Wu, J., Luo, K., Wang, Y., Wang, Z., 2021. Urban road greenbelt configuration: The perspective of PM_{2.5} removal and air quality regulation. *Environ. Int.* 157, 106786.
- Wu, Y., Jiang, B., Zou, Y., Dong, H., Wang, H., Zou, H., 2022. Influence of bacterial community diversity, functionality, and soil factors on polycyclic aromatic hydrocarbons under various vegetation types in mangrove wetlands. *Environ. Pollut.* 308, 119622.
- Xia, J., Yuan, W., Wang, Y.P., Zhang, Q., 2017. Adaptive carbon allocation by plants enhances the terrestrial carbon sink. *Sci. Rep.* 7, 1–11.
- Xiao, H., Wania, F., 2003. Is vapor pressure or the octanol–air partition coefficient a better descriptor of the partitioning between gas phase and organic matter? *Atmos. Environ.* 37, 2867-2878.
- Xiao, J., Chen, G., Li, N., 2018. Ionic liquid solutions as a green tool for the extraction and isolation of natural products. *Molecules* 23, 1-23. Xi, D., Li, J., Kuang, Y.W., Xu, Y.M.,

- Zhu, X.M., 2013. Influence of traffic exhausts on elements and polycyclic aromatic hydrocarbons in leaves of medicinal plant *Broussonetia papyrifera*. *Atmos. Pollut. Res.* 4, 370-376.
- Xie, C., Guo, J., Yan, L., Jiang, R., Liang, A., 2022. The influence of plant morphological structure characteristics on PM_{2.5} retention of leaves under different wind speeds. *Urban For. Urban Green.* 71, 127556.
- Xing, W., Yang, L., Zhang, H., Zhang, X., Wang, Y., Bai, P., Zhang, L., Hayakawa, K., Nagao, S., Tang, N., 2022. Variations in traffic-related polycyclic aromatic hydrocarbons in PM_{2.5} in Kanazawa, Japan, after the implementation of a new vehicle emission regulation. *J. Environ. Sci.* 121, 38-47.
- Xu, H., Wang, W., Wang, H., Sun, Y., Zhong, Z., Wang, S., 2019. Differences in quantity and composition of leaf particulate matter and morphological structures in three evergreen trees and their association in Harbin, China. *Environ. Pollut.* 252, 1772–1790.
- Yaffe, D., Cohen, Y., Arey, J., Grosovsky, A.J., 2008. Multimedia analysis of PAHs and Nitro-PAH daughter products in the Los Angeles basin. *Risk Anal.* 72, 1567–1572.
- Yaghmaei, L., Jafari, R., Soltani, S., Eshghizadeh, H.R., & Jahanbazy, H., 2022. Interaction effects of dust and water deficit stresses on growth and physiology of Persian oak (*Quercus Brantii* Lindl.). *J. Sustain. For.* 41, 134–158.
- Yakovleva, E.V., Gabov, D.N., Beznosikov, V.A., Kondratenok, B.M., Dubrovskiy, Y.A., 2017. Accumulation of PAHs in tundra plants and soils under the influence of coal mining. *Polycycl. Aromat. Comp.* 37, 203-218.
- Yang, B., Liu, S., Liu, Y., Li, X., Lin, X., Liu, M., Liu, X., 2017. PAHs uptake and translocation in *Cinnamomum camphora* leaves from Shanghai, China. *Sci. Total Environ.* 574, 358-368.
- Yang, D., Li, C., Lau, A.K.H., Li, Y., 2013. Long-term measurement of daytime atmospheric mixing layer height over Hong Kong. *J. Geophys. Res. Atmos.* 118, 2422–2433.
- Yang, L., Zhang, L., Chen, L., Han, C., Akutagawa, T., Endo, O., Yamauchi, M., Neroda, A., Toriba, A., Tang, N., 2021. Polycyclic aromatic hydrocarbons and nitro-polycyclic aromatic hydrocarbons in five East Asian cities: Seasonal characteristics, health risks, and yearly variations. *Environ. Pollut.* 287, 117360.
- Yang, W., Lang, Y.H., Bai, J., Li, Z.Y., 2015. Quantitative evaluation of carcinogenic and non-carcinogenic potential for PAHs in coastal wetland soils of China. *Ecol. Eng.* 74, 117-124.

- Yang, Y., Hawthorne, S.B., Miller, D.J., 1997. Class-selective extraction of polar, moderately polar, and nonpolar organics from hydrocarbon wastes using subcritical water. *Environ. Sci. Technol.* 31, 430–437.
- Yan-ju, L., Hui, D., 2008. Variation in air pollution tolerance index of plant near a steel factory: implications for landscape- plant species selection for industrial areas. *WSEAS Trans. Environ. Dev.* 1, 24–30.
- Yatawara, M., Dayananda, N., 2019. Use of corticolous lichens for the assessment of ambient air quality along rural–urban ecosystems of tropics: a study in Sri Lanka. *Environ. Monit. Assess.* 191, 1–14.
- Ye, R., Tian, K., Hu, H., Li, P., & Tian, X., 2023. Extraction process optimization of essential oil from *Melissa officinalis* L. using a new ultrasound-microwave hybrid-assisted Clevenger hydrodistillation. *Ind. Crops Prod.* 203, 117165.
- Yemm, E.W., Willis, A.J., 1954. The estimation of carbohydrates in plant extracts by anthrone. *Biochem. J.* 57, 508–514.
- Yin, H., Tan, Q., Chen, Y., Lv, G., Hou, X., 2011. Polycyclic aromatic hydrocarbons (PAHs) pollution recorded in annual rings of ginkgo (*Ginkgo biloba* L.): Determination of PAHs by GC/MS after accelerated solvent extraction. *Microchem. J.* 97, 138–143.
- Yu, G.G., Wang, T.G., Wu, D.P., 2007. Study on fingerprints of PAHs from the combustion of bavin and coal. *Ecol. Environ.* 16, 285–289.
- Yu, H., Liu, Y., Han, C., Fang, H., Weng, J., Shu, X., Pan, Y., Ma, L., 2020. Polycyclic aromatic hydrocarbons in surface waters from the seven main river basins of China: Spatial distribution, source apportionment, and potential risk assessment. *Sci. Total Environ.* 752, 141764.
- Yu, Z., Lin, Q., Gu, Y., Du, F., Wang, X., Shi, F., Ke, C., Xiang, M., Yu, Y., 2019. Bioaccumulation of polycyclic aromatic hydrocarbons (PAHs) in wild marine fish from the coastal waters of the northern South China Sea: risk assessment for human health. *Ecotoxicol. Environ. Saf.* 180, 742–748.
- Yuan, H., Li, T., Ding, X., Zhao, G., Ye, S., 2014. Distribution, sources and potential toxicological significance of polycyclic aromatic hydrocarbons (PAHs) in surface soils of the Yellow River Delta, China. *Mar. Pollut. Bull.* 83, 258–264.
- Yuan, J., Wang, X., Zhou, H., Li, Y., Zhang, J., Yu, S., Wang, M., Hao, M., Zhao, Q., Liu, L., Li, M., Li, J., 2020. Comparison of sample preparation techniques for inspection of leaf epidermises using light microscopy and scanning electronic microscopy. *Front. Plant Sci.* 11, 1–13.

- Yunker, M.B., Macdonald, R.W., Vingarzan, R., Mitchell, R.H., Goyette, D., Sylvestre, S., 2002. PAHs in the Fraser River basin: A critical appraisal of PAH ratios as indicators of PAH source and composition. *Org. Geochem.* 33, 489–515.
- Zachara, A., Gałkowska, D., Juszczak, L., 2018. Contamination of tea and tea infusion with polycyclic aromatic hydrocarbons. *Int. J. Environ. Res. Public Health* 15, 1-15.
- Zalewski, R.I., Krygowski, T.M., Shorter, J. (Eds.), 1991. Similarity Models in Organic Chemistry, Biochemistry and Related Fields. *Studies in Organic Chemistry* (Vol. 42). Elsevier, p. 342.
- Zarrinmehr, M.J., Daneshvar, E., Nigam, S., Gopinath, K.P., Biswas, J.K., Kwon, E.E., Wang, H., Farhadian, O., Bhatnagar, A., 2022. The effect of solvents polarity and extraction conditions on the microalgal lipids yield, fatty acids profile, and biodiesel properties. *Bioresour. Technol.* 344, 126303.
- Zechmeister, H.G., Dullinger, S., Hohenwallner, D., Riss, A., Hanus-Illanr, A., Scarf, S., 2006. Pilot study on road traffic emissions (PAHs, Heavy Metals) measured by using mosses in a tunnel experiment in Vienna, Austria. *Environ. Sci. Pollut. Res. Int.* 13, 398-405.
- Zhang, C., Yao, F.E.N.G., Liu, Y.W., Chang, H.Q., LI, Z.J., Xue, J.M., 2017a. Uptake and translocation of organic pollutants in plants: A review. *J. Integr. Agric.* 16, 1659-1668.
- Zhang, S., Yao, H., Lu, Y., Yu, X., Wang, J., Sun, S., Liu, M., Li, D., Li, Y.F., Zhang, D., 2017b. Uptake and translocation of polycyclic aromatic hydrocarbons (PAHs) and heavy metals by maize from soil irrigated with wastewater. *Sci. Rep.* 7, 1-11.
- Zhang, J., Liu, G., Wang, R., Huang, H., 2017c. Polycyclic aromatic hydrocarbons in the water-SPM-sediment system from the middle reaches of Huai River, China: Distribution, partitioning, origin tracing and ecological risk assessment. *Environ. Pollut.* 230, 61-71.
- Zhang, J., Zhang, X., Hu, T., Xu, X., Zhao, D., Wang, X., Li, L., Yuan, X., Song, C., Zhao, S., 2022a. Polycyclic aromatic hydrocarbons (PAHs) and antibiotics in oil-contaminated aquaculture areas: Bioaccumulation, influencing factors, and human health risks. *J. Hazard. Mater.* 437, 129365.
- Zhang, X., Wang, J., Feng, S., Yu, X., Zhou, A., 2022b. Morphological and physiological responses of *Dianthus spiculifolius* high wax mutant to low-temperature stress. *J. Plant Physiol.* 275, 153762.
- Zhang, M., Zhu, L., 2009. Sorption of polycyclic aromatic hydrocarbons to carbohydrates and lipids of ryegrass root and implications for a sorption prediction model. *Environ. Sci. Technol.* 43, 2740–2745.

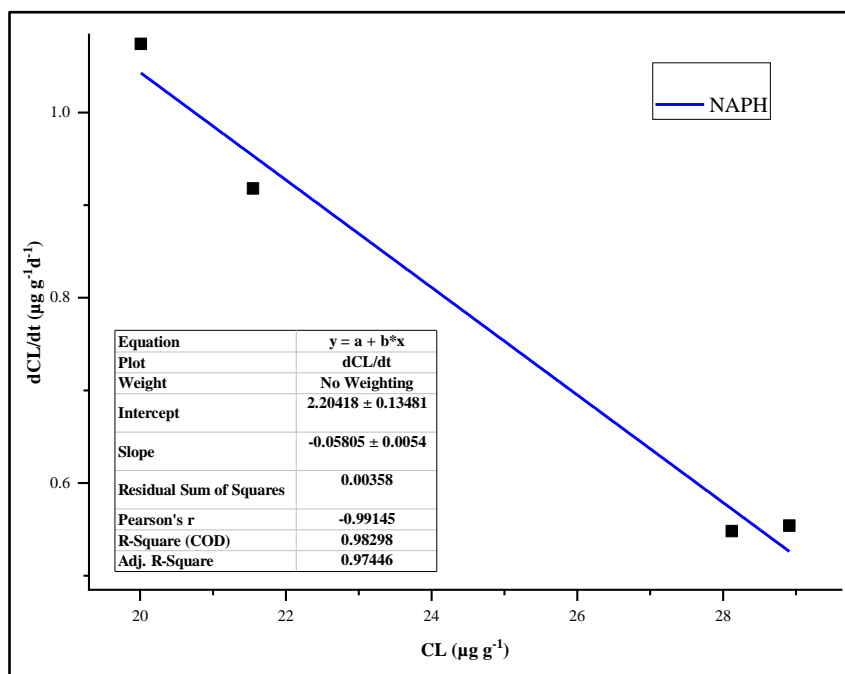
- Zhang, P.Q., Liu, Y.J., Chen, X., Yang, Z., Zhu, M.H., Li, Y.P., 2016. Pollution resistance assessment of existing landscape plants on Beijing streets based on air pollution tolerance index method. *Ecotoxicol. Environ. Saf.* 132, 212–223.
- Zhang, W., Zhang, S., Wan, C., Yue, D., Ye, Y., Wang, X., 2008. Source diagnostics of polycyclic aromatic hydrocarbons in urban road runoff, dust, rain and canopy throughfall. *Environ. Pollut.* 153, 594–601.
- Zhang, W., Zhang, Y., Gong, J., Yang, B., Zhang, Z., Wang, B., Zhu, C., Shi, J., Yue, K., 2020. Comparison of the suitability of plant species for greenbelt construction based on particulate matter capture capacity, air pollution tolerance index, and antioxidant system. *Environ. Pollut.* 263, 114615.
- Zhang, Y., Tao, S., 2009. Global atmospheric emission inventory of polycyclic aromatic hydrocarbons (PAHs) for 2004. *Atmos. Environ.* 43, 812–819.
- Zhao, L., Cao, X., Masek, O., Zimmerman, A., 2013. Heterogeneity of biochar properties as a function of feedstock sources and production temperatures. *J. Hazard. Mater.* 256–257, 1–9.
- Zhao, X., He, M., Shang, H., Yu, H., Wang, H., Li, H., Piao, J., Quinto, M., Li, D., 2018. Biomonitoring polycyclic aromatic hydrocarbons by *Salix matsudana* leaves: A comparison with the relevant air content and evaluation of environmental parameter effects. *Atmos. Environ.* 181, 47–53.
- Zhao, Z., Gong, X., Zhang, L., Jin, M., Cai, Y., Wang, X., 2021. Riverine transport and water-sediment exchange of polycyclic aromatic hydrocarbons (PAHs) along the middle-lower Yangtze River, China. *J. Hazard. Mater.* 403, 123973.
- Zhao, Z., Li, H., Gao, X., 2024. Microwave encounters ionic liquid: synergistic mechanism, synthesis and emerging applications. *Chem. Rev.* 124, 2651–2698.
- Zheng, H., Xing, X., Hu, T., Zhang, Y., Zhang, J., Zhu, G., Li, Y., Qi, S., 2018. Biomass burning contributed most to the human cancer risk exposed to the soil-bound PAHs from Chengdu Economic Region, western China. *Ecotoxicol. Environ. Saf.* 159, 63–70.
- Zheng, H., Yang, D., Hu, T., Li, Y., Zhu, G., Xing, X., Qi, S., 2017. Source apportionment of polycyclic aromatic carbons (PAHs) in sediment core from Honghu Lake, central China: comparison study of three receptor models. *Environ. Sci. Pollut. Res.* 24, 25899–25911.
- Zhong, Y., Zhu, L., 2013. Distribution, input pathway and soil-air exchange of polycyclic aromatic hydrocarbons in Banshan Industry Park, China. *Sci. Total Environ.* 444, 177–82.
- Zhou, L., Dong, L., Huang, Y., Shi, S., Zhang, L., Zhang, X., Yang, W., Li, L., 2014. Spatial distribution and source apportionment of polycyclic aromatic hydrocarbons (PAHs) in

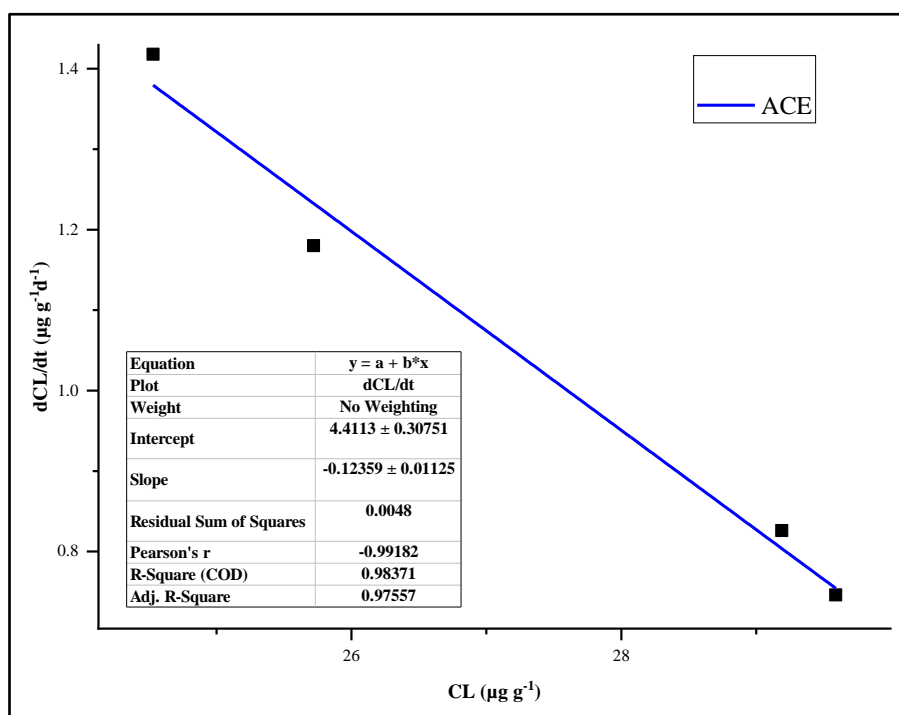
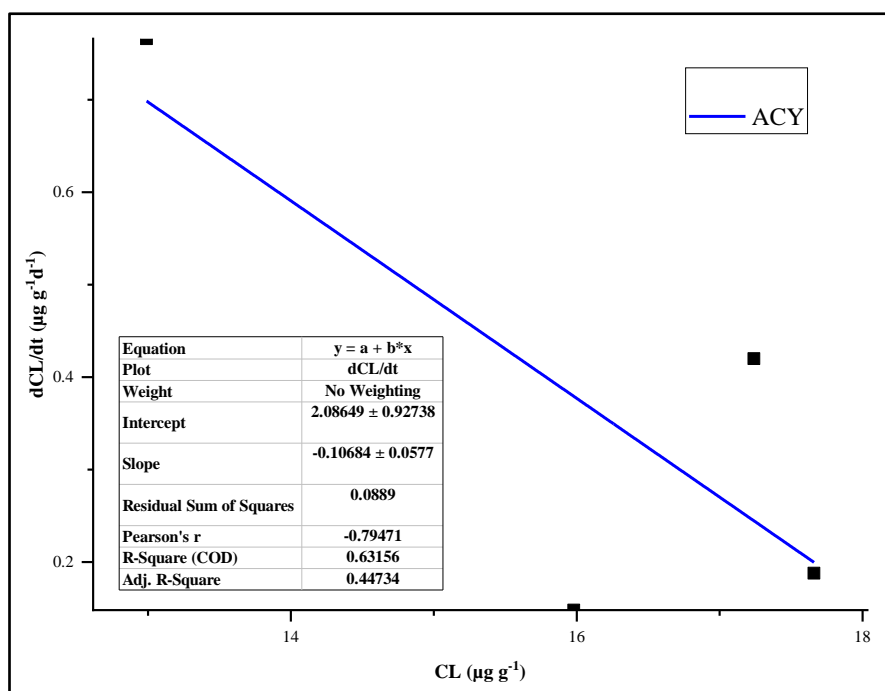
- Camphor (*Cinnamomum camphora*) tree bark from Southern Jiangsu, China. *Chemosphere* 107, 297–303.
- Zhou, Y., Chen, C., Lu, T., Zhang, J., Chen, J., 2022. Season impacts on estimating plant's particulate retention: Field experiments and meta-analysis. *Chemosphere* 288, 132570.
- Zhu, H., Wang, F., Li, B., Yao, Y., Wang, L., Sun, H., 2020. Accumulation and translocation of polybrominated diphenyl ethers into plant under multiple exposure scenarios. *Environ. Int.* 143, 105947.
- Zhu, L.Z., Wang, J., 2005. PAHs pollution from traffic sources in air of Hangzhou, China: trend and influencing factors. *J. Environ. Sci.* 17, 365-370.
- Zilaie, M.N., Arani, A.M., Etesami, H., 2023. Evaluation of air pollution (dust) tolerance index of three desert species *Seidlitzia rosmarinus*, *Haloxylon aphyllum*, and *Nitraria schoberi* under salinity stress. *Environ. Monit. Assess.* 195, 1–13.
- Zoungranan, Y., Ekou, L., Ekou, T., Fane, D., Kouassi, K.D.B., 2018. Accumulation of polycyclic aromatic hydrocarbons from transplanted lichens *Parmotrema dilatatum* in the city of Abidjan (Ivory Coast). *Aust. J. Basic & Appl. Sci.* 12, 12-16.
- Zubeckis, E., 1962. Ascorbic acid content of fruit grown at Vineland, Ontario. In: 1962 Report of the Horticultural Experiment Station and Products Laboratory. Vineland, Ontario, Canada, pp. 90-96.

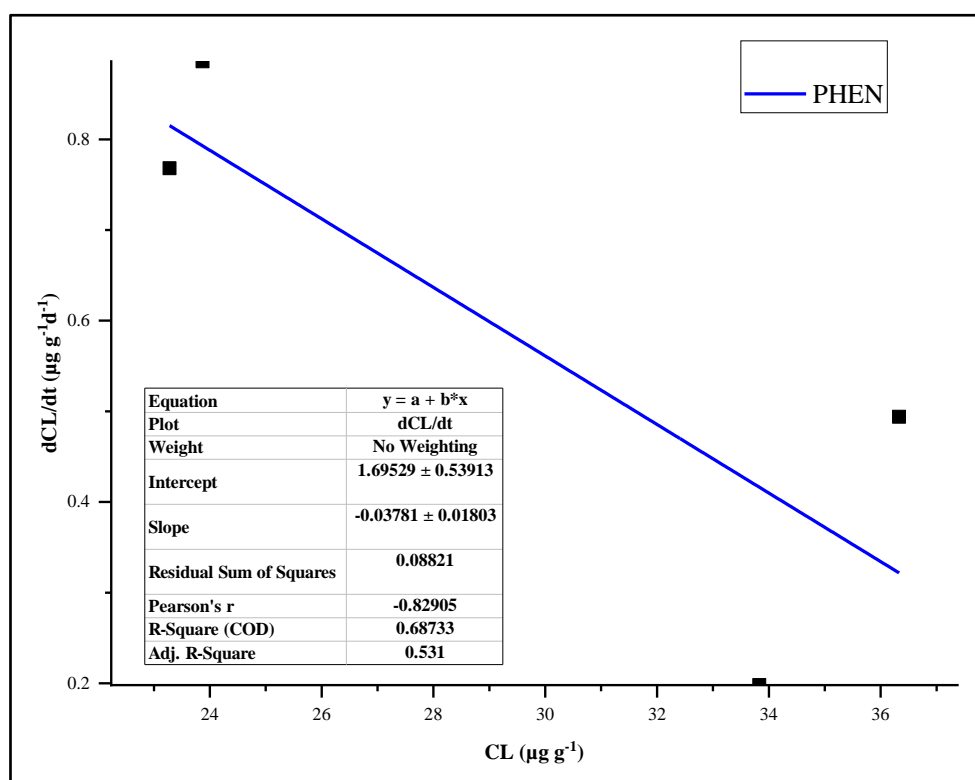
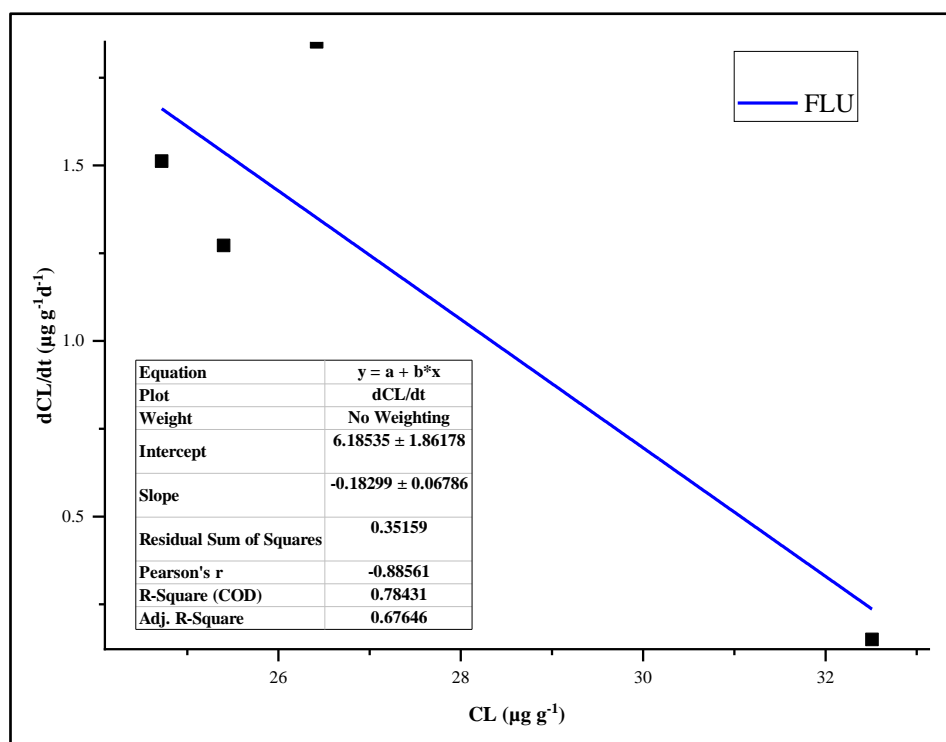
Appendix-I

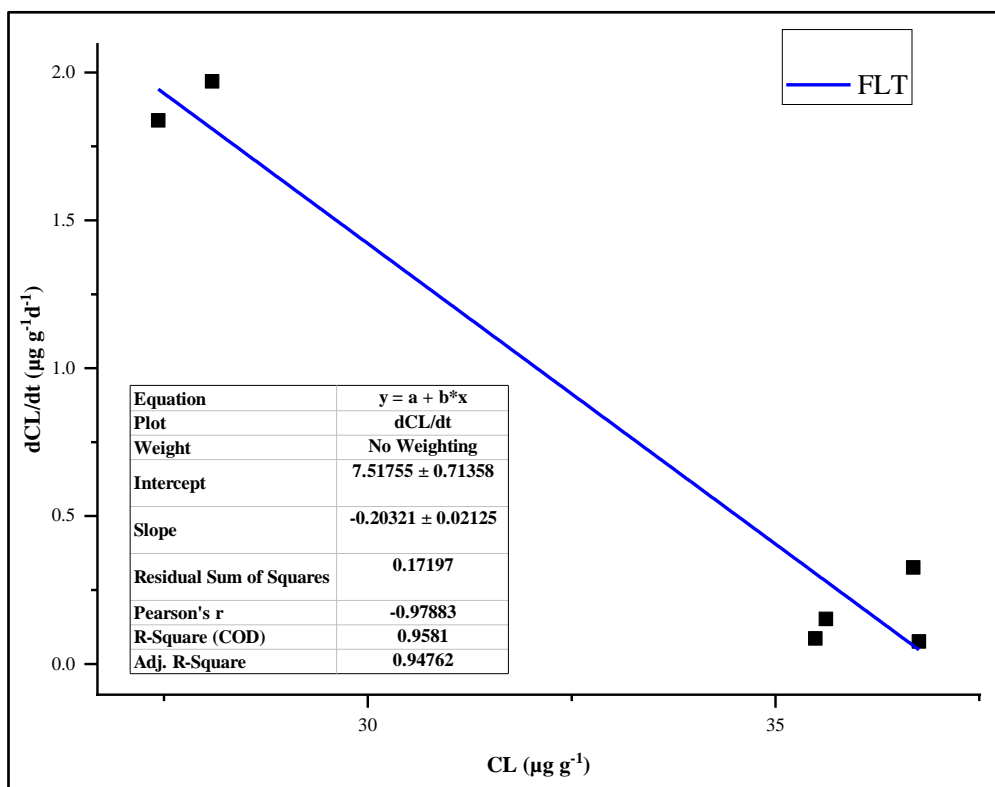
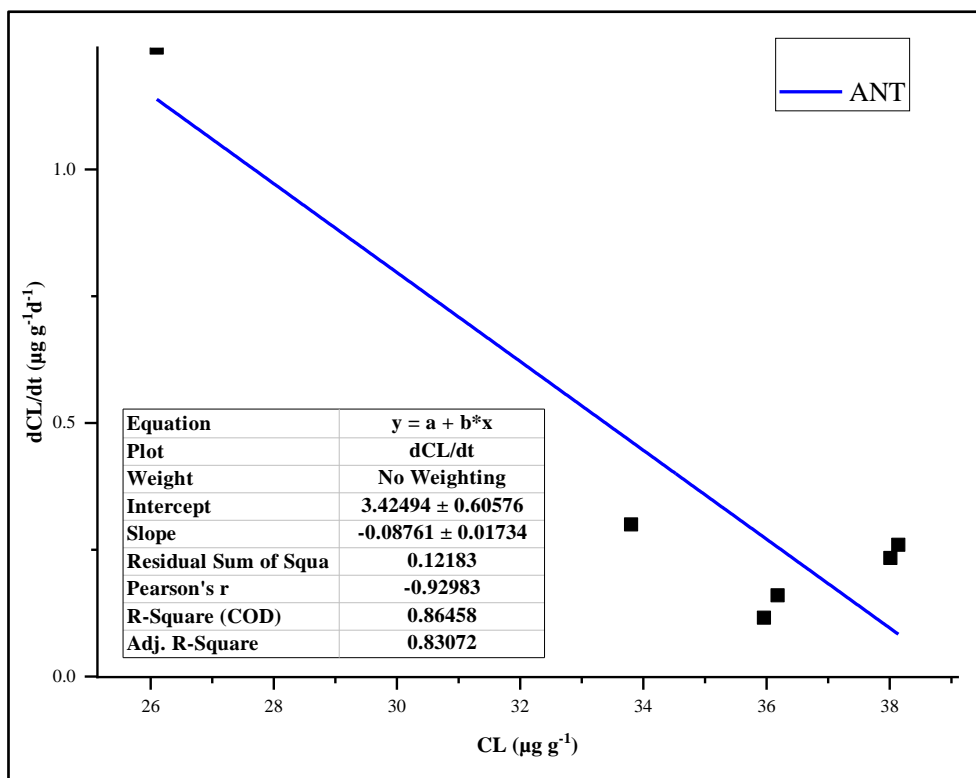
Graphical representation of dC_L/dt ($\mu\text{g g}^{-1} \text{day}^{-1}$) vs. C_L ($\mu\text{g g}^{-1}$) for individual PAHs for estimation of mass transfer coefficient in air-leaf and root-leaf interfaces

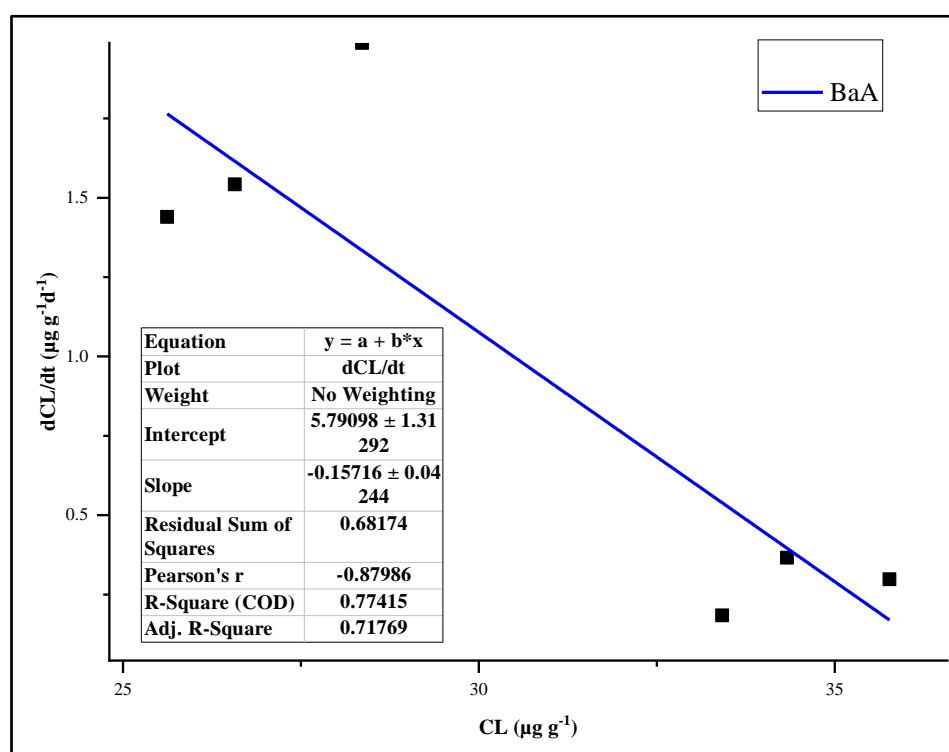
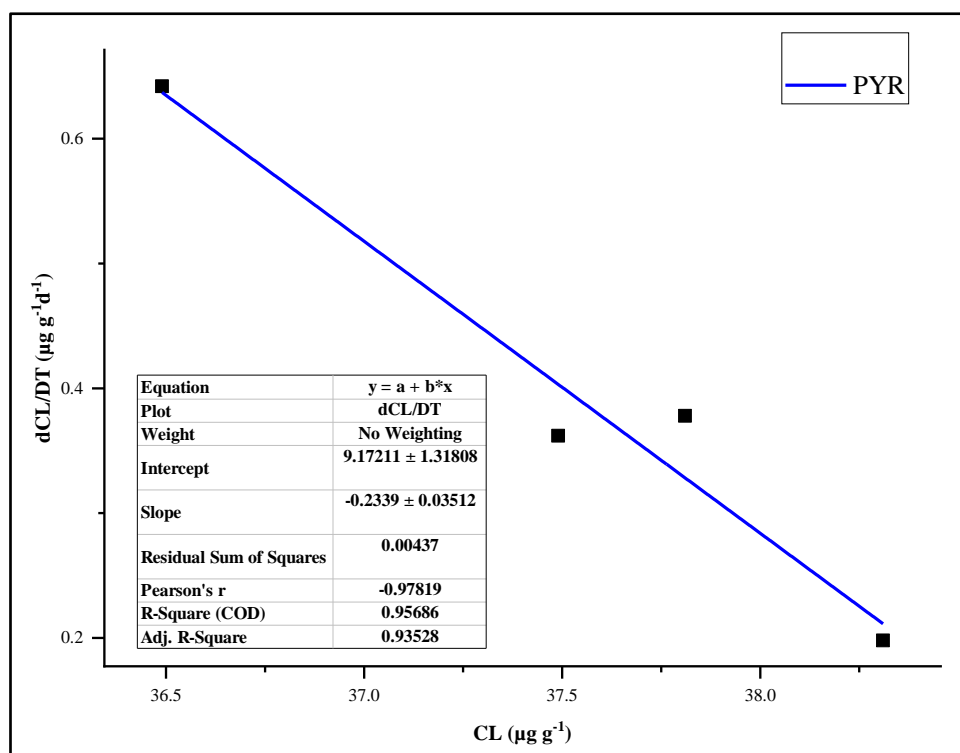
All the plots of dC_L/dt ($\mu\text{g g}^{-1} \text{day}^{-1}$) vs. C_L ($\mu\text{g g}^{-1}$) for individual PAH congeners for evaluation of their mass transfer coefficients considering PAHs uptake from air-plant foliage and roots-plant foliage (as elaborated in **Chapter 7**) have been provided in this section.

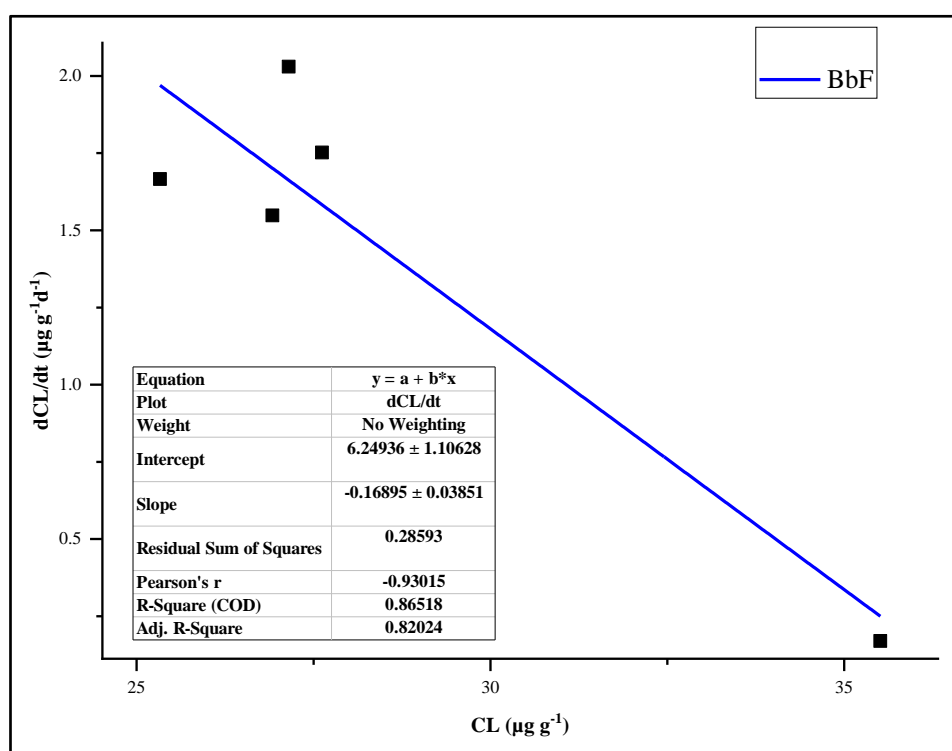
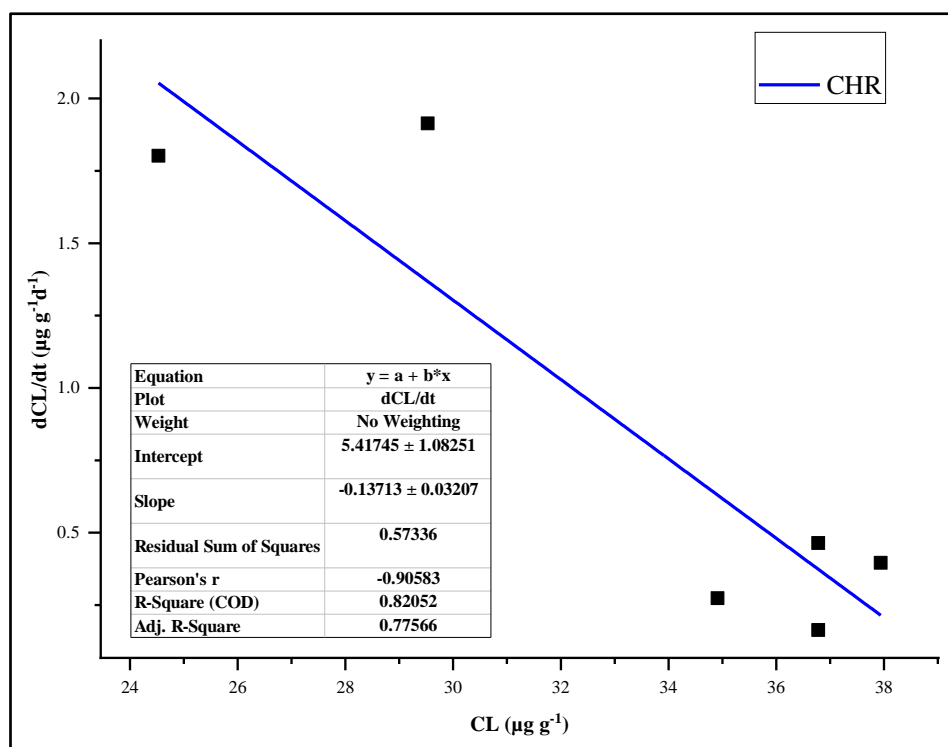


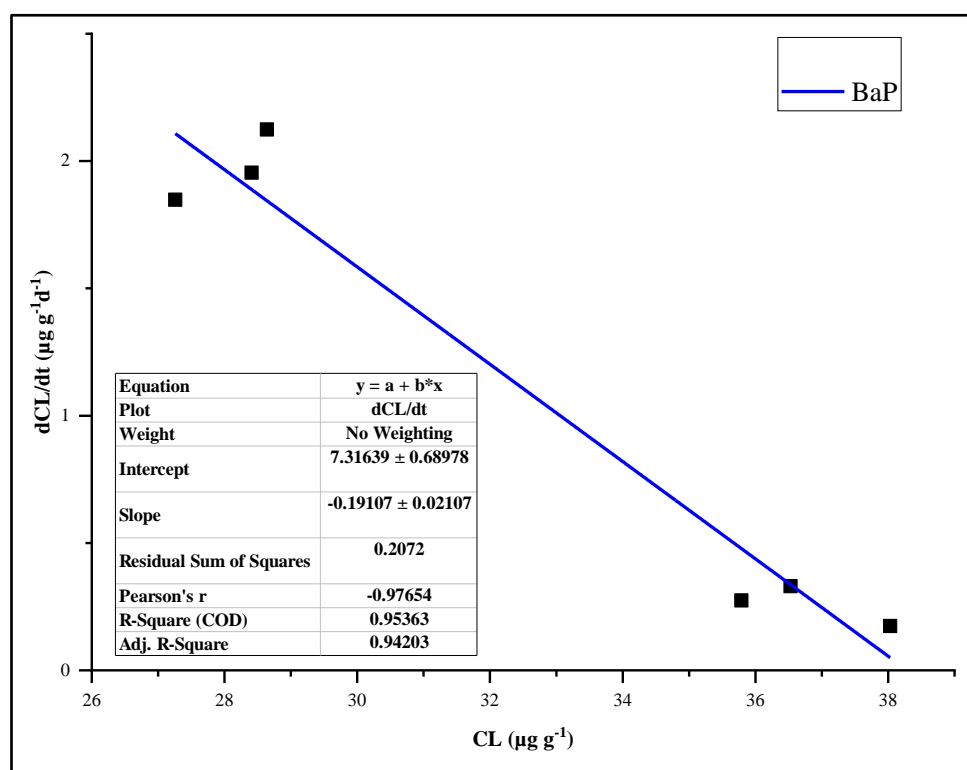
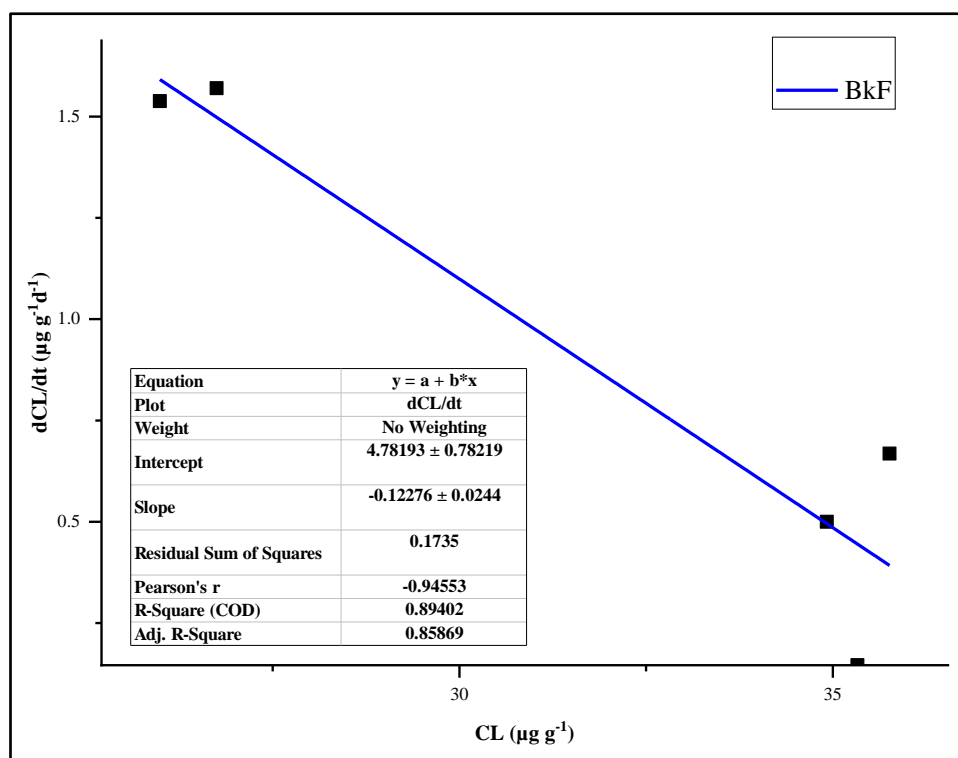


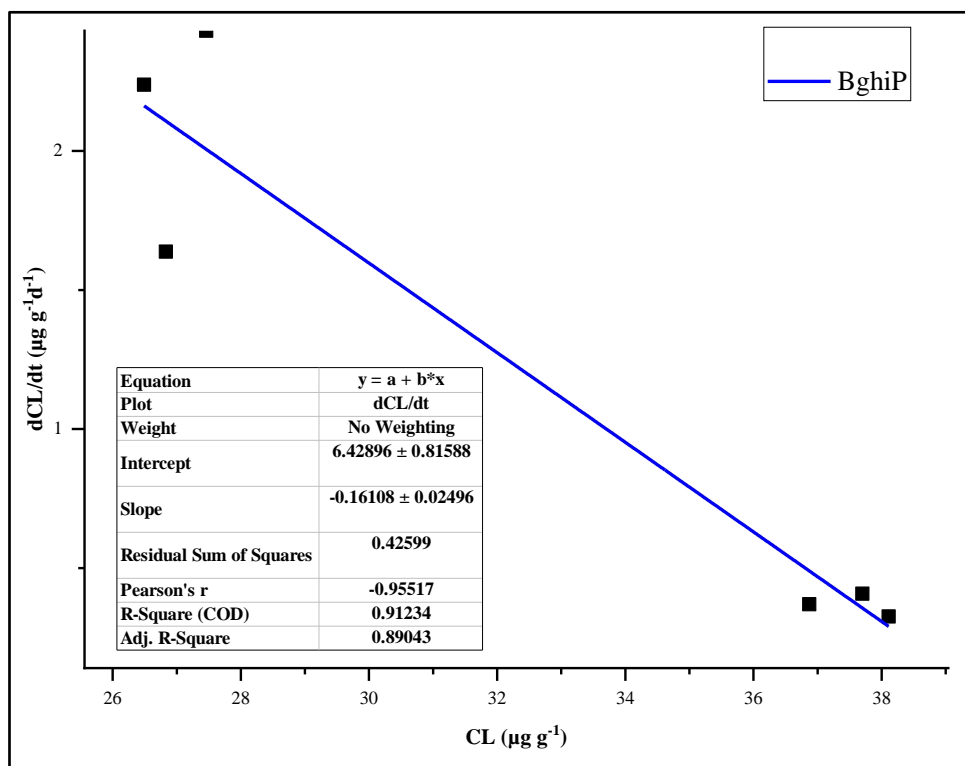
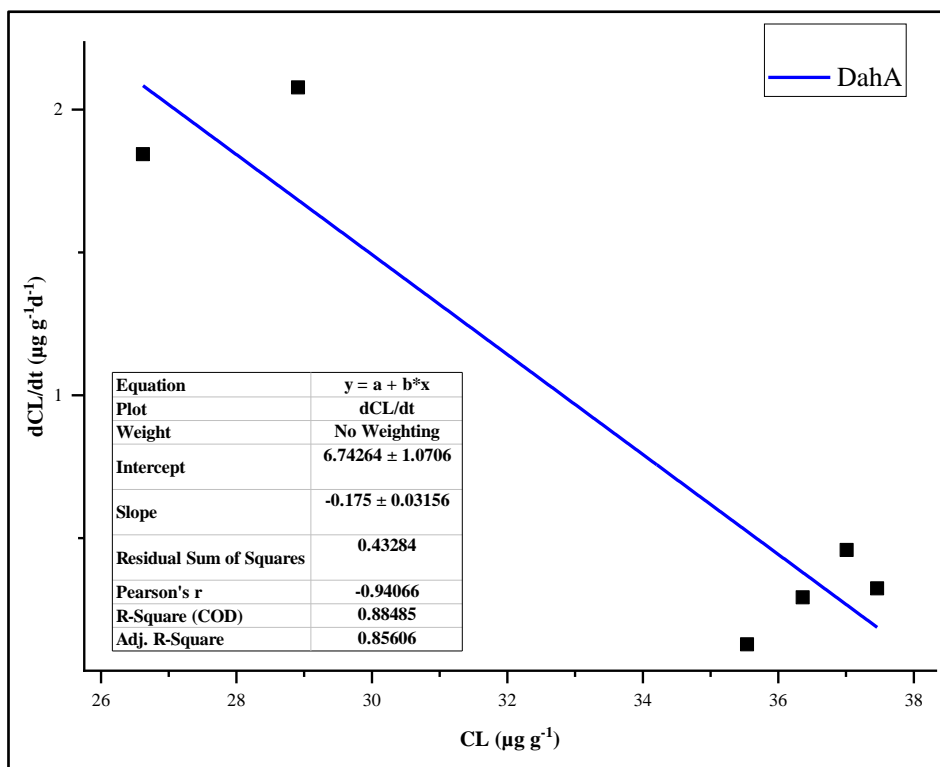












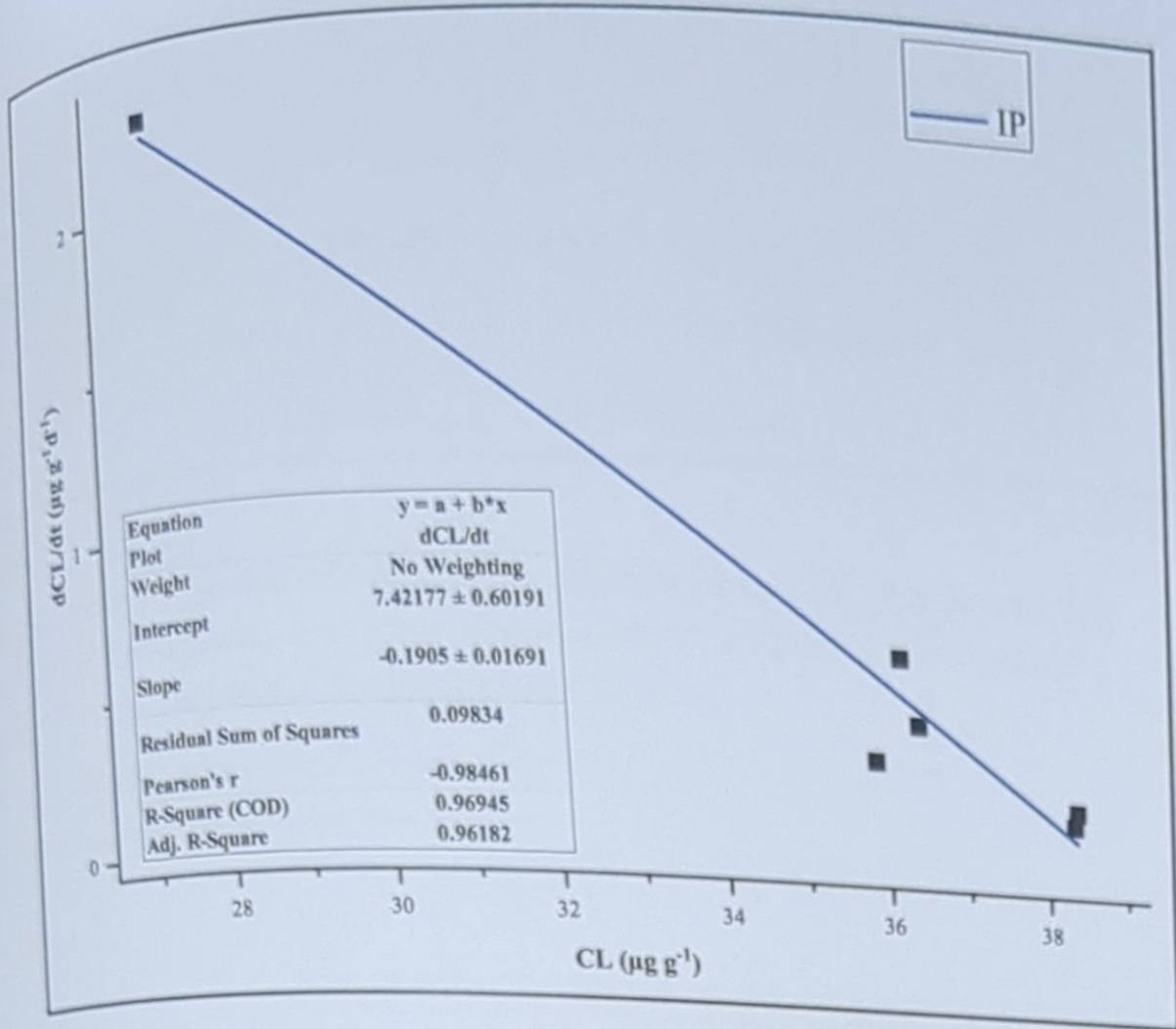


Fig. A1. Plots of dC_L/dt vs. C_L for individual PAH congeners.

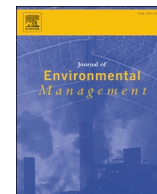
Shritama Mukhopadhyay
23/07/2024

Ratna Dutta
23/07/24

Papita Das
23/07/24

Dr. Ratna Dutta
Associate Professor
Chemical Engineering Department
JADAVPUR UNIVERSITY
Kolkata - 700 032, India

Dr. Papita Das
Professor
Dept. of Chemical Engineering
Jadavpur University, Kolkata



Research article

Greenery planning for urban air pollution control based on biomonitoring potential: Explicit emphasis on foliar accumulation of particulate matter (PM) and polycyclic aromatic hydrocarbons (PAHs)

Shritama Mukhopadhyay, Ratna Dutta^{*}, Papita Das

Department of Chemical Engineering, Jadavpur University, Jadavpur, Kolkata 700032, India

ARTICLE INFO

Keywords:

PM and PAHs
BaP equivalent toxicity
Carcinogenic/mutagenic potential
Leaf micromorphology
Stress responsive leaf traits
APTI/API for green belting

ABSTRACT

In this study, efficiencies of eight indigenous plants of Baishnabghata Patuli Township (BPT), southeast Kolkata, India, were explored as green barrier species and potentials of plant leaves were exploited for biomonitoring of particulate matter (PM) and polycyclic aromatic hydrocarbons (PAHs). The present work focused on studying PM capturing abilities ($539.32\text{--}2766.27\ \mu\text{g cm}^{-2}$) of plants (*T. divaricata*, *N. oleander* and *B. acuminata* being the most efficient species in retaining PM) along with the estimation of foliar contents of PM adhered to leaf surfaces (total sPM (large + coarse): $526.59\text{--}2731.76\ \mu\text{g cm}^{-2}$) and embedded within waxes (total wPM (large + coarse): $8.73\text{--}34.51\ \mu\text{g cm}^{-2}$). SEM imaging used to analyse leaf surfaces affirmed the presence of innate corrugated microstructures as main drivers for particle capture. Accumulation capacities of PAHs of vehicular origin (total index, $\text{TI} > 4$) were compared among the species based on measured concentrations ($159.92\text{--}393.01\ \mu\text{g g}^{-1}$) which indicated *T. divaricata*, *P. alba* and *N. cadamba* as highest PAHs accumulators. Specific leaf area (SLA) of plants ($71.01\text{--}376.79\ \text{cm}^2\ \text{g}^{-1}$), a measure of canopy–atmosphere interface, had great relevance in PAHs diffusion. Relative contribution ($>90\%$) of 4–6 ring PAHs to total carcinogenic equivalent and potential as well as 5–6 ring PAHs to total mutagenic equivalent and potential had also been viewed with respect to benzo[a]pyrene. In–depth analysis of foliar traits and adoption of plant–based ranking strategies (air pollution tolerance index (APTI) and anticipated performance index (API)) provided a rationale for green belting. Each of the naturally selected plant species showed evidences of adaptations during abiotic stress to maximize survival and filtering effects for reductive elimination of ambient PM and PAHs, allowing holistic management of green spaces.

1. Introduction

The severely amplified emission rate of greenhouse gases with other criteria air pollutants results in deterioration of air quality in India which must be tackled on war-footing to ensure sustainable and cleaner environment by avoiding alteration of earth's energy balance and climate. Findings of continuous studies on sustainable practices by the researchers for curbing air pollution have compelled the government bodies of India (like Central Pollution Control Board (CPCB), India) to establish a number of monitoring stations in different states under the National Air Monitoring Programme (NAMP) based on environmental policies and legislative actions (Kaur and Pandey, 2021; NAMP, 2023). Among the major airborne pollutants, particulate matter (PM) (with size

specification: large (aerodynamic diameter, AD: $10\text{--}100\ \mu\text{m}$), coarse (AD: $2.5\text{--}10\ \mu\text{m}$) and fine (AD: $\leq 2.5\ \mu\text{m}$) and polycyclic aromatic hydrocarbons (PAHs) (including low molecular weight PAHs (LMW PAHs) and high molecular weight PAHs (HMW PAHs)) critically affect human health or any other life form in the ecosphere (Delgado-Saborit et al., 2011; Venkatesan, 2016; WHO, 2006). Overshoot in the anthropogenic emissions, being responsible for a sharp increase in pollutants' generation, has already caused irreversible destruction to the natural environment (Ambade et al., 2022). Remediation efforts must be identified by the scientific society to primarily address the life-threatening challenges posed by the carcinogenic or mutagenic impacts of PAHs and PM with their incidences of prevalence. Health risk evaluation of gaseous and particle-bound PAHs (in terms of benzo[a]pyrene equivalents,

^{*} Corresponding author.

E-mail addresses: mukhopadhyayshritama@gmail.com (S. Mukhopadhyay), paul.ratna@gmail.com, ratna.dutta@jadavpuruniversity.in (R. Dutta), papitasaha@gmail.com (P. Das).

<https://doi.org/10.1016/j.jenvman.2024.120524>

Received 5 December 2023; Received in revised form 6 February 2024; Accepted 28 February 2024

0301-4797/© 2024 Elsevier Ltd. All rights reserved.

23/07/2024

Shritama Mukhopadhyay



Biomonitoring of polycyclic aromatic hydrocarbons (PAHs) by *Murraya paniculata* (L.) Jack in South Kolkata, West Bengal, India: spatial and temporal variations

Shritama Mukhopadhyay · Ratna Dutta ·
Aparna Dhara · Papita Das

Received: 19 October 2022 / Accepted: 10 February 2023 / Published online: 23 February 2023
© The Author(s), under exclusive licence to Springer Nature B.V. 2023, corrected publication 2023

Abstract Attempts have been made in the present study for ascertaining the concentrations of atmospheric polycyclic aromatic hydrocarbons (PAHs) using passive biosamplers in preference to conventional air sampling methods. Mechanical stirring, sonication, Soxhlet technique and microwave-assisted Soxhlet extraction (MASE) were employed to extract PAHs from an evergreen plant (*Murraya paniculata*) leaves (having long life-span) sampled from polluted places of South Kolkata, India, with dense population and heavy traffic. Effects of extraction methods and operational parameters (solvent and time) on the recovery levels of PAHs were also investigated. Purified extracts, acquired through adsorption chromatography, were subjected to GC–MS and HPLC–UV analyses for qualitative and quantitative assessment of PAHs. Spatio-temporal distribution of accumulated PAHs across the sampling sites was monitored over premonsoon, postmonsoon and winter supported by pollutant source characterization. The results displayed that the extraction yields of Soxhlet ($272.07 \pm 26.15 \mu\text{g g}^{-1}$) and MASE ($280.17 \pm 15.46 \mu\text{g g}^{-1}$) were the highest among the

four techniques. Conditions of extraction with toluene for 6 h were found to be most favorable for PAHs. In spatio-temporal analysis, total concentrations of PAHs in the foliar samples varied from 200.98 ± 2.72 to $550.79 \pm 10.11 \mu\text{g g}^{-1}$ dry weight, and the highest values being recorded in the samples of Exide More because of daylong inexorable traffic flow/crowding increasing the burden of ambient PAHs. Widespread changes in meteorology exerted influence on seasonal concentrations of PAHs in plant leaves, and extent of leaf contamination by PAHs was observed extreme in winter followed by postmonsoon and then, premonsoon. Foliar accretion of PAHs differed in the study sites with diverse sources of emission from motor vehicles, fossil fuel and biomass burning along with other human interferences.

Keywords Extraction optimization · PAHs · Evergreen plant species · Spatial and temporal variability · Diagnostic ratios · Field study

Introduction

Polycyclic aromatic hydrocarbons (PAHs) are lipophilic environmental carcinogens having pernicious impact on public health owing to their long presence and resistance to biodegradation (Bostrom et al., 2002; IARC, 1983; Mallah et al., 2022; Patel et al., 2020; Zheng et al., 2018). Anthropogenic pollution has been the key contributor of airborne PAHs

Supplementary Information The online version contains supplementary material available at <https://doi.org/10.1007/s10653-023-01506-x>.

S. Mukhopadhyay · R. Dutta (✉) · A. Dhara · P. Das
Department of Chemical Engineering, Jadavpur
University, Kolkata 700032, India
e-mail: ratna.dutta@jadavpuruniversity.in

23/07/2024

Shritama Mukhopadhyay



Assessment of air pollution tolerance index of *Murraya paniculata* (L.) Jack in Kolkata metro city, West Bengal, India

Shritama Mukhopadhyay, Ratna Dutta^{*}, Aparna Dhara

Department of Chemical Engineering, Jadavpur University, Jadavpur, Kolkata 700032, India

ARTICLE INFO

Keywords:

Murraya paniculata (L.) Jack
Air pollution tolerance index (APTI)
Polycyclic aromatic hydrocarbons (PAHs)
Extraction
Biomonitor
Green belts

ABSTRACT

Constant bursting of the city frontiers is taking a massive toll on natural vegetation, deteriorating thereby the purity of the clean air. Biomonitoring of airborne pollutants through creation of green belts has become the only alternative to provide natural filtering barrier. The present study was constructed to evaluate the air pollution tolerance index (APTI) of a commonly found evergreen plant species in Kolkata, *Murraya paniculata*, based on leaf attributes. PAHs accumulating ability of the plant species was also examined so as to establish the species' potential in monitoring of PAHs. *M. paniculata* was found to be tolerant (APTI: 19.78 ± 1.20 – 31.12 ± 0.72) towards air pollution with dust capturing potential between 0.85 ± 0.04 – 2.26 ± 0.02 mg cm⁻². Correlation analysis unveiled the strong relationship of foliar dust with leaf ascorbic acid ($r = 0.931$), leaf extract pH ($r = 0.985$), leaf RWC ($r = -0.822$), total carotenoids ($r = -0.862$) and total chlorophyll ($r = -0.76$). APTI was found to be correlated positively to ascorbic acid and foliar pH and negatively to total chlorophyll and RWC. Changes in leaf surface micromorphology due to particulate pollution were also endorsed by SEM-EDX analysis. Findings revealed that *Murraya paniculata* has the tolerance and efficiency of trapping both lighter and heavier PAHs, proving its ability for biomonitoring of atmospheric pollution.

1. Introduction

Unplanned depletion of agricultural, water and forest lands in and around Kolkata, India, for expansion of city's boundaries to accommodate rapidly growing population including human migration from other places is the primary cause behind the destruction and decay of century-old natural ecosystem. Environmental worsening due to the diversified presence of xenobiotics, gaseous pollutants, heavy metals, persistent organic pollutants (POPs) such as polycyclic aromatic hydrocarbons (PAHs) and dust or particulate matter (PM) imposes toxic air effects on the residents together with native flora and fauna (Haque and Singh, 2017). The situation is also aggravated owing to relentless activities for the construction of infrastructures and industries, power sectors, high traffic density, growth of slum-like settlements, reducing open spaces and boundless emission (local and transboundary) of air pollutants, increasing their level in the atmosphere manifold (Haque and Singh, 2017). Air suspended PM and PAHs are among the deadly air pollutants that are genotoxic in nature. PM has been classified as Group I human carcinogen by The International Agency for Research on Cancer (IARC, 2013). PAHs are a group of hydrophobic organic compounds, ubiquitously present in different environmental compartments and mainly derived from either incomplete combustion of fossil fuels and biomass (anthropogenic inputs) or natural emissions (Mukhopadhyay et al., 2020). Their recalcitrance and persistence in nature make them highly toxic and carcinogenic for which they

^{*} Corresponding author.

E-mail address: paul.ratna@gmail.com (R. Dutta).

<https://doi.org/10.1016/j.uclim.2021.100977>

Received 17 May 2021; Received in revised form 22 July 2021; Accepted 31 August 2021

2212-0955/© 2021 Elsevier B.V. All rights reserved.

23/07/2024

Shritama Mukhopadhyay



Review

A critical review on plant biomonitors for determination of polycyclic aromatic hydrocarbons (PAHs) in air through solvent extraction techniques



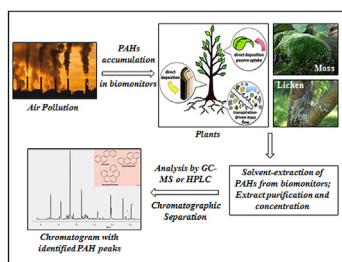
Shritama Mukhopadhyay, Ratna Dutta*, Papita Das

Department of Chemical Engineering, Jadavpur University, Jadavpur, Kolkata, 700032, India

HIGHLIGHTS

- Monitoring of ambient concentration of 16 USEPA PAHs using biomonitors for evaluation of air quality
- Different plant biomonitors based on APTI and IAP values for quantification of ambient PAHs
- Morphological characteristics of plants greatly influence accumulation of PAHs in their tissues over time
- Conventional and modified solvent extraction techniques for determination of PAHs from different biomonitors.
- Different plant bioindicators used till date for assessment of ambient PAHs

GRAPHICAL ABSTRACT



ARTICLE INFO

Article history:

Received 9 January 2020

Received in revised form

5 March 2020

Accepted 6 March 2020

Available online 9 March 2020

Handling Editor: R Ebinghaus

Keywords:

Polycyclic aromatic hydrocarbons (PAHs)

Biomonitoring

Plants biomonitor

Lichen

Moss

Solvent-extraction techniques

ABSTRACT

Polycyclic aromatic hydrocarbons (PAHs) are hydrocarbons having two or more fused aromatic rings, released from natural (like forest fires and volcanic eruption) as well as man-made sources (like burning of fossil fuel & wood, automobile emission). They are persistent priority pollutants and continue to last for a long time in the environment causing severe damage to human health owing to their genotoxicity, mutagenicity and carcinogenicity. The study of PAHs in environment has therefore aroused a global concern. PAHs adsorption to plant cell wall is facilitated by transpiration and plant root lipids which help PAHs transfer from roots to leaves and stalks, causing more accumulation of contaminants with the increase in lipid content. Hence, these bioaccumulators can be utilized as biomonitors for indirect assessment of ambient air pollution. Efficacy of specific plants, lichens and mosses as useful biomonitors of airborne PAHs pollution has been discussed in this review along with prevalent classical and modified extraction techniques coupled with proper analytical procedures in order to gain an insight into the assessment of atmospheric PAHs concentrations. Different modern and modified solvent extraction techniques along with conventional Soxhlet method are identified for extraction of PAHs from accumulative bioindicators and analytical methods are also developed for accurate determination of PAHs. Process parameters like choice of solvent, temperature, time of extraction, pressure and matrix characteristics are usually checked. An approach of biomonitoring of PAHs using plants, lichens and mosses has been discussed here as they usually trap the atmospheric PAHs and mineralize them.

© 2020 Elsevier Ltd. All rights reserved.

* Corresponding author.

E-mail addresses: mukhopadhyayshritama@gmail.com (S. Mukhopadhyay), paul.ratna@gmail.com (R. Dutta), papitasaha@gmail.com (P. Das).

23/07/2024

Shritama Mukhopadhyay



A Review on Seasonal Changes in Particulate Matter Accumulation by Plant Bioindicators: Effects on Leaf Traits

Sayantana Ghosh · Ratna Dutta ·
Shritama Mukhopadhyay

Received: 28 November 2022 / Accepted: 22 July 2023 / Published online: 2 August 2023
© The Author(s), under exclusive licence to Springer Nature Switzerland AG 2023

Abstract Particulate matter (PM), defined as the total mixture of liquid droplets and microscopic solid particles present in the atmosphere, is a major global concern which poses serious threats to human health, causing environmental degradation. In ambient air, PMs are mostly released from both anthropogenic and natural sources which include coal mining activities, thermal power plants, vehicle emissions, strong winds, dust storms, etc. Based on the sources, PMs vary in size (large (PM_{10-100}), coarse ($PM_{2.5-10}$), fine ($PM_{2.5}$) and ultrafine ($PM_{0.1}$) particles) and composition significantly. PM pollution is directly associated with various short and long-term human health effects. Plants, constantly exposed to air, are the principal receptors of both gaseous and suspended particulate pollutants in the atmosphere. Prevalence of PMs exerts a strong influence on plant's morphological, biochemical and physiological traits such as chlorophyll, phyllotaxy, specific leaf area, stomatal distribution, ascorbic acid content, relative water content and pH. Such effects could be studied to identify and screen the tolerant plant species having high Air Pollution Tolerance Index (APTI) as biomonitors for green belt construction through urban plantations for abatement of PM pollution. The present study has

highlighted all the possible changes related to leaf traits because of PM deposition on leaf surfaces of plant species, and seasonal variation-based capturing of PM is also reviewed.

Keywords Particulate matter · Plant bioindicators · Seasonal trends · Leaf traits

1 Introduction

Increasing population density, agriculture-related activities, industrialisation and deforestation have caused pollution of our atmospheric environment, and the most harmful form of an air pollutant is dust. Air-suspended particulate matter (ASPM) poses great threats to most Indian cities, ranging more than $150 \mu\text{g m}^{-3}$ which is appreciably higher than the safe limit of $100 \mu\text{g m}^{-3}$ (PM_{10}) and $60 \mu\text{g m}^{-3}$ ($PM_{2.5}$) in 24-h monitoring (<https://cpcb.nic.in>). Particulate matter (PM) with a diameter of $2.5 \mu\text{m}$ or less is an alarming concern in urban and industrial areas since it can easily penetrate the human respiratory system causing multiple pulmonary and cardiovascular disorders, reproductive and neurological abnormalities and even cancer (Hamanaka & Mutlu, 2018; Manisalidis et al., 2020). It also affects the morphological, physiological and biochemical characteristics of plants (Rai, 2016). Hence, it becomes important to routinely monitor the presence of PM in the atmosphere. Conventional instrument-based air sampling and air

S. Ghosh · R. Dutta (✉) · S. Mukhopadhyay
Department of Chemical Engineering, Jadavpur
University, 188, Raja S.C. Mallick Rd, Kolkata 700032,
India
e-mail: ratna.dutta@jadavpuruniversity.in; paul.ratna@gmail.com

23/07/2024

Shritama Mukhopadhyay



National Symposium on Sustainable Technology & Management for Humanistic Growth

Jointly Organized by

Faculty of Engineering & Technology, Jadavpur University

And

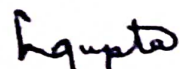
Vivekananda Institute of Environment & Management


22– 23 December 2023

Award for Oral Presentation

*This is to certify that the Paper Titled Efficacy of Mangifera Indica as Biomonitoring Plant Species... authored by Aparna Dhara, Ratna Dutta, Marshal Murmu, Shritama Mukhopadhyay of Department of Chemical Engineering, Jadavpur University was presented in the Symposium and was Adjudged **Second Prize**.*

Kolkata
12 January 2024


Dr Bhaskar Gupta
Professor, ETCE, JU
Organizing Secretary


Swami (Prof.-Dr) Vedajnananda
Chief Mentor & President, VIEM

23/07/2024

Shritama Mukhopadhyay

CERTIFICATE OF PARTICIPATION

International Conference on Chemical Engineering Innovations and Sustainability (ICEIS-2023)

Chemical Engineering Department, Jadavpur University

This is to certify that



Shritama Mukhopadhyay



Jadavpur University, Kolkata, India

Orally presented technical paper entitled “Polycyclic Aromatic Hydrocarbon pollution in the urban wetland soil in South Kolkata” in ICEIS-2023 held during 26th-27th February, 2023 at Jadavpur University, Kolkata, India

Rajat Chakraborty

Ranjana Chowdhury

Kajari Kargupta

P. Das

PROF. RAJAT CHAKRABORTY

PROF. RANJANA CHOWDHURY

PROF. KAJARI KARGUPTA

PROF. PAPITA DAS

Chairman, ICEIS 2023

Joint Conveners, ICEIS 2023

23/07/2024

Shritama Mukhopadhyay



Since-1947

Platinum Jubilee Celebration of
Indian Institute of Chemical Engineers
International Conference on Advances in Chemical & Material Sciences

ACMS-2022

April 14-16, 2022 at HIT Kolkata

Organised by



In Association with



Best Paper Award

This is to certify that Prof./Dr./Mr./Ms.

SHRITAMA MUKHOPADHYAY

JADAVPUR UNIVERSITY

has Presented a paper (Oral/Poster) in ACMS-2022, held at Heritage Institute of Technology, Kolkata, during April 14-16, 2022 and selected for the Best Paper Award.

Title: SEASONAL TRENDS OF ATMOSPHERIC POLYCYCLIC AROMATIC HYDROCARBONS (PAHS) IN KOLKATA METRO CITY OF INDIA: BIOMONITORING USING FOLIAGE OF MURRAYAPANICULATA (L.) JACK

Co-authored by:

RATNA DUTTA, APARNA DHARA, PAPITA DAS

Shri D. M. Butala
President, IIChE

Shri Praveen Saxena
Honorary Registrar, IIChE

Dr. Avijit Ghosh
Organizing Secretary, ACMS-2022
and Assistant Professor
Heritage Institute of Technology

Certificate ID - IICHE/2022/ACMS2022/11616

23/07/2024

Shritama Mukhopadhyay



Since-1947

Platinum Jubilee Celebration of
Indian Institute of Chemical Engineers
International Conference on Advances in Chemical & Material Sciences

ACMS-2022

April 14-16, 2022 at HIT Kolkata

Organised by



In Association with



Certificate

This is to certify that Prof./Dr./Mr./Ms.
SHRITAMA MUKHOPADHYAY

JADAVPUR UNIVERSITY

has Presented a paper (ORAL) in ACMS-2022, held at
Heritage Institute of Technology, Kolkata, during April 14-
16, 2022.

Title: SEASONAL TRENDS OF ATMOSPHERIC POLYCYCLIC AROMATIC HYDROCARBONS (PAHS) IN KOLKATA
A METRO CITY OF INDIA: BIOMONITORING USING FOLIAGE OF MURRAYAPANICULATA (L.) JAC
K

Co-authored by:

RATNA DUTTA, APARNA DHARA, PAPITA DAS

Shri D. M. Butala
President, IIChE

Shri Praveen Saxena
Honorary Registrar, IIChE

Dr. Avijit Ghosh
Organizing Secretary, ACMS-2022
and Assistant Professor
Heritage Institute of Technology

Certificate ID - IICHE/2022/ACMS2022/11292

23/07/2024

Shritama Mukhopadhyay

9th IconSWM-CE 2019



International
Society of
Waste Management,
Air and Water

CRIC

The 9th International Conference on Sustainable Waste Management towards Circular Economy

Venue: Campus 6, Convention Centre, KIIT University, Bhubaneswar, India

November 27 – 30, 2019

CERTIFICATE OF APPRECIATION

Presented to

SHRITAMA MUKHOPADHYAY, APARNA DHARA

For participation and presenting the paper

**Bioindicators for monitoring of ambient air pollution and its
bioremediation -A Review**

in 9th IconSWM-CE during November 27-30, 2019.

Co-authored by: Ratna Dutta

Prof. Dr. Sadhan K Ghosh
Chairman, IconSWM & President, ISWMAW
Dean, Faculty of Engineering and
Technology, Jadavpur University, India



UNITED NATIONS
INDUSTRIAL DEVELOPMENT ORGANIZATION



23/07/2024

Shritama Mukhopadhyay